EPRI



2024 TECHNICAL REPORT

EPRI Materials Degradation Matrix, Revision 5

EPRI Materials Degradation Matrix, Revision 5

3002030559

Final Report, November 2024

EPRI Project Manager
J. Smith

All or a portion of the requirements of the EPRI Nuclear Quality Assurance Program apply to this product.

YES  NO

ELECTRIC POWER RESEARCH INSTITUTE
3420 Hillview Avenue, Palo Alto, California 94304-1338 ▪ PO Box 10412, Palo Alto, California 94303-0813 ▪ USA
800.313.3774 ▪ 650.855.2121 ▪ askepri@epri.com ▪ www.epri.com

DISCLAIMER OF WARRANTIES AND LIMITATION OF LIABILITIES

THIS DOCUMENT WAS PREPARED BY THE ORGANIZATIONS NAMED BELOW AS AN ACCOUNT OF WORK SPONSORED OR COSPONSORED BY THE ELECTRIC POWER RESEARCH INSTITUTE, INC. (EPRI). NEITHER EPRI, ANY MEMBER OF EPRI, ANY COSPONSOR, THE ORGANIZATIONS BELOW, NOR ANY PERSON ACTING ON BEHALF OF ANY OF THEM:

(A) MAKES ANY WARRANTY OR REPRESENTATION WHATSOEVER, EXPRESS OR IMPLIED, (I) WITH RESPECT TO THE USE OF ANY INFORMATION, APPARATUS, METHOD, PROCESS, OR SIMILAR ITEM DISCLOSED IN THIS DOCUMENT, INCLUDING MERCHANTABILITY AND FITNESS FOR A PARTICULAR PURPOSE, OR (II) THAT SUCH USE DOES NOT INFRINGE ON OR INTERFERE WITH PRIVATELY OWNED RIGHTS, INCLUDING ANY PARTY'S INTELLECTUAL PROPERTY, OR (III) THAT THIS DOCUMENT IS SUITABLE TO ANY PARTICULAR USER'S CIRCUMSTANCE; OR

(B) ASSUMES RESPONSIBILITY FOR ANY DAMAGES OR OTHER LIABILITY WHATSOEVER (INCLUDING ANY CONSEQUENTIAL DAMAGES, EVEN IF EPRI OR ANY EPRI REPRESENTATIVE HAS BEEN ADVISED OF THE POSSIBILITY OF SUCH DAMAGES) RESULTING FROM YOUR SELECTION OR USE OF THIS DOCUMENT OR ANY INFORMATION, APPARATUS, METHOD, PROCESS, OR SIMILAR ITEM DISCLOSED IN THIS DOCUMENT.

REFERENCE HEREIN TO ANY SPECIFIC COMMERCIAL PRODUCT, PROCESS, OR SERVICE BY ITS TRADE NAME, TRADEMARK, MANUFACTURER, OR OTHERWISE, DOES NOT NECESSARILY CONSTITUTE OR IMPLY ITS ENDORSEMENT, RECOMMENDATION, OR FAVORING BY EPRI.

THE FOLLOWING ORGANIZATIONS PREPARED THIS REPORT:

EPRI

JLN Consulting

Structural Integrity Associates, Inc.

Dominion Engineering, Inc.

Westinghouse Electric Company

UJV Rez

Trampus Consulting

Canadian Nuclear Laboratories

THE TECHNICAL CONTENTS OF THIS PRODUCT WERE **NOT** PREPARED IN ACCORDANCE WITH THE EPRI QUALITY PROGRAM MANUAL THAT FULFILLS THE REQUIREMENTS OF 10 CFR 50, APPENDIX B. THIS PRODUCT IS **NOT** SUBJECT TO THE REQUIREMENTS OF 10 CFR PART 21.

NOTE

For further information about EPRI, call the EPRI Customer Assistance Center at 800.313.3774 or e-mail askepri@epri.com.

Together…Shaping the Future of Energy®

© 2024 Electric Power Research Institute (EPRI), Inc. All rights reserved. Electric Power Research Institute, EPRI, and TOGETHER…SHAPING THE FUTURE OF ENERGY are registered marks of the Electric Power Research Institute, Inc. in the U.S. and worldwide.

ACKNOWLEDGMENTS

The following organizations prepared this report:

EPRI
3420 Hillview Ave.
Palo Alto, CA, USA 94304

Principal Investigator
J. Smith

JLN Consulting
56 Bradford Farm Road
Mills River, NC, USA 27859

Principal Investigators
P. Andresen
D. Sandusky

Structural Integrity Associates, Inc.
5215 Hellyer Ave., Suite 210
San Jose, CA, USA 95138

Principal Investigator
B. Gordon

Dominion Engineering, Inc.
12100 Sunrise Valley Dr., Suite 220
Reston, VA, USA 20191

Principal Investigator
C. Marks

Westinghouse Electric Company
1000 Westinghouse Dr.
Cranberry Township, PA, USA 16066

Principal Investigator
J. McKinley

UJV Rez
Hlavni 130, Rez
250 68, Husinec, Czech Republic

Principal Investigators
M. Postler
M. Krondak
J. Wandrol
M. Zamboch

Trampus Consulting
20, Zrinyi St.
H-2060, Bicske, Hungary

Principal Investigator
P. Trampus

Canadian Nuclear Laboratories
286 Plant Road
Chalk River, ON, Canada K0J1P0

Principal Investigators
N. Huin
M. Wright
G. Bickel

This report describes research sponsored by EPRI.

This publication is a corporate document that should be cited in the literature in the following manner:

EPRI Materials Degradation Matrix, Revision 5. EPRI, Palo Alto, CA: 2024. 3002030559.

ABSTRACT

The EPRI Materials Degradation Matrix (MDM) is a key part of the industry's materials degradation and issue management initiative. The MDM is a living tool that summarizes the state of industry knowledge regarding degradation mechanisms and related research and development (R&D) activities. The MDM is periodically updated and has progressively included information relating to boiling water reactors and pressurized water reactors outside of the United States, whose operators are members of EPRI. The third and fourth revisions included, for the first time, MDM results for the CANDU pressurized heavy water reactor and VVER designs, respectively. The current Revision 5, includes updates to the MDM tables and explanatory text for all reactor types, based on operating experience and R&D results since the previous revision, to maintain the document consistent with the current industry state-of-knowledge. The MDM is a publicly available document that represents EPRI's perspective on nuclear plant primary system materials degradation.

Keywords
Degradation mechanism
Materials degradation matrix (MDM)
Materials initiative
Materials R&D

Deliverable Number: 3002030559

Product Type: Technical Report

Product Title: EPRI Materials Degradation Matrix, Revision 5

PRIMARY AUDIENCE: Utility personnel responsible for advising EPRI on research addressing nuclear plant primary system materials degradation

SECONDARY AUDIENCE: Research scientists and regulatory authority personnel interested in understanding key materials degradation research and development (R&D) gaps

KEY RESEARCH QUESTION

What are the key materials degradation-related gaps in the industry state-of-knowledge that should be addressed by R&D to promote safe and reliable long-term operation of nuclear power plants?

RESEARCH OVERVIEW

The materials degradation matrix (MDM) presents a broad perspective on materials degradation issues and the state of industry knowledge related to resolving knowledge gaps and mitigating degradation concerns for boiling water reactor (BWR), pressurized water reactor (PWR), Canada deuterium uranium (CANDU) reactor, and Voda-Vodyanoi Energeticheski Reaktor (water-water energetic) (VVER) plants. Results are based on the opinions of industry experts and updated by EPRI staff and consultants to EPRI. The MDM is not intended to be a detailed or comprehensive reference source for current materials degradation issues. Users should refer to the references provided in the MDM for more detailed assessment and characterization of degradation phenomena and discussion of R&D projects.

KEY FINDINGS

Strategic issues identified in Revision 5 of the MDM include the following:

- Stress corrosion cracking (SCC) has been one of the primary materials challenges to light water reactor (LWR) primary system integrity faced by plant operators, and predicting future trends with confidence remains beyond current capabilities, especially for assessing the effect of increasing neutron fluence on SCC susceptibility (irradiation-assisted SCC). There are sufficient instances of SCC in stainless steel components exposed to PWR primary water, along with significant laboratory data, to consider it a generic concern. No precipitous increase in SCC is expected, but inspections will continue to show some incidents of SCC, and it is likely that long-term exposure of materials to environments conducive to SCC will lead to adverse trends in crack initiation and growth in stainless steel components where it has not previously been observed, or at higher incidence than anticipated. As such, improving the capability to predict SCC trends remains an important area of research. While there are some unique elements in reactor types and environments, the majority of SCC dependencies are common. There is a need for this to be reflected in the continuity of modeling across reactor types by rationalizing crack growth models for variables such as temperature, corrosion potential, and water chemistry.
- When exposed to high-energy neutrons, the fracture toughness of austenitic stainless steel is significantly decreased to a saturation value, leading to a decreased critical crack length that can be accommodated by the component without premature failure and, thus, an increased sensitivity to flaws. Currently, there are sufficient data for base metal to identify the embrittlement trend to 90 dpa. This bounds only two-thirds of the expected maximum fluence of the most irradiated PWR internal

components through the period of extended operation. Furthermore, there is a considerable lack of data, at all fluence levels, for stainless steel welds. Overall, there are multiple data gaps to be resolved with respect to the fracture toughness of austenitic stainless steels, which are of strategic importance for core internals during periods of extended operation.

- While not considered a significant issue for BWRs and western-style PWRs due to either low operating temperature or low end-of-life fluence, void swelling is an issue of strategic importance for some VVER 1000 operators, where gamma heating can produce significantly higher peak component temperatures. The specific concern is that there is a lack of data, since the vast majority of available data were produced under non-representative irradiation conditions. The particular risk is that dimensional changes from void swelling in reactor vessel internal components may lead to problems with coolant flow and/or control rod movement.
- The performance of Alloy 690TT steam generator (SG) tubing has been exemplary to date, with zero instances of SCC. Alloy 800NG SG tubing has performed adequately, but operating experience continues to show its vulnerability to secondary side SCC under off-normal chemistry and stress conditions. Concerns remain regarding potential vulnerabilities of these alloys to lead-induced SCC. Additional R&D is needed to provide a clear understanding of the potential vulnerabilities and to ensure that these tube bundles will remain serviceable for extended operations.
- High-chrome nickel-base alloys (Alloy 690 base metal as well as Alloy 52 and Alloy 152 weld filler materials) are being widely applied as replacements for Alloys 600, 82, and 182. Excellent operating experience with no observations of SCC in over 30 years of service supports the superiority of Alloy 690 relative to Alloy 600 in PWR primary water environments—as does extensive laboratory testing. However, ongoing laboratory testing to characterize potential vulnerabilities of Alloy 52 and Alloy 152 for its use in current and new BWR plants has revealed moderate SCC growth rates, indicating that it is not immune, and that its vulnerabilities should continue to be proactively explored.
- Irradiated materials data are needed for additional materials. In western-designed reactors, these materials are associated with components used on the periphery of the core for which additional operating time results in significant end-of-life neutron fluences. For VVER designs, there is a general lack of irradiated materials performance data for the Ti-stabilized stainless steels used.

WHY THIS MATTERS

The MDM results provide a basis for the development of EPRI materials R&D plans and are directly considered by the EPRI Nuclear Materials Management Department in developing long-range materials R&D plans, including the International Materials Research (IMR) Program, the Boiling Water Reactor Vessel and Internals Program (BWRVIP), the Materials Reliability Program (MRP), and the Steam Generator Management Program (SGMP), through consideration of the MDM results in updates to the Issue Management Tables (IMTs) for all BWR, PWR, VVER, and CANDU reactor designs.

HOW TO APPLY RESULTS

EPRI advisors, research organizations, and regulatory authority personnel can use the MDM results as a tool to understand EPRI's perspective on fundamental knowledge gaps associated with primary system material-related degradation. The results should be applied by advisors when providing recommendations to EPRI regarding R&D priorities.

LEARNING AND ENGAGEMENT OPPORTUNITIES

The MDM provides a comprehensive review of age-related degradation mechanisms applicable to nuclear plant primary systems. It can be used by all organizations as a tool to educate staff who are unfamiliar with this topic. It is also a valuable reference tool for staff engaged in aging management activities or related research.

EPRI CONTACT: Jared Smith, Principal Technical Leader, jaredsmith@epri.com

PROGRAMS: Nuclear Power, P41; International Materials Research (IMR), P41.01.01

IMPLEMENTATION CATEGORY: Reference

EPRI
3420 Hillview Avenue, Palo Alto, California 94304-1338 • USA
800.313.3774 • 650.855.2121 • askepri@epri.com • www.epri.com
© 2024 EPRI, Inc. All rights reserved. Electric Power Research Institute, EPRI, and TOGETHER…SHAPING THE FUTURE OF ENERGY are registered marks of the Electric Power Research Institute, Inc. in the U.S. and worldwide.

ACRONYMS AND ABBREVIATIONS

Acronym or Abbreviation	Meaning
AECL	Atomic Energy of Canada Limited
AGS	annulus gas system
ANL	Argonne National Laboratory
ASME	American Society of Mechanical Engineers
ASTM	American Society for Testing and Materials
ATR	advanced test reactor
AVB	anti-vibration bars
AVT	all-volatile treatment
BMI	bottom mounted instrumentation
BWR	boiling water reactor
BWRVIP	Boiling Water Reactor Vessel and Internals Program
C&LAS	carbon and low-alloy steel
C&W	corrosion and wear
CANDU	Canada deuterium uranium (reactor)
CASS	cast austenitic stainless steel
CE	Combustion Engineering
CEDM	control element drive mechanism
CGR	crack growth rate
COG	CANDU Owners Group
CRDM	control rod drive mechanism
CRGT	control rod guide tube
CRVSP	Coordinated Reactor Vessel Surveillance Program
CUF	cumulative usage factor
CVCS	chemical and volume control system
DBTT	ductile-to-brittle transition temperature

Acronym or Abbreviation	Meaning
DHC	delayed hydride cracking
DMW	dissimilar metal weld
DSA	dynamic strain aging
EAC	environmentally assisted cracking
EAF	environmentally assisted fatigue
ECP	electrochemical corrosion potential
EDF	Électricité de France
EDM	electrical discharge machining
Emb.	embrittlement
Env.	environmental
EPR	electrochemical potentiokinetic reactivation
EPRI	Electric Power Research Institute
FAC	flow-accelerated (or -assisted) corrosion
Fat.	fatigue
FIV	flow-induced vibration
FN	ferrite number
GE	General Electric
Gen.	general (corrosion)
GTAW	gas tungsten arc welding
HAZ	heat-affected zone
HCF	high-cycle fatigue
HSLAS(s)	high-strength low-alloy steel(s)
HTH	high-temperature heat (heat treatment)
HTS	heat transport system
HWC-M	hydrogen water chemistry—moderate
IA	irradiation-assisted
IASCC	irradiation-assisted stress corrosion cracking
IC	irradiation creep
ID	inner diameter
IDSCC	inner diameter stress corrosion cracking (applicable to steam generator tubing)

Acronym or Abbreviation	Meaning
IG	intergranular
IGA	intergranular attack
IGSCC (IG)	intergranular stress corrosion cracking
IHSI	induction heating stress improvement
IMR	International Materials Research
IMT	issue management table
INL	Idaho National Laboratory
Irr.	irradiation (effects)
KAIST	Korea Advanced Institute of Science & Technology
KHNP	Korea Hydro & Nuclear Power
LAS	low-alloy steel
LCF	low-cycle fatigue
LISS	liquid injection shutdown system
LPCI	low-pressure coolant injection
LPSCC	low-potential stress corrosion cracking
LTCC	low-temperature creep cracking
LTCP	low-temperature crack propagation
LTO	long-term operation
LWR	light water reactor
MA	mill annealed
MAI	Materials Aging Institute
MDM	Materials Degradation Matrix
MRP	Materials Reliability Program
MSIP	mechanical stress improvement process
NDE	nondestructive evaluation
NEI	Nuclear Energy Institute
NG	nuclear grade
Ni-Alloy	nickel-base alloy
NMCA	noble metal chemical addition
NRC	U.S. Nuclear Regulatory Commission
NWC	normal water chemistry

Acronym or Abbreviation	Meaning
OD	outer diameter
ODSCC	outer diameter stress corrosion cracking (applicable to steam generator tubing)
OE	operating experience
OLNC	On-Line Noble Chem™
OTSG	once-through steam generator
PbSCC	lead-induced stress corrosion cracking
PH	precipitation-hardened
PHT	primary heat transport
PHWR	pressurized heavy water reactor
PMZ	partially melted zone
PSI	Paul Scherrer Institute
PTS	pressurized thermal shock
PWHT	post-weld heat treatment
PWR	pressurized water reactor
PWROG	Pressurized Water Reactor Owners Group
PWSCC	primary water stress corrosion cracking
R&D	research and development
RCS	reactor coolant system
RG	Regulatory Guide
RiFR	reduction in fracture resistance
RIS	radiation-induced segregation
RPV	reactor pressure vessel
RT	radiographic test
RT_{NDT}	reference temperature nil-ductility transition
SCC	stress corrosion cracking
SG	steam generator
SGMP	Steam Generator Management Program
SHE	standard hydrogen electrode
SICC	strain-induced corrosion cracking
SMAW	shielded metal arc welding

Acronym or Abbreviation	Meaning
SMF	stable matrix features
SR	stress relaxation
SS	stainless steel
TEM	transmission electron microscopy
TG	transgranular
TGSCC	transgranular stress corrosion cracking
Th.	thermal
TSP	tube support plate
TSSD	terminal solid solubility for dissolution
TT	thermally treated
TTS	top-of-tubesheet
UMD	unstable matrix defects
USE	upper shelf energy
UT	ultrasonic test
VCD	vacuum carbon deoxidation
VCT	volume control tank
VS	void swelling
VVER	Voda-Vodyanoi Energeticheski Reaktor (water-water energetic) – The Soviet (Russian Federation) designation for a light-water pressurized reactor
Wstg.	wastage

DEFINITIONS

The following set of definitions is provided to clarify terminology used in the Materials Degradation Matrix (MDM). This listing is not intended to be a comprehensive glossary of technical terms, but rather a key listing of terms helpful to the user in understanding terminology used in the MDM.

Beltline. As defined in 10 CFR 50.61(a)(3), the region of the reactor vessel (shell material including welds, heat-affected zones, and plates or forgings) that directly surrounds the effective height of the active core and adjacent regions of the reactor vessel that are predicted to experience sufficient neutron radiation damage to be considered in the selection for the most limiting material with regard to radiation damage.

Casting. An item at, or near, finished shape obtained by solidification of metal in a mold.

Cladding (or **clad**). A thin layer of corrosion-resistant alloy, either stainless steel or nickel-base alloy material, applied to the interior surfaces of a carbon or low-alloy steel component in contact with reactor coolant.

Class 1. The ASME Class 1 primary coolant pressure-retaining boundary.

Degradation matrix results tables. The primary tool used by the EPRI MDM to communicate applicable degradation mechanisms (degradation sub-modes) and the associated state of industry knowledge. Section 2.2 describes the approach used in developing these tables and defines terminology associated with the presentation results in these tables (that is, degradation mechanism applicability, R&D assessment, result categorization tags, and explanatory notes).

Degradation mechanism (also termed **degradation sub-mode**). Describes the degradation processes applicable to nuclear steam supply system (NSSS) materials. IGSCC, PWSCC, IASCC, thermal aging, and irradiation embrittlement are examples of degradation mechanisms.

Degradation mode. A term used to describe broad categories of degradation mechanisms (sub-modes). Degradation modes include SCC, corrosion, wear, fatigue, reduction in fracture properties, and irradiation effects.

Displacements per atom (**dpa**). A measure of neutron damage based on the number of times an atom in a metal lattice is displaced at a given fluence; dpa is used in the industry as a common manner of expressing neutron damage for highly irradiated components—typically reactor internals. At LWR neutron spectra, a neutron fluence of 6.7×10^{20} n/cm^2 (E > 1.0 MeV) corresponds roughly to 1 dpa.

Dissimilar metal weld (**DMW**). A weld between 1) carbon or low-alloy steels to high-alloy steels, 2) carbon or low-alloy steels to nickel-base alloys, or 3) high-alloy steels to nickel-base alloys.

Fluence (**neutron fluence**). The time-integrated neutron flux. Units of fluence are neutrons/cm^2. Unless otherwise noted, neutron fluence values are reported based on fast neutron fluence only (E > 1.0 MeV).

Flux (**neutron flux**). The product of neutron density and neutron speed. Units of flux are neutrons/(cm^2 • sec).

Forging. Plastically deforming metal, usually hot, into a desired shape using localized compressive forces exerted by presses, special forging machines, or by manual or power hammers.

Full structural weld overlay. The deposition of weld reinforcement on the outside diameter surface of the piping, component, or associated weld such that the weld reinforcement can support the design loads without the piping, component, or associated weld lying beneath the weld reinforcement.

High-cycle fatigue (**HCF**). Used to describe fatigue concerns associated with cycling above one million cycles, where high-cycle design fatigue curves are applicable.

Gap. An identified area in which additional R&D is considered warranted to improve the fundamental understanding of degradation mechanisms or to develop improved solutions for prevention of materials degradation or detection of degraded conditions.

Heat-affected zone (**HAZ**). The area of base material that has had its microstructure and properties altered primarily by welding, but also possibly from heat-intensive cutting operations.

Issues management table (**IMT**). EPRI Materials Initiative tool used to identify R&D gaps related to component management. This table summarizes information on materials of construction, degradation mechanisms, consequences of failure, mitigation approaches, repair and replacement technologies, and inspection and evaluation of components. Where there are needs related to mitigation, repair and replacement, or inspection and evaluation, R&D gaps are identified.

Low-cycle fatigue (**LCF**). Used to describe fatigue concerns associated with low numbers of fatigue cycles, well below one million cycles, where low-cycle design fatigue curves are applicable.

Long-term operation (**LTO**). A term used in the nuclear industry to represent operation beyond current license periods (60 years for plants in the United States).

Low-temperature crack propagation (**LTCP**). A term used to describe low-temperature (<150°C) SCC occurring at a preexisting sharp crack.

Mid-cycle fatigue. Used to describe fatigue concerns associated with cycling in the region of one million cycles, which is the transition from the application of low-cycle design fatigue curves to high-cycle design fatigue curves.

Nickel-base alloy. Alloys whose primary constituent is nickel. Examples include Alloys 600, 690, and X-750. In some cases, space constraints result in the use of the term *Ni-alloy* instead of *nickel-base alloy*. The terms are used interchangeably in this report.

Piping components. A general term used to describe pipe segments, pipe fittings, branch connections, welded attachments, thermowell bosses, and thermowells.

Primary pressure boundary. A general term used to indicate Class 1 pressure-retaining components.

Reductions in fracture properties—environmental (**RIFP – Env.**). A general term used to broadly describe several related phenomena, including both high-temperature and low-temperature observations and both K_{IC} (fracture toughness) and J-R tearing (fracture resistance) conditions.

Strategic issue. A general term used in the MDM to describe key knowledge gaps associated with materials degradation phenomena that are broad in nature, encompassing multiple materials or operating environments, and that are considered of high importance for the operating fleet.

Welded attachment. Components that are welded to the interior or exterior surfaces of primary pressure-retaining components.

CONTENTS

ABSTRACT ..... **V**

EXECUTIVE SUMMARY ..... **VII**

ACRONYMS AND ABBREVIATIONS ..... **XI**

DEFINITIONS ..... **XVII**

1 **INTRODUCTION** **1-1**

1.1 Objective 1-1

1.2 MDM Focus and Use 1-1

1.3 Implementation Requirements 1-2

1.4 References 1-2

2 **APPROACH** **2-1**

2.1 Development Approach 2-1

2.2 Degradation Matrix Tables 2-1

2.2.1 Degradation Modes 2-2

2.2.2 Material Classes 2-3

2.2.3 Presentation of Results 2-4

2.2.3.1 Degradation Mechanism Applicability 2-4

2.2.3.2 R&D Assessment 2-5

2.2.3.3 Explanatory Notes 2-5

2.3 References 2-6

3 **STRATEGIC ISSUES** **3-1**

3.1 Western LWR Strategic Issues 3-1

3.1.1 Reactor Vessel Integrity 3-3

3.1.1.1 PWR Vessel Neutron Embrittlement Correlations 3-3

3.1.1.2 BWR Vessel SCC Susceptibility 3-3

3.1.2 SCC Prediction and Modeling 3-3
3.1.2.1 SCC Trends for Thermally Treated Alloy 600 Tube Bundles 3-4
3.1.2.2 BWR SCC in Stainless Steels, Nickel-Base Alloys, and Their Welds 3-5
3.1.2.3 PWR SCC of Stainless Steels 3-5
3.1.2.4 PWR Irradiation-Assisted Stress Corrosion Cracking 3-6
3.1.2.5 BWR Irradiation-Assisted Stress Corrosion Cracking 3-6
3.1.3 Fracture Toughness of Irradiated Stainless Steel 3-6
3.1.4 Void Swelling 3-7
3.1.5 Core Periphery Reactor Internals 3-8
3.1.6 High Chromium Nickel-Base Alloy SCC Vulnerabilities 3-9
3.1.7 ODSCC of Alloy 690 Steam Generator Tubing 3-9
3.1.8 Effect of LWR Environment on Fatigue Resistance 3-10
3.1.9 Additively Manufactured Materials 3-10
3.2 VVER Strategic Issues 3-11
3.2.1 Effect of VVER Environment on Fatigue Resistance 3-12
3.2.2 Irradiated Materials Data 3-12
3.2.3 Void Swelling 3-12
3.3 CANDU Reactor Strategic Issues 3-13
3.3.1 LWR Strategic Issues Applicable to CANDU Plants 3-13
3.3.2 CANDU-Specific Strategic Issues 3-13
3.3.2.1 Fuel Channel Assembly Service Life Margins 3-13
3.3.2.2 Alloy 800NG Steam Generator Tubing Vulnerabilities 3-14
3.3.2.3 The Evolution of End Fitting Mechanical Properties 3-14

_4_ PWR DEGRADATION MATRIX RESULTS 4-1
4.1 Scope and Evaluation Assumptions 4-1
4.2 PWR Results: Degradation Matrix Tables and Explanatory Notes 4-1
4.3 References 4-73

_5_ BWR DEGRADATION MATRIX RESULTS 5-1
5.1 Scope and Evaluation Assumptions 5-1
5.2 BWR Results: Degradation Matrix Tables and Explanatory Notes 5-1
5.3 References 5-30

_6_ VVER DEGRADATION MATRIX RESULTS 6-1
6.1 Scope and Evaluation Assumptions 6-1
6.2 VVER Results: Degradation Matrix Tables and Explanatory Notes 6-2

_7_ CANDU REACTOR DEGRADATION MATRIX RESULTS 7-1
7.1 Scope and Evaluation Assumptions 7-1
7.1.1 Systems Evaluated 7-1
7.1.1.1 Fuel Channel Assemblies 7-1
7.1.1.2 Calandria Vessel and Moderator System 7-1
7.1.1.3 Primary Heat Transport System 7-2
7.1.1.4 Steam Generators 7-2
7.1.1.5 External Surfaces and Pressure-Retaining Bolting 7-3
7.1.2 Components Evaluated 7-3
7.1.3 Evaluation Assumptions 7-3
7.1.3.1 Operating Conditions 7-3
7.1.3.2 Service Life 7-3
7.2 CANDU Results: Degradation Matrix Tables and Explanatory Notes 7-4
7.3 References and Bibliography 7-53

_A_ DEGRADATION MECHANISM SUMMARIES A-1
A.1 Corrosion—General and Localized A-2
A.1.1 General Corrosion A-2
A.1.2 Wastage or Boric Acid Corrosion (Wstg.) A-9
A.1.3 Flow-Accelerated Corrosion (FAC) A-12
A.1.3.1 Effect of Single- or Two-Phase Flow and Turbulence A-13
A.1.3.2 Temperature A-14
A.1.3.3 Water Chemistry A-15
A.1.3.4 Material Composition A-17
A.1.4 Localized Corrosion A-18
A.1.4.1 Galvanic Corrosion A-18
A.1.4.2 Crevice Corrosion A-19
A.1.4.3 Pitting A-23
A.1.4.4 Microbiologically Induced Corrosion (MIC) A-28
A.1.5 Fouling (Foul) A-30
A.1.5.1 Fouling in Primary Coolant Circuits A-31
A.1.5.2 Fouling in Secondary Coolant Circuits A-33

A.2 Wear A-33
A.3 Stress Corrosion Cracking (SCC) A-34
A.3.1 Intergranular Attack (IGA) A-34
A.3.2 Intergranular and Transgranular SCC (IG/TG) A-35
A.3.2.1 The “Blunting Criterion” A-35
A.3.2.2 The Chronology of Events During Stress Corrosion Cracking A-37
A.3.2.3 Life Prediction for Stress Corrosion Cracking A-38
A.3.2.4 Transgranular (TG) SCC of Carbon and Low-Alloy Steels A-43
A.3.2.5 Intergranular (IG) and Transgranular (TG) SCC of Non-Irradiated Stainless Steels in BWRs A-48
A.3.2.6 IGSCC of Nickel-Base Alloys in BWRs A-54
A.3.2.7 SCC of Stainless Steels in PWR Primary Coolant Circuits A-56
A.3.2.8 IGSCC of Nickel-Base Alloys in PWR Primary Water (PWSCC) A-57
A.3.2.9 IGA and SCC of Steam Generator Tubing Alloys in Secondary Circuits A-70
A.3.2.10 SCC of High Strength Alloys A-76
A.3.2.11 Delayed Hydride Cracking (DHC) of Zirconium Alloys A-79
A.3.2.12 Irradiation-Assisted (IA) SCC of Stainless Steels A-81
A.4 Fatigue A-91
A.4.1 Reactor Coolant System and Steam Generator Piping A-92
A.4.2 Reactor Pressure Vessels A-92
A.4.3 Pressurizers A-92
A.4.4 Steam Generator Shell, Tubes, and Internals A-93
A.4.5 RPV Internal Components A-93
A.4.6 High-Cycle Fatigue (HCF) A-94
A.4.7 Low-Cycle Fatigue (LCF) A-95
A.4.8 Corrosion Fatigue (Environmentally Assisted Fatigue [EAF]) A-95
A.5 Fracture—Reduction in Fracture Properties (RiFP) A-98
A.5.1 Thermal Embrittlement (Th) A-99
A.5.1.1 Cast Stainless Steels A-99
A.5.1.2 Ferritic and Low-Alloy Steels A-103
A.5.1.3 Nickel-Base Alloys A-104
A.5.2 Environmentally Induced Reduction of Fracture Resistance (Env) A-104
A.5.2.1 Unusually High SCC Propagation Rates A-106
A.5.2.2 Decreased J-R Tearing Resistance and Fracture Toughness A-106

A.6 Irradiation Effects A-108
A.6.1 Irradiation Embrittlement (Emb) A-109
A.6.1.1 Ferritic Steels A-109
A.6.1.2 Austenitic Stainless Steels A-110
A.6.2 Void Swelling (VS) A-115
A.6.3 Irradiation Creep and Stress Relaxation (IC/SR) A-116
A.7 References and Bibliography A-119

***B* VVER 440 AND 1000 MATERIALS B-1**
B.1 Carbon and Low-Alloy Steels B-1
B.1.1 Service Experience B-1
B.1.2 Material Composition and Properties B-2
B.1.3 Main Limitations B-4
B.2 Carbon and Low-Alloy Steel Welds B-7
B.2.1 Service Experience B-7
B.2.2 Material Composition and Properties B-7
B.2.3 Main Limitations B-8
B.3 Stainless Steels B-10
B.3.1 Service Experience B-10
B.3.2 Material Composition and Properties B-10
B.3.3 Welding and Heat Treatment B-14
B.4 Stainless Steel Welds and Cladding B-14
B.5 References B-17

***C* CANDU OWNERS GROUP REPORT ABSTRACTS C-1**

***D* REVISION LOG D-1**

LIST OF FIGURES

Figure 2-1 MDM table cell content....2-4

Figure 2-2 MDM table cell content—explanatory note numbering....2-6

Figure A-1 Modes of corrosion....A-3

Figure A-2 Pourbaix diagram for iron at 300°C for activities of dissolved cations of 10^{-6} m, modified....A-5

Figure A-3 Solubility of magnetite, NiO and nickel ferrite calculated from the thermodynamic data, and comparison to experimental data....A-6

Figure A-4 Carbon steel corrosion in high temperature water....A-7

Figure A-5 Effect of temperature and dissolved oxygen concentration on the corrosion loss over 200 hours of carbon steels in pure water....A-8

Figure A-6 Corrosion rate for carbon steel in boric acid as a function of temperature....A-11

Figure A-7 Effect of temperature on the flow-accelerated corrosion rate of carbon steel in deoxygenated ammonia all-volatile treatment water....A-15

Figure A-8 Flow-accelerated corrosion data for condensate and moisturizer separator reheater drain systems in four BWR plants as a function of the local dissolved oxygen contents....A-16

Figure A-9 Effect of chromium content of carbon steels on FAC....A-17

Figure A-10 Schematic of crevice in an aerated solution indicating the separation of the metal oxidation and oxygen reduction sites and the consequent changes in pH and anion concentration....A-20

Figure A-11 Schematic of crevice formed at PWR steam generator tube/carbon-steel tube support, together with the phenomena that give rise to localized corrosion and cracking....A-21

Figure A-12 Relation between the pitting resistance equivalent index and resistance to localized corrosion of stainless steels in a 10% FeCl3 solution....A-23

Figure A-13 Potentiostatic polarization curves for Fe-18Cr-8Ni stainless steel in 0.1M NaCl and in 1.0M H_2SO_4 at 25°C....A-25

Figure A-14 Pitting and corrosion potential for Alloy 600 in water containing chloride anions as a function of temperature....A-27

Figure A-15 Microbiological processes occurring on iron or steel....A-30

Figure A-16 Intergranular stress corrosion cracking adjacent to a weld in a 28” (711 mm) BWR Type 304 stainless steel recirculation pipe as observed in many BWR reactor coolant systems, Incipient stress corrosion cracks in a carbon steel BWR feedwater line at ~220°C....A-36

Figure A-17 Sequence of crack initiation, coalescence, and growth during subcritical stress corrosion cracking in aqueous environments....A-37

Figure A-18 Schematic oxidation charge density and time relationship for a strained crack tip and unstrained sides, and changes in oxidation current density following the rupture of the oxide at the crack tip A-39
Figure A-19 Schematic of the elements of the film-induced cleavage mechanism of crack propagation A-41
Figure A-20 Schematic of various reactions at a crack tip associated with hydrogen embrittlement mechanisms in aqueous environments A-42
Figure A-21 Observed and theoretical crack propagation rate/crack tip strain rate relationships for low-alloy steel in 288°C water at various corrosion potentials A-45
Figure A-22 Effect of hardness on the crack propagation rate for various low-alloy steel weldments, plate, and so on, in 8 ppm oxygenated water at 288°C in comparison with the disposition propagation “low sulfur” rate A-47
Figure A-23 Comparison between observed and predicted crack propagation rates for sensitized stainless steel in 288°C water, in 8 ppm oxygenated water under a variety of stressing/straining modes, and oxygenated versus deaerated environments A-50
Figure A-24 Effect of yield strength and martensite on the stress corrosion crack growth rate on stainless steel and Alloy 600 in 288°C, high purity water A-51
Figure A-25 Crack propagation rate/stress intensity dependence for sensitized stainless steel in water at 288°C water with 0.2 ppm oxygen and conductivity 0.3-0.5 µS/cm A-52
Figure A-26 Theoretical and observed crack depth versus operational time relationships for 28” diameter schedule 80, 304 stainless steel piping for two boiling water reactors operating at different mean coolant conductivities A-53
Figure A-27 Predicted and observed effects of average plant water purity on crack incidence in creviced Alloy 600 shroud head bolts A-55
Figure A-28 Predicted and observed effects of average plant water purity on crack incidence in creviced welded access hole covers A-55
Figure A-29 Summary of SCC of austenitic stainless steels in PWR primary circuits A-56
Figure A-30 Tentative SCC domain for Type 304 stainless steel at 200°C in PWR environment containing chloride and sulfate, simulating pressurized aerated conditions A-57
Figure A-31 Time to failure in simulated PWR primary water at 360°C as a function of Cr content of Ni-Cr-10wt% Fe alloys A-60
Figure A-32 Crack propagation rate versus stress intensity data and disposition relationships for nickel-base Alloys 600, 82, 182, and 132 in PWR primary water A-62
Figure A-33 Summary of PWSCC growth rates at constant K_I in Alloy 690 CRDM and plate materials A-63
Figure A-34 Summary of PWSCC growth rate data for Alloys 52 and 152 ..... A-64
Figure A-35 Results of U.S. reactor vessel head penetration inspections updated late 2008 ..... A-67
Figure A-36 Illustration of Monte Carlo simulation of upper head penetration cracking A-69
Figure A-37 Estimated concentrations of species in simulated steam generator crevices versus the concentration in the bulk water A-70
Figure A-38 Mill-annealed Alloy 600 corrosion mode diagram superimposed on the Pourbaix diagram for nickel A-72

Figure A-39 Comparison of IGA/IGSCC susceptibility between Alloy 690TT and Alloy 600MA or TT at temperatures from 280 to 320°C as a function of pH and electrode potential A-73
Figure A-40 Illustration of hydride cracking in a pressure tube A-80
Figure A-41 Hydrogen solubility as a function of thermal history A-80
Figure A-42 Summary of IASCC in light water reactors and associated metallurgical changes in austenitic stainless steels as a function of neutron irradiation in n/cm^2 ..... A-81
Figure A-43 Dependence of IASCC on fast neutron fluence for creviced control blade sheaths in high conductivity BWR coolants where the tensile stress is high due to spot welds and dynamic due to swelling B4C absorber tubes..... A-82
Figure A-44 Weibull plot of the percentage of defective baffle/former bolts on former levels 1 to 5 as a function of neutron dose based on the data for all inspections combined for a French CP0 series PWR A-84
Figure A-45 Crack length versus time for DCB specimens of sensitized Type 304 stainless steel exposed in a BWR core and in the recirculation line..... A-86
Figure A-46 Predicted crack depth versus time response for cracks propagating in the beltline weld of a core shroud illustrating the non-monotonic variation in crack propagation due to the competing effects of fast neutron irradiation on grain boundary chromium depletion and on residual stress relaxation..... A-88
Figure A-47 Crack length versus time predictions and observations for a Type 304 stainless steel BWR core shroud with multiple inspections and multiple cracks, and comparison of observed and predicted crack depth for a number of BWR core shrouds A-89
Figure A-48 IASCC initiation data stress versus time to cracking from constant load tests in PWR primary water..... A-90
Figure A-49 IASCC initiation stress versus neutron fluence from constant load tests in PWR primary water A-91
Figure A-50 Predicted and observed strain amplitude versus cycles to crack initiation relationships for un-notched carbon steel in 288°C, 8 ppm oxygenated water with strain applied at different rates A-97
Figure A-51 Predicted and observed strain amplitude versus cycles to crack initiation relationships for un-notched C&LAS in 288°C water under the worst combination of material and environmental conditions A-97
Figure A-52 Decrease in Charpy impact energy for various heats of cast stainless steels aged at 400°C A-102
Figure A-53 Comparison of experimental and estimated room temperature Charpy impact energy as a function of aging temperature and time for a CASS pump cover plate..... A-103
Figure A-54 Schematic stress corrosion crack propagation rate versus stress intensity curves indicating the divergence from the usual relationship at lower stress intensity . A-105
Figure A-55 Elastic-plastic fracture toughness of Alloy 52 welds in water..... A-107
Figure A-56 Effect of neutron fluence on elevated-temperature yield stress, solution annealed and cold worked..... A-112
Figure A-57 Effect of neutron fluence on fracture toughness—fast reactors..... A-113
Figure A-58 Effect of neutron fluence on fracture toughness—thermal reactors..... A-114

Figure A-59 Void swelling data for austenitic stainless steels irradiated in thermal reactors A-116
Figure A-60 Schematic representation of creep curves under constant load A-117
Figure A-61 Irradiation creep and stress relaxation data and model fits A-118

LIST OF TABLES

Table 3-1 Key LWR knowledge gaps 3-1
Table 4-1 PWR primary pressure boundary 4-3
Table 4-2 PWR reactor vessel internals 4-4
Table 4-3 PWR steam generator tubing, tube plugs, and tubesheet welds 4-5
Table 4-4 PWR steam generator secondary side internals 4-6
Table 4-5 PWR steam generator secondary pressure boundary 4-7
Table 4-6 PWR external surfaces and pressure retaining bolting 4-8
Table 4-7 PWR systems explanatory notes 4-9
Table 5-1 BWR primary pressure boundary 5-3
Table 5-2 BWR reactor vessel internals 5-4
Table 5-3 BWR external surfaces and bolting 5-5
Table 5-4 BWR systems explanatory notes 5-6
Table 6-1 VVER 440 reactor pressure vessel 6-3
Table 6-2 VVER 1000 reactor pressure vessel 6-4
Table 6-3 VVER primary system piping components 6-5
Table 6-4 VVER reactor vessel internals 6-6
Table 6-5 VVER steam generator tube bundle and internals 6-7
Table 6-6 VVER steam generator secondary pressure boundary 6-8
Table 6-7 VVER external surfaces,[1] supports, and pressure-retaining bolting 6-9
Table 7-1 CANDU fuel channel assemblies 7-5
Table 7-2 CANDU calandria vessel and moderator system 7-6
Table 7-3 CANDU primary heat transport system 7-7
Table 7-4 CANDU steam generator tubing 7-8
Table 7-5 CANDU steam generator internals and secondary pressure boundary 7-9
Table 7-6 CANDU external surfaces and pressure-retaining bolting 7-10
Table 7-7 CANDU explanatory notes 7-11
Table A-1 Thermal aging screening criteria for CASS adopted by the NRC A-100
Table B-1 Chemical compositions of RPV steels 15Ch2MFA and 15Ch2NMFA B-5
Table B-2 Specified room temperature mechanical properties for RPV steels 15Ch2MFA and 15Ch2NMFA B-5
Table B-3 Chemical composition of 10GN2MFA steel B-5
Table B-4 Specified room temperature mechanical properties for 10GNMFA steel B-5

Table B-5 Chemical compositions of LAS 25Ch1MF, 40Ch, and 38ChN3MFA B-6
Table B-6 Chemical compositions of carbon steels 20, 22K, and K22MA..... B-6
Table B-7 Chemical compositions of selected filler metals for welding of LAS and CS..... B-9
Table B-8 Chemical compositions of selected stainless steels..... B-13
Table B-9 Specified room temperature mechanical properties of selected stainless steels ... B-14
Table B-10 Chemical compositions of selected FM for welding of SS and BL of DMWs..... B-16
Table C-1 CANDU Owners Group report abstracts C-2
Table D-1 Revision log..... D-2
Table D-2 List of significant changes to the MDM, Revision 5..... D-7
Table D-3 Detailed list of PWR MDM cell result changes for Revision 5 ..... D-8
Table D-4 Detailed list of BWR MDM cell result changes for Revision 5 ..... D-11
Table D-5 Detailed list of CANDU MDM cell result changes for Revision 5..... D-13
Table D-6 Detailed list of VVER MDM cell result changes for Revision 5..... D-16

1
INTRODUCTION

1.1 Objective

The objective of the EPRI Materials Degradation Matrix (MDM) is to identify knowledge gaps associated with degradation phenomena that may detrimentally affect water cooled and moderated power reactor operations or reactor safety. Where gaps are identified, the MDM assesses the status of R&D needed to resolve the knowledge gap.

The EPRI MDM is a key part of the industry's Materials Degradation and Issue Management Initiative and is an important input to the EPRI Issue Management Table (IMT) process for identifying R&D gaps and priorities for boiling water reactors (BWRs) and pressurized water reactors (PWRs) operating in the United States.

The MDM is periodically updated and has progressively included information relating to BWRs and PWRs outside of the United States whose operators are members of EPRI. Starting with Revision 3 [1-1], results for the Canada deuterium uranium (CANDU) pressurized heavy water reactor designs were also included. Revision 4 [1-2] of the MDM included results for VVER reactor designs and further refinement of MDM conclusions for long-term operation (i.e., consideration of 80-year service lives). The current revision includes updates to the MDM tables and the strategic issues for all included reactor designs based on operating experience and R&D results since the previous revision.

1.2 MDM Focus and Use

The MDM presents a broad perspective on materials degradation issues and the state of industry knowledge related to resolving knowledge gaps and mitigating degradation concerns. Results are based on the opinions of industry experts and updated by EPRI staff and consultants to EPRI. The MDM is not intended to be a detailed or comprehensive reference source for current materials degradation issues. Users should refer to the references provided within the MDM for a more detailed assessment and characterization of degradation phenomena and discussion of R&D projects.

The MDM focuses on operating water moderated and cooled reactor designs. Neither advanced large light-water reactor designs nor small modular reactor designs are specifically considered in this version of the MDM. EPRI Advanced Nuclear Technology (ANT) has developed separate degradation matrix products to address advanced light-water reactor designs being proposed for construction in the United States and abroad, and additional related products are under development. For these designs, users should refer to the applicable EPRI ANT degradation assessments (EPRI reports 1019611 [1-3] and 1021088 [1-4] for advanced BWRs and advanced PWRs, respectively).

A consistent effort was made to perform MDM evaluations primarily at a material and environment level, rather than a component level. Although specific component configurations have at times been considered where relatively unique factors associated with a component or limited set of components affect the conclusion reached, there has been no attempt to comprehensively consider all applicable components in the MDM evaluations for each design type.

It is increasingly recognized that materials degradation follows a continuum over the various reactor types, environments, temperatures, etc., and there are considerable common dependencies across reactor types. Thus, it is often beneficial for the MDM, degradation assessment and management, degradation models, and degradation resolution to be viewed in this overall context and not in isolation.

1.3 Implementation Requirements

This report is provided for information only. Therefore, the implementation requirements of Nuclear Energy Institute (NEI) 03-08, Guideline for the Management of Materials Issues [1-5], are not applicable.

NOTE REGARDING NEI 03-08 APPLICABILITY
The NEI 03-08 materials initiative is a U.S. industry initiative developed to ensure proactive management of materials degradation issues. For reactor designs operated by U.S. utilities, the MDM is one of two primary tools applied by EPRI to address the intent of the materials initiative. Additionally, in the context of addressing the intent of NEI 03-08, the Issue Management Tables (IMTs) are the appropriate tool for disposition of the MDM results for the reactor. A component-specific evaluation of degradation issues is addressed in the appropriate Issue Management Table. The MDM is thus considered to be an intermediate product that forms one key part of the basis for IMT conclusions but should not be directly applied to specific component locations in lieu of consulting the appropriate IMT Report.

1.4 References

[1-1] *EPRI Materials Degradation Matrix, Revision 3*. EPRI, Palo Alto, CA: 2013. 3002000628.

[1-2] *EPRI Materials Degradation Matrix, Revision 4*. EPRI, Palo Alto, CA: 2018. 3002013781.

[1-3] *EPRI Materials Management Matrix Project: Advanced Light Water Reactor—Boiling Water Reactor Degradation Matrix (ALWR BWR DM), Revision 0*. EPRI, Palo Alto, CA: 2009. 1019611.

[1-4] *EPRI Materials Management Matrix Project: Advanced Light-Water Reactor—Pressurized Water Reactor Degradation Matrix—Revision 1*. EPRI, Palo Alto, CA: 2010. 1021088.

[1-5] NEI 03-08 Rev. 4, “Guideline for the Management of Materials Issues,” February 2020.

2
APPROACH

For each major reactor type evaluated in the MDM, evaluation results are documented in a set of degradation matrix tables. The approach used to create and present these results is described.

2.1 Development Approach

From initial development through Revision 3, the MDM was based upon an expert elicitation process. A panel consisting of materials experts, industry personnel, and EPRI staff provided the key inputs used to revise the MDM results. The meeting focus was placed on identifying and characterizing important changes occurring since the last MDM panel discussion. Important inputs included relevant recent operating experience, results of completed and ongoing R&D projects, and information regarding newly initiated R&D projects. In the fourth revision, a less formal process was used to revise existing results. Instead of a single expert panel meeting, inputs were solicited from key industry experts and EPRI staff. Inputs provided were used to develop revised MDM content by EPRI staff and consultants. These revised results were subsequently made available for appropriate peer review. One exception to this approach was that an expert panel meeting was used for the purpose of developing MDM results for VVER reactor designs that were added in Revision 4.

In this fifth revision, the expert panel approach was employed. One key benefit of this approach is the development of a common basis for assessments of all the different reactor types. The MDM expert panel consisted of subgroups for each reactor type, that proposed revisions to the MDM content based on operating experience and R&D results obtained since the previous revision. The process culminated with a comprehensive assessment meeting, which, in addition to the MDM panel, included select industry experts and appropriate EPRI subject matter experts. The proposed changes were reviewed and vetted amongst the larger group and assimilated into the current revision.

2.2 Degradation Matrix Tables

Within each section, MDM results are presented in a matrix of degradation mechanisms vs. material classes. Separate degradation matrix tables are provided for groups of components (e.g., Primary Pressure Boundary, Reactor Vessel Internals, Steam Generator Tubes, and Internals).

2.2.1 Degradation Modes

Degradation mechanisms are organized into broad categories (degradation modes), which encompass one or more degradation mechanisms. When possible, similar degradation processes have been combined to simplify the presentation of results. Relevant degradation mechanisms are described in Appendix A: Degradation Mechanism Summaries. The following degradation modes are specified within this revision of the MDM:

- **Corrosion**
  - Wastage (Wstg.)
  - Pitting
  - Flow-Accelerated (or -Assisted) Corrosion (FAC)
  - Fouling
- **Wear**
- **Stress Corrosion Cracking (SCC)**
  - Intergranular and Transgranular SCC (IG/TG)[1, 2, 3]
  - Irradiation-Assisted SCC (IASCC)
  - Outside Diameter SCC (ODSCC)[4]
  - Low Temperature Creep Cracking (LTCC)[5]
  - Delayed Hydride Cracking (DHC)[6]
- **Fatigue (Fat)**
  - High-Cycle Fatigue (HCF)[7]
  - Low-Cycle Fatigue (LCF)
  - Environmentally Assisted Fatigue (EAF)/Corrosion Fatigue (CF)
- **Fracture—Reduction in Fracture Properties (RiFP)**
  - Thermal Aging Embrittlement (Th.)
  - Reduction in Fracture Properties Due to Environmental Effects (Env.)[8]

---

[1] Includes PWSCC. For steam generator tubes, PWSCC is termed “inside diameter SCC” (ID).

[2] Specific forms of environmentally induced cracking, such as Strain-Induced Corrosion Cracking (SICC) and Intergranular Attack (IGA), are considered within the “IG/TG” SCC column.

[3] Includes external surface SCC for the external surfaces of pressure boundary components and for pressure-retaining bolting. See the external surfaces and pressure-retaining bolting tables.

[4] PWR, CANDU, and VVER SG tubes only.

[5] CANDU reactor design carbon steel primary water feeders only. The mechanism refers to environmentally assisted creep cracking.

[6] CANDU reactor design zirconium alloy pressure tubes and calandria tubes only.

[7] Also includes mid-cycle fatigue issues.

[8] This degradation submode is broadly defined to include several related phenomena, including both high temperature and low temperature observations and both K_{IC} (fracture toughness) and J-R tearing (fracture resistance) conditions. Hydrogen embrittlement is also addressed within this degradation mechanism.

- **Irradiation Effects (Irr.)**
  - Irradiation Embrittlement (Emb.)
  - Void Swelling (VS)
  - Irradiation Creep/Stress Relaxation (IC/SR)

2.2.2 Material Classes

Materials are presented in broad material classes. These classes represent groups of specific material grades having similar composition and perform similarly under the same environmental conditions. Descriptions of the material classes used in PWR, BWR, and CANDU reactor designs can be found in the EPRI Materials Handbook [2-1]. Appendix B describes the Russian and Eastern European designated material grades used in VVERs.

The following material classes are used within this Revision 5 of the MDM:

- **Carbon and Low-Alloy Steels (C&LAS)**
  - Low-Alloy Steels (e.g., SA-508, SA-533)
  - Carbon Steels (e.g., SA-516 Gr. 70)
- **Stainless Steels (SS)**
  - Austenitic Stainless Steel Base Metal, Weld Metal, and Cladding
  - Ti-Stabilized Austenitic Stainless Steel Base Metal, Weld Metal, and Cladding (applicable to VVERs)
  - High-Nickel Austenitic Stainless Steel (e.g., Alloy 800)
  - Cast Austenitic Stainless Steel (CASS)
  - Ferritic Stainless Steel
  - Martensitic Stainless Steel
  - Nitrogen-Strengthened Austenitic Stainless Steel (e.g., Alloy XM-19)
  - Precipitation-Hardened Austenitic Stainless Steel (e.g., Alloy A-286, ChN35VT for VVERs)
  - Precipitation-Hardened Martensitic Stainless Steel (e.g., Types 15-5PH, 17-4PH)
- **Nickel-Base Alloys**
  - Wrought and Forged: Alloy 600, Alloy 690
  - Weld metal: Alloy 82 and 182, Alloy 52 and 152 (and Alloy 52 variants)
  - Precipitation-Hardened (e.g., Alloy X-750, Alloy 718)
- **Zirconium Alloys**[9]
  - Zr-2.5 Nb
  - Zr-2, Zr-4

[9] Zirconium alloy evaluation is limited to assessing pressure and calandria tubes in the CANDU reactor design.

For detailed information on these materials, refer to the EPRI Materials Handbook (3002026521) [2-1]. It is noted that hard-facing materials such as Stellite are applied for some reactor internals components (e.g., BWR jet pump wedges and Babcock & Wilcox designed PWR thermal shield restraints). These hard-facing materials are not explicitly considered in the MDM since there are no structural integrity issues resulting from degradation. While hard-facing materials do degrade, the consequences are usually limited to radiological safety concerns. See the EPRI Materials Handbook, Chapter (IV) [2-1] and EPRI 1021103 [2-2] for additional information.

2.2.3 Presentation of Results

Conclusions are presented in each degradation matrix table cell, as illustrated in Figure 2-1.

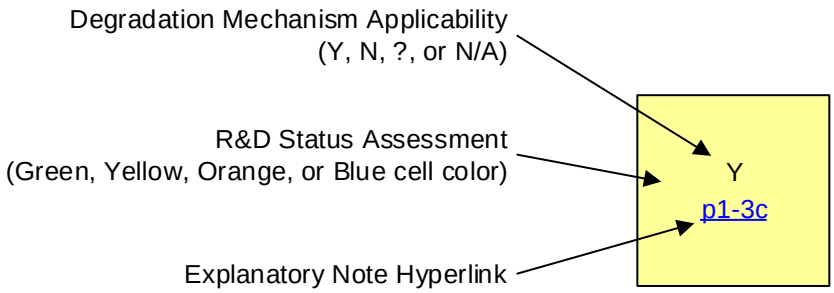

Figure 2-1
MDM table cell content

2.2.3.1 Degradation Mechanism Applicability

The evaluation approach in Revision 5 considers the applicability of each degradation mechanism to each applicable material class (represented as a single "cell" in each Degradation Matrix Table). For each cell, the degradation mechanism applicability result may be one of four choices: *Y*, *N*, *?*, or *N/A*.

"**Y**" signifies that at least one material type or grade included in the material class is known to be, or can be reasonably assumed to be, susceptible to significant damage by the applicable degradation sub-mode. Cells having a "Y" result require an R&D assessment and an associated background color.

"**N**" signifies that none of the material types or grades included in the material class are likely to be susceptible to significant damage by the applicable degradation sub-mode. Cells having an "N" result do not require an R&D assessment and do not have any R&D assessment cell background color applied.

"**?**" signifies that insufficient data are available to reach a "Y" or "N" conclusion. Cells having a "?" result always include a blue R&D assessment cell background color.

"**N/A**" signifies that a "Y," "N," or "?" result is not appropriate for the material class, degradation mechanism, and component assembly service conditions. Cells with an "N/A" result are shaded gray to differentiate them from cells with an "N" result.

Where differing opinions exist regarding a proposed applicability result, a conservative approach is taken, resulting in additional "Y" and "?" determinations. In general, these differences of opinion are noted within the explanatory note text.

2.2.3.2 R&D Assessment

When a cell's degradation mechanism applicability result is either "Y" or "?," the cell background is shaded one of four different colors to indicate how well the degradation phenomenon is characterized and whether ongoing research efforts are expected to resolve uncertainties in a reasonable, near-term time frame.

Blue background color is used for all "?" cells and indicates that a lack of data currently exists to establish degradation mechanism applicability for the material class and expected component service conditions.

Green background color signifies that the degradation mechanism is sufficiently well characterized for the material class and that a reasonable understanding of key characteristics exists. This does not necessarily mean that all attributes of the degradation mechanism are fully characterized. In such cases, additional research may be warranted to quantify specific parameters. Further, the green background color coding does not necessarily mean the degradation mechanism is being adequately managed or can be mitigated, just that the degradation process has been reasonably well characterized by completed research.

Yellow background color signifies that near-term knowledge gaps remain with regard to adequately characterizing, mitigating or managing the degradation mechanism. However, relevant R&D deemed sufficient to address the key knowledge gaps is either in progress or is addressed by specific near-term research program plans.

Orange background color signifies that near-term knowledge gaps remain regarding understanding and adequately characterizing, mitigating, or managing the degradation mechanism. Further, there is insufficient R&D in progress or planned to address the knowledge gaps in a reasonable, near-term time frame.

2.2.3.3 Explanatory Notes

Hyperlinks to explanatory notes are embedded in the Degradation Matrix Tables. The primary function of the explanatory notes is to clarify the degradation mechanism applicability and R&D Assessment determinations.

Explanatory notes are not intended to convey significant technical content such as summaries of ongoing studies or recently completed work. Since the MDM is a summary assessment and not an exhaustive reference review, supporting references provided where available are limited to key documents addressing the issues. Additional technical content is included in the Appendices. However, attention should also be paid to reports generated within individual EPRI R&D programs, as well as data published in the open technical literature, to obtain an up-to-date perspective of the relevant issue.

Explanatory note numbers are defined such that the note number provides an indication of the applicable degradation matrix table cell. A unique note ID is provided for each cell having an explanatory note. Figure 2-2 illustrates the explanatory note numbering approach.

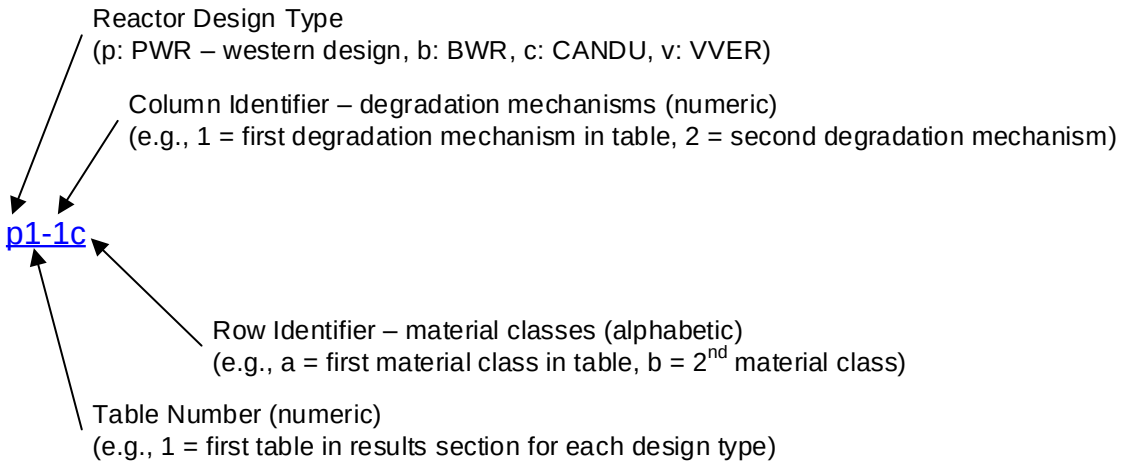

Figure 2-2
MDM table cell content—explanatory note numbering

2.3 References

[2-1] *Materials Handbook for Nuclear Plant Pressure Boundary Applications (IMR-100).* EPRI, Palo Alto, CA: 2024. 3002026521.

[2-2] *Cobalt Reduction Sourcebook*. EPRI, Palo Alto, CA: 2010. 1021103.

3
STRATEGIC ISSUES

Strategic issues are summarized for Western LWR designs, VVERs, and CANDUs in Sections 3.1, 3.2, and 3.3, respectively.

3.1 Western LWR Strategic Issues

Table 3-1 summarizes the significant degradation and material performance concerns resulting from the MDM evaluation. This table contains subsections for PWR Primary System, Steam Generators, BWR Primary System, and Generic Issues. Within the generic issues section, a limited number of broad design-independent industry needs is identified. Although elements of these issues are necessarily design-specific, the intent of this section is to highlight some of the current knowledge gaps. Section reference links within Table 3-1 point to related summary discussion contained in Sections 3.1.1 through 3.1.8.

Table 3-1
Key LWR knowledge gaps

Knowledge Gaps	Examples of Potentially Affected Components	Section Reference
PWR Primary System		
Late occurring damage phenomena and effects on embrittlement trends	Low-alloy steel reactor vessel shells and welds	3.1.1.1
Capabilities to predict IASCC initiation in high fluence components	Baffle former bolts	3.1.2.4
SCC of stainless steel in primary water	Core barrel, piping, safe ends	3.1.2.3
Fracture toughness in irradiated stainless steel	Core barrel, baffle plates	3.1.3
Modeling/prediction of void swelling rates and significance	Baffle/former assemblies, welded core shrouds	3.1.4
Relationship between the effects of neutron fluence and initial microstructure on SCC risks, considering extended operations and initial fabrication	Alloy X-750 CRGT support pins and clevis insert bolts and pins A-286 and X-750 fasteners/bolts, CASS support flanges	3.1.5
Alloy 690, 52, 152 long-term performances/PWSCC resistance	Replacement components, repairs	3.1.6

Table 3-1 (continued)
Key LWR knowledge gaps

Knowledge Gaps	Examples of Potentially Affected Components	Section Reference
Steam Generators		
Prediction of ODSCC, PWSCC initiation trends, and development of effective mitigation technologies	Alloy 600TT tube bundles	3.1.2.1
Evaluation of ODSCC vulnerabilities (e.g., PbSCC)	Alloy 690TT tube bundles	3.1.7
BWR Primary System		
Effect of impurities and increasing yield strength from irradiation on SCC susceptibility of low-alloy steel	Reactor vessel shells and welds	3.1.1.2
Late life IGSCC in nickel-base alloy welds	Instrument nozzle welds Jet pump riser brace RPV ID attachment welds Shroud support welds	3.1.2.2
Key factors influencing IASCC growth in welded stainless steel structures exposed to BWR coolant, including off-axis cracking	Welded structures subject to high fluence (i.e., core shroud, top guide)	3.1.2.5
Thermal/irradiation embrittlement of CASS	Orifice fuel supports and jet pump assembly castings	3.1.3
Effect of extended operations on high-strength core periphery components (irradiated properties including fracture toughness, tensile strength, SCC growth rates)	X-750 jet pump beams and core shroud tie rod repair hardware XM-19 repair hardware	3.1.5
Generic Knowledge Gaps		
SCC initiation prediction, modeling, and mechanistic understanding	All austenitic primary system components	3.1.2
Updating SCC growth rate models and reconciling models as a function of BWR/PWR conditions, temperature, water chemistry, K, etc.	Many components	3.1.2 3.1.2.3
Understanding IASCC processes and characterization of parameters influencing IASCC susceptibility	Near core reactor internals (PWR baffle bolting and core barrels, BWR core shrouds, and top guides)	3.1.2.4 3.1.2.5
Understanding the true effect of coolant exposure on the fatigue resistance of plant components and evaluation of this effect with respect to conservatisms included in original design calculations	Austenitic pressure boundary components with significant fatigue usage (e.g., PWR surge line components)	3.1.8
Understanding the fabrication concerns, degradation modes, mechanical behavior, inspection feasibility, and long-term aging performance of additively manufactured materials for use in LWR applications	Not currently in use	3.1.9

3.1.1 Reactor Vessel Integrity

3.1.1.1 PWR Vessel Neutron Embrittlement Correlations

Current prediction models for neutron embrittlement of reactor vessel low-alloy steel (LAS) correctly emphasize the early and dominant role of copper in the formation of copper-rich precipitates (CRPs), which lead to hardening and an increase in the ductile-brittle transition temperature (DBTT). The current models predict that the increase in DBTT levels off as the matrix copper is consumed by the CRPs – a prediction that is contrary to recent observations in high fluence materials.

There is increasing evidence for the existence of additional damage phenomena that manifest at fluences > ~$5x10^{19}$ n/cm^2 (E > 1.0 MeV), causing continued increases in transition temperature shift (TTS). These high-fluence damage phenomena, which are not fully included in mechanistically guided predictive models, warrant additional consideration. Depending on flux conditions, these embrittlement phenomena likely include a combination of Ni-Mn-Si clustering and stable matrix features. Thermally unstable matrix defects may also form when the flux rates are very high, as seen in some test reactor material irradiations. Ni-Mn-Si clusters have been clearly observed in reactor pressure vessel steels (both in low-copper and higher copper containing steels), resulting in continued embrittlement behavior that needs to be included in power reactor embrittlement models. Appropriate quantification of the effects of these high fluence embrittlement phenomena on TTS represents a key knowledge gap.

3.1.1.2 BWR Vessel SCC Susceptibility

Although most LAS components are clad with stainless steel weld metals, some BWR designs include areas (e.g., nozzles, top head covers) where bare LAS is exposed to the aqueous environment. While the field experience with LAS vessel plate and nozzle material has been excellent, it was demonstrated in the laboratory that small concentrations of chloride (e.g., 3 ppb) can increase the stress corrosion cracking (SCC) crack growth rate (CGR) of reactor pressure vessel steel in BWR environments. A particular concern was the possible crack extension from Alloy 182 attachment pads, which are known to be susceptible to SCC, into the LAS base metal because the crack could be at high K levels. Available data are now considered sufficient to the disposition of these issues. A reduction in the EPRI BWR water chemistry Action Level 1 value for chloride from 5 ppb to 3 ppb was implemented, and work is underway to codify LAS SCC CGRs. While the effects of water impurities such as chloride and, to a lesser extent, sulfate on SCC CGRs are sufficiently understood, there exist very little data on other impurities (e.g., F^-, I^-, Br^-, NO_3^-, PO_4^{3-}). Having been surprised by the high sensitivity of CGRs to chloride, scoping studies to examine the effect of additional impurities may be warranted.

An additional data gap is the paucity of SCC of LAS data for BWR normal operating conditions. The current CGR model (N-896) predicts sustained rapid growth, which is overly conservative compared to the field where there has been essentially no growth (with rare exceptions of shallow growth that then stalls). Much of the data supporting the N-896 model is conservative relative to BWR normal operating conditions, such as intermediate temperature, ripple loading, dynamic strain aging, and impurities above water chemistry Action Level 1. To resolve this gap, LAS SCC data should be obtained under conditions applicable to BWR RPVs (288°C, constant K,

sufficiently large specimens to ensure validity at high K values, water chemistry consistent with VIP-190, etc.), and CGR data points should be taken only near the end of each segment (i.e., wait for the CGR to finish decaying). These new data could be used to develop an updated CGR correlation that is more representative of the phenomena in the field.

3.1.2 SCC Prediction and Modeling

SCC has been one of the primary materials challenges to LWR primary system integrity faced by plant operators. While there are some unique elements and important differences in reactor types and environments, the majority of SCC dependencies are common, and this should be reflected in the understanding and continuity in modeling and disposition curves, or in the management and organizational approach to materials degradation. There is some evidence of stabilizing, or even declining, trends in SCC initiation in LWRs, due to both proactive repair and replacement activities as well as the possibility that remaining components are inherently less susceptible. However, predicting future trends with sufficient confidence remains beyond current capabilities. In many cases, there remain gaps in knowledge of the degradation process and a need to update and rationalize SCC CGR models. Manufacturing factors (e.g., heat-to-heat variability) and fabrication factors (e.g., weld residual stress, fit up stress, and cold work) are known to have significant roles in SCC occurrence, but quantifying the distributions and influence of these variables on SCC remains problematic. Laboratory data provides excellent insights into SCC vulnerabilities and growth rates, but SCC initiation studies are more difficult to leverage. Laboratory initiation tests are typically accelerated by 100-1000X to simulate plant operation, and the effects of such large acceleration on the results are not clear. Furthermore, the effects of the near-surface microstructure (e.g., surface cold work), residual deformation, and stress on crack initiation are poorly known and highly variable. It is also recognized that many phenomena, either alone or synergistically, can contribute to the initiation of cracks at the micro-scale.

Although currently observed trends do not suggest substantial new SCC concerns, it is plausible that long-term exposure of materials to environments conducive to SCC will lead to adverse trends in SCC initiation in materials or components where it has not previously been observed, or to new growth of previously dormant cracks. As such, improving the capability to predict SCC trends remains an important area of research.

3.1.2.1 SCC Trends for Thermally Treated Alloy 600 Tube Bundles

Recent operating experience indicates an ongoing trend of ODSCC indications in Alloy 600TT steam generator (SG) tubes. Cracking is occurring at several axial locations, including areas within the tubesheet, at the top-of-tubesheet region, and at tube supports. Concerns are associated with the impact of deposit buildup, denting, impurities (particularly lead), and anomalous stress conditions (e.g., bulges and over-expansions) or to microstructural deficiencies. In laboratory testing, small amounts of lead have been found to cause rapid cracking (transgranular or intergranular) in Alloy 600, and, coupled with its slow accumulation in many SG deposits, it is now thought that the impact of lead on ODSCC has been previously underestimated. On the primary side, there has now been a limited number of PWSCC indications in SGs tubed with Alloy 600TT. However, most of these indications have been attributed to off-normal stress conditions (i.e., bulges and over-expansions). There is a need for improved understanding of the fundamental factors influencing the SCC observed and for methods to mitigate the progression of SCC to an extent that allows the tube bundle to remain serviceable through the end of plant life.

3.1.2.2 BWR SCC in Stainless Steels, Nickel-Base Alloys, and Their Welds

SCC has occurred in BWRs since the mid-1960s in sensitized and/or cold-worked austenitic stainless steel components, Alloy 600, and their welds. Most of the highly susceptible components fabricated from sensitized or cold-worked materials have been repaired, replaced, or mitigated. Significant improvements in water chemistry, in particular the use of hydrogen water chemistry (HWC) and NobleChem™, have also strongly contributed to the improved SCC resistance. However, it is reasonable to assume that some SCC will continue to occur. Since substantive repairs to, or replacement of, large core support structures like the top guide, core shroud, and shroud support would be very expensive, the capability to estimate the remaining service lives of structural components, particularly irradiated core support structures including the core shroud and top guide, is crucial.

SCC of nickel-base alloy 182 and 82 welds continues to be identified in vessel nozzle dissimilar metal welds and in shroud support welds. Although it has been accepted for many years that Alloy 182 is susceptible to SCC, there is now clear evidence that SCC can also occur in Alloy 82. High residual stresses and strains from weld repairs are the most likely aggravating factors contributing to Alloy 82 SCC. Although most SCC is suspected to have initiated early in plant operations due to these fabrication-related conditions, there are concerns regarding late-in-life SCC occurrence given observations of late occurring PWSCC in these weld alloys in PWRs under low ECP and cold leg temperatures that are not too different from BWR HWC conditions. Significant SCC occurring in shroud support welds that are difficult to access for inspection or repair would represent a challenge to successful LTO for BWRs. As a result, understanding Alloy 182 and 182 material degradation trends remains an important knowledge gap.

Finally, BWRs rely heavily on On-Line NobleChem™ for mitigating SCC. In the context of LTO, U.S. BWRs will ultimately operate with NobleChem™ for the majority of the plant life. Effective NobleChem™ requires an adequate density and distribution of Pt catalyst particles on component surfaces, especially for existing cracks that can grow during startup and operation. However, there is evidence that application of Pt in plants may not be optimal. Understanding application limitations and being able to characterize Pt size-distribution and particle spacing on BWR plant components are important in the context of ensuring optimum SCC mitigation and maximizing component service lives.

3.1.2.3 PWR SCC of Stainless Steels

There are sufficient instances of SCC in stainless steel components exposed to PWR primary water, along with significant laboratory data, to consider it a generic concern. No precipitous increase in SCC is expected, but inspections will continue to show some ongoing incidents of SCC. However, it is likely that long-term exposure of materials to PWR primary water will lead to ongoing SCC initiation and growth in stainless steel components where it has not previously been observed, or at higher incidence than anticipated. One possible example is the recent operating experience of core barrel cracking, which may potentially be indicative of future SCC occurrences. As such, improving the capability to predict SCC trends remains an important area of research. It is recognized that SCC occurs on a continuum from high to low corrosion potential, and from pure water to B/Li chemistry. Efforts should be made to adapt the SCC CGR models to reflect this continuum so that they interface appropriately.

3.1.2.4 PWR Irradiation-Assisted Stress Corrosion Cracking

The primary effects of irradiation on SCC are reasonably well understood and include radiation hardening, radiation-induced segregation, radiation creep relaxation of constant displacement stresses, and the radiolysis of water. Other factors, such as void swelling, helium generation and the evolution of phases, and precipitation at high fluence could have a direct effect on SCC, but their role on SCC is speculative. Void swelling could have an indirect effect by increasing the stress, e.g., as baffle plates swell (in thickness or length). There is no evidence that the origins of IASCC in PWRs differ from those of BWRs, but the individual effects of radiation phenomena on SCC differ quantitatively with water chemistry and temperature. Predicting the integrated effects in plant components of damaging (e.g., radiation hardening and void swelling) and beneficial (e.g., radiation creep relaxation) contributions of irradiation is challenging.

Much of the existing IASCC knowledge comes from BWR experience (e.g., fuel cladding, control rod blades, handles, sheaths, and shrouds) and from PWR operating experience that includes control rod cladding and baffle-to-former bolt cracking. Both solution-annealed and cold-worked austenitic stainless steels are known to be susceptible to IASCC in PWR environments, and there is a significant heat-to-heat variability. Interactions between the relevant materials and environmental parameters have not been adequately quantified, and a single factor is unlikely to dominate IASCC susceptibility. Sufficient data and integrated predictions are not available to adequately characterize the IASCC risk as a function of component, accumulating neutron fluence (and operating time), and location in the PWR internals. Uncertainties associated with data scatter, material variability, irradiation temperature (e.g., from gamma heating), neutron spectrum effects, and water chemistry significantly complicate the prediction of IASCC.

3.1.2.5 BWR Irradiation-Assisted Stress Corrosion Cracking

At neutron fluence levels corresponding to greater than ~0.2 dpa, radiation hardening and radiation-induced segregation increase the yield strength and cause grain boundary Cr depletion. These changes in material properties are known to reduce material resistance to SCC. The result could be an enhanced growth of existing cracks and/or initiation of new cracks. Existing data from an inspection of core shrouds suggest some enhancement of SCC in regions of higher fluence, although there are too few data to conclusively separate the detrimental effect of neutron fluence from fabrication-related factors. It must also be recognized that there are limited test data associated with irradiated stainless steels due to the complexity and costs of irradiated materials testing. As such, the development of improved methods for assessing and characterizing IASCC impacts on the structural integrity of reactor internals subject to significant fluence remains an important knowledge gap for BWRs, especially in the context of LTO.

3.1.3 Fracture Toughness of Irradiated Stainless Steel

When exposed to high-energy neutrons, the fracture toughness of austenitic stainless steel is significantly decreased, asymptotically approaching a saturation value. This leads to a decreased critical crack length that can be accommodated by the component without premature failure and, thus, an increased sensitivity to flaws. The data are consistent in showing a typical saturation of irradiation embrittlement between approximately 5 and 10 dpa and a lower bound fracture toughness (K_{JC}) of approximately 38 MPa$\sqrt{m}$ for fluence values greater than 10 dpa. Currently, there are sufficient data for base metal to identify the embrittlement trend to 90 dpa. However, this bounds only two-thirds of the expected maximum fluence of the most highly irradiated PWR

internal components through the period of extended operation. The lack of PWR component fracture toughness data at peak operating temperatures and very high dpa (>90 dpa) is considered a gap, particularly if additional microstructural evolution occurs due to void swelling or the formation of new phases, which could affect the current lower bound curve. Despite the level of confidence in base metal irradiation embrittlement trends, there are very little fracture toughness data for austenitic stainless steel welds. There is some uncertainty with respect to the effects of varying levels of ferrite in weld metals on embrittlement, and there are little weld metal fracture toughness data beyond 15 dpa. Recent data for material removed from the baffle plate assembly of the Zorita PWR correlated well, showing saturation of mechanical properties above approximately 10 dpa up to the approximately 50 dpa maximum dose tested. However, testing of Zorita core barrel weld metal indicates a reduction in fracture properties for weld material at a lower neutron dose (0.7 to 1.9 dpa) than observed for wrought base metal. Overall, there are multiple data gaps to be resolved with respect to the fracture toughness of austenitic stainless steels, and they are of strategic importance for core internals during extended operation.

For cast austenitic stainless steel (CASS), which generally contains 12-25% ferrite in the austenite phases, thermal and irradiation embrittlement of the ferrite can potentially result in different embrittlement behavior than completely austenitic stainless steels. The industry has demonstrated that there does not appear to be synergistic effects of thermal and irradiation embrittlement (although they both contribute) for CASS materials. However, some key data gaps exist. For example, the assessment of CASS fracture toughness evolution is largely based on weld metal data. The additional weld metal correlations included in BWRVIP-100 Revision 2 shifted the threshold fluence from $6x10^{20}$ n/cm^2 to $<1x10^{20}$ n/cm^2 (E > 1.0 MeV). CASS fracture toughness data are limited (especially in the 0.1 to 1.0 dpa range), and it is unclear to what extent CASS conforms to the same fracture toughness trends of weld metal. Furthermore, there is a lack of data for low Mo materials (CF3/CF8) between 1 and 5 dpa as well as a lack of data for CASS materials with concurrent irradiation dose and thermal exposure for greater than 1 dpa.

3.1.4 Void Swelling

Void swelling is a complex phenomenon that is highly dependent on the material (chemical composition and thermal-mechanical treatment) and on the irradiation conditions (temperature history, fluence, flux, flux-spectrum, and associated transmutation He production). The concern is limited to PWRs and VVERs where the neutron dose and temperature (including the contribution from gamma heating) are substantially higher than those of BWRs. Excessive void swelling can alter component dimensions and loads, degrade fracture toughness, and increase IASCC susceptibility. Although void swelling is projected to be minor for most PWR internals, there are cases where relatively small amounts of void swelling could have a detrimental impact on structures that are not tolerant of changes in dimension. For internal structures, small levels of differential swelling in large volumes of material could produce deformation and increased stress in components. Estimates of the level of void swelling under PWR conditions in the past were based on empirical extrapolations of data from fast reactor irradiations. A recent re-evaluation of the data and models used as the basis for the industry reactor vessel internals guidance showed that the saturation void swelling rate was overestimated by approximately 10X, which, combined with sensitivity studies on relevant PWR component assemblies, indicates that void swelling may be less impactful than previously thought. A cluster dynamics model is available for modeling void swelling of austenitic stainless steel under PWR conditions, which, when

compared to experimental data derived from the GONDOLE program density measurements and TEM characterizations, appears to be quite robust for the prediction of the evolution of the irradiated microstructure under PWR conditions. Data from samples removed from the Zorita plant indicate very limited void swelling under PWR conditions.

The developments listed above have reduced the overall concern for potential void swelling under PWR conditions. There are still some potential gaps in the void swelling data for Type 304 solution annealed and Type 316 cold-worked stainless steels at various neutron fluences, neutron fluxes, temperatures, and stresses. The information needed to fill these gaps includes: 1) more experimental studies of solution-annealed Type 304 and 304L stainless steels; 2) data for intermediate and high doses for temperatures between 340°C and 370°C (644°F and 698°F); 3) data from cumulative doses and operating temperatures representative of subsequent license renewal (SLR) to determine the effects of helium generation rates; 4) data on the combined effect of cold work and alloy composition; 5) the effect of variations in thermal neutron population, local gamma heating rates, and temperature history of the internals on swelling; 6) the uncertainty of determining void swelling values from TEM analyses; 7) the effect of stress on void swelling at PWR-relevant irradiation temperatures; and 8) the interaction of hydrogen with cavities at PWR-relevant temperatures. Developing such data will allow for better calibration of the cluster dynamics modeling and more precise predictions of material microstructural and property evolution during service. These strategic issues, however, represent knowledge gaps that can be adequately addressed only by appropriate examinations of components harvested from PWRs with sufficiently long service lives.

3.1.5 Core Periphery Reactor Internals

While the near-core components exposed to very high neutron fluences are almost exclusively austenitic stainless steels, additional materials are in use around the periphery of the core. These materials receive substantially less neutron fluence, but, in the context of extended operations, their accumulated end-of-life fluences may approach values where neutron effects become of concern. Affected BWR components include jet pump beams, core plate wedge retainers, and shroud repair hardware. These Alloy X-750 and Type XM-19 components are located in the annulus region between the core shroud and reactor vessel and will experience moderate levels of fluence with extended operating periods. Affected PWR components include Alloys A-286 and X-750 core barrel and thermal shield bolting, Alloy X-750 control rod guide tube support pins, and Alloy X-750 clevis insert bolts/pins. The 80-year neutron dose effects for these components will exceed 2 dpa ($1.3x10^{21}$ n/cm^2, E > 1.0 MeV), within a range where irradiation effects may become a concern. SCC growth rate studies of irradiated Alloy X-750 show a limited effect of fluence, but, in general, the irradiated materials data for these alloys are limited. Given that these materials are known to have SCC susceptibility, there is a strategic knowledge gap associated with more confidently predicting SCC behavior and component service lifetimes, and the qualification of more SCC-resistant replacement alloys.

3.1.6 High Chromium Nickel-Base Alloy SCC Vulnerabilities

High chromium nickel-base alloys (Alloy 690 and Alloy 52/152 weld metals) are being widely used for repair of and replacement for components fabricated from Alloys 600, 82, and 182. Excellent operating experience with no observations of PWSCC in 35 years of service supports the superiority of Alloy 690 relative to Alloy 600 in PWR primary water environments, as does extensive laboratory testing. However, these materials are not immune to SCC, and vulnerabilities (such as high cold work or high weld residual strains) need to be avoided.

A database of laboratory SCC growth rates was developed and analyzed by an international expert panel, and shows effects of cold work, yield strength, heat-to-heat variability, weld heat-affected zone structures, crack orientations, stress intensity factor, temperature, and dissolved hydrogen content. In most heats of Alloy 690, the CGRs were considered low for materials with less than 12% cold work; indeed, the low growth rates made it difficult to quantify the effects of the aforementioned variables, and this remains a data gap. However, there were several heats of Alloy 690 that exhibited much higher growth rates, including those with 12% cold work.

For Alloys 52 and 152 weld filler materials, nearly all SCC growth rate testing has yielded "low" or "very low" crack growth rates. However, these higher Cr weld filler metals do have a propensity for developing micro-fissuring during weld deposition, with the micro-fissures potentially presenting sites for PWSCC crack initiation. Work remains in progress to better understand and mitigate the causes of the micro-fissuring by changing the welding processes and procedures, and by developing alternative alloys with improved weldability. ASME code cases are being advanced to leave small weld defects as-is, because weld repairs are almost always more detrimental.

There are also concerns related to the SCC behavior in the first pass or two adjacent to the weld (especially to low alloy or carbon steel), where dilution of the high Cr weld metal occurs. Extensive data show that SCC growth rates decrease rapidly above ~24% Cr, and the dilution zone needs to be characterized. The expert panel is evaluating SCC data, and other studies are underway, to characterize the dilution zone in multiple areas of many dissimilar welds. Another concern relates to the SCC behavior in the low alloy steel HAZ. Moderate SCC growth rates have been observed in the HAZ of temper bead welds in PWR primary water. As the weld metal becomes more resistant (Alloys 52 and 152), vulnerabilities in other areas may develop.

Long-term embrittlement can occur in Ni-Cr-Fe alloys with < 7% iron due to long-range ordering. Although the standard formulation of Alloy 52 contains 7-11% iron, variant formulations are being developed that, in some cases, contain much less than 7% iron. For example, Alloy 52i contains only 2.5% iron, and some alloy development is underway on weld metals with ~0% Fe. There has been only limited evaluation of the potential for long-range ordering in these new high Cr nickel-base weld filler metals during long time service, and this represents another gap of strategic importance.

3.1.7 ODSCC of Alloy 690 Steam Generator Tubing

For Alloy 690TT steam generator tubing, laboratory data suggest that ODSCC is a potential vulnerability, with present concerns focused on potential vulnerabilities associated with lead-induced SCC (PbSCC). There is uncertainty concerning the amount of lead required and the active chemical form needed to cause PbSCC. Exposure to off-normal chemistry conditions appears to also be necessary to promote SCC (including PbSCC) in Alloy 690TT tubing.

Appropriately, much of the ongoing research focuses on off-normal chemistry or on the consequences of operational events. Knowledge gaps include understanding the envelope of electrochemical potential associated with PbSCC, characterizing the film formed on tubing in environments containing lead, and evaluation of remedial actions that can be implemented to mitigate PbSCC (e.g., evaluating the effectiveness of additives that slow plating kinetics and additives that remove lead from solution by precipitating lead compounds). An additional area of concern is the potential for SCC vulnerability to be increased by cold work and stress that can occur due to denting at the top-of-tubesheet region.

3.1.8 Effect of LWR Environment on Fatigue Resistance

Laboratory tests on small specimens in simulated reactor coolant environments show that fatigue resistance in reactor water environments is lower than in a “dry air” environment. It is also recognized that the fatigue design curves that provide the basis for fatigue life assessments of nuclear plant components do not explicitly account for the effects of LWR environments on fatigue life; although, to date, conservatisms included in fatigue design curves and in fatigue calculational methods have been adequate to bound the effects of environment.

Over time, component fatigue usage estimates have been refined through the application of more complex analytical methods to accommodate longer term operation, oftentimes at a significant cost burden to plant owners. This approach, while a pragmatic solution for meeting regulatory requirements, does not directly address the impact of water environments.

A fundamental knowledge gap exists regarding the amount of conservatism that is delivered by the current practice of using correlations based on testing of thin specimens subjected to fully reversed uniaxial loading in air and incorporating environmental sensitivity factors to estimate the fatigue lives of plant components that have complex geometries and are subject to complex pressure/temperature transients.

Assessing the effect of water environments on fatigue crack growth rates is an additional area where gaps remain for some materials and water environment combinations. There are also some areas where additional data or evaluations are needed to generate appropriate correlations of the influence of dissolved oxygen/corrosion potential and material chemistry on environmental multipliers on fatigue life and on fatigue crack growth rates.

3.1.9 Additively Manufactured Materials

Advanced manufacturing methods have been and continue to be considered for fabrication of reactor system components. Leading candidate methods include powder metallurgy/hot isostatic pressing (PM/HIP), additive manufacturing (also called *3D printing*), and advanced joining, cladding, and coating methods (such as cold spray and diode laser cladding). Many of these advanced manufacturing methods are contenders for component fabrication supporting new reactor design and construction. Some of these technologies are also being introduced for replacement components and repair strategies of existing LWRs, notably additive manufacturing (AM). Powder bed fusion (PBF) and directed energy deposition (DED) are some of the prominent AM technologies being researched by EPRI for more widespread use in nuclear reactor metal component fabrication.

Rapid prototyping, resolving supply chain deficiencies, fabrication (coupled with metrology and reverse engineering) to address component obsolescence, and introducing novel design and material functionality with AM methods are some of the reasons such technologies have shown promise for use in the existing LWR plants. While AM technologies have been readily adapted in the past decade or so into the aerospace, medical device, and automotive industries with the advantages of weight reduction and novel designs, it has been slower to get traction with applications in the nuclear industry. Existing LWRs often require like-for-like replacements, and have components with relatively low weight sensitivity for design, such that new manufacturing methods are difficult to economically introduce. Similarly, the nuclear industry requires codification of the material and fabrication specifications into complex codes and standards, including regulatory acceptance, much of which is based upon empirical data collected over many years from conventionally produced materials and parts. EPRI along with others in the industry have been working to optimize manufacturing methods to improve costs and lead time, gather needed empirical data on the pre-service mechanical performance, develop appropriate inspection methods and acceptance criteria, and support standardization of feedstock and fabrication parameters. Similarly, EPRI has implemented research to gather environmental performance data of AM materials, notably fatigue life and stress corrosion cracking growth rates in LWR water chemistries.

While the results to date are promising, they are limited mostly to a small number of alloys and focused on testing in nominal BWR and PWR environments. Extending these positive results to other materials and reactor chemistries requires further testing, as is evaluation in operating reactors. To date components in primary system service are mostly confined to laser-PBF Type 316L stainless steel fuel hardware (installed only in the last several years). Unique grain and cellular microstructures, differing chemistry and dislocation distributions, and the presence of small defects such as porosity and lack-of-fusion are reasons AM materials (with ostensibly the same bulk chemistry as their conventionally produced counterparts) require continued evaluation for equivalency in terms of mechanical performance and/or environmental degradation as a function of time. Irradiated material properties, fatigue performance, and stress corrosion cracking susceptibility are the most strategically important age-related degradation mechanisms to evaluate in this broad class of materials.

3.2 VVER Strategic Issues

VVER materials of construction were specified consistent with Central and Eastern European/Russian/Soviet standards, primarily a set of Soviet state standards in use at the time of design (designated by the acronym GOST, which is derived from Russian words meaning “state standard”). Notable differences between the materials specified for VVER applications and typical Western specifications for LWR service include the use of Titanium-stabilized stainless steels (specified to Russian standards) for components exposed to the primary coolant and use of low-alloy steel grades that contain a nominally higher percentage of Cr and a nominally lower percentage of Mn in comparison with the materials used in Western LWR designs. There are also significantly fewer data available to assess the long-term performance of the materials used in VVERs than there are for the materials used in Western designed reactors. Sections 3.2.1 to 3.2.3 highlight areas for which there are particularly significant needs.

3.2.1 Effect of VVER Environment on Fatigue Resistance

In addition to the generic elements of the R&D needs described in Section 3.1.8, there is a need to understand the effect of the VVER primary water environment on the fatigue resistance of VVER materials. All the work completed to date either do not take into account the effect of environment or have been focused on materials unique to Western-designed LWRs and use environmental conditions typical of Western PWR designs. There are few data addressing the Ti-stabilized stainless steels used in VVER primary system construction. Appropriate databases addressing environmental effects for VVER-specific materials are necessary to address primary system EAF.

Since the evaluation of the environmental effects on fatigue resistance is considered time-critical, a national test program was initiated in the Czech Republic to better understand the degradation mechanism and to potentially reduce the conservatism from present fatigue life calculations. The program includes the testing of non-irradiated Ti-stabilized stainless steels and its weld metals used for RPV welds and cladding. The results are expected to be available by the end of 2024.

3.2.2 Irradiated Materials Data

IASCC of Ti-stabilized stainless steels has occurred to a limited extent to date in VVER baffle bolts. Void swelling is also expected to be significant for VVER reactor internals subjected to high fluence at temperatures above 350°C. However, there is a general lack of data to adequately assess the risk of these degradation phenomena. Similarly, irradiation-assisted stress relaxation data for Ti-stabilized stainless steels are limited. Due to this lack of irradiated materials performance data, current predictive models used to assess VVER reactor internals are largely based on data generated on Western PWR materials. For example, the threshold stress dependence curve for IASCC initiation of reactor vessel internals materials as a function of neutron fluence recommended in the VERLIFE guidelines is based on PWR data since similar data on VVER materials are not available.

Predictions incorporating synergistic effects of irradiation creep, stress relaxation, and swelling on VVER reactor internals are also based on data from non-stabilized stainless steels. A significant amount of R&D was necessary to develop the current state of knowledge for Western PWR materials regarding these degradation mechanisms and the possible synergistic interactions. A similar R&D investment is anticipated to be necessary to address this gap for VVER reactor internals materials. At present, although some work is ongoing and additional R&D is planned, there are still significant gaps remaining.

3.2.3 Void Swelling

According to the current understanding of the phenomena, significant effects of void swelling are primarily limited to RPV internals of VVER 1000 reactors. Due to the lower temperature, including operating temperatures and gamma heating contributions, the effect of void swelling on VVER 440 reactors is currently thought to be negligible.

There are two major issues that would be appropriate to address. The first issue is that the predictions of different models used for the evaluation of void swelling vary significantly, which could lead to incorrect assessments of void swelling effects in reactor components. The benchmarking of available models is currently underway within the DELISA-LTO project in the

framework of the Euratom Research and Training Programme. The second issue is the lack of relevant data. The models are based largely on data obtained from irradiation experiments in fast reactors. Irradiations of this type were performed under conditions that differ significantly from those of VVER plants with respect to irradiation temperature, dose, dose rate, and neutron spectra. As such, there is a degree of uncertainty within the fast reactor data set, which could affect void swelling predictions for VVER plants. Analyzing the void swelling degradation mode on material from the operational VVER1000 reactors therefore remains a priority.

3.3 CANDU Reactor Strategic Issues

Strategic issues applicable to CANDU plants are presented in two categories. Section 3.3.1 presents strategic issues that are similar to those presented for PWRs in Section 3.1 above. Section 3.3.2 describes strategic issues that are uniquely applicable to CANDU reactors.

3.3.1 LWR Strategic Issues Applicable to CANDU Plants

There are sufficient similarities between CANDU plants and PWR systems that some of the strategic issues identified for PWRs in Section 3.1 are considered relevant to CANDU plants. Strategic issues identified in Section 3.1 that are relevant to CANDU plants are as follows:

- PWSCC Mechanistic Understanding and Trend Prediction (Section 3.1.2.1):
  Although there is limited use of Alloy 600/82 components in CANDU reactors in comparison with PWRs (it consists only of Alloy 600 flow elements and associated Alloy 82 dissimilar metal welds in the feeder piping), the knowledge gap related to understanding the underlying mechanisms causing PWSCC and the capability to predict future PWSCC trends is directly applicable to these components.
- High Chromium Nickel-Base Alloy SCC Vulnerabilities (Section 3.1.6):
  Alloy 690 and Alloy 52 weld filler material are currently deployed in CANDU reactors to replace the Alloy 600 and Alloy 82 materials (see first bullet) when feeders are replaced on plant refurbishment. Although LWR qualification testing of Alloy 690, with long-term exposure tests, shows no evidence of crack initiation, even in conditions similar to those that readily produce cracking in Alloy 600, there is a concern that weld dilution effects (lowering of Cr content in weld roots) may require investigation to fully understand the relative risk of crack initiation in these locations.
- Effect of Environment on Fatigue Resistance (Section 3.1.8):
  CANDU primary heat transport (PHT) system materials and operating regimes are sufficiently similar to PWR primary system conditions that R&D providing insight into the effect of environment on PWR components will be broadly applicable to CANDU plant PHT system components.

3.3.2 CANDU-Specific Strategic Issues

3.3.2.1 Fuel Channel Assembly Service Life Margins

Zirconium alloy pressure tubes are unique to the CANDU reactor design. Although the pressure tubes are replaced during mid-life refurbishments and there has been a substantial amount of R&D conducted in this area, improved characterization of pressure tube performance remains an important issue for CANDU plants. Since overly conservative estimates of pressure tube

serviceable life have caused premature shutdown for refurbishment, there is a desire to remove this conservatism to maximize service life. However, the failure of pressure tubes due to delayed hydride cracking (DHC) or fatigue cracking would be a significant event in the life of a plant. Improved characterization of the end-of-life conditions is, therefore, a high priority research area for CANDU plants. While a significant amount of R&D has been directed toward understanding DHC, by comparison, there has been relatively little R&D performed to characterize environmental fatigue effects (including the roles of irradiation and hydrogen/deuterium) and end-of-life structural margins.

A related issue is integrity of annulus spacers (commonly termed “garter springs”). These circular springs retain the appropriate spacing between the calandria tubes and the pressure tubes. In Alloy X-750 spacers, helium concentrations as high as 3 at.% are possible from transmutation reactions. Such concentrations of helium have been shown to cause a loss of ductility, which nearly eliminates the design margin of the component. Alloy X-750 spacers are currently managed by a surveillance program and are being phased out and replaced with a Zr-Nb-Cu alloy during plant refurbishments. However, the Zr-Nb-Cu alloy spacers have been shown to be susceptible to hydrogen ingress, which has led to some observations of brittle cracking in out-reactor component tests. The mitigation of this issue has received little attention to date but is considered a significant strategic issue for CANDU reactors post-refurbishment. The failure of a spacer can lead to contact between the calandria tube and pressure tube that promotes an accumulation of solid hydride and may cause failure of the pressure tube by DHC. Although no spacers have failed in service, the potential for degraded material properties, as already observed, presents a serious concern.

3.3.2.2 Alloy 800NG Steam Generator Tubing Vulnerabilities

The large majority of CANDU reactor SGs contain tubing fabricated from Alloy 800NG. Furthermore, CANDU reactor SGs, which continue to operate with older generation SG tube materials (Alloys 600 and 400), are likely to be replaced with Alloy 800NG during plant refurbishment. Although the performance to date of Alloy 800NG tube bundles in CANDU units has been exemplary, concerns remain regarding possible vulnerabilities that could shorten the serviceable life. European operating experience of Alloy 800 SG tubing in PWR plants includes several instances of ODSCC after long service lives. Based on this experience, as well as laboratory data, ODSCC is a potential vulnerability for CANDU reactor SG tubing.

Key factors that have been identified are: 1) the role of contaminants in promoting crack initiation and 2) the potential for cold work induced during the tube expansion process and differential thermal expansion to cause high stresses at the tube-to-tubesheet junction, which may promote crack initiation. Given the desire to employ Alloy 800NG tubing in replacement SGs, as well as in new plant designs, resolution of the remaining uncertainties regarding Alloy 800NG tubing vulnerabilities is considered a strategic issue for the CANDU reactor fleet.

3.3.2.3 The Evolution of End Fitting Mechanical Properties

A fuel channel life of approximately 400k effective full power hours (EFPH) has been targeted to achieve 90 to 100 effective full power years (EFPY) of reactor life, following a second refurbishment. This represents an increase in service life for fuel channel components of approximately 25%. A key knowledge gap pertaining to the extended operation of end fittings (EFs) is the effect that irradiation and, to a lesser extent, thermal aging may have on the

mechanical properties of Type 403 stainless steel. While a relatively steep neutron flux gradient exists at regions near the core periphery, the inboard end of the EF is expected to receive a small, but possibly significant, dose. Using a representative spectrum, displacement damage of approximately 0.16 to 1.65 dpa has been estimated at the inboard rolled joint groove of EFs for 400k EFPH, depending on the fuel channel configuration. There is only a very small amount of data in this area collected on irradiated material for the purpose of CANDU reactor EF assessment. The fact that relatively little work has been conducted in this area is due to a legacy of assessments performed in the 1980s, when the understanding was that the evolution of mechanical properties saturates or plateaus at a relatively low dose. The examination of ex-service EFs indicated that irradiation could result in increased hardness without any signs of saturation. In the absence of saturation and at a targeted 400k EFPH of component life, irradiation conditions could plausibly lead to hardness levels that would otherwise be considered excessive for Type 403 stainless steel if induced by improper heat treatment or cold working. A significant R&D investment is anticipated to be necessary to address this lack of knowledge and support the risk assessments with respect to EAC susceptibility and the reduction of fracture properties.

4
PWR DEGRADATION MATRIX RESULTS

4.1 Scope and Evaluation Assumptions

The PWR MDM revision is based on a re-evaluation by a panel of knowledgeable experts and in consultation with the appropriate EPRI program and project managers. Changes to the cell colors and explanatory text links reflect new experimental data and plant operating experience. See Section 2.1 for additional discussion and notes regarding the panel assessment process. Assumptions related to component scope and operating conditions used by the panel to facilitate development of consistent results include:

- The scope of PWR systems and components evaluated includes the primary system pressure boundary, reactor vessel internals, and steam generators (primary and secondary sides). Active components (e.g., control rod drives, valve internals, and pump rotating assemblies) and short-lived components (e.g., fuel assemblies and in-core instruments) are not included in the MDM evaluation. For a comprehensive list of PWR components evaluated under the NEI 03-08 materials initiative [4-1], see the EPRI PWR Issue Management Tables.
- All normal operating conditions were considered. These include normal power operations, startup, shutdown, and layup for steam generators. Normal operating conditions are defined to include less controlled environmental conditions, such as significant oxygen ingress that may occur during maintenance periods and persist for some limited time during startup.
- The normal range of secondary water chemistries was considered, together with limited effects of impurities and the way in which these can concentrate (e.g., in heated crevices within steam generators).
- The potential for nominally off-normal environments to occur was considered (e.g., areas subject to oxygen transients for a limited time due to trapped air bubbles).
- The R&D assessment color codes shown in Tables 4-1 through 4-6 are based on the assumption of extended operation, defined as anywhere from 60 to 80 or more years of service.

4.2 PWR Results: Degradation Matrix Tables and Explanatory Notes

The PWR MDM results are presented in the following set of degradation matrix tables:

Table 4-1 PWR Primary Pressure Boundary

Table 4-2 PWR Reactor Vessel Internals

Table 4-3 PWR Steam Generator Tubing, Tube Plugs & Tubesheet Welds

Table 4-4 PWR Steam Generator Secondary Side Internals

Table 4-5 PWR Steam Generator Secondary Pressure Boundary

Table 4-6 PWR External Surfaces and Pressure Retaining Bolting

Hyperlinks within these tables lead to summary notes contained in Table 4-7, PWR Explanatory Notes.

The degradation matrix tables include the use of abbreviations and color coding. Cells *Y*, *N*, *?*, *N/A* results indicate applicability of the degradation mode to a material type. Comprehensive definitions are provided in Section 2.2.3.1.

Cell shading indicates R&D status:

- Green fill indicates that the degradation mechanism is sufficiently well understood.
- Yellow fill indicates sufficient R&D is in progress to address gaps associated with the degradation mechanism in a reasonable time frame.
- Orange fill indicates insufficient R&D is ongoing or planned to address gaps associated with the degradation mechanism in a reasonable time frame.
- Blue fill indicates insufficient data exist to establish degradation mechanism applicability.

Comprehensive definitions of MDM color codes are provided in Section 2.2.3.2.

Within Table 4-7, references are provided in two ways. For EPRI references, a hyperlink to the EPRI abstract webpage is provided. For other references, a citation listing is provided in Section 4.3.

A summary of the changes to cell results for Revision 5 can be found in Appendix D.

Table 4-1
PWR primary pressure boundary[1]

MATERIAL	DEGRADATION MODE													
	Corrosion				Wear	SCC		Fatigue		Reduction in Frac. Properties		Irradiation Effects		
	Wstg.	Pitting	FAC	Foul		IG/TG	IA	HCF	EAF	Th	Env	Emb	VS	IC/SR
C&LAS: Base Metal & HAZ	Y p1-1a	N	N	N	N	Y p1-6a	Y p1-7a	N	Y p1-9a	Y p1-10a	Y p1-11a	Y p1-12a	N	N
C&LAS: Welds	Y p1-1b	N	N	N	N	Y p1-6b	Y p1-7b	N	Y p1-9b	Y p1-10b	Y p1-11b	Y p1-12b	N	N
SS: 300 Series SS Base Metal & HAZ	N	Y p1-2c	N	N	N	Y p1-6c	N	Y p1-8c	Y p1-9c	N	Y p1-11c	N	N	N
SS: 300 Series SS Welds & Clad	N	Y p1-2d	N	N	N	Y p1-6d	N	Y p1-8d	Y p1-9d	Y p1-10d	Y p1-11d	Y p1-12d	N	N
Cast Austenitic Stainless Steel	N	N	N	N	N	Y p1-6e	N	Y p1-8e	Y p1-9e	Y p1-10e	Y p1-11e	N	N	N
Ni-Alloy: 600 Base Metal & HAZ	N	N	N	N	N	Y p1-6f	N	N	Y p1-9f	N	Y p1-11f	N	N	N
Ni-Alloy: 690 Base Metal & HAZ	N	N	N	N	N	Y p1-6g	N	N	Y p1-9g	Y p1-10g	Y p1-11g	N	N	N
Ni-Alloy: 82/182 Welds & Clad	N	N	N	N	N	Y p1-6h	N	N	Y p1-9h	N	Y p1-11h	N	N	N
Ni-Alloy: 52/152 Welds & Clad	N	N	N	N	N	Y p1-6i	N	N	Y p1-9i	Y p1-10i	Y p1-11i	N	N	N

1. The scope of Table 4-1 includes the reactor vessel, pressurizer, steam generator channel head, tubesheet surfaces exposed to primary water, divider plate, and the primary piping system.

Table 4-2
PWR reactor vessel internals

MATERIAL	DEGRADATION MODE													
	Corrosion				Wear	SCC		Fatigue		Reduction in Frac. Properties		Irradiation Effects		
	Wstg.	Pitting	FAC	Foul		IG/TG	IA	HCF	EAF	Th	Env	Emb	VS	IC/SR
STRUCTURAL COMPONENTS AND WELDS														
SS: 300 Series SS Base Metal & HAZ	N	N	N	N	Y p2-5a	Y p2-6a	Y p2-7a	Y p2-8a	Y p2-9a	N	Y p2-11a	Y p2-12a	Y p2-13a	Y p2-14a
SS: 300 Series SS Welds & Clad	N	N	N	N	N	Y p2-6b	Y p2-7b	Y p2-8b	Y p2-9b	Y p2-10b	Y p2-11b	Y p2-12b	Y p2-13b	Y p2-14b
Cast Austenitic Stainless Steel:	N	N	N	N	N	Y p2-6c	? p2-7c	Y p2-8c	Y p2-9c	Y p2-10c	Y p2-11c	Y p2-12c	N	N
Ni-Alloy: 600 Base Metal	N	N	N	N	Y p2-5d	Y p2-6d	N	Y p2-8d	Y p2-9d	N	Y p2-11d	N	N	N
FASTENERS AND HARDWARE														
SS: 300 Series (304, 347, 316CW)	N	N	N	N	N	Y p2-6e	Y p2-7e	Y p2-8e	Y p2-9e	N	Y p2-11e	Y p2-12e	Y p2-13e	Y p2-14e
SS: A-286 Precip. Hardened SS	N	N	N	N	Y p2-5f	Y p2-6f	Y p2-7f	Y p2-8f	Y p2-9f	N	Y p2-11f	Y p2-12f	N	Y p2-14f
SS: Martensitic (403, 410, 431, 17-4PH, 15-5PH)	N	N	N	N	Y p2-5g	Y p2-6g	N	Y p2-8g	Y p2-9g	Y p2-10g	Y p2-11g	N	N	N
Ni-Alloy: X-750	N	N	N	N	Y p2-5h	Y p2-6h	Y p2-7h	Y p2-8h	Y p2-9h	N	Y p2-11h	Y p2-12h	N	Y p2-14h

Table 4-3
PWR steam generator tubing, tube plugs, and tubesheet welds

MATERIAL	DEGRADATION MODE										
	Corrosion				Wear	SCC		Fatigue		Reduction in Frac. Properties	
	Wstg.	Pitting	FAC	Foul		PS (ID)	SS (OD)	HCF	EAF	Th	Env
TUBES											
Ni-Alloy: 600TT	Y p3-1a	N	N	Y p3-4a	Y p3-5a	Y p3-6a	Y p3-7a	Y p3-8a	Y p3-9a	N	Y p3-11a
Ni-Alloy: 690TT	Y p3-1b	N	N	Y p3-4b	Y p3-5b	N	Y p3-7b	Y p3-8b	Y p3-9b	Y p3-10b	Y p3-11b
Alloy 800	Y p3-1c	Y p3-2c	N	Y p3-4c	Y p3-5c	N	Y p3-7c	Y p3-8c	Y p3-9c	? p3-10c	? p3-11c
TUBE PLUGS AND TUBESHEET WELDS											
Ni-Alloy: Tube Plugs	N	N	N	N	N	N	Y p3-9d	N	Y p3-9d	N	Y p3-11d
Ni-Alloy: 52/82 Welds	N	N	N	N	N	N	Y p3-9e	N	Y p3-9e	N	Y p3-11e
Alloy 800 Sleeves	Y p3-1f	Y p3-2f	N	N	N	N	N	Y p3-7f	N	N	N

PS = Primary-Side (Tube ID, primary water chemistry environment)

SS = Secondary-Side (Tube OD, secondary water chemistry environment)

Table 4-4
PWR steam generator secondary side internals

MATERIAL	DEGRADATION MODE									
	Corrosion				Wear	SCC	Fatigue		Reduction in Frac. Properties	
	Wstg.	Pitting	FAC	Foul		IG/TG	HCF	EAF	Th	Env
C&LAS: Base Metal & HAZ	Y p4-1a	Y p4-2a	Y p4-3a	Y p4-4a	Y p4-5a	Y p4-6a	Y p4-7a	Y p4-8a	N	N
C&LAS: Welds	Y p4-1b	Y p4-2b	Y p4-3b	N	Y p4-5b	Y p4-6b	Y p4-7b	Y p4-8b	N	N
SS: Martensitic	N	N	N	Y p4-4c	Y p4-5c	Y p4-6c	Y p4-7c	Y p4-8c	Y p4-9c	N
SS: Ferritic	N	N	N	Y p4-4d	Y p4-5d	Y p4-6d	Y p4-7d	Y p4-8d	N	N
Ni-Alloy: 600 Base Metal	N	N	N	N	Y p4-5e	Y p4-6e	Y p4-7e	Y p4-8e	N	N
Ni-Alloy: 690 Base Metal	N	N	N	N	Y p4-5f	Y p4-6f	Y p4-7f	Y p4-8f	Y p4-9f	N

Table 4-5
PWR steam generator secondary pressure boundary

MATERIAL	DEGRADATION MODE									
	Corrosion				Wear	SCC	Fatigue		Reduction in Frac. Properties	
	Wstg.	Pitting	FAC	Foul		IG/TG	HCF	EAF	Th	Env
C&LAS: Base Metal	N	Y p5-2a	Y p5-3a	N	N	Y p5-6a	N	Y p5-8a	N	N
C&LAS: Welds	N	Y p5-2b	Y p5-3b	N	N	Y p5-6b	N	Y p5-8b	N	N
Ni-Alloy: 600 Base Metal & HAZ	N	N	N	N	N	Y p5-6c	N	Y p5-8c	N	N
Ni-Alloy: 690 Base Metal & HAZ	N	N	N	N	N	Y p5-6d	N	Y p5-8d	N	N
Ni-Alloy: 82/182 Welds & Clad	N	N	N	N	N	Y p5-6e	N	Y p5-8e	N	N
Ni-Alloy: 52/152 Welds & Clad	N	N	N	N	N	Y p5-6f	N	Y p5-8f	N	N

Table 4-6
PWR external surfaces and pressure retaining bolting

MATERIAL	DEGRADATION MODE										
	Corrosion				Wear	SCC	Fatigue		Reduction in Frac. Properties		Irrad. Effects
	Wstg.	Pitting	FAC	Foul		IG/TG	HCF	EAF	Th	Env	Emb
PLATE, FORGINGS, CASTINGS, & WELDS											
C&LAS	Y p6-1a	Y p6-2a	N/A	N/A	N	Y p6-6a	Y p6-7a	Y p6-8a	N/A	N/A	Y p6-11a
SS: 300 Series Base Metal & HAZ	N	Y p6-2b	N/A	N/A	N	Y p6-6b	Y p6-7b	Y p6-8b	N/A	N/A	N/A
SS: Welds & Clad	N	Y p6-2c	N/A	N/A	N	Y p6-6c	Y p6-7c	Y p6-8c	N/A	N/A	N/A
Ni-Alloy: Wrought	N	Y p6-2d	N/A	N/A	N	N	Y p6-7d	Y p6-8d	N/A	N/A	N/A
Ni-Alloy: Welds	N	Y p6-2e	N/A	N/A	N	N	Y p6-7e	Y p6-8e	N/A	N/A	N/A
PRESSURE-RETAINING FASTENERS											
LAS Fasteners	Y p6-1f	Y p6-2f	N/A	N/A	N	Y p6-6f	Y p6-7f	Y p6-8f	Y p6-9f	N/A	N/A
Martensitic SS, A-286 Fasteners	N	Y p6-2g	N/A	N/A	N	Y p6-6g	Y p6-7g	Y p6-8g	Y p6-9g	N/A	N/A
PH SS Fasteners (17-4 PH)	N	Y p6-2h	N/A	N/A	N	Y p6-6h	Y p6-7h	Y p6-8h	Y p6-9h	N/A	N/A

Table 4-7
PWR systems explanatory notes

NOTE ID	EXPLANATORY NOTE
PWR PRIMARY PRESSURE BOUNDARY AND STEAM GENERATOR DIVIDER PLATE	
p1-1a p1-1b	Gaps in the channel head cladding can permit low-alloy steel to contact primary water. Significant corrosion could potentially occur as a result of exposure to oxidizing conditions, occurring most likely after shutdown and draining activities due to concentration of residual primary water by evaporation. There is a general understanding of how corrosion can progress and the overall time frame. There are no fundamental R&D gaps. Any gaps related to management of this issue should be addressed within the PWR IMT report. [R&D Status = GREEN] **References:** EPRI: 3002000473 Other: [4-2]
p1-2c p1-2d	There is field experience associated with cracking and pitting of canopy seals due to trapped air in the CRDM housings during refueling, which is then compressed to the primary system pressure, resulting in a high local partial pressure of oxygen. Low levels of chloride and sulfate impurities are also often present which, because of the extremely high oxidizing conditions at very high oxygen partial pressure, can cause pitting and cracking. There is sometimes also sensitization and cold work associated with seal welding, especially welds remade after upper head replacement. These issues are generally understood and can be managed by venting the CRDM housings or by vacuum filling. [R&D Status = GREEN] **Reference:** EPRI: MRP-236R1

Table 4-7 (continued)
PWR systems explanatory notes

NOTE ID	EXPLANATORY NOTE
p1-6a p1-6b	Although environmentally assisted cracking (corrosion fatigue, SICC, or SCC) in principle is possible for high sulfur steels at low corrosion potential in PWR primary or secondary environments, practical instances of cracking in C&LAS have only been observed in a few cases, mainly in steam generator shells and attached piping and when unusually oxidizing conditions have been allowed to develop (in the event of condenser leaks, for example). It has also been recognized that very low levels of chloride can have a substantial detrimental influence on crack growth rates observed in the laboratory, especially at higher oxidizing potentials associated with the presence of oxygen in solution. However, data indicate that cracking is mitigated by low electrochemical potentials. As such, concerns for PWRs are limited to locations having a potential for transient oxidizing conditions to develop, in combination with loading transients and the presence of small concentrations of ionic impurities. A green R&D result is considered appropriate at present. No fundamental materials R&D is considered needed. [R&D Status = GREEN] **References:** EPRI: 1025133, BWRVIP-233R2 Other: [4-3], [4-4], [4-5]

Table 4-7 (continued)
PWR systems explanatory notes

NOTE ID	EXPLANATORY NOTE
p1-6c	Observations of SCC in wrought stainless steels in the PWR RCS have been confirmed. The instances of SCC in PWR primary water can be classified into two broad categories: 1) events associated with occluded/stagnant/off-chemistry environments and 2) events associated with free flowing, non-contaminated primary water. The mechanism of SCC in occluded or low-flow regions is reasonably well understood. Events reporting some types of contamination were more prevalent in occluded/low-flow environments, and analyses show sensitization does not seem to have any appreciable effect on susceptibility to SCC in occluded/low-flow environments. The incidence of SCC in occluded/low-flow environments has mixed results with respect to cold-work, so no clear conclusions can be drawn regarding that relationship. These findings support conclusions from literature that suggest the primary driving force for SCC in occluded/low-flow regions is a relatively high concentration of ionic contaminants coupled with increased oxygen content. One example is the cracking of a pressurizer heater sleeve that occurred in one plant and was linked to residual oxygen remaining for extended periods after plant shutdown and restart. Pressurizer heater sheaths have also experienced cracking, which has more commonly been linked with significant strain hardening and residual tensile stresses from fabrication. Operating experience suggests that SCC continues to be less prevalent in free-flowing PWR environments. Severe cold work was present for all cases of SCC in free-flowing PWR water. The additional transient exposures that will occur during longer operating periods could potentially affect long-term performance, and extended operation with aerated makeup water could promote late-life SCC events, given the sensitivity to oxidizing conditions. Interaction between SCC and corrosion fatigue is also a possibility. Recent plant operating experience with non-isolable branch piping in the safety injection system is currently being investigated and evaluated by the industry and may result in further actions in the future. Currently, there does not appear to be a fundamental materials knowledge gap for the observed SCC, and tools exist to manage degradation risks. Continued evaluation to address remaining concerns and to monitor OE trends should be addressed as an IMT gap. Specifically, there may be gaps in the identification of susceptible components. Due to these potential gaps and the ongoing work to understand recent OE, the status of this research area has conservatively been assigned as yellow. [R&D Status = YELLOW] **References:** EPRI: MRP-292, MRP-236R1, MRP-458 Other: [4-6], [4-1], [4-8]

Table 4-7 (continued)
PWR systems explanatory notes

NOTE ID	EXPLANATORY NOTE
p1-6d	SCC of stainless steel welds in PWR primary service to date has been relatively rare and has been usually associated with exposure to dissolved oxygen in combination with anionic impurities leading to either transgranular or intergranular cracking, depending on the degree of grain boundary sensitization. The primary field example is cracking of CRDM housing canopy seal weldments due to trapped air in the CRDM housings following an outage, giving a very high local partial pressure of oxygen. Low-level chloride and sulfate impurities, along with sensitization and cold work of the heat-affected zones of the wrought material associated with seal welding, also potentially played a role in the observed cracking. Procedural controls to prevent air entrapment (e.g., vacuum filling) have resolved this issue. Although few test data are available for as-deposited stainless steel weld metals, results are generally consistent with available SCC data for CASS (see p1-6e). In a normal PWR primary water environment, no significant SCC growth has been reported. Under oxygenated conditions, a laboratory study has confirmed that, when thermally aged and embrittled to the maximum extent at 400°C, significant SCC growth can occur in weld metal. However, it was also observed that cracks slowed down and apparently arrested even in the fully aged weld metal when normal hydrogenated primary water conditions were re-established. For stainless steel weld metals, although there may be still a need to confirm whether fully thermally aged weld materials are appropriately addressed by the guidance developed for SCC of wrought and forged stainless steel base metal (see note p1-6c), such evaluation is not considered to be a fundamental knowledge gap requiring additional R&D. SCC of stainless steel welds may also be impacted by the recent OE of non-isolable branch piping in safety injection systems noted in p1-6c; therefore, this research area has been conservatively assigned as yellow. [R&D Status = YELLOW] **References:** EPRI: MRP-236R1 Other: [4-8], [4-9], [4-10]

Table 4-7 (continued)
PWR systems explanatory notes

NOTE ID	EXPLANATORY NOTE
p1-6e	Service history for CASS materials in operating PWRs has been good to date. There have been no SCC occurrences identified in the field. Although test data remain rather limited, SCC testing of CASS in a normal PWR primary water environment indicates good resistance to SCC, with no significant SCC growth reported and no detrimental effect of thermal aging embrittlement identified. However, when thermally aged and embrittled to the maximum extent at 400°C and tested in high temperature oxygenated conditions, significant SCC growth has been observed. In this case, cracks slowed down and apparently arrested even in fully aged CASS when normal hydrogenated primary water conditions were re-established. As a result, SCC concerns for CASS materials in PWR primary service are focused on potential vulnerabilities related to oxygen transients that could occur during startups and shutdowns or due to use of aerated makeup water (see note p1-6c) in combination with the potential for changes in material properties caused by thermal aging (see note p1-10e) to detrimentally affect SCC performance. Finally, characterization of fracture properties associated with exposure to the PWR primary water environment is an additional issue interrelated with both SCC and thermal aging (see note p1-10e). Although reduced fracture properties resulting from exposure to primary system water are not anticipated to be significant by themselves, a synergistic effect between thermal aging and SCC could potentially exist. Additional gaps in state of knowledge include 1) understanding the threshold oxygen concentrations resulting in SCC initiation as a function of exposure temperature and time and 2) characterization of saturation properties for the entire spectrum of relevant CASS material compositions and service temperatures. However, MRP-362 Revision 1 dispositioned the risk of SCC for CASS piping in PWRs, supporting the designation of this research area as green. [R&D Status = GREEN] **References:** EPRI: MRP-276, MRP-175R1, MRP-362R1 Other: [4-10], 0, [4-7]

Table 4-7 (continued)
PWR systems explanatory notes

NOTE ID	EXPLANATORY NOTE
p1-6f p1-6h	PWSCC of Alloy 600, 82, and 182 materials is an ongoing industry concern but is generally well understood and managed. At present, a suite of effective mitigation, repair, and replacement options is available and, thus, most resources are directed toward implementation of long-term PWSCC management, particularly for locations that have not yet experienced significant cracking. Infrequent observations of PWSCC in T_{cold} locations (cold heads, BMI/BMN penetrations) are consistent with a lack of capability to predict initiation times and initiation trends. In some instances, notably T_{cold} reactor pressure vessel heads, evaluating true operating temperatures and their variability may also be important in circumstances where convection currents may be present from hotter regions below. Degradation of steam generator channel head cladding and divider plate components is also known to occur but has been evaluated and dispositioned as adequately managed under the current plant in-service inspection programs. Many unmitigated Alloy 600, 82, and 182 plant components have performed acceptably to date, due either to low material susceptibility (e.g., Alloy 82 welds) or exposure to lower operating temperatures (e.g., cold leg dissimilar metal welds). Plant asset management decision making for these components would benefit from improved understanding of how their vulnerability to PWSCC may change as plants continue to age and from improved characterization of reasonable service life expectations for such materials. Additionally, a more complete understanding of how pre-existing welding defects, including both surface breaking and subsurface micro-fissures, may interact with the PWSCC initiation and crack growth processes would increase confidence in predictions of PWSCC behavior that may, for example, be relevant when addressing the implications of component weld inspection results. These knowledge gaps are not considered critical or urgent, and the existing plant aging management programs continue to be effective; therefore, this research area remains categorized as green. [R&D Status = GREEN] **References:** EPRI: MRP-55R1, MRP-115, MRP-265, MRP-197, MRP-198, MRP-283, MRP-285, MRP-301, MRP-304, MRP-263NP, MRP-267R2, MRP-335R3-A, MRP-420R1, MRP-448, MRP-449, 3002000473, 3002002850 Other: [4-2]

Table 4-7 (continued)
PWR systems explanatory notes

NOTE ID	EXPLANATORY NOTE
p1-6g p1-6i	Alloy 690 and its compatible weld metals (Alloys 52, 152, and variants) have been in PWR primary water service for more than 30 years without any SCC identified. These materials are being widely used for component repairs and replacements for Alloy 600 and its compatible weld metals, Alloys 82 and 182. Laboratory testing continues to indicate that susceptibility to SCC of the as-received material is very low in Alloy 690 and Alloys 52 and 152. PWSCC crack growth has been observed in Alloy 690 in some laboratory studies, although the faster rates of crack growth generally occurred in the presence of excessive cold work (more than approximately 20%), which would not be expected in plant components. Higher crack growth rates were also found on specific directions in some variants of worked materials, although the direction of higher growth was along the rolling plane of the plate materials, again a situation which would not be relevant to plant applications. There remains a question of a heat-to-heat variation of materials susceptibility to SCC, with some heats being more sensitive to lower levels of cold work. The applicability of these results to actual service conditions is not yet fully understood, although factors of improvement for Alloys 690, 52, and 152 over Alloys 600, 82, and 182, respectively, have been developed. These large factors of improvement have been used to justify inspection relief needs in some plants, and the factors of improvement documented in MRP-386 are being implemented in the 2023 ASME Code. Ongoing efforts are judged to be sufficient to address PWSCC of Alloys 690, 52, and 152 (and variants). At issue for Alloy 690 is the magnitude and location of weld residual strain occurring in actual plant components, the potential for the plane of cracking to align with the plane of deformation, and the extent of crack growth enhancement that may occur due to these conditions. For Alloys 52 and 152 weld metals (including variants), excellent SCC resistance is indicated by laboratory testing. Except for welds with significant levels of additional cold work applied, all growth rates observed can be generally described as “low” or “very low.” Remaining PWSCC concerns associated with these welding materials include 1) the potential for weld cracking (i.e., hot cracking and ductility dip cracking) to create an initiation site for EAC and 2) the potential for some weld configurations, some weld processes, or weld repairs to influence long-term SCC performance. Remaining work is also focused on resolving uncertainties due to significant variations in CGRs reported by different labs. Additional research needs include testing of additional HAZ/partial-melting zone material and evaluation of weld dilution effects. [R&D Status = YELLOW] **References:** EPRI: MRP-310, MRP-237R2, MRP-386, MRP-448 Other: [4-12]

Table 4-7 (continued)
PWR systems explanatory notes

NOTE ID	EXPLANATORY NOTE
p1-7a p1-7b	Note p1-6a describes data suggesting occurrences where low-alloy steel resistance to environmentally assisted crack propagation might be reduced. There is an additional consideration for pressure vessel steels located in the beltline region due to the increases in the yield strength of the pressure vessel material that occurs with neutron fluence. There is no ongoing or planned research to characterize the effect of neutron embrittlement on the EAC behavior of low-alloy steels, nor is this judged to be an area of significant concern at present. Note that this conclusion differs from that provided for BWRs due to the impact of potential NWC oxidizing conditions. [R&D Status = GREEN] **References:** None
p1-8c p1-8d p1-8e	High-cycle fatigue due to thermal cycling (turbulence penetration or thermal stratification) or mechanical vibration is design/location dependent phenomena and therefore applicable to primary system piping components. These phenomena are generally well characterized, and no additional research is needed at this time. Although some modeling issues remain unresolved, these are anticipated to be addressed by analysis and not through additional testing. Concern has also been expressed that implementation of low leakage cores could result in some thermal striping which persists into the hot leg, possibly resulting in additional thermal fatigue at component locations having geometric discontinuities or surface imperfections. To date there have not been any systematic studies performed to validate or dismiss this concern. However, R&D to specifically address this concern is not deemed needed at present, and a Green R&D status result is appropriate. This specific issue is retained in the MDM to provide tracking for the concern and to permit reassessment of the issue at a later date. [R&D Status = GREEN] **References:** EPRI: MRP-85R2, MRP-146R2, MRP-192R4, MRP-32R2, MRP-459, MRP-478, MRP-192R4

Table 4-7 (continued)
PWR systems explanatory notes

NOTE ID	EXPLANATORY NOTE
p1-9a p1-9b	Laboratory tests on small specimens in simulated LWR environments show that fatigue resistance in reactor water environments is lower than in a “dry air” environment. This conclusion is supported by a database of laboratory tests on small specimens in simulated reactor coolant environments. It is also recognized that the fatigue design curves that provide the basis for fatigue life assessments of nuclear plant components do not explicitly account for the effects of LWR environments on fatigue life—although, to date, conservatisms included in fatigue design curves and in fatigue calculational methods have been adequate to bound the effects of environment. Environmentally assisted fatigue cracking of low alloy steels in LWR environments has been addressed by the publication of ASME Code Section XI, Appendix Y-3200. Material with sulfur content below 0.004 wt% is not considered susceptible to EAF cracking, while materials with sulfur content greater than, or equal to, 0.004 wt% may be evaluated using the procedure provided in Y-3200. Low alloy steel welds are treated under the same process. With the availability of this non-mandatory appendix, the research needs for low alloy steel EAF are assigned as green. [R&D Status = GREEN] **References:** EPRI: 1026724, 3002010554, 3002010555, 3002007973, 3002013214, 3002020450, MRP-407, MRP-415, MRP-464 Other: [4-12], [4-14]

Table 4-7 (continued)
PWR systems explanatory notes

NOTE ID	EXPLANATORY NOTE
p1-9c p1-9d p1-9e p1-9f p1-9g p1-9h p1-9i	Laboratory tests on small specimens in simulated LWR environments show that fatigue resistance in reactor water environments is lower than in a “dry air” environment. This conclusion is supported by a database of laboratory tests on small specimens in simulated reactor coolant environments. It is also recognized that the fatigue design curves that provide the basis for fatigue life assessments of nuclear plant components do not explicitly account for the effects of LWR environments on fatigue life—although, to date, conservatisms included in fatigue design curves and in fatigue calculational methods have been adequate to bound the effects of environment. A fundamental knowledge gap exists regarding the amount of conservatism that is delivered by the current practice of using correlations based on testing of thin specimens subjected to fully reversed uniaxial loading and environmental sensitivity factors to estimate the fatigue lives of plant components that have complex geometries and are subject to complex pressure/temperature transients. Key steps in addressing this knowledge gap include: 1. Demonstrating a better understanding of methods to predict fatigue crack initiation and growth in actual components under typical plant conditions. 2. Validating this understanding through further laboratory experimental work focused on tests that are more representative of prototypical conditions experienced by actual plant components. 3. Further investigating transient complexities, including non-isothermal loading, multiple hold times, and variable amplitude and strain rate loading occurring concurrently with changes in water chemistry. 4. Generation of additional fatigue test data, as appropriate, for materials that are under-represented in the currently available fatigue (ε-N) database and for assessing the fatigue behavior of welded structures that may be influenced by geometric stress concentration factors, weld defects, residual stress, and multiaxial stress states. Management based on flaw tolerance represents a viable alternative when it is not possible to demonstrate that the accumulated fatigue life will not exceed the allowed value prior to the end of plant life. ASME Code Case N-809 provided a methodology for developing fatigue crack growth rate curves for stainless steel in PWRs. Assessing the effect of water environments on fatigue crack growth rates is an additional area where gaps remain for some materials and water environment combinations. There are also some areas where additional data or evaluations are needed to generate appropriate correlations of the influence of dissolved oxygen/electrochemical potential (ECP) and material chemistry on environmental multipliers and fatigue crack growth rates. The R&D status overall is characterized as orange since it is unclear whether current work plans, and associated funding, are adequate to resolve this issue. [R&D Status = ORANGE] **References:** EPRI: 1026724, 3002010554, 3002010555, 3002007973, TR-106092, MRP-407, MRP-415, MRP-276 Other: [4-15], [4-16], [4-17], [4-22]

Table 4-7 (continued)
PWR systems explanatory notes

NOTE ID	EXPLANATORY NOTE
p1-10a p1-10b	Thermal aging embrittlement remains a possibility for low-alloy steels in PWR primary circuit component assemblies. The thermal aging mechanisms that are likely to affect low-alloy steels were reviewed (precipitation of carbides, nitrides, copper, and nickel-manganese-silicon phases, phosphorus segregation to grain boundaries, and strain aging), and it was concluded, based on the laboratory data reviewed, that phosphorus segregation is the main thermal embrittlement mechanism for typical well-tempered and stress-relieved PWR low-alloy steels. The shift in ductile-to-brittle transition temperature is expected to be modest for 40 years of operation, but the segregation accelerates with time, so long-term embrittlement at current 80-year operating life targets will be larger. The risk of embrittlement is dependent on the phosphorus content and the temperature, with lower phosphorus and lower temperatures resulting in lower embrittlement. Available studies also indicate that HAZ material is more susceptible to thermal embrittlement than either base metal or weldments. Therefore, the location within the primary coolant pressure boundary nominally most susceptible to thermal embrittlement would be HAZ material associated with pressurizer welds and the reactor vessel outlet nozzle welds. Fracture mechanics analyses of the limiting locations based on stress, material, and temperature (pressurizer welds) were performed for Westinghouse, Combustion Engineering, and Babcock & Wilcox PWR designs. These assessments evaluated P-T limit curves for postulated flaws in pressurizer welds with thermal embrittlement and compared the results to P-T limit curves for the reactor pressure vessel. These evaluations can be used as a tool in dispositioning thermal embrittlement of low-alloy steel and its welds. Additionally, low-alloy steel samples have been extracted from a recently decommissioned PWR. Those samples have been tested by EPRI to better understand the actual thermal embrittlement effects in a PWR. Based on the review of thermal embrittlement mechanisms, development of tools to disposition embrittlement, and ongoing research, this R&D status has been assigned as yellow. [R&D Status = YELLOW] **References:** EPRI: MRP-80, MRP-438, MRP-463, MRP-474, MRP-491 Other: [4-18], [4-19], [4-20], [4-13]

Table 4-7 (continued)
PWR systems explanatory notes

NOTE ID	EXPLANATORY NOTE
p1-10d	Thermal aging of stainless steel welds and cladding is related to operating temperature, chemical composition, and ferrite content. Although no significant thermal aging is anticipated for the typical delta ferrite levels (5-10 FN) in austenitic stainless steel welds and cladding, a significant reduction in fracture toughness is likely if the ferrite volume fraction exceeds approximately 10 FN, particularly if the alloy has molybdenum additions. Potential reductions in toughness will be somewhat greater for longer operating lives. However, since thermal aging is a diffusion dependent process, additional reduction in fracture toughness is not likely to be large or to represent a substantial issue, and knowledge about this degradation mechanism in austenitic stainless steel weld metal is considered mature. [R&D Status = GREEN] **References:** EPRI: TR-106092, MRP-276 Other: [4-19]

Table 4-7 (continued)
PWR systems explanatory notes

NOTE ID	EXPLANATORY NOTE
p1-10e	Thermal aging of cast austenitic stainless steel is limited to castings meeting specific screening criteria for component type, casting method, molybdenum content, and ferrite content. Thermal embrittlement processes are generally well understood. Existing research (TR-106092) has indicated that both saturated and partially aged predictions of fracture toughness are very conservative for all but the most extreme cases. However, concern has been expressed regarding anomalies in the kinetics of thermal aging and embrittlement between 350°C and 400°C that imply that the mechanism of aging and embrittlement may not be the same in this temperature range compared to lower PWR service temperatures. Thus, accelerated aging at higher temperatures than 350°C may not necessarily be conservative. The database is dominated by Mo containing CASS (CF-8M) coupled with high ferrite fractions that suffer the greatest thermal aging embrittlement. Correlations between metallurgical and mechanical testing data are being continuously updated as the database steadily increases from laboratory aged archive materials as well as materials recovered from CASS elbows during steam generator replacements. There is a perceived need to extend the database to less susceptible CASS materials and to temperatures as low as 285°C in the context of plant life extension and because the loading of some cold leg elbows can be significantly higher than in the hot leg. For lower thermal aging temperatures, saturation becomes more difficult to demonstrate. Work is ongoing to extend the database. Potential reductions in toughness may continue for operation beyond 60 years. However, since thermal aging is a diffusion-dependent process, reductions in fracture toughness during later operating periods are much less than in earlier operating periods. Although the additional aging associated with extended operations is not considered a significant concern, depending on the results of ongoing testing, there could be a need for additional data to demonstrate saturation properties. [R&D Status = GREEN] **References:** EPRI: TR-106092, TR-016743V2R1, 3002018322, 3002018324 Other: [4-23], [4-24], [4-21]

Table 4-7 (continued)
PWR systems explanatory notes

NOTE ID	EXPLANATORY NOTE
p1-10g	Thermal aging tests indicate that the higher chromium content nickel-base Alloy 690 can be embrittled by formation of a Ni_2Cr phase due to long range ordering when the iron content is very low (i.e., below commercial alloy minimum specification limits). Significant long-term embrittlement has been shown to occur in materials with iron content < 7%. From a practical perspective, the concerns associated with this issue are mitigated by controls on the iron content of Alloy 690 materials that have been recommended to prevent this issue for a number of years. EPRI TR-016743 addresses thermally treated Alloy 690 steam generator tubing. The minimum iron content has been increased from 7% (ASTM SB-163) to 9% (EPRI) to minimize the risk of formation of the ordered (brittle) phase Ni_2Cr during thermal aging in service. As a result, it is thought that most Alloy 690 in use domestically was specified to include iron ≥ 7% and that current EPRI guidance will ensure that future use of Alloy 690 in repair/replacement activities also specifies iron > 9%. This issue is considered an implementation issue associated with confirmation of iron content and identification of any materials in service with < 7% iron. [R&D Status = GREEN] **References:** EPRI: TR-016743V2R1, 3002018322, 1026723, 3002018324 Other: [4-23], [4-24]

Table 4-7 (continued)
PWR systems explanatory notes

NOTE ID	EXPLANATORY NOTE
p1-10i	Thermal aging tests indicate that the higher chromium content nickel-base alloy weld metals can be embrittled by formation of a Ni_2Cr phase due to long range ordering when the iron content is very low. Significant long-term embrittlement has been shown to occur only in Ni-Cr-Fe materials with iron content < 7%. However, the focus of high Cr nickel-base alloy weld filler metal development to date has been on improving weldability and providing a higher degree of assurance that weld repairs and welds in new components using these weld filler metals will be free from hot cracking and/or ductility dip cracking. Although the standard formulation of Alloy 52 contains 7-11% iron, variant formulations are being developed that, in some cases, contain much less than 7% iron. For example, Alloy 52i contains only 2.5% iron. To date, there have been few specific evaluations of the potential for long range ordering to occur in service for new, high Cr nickel-base weld filler metals, particularly those with low iron content. Additionally, if development of the brittle Ni_2Cr phase could occur, there are few data with which to assess the extent and significance of embrittlement. Any effect of extended operations on the potential for the formation, and the subsequent consequences, of the brittle Ni_2Cr phase is presently unclear. EPRI is actively working in this area to enhance the available thermal aging data pertaining to Alloy 52 weld metal. The investigations involve iterative hardness assessments, supplemented by detailed SEM and TEM analyses, for nine distinct variations of Alloy 52 aged at elevated temperatures for up to 20,000 hours. As there is significant ongoing and planned work on this topic, the R&D status is set to Yellow. [R&D Status = YELLOW] **References:** EPRI: 1026723, 3002013280 Other: [4-23], [4-24], [4-21]

Table 4-7 (continued)
PWR systems explanatory notes

NOTE ID	EXPLANATORY NOTE
p1-11a p1-11b	Uncertainties remain regarding the role of hydrogen in the observed phenomena. Hydrogen fugacity in the environment, the diffusivity of hydrogen within the metal, and the interaction of hydrogen with other parameters (e.g., temperature and mechanical loading rate) all remain poorly understood. Specifically considering low alloy steels, there is a need to address potential synergisms with other degradation phenomena, notably SCC and corrosion fatigue. For reactor vessel beltline shells and welds subject to significant neutron fluence, irradiation embrittlement (see note p1-12a) is an additional factor that must be considered, since the elevated yield strengths resulting from irradiation damage likely increase the magnitude of any effect that exists. The R&D status is judged to be Orange since there are no current plans to conduct additional testing. In 2017, EPRI completed a literature review of hydrogen-related degradation on reactor pressure materials. This report concluded with the limited data available that the amount of mobile hydrogen likely to be present in the RPV wall should produce small effects on the average tensile and fracture toughness at room temperature, but no effects at operating temperature. The buildup of hydrogen pressure in voids or flakes within an RPV wall is insufficient to cause a crack to propagate. [*NOTE: Regarding observations of rapid fracture occurring under rising K conditions, similar testing in air concluded that plastic instability resulting from mechanical overload conditions was the primary factor in the observations associated with stainless steels and nickel-base welds. No evidence of an effect of the environment was observed. See EPRI 3002000766. It is likely that similar conclusions can be shown to be valid for low alloy steels.*] [R&D Status = ORANGE] **References:** None
p1-11c	Some effect of the environment on the fracture properties of wrought and forged stainless steel base metals must be considered possible based on available data. However, for non-irradiated structural components (note that this item does not include bolting), these reductions are less significant than those observed for either irradiated materials or for highly cold-worked materials. Although uncertainties remain regarding the role of hydrogen in the observed phenomena, additional near-term R&D is not considered needed for non-irradiated stainless steel structural components. [*NOTE: Regarding observations of rapid fracture occurring under rising K conditions, similar testing in air concluded that plastic instability resulting from mechanical overload conditions was the primary factor in the observations. No evidence of an effect of the environment was observed. See EPRI report 3002000766.*] [R&D Status = GREEN] **References:** None

Table 4-7 (continued)
PWR systems explanatory notes

NOTE ID	EXPLANATORY NOTE
p1-11d p1-11e	Testing of aged CF8 material in simulated PWR primary water chemistry environment identified pronounced reductions in fracture toughness of the material at low temperatures (e.g., during startup, shutdown, and layups). Inadvertent testing of one specimen in high temperature water revealed that substantial reductions in fracture properties can persist at high temperature, even though the magnitude of the effect is less than that identified at low temperature. Presently, there are few data to characterize the extent of this phenomenon for CASS materials, particularly at high temperatures. Due to similarity of microstructure, similar results can also be anticipated for stainless steel weld metals, although the reduced ferrite in weld metals would remove most of the embrittling effect of thermal aging. [*NOTE: Regarding observations of rapid fracture occurring under rising K conditions, similar testing in air concluded that plastic instability resulting from mechanical overload conditions was the primary factor in the observations. No evidence of an effect of the environment was observed. See EPRI report 3002000766. It is likely that similar conclusions can be shown to be valid for CASS and stainless steel welds.*] [R&D Status = ORANGE] **References:** EPRI: MRP-276, MRP-293 Other: [4-9]
p1-11f p1-11g	Recent research shows that Alloy 690 base metal exhibits some reduced fracture resistance properties at low temperatures (e.g., typical of startup, shutdown, and layups) in simulated PWR primary water chemistry environments. However, these reductions are much less significant than those observed for nickel-base alloy weld filler metals and Alloy X-750. Available data also suggest that Alloy 600 is less affected than Alloy 690. Although the phenomenon is not well understood for any material, there are no near-term concerns regarding environmental effects on J-R properties for Alloys 600 and 690, unless the material has been subject to substantial cold work. Additionally, synergisms with thermal or irradiation embrittlement are less likely than for other materials. [R&D Status = GREEN] **Reference:** EPRI: MRP-293

Table 4-7 (continued)
PWR systems explanatory notes

NOTE ID	EXPLANATORY NOTE
p1-11h p1-11i	Research indicates that nickel-base weld metals, including Alloys 82, 182, 52, and 152 all exhibit some reduction in fracture properties at low temperatures (e.g., typical of startup, shutdown, and layups) in simulated PWR primary water chemistry environments. Regarding low temperature effects (LTCP), a recent MRP review of the state of knowledge regarding low-temperature effects for nickel-base alloys concluded that, although some areas of uncertainty remain, additional testing of nickel-base alloy weld materials to evaluate LTCP is unlikely to be of significant benefit to the industry. However, uncertainties do remain regarding the role of hydrogen in the observed phenomena. Hydrogen fugacity in the environment, the diffusivity of hydrogen within the metal, and the interaction of hydrogen with other parameters (e.g., temperature and mechanical loading rate) all remain poorly understood. An additional uncertainty is synergism with PWSCC. A separate, although lesser, concern is the possibility that fabrication-induced micro-fissures in Alloys 52 and 152 weld metals could have a detrimental effect on component fracture properties. There are few test data to characterize performance at higher temperatures. The focus of testing performed to date has been specifically on LTCP. Additionally, since only a few welds have been tested, weld-to-weld variability has not been fully evaluated for either low temperature or high temperature regimes. [*NOTE: Regarding observations of rapid fracture occurring under rising K conditions, similar testing in air concluded that plastic instability resulting from mechanical overload conditions was the primary factor in the observations associated with stainless steels and nickel-base welds. No evidence of an effect of environment was observed. [See EPRI report 3002000766.*] [R&D Status = ORANGE] **Reference:** EPRI: MRP-293

Table 4-7 (continued)
PWR systems explanatory notes

NOTE ID	EXPLANATORY NOTE
p1-12a p1-12b	There are two key elements that need to be better understood and addressed: 1. Effect of neutron flux and spectrum on embrittlement conditions: Much of the available high-fluence data was obtained from test reactors with significantly higher flux (> 100X) than LWRs. Irradiation at LWR-relevant flux may result in more embrittlement of low-alloy steel materials than predicted by high flux data. Additional traditional surveillance data will remain limited since plans for some utilities addressing higher EOL fluence currently rely on deferral of remaining capsule tests, not an increase in the number of tests and the data from remaining surveillance capsules will be obtained over time. 2. Potential for additional high fluence damage phenomena: There is some evidence for the existence of additional damage phenomena that manifest at fluences > ~$5x10^{19}$ n/cm^2 (E > 1.0 MeV), causing continued increases in transition temperature shift. These high-fluence damage phenomena, which may not be currently included in mechanistically guided predictive models, warrant additional consideration. Depending on flux conditions, embrittlement phenomena likely include a combination of Ni-Mn-Si clustering and stable matrix features. Thermally unstable matrix defects may also form when the flux rates are very high, as seen in some test reactor material irradiations. Ni-Mn-Si clusters have been clearly observed in reactor pressure vessel steels (both in low-copper and higher copper containing steels), resulting in continued embrittlement behavior that is included in many power reactor embrittlement models and needs to be validated or adjusted to higher fluence measurements. Appropriate quantification of the effects of these high fluence phenomena on the transition temperature shift represents a key knowledge gap. One program the industry has implemented to address this data gap is to reconstitute remnants of broken Charpy impact specimen from previous irradiated surveillance capsule samples under the PWR Supplemental Surveillance Program. Two capsules with a total of 288 Charpy impact specimen from 27 unique surveillance plates, forgings, and welds were placed into two operating PWRs to achieve increased neutron irradiation. When tested (currently targeting a spring 2027 and fall 2028 withdrawal from the two host plants), the data obtained from these specimens will be used to improve the embrittlement projection models, which account for high fluence effects. HAZ materials were specifically evaluated and removed from consideration in reactor pressure vessel structural integrity assessment based on a comprehensive review of HAZ fabrication requirements from multiple countries. Considering the high fluence data that will be produced from ongoing neutron irradiation of standard surveillance capsules and the PSSP specimens, this R&D area can be moved to yellow for 80 years of plant operation. Longer periods of operation would remain classified as orange based on continued lack of data and potential lack of ability to obtain data. A proposed rule-making letter (SECY-22-0019) has been tabled by the NRC for a vote, which would allow the NRC staff to update RG1.99R2 to Revision 3 to account for the lack of accuracy of the current ETC in the guide to the tested capsule results at high fluence. [R&D Status = YELLOW] **References:** EPRI: MRP-326R1, MRP-412, MRP-439, MRP-473, MRP-475, MRP-484, MRP-485 Other: [4-26], [4-27], [4-28], [4-29]

Table 4-7 (continued)
PWR systems explanatory notes

NOTE ID	EXPLANATORY NOTE
p1-12d	Irradiation embrittlement concerns associated with reactor pressure vessel stainless steel welds and cladding are limited to possible synergisms with thermal aging. There is no specific evidence that cracking of the cladding has a significant impact on the low alloy steel base metal, although a recent wastage event is tracked by note p1-1a. No R&D is presently considered to be needed. [R&D Status = GREEN] **References:** EPRI: MRP-79R1, MRP-80, MRP-276, MRP-175R1, MRP-326R1 Other: [4-30], [4-25]

Table 4-7 (continued)
PWR systems explanatory notes

NOTE ID	EXPLANATORY NOTE
PWR REACTOR VESSEL INTERNALS	
p2-5a	PWR operating experience includes wear issues associated with flux thimbles, guide card wear by control rod cladding contact, and thermal sleeve flanges. Recent operating experience associated with Westinghouse designed reactors in the United States and similar designs in Europe indicates that interactions between control rods and the guide cards in the control rod guide tube assemblies in PWRs can cause significant wear-related degradation, depending on the design-type (CRGT tube design and RCCA design) and operating characteristics (Ref. Westinghouse NSAL-17-1, dated January 2017). The wear tends to be concentrated on the guide cards, and lower continuous guidance structures in certain designs (17x17-style) and extensive wear in this guidance system may impede control rod insertion. The PWROG has performed targeted inspections and surveys of existing examination data to characterize the distribution and extent of wear in the CRGT assemblies. The PWROG studies have resulted in comprehensive guidance, addressing inspections/measurements, evaluation of inspection results, and long-term management of guide card and continuous section wear. The guidance has been included as part of NEI 03-08 requirements of the latest revision of MRP-227. The industry has also provided updated supplemental NEI 03-08 inspection guidance for CRGT guide cards to U.S. plants based on these PWROG studies (Ref. OG-18-46, dated February 1, 2018). Similarly, for the thermal sleeve flange wear issue, operating experience has been identified at non-U.S. PWR plants. Updated acceptance criteria and additional inspection recommendations for affected plants are being developed by the OEM and/or PWROG. For these concerns of wear, the degradation risks are continually monitored, and trending of the operating experience is performed as part of the extent of condition and plant-specific inspection responses. No additional fundamental materials R&D is needed. [R&D Status = GREEN] **References:** EPRI: MRP-175R1, MRP-189R3, MRP-191R2, MRP-227R2, MRP-227R2 Other: [4-32], [4-33], [4-34], [4-35]

Table 4-7 (continued)
PWR systems explanatory notes

NOTE ID	EXPLANATORY NOTE
p2-5d	Wear is a concern for the nickel-base alloy core guide lugs and clevis inserts* because the gaps are increasing for some units. There has also been experience with clevis insert bolt failure at multiple plants, including a recent incident where an insert, with all bolts failed, was displaced from its installed position. There is not a current need for additional research for the core guide lugs. Clevis insert wear has been observed in two locations: 1) on the surface of the insert where wear is expected and 2) around the clevis insert bolts after the bolts failed. In MRP-227 Revision 2, the clevis insert bolts and the clevis insert bearing surface are classified as Existing Programs for management for loss of material (wear), which indicates the use of VT-3 examination methods of all accessible surfaces. A Westinghouse technical bulletin (TB-14-5) recommends an updated inspection scope to manage functional performance. Therefore, wear is being adequately addressed by targeted inspections and tracking of operating experience. Management is considered an implementation issue. * Alloy 600 clevis inserts are hard-faced with Stellite. [R&D Status = GREEN] **References:** EPRI: MRP-175R1, MRP-189R3, MRP-191R2, MRP-227R2 Other: [4-36], [4-37]

Table 4-7 (continued)
PWR systems explanatory notes

NOTE ID	EXPLANATORY NOTE
p2-5f p2-5g p2-5h	For Alloy A-286 and Alloy X-750 reactor internals fasteners, wear may be a concern. The dose on select core barrel and thermal shield bolting may exceed the screening criteria established in MRP-175 for irradiation-enhanced stress relaxation and irradiation creep for 60-80 years for these materials (resulting in potential wear and fatigue concerns), which necessitates the need for aging management related to wear and fatigue. Additionally, wear of reactor vessel internals hold down springs (or rings) is considered plausible, although martensitic stainless steel was specifically selected to replace Type 304 stainless steel hold down rings previously experiencing loss of preload and subsequent wear. Wear has been observed on the stationary gripper latch arm teeth of a control rod drive mechanism latch assembly, as reported in Westinghouse Infogram IG-20-1. The drive rod is fabricated from martensitic stainless steel, while the wear surface is a cobalt-based alloy. The latch assembly wear is not a condition adverse to nuclear safety and can be managed through plant actions and programs. Wear of these high-strength fasteners and hold down springs is adequately managed by ongoing aging management programs, and no additional research is needed. [R&D Status = GREEN] **References:** EPRI: MRP-175R1, MRP-189R3, MRP-191R2, MRP-227R2 Other: [4-38]

Table 4-7 (continued)
PWR systems explanatory notes

NOTE ID	EXPLANATORY NOTE
p2-6a p2-6b	Experience with SCC of austenitic stainless steels and their weld metals in PWR primary water with good chemistry control has been limited. Typically, in good-quality primary water (i.e., with no deleterious species such as halides or sulfates and low electrochemical potential), these alloys do not experience SCC unless subjected to significant cold work. SCC may also occur in occluded conditions if the water chemistry is negatively affected. Test data and operating experience indicate that SCC is not a concern for material with cold work < 20%. Above this level, SCC initiation and propagation may be a concern. This material condition was selected as one of the screening criteria for austenitic stainless steel reactor vessel internals components in MRP-175, Revision 1. Related to the cold work limits, laboratory data have also indicated that material with high microhardness values (Vickers hardness > ~270-310) may also be susceptible to SCC. From a research perspective, these phenomena are reasonably well understood, and no specific additional research is recommended. The environmental and material conditions can be managed or monitored, making this a plant operation and management issue. Recent operating experience of cracking at the upper girth weld of a Westinghouse-designed core barrel may impact this conclusion on the need for additional research. Five crack indications were detected and ranged from 1.1 inches to 17.8 inches (2.8 cm to 45 cm) in length and 37% to 92% through-wall. The indications were only visible from the inner diameter surface of the barrel. The neutron dose at the upper girth weld is below the screening criterion for IASCC, so the potential that these were due to SCC must be considered. This experience is noted here for its relevance, but until the cracks are sampled and examined no additional research areas can be recommended. Additional relevant discussion of SCC in stainless steel materials is provided in notes p1-6c and p1-6d. For reactor internals structures and welds, MRP-175 includes SCC screening criteria based on stress (operational and residual), cold work, and weld ferrite content. [R&D Status = GREEN] **References:** EPRI: MRP-175R1 Other: [4-39]

Table 4-7 (continued)
PWR systems explanatory notes

NOTE ID	EXPLANATORY NOTE
p2-6c	CASS reactor internals typically do not contain welds and are not anticipated to be subject to significant stresses in service. Additionally, MRP-175, Rev. 1, includes SCC screening criteria based on stress (operational and residual) and casting ferrite content. As a result, the R&D status is Green. However, note that this conclusion does NOT extend to pressure-retaining castings (see note p1-6e) and that there are additional concerns associated with castings subject to significant neutron fluence (see note p2-7c). [R&D Status = GREEN] **Reference:** EPRI: MRP-175R1
p2-6d	See note p1-6f. [R&D Status = GREEN] **References:** EPRI: MRP-88, MRP-175R1, MRP-189R3, MRP-190, MRP-191R2, MRP-227R2, MRP-273 Other: [4-40], [4-31], [4-42]
p2-6e	See note p1-6c and p2-6a for general discussion regarding SCC of stainless steels in the PWR RCS. SCC of 300 series stainless steel internals bolting in the absence of irradiation effects has been rare. Where occurring, SCC events are generally attributed to excessive cold work or cases where the as-installed strains likely exceeded the yield strength limit substantially. MRP-175, Rev. 1, contains SCC screening criteria for reactor internals based on stress (operational and residual) and degree of cold work. As a result, the R&D status for stainless steel internals bolting is Green. However, note that this conclusion does NOT extend to irradiated bolting (see note p2-7e). [R&D Status = GREEN] **Reference:** EPRI: MRP-175R1

Table 4-7 (continued)
PWR systems explanatory notes

NOTE ID	EXPLANATORY NOTE
p2-6f	There has been prior field experience with SCC of Alloy A-286 in PWR applications, most notably in thermal shield bolts, with cracking occurring in locations associated with peak stresses (i.e., at or near the fillet region under the bolt head). Other relevant operating experience (though not a reactor vessel internal component) is the cracking of Alloy A-286 turning vane bolts of certain reactor coolant pump designs. For turning vane bolts, the industry was able to develop a probabilistic risk assessment framework to support long-term management of the degradation. The U.S. NRC published Information Notice 90-68 regarding a specific cracking event with this alloy and effectively discouraged its use. SCC of Alloy A-286 has been studied, with laboratory testing indicating that Alloy A-286 performs satisfactorily when peak stresses are limited to 70-80% of the room temperature yield strength. Aging management programs are in place and screening criteria for SCC are contained in MRP-175. Many A-286 bolts have already been replaced, and bolt replacement is an established technology for PWR internals. No additional research is considered warranted. [R&D Status = GREEN] **References:** EPRI: MRP-88, MRP-175R1, MRP-189R3, MRP-190, MRP-191R2, MRP-227R2, MRP-273 Other: [4-40], [4-31], [4-42]
p2-6g	Although the MDM focus is on passive reactor internals, martensitic stainless steels are also widely used for parts immersed in reactor coolant in applications, such as valve and pump hardware and pump shafts. These materials have generally performed satisfactorily, although some cases of SCC have been experienced. The SCC has often been attributed to use of material in too high a hardness condition or loaded beyond 70% of the room temperature yield strength. Early life failures associated with overly hard or highly loaded components are considered historical in nature. Near-term concerns are considered to be adequately addressed by aging management programs in place. [R&D Status = GREEN] **References:** EPRI: 3002018322, MRP-175R1, MRP-227R2

Table 4-7 (continued)
PWR systems explanatory notes

NOTE ID	EXPLANATORY NOTE
p2-6h	There has been substantial field experience with SCC of prior generation Alloy X-750 components due to suboptimal heat treatment and designs that included high stress concentrations and poor surface finish. However, extensive laboratory testing indicates that new Alloy X-750 parts will perform satisfactorily if they meet current specification requirements regarding chemical composition, optimized heat treatment (HTH condition), fabrication sequence, stress/strain limits, and surface finish. Older Alloy X-750 designs are being managed through inspection and replacement, sometimes with the optimized Alloy X-750 parts and sometimes with strain-hardened Type 316 stainless steel. An emerging issue with Alloy X-750 in recent years is the failure of clevis insert bolts, which has occurred in multiple plants. During a routine ISI of the reactor vessel in 2010, one plant reported that seven of 48 Alloy X-750 clevis insert bolts showed evidence of separation between the head and the shank. Clevis insert bolt head/shank failures were evidenced by wearing of the lock bars which retain the torque of the clevis insert bolts. At one location, the clevis insert dowel pin tack welds were fractured, and the dowel pin was slightly rotated and displaced deeper into the clevis insert. The utility later replaced 29 of the 48 bolts and confirmed that all 29 were cracked. Visual examination in 2017 at a different plant found visual indications of clevis insert bolt failure in two of 48 bolts. Then, in 2020, a third plant observed displacement of one of the clevis inserts, indicating complete failure of all the bolts and dowels at that location. The clevis insert bolts are managed as an Existing Component with a VT-3 general visual inspection requirement in MRP-227. The industry has also recently issued OG-21-160 to require volumetric ultrasonic testing or proactive replacement of the bolts. The volumetric inspections required by OG-21-160 have been implemented at several plants, to date, with varying numbers of indications detected in the clevis insert bolts. The known susceptibility of non-optimized Alloy X-750 to SCC and low temperature crack propagation (LTCP) is expected to be a contributor to the observed degradation. Plants have been able to continue operation with the development of analytical dispositions. At present, no additional research is needed. Screening criteria for SCC based on stress are contained in MRP-175. [R&D Status = GREEN] **References:** EPRI: MRP-88, MRP-175R1, 3002018322 Other: [4-36], [4-37], [4-44], [4-45]

Table 4-7 (continued)
PWR systems explanatory notes

NOTE ID	EXPLANATORY NOTE
p2-7a p2-7b	MRP-175 contains IASCC screening criteria based on stress (operational and residual) and dose. MRP-211, Revision 1, now includes IASCC initiation data up to 100 dpa, but there are still testing gaps for temperature (especially > 325°C or > 617°F) and high fluence IASCC initiation data (particularly between 80 and 100 dpa and > 100 dpa). For IASCC crack growth rate (CGR) data, there are two gaps: 1) the range of conditions experienced in BWR and PWR service and 2) confidence that trends and correlations identified will be reliable up to the neutron fluences associated with extended operations. Factors such as the influence of increased temperature (greater than about 340°C) due to gamma heating in PWR internals and grain boundary segregation processes that do not saturate with increasing neutron dose need to be investigated for their effect on IASCC CGRs. Investigations continue to focus on understanding parameters affecting IASCC including heat-to-heat variability, effects of localized deformation, Si segregation at grain boundaries, and inherent strength. There is a need to develop additional data on material irradiated in a LWR environment since much of the existing data has been obtained from irradiation in the BOR-60 fast breeder reactor. There is still some residual criticism as to the applicability of test reactor data to the LWR environment because of neutron spectrum effects, the high helium gas production, and the tiny bubble formation in stainless steels irradiated in PWRs, which is not reproduced in fast reactors. Potentially long incubation effects due to the order of magnitude difference in neutron flux (between the PWR spectrum and the fast reactor spectrum) and the effect of temperature (particularly above 325°C or 617°F) on IASCC initiation are other important issues. These issues have been at least partially mitigated by the completion of IASCC initiation and CGR testing of material removed from the decommissioned Zorita PWR. Extended operation does not fundamentally change the issue but does introduce additional uncertainties that should be considered, particularly synergies with other mechanisms such as void swelling and applicability of the CGR data trends and correlations to high neutron fluences. The detrimental impact of He generation by thermal neutrons on the ability to perform weld repairs is also a concern. Long-term operation will expand the list of components where weld repair options become limited due to He-induced cracking. A Yellow R&D status result is considered appropriate at this time. Although factors influencing IASCC initiation are still not well understood, future R&D needs are largely dependent on the results of the ongoing work. [*NOTE: This cell is applicable to irradiated stainless steel structural components and welds. Cell p2-7e addresses IASCC of stainless steel fasteners.*] [R&D Status = YELLOW] **References:** EPRI: MRP-175R1, MRP-211R1, MRP-214, MRP-320, 1022815, 3002003103, MRP-413, MRP-440, MRP-451, 3002021051 Other: [4-46], [4-47], [4-48]

Table 4-7 (continued)
PWR systems explanatory notes

NOTE ID	EXPLANATORY NOTE
p2-7c	Concerns exist regarding the potential for thermal aging and/or irradiation to increase susceptibility to SCC initiation. There is a need to evaluate the validity of synergistic impacts and, if determined to be needed based on evaluation, to characterize the SCC performance of thermally aged and irradiated CASS materials. Presently, there are relatively few data addressing SCC of CASS materials in light water reactor environments and even fewer data addressing SCC of irradiated CASS materials. Although no serious detrimental interaction has been observed to date and theoretical arguments do not suggest any significant synergistic effect, the subject remains as a knowledge gap. [R&D Status = BLUE] **References:** EPRI: MRP-175R1, MRP-211R1, MRP-276, 3002018322, MRP-320, 1022815, 3002003103

Table 4-7 (continued)
PWR systems explanatory notes

NOTE ID	EXPLANATORY NOTE
p2-7e	See note p2-7a for generic discussion related to IASCC. For stainless steel fasteners, recent OE includes failures of lock bars and many baffle-to-former bolts at various Westinghouse-design (or derivative design) units. Multiple failure mechanisms were indicated, but IASCC is considered the primary failure mechanism. Clustering of baffle-to-former bolt failures was also observed in many of the units; this phenomenon is believed to be the result of random IASCC initiation resulting in neighboring baffle-to-former bolts carrying additional loads leading to cracking. The B&W-designed units have not observed the same level of cracked and clustering of cracked bolts as the Westinghouse-designed units. Increased IASCC susceptibility of the Westinghouse-designed units is attributed primarily to large stresses on the bolts due to a downflow configuration and the installation, fabrication, and design characteristics of the baffle-to-former bolts. The inability to accurately predict the observed cracking highlights limitations of the current models used to assess IASCC susceptibility and forecast initiation and growth of cracks. There are many influencing parameters that complicate prediction modeling efforts, including heat-to-heat variability, the complex evolution of bolt stresses that can occur over time, bolt design factors, and variations in environmental conditions. Based on the OE and design factors affecting key variables like bolt peak stress, the plants have been divided into tiers based on expected baffle-to-former bolt susceptibility. This was combined with updated modeling results from several vendors to develop interim requirements based on plant tier that were later incorporated in MRP-227. The current requirements are adequate for managing the bolts given current knowledge; however, due to the relevant IASCC unknowns already discussed in p2-7a, the continued observation of degradation of baffle-to-former bolts at plants performing MRP-227 inspections is expected. A Yellow R&D status is considered appropriate until a better understanding of the failure mechanism(s) is achieved. [R&D Status = YELLOW] **References:** EPRI: MRP-175R1, MRP-211R1, MRP-214, MRP-227R2, MRP-320, 1020983, 1022815, 3002003103, MRP-413, MRP-425, MRP-443 Other: [4-46], [4-49], [4-50], [4-41], [4-52]

Table 4-7 (continued)
PWR systems explanatory notes

NOTE ID	EXPLANATORY NOTE
p2-7f p2-12f	See note p2-7e regarding IASCC of austenitic stainless steel fasteners. The screening threshold fluence for IASCC is set by MRP-175 at 3 dpa (2.0 x 10^{21} n/cm^2, E > 1.0 MeV) and for IE is set by MRP-175 at 1.5 dpa (1.0 x 10^{21} n/cm^2, E > 1.0 MeV) for Alloy A-286. There are no data regarding IASCC or IE susceptibility for Alloy A-286 and no planned research to address this gap. However, since existing MRP inspection programs adequately address cracking of these fasteners and research continues on IASCC and IW of the more prolific material categories of stainless steel fasteners found in PWRs, a Green R&D status is considered appropriate. [R&D Status = GREEN] **References:** EPRI: MRP-88, MRP-175R1, MRP-189R3, MRP-190, MRP-191R2, MRP-227R2, MRP-273

Table 4-7 (continued)
PWR systems explanatory notes

NOTE ID	EXPLANATORY NOTE
p2-7h p2-12h	Irradiation effects and IASCC of Alloy X-750 materials in the PWR environment have not been considered of significant concern because components fabricated from these materials have relatively low end-of-life neutron dose. Although an effect of irradiation on SCC properties has been shown to exist, MRP-175, Rev. 1, contains screening criteria for IASCC and plants are implementing plant-specific inspection programs for CRGT support pins based on support pin vintage and for core barrel and thermal shield bolts. Although these pins and bolts are readily replaceable (most U.S. units have already replaced the originally installed X-750 CRGT support pins), there are some replacement X-750 support pins in service for which a better understanding of remaining serviceable life would be beneficial. In particular, for plants potentially considering extended operations, there is some need to reconsider prior conclusions since the neutron fluence for CRGT support pins and select core barrel and thermal shield bolts may approach, or possibly exceed, the 3 dpa screening limit in MRP-175, Rev. 1, for IASCC and/or the 1 dpa screening limit in MRP-175, Rev. 1, for irradiation embrittlement. In addition, some experimental work by the Bettis Laboratory suggests that the higher boron levels in X-750 could have an adverse effect on SCC performance even at low neutron fluences. Boron is usually present at higher concentrations for hot workability, particularly on grain boundaries. Since B^{10} has an exceptionally high neutron cross-section, it has been theorized that significant concentrations of helium could be generated by transmutation along grain boundaries, leading to degraded SCC performance. Although existing inspection programs are addressing near-term aging management and replacement is a viable option, it is preferable to proactively address the potential for adverse trends to occur at higher fluences. Although limited studies of X-750 irradiated materials performance are being performed by the BWRVIP, these studies are focused on BWR environments and lower accumulated neutron fluence. There is no ongoing or planned research to characterize environmental parameters that may contribute to IASCC and/or IE of Alloy X-750 at the fluences associated with the extended operational life of PWR internals components. [R&D Status = ORANGE] **References:** EPRI: MRP-175R1, MRP-189R3, MRP-190, MRP-191R2, MRP-227R2 Other: [4-53] 0, [4-55], [4-56]

Table 4-7 (continued)
PWR systems explanatory notes

NOTE ID	EXPLANATORY NOTE
p2-8a p2-8b p2-8c p2-8d p2-8e p2-8f p2-8g p2-8h	See notes p2-14 regarding irradiation creep/irradiation-enhanced stress relaxation. High-cycle fatigue is considered a possible failure mode for all reactor vessel internals materials. Bolted connections that are exposed to sufficient neutron fluence for irradiation creep / irradiation-enhanced stress relaxation to occur may become susceptible to fatigue. There is concern that loss of bolt preload due to irradiation creep could result in increased component vibration and subsequent fatigue damage. However, this concern can be addressed by implementation of aging management programs. There is no fundamental materials R&D gap. [R&D Status = GREEN] **References:** EPRI: MRP-175R1, MRP-189R3, MRP-190, MRP-191R2, MRP-227R2

Table 4-7 (continued)
PWR systems explanatory notes

NOTE ID	EXPLANATORY NOTE
p2-9a p2-9b p2-9c p2-9d p2-9e p2-9f p2-9g p2-9h	For high fluence reactor internals, there are limited data related to the effects of neutron fluence on fatigue life. Component locations of higher concern are fasteners exposed to high neutron fluence. Irradiation-induced effects could have an impact on fatigue strength. For reactor internals not exposed to significant neutron fluence, concerns are less substantial. The NRC published NUREG-6909, Revision 1, in 2018, which details an environmental correction factor for expected fatigue life for carbon and low-alloy steels, wrought and cast austenitic stainless steels, and nickel-based alloys. The maximum environmental correction factor is more than double the factor observed by Chopra et al. in a 2002 ASME PVP paper. Results of testing that attempted to show that the variable loading conditions imposed on actual plant components would be less aggressive than assumed in NUREG/CR-6909 (prior to its revision) were published by EPRI in 2016. Near-term knowledge gaps remain with respect to adequate characterization of EAF. Consideration of extended operations increases fatigue usage relative to original design and initial plant life extension. This increased usage may increase the need for data that address the impact of neutron fluence on fatigue life and for review of fatigue usage estimates to determine whether low fatigue margins exist for any reactor internals components. Current research efforts in progress are focused on pressure-retaining locations since pressure-retaining locations are of greater concern (See notes p1-9c and p1-6f). The focus on pressure boundary locations is consistent with the NRC staff conclusion documented in the safety evaluation on MRP-227, Revision 1-A, that EAF only needs to be addressed for reactor coolant pressure boundary components for license renewal (see Section 3.6.8 of the safety evaluation). While this research can be generically applied to stainless steel and nickel-base alloy reactor internals components, current plans do not include work to evaluate the influence of neutron irradiation on fatigue crack initiation and growth. There may also be other aspects that are different for reactor internals, such as the use of thinner components and components with more complex geometries. However, additional work should be completed relative to pressure-retaining components before considering plans for reactor internals components. Bolt replacement may be a viable alternative for some cases. [R&D Status = ORANGE] **References:** EPRI: MRP-175R1, MRP-189R3, MRP-190, MRP-191R2, MRP-227R2, MRP-415 Other: [5-22], [4-57]

Table 4-7 (continued)
PWR systems explanatory notes

NOTE ID	EXPLANATORY NOTE
p2-10b	See note p1-10d. [R&D Status = GREEN] **References:** EPRI: TR-106092, MRP-276 Other: [4-22]
p2-10c	See note p1-10e for general discussion regarding thermal embrittlement of CASS materials and conclusions regarding R&D status. Potential synergistic effects of thermal aging and irradiation embrittlement specifically applicable to reactor internals castings are addressed by note p2-12c. [R&D Status = YELLOW] **References:** EPRI: MRP-175R1, MRP-276, TR-106092 Other: [4-22]
p2-10g	For martensitic stainless steels (Types 403, 410, and 431), there are relatively few data available to assess thermal aging effects. MRP-175 indicates that most data are related to Type 410 material, which is anticipated to be similar to, or to bound, Types 403 and 431. Thermal embrittlement of martensitic stainless steel is likely linked to grain boundary segregation of impurities, but there is no general increase in material hardness. Initial hardness is controlled by the post-quench tempering heat treatment temperature. Type 17-4PH stainless steel is generally considered more susceptible to thermal embrittlement than the other martensitic stainless steels. Further, it is noted in MRP-175 that Type 17-4 PH embrittlement includes a severe decrease in upper shelf energy (USE) (which is not observed in non-precipitation hardenable martensitic stainless steels). Thermal embrittlement data for Type 15-5PH stainless steels are very limited. Comprehensive data associated with thermal embrittlement are not available for all precipitation-hardened martensitic stainless steels of interest. Since thermal aging is a diffusion-dependent process, further reductions in fracture toughness due to thermal aging occurring with operation beyond 60 years will be less significant than earlier operating periods and are not considered to be a significant concern. However, the potential for reductions in SCC margins to occur over time due to thermal aging is conservatively noted as a concern relative to extended operation. While thermal embrittlement of Type 410 and Type 17-4 PH is relatively well characterized, the data sets are limited for other alloys. [R&D Status = ORANGE] **References:** EPRI: MRP-80, MRP-175R1, 3002018322

Table 4-7 (continued)
PWR systems explanatory notes

NOTE ID	EXPLANATORY NOTE
p2-11a p2-11e	Research shows that wrought and forged stainless steel base metal can exhibit some reduction in fracture resistance properties due to exposure to the primary system coolant. For non-irradiated components, these reductions are less significant than those observed for either irradiated materials or for highly cold-worked materials. However, in the context of irradiated PWR stainless steel structures, the increased yield strengths resulting from irradiation are cause for some additional investigation. Some limited J-R testing (at LWR operating temperature) of irradiated stainless steels was performed on a Type 316 stainless steel control rod blade with 6.7 dpa removed from a Swedish BWR plant. Results from this study show that there is little or no effect of BWR and PWR environments on fracture resistance. However, this conclusion is only true for specimens containing transgranular pre-cracks generated in air at room temperature. There were indications of an effect of the BWR environment on fracture resistances for specimens containing intergranular pre-cracks. Low temperature tests of irradiated SS exposed to PWR primary water have not been performed. [R&D Status = ORANGE] **Reference:** EPRI: 1025124
p2-11b	See note p1-11d. Zorita core barrel weld material, irradiated to approximately 0.7 to 1.9 dpa showed low fracture toughness when tested in air, PWR water at 320°C, and PWR shutdown conditions at 170°C. The toughness did not vary significantly with temperature, dose, or test environment. [R&D Status = ORANGE] **References:** EPRI: MRP-451 Other: [4-62]
p2-11c	See note p1-11e. [R&D Status = ORANGE] **References:** EPRI: MRP-276, MRP-293 Other: [4-9]
p2-11d	See note p1-11f. [R&D Status = GREEN] **Reference:** EPRI: MRP-293

Table 4-7 (continued)
PWR systems explanatory notes

NOTE ID	EXPLANATORY NOTE
p2-11f p2-11g	The increased yield strengths of the precipitation-hardened stainless steel or martensitic stainless steel fasteners addressed by this note are a cause for some additional concern that any effects of environment on fracture resistance could be more substantial than for austenitic stainless materials. There has been no specific testing of precipitation-hardened stainless steel or martensitic stainless steel materials to address environmental effects on fracture properties, and no research is in progress or planned. However, some effect of environment likely exists given the current understanding of the phenomenon. [R&D Status = ORANGE] **Reference:** Other: [4-30]
p2-11h	Alloy X-750 is known to be susceptible to fracture under some relevant operating conditions, particularly low temperature operation under load. Few data exist to characterize this concern for Alloy X-750. Synergism with PWSCC is also of some concern given the material's high yield strength and history of PWSCC. There have been many failures of Alloy X-750 in service. In some of these cases, crack extension at low temperature could have contributed to the failure, although this cannot be proven. Given available data, it is likely that there is some effect of environment at higher temperatures. The effects of irradiation hardening elevate the concern for some component locations. The role of hydrogen in contributing to abnormally high SCC crack growth rates remains a significant uncertainty. Hydrogen fugacity in the environment, the diffusivity of hydrogen within the metal, and the interaction of hydrogen with other parameters, such as temperature and mechanical loading rate, are not well understood. Synergisms with PWSCC and corrosion fatigue must also be considered. There are no current plans for additional evaluation of X-750 regarding rapid fracture. Susceptibility to LTCP has been demonstrated in the laboratory. However, additional work is needed to characterize material responses so that, if needed, guidance for plant operation can be provided. Additional data are also needed to characterize performance at higher temperatures, particularly regarding abnormally high SCC growth rates. See p2-6h for additional information on the potentially relevant operating experience with Alloy X-750 fasteners and on their susceptibility to SCC. [R&D Status = ORANGE] **References:** EPRI: MRP-293, MRP-175R1

Table 4-7 (continued)
PWR systems explanatory notes

NOTE ID	EXPLANATORY NOTE
p2-12a p2-12e	Most of the data for assessing the embrittlement of Type 300 series stainless steels due to neutron irradiation have been obtained from material exposed in fast reactors. The comparison of available thermal reactor data to fast reactor data results for lower fluences has confirmed the relevance of mechanical properties data developed from fast reactor irradiations. Current fast reactor mechanical properties data do not extend to peak doses pertinent to LWR extended operations. The appearance of an apparent plateau in mechanical properties after relatively modest doses, however, suggests that the consequences for life extension for extended operations may not be significant. Recent data for material removed from the baffle plate assembly of the Zorita PWR correlated well, showing saturation of mechanical properties above approximately 10 dpa up to the maximum dose tested (~50 dpa). Irradiation embrittlement and associated R&D needs for PWR stainless steel bolting are essentially the same as for other wrought stainless steel internals. The most highly irradiated bolting is typically baffle-to-former bolts made of Type 316CW, Type 316, Type 304, or Type 347. All these materials are represented in the existing fast reactor and thermal reactor data sets with much of the high fluence data being for cold-worked material. Embrittlement saturation for baffle-to-former bolts will be achieved relatively early in life and, thereafter, the properties will be maintained at stable, predictable levels. The major uncertainty for extended operating periods is the potential for significant void swelling to result in degraded material properties. However, this concern is somewhat mitigated by recent developments in the understanding of void swelling rate and the low swelling observed in material removed from a PWR (see p2-13a for details). Despite the level of confidence in the existing fast and thermal reactor data, MRP-211, Rev. 1, does note gaps in the data sets for irradiated stainless steels at high fluence, including a gap in tensile strength data for fluences greater than 70 dpa (for some cases) and a gap in fracture toughness data for fluences greater than 90 dpa. The impact of void swelling at these high neutron doses may be a factor. Fast reactor data are considered suitable for use in estimating the strength and ductility properties of highly irradiated stainless steels in LWRs since neither a flux nor a helium bubble effect has yet been identified on the mechanical properties of austenitic stainless steels used in LWRs. Unless some as-yet unobserved or unknown embrittlement phenomenon manifests itself with long exposure times and high neutron dose (for example, void swelling), reductions in material toughness can be expected to saturate at some predictable level. The potential for a void swelling effect on mechanical properties is a gap, but its significance is reduced due to the updated understanding and data on swelling. Some research is in progress to address the key knowledge gaps. Work plans include generation of high fluence material property data for materials irradiated in a PWR environment to increase confidence in late life properties. However, more work needs to be done to answer the remaining questions. [R&D Status = ORANGE] **References:** EPRI: MRP-175R1, MRP-211R1, MRP-214, MRP-320, MRP-440, MRP-451, 3002021050, 3002020892 Other: [4-15]

Table 4-7 (continued)
PWR systems explanatory notes

NOTE ID	EXPLANATORY NOTE
p2-12b p2-12c	Despite the level of confidence in the existing fast and thermal reactor data and the gaps in data for wrought materials up to 90 dpa, there are limited fracture data to confirm the lower bound fracture toughness for austenitic stainless steel welds. There is some uncertainty with respect to the effects of varying levels and orientations of ferrite in weld metals on embrittlement, and there is very limited existing high fluence, > 15 dpa (1.0×10^{22} n/cm^2, E > 1.0 MeV) data for welds. Testing of weld material removed from the Zorita PWR core barrel provided results for material irradiated between 0.7 and 1.9 dpa. These data indicated reduction in fracture properties for weld metal at lower fluence than observed for wrought base metal. Data for the possible effects of void swelling with respect to a possible reduction in fracture toughness below current lower bound saturation value also do not exist, but this concern is somewhat mitigated by recent developments in the understanding of void swelling rate and the low swelling observed in material removed from a PWR (see p2-13a for details). Overall, there are multiple areas that still require investigation and testing for irradiation embrittlement of austenitic weld metals, and the assigned category should remain as Orange. There have been recent studies of the synergistic effects of thermal and irradiation embrittlement of austenitic stainless steel weld materials. Older studies by the MRP of CASS reactor internals in PWR service did not identify any evidence supporting synergistic effects of thermal and irradiation embrittlement. A practical result is that lower bound fracture toughness values are controlled by either thermal aging or irradiation damage. The industry (BWRVIP and MRP) has demonstrated that there does not appear to be any synergistic effect. However, there are key gaps in the data for combined thermal aging and irradiation embrittlement of CASS materials, primarily: 1) no data for low molybdenum (CF3/CF8) materials between 1 and 5 dpa and 2) data from CASS materials with irradiation dose and thermal exposure accumulated concurrently with more than 1 dpa of exposure. Sources of data to address this gap are associated with analysis of components removed from service in operating reactors. As such, the development of a proactive specimen test program is not practical. Also see note p1-10e, which addresses current R&D needs related to the thermal embrittlement database associated with stainless steel castings removed from PWR service. Recent work by MRP has indicated that microstructural changes in austenitic stainless steel welds under irradiation at elevated temperatures saturate by about 1 dpa. [R&D Status = ORANGE] **References:** EPRI: MRP-276, MRP-211R1, MRP-440, MRP-441, MRP-451 Other: [4-30], [4-58], [4-59], [4-60], [4-61], [4-62]

Table 4-7 (continued)
PWR systems explanatory notes

NOTE ID	EXPLANATORY NOTE
p2-13a p2-13b	Void swelling is a potential concern for PWR internals because swelling produces dimensional changes. Void swelling in PWR internals is projected to be minor in most cases, but there are still concerns regarding the potential impact of small amounts of void swelling (0.2%) on structures that are not tolerant of changes in dimension. For some structures, small levels of differential swelling in large volumes of material could cause significant extensions and deflections that would have to be accommodated locally (e.g., closure or opening of gaps). There are several data gaps with respect to potential void swelling in PWR internals, including the lack of data for welds, the lack of data at the highest potential PWR component temperatures (when gamma heating effects are included, it is approximately 370°C [698°F]) and complications from issues such as differences in irradiation temperature and fast neutron flux between fast reactors and LWRs, variations between different alloys, and the role of helium generation. Due to the flux effects on void swelling, fast reactor irradiations are generally not viable for generating data for LWRs. Additional information is needed to determine at what fluences void swelling concerns become significant for LWRs. Additionally, there are concerns that significant void swelling could also result in reductions in fracture toughness below the currently defined lower bound saturation values (see note p2-12a). Ongoing programs address some of these gaps. The GONDOLE project, initiated in 2004 and extended to 2018, assessed swelling in stainless steels with a PWR neutron spectrum and PWR operating temperatures (see MRP-327). Microstructural studies of materials from components retired from operating reactors are adding additional information. Examination of baffle plate material from the Zorita PWR showed less than 0.1% swelling for doses between 33 and 47 dpa and temperatures between 299 and 327°C (570 and 621°F). Re-evaluation of the available data has revealed that the previous 1%/dpa saturation void swelling rate for PWR conditions was overestimated and should be closer to 0.07%/dpa. This significantly lower rate is expected to minimize the impact caused by void swelling, as shown by sensitivity studies conducted in MRP-230, Rev. 3. EPRI is also conducting research in NDE for void swelling (report 3002021195). Such technologies could be used to manage void swelling through monitoring rather than prediction. There may be a need to perform further work to address specific gaps that remain, or to investigate doses relevant for long-term operation for periods beyond 80 years. However, based on the various testing and examination results and the significant reduction in expected saturation swelling rate, this item has been updated to an R&D status of Green. [R&D Status = GREEN] **References:** EPRI: MRP-50, MRP-73, MRP-135R2, MRP-175R1, MRP-211R1, MRP-230R3, MRP-257, MRP-259R2, MRP-327, MRP-320, MRP-321, MRP-391, MRP-440, 3002021050, 3002021195 Other: [4-63], [4-64], [4-65], [4-51]

Table 4-7 (continued)
PWR systems explanatory notes

NOTE ID	EXPLANATORY NOTE
p2-13e	The void swelling phenomenon for stainless steel bolting is essentially the same as for other stainless steel PWR internal components (see note p2-13a). However, there are some considerations for bolting, particularly baffle-to-former bolts, that are worth noting. Baffle-to-former bolts will simultaneously experience some of the highest temperatures and highest neutron fluences for PWR internals. It is therefore expected that baffle-to-former bolts are one of the most likely components to experience significant void swelling. A possible mitigating consideration is that many baffle-to-former bolts currently installed are fabricated from cold-worked Type 316 material (316CW), which was investigated extensively as a void swelling resistant material for fast reactor applications. At the least, it was demonstrated to delay the onset of void swelling relative to solution-annealed Type 304, in some cases. For the PWR case, because the peak temperatures are near the lower bound for void swelling anyway, a delay in the onset of swelling may be sufficient to avoid significant dimensional or strain issues over the life of the bolt. In the first phase of the GONDOLE program, little, if any, swelling was reported for Type 316CW stainless steel. Bolts fabricated from solution-annealed stainless steels may be more vulnerable, or at least see an onset of void formation at a lower fluence. In the case of baffle-to-former bolts, because of the high operating temperature and fluence, it is noted that the ongoing test programs are not likely to envelop conditions of extended operations, which gives added incentive to continue to pursue the physically based modeling indicated in note p2-13a. Similar to the base metal in p2-13a, the reevaluation of the available data showing that the previous 1%/dpa saturation void swelling rate for PWR conditions was overestimated and should be closer to 0.07%/dpa is applicable to the 300 series fastener materials. This significantly lower rate is expected to minimize the impact caused by void swelling, as shown by sensitivity studies conducted in MRP-230, Rev. 3. There may be a need to perform further work to address specific gaps that remain or to investigate doses relevant for extended operation for periods beyond 80 years. However, based on the various testing and examination results and the significant reduction in expected saturation swelling rate, this item has been updated to an R&D status of Green. [R&D Status = GREEN] **References:** EPRI: MRP-50, MRP-73, MRP-175R1, MRP-211R1, MRP-230R3, MRP-257, MRP-327, MRP-320, MRP-321, MRP-391, 3002020892 Other: [4-63], [4-64], [4-65], [4-51]

Table 4-7 (continued)
PWR systems explanatory notes

NOTE ID	EXPLANATORY NOTE
p2-14a p2-14e	In general, irradiation creep and irradiation-enhanced stress relaxation are well characterized for stainless steels. Although thermal relaxation occurs relatively early in life and is observed to saturate at about 10-20% reduction in the initial load, irradiation enhanced creep/relaxation can continue with increasing radiation exposure and much greater reductions in stress can be attained. Near-term practical concerns are focused on relaxation of bolted connections that require retention of mechanical preload to maintain their function. Loss of preload could also lead to fatigue and wear. An additional concern is the uncertainty associated with the interaction of irradiation creep with void swelling on the stresses generated within complex structural situations in core internals. In some cases, irradiation creep could significantly relax stresses, while, in other cases, void swelling could negate stress relaxation. Retention of high stress could make a component more vulnerable to IASCC, while a reduction in stress could make a component less vulnerable to IASCC. Because of the potentially different responses of mating materials in reactor vessel internals, the evaluation of the structural response of internals to the combined effects of irradiation creep and void swelling is a complex 3D analytical problem. Sensitivity studies evaluating the effects of the lower saturation void swelling rates discussed in p2-13a showed that loosening of the assembly, rather than significant stress increases, is likely to be a long-term concern. Due to the increased dose in components at longer operating times, the range of components potentially affected during extended operations could expand compared to those considered for previous operations. This expanded range of components may require new and extended evaluations, in addition to existing ones. These concerns are also noted in p2-13a. Despite the large amount of research in the field of irradiation-enhanced creep and stress relaxation over the past three decades, data obtained in a PWR internals environment are limited (to approximately 10 dpa or ~6.67×10^{21} n/cm^2, E > 1.0 MeV). Most of the data were from fast neutron reactor irradiations; therefore, the influence of the dose rate, the temperature, and the spectrum (and hence the helium production rate) remain uncertain. Adequate data to forecast the overall effect of irradiation creep on PWR component items based on tests in a PWR flux spectrum environment currently do not exist. [R&D Status = ORANGE] **References:** EPRI: MRP-175R1, MRP-211R1, MRP-230R3, MRP-320, MRP-135R2, MRP-259R2, 3002020892

Table 4-7 (continued)
PWR systems explanatory notes

NOTE ID	EXPLANATORY NOTE
p2-14b	For welds and cladding, irradiation-enhanced stress relaxation will occur in regions of higher fluence. In general, relaxation of weld residual stress is not detrimental to material performance and may even have beneficial effects. In some cases, stress relaxation could prevent or delay onset of IASCC. However, adverse interactions with void swelling could also occur, possibly offsetting the effects of stress relaxation with a net increase in stress, thereby increasing SCC susceptibility. Currently, the quantitative effects of these interactions are not known. The potential effect of irradiation stress relaxation on beltline core barrel welds was evaluated in the reactor vessel internals functionality analysis documented in MRP-230, Revision 3. These studies showed that long-term neutron exposure of the core barrel welds is expected to reduce the residual stress and the risk of IASCC, based on current models. Currently, the evaluation and modeling results are limited and could be supplemented with further work or examination of other components and structures. Also, the limitations on the available test data relevant to PWR conditions noted in p2-14a for base metal also apply. [R&D Status = ORANGE] **References:** EPRI: MRP-175R1, MRP-211R1, MRP-230R3, MRP-320
p2-14f p2-14h	Irradiation-enhanced stress relaxation and irradiation creep will occur for some Alloy X-750 bolting, most significantly in some core barrel and thermal shield bolting. It may also occur for some Alloy A-286 fasteners. Additionally, MRP-211, Rev. 1, and MRP-175, Rev. 1, identify no irradiation-enhanced stress relaxation and irradiation creep data for Alloy A-286 (and only limited data for austenitic stainless steels and Alloy X-750, on which the screening criteria are based). Some core barrel and thermal shield bolting does exceed the screening set forth in MRP-175, Rev. 1, for Alloy A-286 and Alloy X-750. A review of fleet Alloy A-286 bolting exposure conditions against the screening criteria in MRP-175, Rev. 1, is needed to determine whether there are any new aging management concerns associated with extended operations. [R&D Status = ORANGE] **References:** EPRI: MRP-88, MRP-175R1, MRP-189R3, MRP-190, MRP-191R2, MRP-211R1, MRP-227R2, MRP-293

Table 4-7 (continued)
PWR systems explanatory notes

NOTE ID	EXPLANATORY NOTE
STEAM GENERATOR TUBING, PLUGS, AND TUBESHEET WELDS	
p3-1a p3-1b p3-1c	Wastage (general corrosion) of thermally treated Alloy 600 or Alloy 690 tubing is assumed to be possible in principle, but there is not any field experience to date. Thermally treated Alloy 600 has the same chemical composition as mill annealed Alloy 600 where wastage did occur for some older SGs. In recent years, implementation of improved water chemistry controls has prevented significant wastage of thermally treated Alloy 600 and Alloy 690 tubing. [R&D Status = GREEN] **References:** EPRI: 1024992, 3002018322
p3-1f p3-2f p3-7f	Alloy 800 leak-limiting sleeves are used to repair some tube defects. Due to the possibility that secondary coolant may contact the sleeve and concentrate due to boiling, these sleeves are subject to the same corrosion phenomena as Alloy 800 SG tubes. See p3-1c, p3-2c, and p3-7c. Similarly, the research that addresses degradation of Alloy 800 steam generator tubing is also applicable to Alloy 800 sleeves. [R&D Status = GREEN] **References:** EPRI: 1024992, 3002010397, 3002002853, 3002023844, 3002007860, 3002012933
p3-2c	Some pitting corrosion of PWR Alloy 800 tubing was observed at Biblis, Unit B, but this was associated with phosphate chemistry, which is no longer used (see p3-1c). Pitting experience at Darlington may be relevant to PWR Alloy 800 tubing (see p4-2a). [R&D Status = GREEN] **Reference:** EPRI: 1024992

Table 4-7 (continued)
PWR systems explanatory notes

NOTE ID	EXPLANATORY NOTE
p3-4a p3-4b p3-4c p3-8a p3-8b p3-8c	Fouling of SGs, particularly of tube-to-broached tube support openings, is an issue of concern. Worldwide, a number of SGs experienced heavy buildup of deposits that reduced or blocked water/steam flow through the broached quatrefoil openings (or trefoil in OTSGs). Fouling and flow blockage occurs preferentially at specific locations inside the SG. As a result, additional flow can be forced into the open lane at the center of some tube bundle configurations, resulting in flow well above design values. Blockage can also result in tubes being effectively fixed to a tube support plate allowing for unusual modes of vibration and subsequently leading to tubing fluid-elastic instability and high-cycle fatigue cracking of the tube. Additional research is needed to determine the level of deposit buildup to fix a tube in a quatrefoil tube support and the flow fields involved. Research along multiple paths is being pursued to fully characterize this fouling phenomenon. First, a better understanding of flow fields and the effect of blockages through development of advanced computational fluid dynamics simulation is necessary to predict when flow patterns could induce potentially high degradation rates. Generic evaluations of the thermal hydraulics for each of the Westinghouse SG designs are available to support utilities in evaluating potential fatigue failure of tube U-bends, but further modeling may still be required. Second, work to better understand the phenomenon of fluid-elastic instability is ongoing to better define the margin to the onset of this important phenomenon (see p3-5a). Third, work to better control iron transport and deposit buildup is ongoing to help reduce the growth of fouling and reduce deposit buildup rates. Except for one model SG, other performance issues (level oscillations and loss of thermal performance) appear to manifest sooner than flow-induced vibrations. Mitigation measures taken to address these issues (i.e., chemical cleaning) also fully address the issue of fouling and deposit-related, flow-induced vibration. [R&D Status = YELLOW] **References:** EPRI: 1018344, 1018888, 1020643, 1020994, 1022824, 1024837, 1025127, 1025129, 3002005515, 1025317, 3002001991, 3002005424, 3002007562, 3002007565 Other: [4-67], [4-68], [4-69], [4-70]

Table 4-7 (continued)
PWR systems explanatory notes

NOTE ID	EXPLANATORY NOTE
p3-5a p3-5b p3-5c	Wear is a significant concern for all steam generator tubing. Steam generator tube damage due to the generation of loose parts, intrusion of foreign objects, or anomalous anti-vibration bar and tube gaps currently represents the most significant operational challenge for steam generators in operating PWRs, particularly for SGs with Alloy 690 tubing for which SCC resistance has been good to date. Fluid elastic instability in tube bundles with small pitch-to-diameter ratios that are in a two-phase flow regime is not well-characterized. Laboratory testing of mockup tube bundles was completed in air and freon to simulate in-plane fluid elastic instability in single-phase and two-phase conditions and provides key inputs to future research and modeling. Additional laboratory testing and model development are needed to determine the influence of instability on operating SGs. Steam generator tubes are supported by tube support plates (OTSG) or tube support plates and anti-vibration supports in the U-bend (U-tube SG). The physical parameters (e.g., tube to support gap at cold conditions) that constitute an effective support are not well defined. Fundamental research is needed to develop a measurable definition of, or a means to calculate, an effective support. Thermal hydraulic and fluid-structure interaction tools currently available to analyze tube wear from foreign objects, tube support structures, and high-cycle fatigue are inadequate, and research remains in progress to better understand the wear causes and to improve management techniques. [R&D Status = YELLOW] **References:** EPRI: 1020643, 1014989, 1014991, 1016563, 1020642, 1024838, 3002000322, 3002005090, 3002010355, 3002012939, 3002015956

Table 4-7 (continued)
PWR systems explanatory notes

NOTE ID	EXPLANATORY NOTE
p3-6a	While there has been limited PWSCC of Alloy 600TT experienced to date in U.S. PWRs, there has been more significant occurrence of PWSCC in several foreign units. The main conclusions that can be developed from these experiences are that PWSCC of thermally treated Alloy 600 is clearly possible, and that small changes (either in design parameters or possibly with operational conditions) could result in the significantly increased PWSCC being observed in service. Eddy current testing indications consistent with PWSCC have been observed in a limited number of domestic steam generators. Although most of these indications have been attributed to off-normal stress conditions (i.e., bulges and over-expansions), there is concern that PWSCC could ultimately affect a substantial number of thermally treated Alloy 600 tubes, including tubes without identified off-normal stress conditions. Continued initiation of PWSCC is anticipated. Presently, evaluations given the current rate of PWSCC-related tube plugging suggest that steam generators with thermally treated Alloy 600 are likely to remain serviceable through licensed plant lifetimes. Although no fundamental science-related R&D is needed at present, there is a need to continue to evaluate field observations so that indications of adverse trends that could significantly affect tube bundle service life are identified and investigated. [R&D Status = YELLOW] **References:** EPRI: 1018887, 3002000474, 1019044, 1020991, 1022640, 3002000475

Table 4-7 (continued)
PWR systems explanatory notes

NOTE ID	EXPLANATORY NOTE
p3-7a	Recent operating experience indicates an ongoing trend of ODSCC indications in thermally treated Alloy 600 tubes. Cracking has occurred in a number of tube bundle locations, including areas within the tubesheet, at the top-of-tubesheet region, and at tube supports. Concerns are associated with the impact of deposit buildup, denting, impurities (e.g., lead), and anomalous stress conditions (e.g., bulges and over-expansions). Alloy 600TT units have advanced tube support plate (TSP) designs that minimize tube/support crevices. In addition, secondary chemistry alternate amine use, and high ammonia chemistry have significantly reduced the amount of iron oxides being transported into the SG. However, it is now apparent that over time, tube/TSP and tube/top-of-tubesheet (TTS) deposits develop, which can act as crevices to concentrate bulk water chemistry and increase the tube wall temperature. This can result in aggressive conditions at the tube surface under the deposits and an increased potential for corrosive attack. In laboratory testing, small amounts of lead have been found to cause rapid cracking (transgranular or intergranular) in Alloy 600TT and coupled with its slow accumulation in many SG deposits, it is now thought that the impact of lead on ODSCC has been previously underestimated. Despite current mitigation techniques and relatively low rates of ODSCC, continued initiation of new cracks is anticipated. Research is ongoing to better understand the fundamental factors influencing ODSCC of Alloy 600TT tubing and to improve SG life prediction capabilities. Additionally, work to understand the detrimental role of lead and to identify mitigating actions that can be taken if lead SCC is observed is being pursued. The goal of this research is to manage ODSCC to an extent that Alloy 600TT tube bundles can remain serviceable through the plant's end of life. [R&D Status = YELLOW] **References:** EPRI: 3002000474, 1014990, 1019044, 1018249, 1020993, 1022829, 1018887, 1020991, 3002000475, 3002000490, 3002007860

Table 4-7 (continued)
PWR systems explanatory notes

NOTE ID	EXPLANATORY NOTE
p3-7b	Laboratory data suggest that secondary side SCC (or ODSCC) of Alloy 690TT tubing is a potential vulnerability, but only within a much more limited range of conditions than for Alloy 600. While there has been no field experience with ODSCC of Alloy 690TT tubing to date, thermally treated Alloy 600 tubing operating experience indicates that a significant incubation time exists, after which an upward trend in cracking incidence occurs. Present concerns are focused on potential vulnerabilities associated with lead (Pb) induced SCC (PbSCC). Lead is observed in steam generator deposits from operating plants even when all practical precautions against common causes of lead contamination have been taken. There is uncertainty concerning the amount of lead needed and the active chemical form needed to cause PbSCC. Exposure to off-normal chemistry conditions appears to also be necessary to promote SCC (including PbSCC) in Alloy 690TT tubing. Similar to Alloy 600TT units, Alloy 690TT units have advanced TSP designs, which minimize tube/support crevices, and secondary chemistry alternate amine use and high ammonia chemistry significantly reduce deposit formation. However, over time, tube/TSP and tube/TTS deposits develop, which can act as crevices to concentrate bulk water chemistry and increase the tube wall temperature. This can result in aggressive conditions at the tube surface under the deposits and an increased potential for corrosive attack. The remaining knowledge gap is whether SCC of Alloy 690TT tubing is a practical concern when considering the pH ranges that are possible within crevices in service. Appropriately, much of the ongoing research focuses on off-normal chemistry or operational events. Knowledge gaps include understanding the envelope of electrochemical potentials associated with PbSCC, characterizing the film formed on tubing in environments containing lead, and evaluation of remedial actions that can be implemented to mitigate PbSCC (e.g., evaluating the effectiveness of additives that slow plating kinetics and additives that remove lead from solution by precipitating lead compounds). An additional area of concern is the potential for SCC vulnerability to be increased by cold work and stress due to denting at the top of the tubesheet. [R&D Status = YELLOW] **References:** EPRI: 1019043, 1019044, 1018249, 1020993, 1022829, 1024991, 3002000475, 3002000490, 3002007860

Table 4-7 (continued)
PWR systems explanatory notes

NOTE ID	EXPLANATORY NOTE
p3-7c	PWR plant experience with ODSCC of Alloy 800 steam generator tubes has included the following: • ODSCC has been observed in deep tubesheet crevices formed by tubesheet expansions that included mechanical rolls at the top and bottom of the tubesheet but left the main length of tubing in the tubesheet unexpanded. Corrosion is hypothesized to be related to repeated wetting and drying cycles related to the differential expansion of the tube and tubesheet during startup and shutdown. • ODSCC has been observed at top-of-tubesheet crevices. These flaws are hypothesized to be related to the presence of iron oxide deposits forming an occluded region at the tubesheet. • Denting, which is the constriction of tubes due to corrosion of the surrounding material, has led to ODSCC at a number of units with Alloy 800 tubing. • Circumferential cracks in relatively large numbers (100s) have been observed at one unit near the top of the tubesheet. This degradation is hypothesized to have been caused by the accumulation of anions (especially sulfate) from condenser leaks in regions of restricted flow, possibly due to the accumulation of corrosion products. In addition to the observed vulnerabilities under off-normal chemistry and stress conditions, the knowledge gaps pertaining to the susceptibility to PbSCC, described for Alloy 690TT in p3-7b, are also relevant to Alloy 800 SG tubing since it has shown an increased susceptibility to PbSCC in laboratory testing compared to Alloy 690TT. There is ongoing work, mostly conducted under the COG R&D program, aimed at increasing the understanding of the ODSCC vulnerabilities and potential means of mitigation. As such, the R&D status is set to Yellow. [R&D Status = YELLOW] **References:** EPRI: 1024992, 3002010397, 3002002853, 3002023844, 3002007860, 3002012933 Other: [4-75]

Table 4-7 (continued)
PWR systems explanatory notes

NOTE ID	EXPLANATORY NOTE
p3-7d p3-7e	Failure of Alloy 600 tube plugs is a well-characterized issue that has occurred at multiple plants. In at least one case, a failed tube plug caused an SG tube to rupture and leak primary coolant into the secondary system. Many different plug designs have been used in the industry, and plants manage the potential degradation through inspections. Since this is a mature issue, the various research aspects are well-understood. The industry has documented detailed evaluations of the operating experience, plug designs, failure modes, and inspection and evaluation approaches. Additionally, the SCC degradation of Alloy 600 and its associated weld metals is well understood, as noted in other entries of these tables. Cracking of tube plug welds observed in at least one CANDU unit tubed with Alloy 600 suggested a potential knowledge gap. However, analytical evaluation indicated that the tube end cracking in the CANDU unit is not expected to be a practical concern since the stress fields are not conducive to crack growth that would likely impact pressure boundary integrity. Based on the available information, no further R&D is needed. [R&D Status = GREEN] **References:** EPRI: TR-109495, 3002000636
p3-9a p3-9b p3-9c	Laboratory testing has shown that fatigue resistance of austenitic alloys in a hydrogenated, high temperature water environment is lower than fatigue resistance in an air environment. However, the most significant effects have been found to occur when cyclic frequencies are lower than about 1 Hz. Although some effect of the environment on fatigue resistance does likely exist, since the principal fatigue loads for SG tubes result from high-cycle, flow-induced vibrations, it is unlikely that EAF effects are important in comparison with other degradation phenomena (e.g., ODSCC, wear). The consensus is that no additional R&D is warranted at this time to address EAF of SG tubing. [R&D Status = GREEN] **References:** None
p3-9d p3-9e	Fatigue usage is not anticipated to be a significant consideration for tube plugs and associated tubesheet welds. The consensus is that no R&D is warranted at this time. [R&D Status = GREEN] **References:** None
p3-10b	See note p1-10g.

Table 4-7 (continued)
PWR systems explanatory notes

NOTE ID	EXPLANATORY NOTE
p3-10c	Thermal embrittlement of Alloy 800 SG tubes has not been studied. The current understanding of the thermal embrittlement of Alloy 690 material (see p1-10g) due to the formation of Ni_2Cr indicates that a similar mechanism would not affect Alloy 800 due to its high concentration of iron. High carbon versions of Alloy 800 are routinely used at much higher temperatures than PWR operating temperatures. An evaluation of Alloy 800 superheater tubing from Peach Bottom Unit 1 (high temperature gas reactor) indicated measurable age-hardening after operation for 1349 EFPD at 557°C (superheater outlet) but not at 415°C (superheater inlet). At this time, no additional research is considered necessary. However, there is a general lack of information on this issue. [R&D Status = BLUE] **Reference:** Other: [4-76]
p3-11a p3-11b p3-11d	Some effect of the PWR primary side environment on fracture properties is known to exist for both Alloys 600 and 690 (see note p1-11f). However, a recent evaluation of available data concluded that the primary cause of these observations of rapid fracture is plastic instability due to mechanical overload. Although environmental effects cannot be excluded, any effect of environment is likely small in relatively low strength wrought austenitic alloys. Assuming that some effect of environment exists for Ni-base alloy tubing exposed to PWR primary water, available data show any environmental effects on fracture properties are less significant for Alloy 600 and 690 than for nickel-base alloy weld metals and high strength precipitation hardened Alloy X-750. Finally, any effect is likely limited to the PWR primary environment. Based on these data, there is no need for additional R&D. [R&D Status = GREEN] **Reference:** EPRI: MRP-293
p3-11c	There are limited data available on the possibility of hydrogen embrittlement of Alloy 800. The limited studies available indicate that Alloy 800 may be more susceptible to hydrogen embrittlement than Alloy 600. [R&D Status = BLUE] **References:** Other: [4-77], [4-78]

Table 4-7 (continued)
PWR systems explanatory notes

NOTE ID	EXPLANATORY NOTE
p3-11e	See note p1-11h. Similar susceptibility to an effect of environment on fracture properties exists for tube-to-tubesheet welds as exists for other Ni-base alloy weld metals used elsewhere in the PWR primary circuit. It is also noted that the plugging of neighboring tubes may change the stress profile in some welds. Most U.S. utilities have obtained inspection relief for tubesheet welds based on these welds not posing a significant risk to pressure boundary integrity (leakage or pullout). [R&D Status = GREEN] **References:** EPRI: MRP-285, MRP-293
STEAM GENERATOR SECONDARY SIDE INTERNALS	
p4-1a p4-1b p4-2a p4-2b	Corrosion of carbon steel SG internals components has not been a significant concern for SG operation to date. Substantial corrosion during operations is not expected to occur due to chemistry controls, although losses during chemical cleaning operations need to be monitored. [R&D Status = GREEN] **Reference:** None
p4-3a p4-3b	Flow-accelerated corrosion (FAC) remains plausible for carbon steels, especially in regions of higher velocity/turbulence and/or two-phase flow such as in moisture separator assemblies. OE includes significant material loss due to FAC in carbon steel components within the steam drums of Westinghouse SGs. Several factors play a role in FAC of carbon steels exposed to secondary chemistry conditions, including material chemistry (particularly residual Cr content), component geometry, fluid velocity, turbulence, temperature, steam quality, and galvanic connections (resulting in preferential galvanic attack of weld metals due to lower amounts of trace elements compared to the adjoining base metals). With respect to standard chemistries, there is not a fundamental knowledge gap, and no fundamental materials R&D is needed to address this issue. Instead, addressing long-term uncertainties regarding the potential extent and significance of FAC for a long service life is considered an implementation issue that should be managed within the PWR IMTs. [R&D Status = GREEN] **References:** EPRI: 1022830 Other: [4-71]

Table 4-7 (continued)
PWR systems explanatory notes

NOTE ID	EXPLANATORY NOTE
p4-4a p4-4c p4-4d	Fouling and flow blockage at tube-to-tube support intersections have been found to occur under some conditions. The primary materials performance concern is not with the tube support but with the tubing, since the resulting changes in flow conditions can cause excessive vibration of the tubes near the center of the tube bundle, subsequently leading to tubing fluid-elastic instability and high-cycle fatigue cracking of the tube (note p3-4a). Since the issue of tube material degradation from fouling is tracked by cell p3-4a and there is no significant degradation of the support structures, a Green R&D result is assigned for fouling of SG tube support materials. [R&D Status = GREEN] **Reference:** None
p4-5a p4-5b p4-5c p4-5d p4-5e p4-5f	Wear of SG internals is plausible for all component locations, considering the possibility of loose parts, anomalous anti-vibration bar and tube gaps, and/or tube flow-induced vibrations. However, no additional characterization of the phenomena is needed for SG internals. The primary focus on ongoing work is to assess the impact on SG tubing. (See note p3-5a.) [R&D Status = GREEN] **Reference:** None
p4-6a p4-6b	Consistent with the conclusions for carbon and low-alloy steel pressure boundary components, SCC of carbon and low-alloy steel SG components exposed to secondary water chemistry is considered possible, especially in off-normal chemistry conditions. However, further fundamental research to address this issue is not needed. [R&D Status = GREEN] **Reference:** None

Table 4-7 (continued)
PWR systems explanatory notes

NOTE ID	EXPLANATORY NOTE
p4-6c p4-9c	Martensitic stainless steels have generally performed satisfactorily, although some cases of SCC have been experienced in PWR primary service. In these cases, the SCC has often been attributed to use of material in too high a hardness condition or application of high loads. For SG internals applications, the primary concern is that SCC susceptibility may increase as a result of thermal aging. Although the limited available data suggest that thermal aging is not anticipated to be substantial, there could be some reduction in toughness over a long service life. For such material, even a minor increase in the ductile-to-brittle transition temperature (DBTT) can result in a large deterioration of the room temperature impact energy given that the initial, un-aged DBTT of martensitic stainless steel material is near room temperature. SCC susceptibility could be enhanced at lower temperatures, potentially even under shutdown conditions. To date, there has been no comprehensive review of the available data in relation to steam generator applications nor into the potential for degradation during the long service life of replacement SGs. [R&D Status = ORANGE] **References:** EPRI: MRP-80, MRP-175R1, 3002018322
p4-6d	Ferritic stainless steels used as materials of construction for domestic SG internals are not typically subject to SCC, and operating experience to date has been good. Process controls to limit hardness adequately limit potential for SCC under normal operating conditions. The consensus for this item is that a conservative “Y” is appropriate since SCC is plausible after long-term operation if exposure to off-normal chemistry occurs or if excessive hardness is induced by improper heat treatment or cold working. However, the potential for SCC of ferritic stainless steels in SG service is judged to be minimal. Existing management techniques are currently considered to be adequate. No research is warranted to address near-term operations. [R&D Status = GREEN] **Reference:** EPRI: 3002015322
p4-6e p4-6f	Stress corrosion cracking of nickel-base alloy SG internals components (e.g., tube bundle support wrapper wedges and shims, AVB retainer bars, AVB retaining rings, AVB end caps, thermal sleeves, feedwater spargers, and spray nozzles) is considered plausible but unlikely due to the very low hydrogen fugacity in secondary water. Industry experience to date has been favorable, and this issue is not currently considered to be a significant degradation concern. [R&D Status = GREEN] **Reference:** None

Table 4-7 (continued)
PWR systems explanatory notes

NOTE ID	EXPLANATORY NOTE
p4-7a p4-7b p4-7c p4-7d p4-7e p4-7f	High-cycle fatigue is not considered to be a concern for the SG internals. [R&D Status = GREEN] **Reference:** None
p4-8a p4-8b	See note p5-8a. [R&D Status = GREEN] **Reference:** None
p4-8c p4-8d p4-8e p4-8f	Laboratory tests on small specimens in simulated LWR environments indicate that fatigue resistance in a high-temperature water environment can be lower than previously assumed based on air data. Environmental fatigue testing focused on BWR and PWR primary water chemistry environments has led to significant changes in the guidelines for evaluating corrosion fatigue of BWR and PWR primary components. Given the environmental effects observed in other environments, especially during water chemistry transients, some detrimental effect of environment on fatigue life is anticipated. It is also acknowledged that for some materials (e.g., martensitic stainless steels), there are no experimental data characterizing the effect of environment on fatigue usage. However, overall, fatigue environmental effects associated with the SG secondary chemistry environment with very low hydrogen and oxygen fugacities are anticipated to be much less significant than effects associated with hydrogenated environments. The consensus is that no fundamental materials R&D focused on stainless steel and nickel-base alloy materials exposed to the SG secondary chemistry environment is presently warranted. [R&D Status = GREEN] **Reference:** Other: [4-72]
p4-9f	See note p1-10g. [R&D Status = GREEN] **References:** EPRI: TR-016743V2R1, 3002018322, 1026723, 3002018324 Other: [4-23], [4-24]

Table 4-7 (continued)
PWR systems explanatory notes

NOTE ID	EXPLANATORY NOTE
STEAM GENERATOR SECONDARY PRESSURE BOUNDARY	
p5-2a p5-2b p5-6a p5-6b	Secondary side SG shell pitting and associated environmentally assisted cracking (corrosion fatigue and/or strain-induced corrosion cracking) has occurred in operating PWRs. This phenomenon has been attributed to poor chemistry controls allowing oxygen and copper ion ingress coupled with overly hard closure welds resulting from too low a stress relief temperature. These issues were dealt with satisfactorily in the 1990s with no repetition. TTS crevices are potential locations for denting, even in newer SGs. Slow corrosion of the low-alloy steel tubesheet in the TTS crevice region will occur over the service life of SGs. Denting in this region would increase stresses in the tube wall and increase tube susceptibility to both ID and OD initiated SCC. However, SCC caused by denting is addressed in the MDM cells for SCC of SG tubing (notes p3-6a, p3-7a) and need not be addressed further regarding secondary pressure boundary corrosion. [R&D Status = GREEN] **Reference:** None
p5-3a p5-3b	See note p4-3a. [R&D Status = GREEN] **References:** EPRI: 1022830 Other: [4-71]
p5-6c p5-6d p5-6e p5-6f	Although plausible, SCC of an Alloy 690 or Alloy 600 steam outlet flow limiter and associated attachment welds is unlikely in practice due to the low hydrogen partial pressure and low oxygen content of the main steam environment. Based on laboratory testing and field experience in replacement SGs, these alloys are expected to be resistant to SCC, even if some oxygen is present. Therefore, a “Y” and green conclusion is considered appropriate at present, and no additional R&D is warranted. [R&D Status = GREEN] **Reference:** None

Table 4-7 (continued)
PWR systems explanatory notes

NOTE ID	EXPLANATORY NOTE
p5-8a p5-8b	Corrosion fatigue is an applicable phenomenon for the low-alloy steel steam generator shell and associated nozzles and piping. Girth weld cracking of the SG shells and feedwater nozzle blend radii have been observed, where both hot/cold water thermal fatigue and an environmental contribution were identified. This particular environmental fatigue issue is related to pitting initiated by off-normal chemistry conditions with subsequent corrosion fatigue cracking. Hot and cold water layering in feedwater nozzles and control of water level in the SG downcomer during hot standby are contributory factors. Chemistry controls and improved design/operating practices, particularly during hot standby, have effectively mitigated this issue. A similar conclusion is reasonable for carbon and low-alloy steel steam generator internals p4-8a and p4-8b. [R&D Status = GREEN] **Reference:** None
p5-8c p5-8d p5-8e p5-8f	See note p4-8e. [R&D Status = GREEN] **Reference:** Other: [4-72]

Table 4-7 (continued)
PWR systems explanatory notes

NOTE ID	EXPLANATORY NOTE
PWR EXTERNAL SURFACES AND PRESSURE RETAINING BOLTING	
p6-1a p6-1f	Boric acid corrosion due to borated water leakage onto external surfaces is relatively well understood. Work at EPRI has been focused on modeling corrosion rates in the annulus region of both upper vessel penetrations (e.g., CRDM penetrations) and lower vessel penetrations (e.g., bottom mounted instrumentation penetrations). Corrosion rates observed in full-scale mock-ups were consistent with corrosion rates predicted by analysis. Current inspection programs developed using guidance from the PWROG were found to be adequate. No additional R&D is needed at this time. Further, there is no direct impact of extended operations since the development of conditions conducive to wastage is not directly linked to additional service time. [*NOTE: Boric acid corrosion of component external surfaces and bolting that is accelerated by fluid flow is also considered in this cell.*] [R&D Status = GREEN] **References:** EPRI: MRP-058R2, 3002018322, MRP-308, MRP-110, MRP-205R4, MRP-199 Other: [4-66]
p6-2a p6-2b p6-2c p6-2d p6-2e p6-2f p6-2g p6-2h	External surface pitting is considered plausible for all materials of construction if the material is exposed to moist or wetted conditions continuously or periodically. The panel consensus is that no additional research is presently needed. Pitting on gasket seating surfaces (both vessel and cover plate) of primary and secondary side SG and pressurizer closures has been observed in operating PWRs. The pitting has typically been attributed to poor cleaning of the surfaces prior to assembly of the closure hardware during the previous outage/assembly. [R&D Status = GREEN] **Reference:** EPRI: 3002018322

Table 4-7 (continued)
PWR systems explanatory notes

NOTE ID	EXPLANATORY NOTE
p6-6a	Results of SCC tests using SSRT and J-R specimens of a CrMoV low-alloy steel in concentrated solution (i.e., a maximum effect occurred in a 4.8% solution at 270˚C), which may be indicative of boric acid concentration in a crevice, show that SCC may be possible under such conditions. Additional data are needed to determine whether SCC is possible within the environmental and loading conditions that may develop during plant operations. [R&D Status = ORANGE] **References:** EPRI: 3002018322 Other: [4-74]
p6-6b	ODSCC is known to occur when stainless steel component external surfaces are contaminated with detrimental ionic species. ODSCC of stainless steel piping has been observed at plants throughout the world. Recent U.S. events have occurred at Callaway, Wolf Creek, San Onofre, and Salem. Most of the incidences of ODSCC have occurred in the presence of chlorides. These experiences confirm that austenitic stainless steels are susceptible to chloride-induced SCC, even if non-sensitized, at moderate temperature, and relatively low applied stress. ODSCC is not easily detected prior to development of through-wall cracking and associated leakage. Much of the cracking observed to date has occurred in HAZs. However, cracking can and does occur away from welds in unaffected base metal and has been detected beneath component supports, complicating efforts to detect cracking prior to through-wall penetration. At this time, no additional fundamental research to address the degradation mechanism is needed. However, it is acknowledged that there are remaining implementation gaps, particularly regarding the development and deployment of NDE technologies capable of reliably screening potentially susceptible piping for part through-wall ODSCC indications. [R&D Status = GREEN] **Reference:** EPRI: 3002018322
p6-6c	ODSCC is known to occur when stainless steel component external surfaces are contaminated with detrimental ionic species. However, a review of operating experience does not indicate any cracking observed directly in stainless steel welds or castings. Although ODSCC must be considered plausible, stainless steel welds and castings are clearly less susceptible to ODSCC than stainless steel base metal (p6-6b). No research is needed at present. [R&D Status = GREEN] **Reference:** EPRI: 3002018322

Table 4-7 (continued)
PWR systems explanatory notes

NOTE ID	EXPLANATORY NOTE
p6-6f	Cracking of high strength low-alloy steel bolting is possible (particularly in high hardness bolting) in the presence of unstable lubricants (notably MoS_2), harsh environments, or alternating wet and dry conditions. SCC of some reactor vessel studs having hardness well above Rockwell C40 has been observed. The approach used by the industry to address this problem has been to minimize the use of lubricants that potentially degrade to form aggressive species and sealants with potentially aggressive impurities. The SCC characteristics of low-alloy steel fastener materials are relatively well understood and industry issues surrounding the use of unstable lubricants are generally resolved. Although concern exists that thermal embrittlement could have a detrimental impact on SCC margins, there are few data to characterize the significance of any thermal embrittlement that could occur (see note p6-9f). Since the thermal embrittlement issue is tracked by cell p6-9f, a Green result is appropriate for this cell until additional data become available. [R&D Status = GREEN] **Reference:** EPRI: 3002018322
p6-6g	Martensitic stainless steels are widely applied in nuclear plants, and SCC of martensitic stainless steel pressure retaining fasteners has occurred in a number of cases. The primary causes of SCC failures have been use of material with excessive hardness and use of material with acceptable hardness but undesirable brittleness due to improper heat treatment. Some failures have additionally involved exposure to chlorides or other aggressive species. No additional R&D is needed at this time. The SCC properties of martensitic stainless steel fasteners are relatively well characterized, and most observed failures are associated with excessive hardness or improper heat treatment. [R&D Status = GREEN] **Reference:** EPRI: 3002018322

Table 4-7 (continued)
PWR systems explanatory notes

NOTE ID	EXPLANATORY NOTE
p6-6h	Stress corrosion cracking of precipitation-hardened stainless steel fasteners is known to occur and has been manifested in field experience. Similar to other fastener materials, SCC susceptibility is found to be promoted by excessive hardness. Although the SCC characteristics of these materials are relatively well understood, there is a concern that aging at high temperatures could cause embrittlement that reduces SCC margins. Additional thermal aging due to extended exposure to operating temperatures due to extended operations could potentially have a detrimental impact on fastener performance and promote late-life SCC occurrences. The Orange R&D status result is based on the lack of any systematic study into the relationship between embrittlement resulting from long-term aging and SCC susceptibility (see note p6-9h). [R&D Status = ORANGE] **Reference:** EPRI: 3002018322
p6-7a p6-7b p6-7c p6-7d p6-7e p6-7f p6-7g p6-7h	Externally initiated cracking due to high-cycle fatigue is possible. Typically, externally initiated high-cycle fatigue cracking is the result of acoustic or mechanical loading and is not a progressive, long-term aging phenomenon. While cracking may occur as a result of improper design, these phenomena are well understood, and no additional research is presently needed. [R&D Status = GREEN] **Reference:** EPRI: 3002018322
p6-8a p6-8b p6-8c p6-8d p6-8e	Low-cycle fatigue cracking initiating at a component external surface may occur if the external surface loading dominates over the loading at the internal surface. However, it is noted that internal surface fatigue usage can still be limiting when the effects of reactor coolant on fatigue behavior are considered. Fatigue usage factors for surfaces exposed to air are provided by the ASME Code for all relevant materials. No additional R&D specific to external surfaces is warranted. [R&D Status = GREEN] **Reference:** None

Table 4-7 (continued)
PWR systems explanatory notes

NOTE ID	EXPLANATORY NOTE
p6-8f p6-8g p6-8h	Low-cycle fatigue of pressure-retaining fasteners is well understood. No additional research is warranted at this date. Notably, consideration of extended operations may cause fatigue usage estimates to exceed 1.0 for some ASME Class 1 fastener locations. Where this occurs, affected units would need to either refine existing fatigue analyses to remove conservatisms or replace the fasteners. However, this is not a materials R&D issue, but rather an implementation issue. [R&D Status = GREEN] **Reference:** None
p6-9f	The EPRI Materials Handbook notes that some limited testing of a French 35NCD16 stud material indicated significant embrittlement. This result is notable because the embrittlement was observed at a relatively low aging temperature (536°F). Although the steel involved (35NCD16) is not similar to any of the steels commonly used in U.S. plants, the results indicate that some embrittlement of steels used for bolting in the United States could potentially occur. Embrittlement of low-alloy steel fasteners is considered a significant concern because embrittled materials typically have reduced SCC margins. Available data to characterize the potential for embrittlement of low-alloy steel fasteners as a result of service-induced aging at high temperatures are limited. [R&D Status = ORANGE] **Reference:** EPRI: 3002018322
p6-9g	For the typical martensitic stainless steels applied in nuclear plant pressure retaining applications, thermal embrittlement observed in laboratory testing has been minimal. No additional research is warranted at this date. [R&D Status = GREEN] **Reference:** EPRI: 3002018322

Table 4-7 (continued)
PWR systems explanatory notes

NOTE ID	EXPLANATORY NOTE
p6-9h	The EPRI Materials Handbook notes that 17-4 PH tends to embrittle with service at high operating temperatures. Embrittlement can occur even when fasteners are supplied in correct hardness conditions and service aging embrittlement induced SCC and/or brittle fracture have occurred in a number of cases. Investigation by EDF concluded that embrittlement of 17-4 PH cannot be ruled out for long time exposure to service temperatures of 482°F (250°C) and higher. The specific concern prompting the Orange R&D status result is the lack of any systematic study into the relationship between embrittlement resulting from long-term aging and SCC susceptibility (see note p6-6h). At present, no systematic long-term aging studies have been performed for these precipitation-hardened materials. Over time, increased SCC susceptibility typically occurs and should be studied in parallel with any embrittlement studies. Additional thermal aging due to extended exposure to operating temperatures could potentially have a detrimental impact on fastener performance and promote late-life SCC occurrences. [R&D Status = ORANGE] **Reference:** EPRI: 3002018322
p6-11a	Irradiation embrittlement of reactor pressure vessel supports will become more of an issue as plants extend operation to 80 years or beyond. This must be addressed for license renewal, yet there are almost no data for material exposed under the actual operating conditions. Some test reactor data are used, which shows large scatter and large reduction in toughness. Current plans for research include evaluating the structural stability of the supports through either fracture mechanics evaluations using bounding material properties or materials testing efforts to determine the true level of embrittlement in decommissioned support structures. The ongoing and planned research in this area is considered adequate, at this time. [R&D Status = YELLOW] **Reference:** None

4.3 References

NOTE: References listed here do not include published EPRI reports. Access to the full citation of each EPRI report listed in this section is available through use of the hyperlinks provided. If a hyperlink is not available, this report has been archived and is no longer directly accessible on epri.com.

[4-1] NEI 03-08 Revision 4, Guideline for the Management of Materials Issues, October 2020.

[4-2] NSAL-12-1, Rev. 1, *Steam Generator Channel Head Degradation*, Westinghouse Electric Company, October 2, 2017.

[4-3] K. Kumagai, S. Suzuki, Y. Takagi, M. Morra, P. Andresen, G. Catlin, L. Nelson, and R. Horn, "Effects of K and Anion Impurity Concentrations on Crack Growth Kinetics Near Alloy 182/A533B Weld Overlay Boundaries in BWRs." Presented at the 14th International Conference on Environmental Degradation of Materials in Nuclear Power Systems, Virginia Beach, VA, August 2009.

[4-4] BWRVIP 2016-123, Transmittal of Interim Guidance for BWR Water Chemistry Guidelines, November 2, 2016.

[4-5] Roth, A., et al., "Influence of Dynamic Strain Ageing on the Crack Growth Rates and Crack Tip Plasticity of Low-Alloy Steels in Oxygenated High Temperature Water." Presented at the 14th International Conference on Environmental Degradation of Materials in Nuclear Power Systems, Virginia Beach, VA, August 2009.

[4-6] R. Hosler, S. Fyfitch, H. Malikowski, and G. Ilevbare, "Review of Stress Corrosion Cracking of Pressure Boundary Stainless Steel in Pressurized Water Reactors and the Need for Long-Term Industry Guidance." Presented at 16th International Conference on Environmental Degradation of Materials in Nuclear Power Systems—Water Reactors, NACE International, 2013.

[4-7] P. Andresen, P. Emigh, M. Morra, and J. Hickling, "Effects of PWR Primary Water Chemistry and Deaerated Water on SCC." Presented at 12th International Conference on Environmental Degradation of Materials in Nuclear Power Systems, 2005.

[4-8] Pressurized Water Reactor Owners Group Report WCAP-16913-P, Revision 1, *Operability Assessment and Plant Applicability for Pressurizer Heater Sleeve Leakage in Westinghouse Designed Pressurizers*, PWROG, April 2009.

[4-9] J. R. Hixon, J. H. Kim, and R. G. Ballinger, "Effect of Thermal Aging on SCC and Mechanical Properties of Stainless Steel Weld Metals." Presented at 13th International Conference on Environmental Degradation of Materials in Nuclear Power Systems Whistler, British Columbia, 2007.

[4-10] T. Yamada, T. Terachi, T. Miyamoto, M. Aoki, and K. Arioka, "Potential Dependence of SCC of Welded and Cast Stainless Steels in High-Temperature Water – The Effect of Long Term Thermal Aging on SCC Growth." Presented at International Conference NPC 2012 on Water Chemistry of Nuclear Reactor Systems, Paper P2-57-104, 2012.

[4-11] T. Yamada, T. Terachi, T. Miyamoto, and K. Arioka, "Crack Growth Behavior of Welded and Cast Stainless Steels in Hydrogenated and Oxygenated High-Temperature Water." In: Proceedings of 14th International Conference on Degradation of Materials in Nuclear Power Systems, pp. 684–689, Virginia Beach, VA, ANS, 2009.

[4-12] T. Yamada, T. Terachi, T. Miyamoto, and K. Arioka, "Potential Dependence of SCC Growth of Cast Stainless Steels and Weld Metal in High-Temperature Water." In: Proceedings of Nuclear Plant Chemistry Conference, Quebec, Canada, October 3–7, 2010.

[4-13] P. Andresen and M. Mora, "PWR SCC Growth Rates of Cold-worked Alloy 690 & Alloys 52/152 Weld Metal." Presented at the Alloy 690 Expert Panel Meeting, St. Petersburg, FL, November 2007.

[4-14] ASME Boiler and Pressure Vessel Code, Section XI, Rules for Inservice Inspection of Nuclear Power Plant Components. American Society of Mechanical Engineers, New York, NY, 2021 Edition.

[4-15] NUREG/CR-6960, Crack Growth Rates and Fracture Toughness of Irradiated Austenitic Stainless Steels in BWR Environments. U.S. Nuclear Regulatory Commission, March 2008.

[4-16] O. M. Chopra, "Development of Fatigue Design Curve for Austenitic Stainless Steels in LWR Environments: A Review." ASME PVP 439 January 2002.

[4-17] ASME Code Case N-809, Reference Fatigue Crack Growth Rate Curves for Austenitic Stainless Steels in Pressurized Water Reactor Environments, Section XI, Division 1, June 23, 2015.

[4-18] M. J. DeVan, A. L. Lowe, and S. Wade, "Evaluation of Thermal-aged Plates, Forgings, and Submerged-ARC Weld Metals," *ASTM Special Technical Publication*, 1175, pp. 268–282 (1994).

[4-19] M. J. DeVan, A. L. Lowe Jr., and J. B. Hall, "Fracture Toughness Test Results of Thermal Aged Reactor Vessel Materials," *ASTM Special Technical Publication*, 1270, pp. 660–669 (1996).

[4-20] H. P. Gunawardane, J. B. Hall, and S. T. Rosinski, "Mechanical Property Changes in Reactor Vessel Materials Thermally Aged for 209 000 H at 282C." In: Effects of Radiation on Materials: 22nd Symposium, *ASTM Special Technical Publication*, 1475 STP, pp. 236–244 (2006).

[4-21] Eiselt, C. C., et al., "Investigation of Thermal Ageing in Long Term Operated RPV Materials," PVP2015-45558, *Materials and Fabrication*, 6A (2015).

[4-22] NUREG/CR-4513, Revision 2, Estimation of Fracture Toughness of Cast Stainless Steels During Thermal Aging in LWR Systems, U.S. Nuclear Regulatory Commission, May 2016 (ML16145A082).

[4-23] A. Marucco and E. Signorelli, "Phase Transformations in Long-Term Aged Ni-Cr-Fe Alloys," *Materials Science Forums*, Vols. 126–128, p. 375 (1993).

[4-24] Young, G. A., et al., "Properties and Performance of a High Chromium Nickel Alloy Weld Filler Metal 52i." In: Proceedings of the 17th International Conference on Environmental Degradation of Materials in Nuclear Power Systems—Water Reactors, CNS, 2015.

[4-25] G. A. Young, R. A. Etien, M. J. Hackett, J. D. Tucker, and T. E. Capobianco, "Physical Metallurgy, Weldability, and In-service Performance of Nickel-Chromium Filler Metals Used in Nuclear Power Systems." Paper presented at the 15th International Conference on Environmental Degradation of Materials in Nuclear Power Systems, TMS, Colorado Springs, August 7–11, 2011.

[4-26] R. Nanstad and G. R. Odette, "Development of a Robust Predictive Embrittlement Model for Reactor Pressure Vessel Lifetime Extension," D.O.E. Light Water Reactor Sustainability Newsletter, Issue 6, December 2011.

[4-27] G. R. Odette, "Nuclear Reactors: Pressure Vessel Steels Encyclopedia of Materials," *Science and Technology*, 6369–6376 (2008).

[4-28] Nuclear Regulatory Commission Regulatory Guide 1.99, Revision 2, Radiation Embrittlement of Reactor Vessel Materials, NRC, May 1988.

[4-29] ASTM Standard, E900-21, Standard Guide for Predicting Radiation-Induced Transition Temperature Shift in Reactor Vessel Materials, 2021.

[4-30] Li, Z., et al., "Effects of Thermal Aging and Low Dose Neutron Irradiation on the Ferrite Phase in a 308L Weld." In: Proceedings of the 18th International Conference on Environmental Degradation of Materials in Nuclear Power Systems—Water Reactors. The Minerals, Metals & Materials Series. Springer, Cham, 2019.

[4-31] Bjurman, M., et al., "Microstructural Evolution of Welded Stainless Steels on Integrated Effect of Thermal Aging and Low Flux Irradiation." In: Proceedings of the 18th International Conference on Environmental Degradation of Materials in Nuclear Power Systems—Water Reactors. The Minerals, Metals & Materials Series. Springer, Cham, 2019.

[4-32] TB-07-2 Rev. 3, "Reactor Vessel Head Adapter Thermal Sleeve Wear," Westinghouse Electric Company, December 7, 2015.

[4-33] Pressurized Water Reactor Owners Group Letter, OG-18-46, "Transmittal of Approved 'Needed' Interim Guidance for Addressing Accelerated Guide Card Wear Issue Described in NSAL-17-1, (LTR-RIDA-17-270, Revision 0), PA-MSC-1471," February 20, 2018.

[4-34] Pressurized Water Reactor Owners Group Report, WCAP-17451-P, Revision 2, "Reactor Internals Guide Tube Wear—Westinghouse Domestic Fleet Operational Projections," November 2018.

[4-35] Westinghouse Nuclear Safety Advisory Letter, NSAL-17-1, "Guide Tube Guide Card Wear Attributed to Ion Nitride Rod Cluster Control Assembly," January 16, 2017.

[4-36] Materials Reliability Program Letter, MRP 2020-011, "Notification of Recent Operating Experience (OE) Related to Displaced PWR Clevis Insert Assembly," April 28, 2020.

[4-37] TB-14-5, "Reactor Internals Lower Radial Support Clevis Insert Cap Screw Degradation," Westinghouse Electric Company, August 25, 2014.

[4-38] Westinghouse InfoGram, IG-20-1, "CRDM Latch Assembly Stationary Gripper Wear," July 30, 2020.

[4-39] Materials Reliability Program Letter, MRP 2023-001, "Notification of Recent PWR Core Barrel Cracking Operating Experience and Recommended PWR Plant Actions,"

February 2, 2023.

[4-40] NRC Information Notice 90-68, Stress Corrosion Cracking of Reactor Coolant Pump Bolts, U.S. Nuclear Regulatory Commission, October 1990.

[4-41] Westinghouse Technical Bulletin, NSD-TB-94-06, "Model 93A RCP Turning Vane Bolt IGSCC Issue," August 11, 1994.

[4-42] Westinghouse Nuclear Safety Advisory Letter, NSAL-14-6, "Reactor Coolant Pump Turning Vane Bolt Cracking and Failures," September 24, 2014.

[4-43] P. L. Andresen, P. W. Emigh, and R. M. Horn, "Stress Corrosion Crack Growth Response of AH & HTH Alloy X-750 in High Temperature Water." Paper (#621) presented at Corrosion 2003, NACE, Houston, TX, 2003.

[4-44] Materials Reliability Program Letter, MRP 2017-024, "Notification of Recent Operating Experience (OE) Related to PWR Clevis Insert Bolting Fabricated from X-750," September 19, 2017.

[4-45] Pressurized Water Reactor Owners Group Letter, OG-21-160, "NEI 03-08 Needed Guidance: PWR Lower Radial Support Clevis Insert X-750 Bolt Inspection Requirements," September 1, 2021.

[4-46] NUREG/CR-6965, Irradiation-Assisted Stress Corrosion Cracking of Austenitic Stainless Steels and Alloy 690 from Halden Phase 11 Irradiations, U.S. Nuclear Regulatory Commission, September 2008.

[4-47] ASME Code Case N-889, Reference Stress Corrosion Crack Growth Rate Curves for Irradiated Austenitic Stainless Steels in Light Water Reactor Environments, Section XI, Division 1, July 12, 2018.

[4-48] Nuclear Regulatory Commission, Regulatory Guide 1.147, Revision 20, Inservice Inspection Code Case Acceptability, ASME Section XI, Division 1, December 2021.

[4-49] Materials Reliability Program Letter, MRP 2016-021, "Transmittal of NEI-03-08 'Needed' Interim Guidance Regarding Baffle Former Bolt Inspetions for Tier 1 Plants as Defined in Westinghouse NSAL-16-01," July 25, 2016.

[4-50] Materials Reliability Program Letter, MRP 2017-009, "Transmittal of NEI-03-08 'Needed" Interim Guidance Regarding Baffle Former Bolt Inspection for PWR Plants as Defined in Westinghouse NSAL-16-01 Rev. 1," March 15, 2017.

[4-51] Materials Reliability Program Letter, MRP 2017-010, "Summary 'White Paper' of the Baffle-Former Bolt Prediction Results Provided by Structural Integrity Associated, AREVA, and Westinghouse," March 17, 2017.

[4-52] Westinghouse Nuclear Safety Advisory Letter, NSAL-16-1, Revision 1, "Baffle-Former Bolts," August 1, 2016.

[4-53] W. J. Mills, M. R. Lebo, J. J. Kearns, R. C. Hoffman, J. J. Korinko, R. F. Luther, and G. B. Sykes, "Effect of Irradiation on the Stress Corrosion Cracking Behavior of Alloy X-750 and Alloy 625." Paper presented at the 6th International Symposium on Environmental Degradation of Materials in Nuclear Power Systems—Water Reactors, TMS, Warrendale, PA, 1993.

[4-54] R. Bajaj, W. J. Mills, M. R. Lebo, B. Z. Hyatt, and M. G. Burke, "Irradiation-Assisted Stress Corrosion Cracking of HTH Alloy X-750 and Alloy 625." Paper presented at the 7th International Symposium on Environmental Degradation of Materials in Nuclear Power Systems—Water Reactors, Breckenridge, CO, NACE International, 1995.

[4-55] R. Bajaj, W. J. Mills, B. F. Kammenzind, and M. G. Burke, "Effects of Neutron Irradiation on Deformation Behavior of Nickel-Base Fastener Alloys." In: Proceedings of the Ninth International Symposium on Environmental Degradation of Materials in Nuclear Power Systems—Water Reactors, TMS, Newport Beach, CA, 1999.

[4-56] W. J. Mills, "Post-Irradiation Fracture Toughness of Inconel X-750," *Engineering Fracture Mechanics*, Vol. 18, No. 3, pp. 601–607 (1983).

[4-57] Nuclear Regulatory Commission Report, NUREG/CR-6909, Revision 1, Effect of LWR Water Environments on the Fatigue Life of Reactor Materials, May 2018.

[4-58] BWRVIP 2015-035, Summary of Industry Position on Screening Criteria for Thermal and Irradiation Embrittlement for PWR and BWR Reactor Internals Fabricated of Cast Austenitic Stainless Steel, EPRI, Palo Alto, CA, March 23, 2015.

[4-59] MRP Letter 2015-009, "Summary of Industry Position on Screening Criteria for Thermal and Irradiation Embrittlement for PWR and BWR Reactor Internals Fabricated of Cast Austenitic Stainless Steel," EPRI, Palo Alto, CA, March 23, 2015.

[4-60] U.S. NRC, Final Safety Evaluation of the BWRVIP-234; Thermal Aging and Neutron Embrittlement Evaluation of Cast Austenitic Stainless Steel for BWR Internals (TAC No. ME5060), June 20, 2016, ADAMS Accession No. ML16096A002.

[4-61] BWR Vessel & Internals Project Letter, BWRVIP 2021-030, Potential Non-Conservatism in EPRI Report, BWRVIP-100, Rev. 1-A, 3002008388 and Impacted BWRVIP Reports, March 22, 2021.

[4-62] Materials Reliability Program Letter, MRP 2022-009, "Summary of Reassessment of Irradiated Stainless Steel Fracture Toughness Test Results Discussed in MRP-441 and MRP-450 Technical Reports," March 31, 2022.

[4-63] NUREG/CR-6897, Assessment of Void Swelling in Austenitic Stainless Steel Core Internals, U.S. Nuclear Regulatory Commission, January 2006.

[4-64] Radiation-Induced Voids in Metals, A.E.C. Symposium Series 26, April 1972.

[4-65] F. A. Garner, "Assessment of the Swelling Equation Used to Predict Swelling of AISI Stainless Steel in LWR and LMR Environments." In: Proceedings of the 16th Environmental Degradation, 2013.

[4-66] F. A. Garner, "New Data and Insights on Prediction of Void Swelling in Austenitic Pressure Vessel Internals," Fontevraud 9, Avignon, France, September 17–20, 2018.

[4-67] NRC Information Notice 2007-37, Buildup of Deposits in Steam Generators, U.S. Nuclear Regulatory Commission, November 2007.

[4-68] H. E. Rummens, J. T. Rogers, and C. W. Turner, "The Thermal Hydraulics of Tube Support Fouling in Nuclear Steam Generators," *Journal of Nuclear Technology*, Vol. 148, December 2004.

[4-69] H. Bodineau and T. Sollier, "Tube Support Plate Clogging Up of French PWR Steam Generators." Paper presented at EUROSAFE, Paris, France, November 3–4, 2008.

[4-70] M. Le Calvar, A. Vergnault, H. Bodineau, F. Balestreri, and T. Sollier, "Build-up of Deposits in Steam Generators: A Safety Issue," Institut de Radioprotection et de Sûreté Nucléaire (IRSN). In: 14th International Conference on Environmental Degradation of Materials in Nuclear Power Systems, Virginia Beach, VA, August 2009.

[4-71] Nuclear Regulatory Commission Generic Letter 97-06, Degradation of Steam Generator Internals, December 30, 1997.

[4-72] P. M. Scott and D. R. Tice, "Stress Corrosion in Low Alloy Steels," *Nuclear Engineering and Design*, Vol. 119, pp. 399–413 (1990).

[4-73] WCAP-15988-NP Rev. 3, "Generic Guidance for an Effective Boric Acid Aging Management Program for Pressurized Water Reactors," Westinghouse Electric Company, April 2023.

[4-74] A. Brozova, J. Burda, and D. Karnik, "NRI Studies on the Behavior of Low-alloy Steel Exposed to Boric Acid Solutions at Ambient and Elevated Temperatures," Nuclear Research Institute Rez, Rez (Czech Republic), January 2003.

[4-75] IAEA IRS Number 8779, Indications at Steam Generator Tubes During Eddy Current Testing.

[4-76] J. E. Chafey and D. I. Roberts, "Steam Generator Materials Performance in High Temperature Gas-Cooled Reactors," *General Atomics*, GA-A15836 (1980).

[4-77] K. Kon, S. Tsujikawa, and Y. Hisamatsu, "Embrittlement and Its Recovery Process of Hydrogen-Charged Alloy 800," *Zairyo-to-Kankyo*, Vol. 41 (1992).

[4-78] K. Kon, S. Tsujikawa, and Y. Hisamatsu, "Embrittlement of Hydrogen-Charged Alloy 600 Single Crystals," *Bishoku Gijutsu*, Vol. 39 (1990).

5
BWR DEGRADATION MATRIX RESULTS

5.1 Scope and Evaluation Assumptions

The BWR MDM revision is based on a reevaluation by a panel of knowledgeable experts and in consultation with the appropriate EPRI program and project managers. Changes to the cell colors and explanatory text links reflect new experimental data and plant operating experience. See Section 2.1 for additional discussion and notes regarding the panel assessment process. Assumptions related to component scope and operating conditions used by the panel to facilitate development of consistent results include:

- The scope of BWR systems and components evaluated includes the primary pressure boundary and reactor vessel internals. Active components (e.g., control rod drives, valve internals, and pump rotating assemblies) and short-lived components (e.g., fuel assemblies and in-core instruments) are not included in the MDM evaluation. For a comprehensive list of BWR components evaluated under the NEI 03-08 [5-1], including materials of construction, see the EPRI BWR Issue Management Tables.
- All normal operating conditions were considered. These include normal power operations and startup/shutdown. Normal operating conditions are defined to include less controlled environmental conditions, such as significant oxygen ingress that may occur during maintenance periods and persist for some time during startup.
- Normal Water Chemistry (NWC) is the default chemistry control paradigm assumed in presenting results in Tables 5-1 and 5-2. As appropriate, moderate Hydrogen Water Chemistry (HWC-M), noble metal catalyzed chemistries (NMCA, NobleChem, and OLNC), and minor off-normal chemistry conditions are addressed in the explanatory notes.
- The R&D assessment color codes shown in Tables 5-1 through 5-3 are based on the assumption of extended operation, defined as anywhere from 60 to 80 or more years of service.

5.2 BWR Results: Degradation Matrix Tables and Explanatory Notes

The BWR MDM results are presented in the following set of degradation matrix tables:

Table 5-1 BWR Primary Pressure Boundary

Table 5-2 BWR Reactor Vessel Internals

Table 5-3 BWR External Surfaces and Bolting

Hyperlinks within these tables lead to summaries of the degradation phenomena contained in Table 5-4, BWR Systems Explanatory Notes.

The degradation matrix tables include the use of abbreviations and color coding. Cell *Y*, *N*, *?*, and *N/A* results indicate applicability of the degradation mode to a material type. Comprehensive definitions are provided in Section 2.2.3.1.

Cell shading indicates R&D status:

- Green fill indicates that the degradation mechanism is sufficiently well understood.
- Yellow fill indicates R&D is in progress to address gaps associated with the degradation mechanism in a reasonable time frame.
- Orange fill indicates insufficient R&D is ongoing or planned to address gaps associated with the degradation mechanism in a reasonable time frame.
- Blue fill indicates insufficient data exist to establish degradation mechanism applicability.

Comprehensive definitions of MDM color codes are provided in Section 2.2.3.2.

Within Table 5-4, references are provided in two ways. For EPRI references, a hyperlink to the EPRI abstract webpage is provided. For other references, a citation listing is provided in Section 5.3.

A summary of the changes to the cell results for Revision 5 can be found in Appendix D.

Table 5-1
BWR primary pressure boundary

MATERIAL	DEGRADATION MODE													
	Corrosion				Wear	SCC		Fatigue		Reduction in Frac. Properties		Irradiation Effects		
	Wstg.	Pitting	FAC	Foul		IG/TG	IA	HCF	EAF	Th	Env	Emb	VS	IC/SR
C&LAS: Base Metal & HAZ	N	N	Y b1-3a	N	N	Y b1-6a	Y b1-7a	Y b1-8a	Y b1-9a	N	Y b1-11a	Y b1-12a	N	N
C&LAS: Welds	N	N	Y b1-3b	N	N	Y b1-6b	Y b1-7b	Y b1-8b	Y b1-9b	N	Y b1-11b	Y b1-12b	N	N
SS: 300 Series SS Base Metal & HAZ	N	N	N	N	N	Y b1-6c	N	Y b1-8c	Y b1-9c	N	Y b1-11c	N	N	N
SS: 300 Series SS Welds & Clad	N	N	N	N	N	Y b1-6d	N	Y b1-8d	Y b1-9d	Y b1-10d	Y b1-11d	Y b1-12d	N	N
Cast Austenitic Stainless Steel	N	N	N	N	N	Y b1-6e	N	N	Y b1-9e	Y b1-10e	Y b1-11e	N	N	N
Ni-Alloy: A600 Base Metal & HAZ	N	N	N	N	N	Y b1-6f	N	N	Y b1-9f	N	Y b1-11f	N	N	N
Ni-Alloy: A182 Welds & Clad	N	N	N	N	N	Y b1-6g	N	N	Y b1-9g	N	Y b1-11g	N	N	N
Ni-Alloy: A82 Welds & Clad	N	N	N	N	N	Y b1-6h	N	N	Y b1-9h	N	Y b1-11h	N	N	N
Ni-Alloy: A52/152 Welds & Clad	N	N	N	N	N	Y b1-6i	N	N	Y b1-9i	N	Y b1-11i	N	N	N

Table 5-2
BWR reactor vessel internals

MATERIAL	DEGRADATION MODE													
	Corrosion				Wear	SCC		Fatigue		Reduction in Frac. Properties		Irradiation Effects		
	Wstg.	Pitting	FAC	Foul		IG/TG	IA	HCF	EAF	Th	Env	Emb	VS	IC/SR
STRUCTURAL COMPONENTS AND WELDS														
SS: 300 Series Base Metal & HAZ	N	N	N	Y b2-4a	Y b2-5a	Y b2-6a	Y b2-7a	Y b2-8a	Y b2-9a	N	Y b2-11a	Y b2-12a	N	Y b2-14a
SS: Welds & Clad	N	N	N	Y b2-4b	Y b2-5b	Y b2-6b	Y b2-7b	Y b2-8b	Y b2-9b	Y b2-10b	Y b2-11b	Y b2-12b	N	Y b2-14b
Cast Austenitic Stainless Steel	N	N	N	N	N	Y b2-6c	Y b2-7c	Y b2-8c	Y b2-9c	Y b2-10c	Y b2-11c	Y b2-12c	N	N
Ni-Alloy: A600 Base Metal & HAZ	N	N	N	N	N	Y b2-6d	N b2-7d	Y b2-8d	Y b2-9d	N	Y b2-11d	N	N	N
Ni-Alloy: A182 Welds & Clad	N	N	N	N	N	Y b2-6e	N b2-7e	Y b2-8e	Y b2-9e	N	Y b2-11e	N	N	N
Ni-Alloy: A82 Welds & Clad	N	N	N	N	N	Y b2-6f	N b2-7f	Y b2-8f	Y b2-9f	N	Y b2-11f	N	N	N
FASTENERS AND HARDWARE														
SS: 300 Series	N	N	N	N	N	Y b2-6g	Y b2-7g	Y b2-8g	Y b2-9g	N	Y b2-11g	Y b2-12g	N	Y b2-14g
SS: XM-19	N	N	N	N	N	Y b2-6h	Y b2-7h	Y b2-8h	Y b2-9h	N	Y b2-11h	Y b2-12h	N	Y b2-14h
Ni-Alloy: X-750	N	N	N	N	N	Y b2-6i	Y b2-7i	Y b2-8i	Y b2-9i	N	Y b2-11i	Y b2-12i	N	Y b2-14i

Table 5-3
BWR external surfaces and bolting

MATERIAL	DEGRADATION MODE									
	Corrosion				Wear	SCC	Fatigue		Reduction in Frac. Properties	
	Wstg.	Pitting	FAC	Foul		IG/TG	HCF	LCF	Th	Env
PLATE, FORGINGS, CASTINGS, AND WELDS										
C&LAS	N	Y b3-2a	N/A	N/A	N	N	Y b3-7a	Y b3-8a	N/A	N/A
SS: 300 Series Base Metal & HAZ	N	N	N/A	N/A	N	Y b3-6b	Y b3-7b	Y b3-8b	N/A	N/A
SS: 300 Series Welds	N	N	N/A	N/A	N	Y b3-6c	Y b3-7c	Y b3-8c	N/A	N/A
Cast Austenitic Stainless Steel	N	N	N/A	N/A	N	Y b3-6d	Y b3-7d	Y b3-8d	N/A	N/A
Ni-Alloy: Base Metal & HAZ	N	N	N/A	N/A	N	N	Y b3-7e	Y b3-8e	N/A	N/A
Ni-Alloy: Welds	N	N	N/A	N/A	N	N	Y b3-7f	Y b3-8f	N/A	N/A
PRESSURE-RETAINING FASTENERS										
LAS Fasteners	N	Y b3-2g	N/A	N/A	N	Y b3-6g	Y b3-7g	Y b3-8g	N	N/A
Stainless Steel Fasteners	N	N	N/A	N/A	N	N	Y b3-7h	Y b3-8h	N	N/A

Table 5-4
BWR systems explanatory notes

NOTE ID	EXPLANATORY NOTE
BWR PRIMARY PRESSURE BOUNDARY	
b1-3a b1-3b	FAC concerns are confined to plain carbon steels. For BWRs, the primary concern is carbon steel bottom head drain line piping and, more recently, the reactor water cleanup system in BWRs with NobleChem™. Locations of lesser concern, such as the feedwater piping, where FAC could be exacerbated by low oxygen as a result of operating with HWC-M are managed by monitoring of oxygen levels in feedwater and the addition of oxygen as needed to maintain at least 30 ppb per the EPRI BWR Water Chemistry Guidelines. Current models and inspection programs are considered adequate to address FAC of bottom head drain nozzles and drain lines. No additional research is required. [R&D Status = GREEN] **References:** EPRI: BWRVIP-190R1, BWRVIP-205, BWRVIP-208, BWRVIP-213

Table 5-4 (continued)
BWR systems explanatory notes

NOTE ID	EXPLANATORY NOTE
BWR PRIMARY PRESSURE BOUNDARY	
b1-6a b1-6b	Significant research has been conducted to assess factors affecting SCC of low-alloy steels, including high sulfur effects, intermediate temperature effects, ripple loading effects, and the effect of chloride impurities. Dynamic strain aging (DSA), which depends on the free carbon and nitrogen contents of C&LAS, has been identified as an additional phenomenon having a detrimental effect on SCC initiation resistance and growth rates. This is based primarily on the coincidence of the trends in occurrence of DSA as a function of temperature and susceptibility to SCC, particularly at high corrosion potentials typical of NWC. DSA is at a maximum at about 250°C and has less effect at normal operating temperatures. Recent research shows that 3 ppb chloride can accelerate SCC growth rates at high corrosion potential in the laboratory. Available data are now considered sufficient to disposition these issues. A reduction in the EPRI BWR water chemistry action level 1 value for Cl^- from 5 ppb to 3 ppb has been implemented to address Cl^- effects, and work is ongoing to codify low-alloy steel SCC CGRs. However, having been surprised by the high sensitivity to Cl, scoping studies to evaluate impurities (such as F, I, Br, NO_3, PO_4, etc.) should be undertaken. An additional data gap is the paucity of SCC of LAS data for BWR normal operating conditions. The current CGR model (N-896) predicts sustained rapid growth, which is overly conservative compared to the field where there has been essentially no growth (with rare exceptions of shallow growth that then stalls). Much of the data supporting the N-896 model are conservative relative to BWR normal operating conditions, such as intermediate temperature, ripple loading, dynamic strain aging, and impurities above water chemistry action level 1. To resolve this gap, LAS SCC data should be obtained under conditions applicable to BWR RPVs (288°C, constant K, sufficiently large specimens to ensure validity at high K values, water chemistry consistent with VIP-190, etc.), and CGR data points should only be taken near the end of each segment (i.e., wait for the CGR to finish decaying). These new data could be used to develop an updated CGR correlation that is more representative of the phenomena in the field. For these reasons, the R&D status is set to Orange. [R&D Status = ORANGE] **References:** EPRI: BWRVIP-233R2, BWRVIP-60-A Other: [5-2], [5-3], [5-4], [5-5], [5-6]

Table 5-4 (continued)
BWR systems explanatory notes

NOTE ID	EXPLANATORY NOTE
	BWR PRIMARY PRESSURE BOUNDARY
b1-6c b1-6d	Cracking occurred in early BWRs under NWC in cold worked or in furnace or weld sensitized Type 304 stainless steel. Subsequently, there was significant experience with cracking of low carbon, non-sensitized shrouds and recirculation system piping. Intensive study by researchers shows that crack initiation is also promoted by surface cold work from heavy machining, grinding, cold rolling, etc. Once initiated, IGSCC will propagate in the weld shrinkage strained region of the heat-affected zone (close to the weld fusion line). HWC and NobleChem™ are capable of providing SCC mitigation for many locations (e.g., recirculation system piping, reactor internals in the lower plenum, etc.). Recent work is focused on quantifying the relative effectiveness of NMCA and OLNC to mitigate IGSCC. For example, SCC mitigation requires an adequate density and distribution of Pt particles on component surfaces, especially for existing cracks that can grow during startup and operation. Studies are underway to investigate of the Pt size-distribution and particle spacing on BWR plant components, which are considered critical to ensuring optimum SCC mitigation. Although not commonly observed in the field, laboratory testing and plant data show that SCC growth in the weld metal is possible under oxidizing conditions, with SCC growth rates not significantly different than wrought materials observed in laboratory testing. For welds, there is the additional potential for thermal aging to detrimentally affect SCC resistance. Some cracking of L-Grade weld metals has been observed, although SCC in BWR primary systems of L-grade stainless steel welds remains relatively rare. Issues with the stainless steel cladding on the BWR reactor pressure vessel are related to the cladding application method (e.g., low ferrite, which would make hot cracking more likely), almost certainly not to SCC of the cladding during service. While some clad cracking was observed in early BWRs, this issue has been examined in detail and resolved. Overall, current aging management capabilities are considered adequate for managing IGSCC of stainless steels, although improvements in OLNC implementation should be pursued. [R&D Status = GREEN] **References:** EPRI: BWRVIP-14-A, BWRVIP-190R1 Other: [5-7]

Table 5-4 (continued)
BWR systems explanatory notes

NOTE ID	EXPLANATORY NOTE
BWR PRIMARY PRESSURE BOUNDARY	
b1-6e	Laboratory testing indicates that SCC of CASS components is possible in high carbon, low ferrite samples. Weld metals and CASS can undergo thermal aging, which can increase SCC growth rates. However, EPRI 1019030 showed that thermally aged CF8 samples possessed significant SCC resistance in a low ECP environment. EPRI 1019030 also documents the results of testing performed to evaluate reductions in fracture resistance in thermally aged CASS materials. SCC pre-cracking was attempted as part of the test protocol. SCC growth rates were found to be too low to be of engineering significance. However, at high ECP, there can be a significant acceleration of SCC growth rates with thermal aging. Thus, SCC concerns are focused on high ECP environments, including during startups and shutdowns. No field incidents of SCC in CASS components have been confirmed. SCC is considered to be unlikely if there is good water chemistry in BWRs. The consensus is that further research is not needed. [R&D Status = GREEN] **References:** EPRI: 1020957, BWRVIP-234-A Other: [5-8]
b1-6f	SCC of wrought nickel-base alloys was observed in early BWR operation. This susceptibility is primarily related to welded crevice designs and poor water chemistry or severe water chemistry transients. These included reactor vessel safe ends with creviced thermal sleeve attachments, shroud head bolts with creviced spacer sleeves, and shroud support access hole covers. Most of these components have been removed and replaced. No SCC initiation directly in Alloy 600 has been observed, although crack propagation from adjacent Alloy 182 weld metal is of concern. [R&D Status = GREEN] **Reference:** EPRI: BWRVIP-301

Table 5-4 (continued)
BWR systems explanatory notes

NOTE ID	EXPLANATORY NOTE
BWR PRIMARY PRESSURE BOUNDARY	
b1-6g b1-6h	SCC in Alloy 82 and Alloy 182 welds in shroud supports, access hole cover, and jet pump adapters continues to be identified and monitored. Although most of the cracking reported has been detected in Alloy 182, SCC has also occurred in Alloy 82 weld material, primarily associated with highly restrained and creviced geometries. Although Alloy 82 resistance to SCC initiation has been good, it is noted that SCC crack growth rates observed in laboratory specimens are not dramatically lower than for Alloy 600 or Alloy 182. A recent expert panel analysis of Alloy 82 shows moderately high growth rates, and modern Alloy 182 data need to be evaluated for consistency. Extensive studies on high nickel weld metals show that the SCC growth rate drops rapidly for Cr concentrations above ~24% (Alloy 182 has ~15% Cr, and Alloy 82 has ~20% Cr). Near-term degradation concerns continue to be managed by inspection programs. However, there is concern regarding the possibility of a progressive reduction in the stress threshold for SCC initiation after long exposure to the environment. HWC-M implementation places BWR coolant chemistry at an ECP close to the redox potential of the Ni/NiO phase boundary, where a peak in SCC growth rate is observed; the dissolved hydrogen levels used for OLNC are much lower. As such, HWC-M operation can have a detrimental effect on long-term SCC performance of nickel-base alloys. This R&D status is categorized as Yellow to reflect planned work related to crack growth rates for Alloy 82/182. [R&D Status = YELLOW] **References:** EPRI: BWRVIP-59-A, BWRVIP-222, BWRVIP-180R1 Other: [5-9]
b1-6i	High-chromium nickel-base alloys (e.g., Alloy 690 as well as Alloy 52 and Alloy 152 weld filler materials) are being widely applied as replacements for Alloys 600, 82, and 182 in PWRs. These materials exhibit excellent operating experience to-date in PWR primary water, with no observations of SCC in almost 30 years of service. However, ongoing laboratory testing to characterize potential vulnerabilities of Alloy 52 and Alloy 152 for their use in current and new BWR plants has revealed moderate SCC growth rates. The R&D status is set to Orange to reflect the lack of ongoing or planned work in this area. [R&D Status = ORANGE] **Reference:** None

Table 5-4 (continued)
BWR systems explanatory notes

NOTE ID	EXPLANATORY NOTE
BWR PRIMARY PRESSURE BOUNDARY	
b1-7a b1-7b	As neutron fluence accumulates, increased crack growth rates may be possible due to microstructural changes and increases in yield strength. There is extensive data showing that increased yield strength from composition, heat treatment, and cold work increase the SCC growth rates of low-alloy steel, and it is likely that this also applies to radiation hardening. The increase in yield strength occurs at a lower fluence in low-alloy steels compared to stainless steels, thus, IASCC remains a relevant degradation mode for extended operations. However, the risk of IASCC initiation and growth in the RPV is considered to be low since the regions most susceptible to SCC (e.g., nozzle/penetration weld HAZ) are distant from the core mid-plane—that is, spatially removed from the regions of significant flux. For this reason, the R&D status has been set to Green. [R&D Status = GREEN] **Reference:** None
b1-8a b1-8b b1-8c b1-8d	High-cycle fatigue due to thermal cycling (turbulent mixing of water of different temperatures) is a design/location-dependent phenomenon and is therefore applicable for all materials. There are some issues related to knowledge of plant conditions and modeling of thermal mixing but no knowledge gaps related to understanding of the degradation mechanism. Design-related implementation is appropriately addressed in the IMTs. [R&D Status = GREEN] **References:** EPRI: BWRVIP-155R1, MRP-146R2

Table 5-4 (continued)
BWR systems explanatory notes

NOTE ID	EXPLANATORY NOTE
	BWR PRIMARY PRESSURE BOUNDARY
b1-9a b1-9b b1-9c b1-9d b1-9e b1-9f b1-9g b1-9h b1-9i	Laboratory tests on small specimens in simulated LWR environments show that fatigue resistance in reactor water environments is lower than in a “dry air” environment. This conclusion is supported by a database of laboratory tests on small specimens in simulated reactor coolant environments. It is also recognized that the fatigue design curves that provide the basis for fatigue life assessments of nuclear plant components do not explicitly account for the effects of LWR environments on fatigue life; although, to date, conservatisms included in fatigue design curves and in fatigue calculational methods have been adequate to bound the effects of environment. Over time, component fatigue usage estimates have been refined through the application of more complex analytical methods to accommodate longer term operation, oftentimes at a significant cost burden to plant owners. This approach, while a pragmatic solution for meeting regulatory requirements, does not directly address the impact of water environments. A fundamental knowledge gap exists regarding the amount of conservatism that is delivered by the current practice of using correlations based on testing of thin specimens subjected to fully reversed uniaxial loading and environmental sensitivity factors to estimate the fatigue lives of plant components that have complex geometries and are subject to complex pressure/temperature transients. Key steps in addressing this knowledge gap include: 1. Demonstrating a better understanding of the methods to predict fatigue crack initiation and growth in actual components subjected to typical plant conditions, while allowing for less costly analyses. 2. Validating this understanding through further laboratory experimental work focused on tests that are more representative of prototypical conditions experienced by actual plant components. 3. Further investigation of transient complexities, including non-isothermal loading, multiple hold times, and variable amplitude and strain rate loading occurring concurrently with changes in water chemistry. 4. Generation of additional fatigue test data, as appropriate, for materials that are underrepresented in the currently available fatigue (S-N) database and for assessing the fatigue behavior of welded structures that may be influenced by geometric stress concentration factors, weld defects, residual stress, and multiaxial stress states. Management based on flaw tolerance represents a viable alternative when it is not possible to demonstrate that the accumulated fatigue life will not exceed the allowed value prior to the end of plant life (note that most laboratory initiation data reflect a 25% drop in load, which represents a sizeable crack). Assessing the effect of water environments on fatigue crack growth rates is an additional area where gaps remain for some materials and water environment combinations. The R&D status overall is characterized as Orange since it is unclear whether current work plans and associated funding are adequate to resolve this issue. [R&D Status = ORANGE] **References:** EPRI: 1026724, 3002010554, 3002010555, 3002007973, MRP-407, MRP-415 Other: [5-18], [5-22]

Table 5-4 (continued)
BWR systems explanatory notes

NOTE ID	EXPLANATORY NOTE
BWR PRIMARY PRESSURE BOUNDARY	
b1-10d	Thermal aging of stainless steel welds and cladding is related to operating temperature, chemical composition, and ferrite content. Although no significant thermal aging is anticipated for the typical delta-ferrite levels (5-10 FN) in austenitic stainless steel welds and cladding (FN as high as 13 have been observed in some welds), some reduction in fracture toughness may occur if the ferrite volume fraction exceeds approximately 10 FN, particularly if the alloy has molybdenum additions. However, at BWR operating temperatures, embrittlement effects are modest up to delta-ferrite levels of 20 FN. [R&D Status = GREEN] **Reference:** Other: [5-10]
b1-10e	Thermal aging of cast austenitic stainless steel is limited to castings that meet specific screening criteria for component type, casting method, molybdenum content, and ferrite content. Additionally, all other parameters being equal, L-Grade castings are less subject to thermal aging than higher carbon CASS material. BWR concerns are mitigated by relatively low peak operating temperatures. Embrittlement of BWR CASS materials is bounded by embrittlement of PWR CASS materials due to lower operating temperatures for the BWR design. In addition, BWR CASS piping components are limited to 1) thick-walled valve bodies and pump casings and 2) flow venturi inserts inserted into the wrought recirculation system piping. BWRVIP-234-A documents a study of CASS thermal embrittlement for the BWR environment. This study concludes that thermal embrittlement is not a substantial concern. [R&D Status = GREEN] **Reference:** EPRI: BWRVIP-234-A

Table 5-4 (continued)
BWR systems explanatory notes

NOTE ID	EXPLANATORY NOTE
	BWR PRIMARY PRESSURE BOUNDARY
b1-11a b1-11b	Uncertainties remain regarding the role of hydrogen in the observed phenomena. Hydrogen fugacity in the environment, the diffusivity of hydrogen within the metal, and the interaction of hydrogen with other parameters (e.g., temperature and mechanical loading rate) all remain poorly understood. Specifically considering low-alloy steels, there is a need to address potential synergisms with other degradation phenomena, notably SCC and corrosion fatigue. For components subject to significant neutron fluence, irradiation embrittlement (see note b1-12a) is an additional factor that must be considered since the elevated yield strengths resulting from irradiation damage likely increase the magnitude of any effect that exists. Studies show that H permeation in iron and nickel-base alloys is sufficiently rapid above ~250°C that high local H fugacity is unlikely. H permeation is controlled by the coolant hydrogen fugacity, and neither the oxide formed in high temperature water nor air affect the dissociation or permeation of hydrogen. Thus, high "internal hydrogen pressure" cannot build up, although at a given hydrogen fugacity in the metal, there can be a higher concentration of hydrogen 'stored' at voids, precipitates, carbides, dislocations, etc. The change in hydrogen solubility with temperature can create elevated hydrogen fugacity during cooling. In general, hydrogen effects on cracking are much more pronounced below about 125°C. The R&D status is judged to be Orange since there are no current plans to conduct additional testing. [*NOTE: Observations of rapid fracture under rising K in SCC and fatigue tests can be due to plastic instability resulting from mechanical overload conditions, and subsequent studies have shown no evidence of an effect of environment.*] [R&D Status = ORANGE] **References:** EPRI: 1020957 Other: [5-1]
b1-11c	Some effect of the environment on the fracture properties of wrought stainless steel base metals is possible based on available data. However, for components not subject to significant fluence, these effects are less significant than those observed for irradiated materials or highly cold-worked materials. Uncertainties remain regarding the role of hydrogen in the observed phenomena at various temperatures, although additional near-term R&D is not considered necessary for non-irradiated stainless steel components. [*NOTE: Observations of rapid fracture under rising K in SCC and fatigue tests can be due to plastic instability resulting from mechanical overload conditions, and subsequent studies have shown no evidence of an effect of environment.*] [R&D Status = GREEN] **Reference:** None

Table 5-4 (continued)
BWR systems explanatory notes

NOTE ID	EXPLANATORY NOTE
BWR PRIMARY PRESSURE BOUNDARY	
b1-11d b1-11e	Limited testing of aged CF8 material in simulated PWR primary water chemistry environment identified pronounced reductions in fracture toughness of the material at low temperatures (e.g., consistent with startup/shutdown and layup). Inadvertent testing of one specimen in high temperature water suggested that substantial reductions in fracture properties can persist at high temperature, even though the magnitude of the effect is less than that at low temperature. The data to characterize the extent of this phenomenon for CASS material are limited, particularly at high temperatures. Due to the similarity of as-solidified microstructure, similar results are also observed in stainless steel weld metals, although the lower ferrite content in weld metals limits the magnitude of the effect of thermal aging. [*NOTE: Observations of rapid fracture under rising K in SCC and fatigue tests can be due to plastic instability resulting from mechanical overload conditions, and subsequent studies have shown no evidence of an effect of environment.*] [R&D Status = ORANGE] **References:** EPRI: 1020957 Other: [5-10]
b1-11f	Although the phenomenon is not well understood for any material, there are no near-term concerns regarding environmental effects on J-R properties for Alloy 600. Synergisms with thermal or irradiation embrittlement are much more unlikely for Alloy 600 than for other materials. [R&D Status = GREEN] **Reference:** EPRI: MRP-293

Table 5-4 (continued)
BWR systems explanatory notes

NOTE ID	EXPLANATORY NOTE
BWR PRIMARY PRESSURE BOUNDARY	
b1-11g b1-11h b1-11i	Research indicates that nickel-base weld metals, including Alloys 82, 182, 52, and 152 exhibit some reduction in fracture properties at temperatures below ~125°C (e.g., during startup, shutdown, and layup) in simulated PWR primary water chemistry environments. Few data are available in BWR water. Regarding low temperature effects on toughness (sometimes referred to as “low temperature crack propagation,” or LTCP, although this can also refer to low temperature SCC), a recent MRP review of low-temperature effects for nickel-base alloys concluded that some areas of uncertainty remain, but additional testing of nickel-base alloy weld materials to evaluate LTCP is unlikely to provide significant insights relevant to the industry. Uncertainties remain regarding the role of hydrogen in the observed phenomena. Hydrogen fugacity in the environment, the diffusivity of hydrogen within the metal, and the interaction of hydrogen with other parameters (e.g., temperature and mechanical loading rate) are poorly understood. There are few test data to characterize performance at higher temperatures. The focus of testing performed to date has been on LTCP. Additionally, since only a few welds have been tested, weld-to-weld variability has not been evaluated in detail for either the low temperature or high temperature regimes. [*NOTE: Observations of rapid fracture under rising K in SCC and fatigue tests can be due to plastic instability resulting from mechanical overload conditions, and subsequent studies have shown no evidence of an effect of environment.*] [R&D Status = ORANGE] **References:** EPRI: 1020957, MRP-293
b1-12a b1-12b	Per NRC assessments (ML19203A089, ML21270A002), sufficient data exist to assure that Regulatory Guide 1.99, Rev. 2, remains adequate up to fluence levels well beyond the projected 80-year 1/4T fluence for BWRs, which is less than 1E19 n/cm^2 (BWRVIP-321-A). It is understood that the RG1.99R2 Position 1.1 (surveillance data not available) ETC will not bound all surveillance, but this is addressed by RG1.99R2 Position 1.2 (surveillance data available). The ISP/ISP(E)/SSLR program will continue to remove and test surveillance capsules, as appropriate, to support the performance of RG1.99R2 Position 1.2. Therefore, this material degradation mechanism is adequately addressed by existing programs, and additional R&D is not necessary at this time. As such, the R&D status is set to Green. [R&D Status = GREEN] **References:** EPRI: BWRVIP-216NP, BWRVIP-321-A Other: [5-11], [5-13]

Table 5-4 (continued)
BWR systems explanatory notes

NOTE ID	EXPLANATORY NOTE
BWR PRIMARY PRESSURE BOUNDARY	
b1-12d	Irradiation embrittlement concerns associated with stainless steel welds or RPV cladding are limited to possible synergism with thermal aging. Cracking of the cladding has been shown to have limited impact on the low-alloy steel base metal because the stress intensity factor is very low. No additional R&D is needed to address this issue for cladding. [R&D Status = GREEN] **Reference:** None
BWR REACTOR VESSEL INTERNALS	
b2-4a b2-4b	Jet pump fouling is an ongoing operational concern. Differences in zeta potential cause accumulation of localized crud buildup on jet pump nozzles and inlet mixers. This buildup creates an operational issue by reducing jet pump performance and can also cause increased vibration that may result in an increase in the set screw gap and subsequent wedge wear or fatigue cracking of riser brace welds or sensing lines. Fouling represents a more important consideration for plants implementing an extended power uprate, where increased flow can aggravate jet pump zeta potential induced deposition. Coatings have been developed that minimize crud buildup. This is an implementation issue that should be tracked in the BWR IMTs. No materials research is warranted. [R&D Status = GREEN] **Reference:** None
b2-5a b2-5b	Wear concerns arise in some BWR internal components and are a direct result of flow-induced vibration. Jet pump assembly components with wear include wedges, adjusting screws, labyrinth seals, and restrainer brackets. Some of these jet pump components are hard-faced with Stellite, which increases ^{60}Co in the reactor water. Wear is also a concern for some upper reactor vessel locations such as vessel lugs, feedwater end brackets, and BWR/6 shroud head studs. Improved operational understanding of FIV and associated wear is an implementation issue that should be tracked in the BWR IMTs. No materials research is warranted. [R&D Status = GREEN] **References:** EPRI: BWRVIP-139R1-A, BWRVIP-301, BWRVIP-41R4 Other: [5-14]
b2-6a b2-6b	See notes b1-6c and b1-6d.
b2-6c	See note b1-6e.
b2-6d	See note b1-6f.
b2-6e b2-6f	See notes b1-6g and b1-6h.

Table 5-4 (continued)
BWR systems explanatory notes

NOTE ID	EXPLANATORY NOTE
BWR REACTOR VESSEL INTERNALS	
b2-6g b2-7g	The as-installed condition of bolting includes moderate tensile stress and threaded regions where stress concentrations occur and where off-normal (crevice) chemistry could develop. However, the bolting material is solution annealed and honed, which significantly reduces the potential for SCC. Field experience has been good; no instances of SCC in stainless steel bolting have been identified. There are a limited number of stainless steel fasteners subject to appreciable neutron fluence. These include core plate pins, core plate rim hold-down bolts, and top guide pins. Neutron fluence increases the yield strength and increases the propensity for SCC. It is mitigated by irradiation creep relaxation that reduces the stress. Since the fluence associated with extended operations is only nominally above the conservative IASCC threshold of $5x10^{20}$ n/cm^2 (E > 1.0 MeV) used for stainless steel components, IASCC is not considered to be a significant concern. The consensus is that no additional R&D is needed. [R&D Status = GREEN] **References:** EPRI: BWRVIP-25R1-A, BWRVIP-26-A
b2-6h	Nitrogen-strengthened stainless steels (Type XM-19) exhibit stress corrosion crack growth behavior in NWC but have been found in experimental studies to be generally far less susceptible to SCC initiation than 300 series stainless steels. Application of XM-19 is relatively limited in BWRs. The primary application is core shroud tie rod repair hardware and selected core plate and top guide applications in late vintage BWR designs. In these applications, XM-19 is used in the solution-annealed condition, and BWR field experience has been excellent. The elevated yield strength of XM-19 increases the SCC growth rate above that for Type 304 and Type 316 stainless steel, and cold work or irradiation will produce a further increase. However, this is a design and implementation issue, and more experimental work is not considered necessary. See note b2-7h. [R&D Status = GREEN] **References:** EPRI: BWRVIP-240, BWRVIP-291R1 Other: [5-15], [5-16]

Table 5-4 (continued)BWR systems explanatory notes

NOTE ID	EXPLANATORY NOTE
BWR REACTOR VESSEL INTERNALS	
b2-6i	Although the fleet-wide operating experience for SCC of Alloy X-750 is reasonably good, there have been some incidents of cracking. Laboratory studies show consistently high SCC growth rates at high ECP. The failures in Alloy X-750 have raised concerns regarding its long-term viability as a reliable material in a BWR environment. Alloy X-750, even in its optimal heat treatment condition (all remaining X-750 in BWR structural applications is in the HTH condition, with the exception of some springs in reactor internals in the spring temper condition), exhibits some susceptibility to SCC initiation as well as moderate growth rates. Alloy X-750 has exhibited susceptibility to IGSCC at applied stresses less than the yield strength at operating temperature. Stress intensification around notches and sharp corners has also been shown to promote cracking where the nominal stress was much lower. Recent testing of Alloy X-750 specimens in the HTH condition confirms that, even under HWC conditions, SCC crack growth rates of engineering significance can occur. While HWC-M/NobleChem™ provides significant mitigation benefits for jet pump beams (particularly for SCC growth rate), it is not expected that HWC-M/NobleChem™ is effective in lowering the ECP at higher elevations in the annulus region, such that mitigation of repair hardware in those locations is unlikely. Given the SCC susceptibility observed, the strategic knowledge gap associated with these materials is the capability to predict component service lifetimes with greater confidence, especially including the effects of irradiation. There are promising alternative alloys (such as Alloy 725) that are much more SCC resistant and should receive further evaluation. Currently, the R&D status is set to Orange to reflect the lack of ongoing or planned work in this area. [R&D Status = ORANGE] **References:** EPRI: BWRVIP-84R3, BWRVIP-218, BWRVIP-138R2, BWRVIP-240, BWRVIP-291R1 Other: [5-15], [5-17]

Table 5-4 (continued)
BWR systems explanatory notes

NOTE ID	EXPLANATORY NOTE
BWR REACTOR VESSEL INTERNALS	
b2-7a b2-7b	Irradiation-assisted stress corrosion cracking (IASCC) is an important concern in assessing the long-term viability of BWR near-core welded structures (e.g., core shrouds, top guides, and jet pump risers). IASCC is affected by radiation hardening, radiation segregation, radiolysis of water, and radiation creep relaxation of constant displacement stresses. The latter includes weld residual stress as well as fit-up stresses. Note that fit-up stresses in the core shroud involve the entire shroud and are not just localized to a weld. Because the fluence varies by more than a factor of 10 around the shroud, and less than 20% of the circumference is well above the average fluence, the fit-up stresses relax much less than weld residual stresses. An additional concern suggested by some field data is the possibility of increasing crack growth rates in highly irradiated materials, possibly reflecting a reduction in the effectiveness of HWC-based mitigation at higher neutron fluence. There is also evidence of this in laboratory data. The multiple (both detrimental and beneficial) factors during irradiation and the uncertainty in the effectiveness of mitigation at low corrosion potential complicate the prediction of future degradation and confidently distinguishing between higher and lower risk (regions and plants). Current research plans include additional characterization of materials harvested from decommissioned or operating reactors, characterization of the effectiveness of HWC technologies (i.e., HWC-M, NMCA, and OLNC) at fluences above 0.75 dpa ($5x10^{20}$ n/cm^2, E > 1.0 MeV) in the laboratory and in plant inspection data. The detrimental impact of helium generation by thermal neutrons on the ability to perform weld repairs on BWR internals affected by IASCC is a related concern that contributes to the R&D status. [R&D Status = YELLOW] **References:** EPRI: BWRVIP-99-A, BWRVIP-100R2, BWRVIP-154R2, BWRVIP-174R3, BWRVIP-253, BWRVIP-302, 3002003103, BWRVIP-97R1, 1021174, BWRVIP Letter 2016-030 Other: [5-18], [5-19]

Table 5-4 (continued)
BWR systems explanatory notes

NOTE ID	EXPLANATORY NOTE
BWR REACTOR VESSEL INTERNALS	
b2-7c	IASCC concerns for BWR reactor vessel internal CASS components are limited to the jet pump assembly, BWR/6 LPCI couplings, and fuel support castings. These concerns are mitigated by design considerations. Jet pumps and LPCI couplings are located in the annulus region where the fast neutron fluence is limited to the low end of the fluence range where IASCC is considered plausible for stainless steels. Fuel support castings receive significant fluence (up to several dpa during extended operations). However, these castings do not contain any structural welds (resulting in lower stresses), do not experience high tensile loads under normal operating conditions, and are readily removable and replaceable. Service experience has been excellent with no reported cracking and with the same fuel support casting design used in operating BWRs for more than 50 years. Thus, additional research is not considered to be warranted. [R&D Status = GREEN] **Reference:** EPRI: BWRVIP-234-A
b2-7d b2-7e b2-7f	RAMA models show that fast neutron fluence estimates for components fabricated from nickel-base Alloys 600, 82, and 182 will not approach a range of IASCC concern (at or below 10^{20} n/cm^2), even during extended operations. Therefore, IASCC is not a concern for these alloys in BWRs. **Reference:** None
b2-7h b2-12h	IASCC and irradiation effects associated with nitrogen strengthened stainless steels (Type XM-19) are possible due to their locations and fluence levels. Type XM-19 is used in shroud repair hardware where the fluence exposure may be sufficient to promote IASCC. Although no welds are present in these components, there is a sustained stress from application of preload in the bolted assemblies, as well as some differential expansion loads. Irradiated XM-19 test data obtained at INL indicate that the SCC growth rate increase is small at the relevant fluence levels, although the data are limited and involve only one heat of XM-19. The R&D status is set to Orange to reflect the lack of ongoing or planned testing in this area. [R&D Status = ORANGE] **References:** EPRI: BWRVIP-240, BWRVIP-291R1, BWRVIP-315-A

Table 5-4 (continued)
BWR systems explanatory notes

NOTE ID	EXPLANATORY NOTE
BWR REACTOR VESSEL INTERNALS	
b2-7i b2-12i	Alloy X-750 BWR internals components are located where end-of-life fluence approaches a level at which IASCC can be a concern. SCC of Alloy X-750 in the absence of irradiation is also a concern (see note b2-6i). At present, key concerns for Alloy X-750 are in shroud tie-rod repair hardware and jet pump hold-down beams. EPRI and INL evaluated IASCC growth rates in irradiated Alloy X-750 specimens and found a limited enhancement relative to non-irradiated data. At high corrosion potential, the non-irradiated and irradiated SCC growth rates were high in Alloy X-750, with significant reduction at low corrosion potential. The R&D status of Orange reflects the lack of ongoing or planned work in this area to address the knowledge gap. [R&D Status = ORANGE] **References:** EPRI: BWRVIP-240, BWRVIP-291R1 Other: [5-20], [5-21]
b2-8a b2-8b b2-8c b2-8d b2-8e b2-8f b2-8g b2-8h b2-8i	High-cycle fatigue is a concern for some BWR internals components, particularly steam dryers and jet pumps. High-cycle fatigue of some steam dryer locations has become an acute issue after power uprates. Higher steam velocities at uprated power levels resulted in new acoustic resonance loads being introduced into the upper reactor vessel steam space, leading to dryer damage and replacement of steam dryers in some cases. High-cycle fatigue has also been observed in jet pump assemblies. Cracking is driven by FIV at the slip joint and/or the vane passing frequency of the recirculation pumps. Areas of concern include riser braces, riser pipes near the brace attachment, and sensing lines. High-cycle fatigue concerns for BWR reactor internals are primarily a design and implementation issue. Any gaps related to management of steam dryer and jet pump vibration are appropriately addressed in the BWR IMTs. [R&D Status = GREEN] **References:** EPRI: BWRVIP-41R4, BWRVIP-139R1-A, BWRVIP-252, BWRVIP-266

Table 5-4 (continued)
BWR systems explanatory notes

NOTE ID	EXPLANATORY NOTE
BWR REACTOR VESSEL INTERNALS	
b2-9a b2-9b b2-9c b2-9d b2-9e b2-9f b2-9g b2-9h b2-9i	For irradiated reactor internals, there are relatively limited data related to the effects of neutron fluence on fatigue life and crack growth rates. It is presently not clear whether there is any effect of neutron irradiation with respect to environmental effects on fatigue life, except that irradiation raises the yield strength and thereby potentially decreases the endurance limit. However, fatigue usage values for near-core reactor internals experiencing relatively high neutron fluence (up to 1 dpa) are quite low, generally below 0.1. As a result, no additional R&D is presently needed to address environmental fatigue life effects for highly irradiated reactor internals. Concerning fatigue crack propagation rates, a recently completed study of irradiated stainless steels has identified and modeled a deleterious effect of irradiation in the form of a superposition model with IASCC growth rates. It is considered that the model is robust for NWC conditions. However, the database for combined BWR HWC and PWR primary conditions should be expanded because of the low number of available specimens and high scatter caused by one particular heat. Ongoing programs addressing IASCC are anticipated to generate as a byproduct of additional corrosion fatigue crack growth data required to fill this R&D gap so that “Y” and Yellow are considered appropriate for the stainless steel materials for which management by crack growth is appropriate. This pertains specifically to cells b2-9a and b2-9b. For other materials, there remains little evidence that R&D is needed. The materials are not subject to high fluence and are inspected routinely for the purpose of managing IGSCC concerns. In practical terms, components are managed with the presumption of some cracking due to IGSCC. FCGRs are relatively small in comparison to assumed IGSCC CGRs. Therefore, additional R&D is not considered to be warranted at this time. [R&D Status = YELLOW] (for irradiated stainless steel structures) [R&D Status = GREEN] (for all other material types) [*NOTE: The effect of environment and associated R&D needs described for pressure-retaining components in note b1-9a remain generally applicable to reactor internals. However, the results shown here focus on the unique aspect of irradiation that is applicable to reactor internals only*.] **Reference:** EPRI: 3002007969
b2-10b	See note b1-10d.

Table 5-4 (continued)
BWR systems explanatory notes

NOTE ID	EXPLANATORY NOTE
	BWR REACTOR VESSEL INTERNALS
b2-10c b2-12c	Concerns for BWR reactor internals are limited because of the lower operating temperatures compared to PWRs and the very limited use of high molybdenum castings (CF8M) in BWRs. BWRVIP-234-A documents the results of a comprehensive assessment of thermal and irradiation embrittlement. This assessment, however, was based heavily on weld metal data. The additional weld metal correlations included in BWRVIP-100, Revision 2, shifted the threshold fluence from $6x10^{20}$ n/cm^2 to $<1x10^{20}$ n/cm^2 (E > 1.0 MeV). The end-of-life fluence for the orificed fuel supports and jet pump assembly castings can exceed the radiation-induced embrittlement threshold. With respect to the irradiation embrittlement of CASS, some key data gaps exist. CASS fracture toughness data are limited (especially in the 0.1 to 1.0 dpa range), and it is unclear to what extent CASS conforms to the same fracture toughness trends of weld metal. Furthermore, there is a lack of data for low Mo materials (CF3/CF8) between 1 and 5 dpa as well as a lack of data for CASS materials with concurrent irradiation dose and thermal exposure for greater than 1 dpa. The R&D status of Orange reflects the lack of ongoing or planned work in this area to address these knowledge gaps. [R&D Status = ORANGE] **References:** EPRI: BWRVIP-234-A, BWRVIP-100R2
b2-11a	Research shows that wrought stainless steel can exhibit some reduction in fracture resistance properties due to exposure to the primary system coolant. For non-irradiated components, these reductions are less significant than for irradiated materials or for highly cold-worked materials. The increased yield strengths resulting from irradiation are cause for additional investigation. Some limited J-R testing (at LWR operating temperature) of irradiated stainless steels was performed on a Type 316 stainless steel control rod blade with 6.7 dpa removed from a Swedish BWR plant. Results show that there is little or no effect of BWR and PWR environments on fracture resistance. However, this conclusion is only true for specimens containing transgranular pre-cracks generated in air at room temperature. There were indications of an effect of the BWR environment on fracture resistances for specimens containing intergranular pre-cracks. [*NOTE: Observations of rapid fracture under rising K in SCC and fatigue tests can be due to plastic instability resulting from mechanical overload conditions, and subsequent studies have shown no evidence of an effect of environment.*] [R&D Status = ORANGE] **Reference:** EPRI: 1025124
b2-11b	See note b1-11d.
b2-11c	See note b1-11e.
b2-11d	See note b1-11f.
b2-11e	See note b1-11g.

Table 5-4 (continued)
BWR systems explanatory notes

NOTE ID	EXPLANATORY NOTE
BWR REACTOR VESSEL INTERNALS	
b2-11f	See note b1-11h.
b2-11g	See note b1-11c.
b2-11h	Possible reductions in fracture properties of Type XM-19 due to exposure to the BWR environment have not been sufficiently studied. The present understanding is that some effect of environment likely exists. In addition, strengthening by irradiation hardening may elevate the potential for this phenomenon to occur in this alloy. EPRI and INL studies on the J-R response of irradiated XM-19 showed a reduction above ~0.3 dpa. Due to the lack of ongoing or planned testing in this area, an Orange R&D status is applied. [R&D Status = ORANGE] **References:** EPRI: BWRVIP-240, BWRVIP-291R1, 1025124
b2-11i	Alloy X-750 is susceptible to environmental effects on fracture, particularly at low temperature operation. Crack growth by SCC is a concern because of the material's high yield strength. EPRI and INL evaluated the effects of irradiation on toughness and observed a progressive reduction above about 0.3 dpa. Additional work is needed to characterize material responses so that guidance for plant operation can be provided. Additional data are also needed to characterize performance at higher temperatures, particularly regarding high SCC growth rates. [R&D Status = ORANGE] **Reference:** EPRI: MRP-293

Table 5-4 (continued)
BWR systems explanatory notes

NOTE ID	EXPLANATORY NOTE
BWR REACTOR VESSEL INTERNALS	
b2-12a b2-12b	Some reduction in ductility of stainless steels occurs at fluences as low as $1x10^{20}$ n/cm^2 (E > 1.0 MeV). Above $1x10^{21}$ n/cm^2 (~1.5 dpa), uniform elongation is typically less than 1%. Irradiation also reduces toughness. BWRVIP-76-A establishes a threshold of $3x10^{20}$ n/cm^2 (E > 1.0 MeV) for flaw evaluation, using limit load techniques. Data show that the reduction in toughness with irradiation saturates at some fluence level. However, in some cases, the saturated toughness for this material class is quite low. While higher fluence yields an increased He level (all other parameters being equal), and a small volume fraction of new phases can form, the current understanding is that the observed saturation values of toughness will not be reduced further by levels of irradiation damage calculated for BWR structural components. This degradation mechanism is not a concern for long-term operation of 300-series stainless steel base metal with fluence values below $1x10^{20}$ n/cm^2 (E > 1.0 MeV). Existing data characterize embrittlement trends up to a neutron fluence of approximately 90 dpa (PWR relevant fluence), which exceeds the end-of-life fluence for BWR internals by a large margin. However, the high fluence response of weld and HAZ materials, including assessment of high fluence saturation values, is not as well established. Ongoing work planned to address gaps in the data for PWRs will adequately bound BWR operations. A Yellow R&D status is retained until the ongoing work is completed and the results are evaluated. [R&D Status = YELLOW] **References:** EPRI: BWRVIP-76R1, BWRVIP-99-A, BWRVIP-100R2, BWRVIP-154R2, BWRVIP-221, BWRVIP-294R2, MRP-320 Other: [5-18], [5-19]
b2-12g	Stainless steel bolting located near the core (e.g., core plate hold-down bolts) may experience some irradiation embrittlement. Although some irradiation embrittlement will likely occur, the existing databases exceed the end-of-life fluences anticipated by a large margin. [R&D Status = GREEN] **References:** EPRI: BWRVIP-100R2, MRP-50, MRP-175R1, MRP-211R1
b2-14a b2-14b	This phenomenon is considered generally beneficial for welded stainless steel structures, as reduced internal stresses tend to reduce SCC susceptibility; although, there may be concerns for the extent and asymmetry of stress relaxation for some components. No R&D is needed. [R&D Status = GREEN] **Reference:** None

Table 5-4 (continued)
BWR systems explanatory notes

NOTE ID	EXPLANATORY NOTE
BWR REACTOR VESSEL INTERNALS	
b2-14g	Irradiation-enhanced stress relaxation is a concern only for bolted connections where loss of joint preload can have a detrimental impact on the function of the component or associated assembly (e.g., core plate hold-down bolts). Stainless steel components in shroud restraint assemblies will also receive fast neutron doses that are sufficient to promote irradiation-enhanced stress relaxation. However, this issue is primarily an implementation issue associated with ensuring that adequate fastener preload is maintained. The phenomenon of irradiation-enhanced stress relaxation is relatively well quantified for 300 series stainless steels in the range of fluences applicable to BWRs. Additional R&D is not needed. [R&D Status = GREEN] **References:** EPRI: MRP-50, MRP-175R1, MRP-211R1 Other: [5-15]
b2-14h b2-14i	Irradiation-enhanced stress relaxation concerns are primarily focused on bolted connections where loss of joint preload can have a detrimental impact on the function of the component or associated assembly. Type XM-19 and Alloy X-750 components in shroud restraint assemblies will receive fast neutron doses that are sufficient to promote irradiation-enhanced stress relaxation. The phenomenon of irradiation-enhanced stress relaxation is relatively well understood in the fluence ranges applicable to BWRs. However, for Alloy X-750, there is evidence of higher irradiation-enhanced stress relaxation rates than for 300 series stainless steels. Extended operations and higher neutron fluence may be a concern for some repair hardware components. For Alloy X-750 and XM-19, there are relatively few data to quantify the trend. No R&D is in progress. Although it is possible to manage this issue through ongoing preload checks, improved relaxation correlations would be beneficial. Conservatively, an Orange R&D status is assigned. [R&D Status = ORANGE] **References:** EPRI: BWRVIP-240, BWRVIP-291R1, MRP-50, MRP-175R1, MRP-211R1 Other: [5-15]

Table 5-4 (continued)
BWR systems explanatory notes

NOTE ID	EXPLANATORY NOTE
BWR EXTERNAL SURFACES AND BOLTING	
b3-2a b3-2g	External surface pitting is considered plausible for all materials of construction if the material is exposed to moist or wetted conditions continuously or periodically, especially when chloride is present. Pitting is well understood, and no additional research is needed. [R&D Status = GREEN] **Reference:** EPRI: 3002018322
b3-6b b3-6c b3-6d	It is known that exposure to significant concentrations of contaminants and periodic wetting can initiate SCC in stainless steel piping and welds. Most of the incidences of ODSCC have occurred in the presence of chlorides. The susceptibility of austenitic stainless steels to chloride-induced SCC is widely known, even if it is non-sensitized and exposed at moderate temperature and relatively low stress. ODSCC is not usually detected prior to development of through-wall cracking and associated leakage. Although there are increased concerns regarding ODSCC as a result of recent PWR events, at this time, the phenomenon is well understood, and no additional research is needed. [R&D Status = GREEN] **Reference:** EPRI: 3002018322
b3-6g	Cracking of high-strength, low-alloy steel bolting is possible in the presence of unstable lubricants (notably MoS_2) or harsh environments. Other carbon and low-alloy steel external surfaces are not susceptible to SCC under atmospheric conditions. Cracking susceptibility is typically associated with excessive hardness (Rockwell-C > 40) and is of limited concern because bolting is controlled to Rockwell-C values of 38 or less. No additional R&D is needed since the SCC characteristics of low-alloy steel fastener materials are relatively well understood and the industry understands that unstable lubricants should not be used. [R&D Status = GREEN] **Reference:** EPRI: 3002018322
b3-7a b3-7b b3-7c b3-7d b3-7e b3-7f b3-7g b3-7h	Externally initiated cracking due to high-cycle fatigue is possible. Typically, externally initiated high-cycle fatigue cracking is the result of acoustic or mechanical loading and is affected by time (cycles) but not from aging phenomena. While cracking may occur as a result of improper design, these phenomena are well understood, and no additional degradation mechanism research is needed. [R&D Status = GREEN] **Reference:** None

Table 5-4 (continued)
BWR systems explanatory notes

NOTE ID	EXPLANATORY NOTE
BWR EXTERNAL SURFACES AND BOLTING	
b3-8a b3-8b b3-8c b3-8d b3-8e b3-8f	Low-cycle fatigue cracking initiating at a component external surface may occur if the external surface loading dominates over the loading at the internal surface. It is noted that internal surface fatigue usage can still be limiting when the effects of reactor coolant on fatigue behavior are considered. Fatigue usage of these materials in air is well documented and addressed by ASME Section III. No additional research specific to external surfaces is needed. [R&D Status = GREEN] **Reference:** None
b3-8g b3-8h	Low-cycle fatigue of pressure-retaining fasteners is well understood. No additional research is warranted at this date. Extended operations may result in the fatigue usage estimates exceeding 1.0 for some ASME Class 1 fastener locations. Where this occurs, affected units would need to either refine existing fatigue analyses to remove conservatisms or replace the fasteners. However, this is an implementation issue, and no R&D is needed. [R&D Status = GREEN] **Reference:** None

5.3 References

NOTE: References listed here do not include published EPRI reports. Access to the full citation of each EPRI report listed in this section is available through use of the hyperlinks provided. If a hyperlink is not available, this report has been archived and is no longer directly accessible on epri.com.

[5-1] NEI 03-08, Revision 3, Guideline for the Management of Materials Issues, February 2017.

[5-2] Roth, A., et al., "Influence of Dynamic Strain Ageing on the Crack Growth Rates and Crack Tip Plasticity of Low-Alloy Steels in Oxygenated High Temperature Water." Presented at the 14th International Conference on Environmental Degradation of Materials in Nuclear Power Systems, Virginia Beach, VA, August 2009.

[5-3] K. Kumagai, S. Suzuki, Y. Takagi, M. Morra, P. Andresen, G. Catlin, L. Nelson, and R. Horn, "Effects of K and Anion Impurity, Concentration, on Crack Growth Kinetics Near Alloy 182/A533B Weld Overlay Boundaries in BWRs." Presented at the 14th International Conference on Environmental Degradation of Materials in Nuclear Power Systems, Virginia Beach, VA, August 2009.

[5-4] Ritter, S., et al., "The Environmentally Assisted Behaviour in the Transition Region of Nickel-Base Alloy/Low-Alloy Steel Dissimilar Metal Weld Joints Under Simulated BWR Conditions," Paul Scherrer Institute, Fontevraud 7, September 2010.

[5-5] Z. Que, H. P. Seifert, P. Spaetig, G. S. Rao, and S. Ritter, "Effect of High-Temperature Water and Hydrogen on the Fracture Behavior of Low-Alloy Steels," Paul-Scherrer Institute, Environmental Degradation, 2017.

[5-6] BWRVIP 2016-123, Transmittal of Interim Guidance for BWR Water Chemistry Guidelines, November 2, 2016.

[5-7] S. Suzuki, "BWR Materials Research for Ageing Management in TEPCO." Presented at the International Symposium on the Ageing Management and Maintenance of Nuclear Power Plants, February 22, 2007.

[5-8] N. R. Hughes, W. L. Clarke, and D. E. Delwiche, Stainless Steel Castings, ASTM STP 756. In: V. G. Behal and A. S. Melilli, eds. *Intergranular Stress Corrosion Cracking Resistance of Austenitic Stainless Steel Castings* (pp. 26–47). Philadelphia: American Society for Testing and Materials, 1982.

[5-9] GEH SIL 433, Supplement 2, Shroud Head Bolt Failure.

[5-10] J. R. Hixon, J. H. Kim, and R. G. Ballinger, "Effect of Thermal Aging on SCC and Mechanical Properties of Stainless Steel Weld Metals." Presented at the 13th International Conference on Environmental Degradation of Materials in Nuclear Power Systems, Whistler, British Columbia, 2007.

[5-11] L. A. James and W. C. Porr, "The Effect of an Elevated Temperature Aqueous Environment Upon the J-controlled Tearing of a Low Alloy Steel," *International Journal of Pressure Vessels and Piping*, Vol. 76, pp. 769–779 (1999).

[5-12] Nanstad and Odette, "Development of a Robust Predictive Embrittlement Model for Reactor Pressure Vessel Lifetime Extension," D.O.E. Light Water Reactor Sustainability Newsletter, Issue 6, December 2011.

[5-13] Soneda, N., et al., "Flux Effect on Neutron Irradiation Embrittlement of Reactor Pressure Vessel Steels Irradiated to High Fluences," INIS-FR-11-0561, Conference Fontevraud 7, July 1, 2011.

[5-14] BWRVIP 2009-202, Interim Guidance for Accelerated Inspections of Jet Pump Riser to Riser Brace Welds and Wedges, June 18, 2009.

[5-15] INL/EXT-11-24173, Baseline Fracture Toughness and CGR Testing of Alloys X-750 and XM-19 (EPRI Phase 1), February 2012.

[5-16] M. J. Povich and D. E. Broecker, "The Stress Corrosion Cracking of Austenitic Stainless Steel Alloys in High Temperature Air Saturated Water," *Materials Performance (NACE)*, Vol. 18, No. 10 (1979).

[5-17] BWRVIP 2011-011, Guidance for Evaluating Repair Hardware with X-750 Components, January 19, 2011.

[5-18] NUREG/CR-6960, Crack Growth Rates and Fracture Toughness of Irradiated Austenitic Stainless Steels in BWR Environments, U.S. Nuclear Regulatory Commission, March 2008.

[5-19] NUREG/CR-6965, Irradiation-Assisted Stress Corrosion Cracking of Austenitic Stainless Steels and Alloy 690 from Halden Phase 11 Irradiations, U.S. Nuclear Regulatory Commission, September 2008.

[5-20] R. Bajaj, W. J. Mills, M. R. Lebo, B. Z. Hyatt, and M. G. Burke, "Irradiation-Assisted Stress Corrosion Cracking of HTH Alloy X-750 and Alloy 625." In: Proceedings of the Seventh International Symposium on Environmental Degradation of Materials in Nuclear Power Systems—Water Reactors, American Nuclear Society, 1997.

[5-21] W. J. Mills, "Post-Irradiation Fracture Toughness of Inconel X-750," *Engineering Fracture Mechanics*, Vol. 18, No. 3, pp. 601–607 (1983).

[5-22] O. M. Chopra, *Development of Fatigue Design Curve for Austenitic Stainless Steels in LWR Environments: A Review*. ASME PVP 439, January 2002.

6
VVER DEGRADATION MATRIX RESULTS

6.1 Scope and Evaluation Assumptions

The VVER MDM results presented in this section are based on generic evaluation by a panel of subject matter experts and updated for this Revision 5 after consultation with the appropriate EPRI program and project managers concerning progress made since the last revision. See Section 2.1 for additional discussion and notes regarding the assessment process.

The VVER is a type of pressurized water reactor (PWR) that was developed in Russia (in the former Soviet Union), employing light water as a coolant and moderator. The units considered in this revision of the MDM are the 440 MWe Type 213 (VVER 440) and 1000 MWe Type 320 (VVER 1000) designs operating in Finland, the Czech Republic, and Hungary.

There are some significant differences between VVERs and the PWRs reviewed in Section 4, both in terms of design and materials used. Distinguishing features of the VVER include:

- Horizontal steam generators (SGs) equipped with austenitic stainless steel tube bundles that terminate in vertical cylinders, known as *collectors*, that penetrate the SG pressure boundary to allow primary water to flow through the tubes.
- Hexagonal fuel assemblies.
- Top-mounted in-core instrumentation, thereby avoiding RPV bottom head penetrations.
- High-capacity pressurizers.
- Spent fuel pools located inside the containment building and close to the RPV that are typical in many of the Western-design PWRs.
- Primary water chemistry using KOH for pH control and boric acid for nuclear reactivity control in the range 7.0 to 7.2 at operating temperature, and NH_3 as a source of hydrogen.
- Materials of construction that were specified consistent with Eastern European/Soviet standards, primarily a set of Soviet state standards in use at the time of design (designated by the acronym GOST, which is derived from Russian words meaning “state standard”). Notable differences between these material specifications and typical Western specifications for LWR service include:
  - Use of Ti-stabilized stainless steels using grades specified to Russian standards.
  - Use of low-alloy steels that contain a nominally higher percentage of Cr and a nominally lower percentage of Mn.

The scope of VVER systems and components evaluated includes the RPV; primary system pressure boundary piping, including the pressurizer, main coolant pump, and valve bodies; external bolting and reactor vessel supports; reactor vessel internals; and SGs (primary and secondary sides). Active components (e.g., control rod drives, valve internals, and pump rotating assemblies) and short-lived components (e.g., fuel assemblies) are not included in the evaluation.

All normal operating conditions were considered. These include normal power operations, startup, shutdown, and layup for SGs. Normal operating conditions are defined to include less well controlled environmental conditions, such as significant oxygen ingress that may occur during maintenance periods and persist for some limited time during startup.

The normal range of secondary all-volatile treatment (AVT) water chemistries was considered, together with limited effects of impurities and the way in which these can concentrate (e.g., in SG heated crevices).

The potential for nominally off-normal environments to occur was also considered (e.g., areas subject to oxygen transients for a limited time due to trapped air bubbles after refueling outages).

6.2 VVER Results: Degradation Matrix Tables and Explanatory Notes

The VVER MDM results are presented in the following set of degradation matrix tables:

Table 6-1 VVER 440 Reactor Pressure Vessel

Table 6-2 VVER 1000 Reactor Pressure Vessel

Table 6-3 VVER Primary System Piping Components

Table 6-4 VVER Reactor Vessel Internals

Table 6-5 VVER Steam Generator Tube Bundle and Internals

Table 6-6 VVER Steam Generator Secondary Pressure Boundary

Table 6-7 VVER External Surfaces, Supports, and Pressure-Retaining Bolting

Hyperlinks within these tables lead to summary notes contained in Table 6-8. The degradation matrix tables include the use of abbreviations and color coding. Cell *Y*, *N*, *?*, and *N/A* designations indicate applicability of the degradation mode to a material type. Comprehensive definitions are provided in Section 2.2.3.1.

Cell shading indicates R&D status:

- Green fill indicates that the degradation mechanism is sufficiently well understood.
- Yellow fill indicates R&D is in progress to address gaps associated with the degradation mechanism in a reasonable time frame.
- Orange fill indicates insufficient R&D is ongoing or planned to address gaps associated with the degradation mechanism in a reasonable time frame.
- Blue fill indicates insufficient data exist to establish degradation mechanism applicability.

Comprehensive definitions of MDM color codes are provided in Section 2.3.3.2.

Changes to cell results for Revision 5 can be found in Appendix D.

Table 6-1
VVER 440 reactor pressure vessel

MATERIAL	DEGRADATION MODE												
	Corrosion				Wear	SCC		Fatigue		Reduction in Frac. Properties		Irradiation Effects		
	Wstg.	Pitting	FAC	Foul		IG/TG	IA	HCF	EAF	Th	Env	Emb	VS	IC/SR
C&LAS: Base Metal & HAZ[1]	N	Y v1-2a	N	N	N	N	N	N	N	Y v1-10a	N	Y v1-12a	N	N
C&LAS: Welds[2]	N	N	N	N	N	N	N	N	N	Y v1-10b	N	Y v1-12b	N	N
SS Welds & Cladding[3]	N	N	N	N	N	Y v1-6c	N	N	Y v1-9c	Y v1-10c	N	Y v1-12c	N	N
SS: Ti Stabilized (08Ch18N10T)	N	Y v1-2d	N	N	N	Y v1-6d	N	N	Y v1-9d	Y v1-10d	N	N	N	N

1. Includes the following grades: 15Ch2MFA, 18Ch2MFA, 25Ch3MFA, 22K (carbon steel).
2. Includes the following grades: Sv10ChMFT (flux – AN-42), Sv08A.
3. Includes the following grades: EA 898/21B, ZIO 8, Sv08C19N10G2B.

Table 6-2
VVER 1000 reactor pressure vessel

MATERIAL	DEGRADATION MODE													
	Corrosion				Wear	SCC		Fatigue		Reduction in Frac. Properties		Irradiation Effects		
	Wstg.	Pitting	FAC	Foul		IG/TG	IA	HCF	EAF	Th	Env	Emb	VS	IC/SR
LAS: Base Metal & HAZ[1]	N	Y v2-2a	N	N	N	N	N	N	N	Y v2-10a	N	Y v2-12a	N	N
CS (22K, 20)	N	N	N	N	N	N	N	N	N	Y v2-10b	N	Y v2-12b	N	N
C&LAS Welds[2]	N	N	N	N	N	N	N	N	N	Y v2-10c	N	Y v2-12c	N	N
SS Welds & Cladding[3]	N	N	N	N	N	Y v2-6d	N	N	Y v2-9d	Y v2-10d	N	Y v2-12d	N	N
SS: Ti Stabilized (08Ch18N10T)	N	Y v2-2e	N	N	N	Y v2-6e	N	N	Y v2-9e	Y v2-10e	N	N	N	N

1. Includes the following grade: 15Ch2NMFA.
2. Includes the following grades: Sv-12Ch2NMFTA, Sv-16Ch2NMFTA, Sv-08ChGNMTA, Sv-10ChGNMAA, Sv-08A, Sv-06A.
3. Includes the following grades: EA-395/9, EA-400/10T, Sv-07Ch25N13, Sv-04Ch20N10G2B, ZIO-8, CL-25, EA-898/21B.

Table 6-3
VVER primary system piping components (including the pressurizer)

MATERIAL	DEGRADATION MODE														
	Corrosion					Wear	SCC		Fatigue		Reduction in Frac. Properties		Irradiation Effects		
	Wstg.	Pitting	FAC	Foul	IGA		IG/TG	IA	HCF	EAF	Th	Env	Emb	VS	IC/SR
VVER 440 (ALL PIPING COMPONENTS[1]) AND VVER 1000 (BRANCH LINES ONLY[2])															
SS: Ti-Stabilized (08Ch18N10T, 08Ch18N12T)	N	Y v3-2a	N	N	Y v3-5a	N	Y v3-7a	N	Y v3-9a	Y v3-10a	N	N	N	N	N
CASS and SS: Welds (UONI 13/55)	N	N	N	N	Y v3-5b	N	Y v3-7b	N	Y v3-9b	Y v3-10b	N	N	N	N	N
VVER 1000 (LARGE BORE PIPING COMPONENTS[2]) AND PRESSURIZER[3]															
C&LAS (10GN2MFA) **C&LAS Welds**	N	N	N	N	N	N	N	N	N	N	Y v3-11c	N	N	N	N
SS: Cladding (08Ch18N10T)	N	N	N	N	Y v3-5d	N	Y v3-7d	N	N	Y v3-10d	N	N	N	N	N
CASS and SS: Welds (PT-30)	N	N	N	N	Y v3-5e	N	Y v3-7e	N	N	Y v3-10e	Y v3-11e	N	N	N	N

1. VVER 440 primary system piping components are all austenitic stainless steel construction.
2. VVER 1000 primary system branch lines have austenitic stainless steel construction, similar to VVER 440. However, the VVER 1000 main reactor coolant loop components are clad with stainless steel.
3. Materials applicable to pressurizers include C&LAS and SS cladding.

Table 6-4
VVER reactor vessel internals

MATERIAL		DEGRADATION MODE													
	Corrosion					Wear	SCC		Fatigue		Reduction in Frac. Properties		Irradiation Effects		
	Wstg.	Pitting	FAC	Foul	IGA		IG/TG	IA	HCF	EAF	Th	Env	Emb	VS	IC/SR
SS: Ti-Stabilized[1]	N	Y v4-2a	N	N	Y v4-5a	Y v4-6a	Y v4-7a	Y v4-8a	Y v4-9a	Y v4-10a	N	Y v4-12a	Y v4-13a	Y v4-14a	Y v4-15a
SS: Welds	N	N	N	N	Y v4-5b	Y v4-6b	N	Y v4-8b	Y v4-9b	Y v4-10b	Y v4-11b	Y v4-12b	Y v4-13b	Y v4-14b	Y v4-15b
SS: Martensitic[2] (VVER 440 only)	N	Y v4-2c	N	N	N	Y v4-6c	Y v4-7c	Y v4-8c	Y v4-9c	Y v4-10c	Y v4-11c	Y v4-12c	Y v4-13c	Y v4-14c	Y v4-15c
PH High Ni Stainless Steel[2]	N	N	N	N	N	Y v4-6d	N	Y v4-8d	Y v4-9d	Y v4-10d	Y v4-11d	Y v4-12d	Y v4-13d	N	N

1. Includes both internal structures (base metal and HAZ material) as well as baffle bolts.
2. Material associated with internal fasteners/hardware.

Table 6-5
VVER steam generator tube bundle and internals

MATERIAL	DEGRADATION MODE											
	Corrosion				Wear	SCC		Fatigue		Reduction in Frac. Properties		Stress Relax.
	Wstg.	Pitting	FAC	Foul		PS (ID)	SS (OD)	HCF	EAF	Th	Env	
TUBES, TUBE PLUGS, AND TUBESHEET WELDS												
SS: Ti-Stabilized Austenite	N	Y v5-2a	N	Y v5-4a	Y v5-5a	N	Y v5-7a	Y v5-8a	Y v5-9a	N	N	N/
SECONDARY SIDE INTERNALS												
SS: Ti-stabilized Austenite, SS Welds and HAZ, incl. DMW	N	Y v5-2b	N	Y v5-4b	Y v5-5b	N/A	Y v5-7b	Y v5-8b	Y v5-9b	N	N	N
C&LAS Base Metal and Welds	Y v5-1c	Y v5-2c	Y v5-3c	N/A	Y v5-5c	N/A	Y v5-7c	Y v5-8c	Y v5-9c	N	N	Y v5-12c
PRIMARY CIRCUIT COLLECTORS												
SS: Ti-Stabilized Austenite (VVER 440 only)	N	Y v5-2d	N	Y v5-4d	Y v5-5d	N	Y v5-7d	N	Y v5-9d	N	N	N
LAS (VVER 1000 only)	Y v5-1e	Y v5-2e	Y v5-3e	Y v5-4e	Y v5-5e	N	Y v5-7e	N	Y v5-9e	N	N	N
High Ni Stainless Steel	N	N	N	N/A	Y v5-5f	N	Y v5-7f	Y v5-8f	Y v5-9f	Y v5-10f	N	N

PS = Primary-Side (Tube ID, primary water chemistry environment).

SS = Secondary-Side (Tube OD, secondary water chemistry environment).

Table 6-6
VVER steam generator secondary pressure boundary

MATERIAL	DEGRADATION MODE										
	Corrosion				Wear	SCC		Fatigue		Reduction in Frac. Properties	
	Wstg.	Pitting	FAC	Foul		PS	SS	HCF	EAF	Th	Env
SS: Ti-Stabilized Austenite	N	Y v6-2a	N	N	Y v6-5a	N/A	Y v6-7a	Y v6-8a	Y v6-9a	N	N
SS: Welds and HAZ (incl. DMW)	N	Y v6-2b	N	N	Y v6-5b	N/A	Y v6-7b	Y v6-8b	Y v6-9b	N	N
LAS: Base Metal (VVER 1000 only)	Y v6-1c	Y v6-2c	Y v6-3c	Y v6-4c	Y v6-5c	N/A	Y v6-7c	N	Y v6-9c	Y v6-10c	N
CS: Base Metal (VVER 440 only)	Y v6-1d	Y v6-2d	Y v6-3d	Y v6-4d	Y v6-5d	N/A	Y v6-7d	N	Y v6-9d	Y v6-10d	N
C&LAS: Welds	Y v6-1e	Y v6-2e	Y v6-3e	Y v6-4e	Y v6-5e	N/A	Y v6-7e	N	Y v6-9e	Y v6-10e	N

PS = Primary-Side (i.e., primary water chemistry environment, not applicable to SG secondary pressure boundary components).

SS = Secondary-Side (i.e., secondary water chemistry environment).

Table 6-7
VVER external surfaces,[1] supports, and pressure-retaining bolting

MATERIAL	DEGRADATION MODE													
	Corrosion				Wear	SCC		Fatigue		Reduction in Frac. Properties		Irradiation Effects		
	Wstg.	Pitting	FAC	BAC		IG/TG	IA	HCF	LCF	Th	Env	Emb	VS	IC/SR
RPV SUPPORTS														
C&LAS Base Metal[2]	N	N	N	Y v7-4a	N	N	N	N	N	Y v7-10a	N	Y v7-12a	N	N
C&LAS Welds[3]	N	N	N	Y v7-4b	N	N	N	N	N	Y v7-10b	N	Y v7-12b	N	N
PRESSURE-RETAINING BOLTING														
VVER 440 – LAS[4(a)]	N	N	N	Y v7-4c	Y v7-5c	N	N	N	Y v7-9c	N	N	N	N	N
VVER 1000 – LAS[4(b)]	N	N	N	Y v7-4d	Y v7-5d	N	N	N	Y v7-9d	N	N	N	N	N

1. MDM results for external surfaces of structural components are the same as those for Western PWRs. See Table 4-6.
2. Grades: 11 375.1, 11 378, 12 022.1, 422 643.5, 14 140.9.
3. Grades: UONI 13/55.
4(a). Grades: 38ChN3MA, 25Ch1MF, 12Ch1MF.
4(b). Grades: 25Ch2MFA, 38ChN3MFA.

Table 6-8
VVER explanatory notes

NOTE ID	EXPLANATORY NOTE
VVER 440 REACTOR PRESSURE VESSEL	
v1-2a	The pitting corrosion risk applies to C&LAS locations without cladding, which can only be due either to localized damage or to slag channels present in the cladding of some RPVs. Pitting can only occur if oxygen is present, which implies that the main risk is during refueling and then only if an acidic anion impurity like chloride is also present. [R&D Status = GREEN]
v1-2d	The only potential location for pitting in stainless steel is above the water level during outages (based on the situation at Loviisa) when oxygen is present and with higher concentrations of acidic anionic chemical impurities than specified in the coolant. The mechanism is theoretically possible but has not been observed to date. [R&D Status = GREEN]
v1-6c	SCC (and EAF) is hypothetically possible if there is a through-clad defect, aqueous impurities, and sufficiently high stress. There is a known case in a Loviisa pressure vessel where slag inclusions could possibly interact with the inner surface of the C&LAS vessel. In the case of the Dukovany plant (vessels manufactured by ŠKODA), any breach of the rules for the integrity of such weld overlays would most likely be avoided since the slag channels were detected mainly between the base material and the first weld clad layer. This has been confirmed by the results of NDT. Nevertheless, the emergence of these defects at the internal RPV surface by fatigue crack growth cannot be completely excluded in the future. [R&D Status = GREEN]
v1-6d	IGSCC of stabilized SS is considered possible, with the highest risk associated with stagnant locations. Welded zones are the critical locations. There is some disagreement among specialists as to whether the influencing parameters are sufficiently well characterized. The green color assigned, which is consistent with the present Western PWR position, reflects the VVER plant operators' perspective that additional R&D would not significantly affect plant management of the issue via appropriate primary water chemistry controls. [R&D Status = GREEN]

Table 6-8 (continued)
VVER explanatory notes

NOTE ID	EXPLANATORY NOTE
VVER 440 REACTOR PRESSURE VESSEL	
v1-9c v1-9d	In the fatigue life evaluation procedures of NTD ASI (Normative Technical Documentation of the Czech Association of Mechanical Engineers), the environmental factor influencing the development of fatigue is not addressed adequately. The latest experimental work has shown decreasing fatigue endurance with exposure to the VVER primary water environment similar to that observed in studies of PWR primary circuit austenitic stainless steels. A national research project was initiated in the Czech Republic to better understand the mechanism of EAF and, if possible, to remove conservatism from the present methodologies for fatigue life calculations. Material testing under this project includes non-irradiated stainless steels. In the case of the calculated cumulative usage factors for the RPV, the values are higher in the low irradiated locations. Therefore, EAF testing of irradiated materials was not deemed necessary for the RPV. Due to the considerable work being carried out under this program, the R&D status is set to Yellow. [R&D Status = YELLOW]
v1-10a v1-10b	Laboratory accelerated simulations of 60 years of operation indicate thermal stability of these materials at reactor operating temperatures, typically 270°C in 440 MWe plants (with a primary hot leg water temperature of 297°C). Similar behavior of the weld metal is expected. The pressurizer operates at 325°C, which is the bounding case for thermal embrittlement. Both thermal and irradiation degradation mechanisms (TH and EMB) are monitored and evaluated during operation in the context of RPV surveillance programs that include assessment of the degree of embrittlement of the base material, weld metal, and HAZ. The results obtained are used to modify and add to these surveillance programs, especially with respect to extended operations. [R&D Status = GREEN]

Table 6-8 (continued)
VVER explanatory notes

NOTE ID	EXPLANATORY NOTE
VVER 440 REACTOR PRESSURE VESSEL	
v1-10c	The metallographic structure of austenitic weld metals is similar to CASS, where sensitivity to thermal embrittlement depends on the delta ferrite content. As high as 8 to 10% delta ferrite is expected in plant component weld metals. Thermal aging of stainless steel weld metals has been observed in the laboratory when delta ferrite is low (5 to 15%), using a force indentation curve technique that indicated that fracture properties are slightly reduced. Thermal aging of these stainless steel weld metals has therefore been observed to have a higher impact with smaller amounts of delta ferrite than those considered of concern in CASS, which may be related to the chemical composition of the delta ferrite. The welding process can also influence the concentration of delta ferrite in the weld metal. More research on the effect of the amount of delta ferrite, as well as its composition and its distribution, on the thermal aging behavior of weld metals is needed. Clad material samples have been included in surveillance capsules for the current five-year plan in the Czech Republic (and a similar action was performed in Hungary), and although their primary purpose is to examine irradiation effects, some insight will also be gained into thermal embrittlement. This is not, however, considered a plant operations priority. A weld from the Kola NPP was removed from the primary circuit after 100,000 operating hours, and some changes in precipitation and dislocation structure were thought to have occurred, although detailed information on the original as-fabricated condition was not available. Other unpublished work on material subjected to 200,000 hours of operation has revealed some changes in dislocation structure and sigma phase precipitation, but without any apparent effect on mechanical properties. Hardness measurements have been carried out on primary circuit welds in Hungary, and no increase in hardness was found after 30 years of primary circuit operation. A plan to extract a boat sample from the weld metal from primary piping at Dukovany station is being prepared. [R&D Status = YELLOW]

Table 6-8 (continued)
VVER explanatory notes

NOTE ID	EXPLANATORY NOTE
VVER 440 REACTOR PRESSURE VESSEL	
v1-10d	Ti-stabilized stainless steel is used only for penetrations through the upper closure head. The delta ferrite content of the wrought material (maximum 3%) and the operating temperature of 270°C are considered too low to cause any thermal embrittlement issues. [R&D Status = GREEN]
v1-12a v1-12b v1-12c	Irradiation embrittlement is monitored and evaluated by means of RPV surveillance programs that include assessment of the degree of embrittlement of the base material, weld metal, and HAZ. A high-quality surveillance program is considered key to ensuring safe operation. The results obtained are used to modify and add to these surveillance programs, especially for the case of LTO. Clad material samples have been included in surveillance capsules for the current five-year plans in the Czech Republic and Hungary. The true chemical composition is an important input to enable correct predictions of embrittlement. Some mechanistic aspects of RPV embrittlement are still unknown and more research is needed, for example, into the occurrence and effects of late blooming phases. Synergism between thermal aging and irradiation embrittlement is an issue that will need further investigation. [R&D Status = ORANGE]
VVER 1000 REACTOR PRESSURE VESSEL	
v2-2a	The pitting corrosion risk applies to ferritic RPV steel locations with defective cladding only. Defective cladding is considered unlikely in these more modern RPVs since manufacturing and welding can be done with high quality to eliminate the slag inclusion channels in weld overlay cladding observed previously on 440 MWe plants. Pitting can only occur if oxygen is present, which implies that the main risk is during refueling and then only if an acidic anion impurity like chloride is also present. [R&D Status = GREEN]
v2-2e	In some places with higher concentrations of chemical impurities in the coolant, pitting is a potential degradation mechanism for stainless steel cladding (and primary piping). The only potential location for pitting is above the water level during an outage where higher concentrations of chemical impurities may accumulate, and oxygen is present. The mechanism is theoretically possible but has not been observed to date. [R&D Status = GREEN]
v2-6d v2-6e	IGSCC in stabilized SS is considered possible, but the influencing parameters are relatively well known. The highest risk is in stagnant locations. Welded zones are potentially critical locations. As in the case of the 440 MWe plants, additional R&D is not deemed necessary. [R&D Status = GREEN]

Table 6-8 (continued)
VVER explanatory notes

NOTE ID	EXPLANATORY NOTE
VVER 440 REACTOR PRESSURE VESSEL	
v2-9d v2-9e	In the fatigue life evaluation procedures of NTD ASI (Normative Technical Documentation of the Czech Association of Mechanical Engineers), the environmental factor influencing the development of fatigue is not addressed adequately. The latest experimental work has shown decreasing fatigue endurance with exposure to the VVER primary water environment similar to that observed in studies of PWR primary circuit austenitic stainless steels. A national research project was initiated in the Czech Republic to better understand the mechanism of EAF and, if possible, to remove conservatism from the present methodologies for fatigue life calculations. Material testing under this project includes non-irradiated stainless steels. In the case of the calculated cumulative usage factors for the RPV, the values are higher in the low irradiated locations. Therefore, EAF testing of irradiated materials was not deemed necessary for the RPV. Due to the considerable work being carried out under this program, the R&D status is set to Yellow. [R&D Status = YELLOW]
v2-10a v2-10c	Thermal aging can be evaluated on the basis of laboratory tests at higher temperatures than those applicable to plant operations. Laboratory simulations of 60 years of operation indicate thermal stability of these materials at reactor operating temperatures. The primary hot leg temperature in 1000 MWe plants is 322°C (compared with 297°C in 440 MWe plants). The pressurizer in 1000 MWe plants operates at 335°C, although evaluations may be carried out up to 350°C, which is the bounding case for thermal embrittlement in service. Both thermal and irradiation degradation mechanisms were monitored during operation and evaluated in the context of RPV surveillance programs that include assessment of the degree of embrittlement of the base material, weld metal, and HAZ. The results obtained are used to modify and add to these surveillance programs, especially to support LTO. The Green R&D color result for these two cells reflects the plant specialists' position that thermal aging of C&LAS RPV steels and welds is adequately characterized. However, synergisms between thermal and irradiation degradation mechanisms are an issue that some researchers consider will need further investigation for VVER EPR materials. [R&D Status = GREEN]

Table 6-8 (continued)
VVER explanatory notes

NOTE ID	EXPLANATORY NOTE
VVER 440 REACTOR PRESSURE VESSEL	
v2-10b	Data from laboratory tests simulating 60 years of operation indicate thermal stability of the 22K and 20 carbon steel material grades used for the fabrication of upper closure heads. Similar behavior of the weld metal is expected. High quality carbon steel 22K was originally designed and described as a product without susceptibility to thermal embrittlement. In later updates of the Russian technical standards, it was postulated that the change of the ductile-to-brittle transition temperature could be up to 30°C without considering the length of time of high temperature exposure. For LTO, it would be reasonable to confirm or update that postulate. Although no experimental data are publicly accessible presently, the status is set to Yellow. [R&D Status = YELLOW]
v2-10d	Austenitic weld metals should have metallographic structures similar to CASS, where sensitivity to thermal embrittlement depends on delta ferrite content. The welding process can influence the delta ferrite content of the metal. It is expected that plant component welds can contain up to 8-10% delta ferrite. Thermal aging of weld metals has been observed to have higher impact with smaller amounts of delta ferrite than typically observed in CASS, which may be related to the chemical composition of the delta ferrite. More research is needed on the effect of the amount of delta ferrite, its composition, and distribution on the thermal aging behavior of weld metals. Although identified by research organizations as an R&D need, this issue is not considered a priority by plant operations personnel. [R&D Status = YELLOW]
v2-10e	Ti-stabilized stainless steel is used only for penetrations through the upper closure head. The delta ferrite content of the wrought material (maximum 3%) and the operating temperature of ~300°C are considered too low to cause any thermal embrittlement issues. [R&D Status = GREEN]
v2-12a v2-12b v2-12c v2-12d	Both thermal and irradiation degradation mechanisms (TH and EMB) are monitored during operation and evaluated in the context of the RPV surveillance programs that include assessment of the degree of embrittlement of the base material, weld metal, and HAZ. The current five-year plan also includes SS clad material. Synergism between thermal and irradiation degradation mechanisms is an issue that will need further investigation for VVER RPV materials. [R&D Status = ORANGE]

Table 6-8 (continued)
VVER explanatory notes

NOTE ID	EXPLANATORY NOTE
VVER PRIMARY SYSTEM PIPING COMPONENTS (INCLUDING THE PRESSURIZER)	
v3-2a	The only potential location for pitting in wrought stainless steel is above the water level during outages (based on the situation at Loviisa) when oxygen is present and with higher concentrations of acidic anionic chemical impurities in the coolant than permitted by the primary water specification. The mechanism is theoretically possible but has not been observed to date. [R&D Status = GREEN]
v3-5a v3-5b v3-5d v3-5e v4-5a v4-5b	In Ti-stabilized austenitic stainless steels, Cr and C create carbides on grain boundaries if the component temperature is in the sensitization regime. While Ni and N have an influence on the process by shifting the Time-Temperature-Precipitation (TTP) curves, C is the most dominant element. Stabilized stainless steels are also sensitive to IGA; see RBMK separator tubing degradations. The process is thermally activated depending on time and temperature. So far, relatively short periods were investigated (100,000 hours). In these circumstances, the TTP curve does not predict sensitization at a temperature of 300°C. However, SEM investigations have indicated potential IGA susceptibility of Ti-stabilized stainless steels after long-term operation (> 200,000 hours) even at relatively low temperatures associated with reactor operation. Since sensitization depends on chemical composition, grain size, and temperature, the impact is not equal across all stainless steel reactor components. Taking all into account, future work should focus on: • Stress concentration areas of components operating at a relatively high temperature (e.g., 300°C) • Hot leg components of the reactor coolant system, especially HAZ of welds R&D status = ORANGE
v3-7a v3-7b v3-7d v3-7e	IGSCC of wrought stabilized SS is considered possible, particularly in the presence of severe cold-worked (i.e., > 20%). Welded zones are anticipated to be the critical locations. However, no R&D is in progress or planned for VVER stainless steels. The highest risk is still considered to be in stagnant locations where higher concentrations of deleterious anionic impurities may accumulate, especially during refueling outages. There is some disagreement among specialists as to whether the influencing parameters are sufficiently well characterized. According to recent operating experience with SCC indications in the safety system piping in some Western-style PWR plants as well as the current knowledge of the root causes and influencing parameters, additional R&D is deemed necessary. Specifically, the role of dissolved oxygen and its effect on electrochemical potential in stagnant systems is not clear. This applies to piping made from both Ti-stabilized stainless steel and carbon steel piping with stainless steel cladding. R&D status = ORANGE

Table 6-8 (continued)
VVER explanatory notes

NOTE ID	EXPLANATORY NOTE
VVER PRIMARY SYSTEM PIPING COMPONENTS (INCLUDING THE PRESSURIZER)	
v3-9a v3-9b	High-cycle fatigue due to thermal cycling (turbulence penetration or thermal stratification) or mechanical vibration is a design/location-dependent phenomenon and therefore is applicable to primary system piping components. This phenomenon is generally well characterized, and no additional research is considered necessary. *[NOTE: Only applicable to CASS material if cast fittings are installed in small bore lines having susceptibility to high-cycle fatigue. Since no knowledge gap has been identified, further refinement is not warranted.]* [R&D Status = GREEN]
v3-10a v3-10b v3-10d v3-10e	Environmentally assisted fatigue of components made from 08Ch18N10T RVI and austenitic welds may occur as a result of shutdown/startup transients. A better understanding of the influencing parameters is needed. VERLIFE, in contrast to NTD A.S.I. (Normative Technical Documentation of the Czech Association of Mechanical Engineers), considers the influence of the environment through F_{en} factors (similar to NUREG CR/6909). Note that NTD A.S.I. is based on the PNAEG-Russian standard safety factors n_ε and n_N. A national research project was initiated in the Czech Republic to better understand the mechanism of EAF and, if possible, to remove conservatism from the present methodologies for fatigue life calculations. Material testing under this project is done for the base metal of the primary piping 08Ch18N10T. Welding materials require further investigation. v3-10b, v3-10e: R&D status = ORANGE v3-10a, v3-10d: [R&D Status = YELLOW]
v3-11c	Thermal aging can be evaluated and refined by research on the basis of accelerated laboratory tests. Some solutions were included in a proposed revision to VERLIFE 2015. The higher hot leg operating temperatures of 322°C in 1000 MWe plants and 335°C in the pressurizer are judged to be a factor in the Yellow R&D result. [R&D Status = YELLOW]
v3-11e	Austenitic weld metals and CASS have similar metallographic structures where sensitivity to thermal embrittlement depends on delta ferrite content. The welding process can influence the delta ferrite content of the material. The higher hot leg operating temperatures of 322°C in 1000 MWe plants and 335°C in the pressurizer are judged to be a factor in the Yellow R&D result. Thermal aging of weld metals has been observed to have a higher impact with smaller amounts of delta ferrite compared to CASS, which may be related to the chemical composition of the delta ferrite. More research is needed on the effect of the amount of delta ferrite, its composition, and distribution on the thermal aging behavior of weld metals. [R&D Status = YELLOW]

Table 6-8 (continued)
VVER explanatory notes

NOTE ID	EXPLANATORY NOTE
VVER REACTOR VESSEL INTERNALS	
v4-2a v4-2c	In compliance with the standard water chemistry operating regime, pitting degradation does not occur during normal operation. Pitting corrosion in Ti-stabilized austenitic steels and in martensitic SS may occur during outages with less than optimum chemical control and temperature transients. Pitting corrosion can be an initiator of SCC. The green color reflects the expert panel's judgment that this is a plant operations issue and does not require further R&D input. [R&D Status = GREEN]
v4-6a v4-6b v4-6c v4-6d	Wear occurs as a result of control rod and fuel assembly insertion and during operation due to vibration. It can be related to operating time due to creep and swelling of RVI components such as control rods and their position relative to the fuel. The degradation mechanism is well understood, and no materials knowledge gap exists. [R&D Status = GREEN]
v4-7a	Ti-stabilized stainless steel is considered more resistant to SCC compared to non-stabilized grades, but not fully resistant, particularly in the presence of anionic impurities like chloride and dissolved oxygen. The susceptibility to SCC increases with cold work and deterioration of water chemistry. The possibility of SCC occurring in base materials gives rise to an expectation of higher susceptibility to SCC in weld HAZs (particularly if deterioration of water chemistry occurs during outages). The green color of this cell is consistent with other austenitic stainless steel components exposed to primary water. Irradiation effects on SCC susceptibility are considered separately in the next column (cell v4-8a). [R&D Status = GREEN]
v4-7c	Although martensitic SS fasteners used in the VVER 440 design are potentially susceptible to SCC (TG/IG), operating experience to date has been good, and the components are replaceable. As such, no additional R&D is deemed necessary. [R&D Status = GREEN]
v4-8a v4-8b	IASCC susceptibility in Ti-stabilized stainless steels is proven (Greifswald and Loviisa baffle bolts). The threshold stress dependence curve for IASCC initiation of RVI materials as a function of neutron fluence recommended in the VERLIFE guidelines is based on PWR data. Similar data on VVER materials are not available. An R&D project is needed to determine the initiation curve for 08Ch18N10T and its welds. [R&D Status = ORANGE]

Table 6-8 (continued)
VVER explanatory notes

NOTE ID	EXPLANATORY NOTE
VVER REACTOR VESSEL INTERNALS	
v4-8c	VVER 440 only: Sections of inserted control rods (martensitic SS material 14Ch17N2) may be more susceptible to fast dynamic loading (~1.6 x 10^{-4} s^{-1}) during shutdown at lower temperatures where SCC has been observed in laboratory tests. However, this susceptibility was not confirmed at higher temperatures in laboratory tests (results from an R&D program at Dimitrovgrad). It is not known how it may develop with further plant operation. If any failure is detected, sections fabricated from martensitic SS material can be replaced. [R&D Status = GREEN]
v4-8d	IASCC initiation in components fabricated from high-strength ChN35VT-VD high-Ni stainless steel is possible at doses as low as 1 dpa (experimentally proven), but not confirmed on operational components. Bolts made from high-Ni stainless steel could be replaced if any failure is detected. [R&D Status = GREEN]
v4-9a v4-9b v4-9c v4-9d	High-cycle fatigue is theoretically possible due to coolant pressure pulses through the RVI. However, it is expected that the resulting load/stress or strain amplitude is below the threshold for high-cycle fatigue failure. There is no indication/evidence that the effect may increase during operation. Regardless, there would not be a fundamental materials R&D need warranting additional research. [R&D Status = GREEN]
v4-10a v4-10b	Environmentally assisted fatigue of RVI components made from 08Ch18N10T austenitic stainless steel and its welds may occur as a result of shutdown/startup transients. Thermal fatigue is strongly suspected to be a potential degradation mechanism for CRDMs, although no such degradation has been observed to date. A better understanding of the influencing parameters is needed, including potential synergistic interactions with irradiation damage. The applicable NTD A.S.I. (Normative Technical Documentation of the Czech Association of Mechanical Engineers) standard is based on the PNAEG-Russian standard safety factors n_ε and n_N. By contrast, VERLIFE considers the influence of the environment on fatigue life through F_{en} factors (similar to NUREG/CR-6909). A national research project was initiated in the Czech Republic to better understand the mechanism of degradation and subsequently remove conservatism from present fatigue calculations. The project includes only non-irradiated materials, so the potential influence of irradiation on fatigue material properties should be investigated further. The INCEFA+ project is attempting to create a uniform procedure for the European Union. [R&D Status = ORANGE]
v4-10c	VVER 440 only: Fatigue of RVI martensitic SS in the environment may occur as a result of shutdown/startup transients. Field inspection data have not revealed any problem so far, but large temperature changes are possible and are a concern. No experimental R&D is presently planned or underway. [R&D Status = ORANGE]

Table 6-8 (continued)
VVER explanatory notes

NOTE ID	EXPLANATORY NOTE
VVER REACTOR VESSEL INTERNALS	
v4-10d	Fatigue of RVI high-Ni stainless steel ChN35VT-VD (which is a transition class alloy between highly alloyed SS and Ni-base alloys) in the environment has been demonstrated in laboratory tests and may be significant during shutdown/startup transients. The effect during operation has not yet been detected in service. [R&D Status = ORANGE]
v4-11b	The degree of thermal aging embrittlement of stainless steels at typical LWR operating temperatures depends on the delta ferrite content and is therefore generally absent since the delta ferrite is limited to < 3% volume fraction. The 08Ch18N10T weld metal has a two-phase structure with delta ferrite as high as 8 to 10% volume fraction (while cast components may have up to 12%). It is considered that there is a potential risk of thermal embrittlement of these welds since the welding procedure affects not only the volume fraction of delta ferrite but also its composition. Concerns with thermal aging of CASS are normally only considered significant in non-stabilized stainless steels used in PWRs and BWRs when the delta ferrite exceeds 15% volume fraction. Nevertheless, the VVER expert panel recommends that thermal aging should be considered, and prediction curves based on VVER plant materials should be developed. The current EU research project DELISA-LTO investigates the role of thermal aging on primary components. The results will be valuable for a better understanding of this degradation mechanism on VVER materials. [R&D Status = YELLOW]
v4-11c v4-11d	Some researchers consider that there is a possible risk of thermal embrittlement. However, these small components are replaceable if necessary. As such, the R&D status is set to Green. [R&D Status = GREEN]
v4-12a v4-12b v4-12c v4-12d	The database for environmental effects on fracture toughness in the irradiated condition is insufficient. Measurements of fracture toughness in primary water environments on VVER RVI materials are limited. Assessment is presently based on standard (short term) tests in air. RVI materials can exhibit some reduction in fracture resistance properties due to exposure to the primary system coolant. The increased yield strength resulting from irradiation can cause the environmental effect to be more significant. R&D projects are in progress on wrought Ti-stabilized stainless steel and its welds and are planned for the martensitic stainless steel as well as precipitation-hardened high-Ni stainless steel, thus, justifying the Yellow status of these cells. [R&D Status = YELLOW]

Table 6-8 (continued)
VVER explanatory notes

NOTE ID	EXPLANATORY NOTE
	VVER REACTOR VESSEL INTERNALS
v4-13a v4-13b v4-13d	According to the VERLIFE guidelines, the recommended curve for the formation of small volumes of irradiation embrittled material (denoted "LEA" for Local Embrittlement Area) predicts for RVI materials, that: 1. VVER 440: For the maximum RVI temperature (333°C), there is no risk of LEA formation up to ~55 dpa; according to predictive modeling, the inner surface of the core shroud reaches that dose after 65 years of operation. 2. VVER 1000: For the maximum RVI temperature (434°C), there is no risk of LEA formation up to ~38 dpa exposure; according to the predictive modeling, the inner surface of the core shroud reaches that dose after 20 years of operation. Irradiation embrittlement of these stainless alloys requires additional research that considers these new findings related to void swelling. [R&D Status = ORANGE]
v4-13c	VVER 440 only: Typically, ferritic/martensitic steels have very low void swelling rates under neutron irradiation compared to austenitic stainless steels. However, the ductile-to-brittle transition temperature (DBTT) increases rapidly with neutron irradiation at temperatures below 0.3 T_m (absolute melting temperature). To date, there have been no problems in service. The Green R&D result reflects the operators' perspective that these martensitic SS components are readily replaceable. [R&D Status = GREEN]
v4-14a v4-14b	Swelling is expected to be significant at irradiation temperatures above 350°C. TEM examination of a baffle bolt removed from the Greifswald VVER 440 with a fluence up to 12 dpa and an estimated temperature below 400°C identified initial signs of swelling; < 0.1% was roughly estimated from the cavity volume fraction. It is considered that there is a possible risk of RVI dimensional changes due to swelling leading to problems with coolant flow and/or control rod movement. Temperatures at the core barrel and its welds due to gamma heating should be lower than in baffle bolts. Nevertheless, according to VERLIFE, swelling is predicted at the core barrel, leading to a limitation of the coolant flow rate between the core barrel and core shroud due to dimensional changes. This remains to be verified in service and checked by dimensional measurements. [R&D Status = ORANGE]
v4-14c	VVER 440 only: Temperatures are estimated to be below 400°C and the components are replaceable. Typically, ferritic/martensitic steels have very low void swelling rates under neutron irradiation compared to austenitic stainless steels, but the ductile-to-brittle transition temperature (DBTT) increases rapidly with neutron irradiation at temperatures below 0.3 T_m (absolute melting temperature). The Green R&D result reflects the operators' perspective that these martensitic SS components are readily replaceable. [R&D Status = GREEN]

Table 6-8 (continued)
VVER explanatory notes

NOTE ID	EXPLANATORY NOTE
VVER REACTOR VESSEL INTERNALS	
v4-15a v4-15b	This topic represents an unexplored area for specific VVER RVI structural materials. Synergistic effects of irradiation creep, stress relaxation, and swelling are anticipated, as is also the case for PWR internals where this aspect is considered relatively well characterized for non-stabilized stainless steels. Synergistic interactions between these irradiation-induced degradation mechanisms are considered to require more research on VVER specific materials. [R&D Status = ORANGE]
v4-15c	VVER 440 only: Temperatures are estimated to be below 400°C. Although there is likely some influence of irradiation creep and stress relaxation, these are small components and are replaceable if necessary. [R&D Status = GREEN]
VVER STEAM GENERATOR TUBE BUNDLE, INTERNALS, AND SECONDARY PRESSURE BOUNDARY	
v5-1c v5-1e v6-1c v6-1d v6-1e	General corrosion is a well-known degradation mechanism affecting carbon and low-alloy steel components on the secondary side of SGs. The degradation mechanism is very well established and was accounted for in the component design. Corrosion can be aggravated during out-of-specification secondary water chemistry transients, and during chemical cleaning of the secondary side of SGs. It is necessary to monitor the tube corrosion rate and wall loss during all stages of operation, maintenance, and layup. It is also necessary to periodically/continually remove corrosion product sludge that can harbor locally in poor water chemistry. Knowledge of these corrosion phenomena is considered sufficient, and additional research is not required. [R&D Status = GREEN]

Table 6-8 (continued)
VVER explanatory notes

NOTE ID	EXPLANATORY NOTE
VVER REACTOR VESSEL INTERNALS	
v5-2a v5-2b v5-2d v6-2a v6-2b	Pitting can occur on Ti-stabilized stainless steels when both oxygen and chlorides and possibly other acidic anion impurities are present. It is influenced also by anodic polarization caused by the presence of oxidized copper corrosion products (typically from brass condenser tubes). The risk of pitting of SG tubes is minimized by maintaining good secondary circuit chemistry and monitored by planned in-service inspections. Pitting can take place preferentially inside crevices, e.g., between SG tubes and tube support plates. Pitting can also act as an initiator of SCC, particularly in dissimilar metal welds (DMWs) situated in the lower crevice between the secondary collector and the austenitic piece where crud accumulates. Today, research is in progress due to the observation of defects in DMWs of VVER 440 SG collector-to-intermediate piece connections. However, a number of questions related to this topic remain unanswered. Recent operating experience indicates a need for sludge removal from horizonal SGs and enhanced heat exchanger tube degradation inside a sludge pile when operating with high pH secondary chemistry. A solid link is missing between caustic species concentrations and/or pH and tube degradation. DMWs connecting SS piping to the CS SG vessel (v6-2b) are extensively inspected and repaired at VVER SGs. Such activities mitigate the issue but are a burden for plants due to radiation exposure and resources needed. So far, pitting during outage is considered an initiation point for SCC. v6-2a, v6-2b: [R&D Status = GREEN] v5-2a, v5-2b, v5-2d: [R&D Status = YELLOW]
v5-2c v5-2e v6-2c v6-2d v6-2e	Pitting of carbon and low-alloy steels and their welds is a well-known degradation mechanism, and its characteristics are also well-known. The detection of aging effects due to pitting is difficult. However, additional research focused on pitting is not considered necessary due to limited added value for NPPs. Nevertheless, some data will be generated incidentally from the studies of SCC initiation in the context of cracking observed at the lower DMW between the austenitic SS collectors and the C&LAS SG pressure boundary in some 440-MWe plants. v5-2c, v6-2c, v6-2d, v6-2e: [R&D Status = GREEN] v5-2e: [R&D Status = YELLOW]

Table 6-8 (continued)
VVER explanatory notes

NOTE ID	EXPLANATORY NOTE
	VVER REACTOR VESSEL INTERNALS
v5-3c v5-3e v6-3c v6-3d v6-3e	Flow accelerated corrosion is a significant degradation mechanism attacking carbon steels with very low chromium content (< 0.1%). A component with an extensive history of FAC degradation is the carbon steel secondary feedwater distribution header inside VVER 440 SGs. Most of the headers in operating plants were isolated, left inside the SG heat exchanger tube bundles, and new stainless steel headers were retrofitted. Construction of these retrofitted stainless steel headers differs between plants. Today, FAC is a risk factor for only plants with the original CS headers still in service and for those plants having SS collectors connected to the stub tubes of old CS headers. From an LTO perspective, SG vessels fabricated from carbon steel are also at the same risk of FAC degradation, just like vessels of regenerative heat exchangers, but no FAC has been reported to date. Regular inspection of the inside of the SG vessels is performed. FAC is a well-known degradation mechanism, and no additional research specific to FAC in SGs is needed. Degradation is managed through application and constant improvement of computer codes for FAC aging management and through verification of code predictions by inspection. [R&D Status = GREEN]
v5-4a v5-4b v5-4d v5-4e	The outer diameter surfaces of SG tubes are fouled by corrosion products from the secondary circuit. The structure of this layer has a detrimental effect on the heat transfer coefficient, potentially shifting it outside acceptable limits. Sludge deposits within the tube bundles are present in some VVERs. There is a lack of knowledge concerning the conditions affecting the deposited layer morphology. The reason for sludge pile accumulation inside tube bundles is also unknown, and it is not known why the deposits form preferentially in the middle of the tube bundles. A better understanding of the reasons for fouling and of mitigation methods is needed, as well as better knowledge of the influence of different secondary water chemistry regimes on this phenomenon. Degradation phenomena within the sludge pile include pitting and SCC, and their impact on SG tubing is not well quantified. Several methods for assessment of SG fouling are used, including low frequency ECT, endoscope VT, and high-radiation intensive VT. A guidance and inspection criteria would be beneficial for the fleet. [R&D Status = ORANGE]
v6-4c v6-4d v6-4e	Fouling will occur on the secondary side where loose sludge falls to the bottom of the horizontal cylindrical vessel. This is an advantage of the VVER design (with the exception of the lower collector to SG shell crevice) compared to Western PWR designs with vertically oriented tube bundles where sludge instead collects on the horizontal tube support plates and is much harder to remove. The phenomenon is well understood, and no additional research is considered necessary. [R&D Status = GREEN]

Table 6-8 (continued)
VVER explanatory notes

NOTE ID	EXPLANATORY NOTE
VVER REACTOR VESSEL INTERNALS	
v5-5a v5-5b v5-5c v5-5d v5-5e v6-5a v6-5b v6-5c v6-5d v6-5e	The principal source of mechanical wear is damage introduced by foreign objects. Most of the VVER 440 SGs have abandoned carbon steel feedwater distribution headers inside the SG vessel, which may break into smaller fragments during further operation. Such fragments can then become foreign objects in very unfavorable locations inside tube bundles. The mechanism is well understood, and no additional research is considered necessary. [R&D Status = GREEN]
v5-5f	Nickel alloy washers can be damaged during collector opening/closing. The knowledge level is sufficient for management purposes. [R&D Status = GREEN]
v5-7a	Secondary side SCC (or ODSCC) is a significant degradation mechanism affecting SG tubes, albeit very much less seriously than for Alloy 600 tubes in PWR SGs. Today, a significant discrepancy exists between accelerated autoclave tests carried out with relatively high concentrations of impurities and operational experience that indicates low salt impurity concentrations. Operating experience shows that it is not possible to simply correlate secondary circuit chemistry with the number of plugged tubes due to the low overall numbers of plugged tubes and due to changes of water chemistry during the plant lifetimes. In plants with sludge piles, there seems to be a correlation between the number of indications found by ECT and the sludge piles. More research is needed on NDE methods to detect sludge piles and tube indications, as well as on the root cause for the indications, to address LTO concerns. Today, it is believed that plants are near the bottom of the classical U-shaped curve depicting plugging rates during SG lifetimes. For lifetime management, it is necessary to be able to identify the beginning of any accelerating trend curve to initiate proper and timely corrective measures. A limited number of autoclave tests (UJV, SE) are in progress to answer some of these research questions. Recent operating experience indicates a need for sludge removal from horizonal SGs due to enhanced SG tube degradation inside a sludge pile when operating with high pH secondary chemistry. A solid link is missing between caustic species concentrations and/or pH and tube degradation. Some VVER plants reported an increased number of plugged tubes due to ODSCC. It is not clear what factor is causing this trend. Some indications point to the impact of the collector DMW weld repairs, which have been postulated to introduce additional stresses in associated tubing. [R&D Status = ORANGE]

Table 6-8 (continued)
VVER explanatory notes

NOTE ID	EXPLANATORY NOTE
	VVER REACTOR VESSEL INTERNALS
v5-7b	Austenitic stainless steel is affected by SCC from the secondary water side, mainly in crevice regions. From an LTO perspective, the SCC performance of tube support plates (TSPs) is uncertain. There is a possible risk of TSP cracking when stress is applied due to deformation in service. This is not supported by operational experience to date, but a high TSP cracking rate could have a detrimental effect on SG lifetimes. [R&D Status = YELLOW]
v5-7c v6-7c v6-7d v6-7e	Carbon and low-alloy steel can be susceptible to SCC (or SICC), but VVER operating experience does not provide any indication of its significance for the SG internals and pressure boundary, with the exception of the primary collector to SG vessel weld addressed in the preceding note (v5-7d) and the next note (v5-7e). For the carbon steel SG pressure boundary in VVER 440 plants, synergistic effects of impurities together with boric acid are not fully characterized. However, all four cells relate to field repairable components. [R&D Status = GREEN]
v5-7d v6-7b	Dissimilar metal welds of VVER-440 SG primary collectors are affected by SCC (or SICC); cracks have previously been detected in the weld area. It appears to initiate in the austenitic weld metal and propagate along the weld metal/C&LAS interface. This damage is being addressed by a comprehensive research program. Since the investigations performed on the mechanism of cracking have not been published in the open literature, it remains a serious problem for several operating VVER 440s. Information is needed on the cracking mechanism, on material properties, residual stresses, crack growth rates, NDE, LBB issues, and on the consequences of a failure. However, the repair technology is available and has been applied on a number of collectors at different VVER plants. Also, the NDE for this weld is available and qualified. The cleaning of the area around this DMW ("pocket") is accepted as a good practice, which should mitigate the initiation of SCC cracks. Other problematic parts are threads at the top of the collector in the region of thread holes (stainless steel part) since the collector to closure head junction is considered the weakest link in the VVER LOCA analysis. The threaded holes in the upper part of the collector have a history of cracking at Dukovany and Paks stations. Some VVER plants reported an increased number of defects of DMW (following sludge removal) of draining piping at the bottom of the SG. As this piping is thin-walled, the SCC cracks may propagate through-wall in a relatively short period of time. Some welds have cracked repeatedly even though the repair weld is made with maximum care and in the shop. [R&D Status = ORANGE]

Table 6-8 (continued)
VVER explanatory notes

NOTE ID	EXPLANATORY NOTE
VVER REACTOR VESSEL INTERNALS	
v5-7e	The primary circuit collectors of VVER1000 SGs have a significant history of inter-tube hole ligament SCC (or SICC) resulting in replacement of many of these SGs. This issue was widely addressed by the IAEA.[1] As a result, the method of tube expansion into the holes of the collectors during SG manufacture was changed from explosive expansion to hydraulic expansion, which resolved the issue. The second issue being studied today is cracking of the weld "111" connecting the lower end of the primary collector and the SG vessel. This is based on operating experience in Russia that has been attributed to poor water chemistry following the accumulation of sludge in a dead-leg crevice (similar to the VVER 440 case, but without the dissimilar metal weld). Two color codes could be assigned to this cell of the MDM: green for ligament cracking and orange for "111" weld cracking. The overall color code category displayed is Orange. [R&D Status = ORANGE]
v6-7a	Austenitic impulse tubes (small bore piping for the detection of leaks and monitoring purposes) and blowdown lines form part of the SG pressure boundary. Both components have a history of SCC damage, but these adjacent lines are repairable without an effect on LTO. Additional research would be beneficial only in the case of a significant increase in the damage rate. [R&D Status = GREEN]
v5-7f	Nickel alloy washers are subject to SCC because a significant stress is applied, and they are situated in a crevice with likely poor water chemistry compared to bulk. Historically, cracking was due to temper embrittlement. The level of knowledge is considered sufficient. [R&D Status = GREEN]
v5-8a v5-8b v5-8c v5-8f	High-cycle fatigue is possible for SG tubes and internals, particularly the feedwater collector, but no indications of this mechanism are known for VVER SGs. This degradation mechanism should be evaluated, especially in connection with power uprates and other changes affecting fluid dynamics. Some plants address high-cycle fatigue by Time Limited Ageing Analysis (TLAA) showing a high frequency of vibration, but no effect on fatigue has been observed to date. The Green R&D result reflects the position that high-cycle fatigue damage is considered an assessment issue for the IMT and not a fundamental materials R&D issue applicable to the MDM. [R&D Status = GREEN]

[1] IAEA-EBP-WWER-07 WWER-1000 Steam Generator Integrity, IAEA, July 1997.

Table 6-8 (continued)
VVER explanatory notes

NOTE ID	EXPLANATORY NOTE
VVER REACTOR VESSEL INTERNALS	
v6-8a v6-8b	Impulse tubes (small bore piping for detection of leaks and monitoring purposes) connected to the SG vessel are at risk of high-cycle fatigue damage, but these lines are repairable without a significant adverse effect on LTO. [R&D Status = GREEN]
v5-9a v5-9d v5-9e v5-9f	Low-cycle fatigue is a potential degradation mechanism for SG tubes and collectors, particularly in relation to cracking of weld “111” (= weld DN1200) in VVER 1000 SGs. These welds have been repaired in Russia, and cracks have been found in the Czech Republic as well. EAF is considered a possible degradation mechanism. Any effect of environment on low-cycle fatigue could be important because it would increase the calculated cumulative usage factor (CUF). Current data are from a rather fragmentary research project, and comprehensive data are lacking. Many experts consider the available methods for low-cycle fatigue evaluation as overly conservative. To introduce a more realistic approach to low-cycle fatigue and EAF, further research work is necessary to derive accepted assessment methods based on high-quality data. A national research project has been initiated in the Czech Republic to better understand the mechanism of degradation and subsequently remove conservatism from present fatigue calculations. Material testing under this project is done for the base metal of the primary piping 08Ch18N10T. Welding materials require further investigation. v5-9a and v5-9d: [R&D Status = YELLOW] v5-9e and v5-9f: [R&D Status = ORANGE]
v5-9b v5-9c	SG internals are subject to temperature changes during unit startup and shutdown and during ingress of cold feedwater. Such transients contribute to increasing the calculated CUF. Low-cycle fatigue is a potential degradation mechanism. Any effect of environment on low-cycle fatigue is important because it would increase the calculated CUF. Current data are from a rather fragmentary research project, and comprehensive data are lacking. Many experts consider the available methods for low-cycle fatigue evaluation as overly conservative. To introduce a more realistic approach to low-cycle fatigue and EAF, further research work is necessary to derive accepted assessment methods based on high-quality data. [R&D Status = ORANGE]

Table 6-8 (continued)
VVER explanatory notes

NOTE ID	EXPLANATORY NOTE
	VVER REACTOR VESSEL INTERNALS
v6-9a v6-9b v6-9c v6-9d v6-9e	Feedwater nozzles are the most fatigue-susceptible parts of the SG secondary pressure boundary. Due to high fatigue loading, it is considered advisable to initiate research that would result in a better understanding of environmentally assisted fatigue and developing new less conservative assessment methods. Low-cycle fatigue is a potential degradation mechanism. Any effect of environment on low-cycle fatigue is important because it would increase the calculated CUF. Current data are from a rather fragmentary research project, and comprehensive data are lacking. Many experts consider the available methods for low-cycle fatigue evaluation as overly conservative. To introduce a more realistic approach to low-cycle fatigue and EAF, further research work is necessary to derive accepted assessment methods based on high-quality data. A national research project has been initiated in the Czech Republic to better understand the mechanism of degradation and subsequently remove conservatism from present fatigue calculations. Material testing under this project is done for the base metal of the primary piping 08Ch18N10T. Welding materials require further investigation. v6-9a: [R&D Status = YELLOW] V6-9b, v6-9c, v6-9d, v6-9e: [R&D Status = ORANGE]
v5-10f	Thermal aging embrittlement has been identified as a degradation mechanism for primary collector cap washers. It is not necessary to carry out any additional research due to the low cost of the washers and their ease of replacement. [R&D Status = GREEN]
v6-10c v6-10d v6-10e	Thermal aging embrittlement of C&LAS SG pressure boundary materials is considered inherently unlikely at normal operating temperatures. Nevertheless, there are rules in Hungary about zones where the temperature analysis is uncertain and where these uncertainties must be compensated for in analysis by adding 30°C to the best estimate. This conservatism gives rise to some concern, despite that there is no evidence of any practical problems in similar materials even at pressurizer operating temperatures after 30 years of operation of 440-MWe plants. However, since thermal embrittlement of RPV and pressurizer components will bound embrittlement of SG components, a Green R&D result is assigned to these cells. [R&D Status = GREEN]
v5-12c	Some designs of retrofitted stainless steel feedwater distribution headers employ a flange connection using bolts. These bolts are subject to a stress relaxation degradation mechanism. The mechanism is known, and it is managed by an in-service inspection program. There is no need for additional research. [R&D Status = GREEN]

Table 6-8 (continued)
VVER explanatory notes

NOTE ID	EXPLANATORY NOTE
RPV SUPPORTS AND PRESSURE RETAINING BOLTING	
v7-4a v7-4b v7-4c v7-4d	Boric acid corrosion is a degradation mechanism, which may be present on external supports and bolting. In the case of VVER plants, the source of boric acid is leaks from the spent fuel pools or fuel transfer channel. The pools are located inside the containment building close to the reactor pressure vessel, and the leaks present a specific concern. A VVER plant has reported boric acid residue on the surface of the RPV; the cleaning had to be performed to allow NDE of weld area. This degradation is addressed by visual inspections of external surfaces and NDE of bolting. [R&D Status = GREEN]
v7-5c v7-5d	Damaged threads have been observed on some bolts, but the root cause was not determined. Regular NDE is performed, and damaged bolts can be easily removed from service and replaced. [R&D Status = GREEN]
v7-9c v7-9d	Low-cycle fatigue calculations are performed on the RPV closure studs and refined throughout the plant's lifetime. Computational models (VERLIFE), however, contain conservatism and uncertainty. Therefore, monitoring systems to measure metal temperatures are installed in the primary circuit to refine the measurements of temperature transients. Some locations are verified by leak detectors in the main seal groove. [R&D Status = GREEN]
v7-10a v7-10b	Laboratory simulations of 60 years of operation indicate thermal stability of these materials at reactor operating temperatures. The RPV supports are likely to be at ~250°C during power operation. Work is in progress to provide more detailed information on the thermal stability (and irradiation conditions) for RPV supports, and the results will provide guidance as to whether any further R&D is required. [R&D Status = YELLOW]

Table 6-8 (continued)
VVER explanatory notes

NOTE ID	EXPLANATORY NOTE
RPV SUPPORTS AND PRESSURE RETAINING BOLTING	
v7-12a v7-12b	The study of irradiation embrittlement effects on RPV support structures is in its infancy. Researchers are concerned that two conflicting effects are likely where the expected lower fluence decreases the risk but higher impurity contents in the C&LAS grades used may increase it. Work is in progress to provide more detailed information on the irradiation (and thermal conditions) for RPV supports, and the results will provide guidance as to whether any further R&D is required. [R&D Status = YELLOW]

7
CANDU REACTOR DEGRADATION MATRIX RESULTS

The CANDU reactor MDM results presented in this section are based on a generic evaluation by a panel of subject matter experts and updated for this Revision 5 after consultation with the appropriate EPRI program and project managers concerning progress made since the last revision. See Section 2.1 for additional discussion and notes regarding the assessment process.

- Section 7.1 describes the scope of the MDM evaluation for CANDU reactors.
- Section 7.2 provides the evaluation details, including a set of component level tables and an associated set of explanatory notes.

7.1 Scope and Evaluation Assumptions

7.1.1 Systems Evaluated

The MDM scope for the CANDU pressurized heavy water reactor design includes the fuel channel (FC) assemblies, calandria vessel and moderator system, primary heat transport (PHT) system, and steam generators (SGs). Each of these systems is summarized in the following:

7.1.1.1 Fuel Channel Assemblies (Table 7-1)

Fuel channel assembly components evaluated include the zirconium alloy (Zr-2.5wt% Nb) pressure tube, Type 403 stainless steel (quenched and tempered) end fittings, the Zircaloy-2 calandria tube, and annulus spacers fabricated from either X-750 or a Zr-Nb-Cu alloy. The pressure tubes serve as the in-core pressure boundary and contain fuel bundles as well as lithiated and hydrogenated, heavy water reactor coolant. The pressure tubes are roll-expanded into end fittings (EFs), which, among other functions, provide the connection to the out-of-core primary piping. Each pressure tube is thermally insulated from the low-temperature, low-pressure moderator by a carbon dioxide filled (dry) gas annulus between the pressure tube and the calandria tube. Annulus gap spacers are spiral-wound annular springs, often termed “garter springs” that are positioned along the length of the pressure tube and prevent contact of the pressure tube with the calandria tube.

7.1.1.2 Calandria Vessel and Moderator System (Table 7-2)

The scope of MDM evaluation for the calandria-shield tank assembly includes only components that are exposed to the heavy water moderator. Calandria vessel pressure boundary components evaluated include the horizontal/cylindrical calandria shell and the associated end walls (or tubesheets) that are joined to the ends of the calandria tubes. The calandria vessel is exposed to a significant neutron flux. In addition, the assessment includes the large bore piping used to circulate the vapor moderator headspace (i.e., calandria relief ducts). The primary material

used for the calandria vessel and end walls as well as the relief ducts is Type 304L stainless steel with Type 308L weld filler material. Shield tank and end shield components exposed to light water are considered beyond the "primary systems" scope of the MDM and were not included in the evaluation.

The MDM evaluation also includes components internal to the calandria: Liquid Injection Shutdown System (LISS) nozzles and control rod guide tube assemblies. These components are primarily fabricated from Zircaloy-2, but nickel-base alloys are used for support pins (X-750) and springs (Alloy 718).

Moderator system components evaluated include piping, valve bodies, pump casings, and heat exchangers. The moderator system is a low-pressure and low-temperature system that maintains the temperature of the heavy water in the calandria vessel. During normal operation, heavy water moderator is drawn from the calandria via outlet ports located near the top of the calandria vessel, cooled, and returned to the calandria via inlet nozzles located just beneath the outlet ports. The primary material of construction for the moderator system is Type 304L stainless steel. Moderator heat exchange is provided by shell and tube heat exchangers fed by untreated water. Note that, due to the high cost of heavy water, the moderator water flows through the tube interior with untreated water on the shell side. Moderator system heat exchanger tubing materials evaluated include Alloy 800 and titanium.

7.1.1.3 Primary Heat Transport System (Table 7-3)

The PHT system circulates pressurized heavy water coolant through the reactor fuel channels to transfer the heat produced by fission of natural uranium fuel to the SGs. The most prevalent material in the PHT system is unclad carbon steel, used for piping, feeders, and main headers. Other materials used to a lesser extent include low-alloy steel and nickel-base alloys (Alloys 600, 690, 52, and 82). The pressurizer[10] and SG channel heads[11] are fabricated from low-alloy steel. Use of nickel-base alloys is limited to feeder flow elements. These flow elements are fabricated from Alloy 600 or Alloy 690 and welded by Alloy 82 or Alloy 52 to the adjacent carbon steel feeder piping.

PHT system environmental conditions include temperatures in the range of 260–310°C and exposure to high purity, deoxygenated, hydrogenated, and lithiated heavy water coolant. However, oxidizing conditions are plausible during startup and may be possible in some locations during normal operation due to boiling and radiolysis if sufficient dissolved H_2 is not maintained.

7.1.1.4 Steam Generators (Table 7-4 [Tubing] and Table 7-5 [Internals/Secondary Shell])

The CANDU SGs consist of an inverted U-tube bundle within a cylindrical shell. Heavy water coolant from the PHT system passes through the U-tubes. Some SGs include an integral preheater on the secondary side of the U-tube outlet section or integral steam separating equipment in the steam drum above the U-tube bundle.

[10] All pressurizer nozzles and penetrations are also fabricated from low-alloy steel.

[11] SG channel heads are included in the PHT system evaluation because the environmental exposure and degradation issues are most similar to other PHT system components. Different than other PHT low-alloy steel components, the SG channel heads are internally clad with Alloy 82.

Steam generator tubing evaluation is focused primarily on Alloy 800 tubing, although some evaluation of older alloys remaining in service at some CANDU plants is also included (i.e., stress relieved Alloy 600 and Alloy 400). Alloy 600 and Alloy 400 (often referred to by a supplier trade name Monel® 400) are generally considered "sunset" materials for which significant additional materials R&D is not warranted.

Steam generator secondary-side internals are generally constructed from materials similar to those used in PWR designs. Design evolution for CANDU SGs is also similar to that observed for PWR SGs. Over time, designers have progressively replaced carbon steels with more corrosion-resistant alloys and have sought to optimize tube-to-tube support interfaces. Carbon and low-alloy steel is used for tube supports in older designs and is generally applied in SG dryer assemblies. Martensitic and austenitic stainless steels are specified for tube support applications in newer designs. Most CANDU SGs employ lattice bar style tube supports.

Steam generator secondary water chemistry is maintained consistent with EPRI guidelines.

7.1.1.5 External Surfaces and Pressure-Retaining Bolting (Table 7-6)

The scope of MDM evaluation for external surfaces and bolting includes the outer surfaces of the high-temperature portions of the systems and components evaluated in Tables 7-1 through 7-5. Specifically, this includes PHT system components, SG shells and heads, and applicable pressure-retaining bolting for these systems. Pressure-retaining bolting identified by the CANDU expert panel included high-strength, low-alloy steel (HSLAS) SA-193 Gr. B7 and nickel-base Alloy 718. These components are exposed to the reactor building atmosphere. Although some exposure to leakage may occur, CANDU plants aggressively detect and minimize leakage due to the costs associated with replacing heavy water coolant.

7.1.2 Components Evaluated

The scope of components evaluated includes only "passive" components. Passive components are those that perform their safety function without moving parts or changes in configuration. Examples of passive components include pressure tubes, piping, welds, pump casings, valve bodies, and bolting. Active components such as rotating assemblies and valve stems and internals are not considered in the MDM evaluation.

7.1.3 Evaluation Assumptions

Results presented in the component level tables are based on generic evaluation by a panel of subject matter experts. Assumptions used by the panel to facilitate the development of consistent results for different materials, systems, and reactor designs are described in the following sections.

7.1.3.1 Operating Conditions

All normal operating conditions are considered. These include normal power operations, startup, shutdown, and layup for SGs. Normal operating conditions are defined to include less well-controlled environmental conditions, taking into consideration actions such as the significant oxygen ingress that may occur during maintenance periods and persist for some time during startup. Specific off-normal conditions assumed by the panel for the purposes of MDM evaluation include pressure tube leakage and extended SG layup. Although pressure tube leakage is an infrequent event, exposure of the spacers and calandria tubes to wetting can

detrimentally affect performance. On this basis, the conditions and effects developing from pressure tube leakage were considered relevant by the expert panel. Due to mid-life refurbishment and based on experience with extended outages in CANDU plants, extended SG layup was also considered to be a relevant consideration for the SG tubes and internals. Severe, and exceptionally infrequent, off-normal operating conditions, such as resin or raw water intrusion events, were not considered in developing the MDM results.

7.1.3.2 Service Life

MDM evaluations for the CANDU reactor design assume a 60-year service life. However, a mid-life refurbishment that includes replacement of the fuel channel assemblies is also assumed. As a result, the service life assumed for the fuel channel assemblies is 30 years.

7.2 CANDU Results: Degradation Matrix Tables and Explanatory Notes

Component level result tables for the CANDU design include:

Table 7-1 Fuel Channel Assemblies

Table 7-2 Calandria Vessel and Moderator System

Table 7-3 Primary Heat Transport System

Table 7-4 Steam Generator Tubing

Table 7-5 Steam Generator Internals and Secondary Pressure Boundary

Table 7-6 External Surfaces and Pressure-Retaining Bolting

Hyperlinks within these tables lead to summary notes contained in Table 7-7, Explanatory Notes.

The degradation matrix tables include the use of abbreviations and color coding. Cell *Y*, *N*, *?*, and *N/A* designations indicate applicability of the degradation mode to a material type. Comprehensive definitions are provided in Section 2.2.3.1.

Cell shading indicates R&D status:

- Green fill indicates that the degradation mechanism is sufficiently well understood.
- Yellow fill indicates R&D is in progress to address gaps associated with the degradation mechanism in a reasonable time frame.
- Orange fill indicates insufficient R&D is ongoing or planned to address gaps associated with the degradation mechanism in a reasonable time frame.
- Blue fill indicates insufficient data exist to establish degradation mechanism applicability.

Comprehensive definitions of MDM color codes are provided in Section 2.2.3.2.

Within Table 7-7, references are provided in two ways. For EPRI references, a hyperlink to the EPRI abstract webpage is provided. For other references, a citation listing is provided in Section 7.3. Changes to cell results for Revision 5 can be found in Appendix D.

Table 7-1
CANDU fuel channel assemblies[1]

MATERIAL	DEGRADATION MODE															
	Corrosion				Wear	SCC				Fatigue		RiFP		Irradiation Effects		
	Gen.	Local	FAC	Foul		IG/TG	IA	LTCC	DHC	HCF	EAF	Th.	Env.	Emb.	VS	IC/SR
Zr-2.5 Nb[2]	Y c1-1a	Y c1-2a	N	N	Y c1-5a	N	N	N	Y c1-9a	N	Y c1-11a	N	Y c1-13a	Y c1-14a	N	Y c1-16a
Zircaloy: Zr-2[3]	N	N	N	N	Y c1-5b	N	N	N	Y c1-9b	Y c1-10b	N	N	N	Y c1-14b	N	Y c1-16b
Ni-base Alloy: X-750[4]	N	N	N	N	Y c1-5c	Y c1-6c	Y c1-7c	N	N	N	N	Y c1-12c	Y c1-13c	Y c1-14c	Y c1-15c	Y c1-16c
Zr-Nb-Cu[5]	N	N	N	N	Y c1-5d	N	N	N	Y c1-9d	N	N	Y c1-12d	Y c1-13d	Y c1-14d	N	Y c1-16d
SS: Martensitic: (403, 410)[6]	N	Y c1-2e	N	N	N	Y c1-6e	N	N	N	N	Y c1-11e	Y c1-12e	Y c1-13e	Y c1-14e	N	N

Notes:

1. The CANDU fuel channel assembly components evaluated in Table 7-1 have a 30-year nominal life. These components are replaced during a mid-life refurbishment.
2. Pressure tubes.
3. Calandria tubes.
4. Annulus spacers, also termed “garter springs.”
5. Newer design annulus gas system (AGS) spacer spring.
6. Fuel channel assembly end fittings.

Table 7-2
CANDU calandria vessel and moderator system

MATERIAL	DEGRADATION MODE															
	Corrosion				Wear	SCC				Fatigue		RiFP		Irradiation Effects		
	Gen.	Local	FAC	Foul		IG/TG	IA	LTCC	DHC	HCF	EAF	Th.	Env.	Emb.	VS	IC/SR
CALANDRIA VESSEL AND INTERNALS, MODERATOR SYSTEM PIPING COMPONENTS																
SS: L-Grade	N	Y c2-2a	N	N	N	Y c2-6a	? c2-7a	N	N/A	N	N	N	? c2-13a	Y c2-14a	N	Y c2-16a
SS Welds: 308L	N	Y c2-2b	N	N	N	Y c2-6b	? c2-7b	N	N/A	N	N	N	? c2-13b	Y c2-14b	N	Y c2-16b
Zircaloy: Zr-2[1]	N	N	N	N	Y c2-5c	N	N	N	Y c2-9c	Y c2-10c	N	N	N	Y c2-14c	N	Y c2-16c
Ni-base Alloy: X-750, 718[2]	N	Y c2-2d	N	N	N	? c2-6d	? c2-7d	N	N	N	Y c2-11d	N	? c2-13d	? c2-14d	N	Y c2-16d
MODERATOR SYSTEM HEAT EXCHANGER TUBING																
Alloy 800/ Duplex SS	N	Y c2-2e	N	Y c2-4e	N	N	N/A	N	N	N	N	N	N	N/A	N/A	N/A
Titanium	N	N	N	Y c2-4f	N	N	N/A	N	N	N	N	N	N	N/A	N/A	N/A

Notes:

1. Includes control rod guide tubes and liquid injection shutdown system (LISS) nozzles (spargers) internal to the calandria vessel.
2. Includes guide tube springs and LISS nozzle nose pieces (support pins).

Table 7-3
CANDU primary heat transport system

MATERIAL	DEGRADATION MODE											
	Corrosion				Wear	SCC				Fatigue		RiFP	
	Gen.	Local	FAC	Foul		IG/TG	IA	LTCC	DHC	HCF	EAF	Th.	Env.
CS: Base Metal	Y c3-1a	N	Y c3-3a	N	N	Y c3-6a	N/A	Y c3-8a	N	Y c3-10a	Y c3-11a	N	? c3-13a
CS: Welds	Y c3-1b	N	Y c3-3b	N	N	Y c3-6b	N/A	Y c3-8b	N	Y c3-10b	Y c3-11b	N	? c3-13b
LAS	N	N	N	N	N	Y c3-6c	N/A	N	N	Y c3-10c	Y c3-11c	Y c3-12c	? c3-13c
Ni-base Alloy: Alloy 600	N	N	N	N	N	Y c3-6d	N/A	N	N	N	Y c3-11d	N	Y c3-13d
Ni-base Alloy Welds: A82	N	N	N	N	N	Y c3-6e	N/A	N	N	N	Y c3-11e	N	Y c3-13e
Ni-base Alloy: Alloy 690	N	N	N	N	N	Y c3-6f	N/A	N	N	N	Y c3-11f	N	Y c3-13f
Ni-base Alloy Welds: A52	N	N	N	N	N	Y c3-6g	N/A	N	N	N	Y c3-11g	N	Y c3-13g

Table 7-4
CANDU steam generator tubing

MATERIAL	DEGRADATION MODE											
	Corrosion					Wear	SCC		Fatigue		Reduction in Frac. Properties	
	Wstg.	Pitting	FAC	Foul (OD)	Foul (ID)		OD	ID	HCF	EAF	Th.	Env.
STEAM GENERATOR TUBING												
Alloy 800	Y c4-1a	Y c4-2a	N	Y c4-4a	Y c4-5a	Y c4-6a	Y c4-7a	N	Y c4-9a	Y c4-10a	N	N
Ni-base Alloy: 600 (Stress Relieved)	Y c4-1b	Y c4-2b	N	Y c4-4b	Y c4-5b	Y c4-6b	Y c4-7b	Y c4-8b	Y c4-9b	Y c4-10b	N	Y c4-12b
Ni-base Alloy: 400	Y c4-1c	Y c4-2c	Y c4-3c	Y c4-4c	Y c4-5c	Y c4-6c	N	N	Y c4-9c	Y c4-10c	N	N
TUBE PLUGS AND TUBESHEET WELDS												
Ni-base Alloy: Alloy 600 Plugs	N	N	N	N		N	N	Y c4-8d	N	Y c4-10d	N	Y c4-12d
Ni-base Alloy: Alloy 82 Welds	N	N	N	N		N	N	Y c4-8e	N	Y c4-10e	N	Y c4-12e

Table 7-5
CANDU steam generator internals and secondary pressure boundary

MATERIAL	DEGRADATION MODE									
	Corrosion				Wear	SCC	Fatigue		Reduction in Frac. Properties	
	Wstg.	Pitting	FAC	Foul		IG/TG	HCF	EAF	Th.	Env.
STEAM GENERATOR INTERNALS										
C&LAS	Y c5-1a	Y c5-2a	Y c5-3a	Y c5-4a	Y c5-5a	Y c5-6a	Y c5-7a	Y c5-8a	N	N
SS: Martensitic	N	N	N	Y c5-4b	Y c5-5b	Y c5-6b	Y c5-7b	Y c5-8b	Y c5-9b	N
Ni-Alloy: Wrought A600	N	N	N	N	Y c5-5c	Y c5-6c	Y c5-7c	Y c5-8c	N	N
Ni-Alloy: Wrought A800H	N	Y c5-2d	N	N	Y c5-5d	? c5-6d	Y c5-7d	Y c5-8d	N	N
STEAM GENERATOR SECONDARY PRESSURE BOUNDARY										
LAS	N	Y c5-2e	N	N	N	Y c5-6e	N	Y c5-8e	N	N

Table 7-6
CANDU external surfaces and pressure-retaining bolting

MATERIAL	DEGRADATION MODE										
	Corrosion				Wear	SCC		Fatigue		Reduction in Frac. Properties	
	Wstg.	Pitting	FAC	Foul		IG/TG	LTCC	HCF	EAF	Th.	Env.
EXTERNAL SURFACES											
CS	N	Y c6-2a	N/A	N/A	N	Y c6-6a	Y c6-7a	Y c6-8a	Y c6-9a	N/A	N/A
LAS	N	Y c6-2b	N/A	N/A	N	N	N	Y c6-8b	Y c6-9b	N/A	N/A
Ni-Alloy	N	Y c6-2c	N/A	N/A	N	N	N	Y c6-8c	Y c6-9c	N/A	N/A
PRESSURE-RETAINING FASTENERS											
LAS: High Strength	N	Y c6-2d	N/A	N/A	N	Y c6-6d	N/A	Y c6-8d	Y c6-9d	? c6-10d	N/A
Ni-Alloy: Alloy 718	N	Y c6-2e	N/A	N/A	N	Y c6-6e	N/A	Y c6-8e	Y c6-9e	N	N/A

Table 7-7
CANDU explanatory notes

NOTE ID	EXPLANATORY NOTE
CANDU FUEL CHANNEL ASSEMBLIES	
c1-1a	Although pressure tubes undergo superficial general corrosion along the entire length of the pressure tube in the high temperature coolant, the associated wall loss is inconsequential. However, the acquisition of deuterium resulting from the corrosion reaction does increase the hydriding potential of the tube. This potential effect of hydrogen ingress on pressure tube DHC susceptibility is addressed in cell c1-9a. The cell result for general corrosion is Green, and no R&D is warranted. [R&D Status = GREEN] **Reference:** COG: [7-1]
c1-2a	Pressure tubes may undergo localized corrosion reactions, particularly at the ends of the tube where it is rolled into the martensitic stainless steel end fitting. These are of no concern other than the rolled joint region forms the pressure boundary between the coolant and the AGS. The mechanical joint creates a crevice condition and galvanic couple resulting in the possibility for corrosion mechanisms at the ends of the pressure tube. A second localized corrosion reaction also occurs in the outlet half of pressure tubes beneath fuel bundle bearing pads. A crevice condition occurs beneath the bearing pads in contact with the pressure tube. This crevice condition leads to local concentration of lithium hydroxide. High concentrations of lithium hydroxide have led to very rapid corrosion rates in zirconium alloys. The result of this localized corrosion is the development of small, shallow, rounded cavities extending in depth up to approximately 10% of the wall thickness of the pressure tube. A third instance of localized corrosion has been reported in some pressure tubes downstream of the inlet shield plug. It extends about 100 mm into the pressure tube. It is characterized by heavy oxide buildup that becomes friable. The mechanism is thought to be related to the flux spectrum and flow conditions at the channel inlets. Although not an integrity concern, it does adversely affect inspection capability in the rolled joint region. Localized corrosion at the ends of the pressure tube is a current concern, and ongoing R&D is focused on generating models to enable future predictions. There are currently limits on the hydrogen concentration of 70 to 100 ppm ranging across the channel from the inlet to outlet. The reason for the limits is fracture toughness related and the effect that it has on shifting the transition temperature behavior. [R&D Status = YELLOW] **References:** COG: [7-2], Other: [7-50]

Table 7-7 (continued)
CANDU explanatory notes

NOTE ID	EXPLANATORY NOTE
c1-2e	Although localized corrosion of the martensitic stainless steel end fittings is plausible, low corrosion rates are observed in the deoxygenated, lithiated, and high pH heavy water coolant. As a result, there are no plant integrity concerns. A “Y” and Green R&D status are considered appropriate. [R&D Status = GREEN] **Reference:** EPRI: 3002018322
c1-5a	There are documented instances of flaws developing in the vicinity of bearing pads, particularly at the inlet half of the pressure tube. It is speculated that localized wear at bearing pads is responsible. The wear damage itself is shallow and innocuous. The primary wear damage reported in pressure tubes is caused by debris that is entrained in the PHT system. The extent and severity of such damage is related to the cleanliness standards employed during construction and maintenance when the primary system is open (e.g., inspection/repairs of PHT system components). Debris becomes entrapped by fuel bundles and under PHT system flow conditions can fret cavities into the pressure tube wall. In the operating plants, most debris damage occurs during commissioning and early operation as a result of the high debris inventory from construction activities. Debris can also become entrained in the PHT system during operation as a result of component failures. Rigorous implementation of FME practices will help mitigate sources of debris. Due to the nature of the damage, debris frets can occur along the full length of the pressure tube. Debris frets have been observed ranging in depth from superficial to >1 mm in depth. Some pressure tubes undergo active wear caused by vibration of fuel bundles in the HTS flow. The wear occurs in channels containing 13 fuel bundles at the inlets of pressure tubes where turbulence and flow-related harmonics lead to fuel string vibration. Cavities of depths exceeding 10% of wall thickness have been reported. The current strategy for wear due to vibration is to manage the degradation by mitigating damage potential. In Darlington, the wear was caused by harmonics established by the PHT system pump. The number of vanes in the impellers was changed and harmonics reduced. In addition, a long bundle program was also instituted to shift the bearing pads outboard, thereby avoiding fretting in the higher stress roll transition region. In Bruce B, the cores are being converted to 12 bundle units, thereby eliminating the problem. Given the success of these actions, additional R&D is not planned at this time. [R&D Status = GREEN] **Reference:** None

Table 7-7 (continued)
CANDU explanatory notes

NOTE ID	EXPLANATORY NOTE
c1-5b c1-10b	The loads imposed by the pressure tube, coolant, and fuel are translated to the calandria tube via the annulus spacers. Hence, calandria tubes experience wear caused by contact with annulus spacers. Although the observed wear is usually superficial, there has been one instance of more serious wear leading to initiation of a fatigue crack and subsequent calandria tube leakage. Specifically, high-cycle fatigue and fretting centered on an inlet annulus spacer in Pickering B Unit 7, Channel A17, led to the initiation of an axial through-wall fatigue crack in the calandria tube. Wear on the spacer, calandria tube, and pressure tube was observed. The ongoing action is to continue inspecting channels to determine whether there are wear marks on the pressure tube at spacer locations. In addition to concerns over calandria tube wear and possible failure, spacer wear will result in a reduced pressure tube to calandria tube gap, leading to associated concerns over hydride blister formation. The consensus of the expert panel is that no additional R&D is warranted to further characterize the potential for similar events to occur. [R&D Status = GREEN] **Reference:** COG: [7-3]
c1-5c	Spacer wear will result from interaction loads between the pressure tube and calandria tube. Examination of ex-service spacers has indicated X-750 spacers are not subject to significant wear. No additional R&D is considered warranted at this time. [R&D Status = GREEN] **Reference:** COG: [7-3]
c1-5d	Spacer wear will result from interaction loads between the pressure tube and calandria tube. Examination of ex-service spacers has indicated that Zr-Nb-Cu spacers can be subject to significant wear in the pinched region as a result of continual spalling of the hydrides that accumulate at the cold contact points with the calandria tube. A conservative Yellow is assigned to the R&D Status because an insufficient number of spacers has been examined to establish the possible extent of wear and impact on function. If the wear becomes severe and unexpected late-life contact between pressure tube and calandria tube occurs, there is a substantial risk of pressure tube failure. [R&D Status = YELLOW] **References:** COG: [7-3], [7-4], [7-5]

Table 7-7 (continued)
CANDU explanatory notes

NOTE ID	EXPLANATORY NOTE
c1-6c c1-7c	The normal operating environment for the X-750 spacers is dry CO_2 annulus gas that would not be expected to promote SCC. Unless a situation arises where a unit knowingly operates with severe leakage (the AGS functions as a leak detection system), there is no risk of SCC. Consequently, additional R&D is not required. In the rare event of AGS flooding, the primary SCC concern is related to the effect this flooding could have on spacer integrity and serviceable life, particularly if the spacer material properties are degraded by embrittlement (see notes c1-12c and c1-13c). [R&D Status = GREEN] **References:** COG: [7-6], [7-8], [7-10] EPRI: MRP-88, MRP-175R1
c1-6e	The martensitic stainless steel end fitting material has potential susceptibility to SCC, but, based on CANDU operating experience, it seems to be resistant to this mechanism in the lithiated, pH 10, high temperature (> 300°C) heat transport system environment. While a relatively steep neutron flux gradient is known to exist in regions near the core periphery, the inboard end of the end fitting is expected to receive a small, but significant, dose. Examination of ex-service end fittings indicated that irradiation results in increased hardness without any signs of saturation. In the absence of saturation and at a targeted 400k EFPH of reactor life, irradiation conditions could plausibly lead to hardness levels that would be considered sufficient to render the material susceptible to SCC if the high hardness had been induced by other means such as improper heat treatment or cold working. Currently, there is no ongoing or planned R&D to evaluate the role of irradiation increasing the SCC susceptibility of martensitic stainless steels. In the absence of irradiation effects, SCC is plausible only if exposure to off-normal chemistry occurs or if excessive hardness was induced by improper heat treatment or cold working. [R&D Status = ORANGE] **References:** COG: [7-7] EPRI: 3002018322

Table 7-7 (continued)
CANDU explanatory notes

NOTE ID	EXPLANATORY NOTE
c1-9a	The Zr-2.5Nb pressure tubes acquire deuterium via corrosion reactions in the hot and pressurized HTS coolant. In addition, the solubility of hydrogen in zirconium alloys is low; hence, hydrogen can readily precipitate as a brittle hydride phase. Hydrides tend to accumulate at sites of high tensile stress. If the stress levels are sufficiently high, the hydride can grow to a critical size and cracks develop in a stepwise progression to leakage. Although a number of DHC-related cracking events occurred early in CANDU history, improved design, maintenance, and fabrication practices have been successful in preventing subsequent failures. Current aging management concerns are associated with improved characterization/prediction of the end of service life. For end-of-life prediction, the ends of the pressure tubes are of most interest. There is an increased probability of hydride formation at these locations due to the diffusion of hydrogen from end fittings (see note c1-13e), in addition to increased levels of cold work associated with the rolling process. These additional factors can influence the formation of hydrides at this location. Hydride blisters are accumulations of solid hydride that can form in pressure tube material if the hot pressure tube sags into contact with the cooler calandria tube. Under a contacting condition, a temperature gradient is established through the pressure tube wall, and if the protium + deuterium concentration (H_{eq}) is sufficiently high, the hydrogen in solution migrates to the contact site, eventually resulting in solid hydride accumulation. This mechanism was the cause of a pressure tube rupture in 1983 in Pickering Unit 2, Channel G16. Ongoing and planned R&D is directed toward supporting demonstrations of continued serviceability and improved characterization of the pressure tube service life limits. Areas of R&D interest include: • Improved data sets to fully characterize the effect of hydrogen solubility hysteresis • Hydrogen uptake at fuel bundle bearing pads and at pressure tube end fitting joints (See note c1-2a for additional discussion.) • Circumferential variability (including localized exceedance of terminal solid solubility limits observed at inlets) • Material variability effects Completion of ongoing and planned R&D is considered adequate to address the remaining pressure tube DHC data needs. [R&D Status = YELLOW] **References:** COG: [7-11], [7-12] Other: [7-51], [7-52], [7-53], [7-54], [7-55], [7-56], [7-57], [7-58], [7-59]

Table 7-7 (continued)
CANDU explanatory notes

NOTE ID	EXPLANATORY NOTE
c1-9b	Although DHC is plausible for the Zr-2 calandria tubes, the risk is considered low because Zr-2 is a lower yield stress alloy and less susceptible to DHC. To date, there have been no instances of DHC in calandria tubes in any CANDU reactor, despite the presence of high residual stresses caused by rolling the calandria tube into the end shield tube sheet. Conservatively, a "Y" degradation mechanism applicability result is applied. [R&D Status = GREEN] **References:** Other: [7-84], [7-85], [7-86]
c1-9d	DHC is plausible for the Zr-Nb-Cu spacers and the risk has not been fully evaluated. Brittle fracture has been observed during component (crush) testing of ex-service spacers. However, in these instances, the spacers retain sufficient strength to function as designed. Currently, the condition of spacers is being monitored through surveillance, but R&D work is necessary to understand the extent and implications of the observed cracking. [R&D Status = ORANGE] **References:** COG: [7-5], [7-9]
c1-11a	No pressure tube failures attributed to low-cycle fatigue mechanisms have occurred. However, there are no fatigue life data addressing environmental effects for irradiated pressure tube materials. Additionally, pressure tubes have somewhat less structural margin than is typical for primary system pressure-retaining components. The tubes are thinner than most other primary pressure-retaining components (approximately 40 mm in thickness), and once a fatigue crack is initiated, subsequent flaw growth would likely occur by hydride formation and DHC. R&D needs include development of irradiated materials data in the primary coolant environment, understanding the potential role of hydrogen in affecting fatigue life, and characterizing the effects of material variability. At present, an Orange R&D Status result is deemed appropriate. Ongoing and planned R&D is considered insufficient to address these concerns. [R&D Status = ORANGE] **References:** COG: [7-13], [7-14]

Table 7-7 (continued)
CANDU explanatory notes

NOTE ID	EXPLANATORY NOTE
c1-11e	For the martensitic stainless steel end fittings, there are few fatigue life data addressing environmental effects. Additionally, these fittings are subject to neutron fluence during a normal operating life. Irradiation hardening could have further detrimental effect on fatigue life. Regardless, performance to date has been good with no fatigue cracking events. The primary R&D needs are to generically resolve the apparent discrepancy between performance predicted by laboratory data and performance observed in the field and to ensure that the margins existing in current fatigue analyses are sufficient to envelop the effect of environment. Further complicating the issue for martensitic stainless steels is the lack of any relevant environmental fatigue test data. Although EPRI work is underway to address the apparent discrepancy between results obtained by the testing of small, uniaxially loaded specimens and actual plant components, there are no plans to test martensitic stainless steels. Despite the absence of operating experience, an Orange R&D cell result is conservatively applied. Irradiation effects might raise some additional concerns (see notes c1-6e, c1-12e, c1-14e). [R&D Status = ORANGE] **Reference:** EPRI: 3002018322
c1-12c c1-13c	After removal from service, all X-750 spacers have been found embrittled as a result of irradiation-induced He bubble generation (see note c1-14c). Thermal effects are secondary as the spacers have portions in contact with the cool calandria tube and with the hot pressure tube; however, the embrittlement concern dominates at either location. There are no environmental effects of concern (see notes c1-6c and c1-7c). Additional study apart from that being planned is not warranted. [R&D Status = GREEN] **References:** COG: [7-6], [7-8], [7-15], [7-15], [7-1], [7-18]

Table 7-7 (continued)
CANDU explanatory notes

NOTE ID	EXPLANATORY NOTE
c1-12d c1-13d c1-14d c1-16d	To date, Zr-Nb-Cu spacers have not shown obvious signs of unacceptable material condition apart from those noted in c1-9d. Since this material is currently being used in fuel channel assembly refurbishments, continued surveillance is warranted, and those observations will inform the need for further R&D. [R&D Status = GREEN] **References:** COG: [7-15], [7-18], [7-19]
c1-12e	For martensitic steels (Types 403 and 410), there are relatively few data available to assess thermal aging effects. MRP-175 indicates that most data are related to Type 410 material, which is anticipated to be similar to, or to bound, Type 403. Thermal embrittlement of martensitic stainless steel is likely linked to grain boundary segregation of impurities. However, the effect observed in the available data is not an increase in material hardness, but rather a shift in the ductile to brittle transition temperature. Although not considered a high priority concern, some embrittlement due to thermal aging is likely to occur, and available data to characterize the significance of any thermal aging embrittlement are limited. An Orange R&D Status result is conservatively applied. [R&D Status = ORANGE] **References:** EPRI: MRP-175R1, 3002018322

Table 7-7 (continued)
CANDU explanatory notes

NOTE ID	EXPLANATORY NOTE
c1-13a	Pressure tubes exhibit ductile-to-brittle transition as a function of temperature with apparent lower shelf properties persisting at reduced temperatures and upper shelf properties at temperatures exceeding 150°C. Increasing the hydrogen concentration to high levels shifts the transition temperature behavior to higher temperatures. As a result, lower shelf properties persist at temperatures exceeding 150°C, posing significant operational concerns as pressure tubes age. High temperature (> 300°C) corrosion reactions in the pressure tube lead to increasing concentrations of deuterium, which has an adverse impact on fracture toughness transition temperature behavior, particularly at high H_{eq} levels; i.e., H_{eq} levels above the terminal solid solubility for dissolution (TSSD) limit. TSSD is expected to be exceeded near outlets late in life for most reactors and at rolled joints in mid-life (see note c1-9a). This results in increased concern regarding fracture prevention and available structural margins, potentially affecting leak-before-break evaluations. The current R&D focus is placed on improved characterization of serviceability and structural margins for pressure tubes in service. The current consensus is that ongoing and planned R&D is inadequate to address the outstanding data needs in the required time frame. [R&D Status = ORANGE] **References:** Other: [7-51], [7-60]
c1-13e	Testing and evaluation of available materials property data performed by EPRI to assess PWR reactor internals indicate that, in general, higher strength and cold-worked materials are likely to have increased susceptibility to this phenomenon. Some effect is likely to occur for martensitic stainless steels, but there has been no specific testing of martensitic stainless steel materials to address environmental effects on fracture properties. Furthermore, there is likely to be a significant flux of corrosion-generated hydrogen through the end fitting during normal operation (see note c1-13a), the effect of which is unknown. The added contribution of irradiation remains unclear, although a negative effect is expected (see note c1-14e). [R&D Status = ORANGE] **References:** EPRI: MRP-285, MRP-293

Table 7-7 (continued)
CANDU explanatory notes

NOTE ID	EXPLANATORY NOTE
c1-14a	Although exposed to significant fluence over a 30-year operating life ($3x10^{22}$ n/cm^2), neutron damage saturates in pressure tubes after about 1 year of irradiation. Of concern for pressure tube performance is the synergistic effect of high H_{eq} and neutron damage that results in a shift in the fracture toughness transition temperature behavior (see note c1-13a). The primary effect of irradiation embrittlement is being addressed in relation to its effect on fracture toughness transition temperature behavior in c1-13a. Conservatively, the R&D Orange Status indicated is consistent with c1-13a to ensure that neutron fluence effects are considered in future R&D planning. [R&D Status = ORANGE] **Reference:** Other: [7-61]
c1-14b	Embrittlement (strengthening and some loss of ductility) of the Zr-2 calandria tubes will occur. However, such embrittlement does not reduce the functional performance under normal operating conditions. As such, no R&D is needed to address this phenomenon. [R&D Status = GREEN] **Reference:** None
c1-14c	**Operating Experience/Susceptibility:** X-750 spacers become embrittled due to helium production via neutron transmutation reactions. Strength decreases to a point where the spacer has zero remaining ductility late in life. Spacers will retain sufficient strength to support the pressure tube at operational loads, and surveillance is prescribed to monitor the condition of these spacers through life. The nature and evolution of the embrittlement are well understood following a decade of COG-funded research projects, and additional research is not warranted. [R&D Status = GREEN] **References:** COG: [7-6], [7-8], [7-15], [7-15], [7-1], [7-18] EPRI: BWRVIP-262NP, BWRVIP-291R1, BWRVIP-240 Other: [7-62]

Table 7-7 (continued)
CANDU explanatory notes

NOTE ID	EXPLANATORY NOTE
c1-14e	Examination of ex-service end fittings indicated that irradiation could result in increased hardness without any signs of saturation. The fact that relatively little work has been conducted in this area is due to a legacy of assessments performed in the 1980s, when the understanding was that the evolution of mechanical properties saturates or plateaus at a relatively low dose. In the absence of saturation and at a targeted 400k EFPH of reactor life, no clear data exist to support any realistic assessment, and some reduction of fracture toughness remains plausible. The expected irradiation conditions could lead to hardness levels, at which, in the case of tempering and/or cold work, would lead to an increased risk of EAC (see c1-13e). [R&D Status = ORANGE] **Reference:** COG: [7-7]
c1-15c c1-16c	Tight fitting X-750 annulus spacers de-tension primarily as a result of stress relaxation, although irradiation-induced creep and void swelling may play a secondary role. Of concern is the potential for spacer movement resulting from de-tensioning. Once spacers become pinched between the pressure tube and calandria tube, spacer movement is precluded. Sufficient surveillance examinations of spacers and modeling of pressure tube sag and diametral creep have shown that stress relaxation, irradiation creep, and void swelling will not fully de-tension a spacer prior to pinching. [R&D Status = GREEN] **References:** COG: [7-6], [7-8], [7-21]

Table 7-7 (continued)
CANDU explanatory notes

NOTE ID	EXPLANATORY NOTE
c1-16a c1-16b	Both pressure tubes and calandria tubes undergo irradiation creep effects leading to sag and relaxation of stresses. Pressure tube sagging into contact with the calandria tube leading to hydride blister formation is a major issue for operability (see c1-9a). Other creep effects and adverse impacts on the pressure tube include: • **Elongation**: Pressure tubes elongate to an extent whereby the fuel channel assembly is no longer supported on its bearings. An unsupported fuel channel is a non-design condition that could result in large stresses being imparted to the pressure tube and end shield components if the bearings lock up rather than returning to the design condition when the unit is cooled from the hot condition. Other elongation impacts include: – **Burnish mark interaction**. Affects fuel channels containing 13 fuel bundles. The 13 bundle fuel string results in the inlet fuel bundle extending into the inlet roll expanded region of the pressure tube. With channel elongation, a fuel bundle bearing pad of this bundle will come to reside over the higher stress/high H_{eq} burnish mark transition region, and it can fret flaws into the pressure tube wall. – **Power pulse**. The condition arises from an accident scenario whereby reverse flow into fuel channels can cause the fuel string to shift toward the inlet end, resulting in a large uncontrolled increase in reactivity. – **Fueling machine access**. Differential elongation rates vary across the reactor due to differences in channel power. – **Feeder impacts**. Differential elongation also affects feeder pipes by decreasing the clearance between adjacent feeders. • **Diametral expansion**: Diametral expansion involves the creep-related increase in diameter along the length of a fuel channel caused by neutron fluence, pressure, and temperature. Issues related to diametral expansion include exceeding design limits, spacer nip-up, increasing hoop stress, flow bypass impinging on trip margins, and a small effective increase in D_2 uptake. • **Wall thinning**: Wall thinning affects pressure tube loading through increased hoop stresses and results in small, effective increases in the deuterium uptake rate. This has adverse impacts on fitness-for-service assessments. These effects are considered relatively well understood. No additional fundamental materials R&D is needed. [R&D Status = GREEN] **Reference:** Other: [7-61]

Table 7-7 (continued)
CANDU explanatory notes

NOTE ID	EXPLANATORY NOTE
CANDU CALANDRIA VESSEL AND INTERNALS, MODERATOR SYSTEM PIPING COMPONENTS	
c2-2a c2-2b	The threshold of halogen concentration for localized corrosion is not known in the presence of typical moderator environments containing nitrates, especially in the condensation regions of the calandria relief ducts. Presently, there is ongoing and planned work to address this knowledge gap as well as the knowledge gap pertaining to difficulties associated with weld repair (i.e., avoiding helium-induced cracking when welding high-He irradiated stainless steel). See notes c2-6a and c2-6b. [R&D Status = YELLOW] **Reference:** None
c2-2d	Localized corrosion (i.e., pitting, crevice corrosion) of the LISS nozzle nose pieces and control rod guide tube springs is considered plausible. However, no significant corrosion has been identified to date in the low impurity and deoxygenated moderator system coolant. No materials R&D is considered needed. [R&D Status = GREEN] **Reference:** None
c2-5c c2-10c	Wear and high-cycle fatigue of control rod guide tubes and LISS nozzles is possible. Contact with calandria tubes can occur due to calandria tube sag and results in wear or possibly some high-cycle fatigue loading. However, the risk of occurrence is low, and no materials R&D is considered needed. Also see c1-5b. [R&D Status = GREEN] **Reference:** None

Table 7-7 (continued)
CANDU explanatory notes

NOTE ID	EXPLANATORY NOTE
c2-6a c2-6b	The operating experience includes occurrences of SCC in the upper region of the calandria vessel (ducts) where the water/cover gas interface occurs. Such regions are prone to accumulation of residual pollutants from the moderator system, by condensation, leading to significant accumulation of halogens. SCC has been observed away from welds and has, in at least one case, grown through-wall. The threshold of halogen contamination to initiate SCC in the presence of typical moderator chemistries containing nitrates in the condensation regions of the calandria relief ducts is not known. Furthermore, the issue has elevated importance due to the difficulty of weld repair (risk of helium-induced cracking) in these locations. Presently, there is ongoing and planned work to address this knowledge gap as well as the knowledge gap pertaining to difficulties associated with weld repair. [R&D Status = YELLOW] **Reference:** COG: [7-22]
c2-6d c2-7d	Nickel-base alloys, particularly alloys heat treated to obtain high strength properties, are known to be susceptible to SCC. For the calandria vessel internals, SCC may be a concern for the Alloy 718 control rod guide tube springs since these springs are heat treated for increased strength and are subject to tensile stress during normal operation. These springs are additionally subject to neutron fluence. Anticipated fluence is sufficiently high to induce material property changes and could potentially increase SCC susceptibility. For stainless steel calandria vessel materials, there is some uncertainty regarding the effect of thermal neutrons on material properties (c2-14a). Since this effect would also occur in nickel-base alloys, a similar uncertainty exists for the Alloy 718 control rod guide tube springs. There are few relevant irradiated materials data that address the expected operating temperatures or the effects of neutron fluence. There is no applicable ongoing or planned R&D. SCC is not likely to be relevant for the X-750 LISS nozzle nose pieces, which are thick in comparison to the Alloy 718 control rod guide tube springs and are not loaded in tension. [R&D Status = BLUE] **References:** EPRI: MRP-88, MRP-175R1, BWRVIP-240, BWRVIP-262NP, BWRVIP-291R1 Other: [7-63]

Table 7-7 (continued)
CANDU explanatory notes

NOTE ID	EXPLANATORY NOTE
c2-7a c2-7b	End-of-life (60 EFPY) dose is estimated to reach 3.5 dpa for the most highly irradiated regions of the calandria vessel. Since the calandria vessel is not replaced during refurbishments, 90 EFPY doses are expected to be greater. It is unclear how this will affect the properties of the 304L SS and 308L SS tubesheet plate and welds since there are few low-temperature irradiated materials data for stainless steels. Some irradiation embrittlement will occur. However, it is not known how this might affect the susceptibility of the material to IASCC. While the dose limits are expected to exceed the engineering threshold values for IASCC initiation, there are limited data on the specific environmental conditions in the moderator system, which differ significantly from LWR environments in that they are relatively low temperature (some regions of the calandria vessel have predicted operating temperatures approaching 100°C, with gamma heating) but highly oxidizing environments. If IASCC were to occur, conventional weld repair options will not be available due to the accumulation of 100s of appm He in the material. Given the lack of IASCC test data relevant for the calandria vessel environmental conditions, a "?" status is considered appropriate. However, work is currently underway within the COG Strategic R&D Program to address many of these knowledge gaps. [R&D Status = BLUE] **References:** COG: OP-17-7006, COG: OP-17-7007, COG: OP-18-7014, COG: OP-18-7034
c2-9c	The control rod guide tubes and LISS nozzles located inside the calandria vessel are fabricated from Zr-2. Consistent with the result for calandria tubes (c1-9b), DHC is considered plausible but represents a very low risk. The consensus of the expert panel is that no additional R&D is needed. [R&D Status = GREEN] **Reference:** None
c2-11d	Fatigue cracking of the Alloy 718 control rod guide tube springs is plausible, as these springs experience some cyclic loading during startup and shutdown. While there are no relevant data to characterize environmental effects for these higher hardness nickel-base alloys, operating temperatures are low, well below threshold values found to be necessary for introduction of significant environmental effects for austenitic stainless steels. Based on the operating conditions and EAF threshold for stainless steel, low-cycle/environmentally assisted fatigue failures are not considered a significant risk for Alloy 718. The consensus of the expert panel is that no additional R&D is needed. [R&D Status = GREEN] **Reference:** None

Table 7-7 (continued)
CANDU explanatory notes

NOTE ID	EXPLANATORY NOTE
c2-13a c2-13b	Although there are concerns that stainless steel materials could be subject to reductions in fracture properties after exposure to a coolant environment, there are mitigating factors that lessen concerns for the calandria vessel and moderator system materials. Lower operating stresses and reduced fatigue usage exist. Normal operating temperatures are around 60°C. The area of most concern would be the calandria vessel tubesheet rolled connections to the calandria tubes. This region of the calandria vessel is exposed to operating temperatures approaching 100°C, significant neutron fluence at some locations (up to 3.5 dpa at 60 EFPY), and cold work at the rolled connection to the calandria tubes. An additional uncertainty is the effect of thermal neutron fluence and the higher concentrations of He and H that occur with a thermalized neutron spectrum. Given the lack of data relevant for the calandria vessel environmental conditions, a “?” status is considered appropriate. [R&D Status = BLUE] **Reference:** None
c2-13d	Alloy X-750 is known to be susceptible to fracture under some relevant operating conditions, particularly low-temperature operation under load. Few data exist to characterize this concern. Synergism with SCC is also of some concern given the material's high yield strength and significant history of SCC in other reactor designs. The Alloy 718 control rod guide tube springs may be similarly susceptible to this phenomenon. Given the lack of data relevant for the calandria vessel environmental conditions and the potential for synergism with SCC or fatigue, a “?” status is considered appropriate. [R&D Status = BLUE] **Reference:** EPRI: MRP-293

Table 7-7 (continued)
CANDU explanatory notes

c2-14a c2-14b	End-of-life (60 EFPY) dose is estimated to reach 3.5 dpa for the most highly irradiated regions of the calandria vessel. Historical assessments considering the 60-year fluence indicated no plausible degradation because irradiation is taking place in a point defect recombination dominated temperature range. However, the effect of thermal neutrons was not taken into consideration in those assessments. Thermal neutron irradiation results in a higher concentration of He and H from the Ni-59 + n transmutation than is the case with fast neutrons. It is unclear how this will affect the properties of the 304L SS and 308L SS tubesheet plate and welds since there are few low temperature irradiated materials data for stainless steels. Some irradiation embrittlement will occur. However, it is not known whether the effect is significant for planned operating periods. Additionally, there will be a need to address repair of this irradiated material if cracking occurs. Conventional weld repair options will not be available due to the accumulation of 100s of appm He in the material. The status is set at Yellow to reflect a comprehensive accelerated irradiation program and subsequent test program currently underway within the COG Strategic R&D Program to address many of these knowledge gaps. [R&D Status = YELLOW] **References:** COG: [7-23] EPRI: MRP-175R1 Other: [7-63], [7-64]
c2-14c	Some effect of irradiation will occur. However, the effect will be bounded by the effect observed in the calandria tubes. See c1-14b for discussion related to the calandria tubes. A similar “Y” and Green result is conservatively applied. [R&D Status = GREEN] **Reference:** None
c2-14d	The X-750 LISS nozzle nose pieces and Alloy 718 control rod guide tube springs will accumulate sufficient fluence over the plant operating life that some effect of irradiation could occur. However, there are few data to quantify the effect of irradiation at the relatively low temperatures that occur for these components. For stainless steel calandria vessel materials, there is some uncertainty regarding the effect of thermal (slow) neutrons on material properties (c2-14a). Since the effect would also occur in nickel-base alloys, a similar uncertainty exists for the Alloy 718 control rod guide tube springs. There are few relevant irradiated materials data that address the expected operating temperatures or the effects of neutron fluence. There is also no ongoing or planned R&D to develop the needed data. [R&D Status = BLUE] **References:** EPRI: MRP-175R1, BWRVIP-240, BWRVIP-262NP, BWRVIP-291R1

Table 7-7 (continued)
CANDU explanatory notes

NOTE ID	EXPLANATORY NOTE
c2-16a c2-16b	With end-of-life fluences estimated to reach 3.5 dpa in some locations, some irradiation-induced creep and stress relaxation are expected. In general, relaxation of welds is without structurally significant consequences and not detrimental to materials performance. Since the welds were not stress relieved, any irradiation-induced stress relaxation is expected to be beneficial. These phenomena are well characterized for stainless steels, and further R&D is not warranted. [R&D Status = GREEN] **Reference:** None
c2-16c	Some irradiation-induced creep and sagging of the control rod guide tubes and LISS nozzles could occur over a 60-year service life. However, these effects were not considered to be particularly significant in comparison with those occurring in the calandria tubes. See c1-16b for discussion of this phenomenon as applicable to the calandria tubes. [R&D Status = GREEN] **Reference:** None
c2-16d	Some irradiation-induced stress relaxation of the control rod guide tube support springs will occur over the plant service life. However, irradiation-induced stress relaxation and creep are well understood, and no additional materials R&D is considered needed. [R&D Status = GREEN] **Reference:** None

Table 7-7 (continued)
CANDU explanatory notes

NOTE ID	EXPLANATORY NOTE
CANDU MODERATOR SYSTEM HEAT EXCHANGER TUBING	
c2-2e	Alloy 800 moderator system heat exchanger tubes can suffer from under-deposit corrosion and microbiologically induced corrosion due to exposure to raw cooling water. Fouling, which is a precursor for this form of degradation, is controlled by chlorination (c2-4e). Degradation is adequately managed by existing programs. [R&D Status = GREEN] **Reference:** None.
c2-4e c2-4f	Heat exchanger fouling, including biofouling, sediment accumulation, and zebra mussel ingress, is managed continuously by chlorination from spring to fall at residual concentrations of 0.1 ppm and by tube cleaning and inspection. [R&D Status = GREEN] **Reference:** Other: [7-65]
CANDU PRIMARY HEAT TRANSPORT SYSTEM	
c3-1a c3-1b	General corrosion of carbon steels will occur in the PHT system. However, general corrosion rates are linear and predictable. The phenomenon is well characterized, and no R&D is needed. Wall losses associated with FAC are a more substantial concern due to the potential influence of the corrosion-induced deuterium flux through the material on feeder pipe cracking. See notes c3-6a and c3-3a. [R&D Status = GREEN] **Reference:** None.

Table 7-7 (continued)
CANDU explanatory notes

NOTE ID	EXPLANATORY NOTE
c3-3a c3-3b	FAC is an active degradation mode in outlet feeder pipes. Wall thinning has been observed to various degrees (depending on steel Cr content and flow conditions) in all outlet feeder locations from the fuel channel end fitting up to the header. Within an outlet feeder, the highest thinning rates are observed in the tight radius bends immediately downstream of the Grayloc hub. At this location, there is significant turbulence and the presence of coolant unsaturated in dissolved iron. To date, no preferential FAC of the Grayloc hub to feeder pipe welds has been reported. Notably, the FAC and feeder pipe cracking (at the one unit affected by cracking) occurred in the same region of the PHT system. FAC is known to induce a flux of atomic deuterium through the feeder pipe wall, affecting material properties and crack stability. FAC is a well understood phenomenon, and management of FAC is a mature industry capability. As such, there are no R&D needs specific to FAC. R&D needs associated with understanding FAC interactions with feeder pipe cracking are captured by cell c3-6a. [R&D Status = GREEN] **References:** Other: [7-66], [7-67]

Table 7-7 (continued)
CANDU explanatory notes

NOTE ID	EXPLANATORY NOTE
c3-6a c3-8a	Field observations of CANDU PHT feeder pipe bend cracking remain limited to a single CANDU reactor. All the cracking detected has been in outlet feeders at the 1st or 2nd tight-radius (1.5D) bends immediately downstream of the fuel channel assembly outlet. The material is SA-106 Gr. B carbon steel. Factors influencing feeder cracking include residual stresses, high degrees of cold work and elevated material hardness, temperature (cracking is limited to outlet feeder bends), possibly FAC-generated deuterium (see note c3-3a), and possibly transient operating stresses. Although both ID-initiated and OD-initiated cracking has been reported, only ID-initiated cracking is specifically addressed in this cell explanatory note. Note c6-6a, associated with the evaluation of component external surfaces (see Table 7-6), addresses the OD-initiated cracking observed. Three mechanisms, potentially interacting with each other, have been proposed. SCC resulting from exposure to oxygenated conditions is considered a plausible degradation mode for the ID-initiated cracking, although laboratory test results are not conclusive. Oxidizing conditions may develop during startup after maintenance, where significant oxygen ingress to the PHT system occurs. Additionally, some concern was expressed by the expert panel that oxidizing conditions could locally develop in the outlet feeders due to a combination of radiolysis and local boiling. Hydrogen-induced cracking, resulting from deuterium flux through the material, is a second mechanism considered to detrimentally affect material properties and thus potentially promote cracking. An additional FAC-related consideration is the reduction in structural margin that results from local material removal. Low-temperature creep cracking is the third mechanism. Although the LTCC mechanism is generally noted in the context of OD-initiated cracking, LTCC may also influence ID-initiated cracking. Although this issue has been researched for a number of years, there remain significant gaps in mechanistic understanding of the observed cracking. Also see notes associated with FAC (see c3-3a) and reductions in fracture properties associated with exposure to the coolant environment (see c3-11a). Extensive R&D has been conducted on this topic in the past. While cracking is currently managed by inspection, an Orange R&D result is conservatively applied to highlight the potential influence of hydrogen-induced environmental effects. There is no current R&D ongoing or planned to address this issue. [R&D Status = ORANGE] **References:** Other: [7-66], [7-67]

Table 7-7 (continued)
CANDU explanatory notes

NOTE ID	EXPLANATORY NOTE
c3-6b c3-8b	Similar cracking to that observed in feeder pipe outlet bends (see c3-6a) has been observed in a single repair weld and is considered plausible for all welds and weld HAZs since the factors thought to influence cracking in the tight radius bends are also present in some form at welds. Similar exposure to high residual stress, elevated hardness, and FAC-generated deuterium exists. Exposure to plant transient stresses and associated operating cyclic stresses also occurs. Weld shrinkage contributes to significant residual stresses and may induce cold work in the material. Although R&D has been conducted on this topic in the past and cracking is currently managed by inspection, there is no additional R&D ongoing or planned to further investigate the potential for cracking at welds. [R&D Status = ORANGE] **Reference:** None
c3-6c	For low-alloy steels, SCC-related cracking similar to that postulated to explain the observed feeder pipe outlet bend cracking is considered plausible for low-alloy steel locations subject to higher levels of cold work and weld residual stresses. In these locations, the factors thought to influence cracking in the tight radius bends could be present in some form. Similar exposure to oxidizing conditions would exist. Exposure to fatigue transients and associated operating cyclic stresses occurs. Weld shrinkage contributes to significant residual stresses and may induce cold work in the material. Environmentally assisted cracking (EAF, SICC, or SCC) is in principle also possible, although occurrences in LAS are rare and have been mainly in SG shells and attached piping. Cracking has been attributed to poor chemistry controls and/or exposure to unusually oxidizing conditions (e.g., condenser leaks). However, recent laboratory testing does suggest some vulnerability of low-alloy steels to environmentally assisted cracking in relatively pure water. Specifically, the test results indicate that, at higher oxidizing potentials, very low concentrations of chloride (as low as 3 ppb) can have a detrimental influence on crack growth rates. These effects have been confirmed through multiple tests, and the effect has been shown to be significant only for high ECP conditions (see note b1-6a). CANDU reactor startups include periods of time where oxygenated conditions could co-exist with loading transients and the presence of small concentrations of ionic impurities. As such, these test results are considered to have some relevance to the CANDU design. An R&D status consistent with that for LWRs is deemed appropriate. No additional R&D is needed, although CANDU units may need to disposition the results in the specific context of CANDU operations. [R&D Status = GREEN] **References:** EPRI: BWRVIP-233R2 Other: [7-68], [7-69]

Table 7-7 (continued)
CANDU explanatory notes

NOTE ID	EXPLANATORY NOTE
c3-6d c3-6e	Use of Alloy 600 base metal and Alloy 82 weld metal in the PHT system is limited to flow element installations at some units of SA-106 Gr. B/C carbon steel feeders. From a generic perspective, using PWR experience, these materials would be anticipated to have some susceptibility to PWSCC initiation and growth. Regardless, no cracking has been detected to date. However, these locations are difficult to inspect, and there have been no volumetric examinations performed to detect part through-wall cracking. At issue then is the specific susceptibility of these flow element installations to the CANDU PHT environmental conditions. Regarding Alloy 82 weld filler metal, this material has been found to have a long incubation period for crack initiation in PWR primary conditions. PWSCC initiating in the adjacent Alloy 600 material could extend into the Alloy 82 weld. The HAZ at the interface between Alloy 82 and the carbon steel does not differ significantly from the Alloy 82/LAS dissimilar metal weld configuration (in the absence of cladding) in PWRs to warrant any additional risk. Examinations of ex-service flow elements were undertaken and did not identify any specific degradation. Due to the combination of these results, the significant literature in this area, and the plan to replace these materials with Alloys 690 and 52 upon refurbishment, no additional R&D is warranted. [R&D Status = GREEN] **References:** COG: [7-20] [7-24] EPRI: MRP-55R1, MRP-115

Table 7-7 (continued)
CANDU explanatory notes

NOTE ID	EXPLANATORY NOTE
c3-6f c3-6g	Flow elements in the PHT system are progressively replaced with Alloy 690 base metal and Alloy 52 weld metal directly welded to the SA-106 Gr. B/C CS feeders. While the experience of PWRs operating at higher temperature is conservative to CANDU flow elements, the specificities of the CS/Alloy 52 interface could lead to some concerns. In some qualification mockups, due to the dilution of C from the SA-106 Gr. C (< 0.35 wt%), Alloy 52M was found to be sensitized. While sensitization, in the absence of oxygen ingress, is not considered to constitute a significant risk in PWRs, oxidizing conditions are plausible in CANDU designs during startup and during normal operation due to local boiling and radiolysis. However, the locations of flow elements are difficult to inspect, and there have been no volumetric examinations performed. At issue then is the specific susceptibility of these flow element installations to the CANDU PHT environmental conditions. Although R&D is currently ongoing on the generic topic of Alloy 690 and Alloy 52 in LWR nominal environments, no additional R&D is ongoing or planned to further investigate the risk of SCC of sensitized Alloy 52. Alloy 690: [R&D Status = YELLOW] Alloy 52: [R&D Status = ORANGE] **Reference:** COG: [7-20]
c3-10a c3-10b c3-10c	High-cycle fatigue has been generally considered plausible for small diameter piping components. The CANDU PHT system operating experience includes a small number of vibration-related and thermal-fatigue-induced events associated with unanticipated cyclic loading. These phenomena are generally well characterized, and no additional R&D is required. [R&D Status = GREEN] **Reference:** None

NOTE ID	EXPLANATORY NOTE
c3-11a c3-11b c3-11c	Laboratory tests on small specimens in simulated LWR environments show that fatigue resistance in reactor water environments is lower than in “dry air” environments. This conclusion is supported by a database of laboratory tests on small specimens in simulated reactor coolant environments. It is also recognized that the fatigue design curves that provide the basis for fatigue life assessments of nuclear plant components do not explicitly account for the effects of LWR environments on fatigue life, although, to date, conservatisms included in fatigue design curves and in fatigue calculational methods have been adequate to bound the effects of environment. The information documented in NUREG/CR-6909 is considered applicable to the conditions of CANDU reactor operation. Due to the limited fatigue usage in CANDU designs, no additional R&D is needed. [R&D Status = GREEN] **References:** EPRI: 1026724, 3002010554, 3002010555, 3002007973, MRP-407, MRP-415 Other: [7-87], [5-22]
c3-11d c3-11e c3-11f c3-11g	Generically, fatigue environmental effects are applicable, and, for these austenitic alloys, environmental factors could be significant for transients occurring under deoxygenated conditions. However, the use of Alloy 600 and Alloy 690 base metal and Alloy 82 and Alloy 52 weld metal in the PHT system is limited to flow element installations at some units. As a result, there is a limited scope of components to consider. Since usage is anticipated to be relatively low for these locations, low-cycle fatigue, even with consideration of environmental factors, is not viewed to be a significant concern. No R&D is warranted at this time to address EAF for the nickel-base alloy PHT system components. Although environmental effects are applicable, fatigue usage at these locations is low, such that the components will not be limiting. It is additionally noted that additional data relevant to the CANDU design will be generated by ongoing EPRI R&D focused on addressing EAF for PWR primary system nickel-base alloys. [R&D Status = GREEN] **Reference:** None

Table 7-7 (continued)
CANDU explanatory notes

NOTE ID	EXPLANATORY NOTE
c3-12c	Thermal embrittlement of low-alloy steels is noted as a potential long-term concern at high operating temperatures. Within the context of light water PWRs, the focus is on materials exposed to pressurizer temperatures (up to 343°C), although there are concerns that thermal aging could occur at lower temperatures. CANDU peak operating temperatures are not significantly different than PWR operating temperatures. As such, similar concerns are applicable, particularly for the low-alloy steel pressurizer components. Considerable work is being undertaken or planned in this area (see PWR note p1-10a). Consistent with the PWR MDM, the R&D status is set to Yellow. [R&D Status = YELLOW] **References:** EPRI: MRP-80, MRP-438, MRP-463, MRP-474 Other: [7-70]
c3-13a c3-13b c3-13c	The CANDU PHT system is constructed primarily from carbon and low-alloy steels. To date, there has been relatively little testing of carbon or low-alloy steels to address environmental effects on fracture properties.[1] Of particular concern is the possible role of this phenomenon in feeder pipe cracking occurrences (see note c3-6a). The tight radius bends of concern are highly stressed and cold worked and are subject to a substantial hydrogen flux resulting from FAC occurring at the material interface with the PHT system coolant. Further, because the feeder pipes are relatively small in diameter, there is less structural margin available for crack extension than for larger diameter components because of the smaller wall thicknesses. Significant wall loss from FAC occurring in this area is yet another factor of concern (see note c3-3a). For the CANDU reactor design, there is no ongoing or planned R&D to develop an improved understanding of this phenomenon as it relates to the PHT system, particularly for the carbon steel feeder outlet bends in the presence of a hydrogen flux. [R&D Status = BLUE] **Reference:** Other: [7-71] Note: 1. Prior work by James and Porr [7-71] was cited by panel participants. This work is noted because it indicates some effect of environment in J-R tests performed at 243°C. However, similar testing at 288°C failed to indicate any effect of environment. Although some effect of environment could exist in deoxygenated water, the effect is small in comparison with that occurring in oxygenated water.

Table 7-7 (continued)
CANDU explanatory notes

NOTE ID	EXPLANATORY NOTE
c3-13d c3-13f	Available data developed by EPRI to address light water PWR concerns indicate that in comparison with other materials that have been tested, Alloys 600 and 690 are not particularly susceptible to reductions in fracture properties due to coolant exposure. Although the phenomenon is not well understood for any material, there are no near-term concerns regarding environmental effects on J-R properties for Alloys 600 and 690 unless the material has been subject to substantial cold work. Additionally, synergisms with thermal embrittlement are less likely than for other materials. Based on available R&D data for Alloy 600 and Alloy 690, there is not a significant near-term need for additional R&D for this material. Consistent with the light water PWR MDM result for these alloys' (see p1-11f, p1-11g) susceptibility to this phenomenon, a Green R&D Status result is considered appropriate. [R&D Status = GREEN] **Reference:** EPRI: MRP-293
c3-13e c3-13g	Within the context of nickel-base weld metals, work to date has been focused on Alloy 182 and Alloys 52 and 152, although the possibility of low temperature cracking (via LTCP) of Alloy 82 has been studied. Based on available data, low-temperature effects have not been observed to have engineering significance. However, the potential for fracture property reductions to occur at operating temperature is less well defined for Alloys 82 and 52, particularly in the presence of a flux of FAC-generated hydrogen. To date, EPRI R&D at higher temperatures has been focused on the evaluation of materials of greater concern, particularly X-750 and cold-worked stainless steels. Although there are limited data to quantify the nature and significance of this phenomenon for Alloys 82 and 52, some effects are anticipated. Conservatively, an Orange R&D Status result is applied. There have been few tests to characterize performance at higher temperature, even though there have been some observations of abnormally high crack growth rates. Additionally, since only a few welds have been tested, weld-to-weld variability is not considered to have been fully evaluated for either low-temperature or high-temperature regimes. For the CANDU reactor design, there is no ongoing or planned R&D to develop an improved understanding of this phenomenon. [R&D Status = ORANGE] **References:** EPRI: MRP-285, MRP-293

Table 7-7 (continued)
CANDU explanatory notes

NOTE ID	EXPLANATORY NOTE
CANDU STEAM GENERATOR TUBES	
c4-1a c4-1b	Wastage of either Alloy 800 or Alloy 600 tubing is assumed to be possible in principle, but there is not any recent field experience indicating a concern. Wastage of Alloy 600 did occur for some older SGs. The cause was determined to be deep sludge piles and poor water chemistry. In recent years, the implementation of improved water chemistry controls and increased attention to cleaning has prevented significant wastage. To date, wastage of Alloy 800 has not been observed in service. No additional R&D is warranted. [R&D Status = GREEN] **References:** EPRI: 3002018322 COG: [7-25], [7-26] Other: [7-78]
c4-1c c4-2c c4-3c	Based on extensive operating experience, Alloy 400 is susceptible to wastage, pitting, and FAC/erosion-corrosion. Additionally, there is significant susceptibility to crevice corrosion associated with deposits in the presence of anionic impurities and oxidizing potentials (air ingress). An additional concern is the potential for significant corrosion of Alloy 400 tubing under high hydrazine layup conditions. Alloy 400 is considered a mature material being managed to the end of serviceable life. [R&D Status = GREEN] **References:** COG: [7-27] EPRI: 3002018322

Table 7-7 (continued)
CANDU explanatory notes

NOTE ID	EXPLANATORY NOTE
c4-2a	Considering only “at power” conditions, localized pitting corrosion is unlikely. In general, only minor pitting of Alloy 800, influenced by chloride exposure and cold work, has been observed to date. One unit did experience through-wall pitting of Alloy 800 SG tubes as a consequence of chloride attack due to condenser tube leaks. In this incident, only two tubes leaked, but others suffered minor pitting. In other cases, minor corrosion has been detected but appeared coincident with shallow fretting and with plastic strains in the near surface region in the vicinity of the fretting wear scars. Corrosion testing of removed tubes revealed that they were somewhat more susceptible to pitting corrosion than Alloy 800 tubing that has never been in service. The main contributing factors to pitting of Alloy 800 are considered well known, and no additional R&D is warranted. [R&D Status = GREEN] **References:** COG: [7-28], [7-29] EPRI: 3002018322
c4-2b	Alloy 600 tubing was included in a recent evaluation performed by EPRI to assess the adequacy of current layup guidance. As a result of this evaluation, layup guidance was updated. Testing performed as a part of this evaluation did not identify any significant concerns as long as the recommended guidance was implemented. Although the EPRI evaluation may not bound layup conditions reasonably anticipated for CANDU plants due to the occurrence of longer refurbishment outages, use of Alloy 600 in CANDU plants is limited. Alloy 600 is considered a “sunset” material for which additional R&D is not warranted. [R&D Status = GREEN] **References:** EPRI: 1014988, 3002018322

Table 7-7 (continued)
CANDU explanatory notes

NOTE ID	EXPLANATORY NOTE
c4-4a c4-4b c4-4c	Some SGs have experienced a heavy buildup of deposits, which reduced or blocked water/steam flow. In CANDU units, fouling of central tube to tube support openings, causing flow diversion to peripheral openings, even into the cold leg, has been observed. Due to this fouling, cavitation damage and increased vibration have occurred, resulting in significant support plate degradation in at least one case. Fouling of some preheater baffle plates has led to cavitation damage in at least one unit.[1] Although some modeling of fouling for broached tube support plate designs remains in progress, the current consensus is that no additional R&D is warranted to address this issue for CANDU plants. [R&D Status = GREEN] **References:** COG: [7-29], [7-31] EPRI: 1018344, 1020994, 1022667, 1022824 Other: [7-72], [7-73], [7-74], [7-75] **Note**: 1. Cavitation damage to Alloy 800 SG tubing, observed as a consequence of fouling, is considered to be a secondary effect resulting from a specific configuration used at only one site. As a result, cavitation is not explicitly shown in Table 7-4.
c4-5a c4-5b c4-5c	For CANDU units, SG tube ID fouling occurs because the PHT system is predominantly constructed from carbon steel materials, with a majority of the surface area associated with feeder pipes. Iron removal and dissolution by FAC at the feeder outlets are deposited as magnetite inside the SG tubing. Over time, ID fouling can become significant, causing ECT probe interference. To remove the magnetite buildup, a shot blast process was developed. Shot is directed axially along the tube length and captured, along with the removed magnetite at the opposite end of the U-tube. It is noted that some shallow surface cold work is potentially introduced by this process. To date, application of this process has not been associated with increased tube susceptibility to degradation. No R&D is considered warranted to address this issue. [R&D Status = GREEN] **Reference:** Other: [7-75]

Table 7-7 (continued)
CANDU explanatory notes

NOTE ID	EXPLANATORY NOTE
c4-6a c4-6b c4-6c	Wear is a significant concern for SG tubing. Steam generator tube damage due to generation of loose parts, intrusion of foreign objects, or tube support fretting currently represents the most significant operational challenge for replacement SGs where tubing SCC resistance is good. Within CANDU plants, most SGs include lattice bar tube supports. To date, fretting wear performance for this design is good. Additionally, AECL has developed models to predict wear rates and to assess the effectiveness of support designs and thermal-hydraulic configurations and conditions. [R&D Status = GREEN] **References:** EPRI: 1020990, 1020642 COG: [7-29], [7-31] Other: [7-77]

Table 7-7 (continued)
CANDU explanatory notes

NOTE ID	EXPLANATORY NOTE
c4-7a	ODSCC performance of Alloy 800 tubing in CANDU reactors has been good to date, with no cracking detected. However, of some concern is recent experience from European PWRs that include ODSCC in deep tubesheet crevices, at tube support plates, and at the top of the tubesheet. Some of this cracking has been associated with tube denting occurring at the top-of-tubesheet region, but the majority of cases were not associated with denting. Current CANDU SG designs include a hydraulic tube expansion on relatively small SG tubing, 1/2-5/8 inches (12.7-15.9 mm), while the affected European utilities were found to involve, in all cases, a last step of mechanical expansion with mostly 22 mm tubing. A specific concern for Alloy 800 is the larger difference in thermal expansion coefficients between Alloy 800 and low-alloy steel in comparison to the difference between Alloy 600 and low-alloy steel. Thermal cycles associated with startup and shutdown could, over time, impact relaxation at these hydraulically expanded joints. Also of interest in this area are cold work effects, which are not well understood. While a substantial amount of R&D has been completed to quantify the ODSCC performance of Alloy 800, the R&D status of Orange reflects the expert panel's opinion that insufficient R&D is planned or underway to understand the susceptibility of CANDU Alloy 800 SG tubing to ODSCC late in plant life. Remaining R&D gaps include: • Susceptibility to crevice chemistries and to better quantify SCC initiation times. • Alloy 800 performance in comparison with Alloy 690TT, 600TT, and 600 to define relative performance. • Impact on the tube-to-tubesheet expansion design on the SCC susceptibility of Alloy 800. [R&D Status = ORANGE] **References:** COG: [7-28], [7-29], [7-32], [7-33], [7-34], 0, [7-36], [7-37], [7-38], [7-39], [7-40] EPRI: 1024992, 3002018322 Other: [7-78], [7-79], [7-80]

Table 7-7 (continued)
CANDU explanatory notes

NOTE ID	EXPLANATORY NOTE
c4-7b	Currently, only four CANDU units are tubed with Alloy 600, which are scheduled for progressive replacement by 2033. The Alloy 600 tubing used in CANDU designs is mill annealed and slightly sensitized by the stress relief heat treatment given to the SG tube bundles. Bruce A material suffered significant ODSCC, much of which was PbSCC. Bruce B SGs have shown no degradation due to ODSCC after more than 20 years of service. Alloy 600 is considered a mature and sunset material for which no additional R&D is warranted to better characterize ODSCC performance. As a result, the R&D status result is Green. [R&D Status = GREEN] **References:** COG: 0, [7-36], [7-40] Other: [7-78], [7-79], [7-80], [7-81], [7-82]
c4-8b	From a practical perspective, Alloy 600 tube bundle service lives are more likely to be limited by ODSCC. Given the position regarding ODSCC (c4-7b), a similar cell result is appropriate. Additional R&D, addressing the mechanistic understanding of PWSCC in Alloy 600 SG tubing, is not required. [R&D Status = GREEN] **Reference:** None
c4-8d c4-8e	Cracking of manual tubesheet plug welds has been observed and was suspected to have been initiated from the primary side. Substantial R&D has been conducted on the topic of PWSCC of nickel-base alloys. Although there has been no specific R&D to evaluate the potential for the observed cracking to occur in other welds across the CANDU fleet, the consensus of the expert panel is that this does not represent a fundamental materials R&D need. [R&D Status = GREEN] **Reference:** None

Table 7-7 (continued)
CANDU explanatory notes

NOTE ID	EXPLANATORY NOTE
c4-9a c4-9b c4-9c	High-cycle fatigue is possible for SG tubes and internals components subject to high flow conditions (e.g., tube support plates and AVBs). Present concerns are focused on tube interface locations where fluid-elastic instabilities have been identified. CANDU SGs currently use lattice bar supports, which reduce susceptibility to fatigue. Only very few CANDU SG tubes have failed as a consequence of this mechanism. Failures occurred early in life, as typified by high-cycle fatigue. However, recent service experience highlights that if fouling occurs at tube-to-tube support openings, changes in flow pattern, increased vibration, and high-cycle fatigue damage to tubes can result (see c4-4a). Although there is no ongoing work specific to CANDU SGs, a Yellow R&D status result is conservatively retained for this issue. There is a need to follow research being conducted globally (across reactor designs) and evaluate the results for applicability to CANDU SGs. [R&D Status = YELLOW] **References:** COG: [7-41], [7-42] EPRI: 3002018322 Other: [7-72], [7-73], [7-74]
c4-10a c4-10b c4-10c	Laboratory testing has shown that fatigue resistance of austenitic materials in deoxygenated and/or hydrogenated environments can be lower than fatigue resistance in an air environment. However, the most significant effects have been found to occur when cyclic frequencies are lower than about 1 Hz. Although some effect of environment on fatigue resistance likely exists, since the principal fatigue loads for SG tubes result from high-cycle, flow-induced vibrations, it is unlikely that fatigue environmental effects are important in comparison with other degradation phenomena (e.g., ODSCC, wear). The current consensus is that no R&D is warranted. [R&D Status = GREEN] **References:** COG: [7-41], [7-42]
c4-10d c4-10e	Fatigue environmental effects are not anticipated to be a significant consideration for tube plugs and associated tube-to-tubesheet welds. [R&D Status = GREEN] **Reference:** None

Table 7-7 (continued)
CANDU explanatory notes

NOTE ID	EXPLANATORY NOTE
c4-12b c4-12d	Available data developed by EPRI to address PWR concerns indicate that, in comparison with other materials that have been tested, Alloy 600 is not particularly susceptible to reductions in fracture properties due to coolant exposure. Although the phenomenon is not well understood for any material, there are no near-term concerns regarding environmental effects on J-R properties for Alloy 600, unless the material has been subject to substantial cold work. Additionally, synergisms with thermal embrittlement are less likely than for other materials. Finally, Alloy 600 is considered a “sunset” material, for which additional R&D is generally not warranted. [R&D Status = GREEN] **Reference:** EPRI: MRP-293
c4-12e	EPRI research indicates that nickel-base weld filler metals, including Alloy 82, exhibit some reduction in fracture properties at low temperatures (e.g., typical of startup/shutdown and layups) in simulated PWR primary water environments. However, a review of the state of knowledge regarding LTCP of nickel-base alloys conducted by MRP for PWRs concluded that low-temperature effects are not observed to have any engineering significance for Alloy 82 and, although some areas of uncertainty remain, additional testing of Alloy 82 to evaluate LTCP is unlikely to be of significant benefit. At higher temperatures, there is the potential for interaction with PWSCC. There have been few tests to characterize performance of Alloy 82 at higher temperatures, even though there have been some observations of abnormally high crack growth rates. The focus of testing performed to date has been specifically on LTCP. Additionally, since only a few welds have been tested, weld-to-weld variability has not been fully evaluated for either low-temperature or high-temperature regimes. Despite this risk, the conservative bounding case is considered the dissimilar metal welds in feeder flow element installations due to the presence of a FAC-generated hydrogen flux. R&D in this area is considered bounding for SGs. As such, a Yellow R&D status is applied. [R&D Status = YELLOW] **Reference:** EPRI: MRP-293

Table 7-7 (continued)
CANDU explanatory notes

NOTE ID	EXPLANATORY NOTE
CANDU SG INTERNALS AND SECONDARY PRESSURE BOUNDARY COMPONENTS	
c5-1a c5-2a	Corrosion of carbon steel SG internals components has generally not been a significant concern for SG operation to date. However, recent field experience does include under-deposit corrosion of carbon steel tie rods at some early design CANDU plants. In some cases, the corrosion was significant enough to warrant structural integrity concerns and that surrounding tubes were found to have indications of deformation due to forces exerted by corrosion products. The corrosion is thought to have been accelerated by poor water chemistry and significant accumulation of deposits at the top of tubesheet region and is being managed through increased attention to water chemistry, removal of deposits, and periodic inspection. Substantial corrosion is not anticipated to be a fleet-wide concern, and factors influencing observations of corrosion are well understood. No additional materials R&D is warranted. [R&D Status = GREEN] **Reference:** None
c5-2d	There are few nuclear industry-based data to characterize the performance of Alloy 800H. Although significant localized corrosion would not be anticipated, some localized corrosion is possible. However, given the limited usage of Alloy 800H in the SG internals, it is unlikely that localized corrosion would have a significant adverse effect on component function. [R&D Status = GREEN] **Reference:** None
c5-2e c5-6e c5-8e	Secondary side SG shell pitting and associated EAC (EAF and/or SICC) have occurred in CANDU plants, as well as in PWRs. Regardless of the design, the phenomenon has been attributed to poor chemistry controls allowing oxygen and copper ion ingress, coupled with overly hard closure welds resulting from insufficient stress relief temperature. These issues were dealt with satisfactorily in the early 1990s, and there has been no reoccurrence. No additional R&D is needed. [R&D Status = GREEN] **References:** EPRI: 1019628, 3002018322

Table 7-7 (continued)
CANDU explanatory notes

NOTE ID	EXPLANATORY NOTE
c5-3a	FAC-related material loss has been detected in several CANDU SGs in carbon steel support plates, scallop bars, and secondary steam separators. Several factors are known, or are postulated, to play a role in FAC of carbon steels exposed to secondary side chemistry conditions, including material chemical composition (particularly Cr content), fluid velocity, turbulence, temperature, and steam quality. Many of these factors are now relatively well understood and managed by periodic inspection and, if necessary, repair. New CANDU SG designs replace carbon steels with more corrosion-resistant materials. For carbon and low-alloy steel weld materials, operating experience and experimental data have shown that preferential galvanic attack of welds can occur when significant differences exist in trace alloy composition between the welds and adjacent carbon steel materials. EPRI reports 1009695 and 1007772 describe the issue. While a significant galvanic component exists, there is no certainty that flow is not involved in enhancing corrosion rates. This issue is captured under the FAC column, even though galvanic attack is known to be a significant, if not the predominant, contributor. EPRI NSAC-202L provides general guidance to address this issue by inspection. There has been recent operating experience of significant, and unexpected, FAC of SG upper internals of CANDU SGs with particular design characteristics. In addition, recent application of film forming products within CANDU plant secondary systems raised some concerns on the increase of FAC rates. R&D is planned or underway to improve the understanding of these phenomena. For this reason, the R&D status is set to Yellow. [R&D Status = YELLOW] **References:** COG: [7-43], [7-44] EPRI: 1009695, 1007772, 1015425, 3002000563 Other: [7-78]
c5-4a c5-4b	CANDU units now specify lattice bar supports to reduce fouling susceptibility, based on COG-funded R&D, and are validated by good performance in service. No R&D is required in this area. [R&D Status = GREEN] **Reference:** None

Table 7-7 (continued)
CANDU explanatory notes

NOTE ID	EXPLANATORY NOTE
c5-5a c5-5b c5-5c c5-5d	Wear of SG internals is plausible for all component locations, considering the possibility of loose parts, anomalous tube support to tube gaps, and/or tube flow-induced vibrations. However, the current consensus is that no additional characterization of the related phenomena is needed. [R&D Status = GREEN] **Reference:** None
c5-6a	Consistent with the conclusions for carbon and low-alloy steel pressure boundary components, SCC of carbon and low-alloy steel SG internals components exposed to secondary water chemistry is considered possible, especially in off-normal chemistry conditions. However, SCC has not been observed in the field other than some early life corrosion-induced cracking of SG shell girth welds occurring at one CANDU site. This cracking was determined to result from poor early life water chemistry (see note c5-6e). Additional R&D is not required. [R&D Status = GREEN] **Reference:** None
c5-6b	Martensitic stainless steels used as materials of construction for SG internals are not typically subject to SCC. Operating experience to date has been good. Process controls to limit hardness adequately limit the potential for SCC under normal operating conditions. The panel consensus for this item is that a conservative “Y” is appropriate since SCC is plausible after long-term operation, if exposure to off-normal chemistry occurs, or if excessive hardness is induced by improper heat treatment or cold working. However, existing management techniques are currently considered adequate, and no research is warranted at this time. [R&D Status = GREEN] **Reference:** EPRI: 3002018322

Table 7-7 (continued)
CANDU explanatory notes

NOTE ID	EXPLANATORY NOTE
c5-6c	There is some limited application of Alloy 600 in CANDU SG internals. Stress corrosion cracking of nickel-base alloy SG internals components is considered plausible but unlikely due to the low hydrogen fugacity in secondary water. Industry experience to date has been favorable, and this issue is not currently considered a significant degradation concern. [R&D Status = GREEN] **Reference:** EPRI: 3002018322
c5-6d	In CANDU SGs, the use of Alloy 800H is limited to tube support tie rods. There is virtually no nuclear industry experience with Alloy 800H. However, testing found that, although Alloy 800H is susceptible to sensitization, corrosion tests performed in high temperature water found high SCC resistance. Although no performance issues have been identified, the limited nature of available data causes some uncertainty. A "?" result is deemed appropriate. [R&D Status = BLUE] **Reference:** Other: [7-83]
c5-7a c5-7b c5-7c c5-7d	High-cycle fatigue is possible for SG internals components subject to high flow conditions (e.g., tube support plates and AVBs). Present concerns are focused on tube interface locations where fluid-elastic instabilities have been identified. CANDU SGs currently use lattice bar supports, which reduce susceptibility to fatigue. Although there is no ongoing work specific to CANDU SGs, a Yellow R&D status result is conservatively retained for this issue. There is a need to follow research being conducted globally (for all reactor designs) and evaluate the results for applicability to CANDU SGs. [R&D Status = YELLOW] **Reference:** None

Table 7-7 (continued)
CANDU explanatory notes

NOTE ID	EXPLANATORY NOTE
c5-8a c5-8b c5-8c c5-8d	Laboratory testing has shown that fatigue resistance in a water environment can be lower than fatigue resistance in an air environment. Therefore, some effect of environment on fatigue life is anticipated, especially during water chemistry transients. However, the most significant effects have been found to occur when cyclic frequencies are lower than about 1 Hz. Since the principal fatigue loads are likely to result from high-frequency, flow-induced vibrations, it is unlikely that environmental effects are important for SG internals. [R&D Status = GREEN] **Reference:** None
c5-9b	For Type 410 martensitic steel, there are some data to characterize thermal aging. Although not anticipated to be substantial, there could be some reduction in toughness over a long service life. For this material, even a minor increase in DBTT can result in a significant reduction of the room temperature impact energy because the initial DBTT of martensitic stainless steel material is near room temperature. Another long-term concern noted is the potential interaction of embrittlement with long-term SCC initiation. To date, there has been no comprehensive review of the available data in relation to SG applications and considering long service life. Any thermal embrittlement occurring in SG components will be bounded by PWR reactor internals components fabricated from similar material. [R&D Status = ORANGE] **References:** EPRI: 3002018322, MRP-175R1

Table 7-7 (continued)
CANDU explanatory notes

NOTE ID	EXPLANATORY NOTE
CANDU EXTERNAL SURFACES AND BOLTING	
c6-2a c6-2b c6-2c c6-2d c6-2e	External surface pitting is considered plausible for all materials of construction if the material is exposed to moist or wetted conditions continuously or periodically. The consensus is that no additional research is needed. [R&D Status = GREEN] **Reference:** EPRI: 3002018322
c6-6a c6-7a	Field observations include detection of OD-initiated cracking in two outlet feeder tight-radius (1.5D) bends. The material is SA-106 Gr. B carbon steel. In the same area of the feeder pipe, ID-initiated cracking was also observed (see c3-6a). The observed OD-initiated cracking occurs at the bend outer radius region that is highly stressed and cold worked due to the bending process. Due to the limited operating temperature of CS external surfaces and bolting, and the absence of a significant FAC hydrogen flux in comparison to feeder piping, the risk can be reasonably ruled out, and no specific R&D is warranted. [R&D Status = GREEN] **Reference:** Other: [7-67]
c6-6d	Cracking of high-strength, low-alloy steel (HSLAS) bolting is possible (particularly in high hardness bolting) in the presence of unstable lubricants, harsh environments, or alternating wet and dry conditions. SCC of some LWR reactor vessel studs having hardness well above Rockwell C40 has been observed. However, the SCC characteristics of low-alloy steel fastener materials are relatively well understood, and industry issues surrounding the use of overly hard bolting material and unstable lubricants are generally resolved. Performance of HSLAS bolting without these aggravating factors has been good. No additional R&D is considered warranted. [R&D Status = GREEN] **Reference:** EPRI: 3002018322

Table 7-7 (continued)
CANDU explanatory notes

NOTE ID	EXPLANATORY NOTE
c6-6e	Alloy 718 can be susceptible to SCC under wetted conditions and possibly under alternating wet and dry conditions. Susceptibility can be mitigated by control of microstructure and hardness (including surface hardness from thread forming or machining). However, no additional research is currently warranted. [R&D Status = GREEN] **Reference:** EPRI: 3002018322
c6-8a c6-8b c6-8c c6-8d c6-8e	Externally initiated cracking due to high-cycle fatigue is possible. Typically, externally initiated high-cycle fatigue cracking is the result of acoustic or mechanical loading and is not a progressive, long-term aging phenomenon. While cracking may occur as a result of improper design, these phenomena are well understood, and no additional research is needed. [R&D Status = GREEN] **Reference:** None
c6-9a c6-9b c6-9c c6-9d c6-9e	Low-cycle fatigue cracking initiating at a component external surface may occur if the external surface loading dominates over the loading at the internal surface. It is noted that internal surface fatigue usage can still be limiting when the effects of reactor coolant on fatigue behavior are considered. Fatigue usage of these materials in air is well documented and addressed by design codes. No additional research specific to external surfaces is needed. [R&D Status = GREEN] **Reference:** None
c6-10d	The EPRI Materials Handbook notes that limited testing of a French 35NCD16 stud material indicated significant embrittlement. This result is notable for CANDU plants because the embrittlement was observed at a relatively low aging temperature (536°F). Although the steel involved (35NCD16) is not the same grade that is used in CANDU plants, the results indicate that some embrittlement of high-strength, low-alloy steel could potentially occur. Embrittlement of low-alloy steel fasteners is considered a concern because embrittled materials typically have reduced SCC margins. Available data to characterize the potential for embrittlement of low-alloy steel fasteners, as a result of service-induced aging at high temperatures, are limited. [R&D Status = BLUE] **Reference:** EPRI: 3002018322

7.3 References

NOTE: References listed here do not include published EPRI reports. Access to the full citation of each EPRI report listed in this section is available through use of the hyperlinks provided. If a hyperlink is not available, this report has been archived and is no longer directly accessible on epri.com.

[7-1] V. F. Urbanic and R. A. Ploc, "State of the Art Report (SOTAR) on Corrosion and Deuterium Ingress in CANDU Pressure Tubes," COG-05-1064, June 2006.

[7-2] V. F. Urbanic and A. A. Bahurmuz, "State of the Art Report (SOTAR) on Corrosion and Deuterium Ingress at Rolled Joints in CANDU Pressure Tubes," COG-07-1042, March 2009.

[7-3] D. Metger and A. Gagnon, "Assessment of Fuel Channel Annulus Spacer Wear," COG-JP-4363-V203, March 2019.

[7-4] G. A. Bickel and K. Dunn, "P7O07 Annulus Spacers: Visual Examinations, Sectioning and Metallography," COG-JP-4491-V200, November

[7-5] G. A. Bickel, M. Bagheripoor, J. Curilla, and K. Dunn, "Surveillance Report: P5N09 ZrNbCu Annulus Spacers," COG-JP-4695-V005 (unpublished).

[7-6] G. Moan, P. Simons, S. Kim, and A. Gagnon, "Effect of Irradiation on Inconel X-750 Fuel Channel Spacers," COG-JP-4363-V067, December 2010.

[7-7] B. P. Payne, J. M. Smith, and C. D. Judge, "Investigating the Effects of Irradiation and Thermal Ageing on Mechanical Properties of End Fittings – Comprehensive Test Plan," OP-18-7001, February 2006.

[7-8] M. D. Wright and M. Griffiths, "Assessment of Inconel X-750 Material Degradation," COG-JP-4363-V185, November 2011.

[7-9] G. A. Bickel, M. Latour, D. Poff, M. Bagheripoor, and M. Rebello, "Surveillance Report: B6S13 ZrNbCu Annulus Spacers," COG-JP-4680-V005, June 2022.

[7-10] S-H Wang, M.D. Wright, and J. M. Smith, "Assessment of the Potential of Stress Corrosion Cracking of Alloy X-750 Fuel Channel Spacers," COG-JP-4363-V202, March 2012.

[7-11] C. E. Coleman, "Delayed Hydride Cracking in Zirconium Alloys – State of the Art Report (SOTAR)," COG-07-1092, September 2009.

[7-12] P. J. Richinson and N. P. Singh (editors), "Technical Basis of Fitness-for-Service Guidelines for Zirconium Alloy Pressure Tubes in Operating CANDU Reactors," COG-96-651, 1996.

[7-13] Kinectrics Inc.; D. A. Scarth, "Engineering Fatigue Crack Initiation Evaluation Curves for Axial Flaws in Zr-Nb Pressure Tubes," COG-06-1003, April 2007.

[7-14] D. A. Scarth and S. X. Xu, "Interim Approach Fatigue Crack Initiation Evaluation Curves for Axial Flaws in Zr-Nb Pressure Tubes," COG-09-1008, December 2009.

[7-15] C. Moreau, P. Poruks, and J. M. Smeltzer, "Ex-Service Inconel X-750 and Zr-Nb-Cu Garter Springs," COG-06-1065, February 2008.

[7-16] M. Sanderson, "Inconel X-750 Fuel Channel Annulus Spacer Integrity

[7-17] G. A. Bickel, "Results of He and H Analysis in Ex-Service Inconel X-750 Annulus Spacers," COG-JP-4363-V158, December 2011.

[7-18] D. Poff, "Test Report for Ex-Service Spacer Crush Testing," COG-JP-4363-V165, December 2011.

[7-19] G. K. Shek, M. Shanahan, and J. Cui, "FUEL CHANNEL LIFE MANAGEMENT, Assessment of Delayed Hydride Cracking in Zr-2.5Nb-0.5Cu Spacers," COG-JP-4363-V204 (DRAFT), March 2012.

[7-20] M. Mattucci, "Examination of the Heat Affected Zone in the Weld Between Alloy 52M and Carbon Steel," COG-20-4067, November 2021.

[7-21] M. Griffiths, P. Feenstra, G. A. Bickel, S. A. Donohue, C. D. Judge, and L. C. Walters, "Assessment of Inconel X-750 Spacer Detensioning," COG-JP-4363-V197, February 2012.

[7-22] S.-H. Wang and M. D. Wright, "Effects of Chloride and Sulphate on SCC Thresholds for Cold Worked Type 316L Stainless Steel at Intermediate Temperatures," COG-11-4055-DRAFT, December 2011.

[7-23] Z. L. Pan and S. St. Lawrence, "The Effect of Neutron Irradiation on the Mechanical Properties of CANDU Calandria Vessel Material," COG-02-4070-R01, January 2005.

[7-24] D. Finlayson and M. D. Wright, "Potential Risk of Primary Water Stress Corrosion Cracking in Dissimilar Metal Welds at CANDU Feeder Tube Flow Devices," COG-08-4054, January 2009.

[7-25] G. Goszczynski, "Layup Induced Corrosion of UNS N06600 (INCONEL 600) Steam Generator Material and Hydrazine Optimization," COG-03-4059, 2004.

[7-26] G. Goszczynski, "Layup-Induced Corrosion of UNS N08800 (INCOLOY 800) Steam Generator Material and Hydrazine Optimization," COG-02-4075, 2003.

[7-27] G. Goszczynski, "Layup-Induced Corrosion of UNS N04400 (Monel 400) Steam Generator Material and Hydrazine Optimization," COG-05-4069, 2005.

[7-28] Y. C. Lu, "Factors Leading to Corrosion Degradation of Alloy 800," COG-08-4072, 2009.

[7-29] Y. C. Lu, "A Survey on the Corrosion Susceptibility of Archived Alloy 800 Tubing from CANDU Steam Generators," COG-08-4075, 2008.

[7-30] S. Laroche, "Analysis of Tube Degradation in Steam Generator Preheater of Darlington Steam Generator," COG-09-4086, 2010.

[7-31] S. Laroche, "Cavitation Susceptibility of Tubes in Steam Generator Preheaters for CANDU 6 Internal and Bruce External Preheaters," COG 10-4077, 2011.

[7-32] Y. C. Lu, "EAC of Alloy 800 – Current Knowledge and Future Work Required for Supporting SG Life Predictions," COG-08-4080, 2009.

[7-33] N. Briden, "Implications of Intra-Tubesheet Cracking at Biblis A to CANDU Alloy 800 Steam Generator Tube Performance," COG-08-4081, 2009.

[7-34] Y. C. Lu, "Summary Notes on an Optimized Materials Improvement Factor Approach for Alloy 800 CANDU Steam Generator Tubing," COG-08-4082, 2009.

[7-35] C. Turner, "The Basis for Chemistry Control in the Steam Generator During Wet Layup and Startup," COG-09-4008, 2010.

[7-36] Y. C. Lu, "The Interactive Effects Between Steam Generator Impurities on CANDU Steam Generator Tube Corrosion – A Final Report," COG-09-4058, 2009.

[7-37] G. Goszczynski, "Examination of Ex-Service DNGS Steam Generator Tubes (Intra-Tubesheet Region)," COG-09-4078, 2010.

[7-38] N. Briden, "Evaluation of Implications of New Indications of Steam Generator Alloy 800 Tube Degradation," COG-09-4084, 2010.

[7-39] Y. C. Lu, "An Aging Assessment of CANDU Alloy 800 SG Tubing," COG-10-4075, 2011.

[7-40] G. Ogundele, "Summary Report on the Interactive Effects of Impurities on CANDU Steam Generator Tube Cracking," COG-10-4091, 2010.

[7-41] G. Ogundele, "Fatigue of Alloy 800," COG-05-4034, 2005.

[7-42] G. Ogundele, "Fatigue of Alloy 400," COG-07-4030, 2007.

[7-43] J. Pietralik, "Flow-Accelerated Corrosion Rate for Bruce B Steam Generator Secondary Side Internals," COG-02-4055, 2003.

[7-44] C. S. Schefski, "FAC Degradation of Secondary-Site Internals of a Steam Generator with an Internal Preheater," COG-03-4043, 2004.

[7-45] M. Trelinski, "Garter Spring to Pressure Tube Wear Marks – Review of Ultrasonic Inspection Data for Darlington NGS," COG-JP-4363-V072, OPG Report # I-REP-31100-50039 R000, October 2010.

[7-46] M. Trelinski, "Garter Spring to Pressure Tube Wear Marks – Review of Ultrasonic Inspection Data for Bruce B NGS," COG-JP-4363-V073, OPG Report # I-REP-31100-50040 R000, October 2010.

[7-47] S. Khjehpour, J. Xu, and I. Ariani, "Garter Spring (Inconel X-750) Circumferential Distribution of Flux and Temperature," COG-JP-4363-V077, January 2011.

[7-48] C. D. Judge and O. T. Woo, "Preliminary TEM and SEM Examinations of Inconel X-750 Spacer Material Removed from Reactors," COG-JP-4363-V087.

[7-49] M. Sanderson and R. Bravo, "Irradiated Inconel X-750 Annulus Spacer Endurance Fitness for Service Assessment," COG-JP-4363-V097 R0, September 2011.

[7-50] "Industry Meeting on Geometry Characterization of Crevice Corrosion Flaws for Flaw Evaluation – Revision 1" (Notes of Meeting), OPG File: N-31100 P NSATD, July 27, 2006.

[7-51] *Delayed Hydride Cracking in Zirconium Alloys in Pressure Tube Nuclear Reactors*, IAEA-TECDOC-1410, IAEA, Vienna, 2004.

[7-52] Durance, D., et al., "Inducement of IGA/SCC in Inconel 600 Steam Generator Tubing During Unit Outages." In: Proceedings of the 8th International Conference on CANDU Maintenance, Toronto, ON, November 2008.

[7-53] Y. S. Kim (KAEPRI), "Initiation and Arrest of Delayed Hydride Cracking in Zr–2.5Nb Tubes," *Journal of Pressure Vessel Technology*, Vol. 131, No. 1, February (2009).

[7-54] J. J. Kearns, "Terminal Solid Solubility and Partitioning of Hydrogen in the Alpha Phases of Zirconium, Zircaloy-2 and Zircaloy-4," *Journal of Nuclear Materials*, Vol. 22, No. 87, pp. 292–303 (1967).

[7-55] M. Leger and T. P. Byrne, "Hydride Blister Growth in Zr-2.5wt% Nb Pressure Tube Material." In: Proceedings of 12th Conference on Simulation Symposium on Reactor Dynamics and Plant Control, Hamilton, Canada, April 1986.

[7-56] E. C. W. Perryman, "Pickering Pressure Tube Cracking Experience," *Nuclear Energy*, Vol. 17, pp. 95–105 (1978).

[7-57] D. A. Scarth and E. Smith, "Developments in Flaw Evaluation for CANDU Reactor Zr-Nb Pressure Tubes." In: Proceedings of the 1999 ASME Pressure Vessels and Piping Conference, Boston, Massachusetts, August 1–5, PVP-Vol. 391, pp. 35–45; also published in the *ASME Journal of Pressure Vessel Technology*, Vol. 123, pp. 41–48, February 2001.

[7-58] D. A. Scarth and E. Smith, "The Effect of Plasticity on Process-Zone Predictions of DHC Initiation at a Flaw in CANDU Reactor Zr-Nb Pressure Tubes." In: Proceedings of the 2002 ASME Pressure Vessels and Piping Conference, Vancouver, Canada, August 4–8, 2002; PVP-Vol. 437, pp. 19–30.

[7-59] "Technical Requirements for In-Service Evaluation of Zirconium Alloy Pressure Tubes in CANDU Reactors," CSA Standard N285.8, Canadian Standards Association, 2005 Edition N285.8-05 and 2010 Edition N285.8-10.

[7-60] D. Khatamian and J. H. Root, "Comparison of TSSD Results Obtained by Differential Scanning Calorimetry and Neutron Diffraction," *Journal of Nuclear Materials*, Vol. 372, pp. 106–113 (2008).

[7-61] "Assessment and Management of Ageing of Major Nuclear Power Plant Components Important to Safety: CANDU Pressure Tubes," IAEA-TECDOC-1037, IAEA, Vienna, 1998.

[7-62] "Baseline Fracture Toughness and CGR Testing of Alloys X-750 and XM-19 (EPRI Phase 1)," INL/EXT-11-24173, February 2012.

[7-63] G. Stewart, "OPG Calandria Vessel Integrity Assessment," AMEC NSS Report: P1170/RP/001 R00, November 26, 2008.

[7-64] D. Côte, "Irradiated Stainless Steel Tensile Property Review," N-REP-31200-10000-R00, February 2010.

[7-65] P. E. Doherty and M. W. Shanahan, "The Corrosion Performance of Nickel Alloy Heat Exchanger Bundles in Freshwater Service." In: Proceedings of the 3rd International Symposium on Environmental Degradation of Materials in Nuclear Power Systems – Water Reactors, Traverse City, Michigan, August 30–September 3, 1987.

[7-66] "Flow Accelerated Corrosion and Cracking of Carbon Steel Piping in Primary Water – Operating Experience at the Point Lepreau Generating Station." *In: Proceedings of the 12th International Conference on Environmental Degradation of Materials in Nuclear Power Systems – Water Reactors*, Salt Lake City, Utah, April 14–18, 2005.

[7-67] M. D. Wright, "Concurrent Creep-Cracking and SCC in Carbon Steel Pipes (CANDU PHTS Feeder Pipes)." Presented to the Quantitative Micro-Nano (QMN) Approach to Predicting SCC of Fe-Cr-Ni Alloys, Sun Valley, Idaho, USA. Staehle Consulting, June 2011.

[7-68] W. A. Stevenson, WA. H. P. Seifert, S. Ritter, and J. Hickling, *"Environmentally Assisted Cracking of Low-Alloy RPV and Piping Steels Under LWR Conditions."* In: Proceedings of the 11th International Conference on Environmental Degradation of Materials in Nuclear Power Systems – Water Reactors, Stevenson, Washington, August 10–14, 2003.

[7-69] R. Wu, R. Sandström, and F. Seitisleam, "Low Temperature Creep Crack Growth in Low Alloy Pressure Vessel Steel," *Journal of Nuclear Materials,* Vol. 336, pp. 279–290 (2005).

[7-70] H. P. Gunawardane, J. B. Hall, and S. T. Rosinski, "Mechanical Property Changes in Reactor Vessel Materials Thermally Aged for 209 000 H at 282C." In: ASTM Special Technical Publication (STP), "Effects of Radiation on Materials: 22nd Symposium," Vol. 1475, pp. 236–244 (2006).

[7-71] L. A. James and W. C. Porr, "The Effect of an Elevated Temperature Aqueous Environment Upon the J-controlled Tearing of a Low Alloy Steel," *International Journal of Pressure Vessels and Piping*, Vol. 76, pp. 769–779 (1999).

[7-72] H. E. Rummens, J. T. Rogers, and C. W. Turner, "The Thermal Hydraulics of Tube Support Fouling in Nuclear Steam Generators," *Journal of Nuclear Technology*, Vol. 148, pp. 268–286 (2004).

[7-73] H. Bodineau and T. Sollier, "Tube Support Plate Clogging Up of French PWR Steam Generators." Presented at EUROSAFE 2008, Paris, France, November 3–4, 2008.

[7-74] M. Le Calvar, A. Vergnault, H. Bodineau, F. Balestreri, and T. Sollier; Institut de Radioprotection et de Sûreté Nucléaire (IRSN), "Build-up of Deposits in Steam Generators: A Safety Issue." Proceedings of the 14th International Conference on Environmental Degradation of Materials in Nuclear Power Systems, Virginia Beach, Virginia, August 23–27, 2009.

[7-75] M. Yetisir, C. W. Turner, and J. Pietralik, "Contribution of SG Degradation Mechanisms to PIHT Behaviour." Proceedings of the 5th CNS International Conference on CANDU Maintenance, Toronto, ON, November 2000.

[7-76] NRC Information Notice 2007-37, Buildup of Deposits in Steam Generators, U.S. Nuclear Regulatory Commission, November 2007.

[7-77] A. Mohany and V. Janzen, "Flow Induced Vibration and Fretting-Wear Performance of ACR Steam Generator U-Tubes: Instrumentation." Proceedings of Pressure Vessels and Piping Division Conference, Prague, Czech Republic, July 2009.

[7-78] R. L. Tapping, J. Nickerson, P. Spekkens, and C. Maruska, "CANDU Steam Generator Life Management," *Nuclear Engineering and Design,* Vol. 197, pp. 213–223 (2000).

[7-79] R. L. Tapping, "Materials Performance in CANDU Reactors: The First 30 Years and the Prognosis for Life Extension and New Designs, *Journal of Nuclear Materials*, Vol. 383, pp. 1–8 (2008).

[7-80] Y. C. Lu, R. L. Tapping, and M. D. Pandey, "Degradation of Alloy 800 Steam Generator Tubing and Its Long-Term Behaviour Predictions for Plant Life Management." Proceedings of the 6th International Steam Generator Conference, Toronto, ON, November 2009.

[7-81] Durance, D., et al., "Inducement of IGA/SCC in Inconel 600 Steam Generator Tubing During Unit Outages." Proceedings of the 8th International Conference on CANDU Maintenance, Toronto, ON, November 2008.

[7-82] R. L. Tapping, "Steam Generator Aging in CANDUs: 30 Years of Operation and R&D." Proceedings of the 8th International Conference on CANDU Maintenance, Toronto, ON, November 2008.

[7-83] J. S. Janssen, M. M. Morra, and D. J. Lewis, "Sensitization and Stress Corrosion Cracking of Alloy 800H in High Temperature Water," *Corrosion*, Vol. 65, No. 2, pp. 67–78 (2009).

[7-84] P. Efsing and K. Pettersson, "The Influence of Temperature and Yield Strength on Delayed Hydride Cracking in Hydrided Zircaloy-2." In: ASTM Symposium on Zirconium in the Nuclear Industry, Eleventh International Symposium, Garmisch-Partenkirchen, Germany, ASTM International, 1995.

[7-85] V. Grigoriev and R. Jakobsson, "Delayed Hydride Cracking Velocity and J-Integral Measurements on Irradiated BWR Cladding." In: ASTM Symposium on Zirconium in the Nuclear Industry, Fourteenth International Symposium, Stockholm, Sweden, ASTM International, 2004.

[7-86] J. S. Schofield, E. C. Darby, and C. F. Gee, "Temperature and Hydrogen Concentration Limits for Delayed Hydride Cracking in Irradiated Zircaloy." In: G. D. Moan and P. Rudling, Eds. ASTM Symposium on Zirconium in the Nuclear Industry, Thirteenth International Symposium, Annecy, France, ASTM International, 2001.

[7-87] NUREG/CR-6960, Crack Growth Rates and Fracture Toughness of Irradiated Austenitic Stainless Steels in BWR Environments, U.S. Nuclear Regulatory Commission, March 2008.

[7-88] O. K. Chopra, "Development of Fatigue Design Curve for Austenitic Stainless Steels in LWR Environments: A Review." ASME PVP 439, presented at the ASME Pressure Vessel and Piping Conference, Vancouver, BC, August 4–8, 2002.

A
DEGRADATION MECHANISM SUMMARIES

This appendix describes materials degradation modes and their mechanisms identified in the Materials Degradation Matrix that are relevant to the reactor coolant systems and internals of current (Gen. II) light water and heavy water moderated power reactors. It provides a broad treatment of the degradation mechanisms considered and their relevance to mitigation actions. More fundamental treatments are provided in textbook references [A1] through [A7].

NOTE:
The acronyms and abbreviations used throughout this appendix are provided in the front matter of this report.

The degradation modes described in this appendix are as follows:

A.1 Corrosion—General and Localized[12]

- A.1.1 General Corrosion
- A.1.2 Wastage or Boric Acid Corrosion (Wstg.)
- A.1.3 Flow-Accelerated Corrosion (FAC)
- A.1.4 Localized Corrosion[13]
- A.1.5 Fouling (Foul)

A.2 Wear

A.3 Stress Corrosion Cracking (SCC)

- A.3.1 Intergranular Attack (IGA)
- A.3.2 Intergranular and Transgranular SCC (IG/TG)[14]

A.4 Fatigue

- A.4.1 Reactor Coolant System and Steam Generator Piping
- A.4.2 Reactor Pressure Vessels
- A.4.3 Pressurizers

[12] General and localized corrosions are included in this appendix for completeness and as background information to aid understanding of the more structurally significant accelerated or localized corrosion and corrosion cracking modes that are considered important for primary system components. However, note that these corrosion mechanisms can be very significant for lower temperature reactor components, such as service water systems.

[13] Including galvanic corrosion, crevice corrosion, and pitting.

[14] Including irradiation-assisted stress corrosion cracking (IASCC) and delayed hydride cracking (DHC) of zirconium-base alloys.

A.4.4 Steam Generator Shell, Tubes, and Internals

A.4.5 RPV Internal Components

A.4.6 High-Cycle Fatigue (HCF)

A.4.7 Low-Cycle Fatigue (LCF)

A.4.8 Corrosion Fatigue (Environmentally Assisted Fatigue [EAF])

A.5 Fracture—Reduction in Fracture Properties (RiFP)

A.5.1 Thermal Embrittlement (Th)

A.5.2 Environmentally Induced Reduction of Fracture Resistance (Env)

A.6 Irradiation Effects

A.6.1 Irradiation Embrittlement (Emb)

A.6.2 Void Swelling (VS)

A.6.3 Irradiation Creep and Stress Relaxation (IC/SR)

A.1 Corrosion—General and Localized

"Uniform" degradation modes include general corrosion, boric acid corrosion (wastage), and flow-accelerated corrosion, whereas localized corrosion modes address galvanic corrosion, crevice corrosion, and pitting. General corrosion modes result in loss of material over reasonably large areas, defined broadly as greater than 1-2 cm^2, as opposed to localized corrosion that may occur over areas governed by metallurgical inhomogeneity or a structural crevice feature. These mechanisms are summarized schematically in Figure A-1. Additionally, considerations associated with fouling resulting from the accumulation of corrosion products are also addressed in this section.

A.1.1 General Corrosion

General corrosion is characterized by uniform surface loss through metal oxidation. In aqueous solutions, including reactor coolants, it is primarily an electrochemical process involving an anodic oxidation reaction to form positively charged metal cations, which is balanced electrically by a cathodic reaction involving the reduction of oxygen in solution (if present) and/or reduction of hydrogen ions to hydrogen atoms that may then evolve as molecular hydrogen gas. The point of balance between the anodic and cathodic currents determines the characteristic corrosion or electrochemical corrosion potential (often called *ECP*) that can, in principle, be measured with a voltmeter relative to any practically viable standard reference electrode. The scale of corrosion potentials most commonly used in the context of corrosion in high temperature reactor coolants is referenced to the Standard Hydrogen Electrode (SHE).

General corrosion of all structural materials in reactor coolants typically proceeds at a few microns (~0.1 mils) per year, at most. Nevertheless, it is potentially deleterious to plant operation because of 1) the in situ formation or displaced deposition of corrosion products (i.e., fouling), which may perturb the hydraulic flow characteristics and decrease heat transfer efficiency, e.g., on steam generator tubes or fuel cladding; and 2) the neutron activation of corrosion products on fuel cladding surfaces that, upon release to the fluid, increase radioactivity levels in the reactor coolant system or, in the case of direct cycle BWRs, in the balance of plant.

General corrosion rates of structural materials are integrated into the design basis for water-cooled nuclear reactors in terms of conservative estimates of loss of section thickness over the design lifetime based on a large body of research and operating experience over many decades. Thus, there is good reason for the judgment that general corrosion is a manageable issue. Nevertheless, there is much current emphasis on reducing corrosion product formation and transport that lead to radiation fields in reactor primary coolant systems arising from corrosion product activation, particularly of cobalt and nickel.

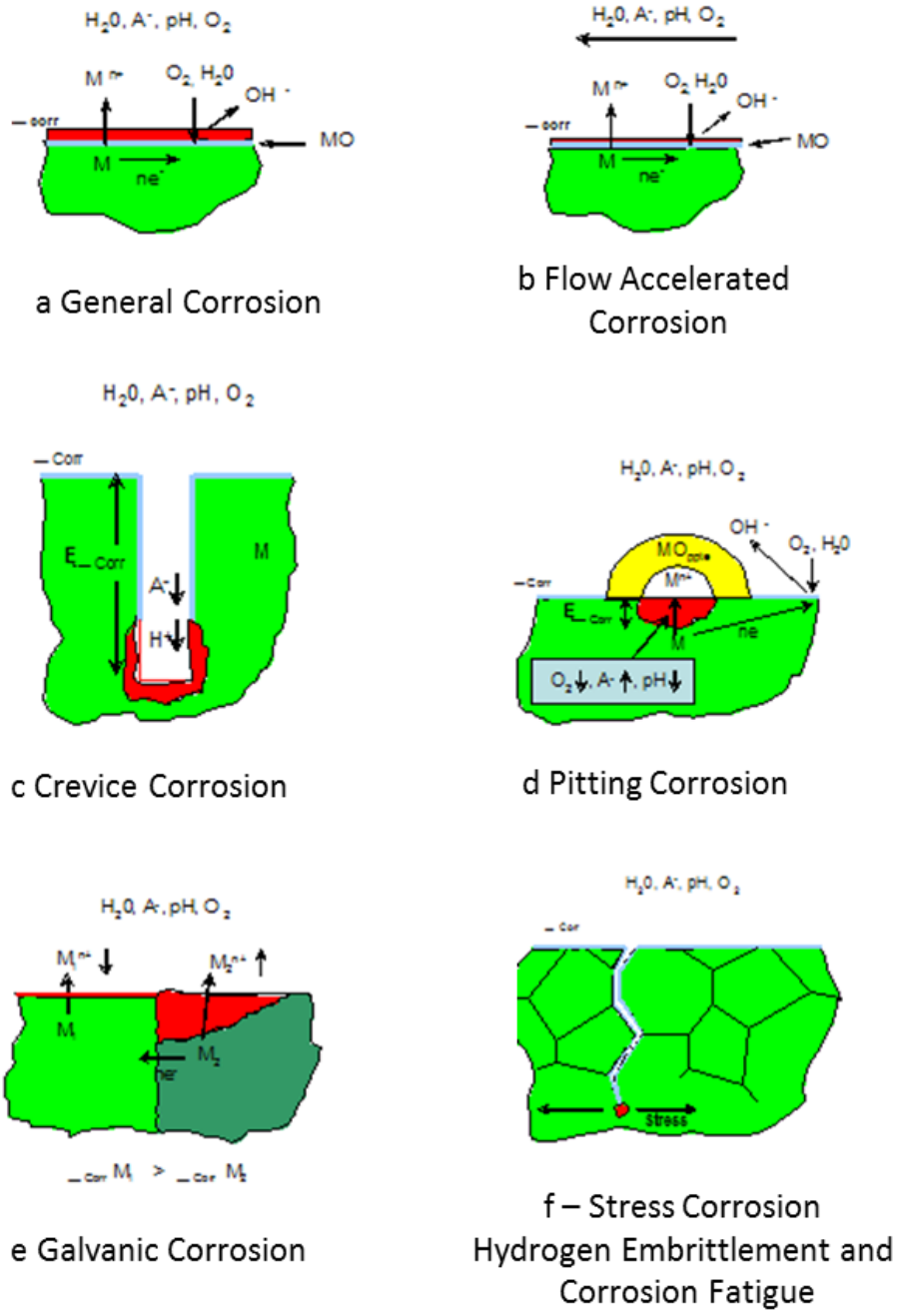

Figure A-1
Modes of corrosion (A- = anions, φ_{corr} corr = corrosion potential)

The red coloration in the figure denotes anodic sites where oxidation reactions occur, and the light blue regions indicate where an oxide (which may be protective) is thermodynamically stable. The arrows in each figure image indicate the direction of movement of the various species.

The following more detailed discussion of general corrosion is included here since the electrochemical details of general corrosion in water cooled reactors form a basis for understanding other corrosion-based degradation modes that have the potential to impact structural integrity.

General corrosion rates may be managed by 1) consideration of the thermodynamically stable (or metastable) species (dissolved metal cations, oxides, salts, etc.) at the metal/water interface and 2) control of the relevant oxidation and reduction kinetics. Corrosion protection of structural alloys in reactor coolants primarily depends upon the formation of stable protective oxide films and maintaining water chemistry conditions that avoid damaging them.

Taking the case of carbon and low-alloy steels (C&LAS), as an example, a Pourbaix diagram (named after its originator [A8]) may be constructed by considering all possible individual electrochemical reactions as a function of solution pH and corrosion potential in order to predict the thermodynamically stable species that may form in the solid state and in solution. Figure A-2 indicates that magnetite, Fe_3O_4, is the stable oxide that forms on iron in neutral, deaerated environments at 300°C, for example. The anodic oxidation reaction may be represented by Equation A-1:

$$3Fe + 4H_2O \rightarrow Fe_3O_4 + 8H+ + 8e- \quad \textbf{Eq. A-1}$$

The counterbalancing cathodic reduction process in a deaerated acidic environment is shown in Equation A-2:

$$2H^+ + 2e^- \rightarrow H_2 \quad \textbf{Eq. A-2}$$

or equivalently in deaerated neutral or alkaline solutions (Equation A-3):

$$2H_2O + 2e^- \rightarrow H_2 + 2OH^- \quad \textbf{Eq. A-3}$$

The equilibrium potential/pH characteristics of these two cathodic reactions resulting in hydrogen evolution are shown by *Line a* in Figure A-2.

In solutions containing dissolved oxygen, however, the main cathodic reaction (Equation A-4) is:

$$O_2 + 2H_2O + 4e^- \rightarrow 4OH^- \quad \textbf{Eq. A-4}$$

whose equilibrium potential/pH characteristics are shown by the dashed *Line b* in Figure A-2.

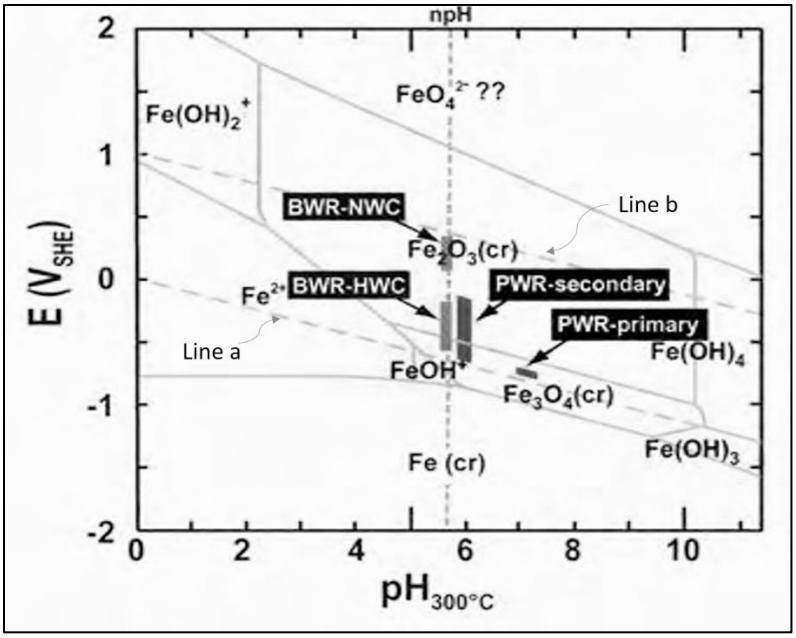

Figure A-2
Pourbaix diagram for iron at 300°C for activities of dissolved cations of 10^{-6} m, modified [A9]

Due to the requirement for electrical neutrality to balance the anodic and cathodic reactions, the corrosion potential of carbon steel in deaerated water is restricted to a range of approximately -600 mV_{SHE} to -800 mV_{SHE} (depending on the pH and dissolved hydrogen partial pressure). The corresponding corrosion potentials in oxygenated water are significantly higher, and hematite, Fe_2O_3, is the predicted stable oxide.

The release of iron to deaerated aqueous environments is determined by the solubility of magnetite, Fe_3O_4. This solubility is highly dependent on the pH, as shown in Figure A-3 (a), with a minimum being observed in the relatively narrow $pH_{300°C}$ range of 6-8, from which come the requirements of water chemistry specifications to maintain these slightly alkaline conditions (the neutral pH of water at 300°C is 5.65). Very similar solubility relationships are observed for nickel oxide and nickel ferrite, as indicated in Figure A-3 (b) and (c). Chromium, on the other hand, is highly insoluble at low potential (e.g., PWR, VVER, or CANDU primary water or BWR HWC) but may be oxidized to soluble hexavalent chromium, as observed in BWRs with oxygenated NWC. The corrosion rate of ferritic iron base alloys in deaerated water tracks the solubility/pH relationship for magnetite, with low rates being observed under slightly alkaline conditions and much higher rates being observed in acidic or more highly alkaline conditions. Such acidic or highly alkaline conditions are not normally allowed under current water chemistry specifications, but they may occur under specific circumstances such as regions of boiling in occluded crevices (e.g., in tube support structures in PWR, VVER, and CANDU steam generators).

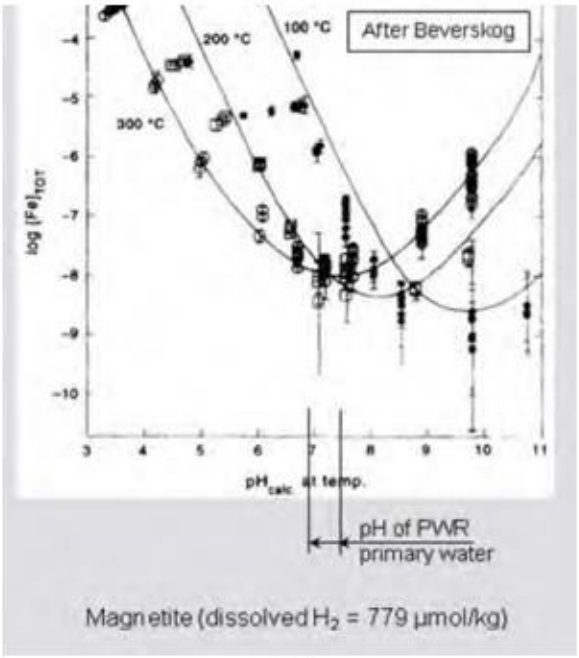

(a)

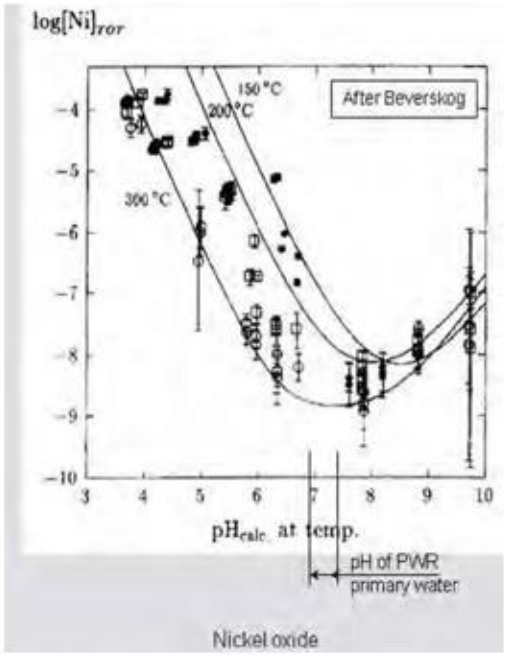

(b)

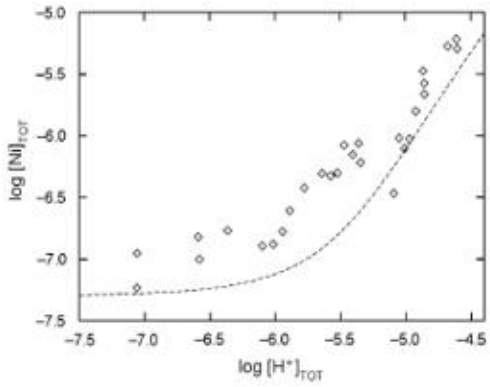

(c)

Figure A-3
(a) Solubility of magnetite, (b) NiO and nickel ferrite calculated from the thermodynamic data, and (c) comparison to experimental data [A9], [A10], [A11]

The corrosion rate of carbon and low-alloy steels in high temperature, neutral or slightly alkaline, deaerated water decreases after initial immersion due to the growth of thermodynamically stable magnetite [A12]. The oxidation rate follows a cubic or parabolic corrosion damage versus time dependency. The magnetite that forms initially in high temperature, deoxygenated water is not particularly protective of the underlying metal.

However, the oxide rapidly grows, initially epitaxially, into the metal substrate and then transforms to a fine grained, randomly oriented crystalline film (Figure A-4). Larger magnetite crystallites, > 0.5 µm size, deposit on the outer surface of this base layer via a dissolution-precipitation reaction. The deposited oxide then grows and coalesces to form a relatively thin but compact layer whose metal protection capability is enhanced by the deposition of fine Fe_3O_4 precipitates in the pores of the outer oxide.

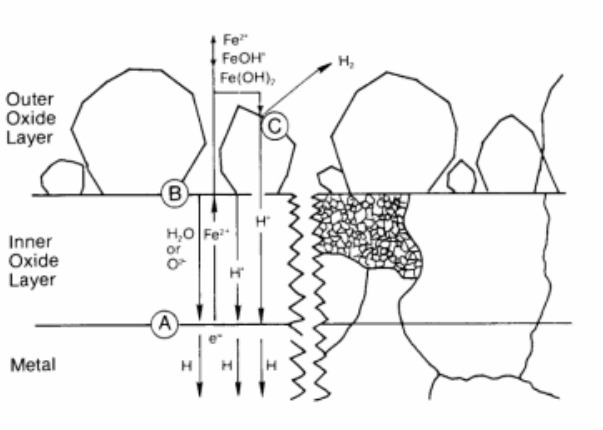

Figure A-4
Carbon steel corrosion in high temperature water (Diffusing species are shown on the left and grain structure appear on the right of the diagram [A13].)

Radiolysis of water in direct cycle BWRs produces stoichiometric amounts of oxygen and hydrogen, as well as some hydrogen peroxide. However, an excess of oxygen (and hydrogen peroxide) forms in the water phase that is retained in the reactor pressure vessel since hydrogen is preferentially partitioned to the steam phase. This introduces an additional cathodic oxygen reduction reaction that markedly increases the potential/pH region where corrosion can occur. Consequently, the corrosion potential of carbon or low-alloy steel moves in a positive direction by an amount that is a function of dissolved oxygen (and hydrogen peroxide) concentration, flow rate, and temperature [A14].

The positive increase in corrosion potential due to the higher dissolved oxygen (and hydrogen peroxide) concentration can lead to an increase in corrosion rate of the carbon steel (Figure A-5), especially at lower temperatures. However, as the temperature increases beyond approximately 150°C, this deleterious effect decreases due to the protective nature of the ferric (Fe-III) oxide (hematite) films now formed on top of the magnetite. Indeed, small amounts of dissolved oxygen in water at temperatures ~288°C can lead to a substantial *decrease* in corrosion rate such that the release of iron cations to the environment is negligible because the solubility of the outer layer of hematite is about a thousand times lower at ~288°C than that of magnetite [A14], [A15]. This point will be returned to later in relation to defining mitigating actions for flow-accelerated corrosion in carbon steel feedwater piping. At higher dissolved oxygen contents (>150 ppb), the corrosion potential is high enough that α-Fe_2O_3 is thermodynamically stable, and this may deposit on top of the double layer at high temperatures. However, as indicated in Figure A-5, although this mixed magnetite/hematite film is protective at high temperatures, it is not protective at lower temperatures.

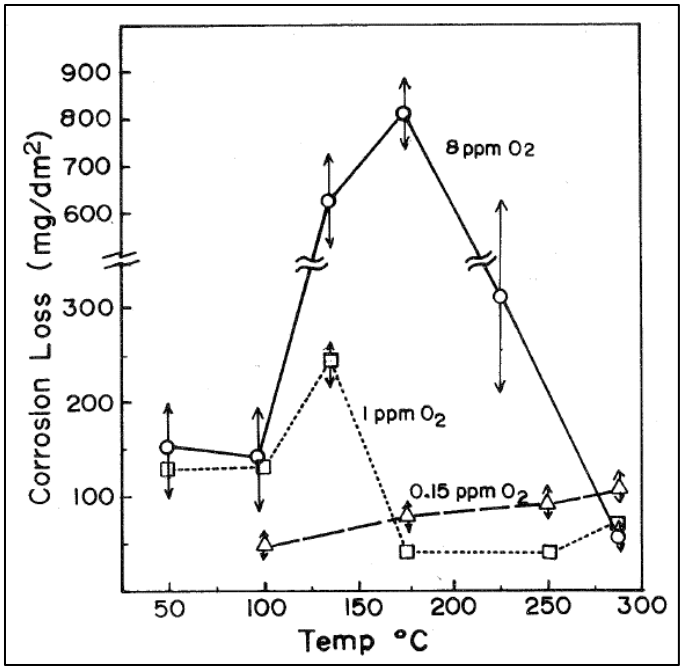

Figure A-5
Effect of temperature and dissolved oxygen concentration on the corrosion loss over 200 hours of carbon steels (SA 106 Grade B, SA 333 Gr 6) in pure water [A14]

NOTE:
The corrosion loss data in this figure should be multiplied by 3.6 to give corrosion rate values in units of mg/dm^2/mo. For calibration purposes, a corrosion loss of 100 mg/dm^2/mo would correspond to a corrosion rate of 1.98 mils/yr or 5.04 µm/yr.

The corrosion rates of stainless steels and nickel-base alloys in water at all temperatures relevant to water-cooled reactors are lower than those of carbon steels, due to the presence of adherent, protective surface spinel-type oxides composed of a mixture of $NiFe_2O_4$, Fe_3O_4, and $FeCr_2O_4$. These are double-layer oxide films with the inner layer being a chromium-rich normal spinel (chromites) and the outer layer an inverse spinel magnetite/nickel ferrite (ferrites), the latter being formed by a metal cation dissolution-precipitation reaction.

The oxide solubility/pH relationships for nickel oxide and nickel ferrite are similar to those of magnetite on iron (see Figure A-3 (b)) so that corrosion protection is maximized in slightly alkaline water conditions. Chromites are very insoluble at low corrosion potential (e.g., in PWR, VVER, and CANDU primary water or BWR HWC conditions) so that the corrosion rates of Type 304 stainless steel, after long exposure times, do not exceed a few tenths of µm/yr in near neutral water at ~300°C [A16]. However, unlike the experience with carbon steels, there is little effect of dissolved oxygen concentration and temperature on the general corrosion rate of stainless steel in the higher temperature range associated with the PWR, VVER, BWR, and CANDU reactor coolant systems (see Figure A-5 for carbon steel) even though at high corrosion potential in BWR NWC chromium can dissolve as hexavalent chromium cations. Nevertheless, this latter process does not seem to affect the innermost chromite spinel layers on stainless steel. Thus, the protective nature of the oxide remains constant over a wide range of electrode

potentials and temperature in these reactor coolant systems. The changes in corrosion potential that are noted are therefore not due to changes in the metal oxidation rate but rather to the equilibrium between the reduction rates of dissolved oxygen and/or hydrogen peroxide, and the oxidation rates of dissolved hydrogen [A17].

This is *not* to imply, however, that the corrosion potential is unimportant regarding all corrosion phenomena on these austenitic alloys. It is, in fact, of extreme importance in defining the localized environments that are relevant to crevice corrosion, pitting, and stress corrosion cracking, as discussed later.

The effects of general corrosion are accounted for in the design basis for PWR, VVER, BWR, and CANDU primary pressure boundary carbon steel and low-alloy steel components since there is a corrosion allowance to account for the loss of section thickness over the component service life. Actual long-term corrosion rates have usually been found to be significantly below the design-basis allowable values, usually because the specified corrosion allowance is conservatively assumed to be a linear function of design life. In the case of BWR carbon steel piping, for example, the design specification provides a general corrosion allowance of 120 mils for the main steam system, but the actual general corrosion rate for carbon steel piping in this environment is now known to be less than 0.16 mils per year [A18], allowing for hundreds of service years.

Similarly, the corrosion allowance for stainless steel piping operating in the 250-300°C range in BWRs is 2.4 mils. The actual general corrosion rate for stainless steel in this temperature range is 0.01 mils/yr of service life, which would allow 240 years of service before the corrosion allowance would be compromised. Moreover, as mentioned earlier, these rates are conservative since corrosion rates generally decrease as an approximately parabolic or inverse cubic function with time. Cast stainless steel components (e.g., recirculation pump bowl, valve bodies) also exhibit similarly low general corrosion rates.

Although general corrosion rates are low for both carbon and low-alloy steels under controlled chemistry conditions, the actual amount of corrosion product formed (in terms of weight) can be very large given the area of exposed steel, and this can give rise to buildups that affect local corrosion and/or heat transfer, as well as corrosion product activation and consequent radioactive contamination problems out of core. It can be argued that the radioactivity buildup situation may be minimized for carbon and low-alloy steels due to the relatively low nickel and cobalt contents in these alloys, and this is supported by the satisfactory performance of unclad carbon and low-alloy steel components in the primary systems of CANDU and some early VVERs. However, cladding the surface area of exposed carbon and low-alloy steel in primary reactor coolant systems with weld overlays of stainless steel decreases the general corrosion rate, especially at high coolant flow rates (due to increased resistance to flow-accelerated corrosion) and under low temperature, oxygenated conditions during shutdown.

A.1.2 Wastage or Boric Acid Corrosion (Wstg.)

As discussed in the previous section, uniform corrosion rates of the principal materials of construction of water-cooled reactors are well below those necessary to compromise the structural integrity of components over their design lives, including presently envisaged plant life extensions. Nevertheless, there are some situations where very high corrosion rates can occur over significant areas and structural integrity may be compromised, of which wastage of carbon and low-alloy

steels due to boric acid leaks from PWR and VVER primary circuits and flow- accelerated corrosion of carbon steel and copper alloys (discussed in the following section) are the most important. Stainless steels and nickel-base alloys [A19] are not affected by either phenomenon, although erosion by escaping steam jets (sometimes called *steam cutting*) is possible.

Although the internal surfaces of carbon and low-alloy steel PWR and most VVER primary circuit components are clad with stainless steel to minimize general corrosion, the stainless steel cladding has occasionally been damaged or deliberately removed locally that exposes the underlying ferritic steel. In these cases, the corrosion rate at 300°C is very low (~2-3 µm per year) because, even in the presence of up to ~1% boric acid (at the beginning of a fuel cycle), the pH is adjusted by lithium hydroxide additions in PWRs or by potassium hydroxide in VVERs so that the solubility of protective oxides, such as magnetite and other spinels, is at a minimum (see Figure A-3) and a protective oxide layer is formed. However, problems have occurred when borated water leaks from the primary coolant circuit have contacted carbon or low-alloy steel surfaces that are normally only exposed to the containment air environment [A19], [A21], [A22], [A23]. The observed severe corrosion or wastage is caused by boric acid and its concentration due to steam flashing at near atmospheric pressure in the containment building and by alternating wetting and drying cycles that produce, ultimately, a concentrated boric acid slurry. Under such highly acidic conditions, the corrosion rate would be expected to increase significantly due to the high solubility of magnetite at low pH, and corrosion rates up to several inches per year are possible. Flow-accelerated corrosion also probably plays a role when carbon and low-alloy steels are exposed to high velocity primary water and steam jets.

The primary water leak rate, location, fluid temperature, and the temperature of the carbon and low-alloy steel surfaces exposed to the leak play important roles in the local concentration of primary water additives (boric acid and lithium hydroxide) that can be achieved and, consequently, the corrosion rate that will be observed. Relatively low temperature leaks, such as those from canopy seals of PWR CRDM housings or faulty valve gaskets, can allow primary water to flow in the liquid state at atmospheric pressure onto hot surfaces where it evaporates and concentrates. The balance between the leak rate and the evaporation rate is critical to whether a concentrated fluid, a moist paste, a molten salt, or a dry powder forms. Since the presence of water in some form is a necessary condition for corrosion of carbon and low-alloy steels (C&LAS) [A30], it follows that the leak rate must exceed or at least balance the evaporation rate at the metal surface for any significant corrosion to occur.

Many experimental studies have been carried out to try to reproduce the corrosion damage of C&LAS observed in PWR systems due to primary water leaks [A19]–[A32]. A high proportion of these experiments has been conducted using aerated or deaerated aqueous solutions with various concentrations of boric acid, and have enabled the influences of concentration, pH, temperature, and dissolved oxygen on corrosion rates to be quantified. Simulated leak tests incorporating the effects of high velocity steam jets have also been carried out. However, corrosion of C&LAS in molten salts with low fractions of water has received much attention relatively recently [A30].

High corrosion rates in excess of half an inch (12.7 mm) or more a year are observed in the presence of concentrated boric acid solutions, usually aerated, or moist boric acid pastes at intermediate temperatures around 100°C. The wastage rates can be ~100 times faster than at ambient temperature and are comparable to those observed in service caused by primary water

leaks. For example, wastage rates of 4 to 6 inches (101.6 to 152.4 mm) per year were observed when solutions containing 15 wt% boric acid were allowed to drip onto surfaces at 95°C. The effect of temperature is in accordance with that which would be expected from the increase in dissociation constant of boric acid up to about 150°C, as well as from thermal activation (Figure A-6). Above about 150°C, corrosion reaction rates stabilize or slow, probably due to the increasing ionic association of boric acid. The stability of the various boric acid phases in the presence of low concentrations of water, as well as the dissociation constants of boric acid and lithium or potassium hydroxide, may also play a role in the non-monotonic dependence of wastage corrosion on temperature.

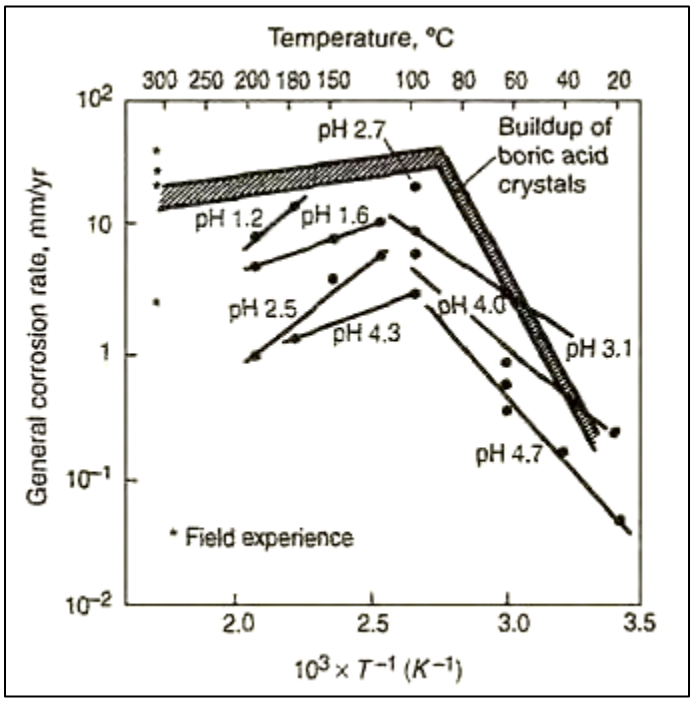

Figure A-6
Corrosion rate for carbon steel in boric acid as a function of temperature [A28]

At very high boric acid concentrations, the role of aeration is less important at pH values of less than about 4.5 because C&LAS easily displaces hydrogen from acidic solutions during corrosion. Recent tests in concentrated boric acid and lithium hydroxide, where the ratio of B/Li was maintained as it would be at the beginning of a fuel cycle, have also shown that very high corrosion rates up to around 5 inches (127 mm) per year were maintained at temperatures around 100°C.

In stagnant or low flow concentrated boric acid solutions, the wastage rate is observed to decrease over a period of a few hours, whereas, in strongly flowing solutions, such a decrease in the wastage rate is not observed. The adverse effect of flow on the corrosion kinetics can be explained by the elimination of corrosion products as they are formed and avoiding iron cation saturation of the solution.

Experiments have also been performed using mockups to simulate in-service leaks of primary water. For example, a leak of primary water at 316°C through a cracked stainless steel tube in a ferritic steel plate gave rise to a maximum corrosion rate of 2 inches (50.8 mm) per year at the point where the leak escaped from the crevice between the tube and steel plate. Similarly,

experiments have been carried out using jets of superheated steam from borated water at 316°C directed at carbon steel surfaces. Corrosion rates up to an inch (25.4 mm) per year were observed just outside the zone directly impacted by the steam jet, whereas even higher rates were measured in the impact zone where erosion also undoubtedly contributed to metal loss. Questions arise in this type of test regarding the degree of cooling experienced by the target relative to in-service conditions and whether the metal removal rates can be exaggerated by use of solutions containing boric acid alone rather than boric acid and lithium hydroxide that are present in PWR primary water. However, the second of these concerns appears to be allayed by the more recent tests in boric acid and lithium solutions described earlier.

Some tests have also been carried out using molten salts of boric acid at temperatures from 150 to 320°C. If no moisture was present, then there was no corrosion of C&LAS, but very high rates of corrosion up to 6 inches (152.4 mm) per year were observed when water was added (at atmospheric pressure). The addition of water also caused the temperatures of the test pieces to converge in the range of 140 to 170°C during these tests.

The beneficial effects of chromium additions to steels and nickel-base alloys have also been demonstrated. At the levels of chromium normally encountered in stainless steels and nickel-base alloys used in PWRs and VVERs, corrosion rates are reduced by two to three orders of magnitude relative to C&LAS and generally pose no problems for structural integrity.

From a practical viewpoint, these observations lead to the following criteria that contribute to high wastage rates that can reach up to 10 inches (254 mm) per year:

- The leak rate must be sufficient to impart a measure of evaporative cooling to the surface of the carbon or low-alloy steel (see the non-monotonic temperature behavior in Figure A-6), since maximum wastage rates are observed between 100 and 150°C.
- The leak rate must be sufficient to maintain the boric acid crystals in a wet condition, since corrosion rates with dry boric acid on a carbon or low-alloy steel surface are negligible [A30].
- Neither high flow rates nor oxygen from air is a necessary condition for high rates of wastage of carbon steel or low-alloy steel under highly concentrated boric acid conditions, although high flow rates can exacerbate wastage under certain circumstances such as in escaping jets in narrow crevices. Oxygen can have an aggravating effect in less concentrated, less acidic boric acid solutions.
- Erosion effects from high velocity steam jets (steam cutting) can exacerbate the damage and will also rapidly cut grooves in stainless alloys.

In conclusion, the phenomenology and mechanisms of boric acid wastage are generally understood and manageable [A29], [A33], [A34].

A.1.3 Flow-Accelerated Corrosion (FAC)

Flow-accelerated corrosion (FAC), sometimes known as flow-assisted corrosion, describes the enhanced loss of metal that can occur in water or steam under single- or two-phase flow conditions, especially at areas of high turbulence that are often associated with geometrical discontinuities or abrupt changes in flow direction. It is most observed in carbon steel used in feedwater systems, extraction steam and drain lines, and in copper-based alloys used in

condensers and heat exchangers. Fundamentally, this acceleration in corrosion rate is associated with changes in the mass-transport controlled oxidation and reduction reaction rates occurring on the surface oxide.

The term *erosion-corrosion* is sometimes used erroneously as a synonym for FAC, although it should only be employed where there is an additional abrasive effect that mechanically removes the protective oxide on a metal surface. Mechanical abrasion assisting the removal of the oxide layer can be due to 1) the impact of water droplets on the surface in two-phase flow steam systems (e.g., wet steam in main steam lines, upper support plates in steam generators, or cross-over piping in turbines); 2) cavitation effects due to imploding vapor bubbles (e.g., impeller blades in pumps); and 3) entrained particles, such as sand, in tertiary coolant systems served by a lake, river, or seawater.

The consequences of FAC include 1) outright failure of the component by mechanical overload when the wall thickness is sufficiently thinned, 2) a significant contribution to feedwater iron content, 3) an increase in radiation levels in BWR balance-of-plant, and 4) the fouling of flow measurement devices and ion exchange polishers by released iron oxides. Extreme examples are the ruptures of an 18-inch (457-mm) diameter carbon-steel condensate line on the secondary side of the Surry-2 PWR in 1986 [A35] and of a 24-inch (610-mm) diameter carbon-steel steam line between the low pressure heater and deaerator at the Mihama-3 PWR in 2004 [A36], [A37]. In both cases, the accelerated corrosion occurred adjacent to pipe geometries such as elbows and/or orifices that disturbed the fluid flow.

Several factors such as flow rate, temperature, pH, water chemistry, and material composition influence the FAC rate. For carbon steels, increases to several millimeters per year can occur depending on specific combinations of these factors [A38]–[A42]. These references include a detailed EPRI-led review of the subject. At the simplest level, the increase in corrosion rate with flow rate under both laminar and turbulent flow regimes may be understood in terms of an increase in removal rate of oxidized species from the metal surface, and/or in some specific circumstances, an increase in diffusion rates of the cathodic reactant, dissolved oxygen or hydrogen, toward the metal surface. In this way, the corrosion current density changes with the mass-transport limited kinetics of the electrochemical oxidation and reduction reactions. The following is a more detailed description of the influence of these various parameters on the metal loss rate.

A.1.3.1 Effect of Single- or Two-Phase Flow and Turbulence

As noted earlier, in single-phase flow, FAC is observed mainly where there are geometric aspects that alter flow direction provoking turbulence in the fluid, for example, at elbows, T- and Y-junctions, valves, diaphragms, orifices, and even welds. It is generally accepted that the parameter that best describes the loss of metal due to FAC is the mass transfer coefficient, which depends on the diffusion of soluble species across the boundary layer between the oxidizing metal surface and the fluid. It is usual to consider the mass transfer coefficient for a straight tube and then apply a coefficient for each specific geometry. The mass transfer coefficient is proportional to the non-dimensional Sherwood parameter, Sh, where:

$$Sh = C.\ Rex.\ Scy \qquad \textbf{Eq. A-5}$$

In the above Equation A-5, Re is the Reynolds number (which integrates the fluid velocity, the hydraulic diameter, and the kinematic viscosity), Sc is the Schmidt number (which integrates the kinematic viscosity and the diffusion coefficient for iron in solution), and C, x, and y are constants.

The kinetics of FAC in smooth straight tubes increase generally as a function of $Re^{0.8}$, whereas, in straight tubes with a rough surface, the FAC rate is directly proportional to the fluid velocity. These dependencies have been verified in the laboratory for single-phase flow mainly in the temperature range from 150 to 250°C. However, the results for two-phase flow are consistent with the dependencies for single-phase flow.

Despite these well characterized dependencies of FAC on hydraulic flow parameters, metal losses greater than predicted have been observed, particularly in single-phase flow conditions where the mass transfer coefficient is very high or in two-phase annular flow [A40], [A41]. The interpretation of these results has been controversial. The role of surface roughness under high mass transfer conditions has been emphasized by certain authors [A38], whereas others have focused on the effect of fluid flow on the cathodic reaction rate in the corrosion process [A40], which is usually neglected in most attempts to quantify FAC kinetics. The latter approach has the advantage of explaining locally increased solubility of magnetite due to a decrease in local corrosion potential caused by the effect of flow on the rate of the cathodic hydrogen evolution reaction. In this case, FAC is seen to accelerate as a function of high mass transfer rates after initially following the $Re^{0.8}$ dependence at lower mass transfer rates.

FAC of carbon steels also depends strongly on the steam quality of two-phase flows [A38]. The kinetics of FAC increase very quickly when the steam quality attains 20 to 40% and is maximum between 40 and 80%. It is also observed that the range of temperatures normally associated with FAC in single-phase water extends to higher temperatures in a two-phase flow. FAC has been seen at temperatures as high as those associated with the secondary side of PWR, CANDU, and VVER steam generators where significant loss has been observed in PWR upper support plates, steam separators, and blowdown piping [A42]. The deleterious effect of two-phase flow is exaggerated as the pH of the feedwater decreases or with increasing partition of volatile chemicals to the vapor phase.

A.1.3.2 Temperature

FAC is significantly affected by temperature with a maximum in dissolution rates of carbon steels occurring at about 130°C in a single-phase flow (Figure A-7) and at about 180°C in a two-phase flow. The effect of temperature on the FAC rate is similar to the effect on the Schikorr reaction (Equation A-6):

$$3Fe(OH)_2 \rightarrow Fe_3O_4 + 2H_2O + H_2 \qquad \textbf{Eq. A-6}$$

Which becomes progressively more efficient as the temperature increases above ~150°C and effectively counterbalances the thermal activation of iron oxidation by forming a more protective layer of magnetite at higher temperatures.

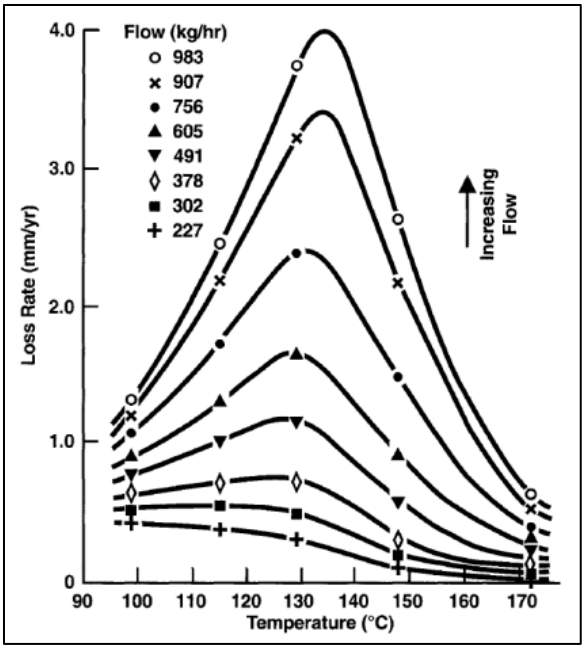

Figure A-7
Effect of temperature on the flow-accelerated corrosion rate of carbon steel in deoxygenated ammonia all-volatile treatment (AVT) water [A38]

The influence of temperature can be marked as a function of the pH, single- or two-phase flow, and fluid velocity. Although FAC rates decrease at temperatures on either side of the peak temperature, FAC is often localized because of mass transfer effects, and rates of metal loss at higher or lower temperatures may still be sufficient to result in wall thinning and piping failure in thin-walled pipes. Operating experience with PWR steam generators shows, for example, that feedwater distribution U-tubes fabricated from carbon steel can lose metal at up to 1 mm/yr in single-phase water at 220°C flowing at 8 to 9 m/s. Consequently, significantly more highly alloyed materials are used today to fabricate the J-tubes in replacement steam generators. A similar strategy has been adopted for the feedwater system in VVER steam generators.

Carbon steel feedwater systems for both BWRs and PWRs are particularly at risk from FAC and are typically routinely inspected to ensure that wall thinning is monitored. In unfavorable conditions, metal loss rates up to 10 mm/yr have been observed [A42]. This is of significance for LWR operators applying for power uprates, since one way in which extra power can be achieved is by increasing the coolant and feedwater flow rates.

A.1.3.3 Water Chemistry

For carbon steels, the pH of typical boiler feedwater, as measured at 25°C, should be between 9 and 10 to minimize corrosion in water due to the minimum in magnetite solubility in this range (see Figure A-3 (a)). On the secondary side of PWR steam generators, this is usually achieved using an all-volatile treatment (AVT) or with ammonia/hydrazine and/or organic amines such as morpholine or ethanolamine. Based on operating experience and the desire to minimize both FAC and sludge accumulation in steam generators, the current industry approach is to operate at the high end of that range if only ammonia/hydrazine is used, even up to a pH of 10.2. However, such a high pH value cannot be used if there are any copper alloy components in the secondary circuit, in which case the pH must not exceed 9.4 and an organic amine is normally employed.

It has been shown, for example, that, in secondary water at a pH of 9.2 and a temperature of 225°C, the loss of metal from carbon steel in ammonia AVT is five times higher than with morpholine. This result occurs because morpholine and other organic amines are stronger bases at higher temperatures than ammonia for the same pH at 25°C. In addition, their partition coefficients between steam and water are lower than those of ammonia, which also favors a higher pH in the liquid phase of two-phase mixtures of water and steam.

Another factor that can influence metal loss rates by FAC in PWR secondary circuits, particularly of carbon steel support plates in the steam generator, is the presence of impurities and their concentration in the liquid phase as steam quality increases. Leaks of seawater through condenser tubes can allow the concentration of chloride in the liquid phase to increase and acidify, especially due to hydrolysis of magnesium chloride. This can then increase the FAC rate of carbon steel support plates to a greater or lesser extent, depending on whether ammonia AVT or organic amines are in use, the latter being, in principle, more effective in the presence of acidic impurities.

The influence of water chemistry on corrosion potential is another important factor affecting the FAC of carbon steels. Oxygen at concentrations ranging from a few ppb to a few tens of ppb, depending on the flow rate (which affects the efficiency of mass transport to and from the corroding surface), can have a dramatic effect on increasing the corrosion potential by 600 to 700 mV and on decreasing, very significantly, the solubility of iron oxides. Hematite (Fe_2O_3), the oxide of iron that forms at high corrosion potential, is about three orders of magnitude less soluble in water than magnetite, the oxide form that forms at low corrosion potential. This has led to the practice of adding 20-30 ppb oxygen to feedwater in BWRs (Figure A-8), as well as in conventional boilers in Germany and in the once-through boilers of the British Advanced Gas Cooled Reactors [A40], [A43], [A44], [A45]. The amount of oxygen required to minimize FAC in two-phase wet steam main lines in BWRs is a function of the amount of radiolysis occurring in the reactor core, the degree of hydrogen water chemistry/NobleChem™ applied, and the extent of venting applied in the moisture separators.

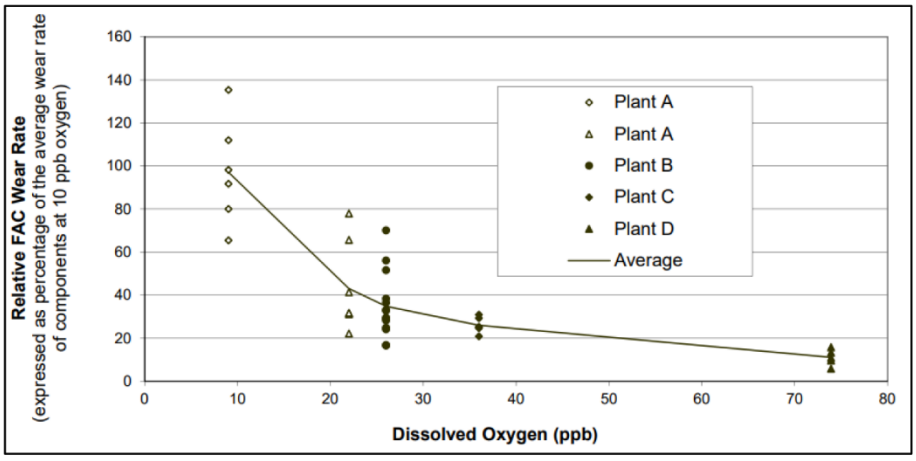

Figure A-8
Flow-accelerated corrosion data for condensate and moisturizer separator reheater drain systems in four BWR plants as a function of the local dissolved oxygen contents [A44]

Other water chemistry parameters that influence FAC of carbon steels are the dissolved iron content and the dissolved hydrogen concentration. The former exerts an influence on the efficiency of the mass transfer of dissolved iron from the corroding surface, whereas the latter directly influences the solubility of magnetite. High dissolved hydrogen concentrations can enhance reductive dissolution of magnetite.

A.1.3.4 Material Composition

The elemental composition of carbon (and low-alloy steels) has a significant impact on FAC rates. The most important alloy variable is the chromium content of the alloy (Figure A-9), which is understandable given the protective nature of the oxides that are formed on chromium-containing alloys. Copper and molybdenum alloying additions have also been suggested to have beneficial effects, although such effects are typically smaller. An empirical expression quantifying the gain (g) from the beneficial alloying additions (in wt%) has been proposed based on laboratory testing [A38], as shown in Equation A-7:

$$g = 83[\text{Cr wt\%}]^{0.9} \times [\text{Cu wt\%}]^{0.25} \times [\text{Mo wt\%}]^{0.2} \qquad \textbf{Eq. A-7}$$

Current practice is to specify chromium levels of > 0.15 or 0.2 wt% for the construction of PWR secondary side feedwater piping with single-phase flow. In two-phase flows, which typically have much higher velocity than single-phase flows, Cr-Mo steels or, preferably, stainless steels may be appropriate. Recognized low-alloy steels such as 1¼Cr-Mo or 2¼Cr-Mo have been widely adopted in some countries, but this necessitates stress relief heat treatments of welds and extra cost. Stainless steel has also been used in PWR steam generator feedwater piping in newer plants, for example, in all the Konvoi units in Germany. In situations where a complete alloy change is not economical, overlays with a higher chromium content coating deposited by thermal spray or welding have been used.

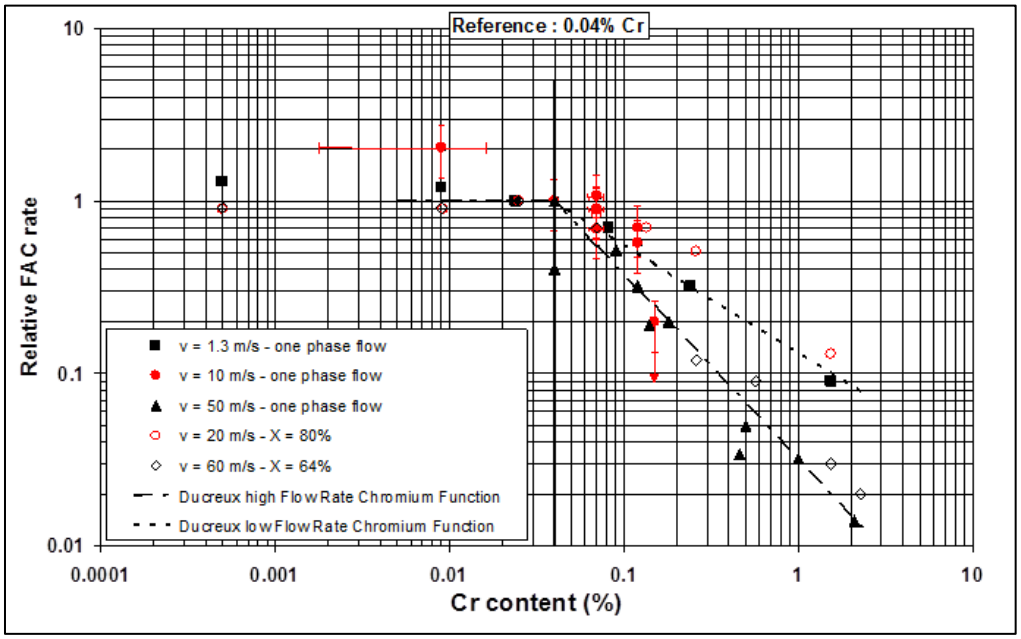

Figure A-9
Effect of chromium content of carbon steels on FAC [A38]

One curious unwanted feature of the effect of chromium on FAC behavior has been observed on several components where a characteristic groove has appeared just downstream of butt welds. In these cases, the butt weld metal was FAC resistant because it contained traces of chromium, and the downstream material did not [A46]. The phenomenon is known as the "entrance effect." Similar situations can arise when FAC-susceptible carbon steel piping is replaced by a more resistant alloy and some of the less resistant material is left in place downstream either by accident or by design.

FAC of copper-based alloys, and especially Cu-Zn Admiralty brass, has been a significant problem in both nuclear and fossil plants. In seawater systems fabricated from Admiralty brass, fluid velocities of > 1 m/s can cause FAC or impingement attack problems while the cupro-nickels can be used up to about 3 m/s [A47]. In nuclear plants, the release of copper cations from heat exchangers has exacerbated various corrosion modes where it plates out downstream and raises the corrosion potential. Copper deposits can exacerbate various corrosion modes on fuel cladding in direct cycle BWRs, whereas on the secondary side of Alloy 600 steam generators tubes in PWRs, copper deposits have been implicated in aggravating IGA/IGSCC. Consequently, this has led to the replacement of Cu-Zn, Cu-Ni, or Cu-Al condenser and heat exchanger tubing, typically by stainless steels for freshwater cooled plants or titanium tubing for seawater-cooled stations.

Steam droplet impingement erosion, like the degradation phenomenon found in turbines, has also occurred on the outer tube bundles of condensers where the steam inlets are located [A42]. This phenomenon has even occurred in condensers with titanium alloy tubes but can be resolved by design changes to the flow inlets and/or by using stainless steels in this area.

A.1.4 Localized Corrosion

This section includes pitting, crevice corrosion, and galvanic corrosion modes of localized corrosion that are illustrated diagrammatically in Figure A-1 (c), (d), and (e). As will be seen, they cannot occur in reactor coolant environments without significant perturbation of the intended water chemistry. For this reason, localized corrosion modes in water-cooled reactors mainly concern tertiary water systems, which are not specifically addressed in the MDM. Also, for convenience, microbiological corrosion is included in this section since the usual result of microbial activity is the generation of an aggressive environment over a confined area, wherein attack is localized. Discussion of intergranular corrosion is, however, deferred until the next section that also addresses stress corrosion cracking.

Localized modes of corrosion can occur at relatively rapid penetration rates. Since they are often hard to detect, they present a significant management challenge and are a significant cause of costly repairs to tertiary water systems.

A.1.4.1 Galvanic Corrosion

Galvanic corrosion (see Figure A-1 (e)) is observed at the junction of two dissimilar metals, which are in electrical contact in a conductive aqueous environment. A similar localized corrosion mode is observed on a single metal surface exposed to environments that have different concentrations of reducible species, usually dissolved oxygen in the context of water-cooled reactors. This can give rise to differential aeration cells and, for example, "waterline attack" for partially immersed structures.

Localized galvanic attack is associated with a macroscopic separation of the anodic and cathodic reaction sites, which, when electrically unconnected, would have markedly different corrosion potentials. The metal with the more negative (unconnected) corrosion potential undergoes an increased corrosion rate when connected to a metal with a more positive (unconnected) corrosion potential close to the region of dissimilar metal contact. The converse is also true in that the corrosion rate of the more noble metal will be decreased by connection with an active metal. This is the basis of cathodic protection of, for example, mild steel by zinc galvanizing or by coupling to a sacrificial zinc (or other active metal) anode. Since the corrosion potentials of the materials of construction in high temperature reactor coolant systems are controlled principally by redox reactions involving hydrogen, water, and oxygen, the corrosion potentials of the unconnected materials are not very different, and galvanic attack is, therefore, not a significant factor.

Another requirement for galvanic corrosion is that the current must also flow through the aqueous environment to complete the electrical circuit between the anode and cathode. Thus, as the distance in the solution between the anode and cathode increases, the solution resistance increases and galvanic attack decreases. Due to the high electrical resistivity of BWR, PWR, VVER, and CANDU primary and secondary coolants, galvanic corrosion cannot be a significant degradation mode (in contrast to some lower temperature tertiary systems, especially in seawater; e.g., steam turbine condensers). In this latter case, the corrosion potentials of the unconnected materials of construction would be very different, and the conductivity of seawater is high so that there can be efficient electrical coupling between anodic and cathodic sites.

The kinetics of galvanic corrosion in low temperature, conductive, aqueous environments is also affected by the relative surface areas of the anodic and cathodic sites. A larger area of the more noble metal compared to that of the more active metal will give a significantly enhanced galvanic corrosion rate of the latter in a conductive solution. For example, the corrosion rate of mild steel condenser tube sheets exposed to seawater may be increased by a factor of 3 to 7 times that in the area adjacent to a copper alloy condenser tube that is rolled into it, with the precise acceleration factor being a function of the excess area of the copper tubes. Similarly, in service water environments, carbon and low-alloy steels have substantially lower corrosion potentials than stainless steels and titanium alloys and would be preferentially attacked in a galvanic couple with them.

As with general corrosion, galvanic corrosion is a very well understood phenomenon, being the theoretical basis for sacrificial anode protection techniques used in many industries for immersed and buried structures. Consequently, although the possibility of galvanic corrosion exists in water-cooled reactor systems, it is generally accounted for at the reactor design and construction stage and concerns mainly the lower temperature systems involving large surface areas in service and cooling water such as in condensers [A48].

A.1.4.2 Crevice Corrosion

Crevice corrosion is associated with occluded volumes inside which a quasi-stagnant solution is present and where there is a mechanism to make that solution more aggressive (e.g., increased impurity concentration with increased acidity or alkalinity). Crevices may be inherent in the component design (such as at gasket joints, lap joints, bolt heads, and threads) or may occur due to corrosion deposits and sludge piles. The critical factors controlling this form of attack are the geometry of the crevice and the electrochemical or thermal hydraulic mechanisms that change the cation and anion concentrations within the crevice.

Electrochemical crevice corrosion occurs when a galvanic couple can be stabilized between an occluded cell, within which no oxidant other than water is present to take part in a cathodic reaction, and an external surface where the reduction of an oxidizing species (e.g., dissolved oxygen) can balance excess anodic current from the occluded cell. The reason for this gradient in the concentration of oxidizing species is that the convection-controlled transport rate of dissolved oxygen into the crevice cannot balance its removal due to general corrosion on the crevice sides. The resultant separation of the cathodic reduction of oxygen at the crevice mouth from the metal oxidation site within the crevice imposes a potential gradient down the crevice, which gives rise to potential-driven migration of anionic impurities (e.g., chloride) into the crevice and of cations toward the free surface outside the occluded cell (Figure A-10). Hydrolysis of dissolved metallic cations within the occluded cell, combined with the transport of anions such as chloride toward the occluded cell, can result in a local pH reduction and very high concentrations of chloride and hydrolyzed metallic cations. Thus, environmental conditions of low pH and high anionic impurity concentration can be created within the crevice, and this can lead to large increases in the local metal corrosion rate if the anions, like chloride, are deleterious to passivity. Sulfate ions can also cause a pH drop in occluded cells but are not deleterious to passive layers on stainless steels, for example, and, thus, very rarely cause localized crevice corrosion (or pitting) by themselves.

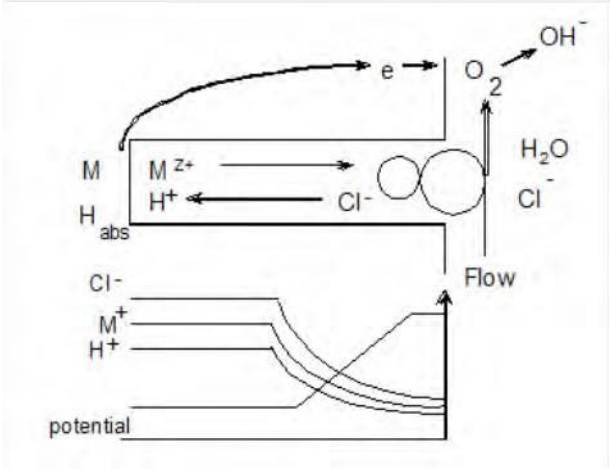

Figure A-10
Schematic of crevice in an aerated solution indicating the separation of the metal oxidation and oxygen reduction sites and the consequent changes in pH and anion concentration

In BWR NWC water, which contains dissolved oxygen and hydrogen peroxide, electrochemically driven concentration of anions in crevices is possible in principle. Classic examples of such environmental chemistry changes in crevices in BWR RCS components are associated with safe-ends, access hole covers, shroud head bolts, and IRM/SRM dry tube assemblies [A49][A50]. In these cases, the potential drop into the crevice is of the order of 700-800 mV and can give rise to an anionic concentration increase on the order of 10-100x and an accompanying pH decrease of approximately 1-2 units [A51]. Such changes in crevice chemistry are not enough to cause excessive crevice corrosion of the austenitic stainless steel or Alloy 600 components, but they are sufficient to promote intergranular stress corrosion cracking of these alloys at the tip of the crevice. Obvious remedies for mitigating this crevice concentration effect are to improve the water purity and/or remove the potential gradient that is

required for the creation of the crevice chemistry. As in the case of the hydrogenated PWR, VVER, or CANDU primary water environments, in BWRs using "hydrogen water chemistry" (HWC), there is no potential difference between the mouth of a crevice and its tip and, therefore, no electrochemical driving force for anion concentration within the crevice.

Other examples of this potential-driven mechanism of crevice chemistry formation are found in service water systems where the liquid may be naturally aerated [A48], [A52] and may contain substantial amounts of chloride. A significant number of these examples concern crevice corrosion of condenser tubes in seawater service. In most cases, the problem has arisen due to poor geometrical design. In those cases where this cannot be changed, remedies rely on re- tubing with stainless steels that contain increased amounts of chromium, nickel, and molybdenum that have higher resistance to crevice corrosion. As would be expected, such alloys have a more protective surface oxide that can better resist the acidic, chloride environments that develop in crevices. Effective crevice corrosion resistance may also be achieved by re-tubing with titanium alloys [A48], [A52].

An alternative mechanism for creating a localized aggressive environment in water reactor plant components occurs on heat transfer surfaces, where concentrations of dissolved species change due to their partition between the aqueous and gaseous (i.e., steam) phases or the evaporation of volatile species. This concentration of acidic, alkaline, or other aggressive non-OH^- anions may be retained under specific geometrical conditions that inhibit solution redistribution. An example of this is the localized corrosion of carbon steel tube support plates in PWR steam generators, as illustrated in Figure A-11, which has led to denting of Alloy 600 tubes, as well as stress corrosion cracking of the tubes.

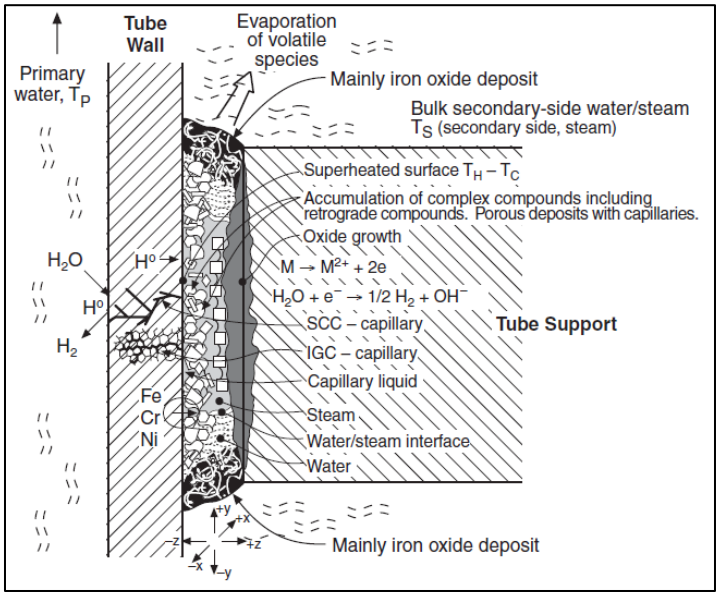

Figure A-11
Schematic of crevice formed at PWR steam generator tube/carbon-steel tube support, together with the phenomena that give rise to localized corrosion and cracking [A53]

The mechanisms for the creation of such concentrations of impurity species are well recognized, having their origin in corrosion of heat transfer surfaces in fossil-fired plants. Any stable liquid phase adjacent to the heat transfer surface must have a boiling point equal to the temperature of that surface, but the vapor pressure above that liquid must be equivalent to that of the steam pressure. The temperature difference between the primary and secondary sides of a PWR (recirculating) steam generator tube can vary from 45°C at the hot leg to 22°C near the top of the U-bends. Considerable solute concentrations are required to accommodate these amounts of superheat and to maintain a liquid phase on the outside of the tube at the secondary side pressure. Different solutes can support different amounts of superheat due to their different solubilities [A54], [A55], [A56]. For example, NaOH will support > 25°C superheat, whereas NaCl will only support < 25°C superheat before precipitation occurs [A57]. Thus, as the extent of superheat changes along a steam generator tube between the primary water entrance and exit, the composition of the precipitates trapped in the tube support plate crevice and the pH of the liquid phase in that location will change. The changes in composition can be remarkable; for instance, chloride concentrations on the order of 4000 ppm are possible 0 in tube support plate crevices compared to concentrations of < 0.03 ppm in the bulk secondary environment. Thermodynamics-based prediction models [A59], in conjunction with thermal- hydraulic analyses [A60], [A61], are available to estimate the kinetics of composition development within PWR steam generator crevices. However, there is still some uncertainty in this understanding due to its inherent complexity and, not infrequently, the lack of adequate high temperature thermodynamic data for the various chemical species that are formed.

Because of the complexity of the environments that can accumulate in PWR steam generator support plate crevices, a variety of degradation modes are possible, including denting of the Alloy 600 tubes (due to excessive corrosion of the adjacent carbon steel resulting in deformation of the tubes by the volume expansion of the oxide). In addition, intergranular attack (IGA) and intergranular stress corrosion cracking of (mainly) Alloy 600MA tubing can occur in tube-to-tube support plate crevices. However, there is sufficient knowledge of both the electrochemical and thermal hydraulic mechanisms of crevice corrosion to make sound engineering judgments regarding where crevice corrosion problems might arise and how the risks of crevice corrosion may be minimized via changes in mechanical design or operating conditions.

The redesign of a crevice region can be appropriate to ensure good liquid flow through it, as illustrated by the redesign of both BWR pressure vessel inlet safe ends and PWR, VVER, and CANDU steam generator tube support structures. The creviced components may also be fabricated using more corrosion-resistant materials, such as stainless steels in the case of the steam generator tube supports or of condensers. Obvious remedies associated with control of the environment include decreasing both the amount of oxidant in the environment at the mouth of the crevice and the anionic impurity concentration in the bulk environment. Examples of these control methods are the adoption of hydrogen water chemistry in BWRs and strict control of secondary feedwater quality plus the appropriate use of hydrazine in PWR, VVER, and CANDU secondary systems. Crevice corrosion will, however, be minimal in systems that are deaerated and/or do not have water/steam phase changes occurring at occluded heat transfer surfaces.

A.1.4.3 Pitting

Pitting corrosion has very similar attributes to electrochemical crevice corrosion in that it depends in part on the creation of a localized environment within the pit. However, an important difference is that the features that lead to pit initiation are inherent in the material microstructure (e.g., the presence of non-metallic inclusions), in contrast with the macroscopic features that are associated with crevice corrosion. Pitting has received much attention and research [A62]–[A66]. This is because of the consequence of through-wall leakage in tubing and that there is uncertainty in predicting the time before it is observed because of the stochastic nature of the initiation process. The overall judgment is, nevertheless, that there is adequate understanding to manage this phenomenon in water-cooled reactors, with the biggest uncertainty being associated with systems where there might be unforeseen water chemistry transients.

In stainless steels, resistance to localized corrosion increases with increasing chromium and molybdenum content. Nitrogen also has a beneficial effect, at least for stainless steels containing molybdenum. Modern stainless steels designed to resist localized corrosion in severe environments such as seawater typically contain 6 to 7% Mo and 0.25 to 0.4% N. Nickel is also reported to be beneficial but to a lesser extent. The beneficial effect of Cr, Mo, and N is often estimated by use of an empirical parameter called the *pitting resistance equivalent* index (PREN), which has the form shown in Equation A-8:

$$\text{PREN} = (\text{wt\%Cr}) + (3.3)(\text{wt\%Mo}) + (16 \text{ to } 30)(\text{wt\%N}) \qquad \textbf{Eq. A-8}$$

Where the factor of 16 is appropriate for austenitic stainless steels and 30 is appropriate for duplex stainless steels.

Figure A-12 illustrates the relation between the values of PREN and resistance to localized corrosion in a conventional standard test solution.

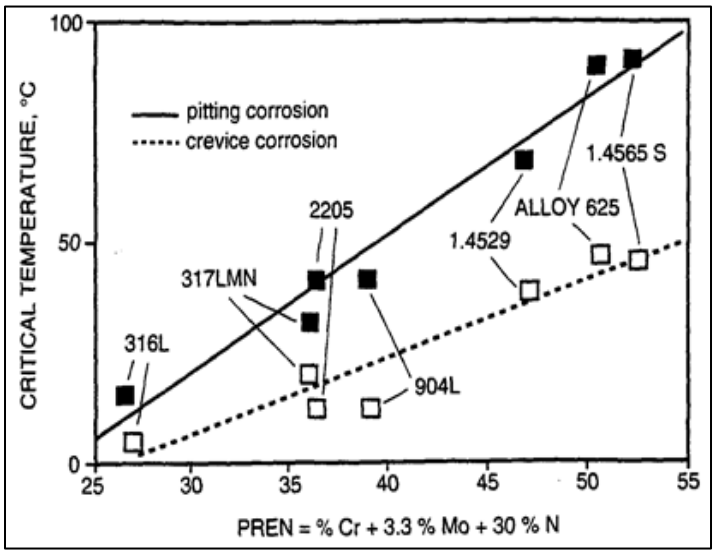

Figure A-12
Relation between the pitting resistance equivalent index and resistance to localized corrosion of stainless steels in a 10% FeCl3 solution [Thyssen Stahl AG Technical Document, 1995]

Pit Initiation

Pit initiation on alloys that have a very protective surface oxide (such as stainless steels, titanium alloys, and nickel-base alloys) is associated with specific localized material and environment conditions that lead to the breakdown of that oxide. There have been numerous mechanistic arguments proposed to predict the onset of oxide breakdown and pit nucleation, ranging from those that invoke competitive absorption, complex ion formation, ion penetration, the formation of halide nuclei, to the point defect model proposed by Macdonald and colleagues [A64]. Discussion of the details of these models is beyond the scope of this review, but in essence they attempt to explain that there is a combination of electrode potential and anion concentration that needs to be met before the oxide loses its protective nature and localized corrosion can occur.

Oxide breakdown and pit initiation are often associated with the presence of halide anions, particularly chloride, and the presence of surface breaking non-metallic inclusions. Non-reactive inclusions such as oxides, silicates, aluminates, etc. may be initiation sites for pitting, particularly those that have been deformed during hot and/or cold working. This is possibly because their interfaces with the base metal have been damaged by deformation and can act as micro-crevices. Globular inclusions are far less deleterious. The more deleterious inclusions are those containing manganese (or calcium) sulfide [A67], [A68], [A69]. Among the sulfide containing inclusions, the complex oxide/sulfides are the most deleterious. This is why clean stainless steels with low sulfur content exhibit improved resistance to chloride environments. Other surface singularities that favor pit initiation may be geometrical (e.g., roughness, metal laps) or chemical (e.g., the presence of iron left on the material surface due to use of carbon steel tools).

The onset of pitting can be characterized by a parameter termed *pitting potential*. This is illustrated in Figure A-13 for the case of a Fe-18Cr-8Ni alloy in 1M H_2SO_4 and in 0.1M NaCl. In 1M H_2SO_4 without chloride impurity, this austenitic alloy exhibits a classical active-to-passive transition at ~0 V_{SHE}, followed by passivity over a relatively wide potential range until the oxide dissolves rapidly (i.e., transpassivity) at more positive electrode potentials > 1.0 V_{SHE}. In the chloride solution, however, it is seen that passivity is lost when the potential is increased to only +0.35 V_{SHE}. This breakdown potential corresponds to the appearance of randomly distributed pits on the surface and is known as the *pitting potential* (E_p). In reality, pit initiation is more complicated than simply exceeding a critical pitting potential. When the corrosion potential increases, an increasing number of “metastable” pits initiate, but many re-passivate after very limited propagation because they cannot attain a large enough size for stable propagation. However, when the corrosion potential becomes high enough (i.e., in the range of the “classical” pitting potential), the probability that a small pit reaches the stable propagation stage increases.

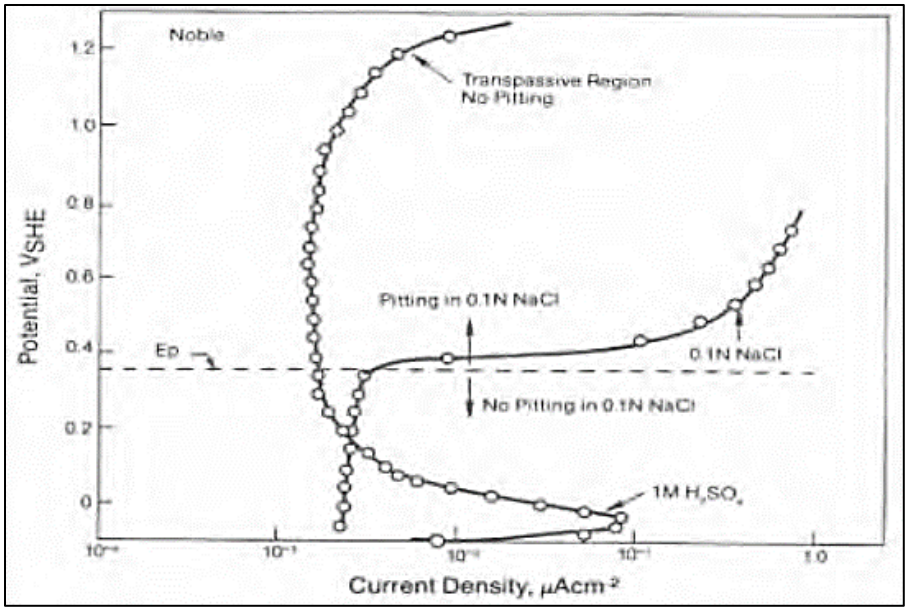

Figure A-13
Potentiostatic polarization curves for Fe-18Cr-8Ni stainless steel in 0.1M NaCl and in 1.0M H_2SO_4 at 25°C [A64]

The pitting potential is a sensitive function of several system parameters, including the anion type and concentration, temperature, and material composition. Chloride anions are usually associated with pitting of stainless steels and nickel-base, titanium-base and copper-base alloys, although pitting can occur (albeit to a lesser extent) with other halides such as bromide and iodide. In some cases, a minimum anion concentration is required, but, in all cases, the pitting potential will decrease with increasing halide concentration. The propensity for pitting will also increase in a given chloride-containing environment with the additional presence of sulfides and other sulfur-containing species ($S_2O_3^{2-}$, $S_4O_6^{2-}$) [A70], [A71]. This observation correlates with extensive pitting of Type 304 stainless steel in polluted, brackish seawater and in areas where microbiologically influenced corrosion can occur. In contrast, other anions can inhibit the pitting of stainless steel, including OH^-, CrO_4^{2-}, NO_3^-, ClO_4-, and SO_4^{2-} [A70], [A72].

Increasing temperature invariably moves the pitting potential in the negative direction for ferritic stainless steels [A71], austenitic stainless steels [A73], [A74], and nickel-base alloys [A74], [A75], although the rate of decrease over the range 25-300°C usually slows at higher temperatures. Alloying additions also have a marked effect on the pitting potential, especially at lower temperatures. For example, the pitting potential of stainless steel moves in a positive direction with increasing molybdenum content (i.e., Type 316 stainless steel) and with chromium
content [A76].

The sites where oxide breakdown occurs may be random but can often be associated with inhomogeneities, such as surface breaking precipitates or with grain boundaries over which the oxide is less protective. Pitting of low-alloy steels in BWR environments at higher temperatures is usually associated with surface breaking manganese sulfide (MnS) precipitates while pitting of stainless steels can be exacerbated by grain boundary sensitization and the resultant localized decrease in the chromium content. Pitting may also be encouraged by the presence of crevices since, as discussed earlier, these can concentrate anionic species when the bulk environment

contains an oxidizing agent in addition to water. An example of such localization of pitting is that which occurs on PWR Alloy 600 steam generator tubing in the sludge pile on top of the tube sheet where it is probably driven by copper deposits from copper cations released by brass condenser tubing [A77]. Another example of the role of crevices or deposits in promoting pitting is the observation of pitting of stainless steel condenser tubing in fresh water when the steel surface has deposits of calcium carbonate.

Since pit initiation occurs when the corrosion potential of the alloy surface is equal to or greater than the pitting potential, the likelihood of pitting occurring will increase with the presence of oxidants (which will result in an increase in the corrosion potential). In water-cooled reactor systems, common oxidizing species are dissolved oxygen (or hydrogen peroxide) and dissolved copper cations.

The interaction between the pitting potential and the corrosion potential and their impact on pit initiation is illustrated in Figure A-14 by the temperature dependence of the corrosion potential and pitting potential of Alloy 600 in water with chloride anions [A75], [A78]. In this case, the corrosion potential changed with different dissolved oxygen concentrations, and the pitting potential varied with different chloride concentrations. It is seen that the pitting potential (i.e., the solid lines in Figure A-14) decreases with increasing temperature and with increasing chloride concentration. However, the corrosion potential is always lower than the pitting potential (for the indicated range of chloride concentrations) under low dissolved oxygen conditions. Thus, at low oxygen levels, pitting is not a concern over a wide temperature range. By contrast, pitting becomes a concern as the dissolved oxygen concentration increases since the corrosion potential moves in the positive direction and eventually is equal to or greater than the pitting potential. Therefore, under these oxygenated conditions, pitting is expected with higher chloride concentrations at temperatures above 100-150°C. It is for this reason that pitting of PWR Alloy 600 steam generator tubing is observed in the sludge piles at temperatures of approximately 150°C in the presence of chloride anions and reducible Cu^{2+} cations that originate from degrading brass condenser tubes [A79].

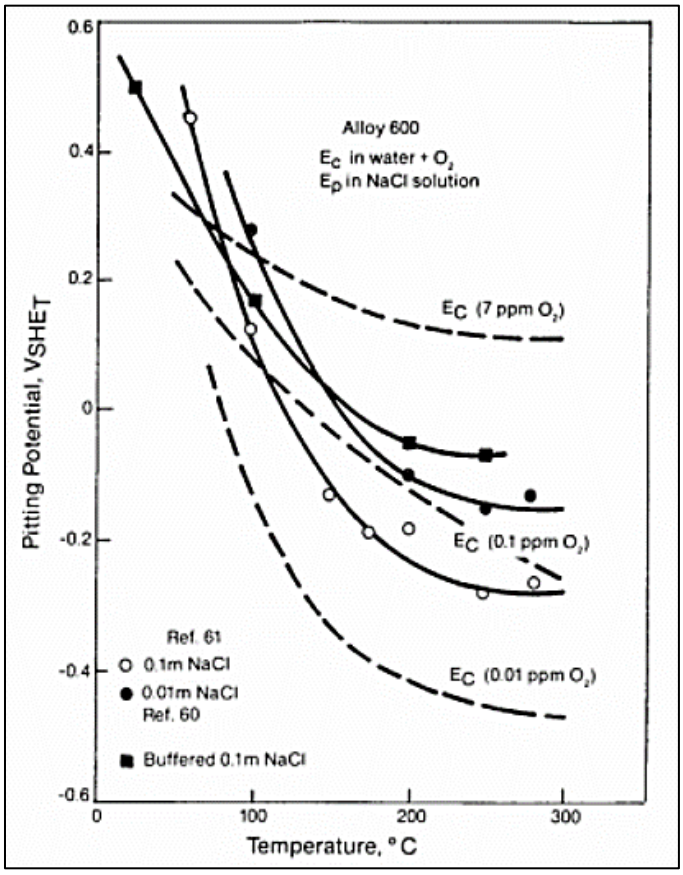

Figure A-14
Pitting and corrosion potential for Alloy 600 in water containing chloride anions as a function of temperature [A75], [A78]

NOTE:
Solid lines denote the pitting potential. Dashed lines denote the corrosion potential.

The situation for carbon and low-alloy steels is slightly different than that for the "passive" Ni- Fe-Cr alloys discussed so far. These steels do not have a very protective oxide at lower temperatures, and, although chloride anions will certainly exacerbate pitting, they are not always necessary for the initiation of pits. Carbon and low-alloy steels have surface-breaking MnS precipitates that dissolve in high temperature water to form a local sulfur-rich environment, which can lead to pitting under specific oxygen/temperature conditions, even in pure water [A80]. The pits formed in carbon and low-alloy steels are often relatively broad and shallow in nature, as opposed to the higher aspect ratio pits observed in austenitic alloys.

Pit Growth

Once the conditions for oxide breakdown have been met, localized corrosion, or pit growth, may then occur at rates that can be rapid and may lead to perforation of thin wall tubing in weeks or months. Pitting rates are a function of the extent to which the corrosion potential exceeds the pitting potential and of the extent to which an aggressive acidic environment can be maintained

in the growing pit. This latter condition was discussed in the previous subsection in relation to the formation of potential drops in crevices and is the same for pitting. In pits, however, the maintenance of an aggressive pit chemistry is facilitated by the possibility that a solid corrosion product can form at the pit mouth, thereby hindering flushing out the local pit environment.

Inside well-developed pits, the solution is so concentrated that a metallic salt film can precipitate on the dissolving surfaces, leading to a more uniform dissolution. This contributes to stabilizing pit propagation [A81], [A82] even though the presence of this film does not seem necessary for pit propagation [A83]. At this point, the surface inside the pit becomes smooth (electropolished), and dissolution is controlled either by diffusion, by ohmic drop, or, in some instances, by the cathodic reaction rate on the external surface.

Both diffusion control and ohmic drop control lead to a parabolic law for pit propagation [A66], shown in Equation A-9:

$$dr/dt \propto t^{0.5} \qquad \textbf{Eq. A-9}$$

where r is the pit radius (depth). In practice, different t^n laws have been observed. For example, pit depth was observed to increase in stainless steel as $t^{0.75}$ at room temperature, but the exponent rapidly decreased as the temperature increased [A84].

The essential controlling parameters of importance in the initiation and growth of pits are known, and deterministic models exist [A85]. However, it is also apparent that many of the controlling parameters for pit initiation and growth are dependent on random events. Consequently, probabilistic models also exist [A86], [A87] that predict the distribution of pitting potentials and the probability that pits propagate or re-passivate. Regardless of these uncertainties, the basic knowledge of the conjoint conditions for pit initiation and growth is in place, thereby allowing management of potential pitting damage in water-cooled reactor systems. This knowledge includes material choices and the required degree of environmental control (water purity, flow rate).

A.1.4.4 Microbiologically Induced Corrosion (MIC)

Biologically influenced corrosion of metallic components may be associated with both bacterial action and macro-fouling due to the presence of other organisms such as algae, slimes, mussels, and barnacles. The individual bacteria are small (typically 0.2-10 µm in dimension), which allows them to penetrate tight crevices. However, bacterial and fungal colonies can grow to macroscopic proportions, given the presence of an aqueous environment with sufficient nutrients. It is important to point out that MIC does not provide a new degradation mode but merely accelerates corrosion by creating chemical environments conducive to other, usually localized, corrosion modes (such as crevice corrosion, pitting, under-deposit corrosion, and dealloying).

The phenomenology and mechanisms of MIC have been reviewed for a number of industries, including nuclear power [A88], [A89], [A90]. Such attack has been observed on Cu-Al, Cu-Zn, and Cu-Ni copper base alloys, as well as carbon and stainless steels. The affected components include piping, tanks, and fire protection lines, which may contain untreated water under stagnant or low flow situations. Degradation occurs primarily in water in the pH range 4-9 and at temperatures from 10 to 50°C, but these ranges can be expanded for specific bacterial strains.

There are hundreds of bacteriological genera that can influence localized corrosion of structural alloys, and biological/corrosion research continues to define the ways that the specific bacteria change the various oxidation and reduction reactions occurring on metals. A discussion of the mechanisms by which these various bacteria accelerate corrosion can be divided in terms of whether the bacteria are anaerobic or aerobic—that is, whether the bacteria can survive in either deaerated environments or aerated environments.

Anaerobic Bacteria

Anaerobic bacteria survive primarily in deaerated water in the pH range 6-12 that contains the required nutrients. These bacteria can reduce sulfate (present as free anions or as a protein) to sulfide (S^{2-}) or bisulfide (HS^-) anions, and, consequently, they are commonly catalogued as "sulfate reducing bacteria" (SRB). Corrosion of metals in deaerated water upon which the sulfate reduction takes place is enhanced due to an acceleration of the dominant H^+ or H_2O reduction reaction, which in turn, increases the corrosion potential and local corrosion rate.

An additional potential degradation mode that may be affected by the presence of S^{2-} or HS^- anions at the surface is hydrogen embrittlement of high strength steels (e.g., bolting) since such sulfur species can inhibit the recombination of adsorbed hydrogen atoms, thereby enhancing the absorption of hydrogen atoms by the metal substrate and potentially leading to hydrogen embrittlement.

SRB also have the ability to oxidize some organic substances to short chain fatty acids (acetic, formic, lactic), which accelerate the corrosion rate due to an associated decrease in pH.

Aerobic Bacteria

Aerobic bacteria depend on the presence of oxygen (and nutrients) for survival and may degrade metal (and concrete) surfaces by a variety of mechanisms. Such bacteria excrete a slime-forming polymer that adheres to the surface. Further surface depositions may occur due to bacteriological oxidation of ferrous to ferric cations that subsequently deposit as hard ferric oxide tubercules on the surface. In severe cases, the surface deposit may be so large (in terms of volume) that water flow in piping can be stopped.

From a corrosion viewpoint, various degradation reactions may be accelerated beneath these surface deposits due to the formation of differential aeration cells (Figure A-15). The localized corrosion rate can be very high since the cathodic area where oxygen reduction is occurring is much larger than the area under the biologically formed tubercule. Another repercussion of the formation of surface deposits is the ability of anaerobic bacteria to survive in the deaerated environment under the surface deposit and to degrade the metal via the sulfate reduction mechanism discussed above. Alternatively, localized degradation may occur by an increase in localized acidity and chloride concentration via the same mechanisms discussed earlier for crevice corrosion and for pit growth. Others such as manganese oxidizing microorganisms can generate MnO_2 deposits that ennoble the surface, thereby raising the potential above the pitting potential.

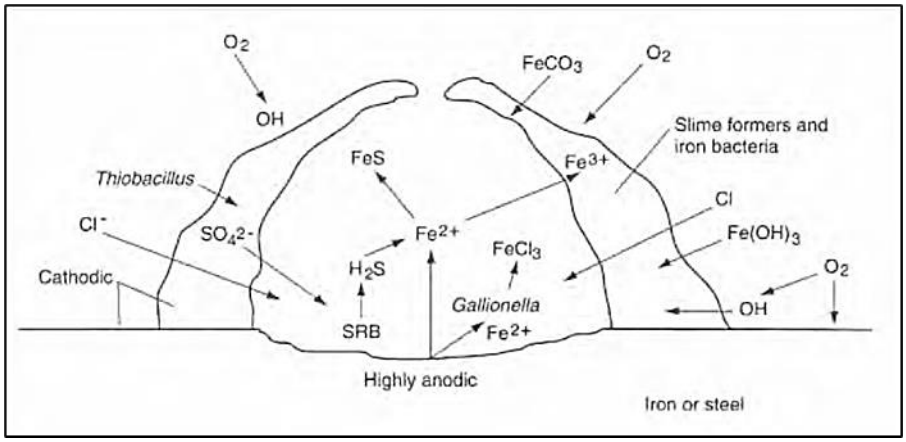

Figure A-15
Microbiological processes occurring on iron or steel [A91]

MIC Management

In all cases, the supply of nutrients to the bacteria is an important factor in managing MIC. Although stagnant conditions are often cited as a requirement for MIC and macro-fouling, the damage can arrest with time due to a reduction in the supply of nutrients. Conversely, periodic flushing of the system or mechanical removal of biological fouling can potentially increase the damage since such intermittent actions may increase the nutrient supply. Thus, mitigation actions must be holistic and take into account the design of the system and the nature of the specific bacteria present. With that caveat, various mitigation actions can be used, including:

- Avoidance of stagnant, untreated water pools that might form in crevices or dead legs after, for example, hydrostatic tests
- Temperature and pH control, the details of which depend specifically on the bacteria present and their ability to survive outside a given pH/temperature range
- Use of organic biocides, the specific use of which is very dependent on the particular bacteria present

A.1.5 Fouling (Foul)

As noted in the section on general corrosion, all metallic alloys used for pressure boundary components release corrosion products to the aqueous environment as dissolved cations. In addition, colloids and particles of corrosion products are often released in response to changes of circuit temperature, pressure, and flow rate during plant transients. Subsequent deposition of these dissolved and suspended corrosion products in response to changes in local environmental conditions (e.g., temperature, pH, turbulence) results in fouling of those surfaces. The consequences can be loss of heat transfer efficiency, increased flow resistance leading in extreme cases to flow-induced vibrations, and buildup of radiation fields on out-of-core primary circuit components.

A.1.5.1 Fouling in Primary Coolant Circuits

The main concern associated with cation release in primary coolant circuits of all water-cooled reactors is the transport and deposition of activated isotopes of the constituent elements of the corroding alloys from within the core to out-of-core primary circuit components where the radiation fields can be a considerable impediment to maintenance activities. In deaerated (and hydrogenated) PWR, VVER, and CANDU primary water, chromium and chromium rich oxides are practically insoluble so that the contribution of the inner chromium-containing oxide layers on Fe-Ni-Cr alloys to cation release is negligible, and iron and nickel constitute the major part of the cations that are dissolved and transported in the primary water environment. In BWR water under-oxygenated NWC conditions (i.e., at high corrosion potential), iron is practically insoluble, but chromium may be oxidized to soluble chromate.

Both in-service and laboratory tests show that cation release is time dependent, with rates decreasing with time. Cation release is often represented as the sum of a steady-state term and an "injection" term that accounts for the time dependence [A92]. Laboratory results are frequently consistent with a power law that is similar, but not identical to general oxidation laws, $w=a.t^b$, where differing values of the exponent b from 1 to 1/3 have been measured [A92].

Laboratory measurements of cation release depend on the experimental conditions used and on the flow rate and the degree of saturation of the aqueous environment by dissolved cations. Cation release measurements performed in saturated solutions can even produce negative results, that is, more Ni and Fe cations can be picked up from the solutions then released by alloy oxidation. Thus, in order to measure the maximum possible cation release, laboratory measurements should be performed in aqueous environments initially free of dissolved Ni and Fe cations and under hydrodynamic conditions that prevent the formation of outer oxide layers precipitated from the environment, for example, by using a flowing loop where dissolved cations are removed on fine zirconia powder [A93] or an experimental loop built with titanium alloys [A94].

In PWRs, VVERs, and CANDUs, the steam generator tube surfaces constitute more than three quarters of the corroding surfaces of the primary coolant circuits (excluding the fuel heat transfer surface). Thus, the steam generator tube alloys can have a major impact on cation release. The release of Ni and Co into primary water is the main contributor to activity buildup in coolant so that the nickel-base Alloys 600 and 690 are at a disadvantage in this respect, relative to Alloy 800 and stainless steel. Cobalt is present as an impurity in alloys containing nickel and is also a major alloying element in Stellites used for hard-facing valve seats and other components where wear resistance is vital to their function. The radioactivity arises from the formation of isotopes ^{58}Co and ^{60}Co in the core from nickel and cobalt cations, respectively. Since chromium is practically insoluble in deaerated aqueous environments, Cr release in PWR and CANDU primary circuits is negligible unless transient oxygen ingress occurs [A95]. The source of cation release into the primary water environment is the flux of Ni and Fe (and Co) cations through the inner oxide layer. However, the actual cation release into the bulk environment also depends on the formation of the outer oxide layer, i.e., on the concentration of cations dissolved in the bulk environment and on the hydrodynamic conditions.

The order of magnitude of the total cation release rate, expressed as the equivalent loss of thickness, for Alloys 600 and 690 is on the order of a few tens of nm per year after long exposure times. However, laboratory studies have shown consistently that for given surface conditions and test environment chemistry, the oxidation and cation release rates of Alloy 690 are significantly lower than those of Alloy 600 [A94], [A96]–[A99], [A193]. Accordingly, oxide layers are generally thinner on Alloy 690 than on Alloy 600.

Although the immediate benefit in terms of primary circuit radiation fields after the replacement of Alloy 600 steam generators by Alloy 690 steam generators has often been lower than expected, lower deposited ^{58}Co activity has eventually been observed [A100]. However, only part of this benefit may be attributed to the steam generator tube alloy composition, the other part being related to the surface condition left by the tube manufacturing processes [A101]. Two parameters are of importance: cold work (particularly surface cold work) and surface chemistry (i.e., near surface composition and preexisting oxide layers). In addition, Alloy 690 introduced in replacement steam generators may not necessarily bring immediate improvement because no protective oxide layer is built up before operation, unlike the development of protective layers that occur as a result of Hot Functional Tests that are performed during initial plant commissioning. Consequently, the corrosion rate is high during the first fuel cycle after steam generator replacement, which produces significant amounts of nickel corrosion products.

The specifications of PWR, VVER, and CANDU primary coolant chemistries also impose a tight range on pH to ensure minimum oxide solubility (see Figure A-3) and minimize activity buildup. In addition, injection of soluble Zn has been introduced in several PWRs to decrease activity pickup on primary coolant circuits, which improves the protective character of the oxide films, minimizes the release of metallic cations, and reduces the incorporation of cobalt into the outer oxide layers.

In BWRs, most of the surface area in contact with the coolant (excluding the fuel heat transfer area) is stainless steel. In the case of plants operating on HWC, the fundamentals governing cation release are similar to PWR, VVER, and CANDU primary conditions. In the case of oxygenated NWC, iron is the main corrosion product present in the circuit (up to 90% in some plants). Nickel may also be present in significant amounts (up to 20% in some cruds), and soluble chromium is also released by stainless steel and may reach concentrations of about 3 to 20 ppb [A102]. Activity of BWR circuits is mainly (70 to 90%) due to ^{60}Co, which is released by cobalt-base alloys (Stellites) and by nickel-base alloys and stainless steels that contain cobalt as an impurity. The contribution of ^{58}Co (5 to 15%) to activity is mainly due to nickel released by nickel-base alloys used for fuel grid spacers and to a smaller extent by stainless steels. When applying HWC to BWRs that previously operated with NWC, the restructuring of oxide layers on stainless steels (and other alloys) can occur, and this can be responsible for some increase in activity due to changes in the solubilities of the different corrosion products. An efficient way to reduce cation release from stainless steels in BWR water is to inject Zn cations, as is done in PWR primary circuits [A102].

A.1.5.2 Fouling in Secondary Coolant Circuits

In the secondary circuits of PWRs, VVERs, and CANDUs, fouling is mainly observed in the steam generators where deposits known as *crud* build up on the tubes, in tube-to-tube support crevices, and on the tubesheet of vertical steam generators in PWRs and CANDUs. The source of fouling of steam generators is well known and is essentially due to the transport of iron oxides from general corrosion and FAC of carbon steel in the feedwater train. Remedies include those described earlier to minimize general corrosion and FAC of carbon steels, as well as sludge lancing with high pressure water jets and chemical cleaning during plant shutdown.

A more serious and phenomenologically different form of steam generator fouling known by the special term *steam generator clogging* refers to the blockage of tube-to-tube support plate (TSP) gaps by corrosion products. Steam generator clogging is more insidious as it may not initially have any obvious effect on steam generator performance but may impair safety as it decreases the recirculation ratio of the steam generator and its water inventory [A103]. Clogging has also been known to cause thermal-hydraulic instabilities (known as *chugging*) and could also increase the loading of tube support plates during transients [A104].

There have been several known cases of TSP blockage in recirculating steam generators starting in 1986 with a CANDU plant after secondary water level oscillations were detected. Further incidences occurred in the early 1990s in PWR steam generators where severe secondary water level oscillations were also observed at two units in the United States that necessitated operating at reduced power levels in order to increase the recirculation ratio and stop the water level oscillations [A105]. The cause of these PWR steam generator water level oscillations was severe deposit buildup in the quatrefoil broached flow holes of the tube support plates that was corrected by chemically cleaning all steam generators at both units. A similar observation was made in 2004 at a South Korean PWR, which also reduced power initially to 97% of nominal power and then to 95%. Steam generator chemical cleaning was carried out at the next outage, after which the secondary water level oscillations disappeared. There is also a current concern with the formation of hard crud deposits within the stainless steel tube bundles of some VVERs.

Clogging of broached TSP flow holes has also been observed in some French PWRs [A104], [A105]. In two of these French plants, the clogging caused the flow velocities to increase locally at very unusual locations in the tube bundle leading to flow-induced vibrations and circumferential high-cycle fatigue cracks that resulted in three primary-to-secondary leaks at the highest tube support plate level. Corrective actions were mainly based on chemical cleaning and an increase in the secondary feedwater $pH_{25°C}$ from 9.2 to 9.6 to decrease the iron corrosion product source term [A105]. Online addition of dispersants can also be used to reduce steam generator fouling [A106]–[A111].

The mechanism of clogging of steam generator broached flow holes and formation of hard deposits is a source of current debate. Some favor explanations based mainly on magnetite particle deposition, while others consider that the phenomenon is dominated by crystal growth due to cation precipitation under the influence of streaming currents generated by local turbulence at the flow hole corners [A112]. Hard deposits tend to form as annuli emanating from the point of flow disturbance. It has been confirmed that pH is a major parameter impacting deposit buildup under PWR secondary water chemistry conditions, particularly when pH_T is < 6. However, this critical value of pH is also influenced by the type of chemical conditioning and by substrate alloy composition.

A.2 Wear

Wear is the loss of material, generally measured as the rate of removal of surface material, caused by the relative motion between adjacent metal surfaces or by the action of hard, abrasive particles in contact with a metal surface. Mechanical wear, for example, is observed in bolted or clamped joints, where relative motion is not intended but can occur due to the reduction or loss of preload. Flow-induced vibration is also known to be a cause of wear through intermittent contact of adjacent metal surfaces.

A limited number of the PWR, VVER, BWR, and CANDU primary pressure boundary components are potentially subject to relative motion, but none are subject to the action of hard, abrasive particles under normal conditions of operation. However, safety and relief valve seats and disks are subject to intermittent relative motion due to operation and testing. Reactor coolant pump and safety/relief valve closure parts, such as the cover and bonnet flanges, the casing and body flanges, and the closure bolting, are subject to some degree of relative motion, especially if preload is lost, or during infrequent disassembly and reassembly operations. Therefore, mechanical wear could be an issue for some primary pressure boundary components, such as the reactor coolant pump and safety/relief valve closure elements, safety/relief valve seats and disks for PWRs, and recirculation pump seal flange and valve closure flanges for BWR primary coolant pressure boundary. Wear can also be encountered between steam generator tubes and support plates and anti-vibration bars in PWRs and CANDUs. Wear is also a potential issue for Zr-2.5Nb pressure tubes under the bearing pads of the fuel bundles used in CANDUs and for control rods and guide cards in the upper internals of PWRs and VVERs. Finally, wear is a known concern for BWR jet pump wedge assemblies and steam dryer bracket interfaces.

A.3 Stress Corrosion Cracking (SCC)

Stress corrosion cracking is a form of tensile stress-assisted environmental attack of structural materials that leads to fracture surfaces with a macroscopically brittle appearance that may be intergranular, transgranular, or mixed. The morphology of SCC may change in any given alloy/environment system in response to relatively subtle changes in the combinations of material, stress, and environmental conditions. Strictly speaking, intergranular attack is more akin to the localized modes of corrosion described earlier since it does not require stress for its propagation but which, nevertheless, shares many characteristics with intergranular stress corrosion cracking (IGSCC) and, in practice, often occurs together with IGSCC.

These forms of environmental attack of structural alloys have been relatively prevalent in water-cooled reactors since their inception, and they have also been a significant source of plant unavailability and costly repairs. The initiation of attack is particularly difficult to predict in advance due to the intrinsic stochastic nature of many of the fundamental subprocesses involved. Thus, the first failure of a given type should never be hastily written off as a special case or unique since it is more likely to be the first incident of a statistically predictable wave of similar events.

A.3.1 Intergranular Attack (IGA)

Intergranular attack, usually abbreviated IGA, is a form of generalized intergranular corrosion that affects all grain boundaries over a more or less homogeneous depth. IGA can occur on unstressed surfaces, although more commonly the presence of tensile stresses promotes the formation of discrete fingers of attack ahead of a uniform layer of oxidized grain boundaries.

One form of IGA can affect irradiated stainless steels when exposed to moist air environments. Radiolysis of moist air by γ-rays emitted by the irradiated stainless steel forms surface films of nitric acid which, when combined with very narrow (< 10 nm) zones of Cr-depletion induced by neutron irradiation (see the later subsection of irradiation-assisted SCC), allows the grain boundaries to be corroded away preferentially, which can promote significant grain dropping. The phenomenon has been called "hot cell rot" after irradiated stainless steel specimens stored in hot cells without adequate humidity control that have been observed to disintegrate after months or years in storage.

More commonly, in the context of water-cooled reactors, IGA has affected (mainly mill-annealed) Alloy 600 steam generator tubes in the crevices formed between the tubes and the carbon steel drilled support plates or under sludge piles on the tubesheet where impurities hide out and become concentrated (as described in the subsection on crevice corrosion). IGA is usually associated with strongly caustic environments and observed in association with IGSCC. The latter requires the presence of a tensile stress and results in the formation of discrete IG cracks normal to the maximum applied (or residual) principal stress. However, the propagation rate of IGA is relatively slow, being about one order of magnitude slower than IGSCC, although the kinetics do increase with increasing temperature.

Due to the close association of IGA with IGSCC of Alloy 600 in crevices on the secondary side of PWR steam generators, further description is postponed until the characteristics of combined IGA/IGSCC are described later in more detail.

A.3.2 Intergranular and Transgranular SCC (IG/TG)

Stress corrosion cracking forms one end of a spectrum of environmentally assisted cracking phenomena that embraces cracking under constant tensile load or displacement (i.e., stress corrosion cracking), monotonically increasing load (i.e., strain-induced corrosion cracking), and cyclic loading (i.e., corrosion fatigue). The main features of stress corrosion and strain-induced corrosion cracking that have affected water-cooled reactors in their primary and secondary coolant systems are summarized here from the viewpoint of the likely mechanisms of attack and salient factors required for the life prediction of components. An adequate appreciation of the mechanism of cracking and the ability to predict its progression in service are usually necessary precursors for reliable long-term mitigation actions [A113]. Corrosion fatigue is discussed separately in a later section devoted to fatigue under cyclic loading.

A.3.2.1 The "Blunting Criterion"

Stress corrosion cracks may initiate and propagate either in an intergranular (i.e., along grain boundaries) or transgranular (i.e., through grain interiors) manner. The crack tips can often be extremely sharp with crack tip widths of the order of 1-5 nm or, less commonly, relatively broad. However, the first criterion that must be met for an incipient crack to continue to propagate is that there must be a mechanism to protect the crack sides so that an incipient sharp crack does not

become a blunt notch that will probably arrest. This criterion is readily met in stainless steels and nickel-base alloys commonly used in water reactor primary coolant circuits that easily form protective oxide films over a wide range of pH/potential/temperature conditions in high temperature water; see Figure A-16 (a) for an example. However, the degree of protection provided by oxides on carbon and low-alloy steels in water can be less effective, especially as the temperature is lowered, and localized corrosion/pitting leading to crack blunting may occur (see Figure A-16 (b)). In the latter case, crack propagation may be sustained if some level of dynamic stressing is applied [A114]. At lower temperatures (150°C), incipient intergranular cracks in low-alloy steel in oxygenated water are consistently blunted by corrosion in the slightly acidic conditions associated with the presence of dissolved carbon dioxide [A115].

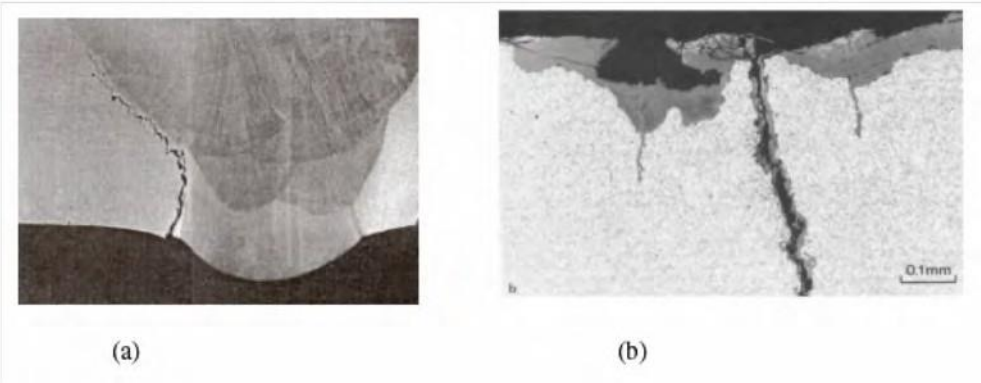

Figure A-16
(a) Intergranular stress corrosion cracking adjacent to a weld in a 28" (711 mm) BWR Type 304 stainless steel recirculation pipe as observed in many BWR reactor coolant systems. (b) Incipient stress corrosion cracks in a carbon steel BWR feedwater line at ~220°C [A114]

Thus, at lower temperatures where the magnetite film on carbon and low-alloy steels is not very protective, the surface is liable to undergo pitting depending on the dissolved oxygen concentration. At intermediate oxygen levels, the pits may initiate cracks, but, at higher concentrations, the incipient cracks have a tendency to blunt and arrest. In contrast, at temperatures > 150-200°C, the oxide that forms on carbon and low-alloy steels in water is a duplex magnetite/hematite film that is relatively protective, and, therefore, propagation of a sharp crack in these steels is possible at these more elevated temperatures.

The crack blunting and arrest tendencies for various alloys can be changed by circumstances that alter the relative rates of corrosion on the crack sides and the strained crack tip. Thus, sustained crack propagation can be achieved by:

- The presence of anions that form surface films, which, in conjunction with the existing stable or metastable oxides, confer the necessary protection to the crack sides. For carbon steels, these anions are phosphate, nitrate, molybdate, and carbonate/bicarbonate. These considerations lead to relatively narrow ranges of corrosion potentials where cracking can be sustained. This is of significance for carbon steels in inhibited closed coolant water (CCW) systems in water-cooled reactors [A116], as well as cracking of nickel-base alloys in concentrated environments created by hideout of impurities in crevices in PWR, VVER, and CANDU steam generators.

- The imposition of dynamic loading (either monotonically increasing or low-frequency cyclic) that increases the crack propagation rate and effectively counteracts the blunting action due to corrosion on the crack sides.

A.3.2.2 The Chronology of Events During Stress Corrosion Cracking

The chronology of stress corrosion cracking follows a sequence that is common to many, if not all, cracking systems in reactor materials (Figure A-17).

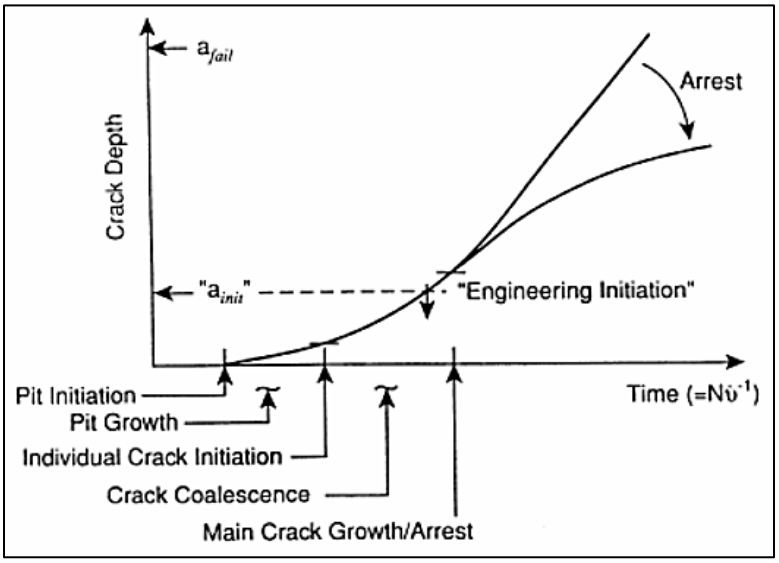

Figure A-17
Sequence of crack initiation, coalescence, and growth during subcritical stress corrosion cracking in aqueous environments

NOTE:
Note the arbitrary definition of "Engineering Initiation," which generally coincides with the NDE resolution limit.

Three separate phases of crack development can be identified:

1. A *precursor period* during which specific metallurgical or environmental conditions are created at the metal/solution interface that are conducive to subsequent crack initiation. For example, the condition at the end of the precursor period may be the breakdown of the normally protective surface oxide film leading to the initiation and growth of pits on the surface (that may be created during reactor shutdown or layup). Other precursor phenomena might be associated with an intergranular attack or the creation of localized environments in crevices.
2. These "precursor" periods may be very short when associated with the presence of high stresses or with excessive water impurity transients during initial reactor operations. On the other hand, precursor events associated with a change in metallurgical microstructure, e.g., involving thermal aging or irradiation embrittlement, or with the creation of a "wedging" stress due to buildup of corrosion product, may take years. An example of this is the cracking consequent to denting of PWR Alloy 600MA steam generator tubing due to the buildup of

stresses over time caused by the accumulation of corrosion product in the crevice between carbon steel support plates and the tubes. Another example is the cracking of L-grade stainless steels in BWR and PWR core internals where the initiation of cracks requires a degree of irradiation-induced changes to the alloy microstructure that may take decades.

3. The *initiation of cracks* when the local environment, microstructure, and stress conditions have reached a critical combination. The criteria for crack initiation (and subsequent short crack growth and coalescence with neighboring cracks) have been extensively reviewed [A117]. Crack initiation sites can include pits, intergranular corrosion, machining marks, crevice corrosion, and stress raisers such as sharp bolt head to shank radii, or the presence of re-entrant angles at welds between misaligned pipes.
4. The *propagation of a dominant crack* at a rate that is very dependent on the material, stress, and environmental conditions. The growth rate is rarely constant, as is often assumed, but may accelerate or decelerate over time, depending on the stress and strain profiles (which can be complicated adjacent to welds) and material microstructure.

A.3.2.3 Life Prediction for Stress Corrosion Cracking

There are basically three approaches to life prediction:

1. *Experiential and probabilistic analyses of past plant failures*, which can lead to the definition of risk-based inspection priorities and to the prediction of future frequencies of failure.
2. *Analyses of laboratory data* to develop empirical life prediction algorithms between the degradation rate and the interacting effects of various system parameters.
3. *The development of mechanism-based life prediction algorithms* in conjunction with good-quality laboratory degradation rate data.

These three approaches have been reviewed [A113], and aspects of each will be discussed below for specific material/reactor system combinations. Before discussing these component-specific issues, however, an overall synopsis is given of the candidate crack propagation mechanisms.

With the advent in the last 30 years of more sensitive analytical capabilities, many of the early stress corrosion cracking hypotheses have been shown to be untenable, and the candidate mechanisms for environmentally assisted crack propagation for alloys in water-cooled reactors have narrowed down to slip-oxidation, film-induced cleavage, internal oxidation, and hydrogen embrittlement. These mechanisms are briefly described below.

Slip-Oxidation Mechanism

The slip-oxidation model relates crack propagation to the rapid oxidation that occurs transiently when the protective film at the crack tip is ruptured. Quantitative predictions of the crack propagation rate via the slip-oxidation mechanism are based on the relationship between the oxidation charge density on a surface and the amount of metal transformed from the metallic state to the oxidized state. The change in oxidation charge density with time following the rupture of a protective film at the crack tip is shown schematically in Figure A-18 (a), and the associated oxidation current density versus time relationship is shown in Figure A-18 (b). Once the protective oxide is ruptured, the crack will advance rapidly into the metal by oxidation/

dissolution on the bared surface but within a matter of milliseconds will begin to slow down as the thermodynamically stable and protective oxide reforms at the crack tip. Sustained crack advance depends, therefore, on maintaining a strain rate in the vicinity of the crack tip that will promote repeated rupture of the oxide film.

Thus, the crack propagation rate, V, is governed by the relationship in Equation A-10 [A118]:

$$\boldsymbol{V = \left(\frac{M}{zpF}\right)\left(\frac{i_o^{\,n} t_o^{\,n} \varepsilon_f^{\,n}}{(1-n)}\right)(d\varepsilon/dt)_{ct}} \qquad \textbf{Eq. A-10}$$

where:

M, p	=	Atomic weight and density of the crack tip metal
F	=	Faraday's constant
z	=	Number of electrons involved in the overall oxidation of an atom of metal
i_o, t_o	=	Bare surface oxidation (dissolution) current density and its duration
ε_f	=	Fracture strain of the oxide at the crack tip
$(d\varepsilon/dt)_{ct}$	=	Crack tip strain rate

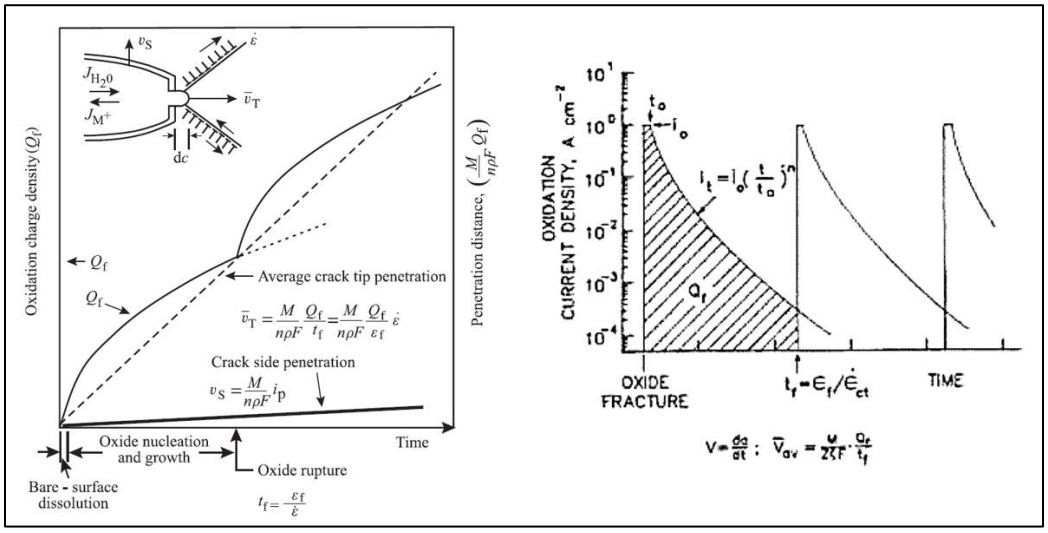

Figure A-18
Schematic oxidation charge density and time relationship for a strained crack tip and unstrained sides [A120] (left), and changes in oxidation current density following the rupture of the oxide at the crack tip (right) (The crack advance is related faradaically to the oxidation charge density, Q_f, which will be a function of the bare surface dissolution rate, i_o, the passivation rate exponent, n, the fracture strain of the oxide, ε f, and the crack tip strain rate [A121].)

In general form, the previous equation collapses, as shown in Equation A-11:

$$V = A(d\varepsilon/dt)_{ct}^{n} \qquad \textbf{Eq. A-11}$$

The parameters A and *n* are related to the dissolution and passivation kinetics at the strained crack and to the mechanical rupture properties of the oxide at the crack tip (i.e., functions of the local material and environment conditions). The crack tip strain rate, $(d\varepsilon/dt)_{ct}$, is a function of the stress/strain/time conditions [A119][A123].

These parameters are directly relatable to the interactions between the stress, material, and environmental parameters that have been empirically associated with environmentally assisted cracking. Thus, this fundamental modeling [A119] is not introducing new concepts contrary to experience but is introducing a more fundamental framework for analyzing changes in the crack propagation rate. The required elements for this model have been experimentally verified for its application to stainless steels and nickel-base alloys in BWR NWC and HWC environments.

Film-Induced Cleavage Mechanism

It has been observed in some examples of environmentally assisted cracking that the equivalent of the oxidation charge density at a strained crack tip is insufficient to explain the observed crack advance. Moreover, for cases where the cracking is transgranular, cleavage-like crystallographic features on the fracture surfaces are hard to rationalize convincingly in terms of the slip-oxidation model by itself. Although there is evidence for a film-induced mechanism in copper-base alloys and austenitic nickel-base alloys and stainless steels in low-temperature environments (i.e., < 115ºC), it has not been extensively tested so far for other alloy systems, and especially those relevant to high temperature water-cooled reactor operations.

The concept of the film-induced cleavage mechanism is that environmentally assisted crack propagation may occur by a combination of oxidation-related and brittle-fracture mechanisms. Specifically, it has been suggested that after rupture of the oxide at the crack tip, the crack initially propagates by an oxidation process that is controlled by the same rate-determining steps as those in the slip-oxidation model described above. However, in the film-induced cleavage model, the crack in the film may then also rapidly propagate a further amount, a*, into the underlying metal matrix by a “cleavage mechanism” (Figure A-19). The brittle extension may be further enhanced if the oxidation process creates an embrittled zone in front of the crack tip by selective dissolution of one of the alloying elements or by in situ oxidation. The extent of the additional fast cleavage propagation into the matrix can be of the order of 1 µm, the exact amount being a function of a combination of various plasticity and microstructural factors.

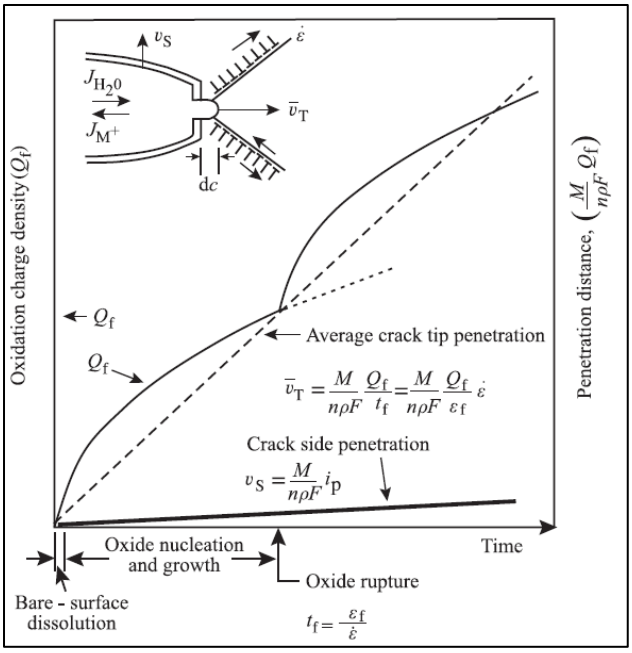

Figure A-19
Schematic of the elements of the film-induced cleavage mechanism of crack propagation [A118], [A124]

Internal Oxidation Mechanism

Somewhat similar to the film-induced cleavage mechanism described above, the internal oxidation mechanism is based on a fracture occurring in an oxide forming ahead of the crack tip [A117], [A125], [A126], [A344], [A345]. It was proposed specifically for intergranular cracking of Alloy 600 and associated weld metals where selective "internal oxidation" of chromium on grain boundaries to Cr_2O_3 is observed ahead of the growing crack tip. An associated chromium-depleted, nickel-enriched zone is created in front of the advancing intergranular crack. In this proposed mechanism, however, there was no suggestion of any additional fast cleavage propagation into unoxidized metal.

The term *internal oxidation* was originally used because intergranular cracking of Alloy 600 in PWR primary water, just like the well-known internal oxidation mechanism in gaseous environments at higher temperatures, is always associated with corrosion/oxidation potentials close to the redox potential of the solvent metal (nickel in this case). Quantitative treatment of crack extension rates has thus far been based on estimating the kinetics of the solid-state diffusion-controlled oxidation process ahead of the crack tip and assuming that it fractures once the crack tip stress intensity exceeds a given threshold value, after which the oxidation-fracture cycle repeats. The concept may also be applied to modeling crack initiation.

Hydrogen Embrittlement Mechanisms

The general concepts and concerns behind subcritical crack propagation due to hydrogen embrittlement in aqueous environments depend on a sequence of events in the following order (Figure A-20):

1. Diffusion of a reducible hydrogen-containing species (e.g., H_3O^+) to the crack-tip region.
2. Reduction of the hydrogen-containing ions to give adsorbed hydrogen atoms.
3. Absorption of the hydrogen atoms followed by interstitial diffusion of these hydrogen atoms to a "process" zone at a distance, X, in front of the crack tip.
4. Once the hydrogen concentration in the "process" zone has reached a critical level, C_{crit}, over a critical volume, d_{crit}, then localized crack initiation can occur within this zone followed by rapid propagation back to the main crack tip. In alloys of titanium, zirconium, and hafnium, stable hydrides can form at stress concentrations and at crack tips, and crack advance occurs by fracture of these hydrides.

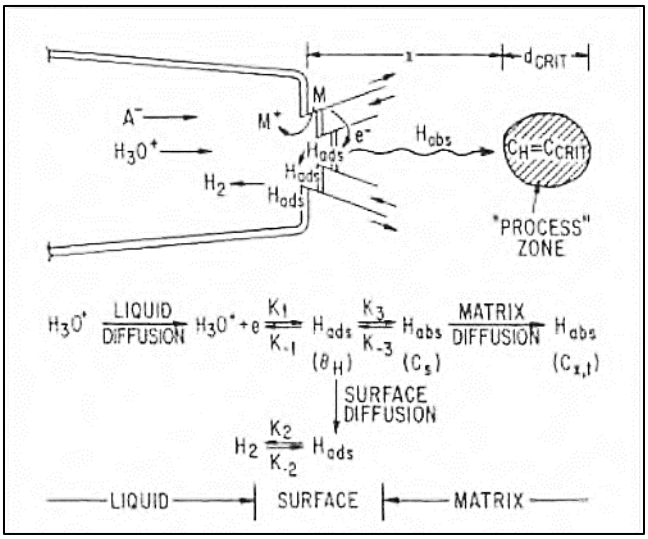

Figure A-20
Schematic of various reactions at a crack tip associated with hydrogen embrittlement mechanisms in aqueous environments [A119]

Thus, disregarding the specifics of these localized fracture mechanisms in the "process" zone for the present, it is apparent that hydrogen embrittlement models predict discontinuous crack propagation at an average rate given by Equation A-12:

$$\bar{V}_t = \frac{X}{t_c}$$

Eq. A-12

where X is the distance from the main crack tip to the "process" zone, which, in turn, is defined by the values of C_{crit} and d_{crit}, and t_c is the time for the concentration of absorbed hydrogen, $C_{x,t}$, to reach a critical value, C_{crit}, in the volume, d_{crit}.

Although, traditionally, such hydrogen embrittlement mechanisms have been applied qualitatively to high strength alloys, it has been suggested that a hydrogen embrittlement mechanism could operate in relatively ductile pressure vessel steels in water at 288ºC [A127], [A128]. More recently, such a mechanism has been proposed, albeit somewhat controversial, for stress corrosion cracking of nickel-base alloys in PWR primary environments [A129]. Hydride formation as a precursor to cracking, however, is a well proven, especially important mechanism for zirconium-base alloys like Zr-2 and Zr-2.5Nb.

A.3.2.4 Transgranular (TG) SCC of Carbon and Low-Alloy Steels

- Carbon and low-alloy steels (C&LAS) used in the primary reactor coolant systems of PWRs, VVERs, and most BWRs for pressure boundary components are clad on the inside surface with a weld overlay of austenitic stainless steel or nickel-base alloy. However, BWR feedwater and main steam lines and some older reactor pressure vessel heads are not clad, as is also the case for the C&LAS pressure boundaries of secondary circuits of PWRs, some early VVER primary circuits and all VVER secondary circuits, and the primary and secondary circuits of CANDUs. Where C&LAS are not exposed to primary coolant, SCC should not be an issue, although at dissimilar metal welds, weld butters of stainless steel or Alloy 182 are often deposited directly onto the pressure vessel steel so that the known SCC susceptibility of Alloy 182 in both PWRs and BWRs raises special concerns. SCC could propagate to the interface between the nickel- base weld metal and ferritic alloys and conceivably into the underlying low-alloy pressure vessel steel. No SCC of carbon or low-alloy steel has been observed in the RPV of PWRs or BWRs, even though there are many cases of exposed low-alloy steel. In fact, the operating experience to date indicates that SCC in cladding blunts when it contacts low-alloy steel [A144]. However, examples have been observed of SCC initiating at dissimilar stainless steel/C&LAS welds on the secondary side of VVER steam generators and then propagating at, or near, the fusion line.

In general, the resistance of C&LAS to stress corrosion cracking in the high temperature reactor systems has been very good, but isolated incidences have occurred, including:

- *Strain-induced transgranular cracking (SICC)* of BWR steam, feedwater, and condensate piping [A130]. This form of cracking usually involves a measure of dynamic loading due to reactor transients such as startup and shutdown.
- *Transgranular stress corrosion cracking (TGSCC)* of a few PWR secondary-side steam generator girth welds with high residual stress and hardness due to improper stress relief heat treatment and the presence of oxidizing species from condenser leaks [A131], [A132], [A133]. Cracking has also occurred in some attached carbon and low-alloy steel piping [A131], [A134].

Crack initiation of C&LAS in high temperature water is a complex process governed by the interaction of several critical parameters so that times to crack initiation can be very long and may also reveal significant statistical variation or scatter due to the probabilistic nature of the process. The latest review [A136] summarizes the following key features for crack initiation.

From laboratory tests, it has been observed that:

- Crack initiation due to SCC and SICC (and corrosion fatigue) can occur at smooth surfaces of C&LAS in oxygenated high temperature water. Note that in deoxygenated high-purity water, crack initiation may also occur due to corrosion fatigue loading but can be ruled out for SCC and SICC.
- Crack initiation needs enhancing factors, e.g., coarse inclusions (MnS), flaws with notch effects, critical (local) conditions regarding water chemistry, and/or severe loading.
- A three-dimensional stress state is assumed to be a further, but so far unverified, enhancement factor.
- Corrosion pits alone are not a necessary precursor for crack initiation, but active pitting can promote susceptibility.
- Other localized or selective corrosion processes at grain boundaries are probably not a necessary precondition or an enhancing factor.
- Material sensitivity to dynamic strain aging is a contributor to initiation due to environmentally assisted cracking.

From BWR operational experience, the following was concluded:

- Environmentally assisted crack initiation in low-alloy steel has not been observed from smooth surfaces, although, as noted earlier, many such component surfaces are clad with stainless steel or Ni-base alloys.
- Crack initiation in low-alloy steel needs additional enhancement factors, such as active, localized corrosion (e.g., by shallow pitting), although the mere existence of pits is not necessarily detrimental.
- Aggressive environments (e.g., contaminated by chlorides, sulfates).
- Flaws (e.g., weld defects, size mismatch) from manufacturing, or even pre-cracks created during operation.
- Environmentally assisted crack initiation under nominal PWR secondary side conditions (low oxygen, i.e., low corrosion potential) is not a critical issue for C&LAS but may occur after oxygen access during outages or during condenser leaks.

A considerable amount of attention has been focused on the mechanism and kinetics of crack propagation in C&LAS used in BWRs and PWRs. The hypothesis that has been most widely accepted for crack propagation in the C&LAS/water system is the slip–oxidation mechanism.

Both the dissolution and passivation kinetics on a bare low-alloy steel surface depend critically on the surface corrosion potential and the anionic activity at the crack tip [A137], [A138], [A139]. The kinetics are bounded asymptotically by two limiting environmental conditions associated with the maintenance of either > 500 ppb or < 20 ppb dissolved S^{2-} at the crack tip [A140].

This, in turn, leads to a predicted range in crack growth rate versus crack tip strain rate responses, which are bounded by two relationships known as the "high sulfur" and "low sulfur" lines (Equations A-13 and A-14; Figure A-21):

High sulfur

$$da/dt = 2.25 \times 10^{-3} (d\varepsilon/dt)_{ct}^{0.35} \text{ mm.s}^{-1} \qquad \textbf{Eq. A-13}$$

Low sulfur

$$da/dt = 10^{-1} (d\varepsilon/dt)_{ct}^{1.0} \text{ mm.s}^{-1} \qquad \textbf{Eq. A-14}$$

Note, however, that although earlier investigations focused primarily on the deleterious effect of sulfur-rich anions, more recent investigations indicate that surprisingly low concentrations of chloride anions also strongly affect crack propagation rates [A141].

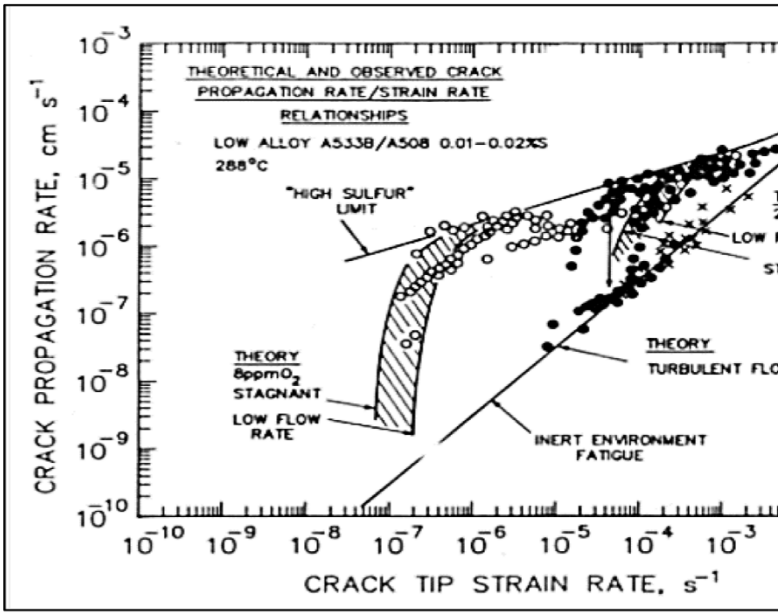

Figure A-21
Observed and theoretical crack propagation rate/crack tip strain rate relationships for low-alloy steel in 288°C water at various corrosion potentials [A140]

NOTE:
The strain rate values are pertinent to tests conducted under corrosion fatigue (at the higher end), slowly increasing applied strain, and constant load creep (at the lower end).

As can be seen in Figure A-21, the theoretical bounding crack propagation rates described by the "high sulfur" relationship cannot be maintained at the lower crack tip strain rates. It is also apparent that the divergence from the maximum theoretical rates depends on the dissolved oxygen concentration and flow rate of the water, the former tending to concentrate anions in the crack, whereas the latter has the opposite effect. If the crack propagation rate falls below a critical value, such that a dissolved sulfur activity > 500 ppb S^{2-} cannot be maintained, then crack arrest may well occur in high purity water, and especially under the high-water flow rate conditions expected for many plant situations that tend to flush aggressive anions out of short cracks.

Thus, there are two phenomena that indicate that stress corrosion cracks should arrest under normal BWR system conditions. The first is due to a failure to maintain a critical dissolved sulfur concentration at the crack tip, as described above, and the second is an inadequate crack tip strain rate associated with the dominance of creep processes under constant load. In fact, crack arrest is frequently observed [A142].

The maintenance of crack propagation rates associated with the "high sulfur" rates depends, therefore, not only on conserving a high crack tip sulfur anion activity, but also on a sustainable crack tip strain rate. Thus, the practical system conditions that meet all these criteria are combinations of:

- High sulfur content steels, mainly in the form of MnS inclusions
- High corrosion potentials
- Stagnant or low flow rate water
- Impure water conditions, primarily chloride
- Unconstrained plane stress crack tip conditions
- Cold work and/or high yield stress
- High tensile residual stress and/or stress concentration due to poor weld design
- Lack of effective stress relief heat treatment
- Dynamic loading due to slow thermal or mechanical cycling

Such combinations do not generally exist for extended periods in operating water-cooled reactors.

Taking into account that there is an observed and understood tendency for crack arrest under closely controlled water chemistry (with no significant transients) and constant load conditions, the current engineering judgment [A143]–[A146] is that, for BWR disposition purposes, the crack propagation rate for crack growth at constant load under full power operation or during transients is given by the following Equations A-15 and A-16:

$$da/dt = 2 \times 10^{-8} \text{ mm/s for } K < 55 \text{ MPa}\sqrt{m} \qquad \textbf{Eq. A-15}$$

$$da/dt = 3.29 \times 10^{-14} K^4 \text{ mm/s for } K \geq 55 \text{ MPa}\sqrt{m} \qquad \textbf{Eq. A-16}$$

equivalent to the "low sulfur" line described earlier. This disposition includes safety margins for crack growth rates, da/dt, below 55 MPa√m (since experiments reveal $da/dt < 10^{-8}$ mm.s^{-1}) and the critical stress intensity factor, K_I, for transition to higher crack growth rates (since experiments show K > 60 MPa√m). This proposal was accepted by the U.S. Nuclear Regulatory Commission (NRC) for implementation in the EPRI BWR VIP program. Revised disposition equations have been prepared considering newer data for C&LAS with ≤ 0.015% S and those with > 0.015% S [A147].

It should be emphasized that, although crack arrest is both predicted and observed, this may be counter-balanced by other material and environmental stress factors and, thereby, may challenge the appropriateness of the disposition relationships if the strict water chemistry and loading caveats associated with these equations are violated [A145], [A146]. Such factors may be categorized as those that increase the effective crack tip strain rate and/or markedly increase the crack tip anionic impurity concentration. These include:

- Enhanced crack tip plasticity due to a loss of plastic constraint.
- Factors that may increase the effective crack tip plasticity such as major increases in yield strength or hardness due to heat treatments that produce a (hard) martensitic microstructure (Figure A-22) and/or in the degree of dynamic strain aging [A148], [A149], [A151], [A152].
- Small, repeated transients in loading (often called "ripple loading") can accelerate crack propagation due to the Bauschinger effect that leads to enhanced plasticity at the crack tip [A141].
- Crack tip chemistry, which impacts on the required degree of water purity control during steady state operation, and control of the magnitude and duration of water chemistry transients, particularly chloride.

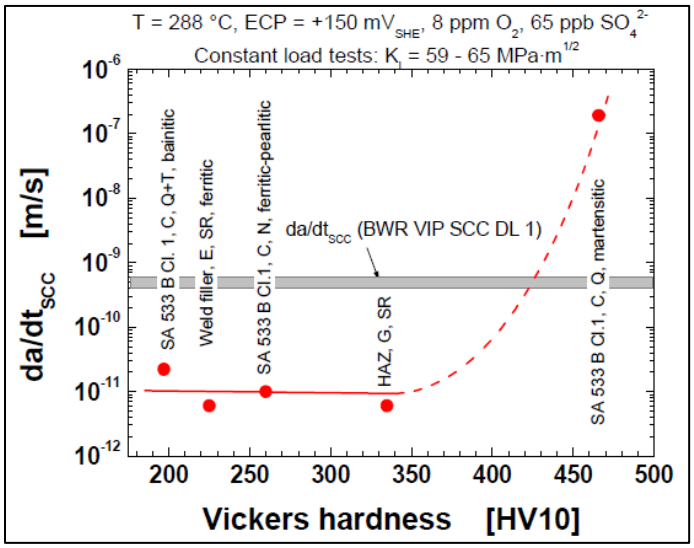

Figure A-22
Effect of hardness on the crack propagation rate for various low-alloy steel weldments, plate, and so on, in 8 ppm oxygenated water at 288°C in comparison with the disposition propagation "low sulfur" rate [A141]

In summary, there is an extensive experimental database on SCC/SICC (and corrosion fatigue) of C&LAS in high temperature water, and there is a viable life prediction methodology based on the slip-oxidation mechanism of crack propagation that is in quantitative agreement with the experimental data.

A.3.2.5 Intergranular (IG) and Transgranular (TG) SCC of Non-Irradiated Stainless Steels in BWRs

It has been well documented since the mid-1960s that intergranular stress corrosion cracking can occur in austenitic stainless steel components in BWRs. This phenomenon has been related to the conjoint requirements of having:

- A sensitized grain boundary microstructure that involves $Cr_{23}C_6$ precipitation and an associated chromium-depleted zone adjacent to the grain boundary. Such sensitization may occur due to temperature/time conditions during welding and, in this case, the cracking occurs adjacent to the weld (see Figure A-16 (a)). Sensitization may also occur due to thermal treatments associated with post-weld heat treatments of adjacent low-alloy steels.
- Excessive cold work, typically > 20%, which could occur due to weld shrinkage, or heavy grinding, or fit-up strains.
- An oxidizing environment that is present in BWRs, particularly those on NWC, due to radiolysis of the coolant in the core, and the presence of anionic impurities (primarily chloride or sulfate) at the ppb level.
- A tensile stress on the internal surface of the component, which may be due to the coolant pressure, fit-up stresses, surface cold work, and, most often, residual stresses adjacent to welds.

These effects have been well characterized, and suitable mitigation actions have been developed. These include, for example, the use of low carbon or stabilized stainless steels, the adoption of HWC and "noble metal technology" in conjunction with water purity control, and, finally, various mechanical engineering approaches to reduce tensile stress and cold work on water wetted surfaces.

The slip-oxidation mechanism of crack propagation described earlier was adopted as a working hypothesis predicting the growth of flaws found in service. Its success has given confidence to empirically derived mitigation actions and has provided the basis for expanding prediction capabilities to systems for which there is a more limited database. Examples of the latter include irradiation-assisted cracking and the cracking of nickel-base alloys in BWR core internals.

The relevant phenomena that need to be quantified for applying the slip-oxidation model to non-irradiated austenitic alloys in BWRs are:

- The *crack tip environment*, which may be markedly different from the bulk environment due to the mass transport (controlled by potential-drop, convection, etc.) of solvated cations, water, and anions within the crack enclave.
- The *metal oxidation rate* of the crack-tip alloy whose composition may be significantly different from the bulk alloy (due to, e.g., chromium depletion at the grain boundaries in sensitized materials).
- The *fracture of the oxide* at the crack tip at a periodicity dependent on its fracture strain and the anelasticity in that strained region.

The approach taken by General Electric and formulated in the PLEDGE model (**P**lant **L**ife **E**xtension **D**iagnosis by **GE**) equates the propagation rate to the oxidation kinetics of the strained crack tip material in the *localized* crack tip environment [A51], [A119]. It emphasizes the importance of the corrosion potential at the crack mouth as a controlling parameter for anion and acidity concentration at the crack tip and thereby on the re-passivation kinetics when the protective oxide film at the crack tip is ruptured by applied strain. Application of the model to BWRs involves 1) defining the crack tip alloy/environment composition in terms of the bulk alloy composition and heat treatment, anionic concentration or water conductivity, and the corrosion potential at the crack mouth; 2) measuring the reaction rates for the crack tip alloy/ environment system that correspond to the conditions defined in *1)*; and 3) defining the crack tip strain rate in terms of continuum parameters such as stress, stress intensity, and loading rate. There has been extensive work conducted in these areas for austenitic (and ferritic) alloys in BWR systems, and a few examples are given here to illustrate how the predictions relate to observations.

The predicted crack propagation rates at various computed crack tip strain rates for sensitized stainless steel in oxygenated water at 288°C are compared with observation in Figure A-23. The figure shows a comparison between observed and predicted crack propagation rates for sensitized stainless steel in 288°C water, in 8 ppm oxygenated water under a variety of stressing/straining modes (left image), and in oxygenated versus deaerated environments (right image) (see Figure A-23, left image) [A119]. In this case, the various strain rates have been associated with creep (under constant load), monotonically increasing strain rates (as in a slow strain rate test), or under cyclic loading at various load amplitudes, mean load, and loading frequencies. Good agreement between observation and theory is noted. The practical impact, however, is that there is no fundamental difference in mechanism between “stress corrosion cracking” and “strain-induced corrosion cracking” (and indeed “corrosion fatigue”), which are represented by these loading modes. Thus, it is valid theoretically to view these degradation phenomena as part of a continuous spectrum of “environmentally assisted cracking” phenomena [A153], [A154]. The crack propagation rate versus crack tip strain rate relationships naturally changes with environmental chemistry, and this is illustrated in Figure A-23 (right image), both theoretically and via observation, where the crack propagation rate for sensitized stainless steel in HWC is compared with NWC.

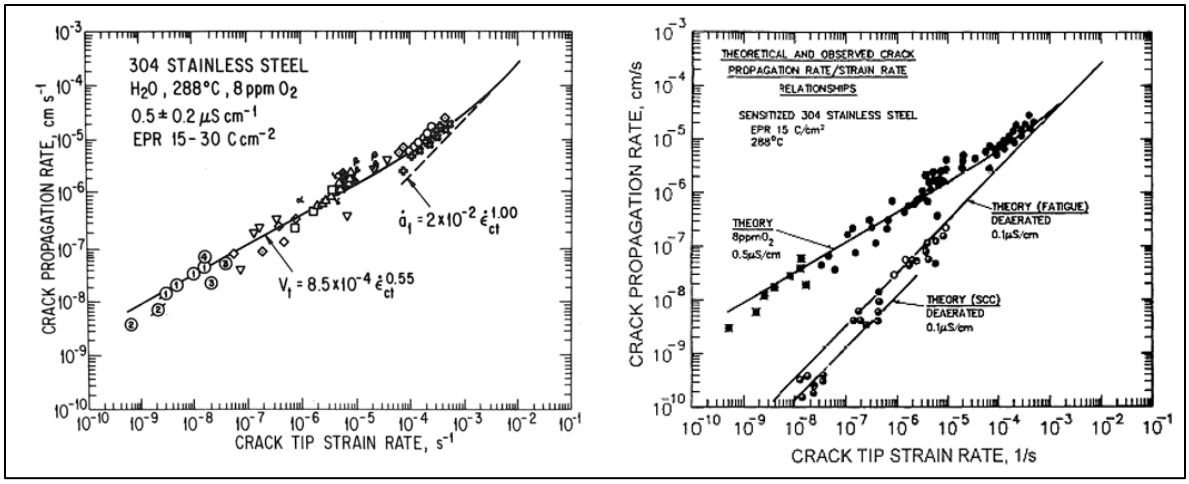

Figure A-23
Comparison between observed and predicted crack propagation rates for sensitized stainless steel in 288°C water, in 8 ppm oxygenated water under a variety of stressing/straining modes (left image), and oxygenated versus deaerated environments (right image) [A119]

Important predicted effects of changes in the crack tip strain rate associated with changes in yield strength and stress intensity are indicated in Figure A-24 and Figure A-25, respectively, under various material and environmental conditions. The practical impact here is that increases in yield stress will increase the crack propagation rate, and this can be related to fabrication practices that alter the bulk yield stress (cold bending) or the localized yield stress (surface grinding) and, indeed, irradiation damage (see later). A further factor shown in Figure A-25 is that there will be a predictable range of crack propagation rate versus stress intensity relationships (bounded by the hatched region in Figure A-25) if the environment is inadequately defined or controlled. This has an impact on the definition of the disposition curve (note the NRC disposition line in Figure A-25) and indicates the degree of experimental control that is required during the acquisition of data for the purpose of formulating a disposition relationship.

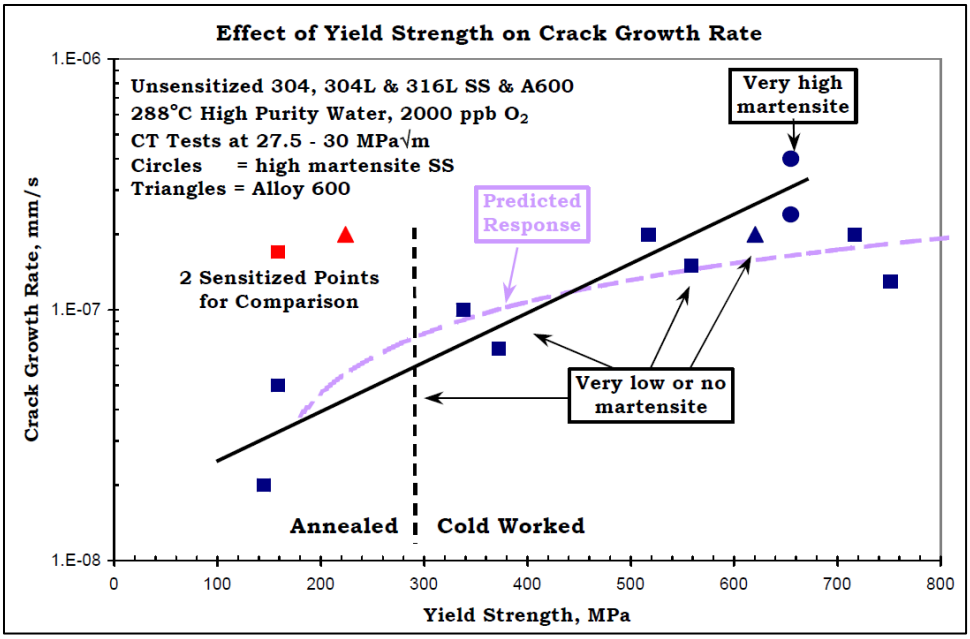

Figure A-24
Effect of yield strength and martensite on the stress corrosion crack growth rate on stainless steel and Alloy 600 in 288°C, high purity water (< 0.10 S/cm outlet) [A155], [A156]

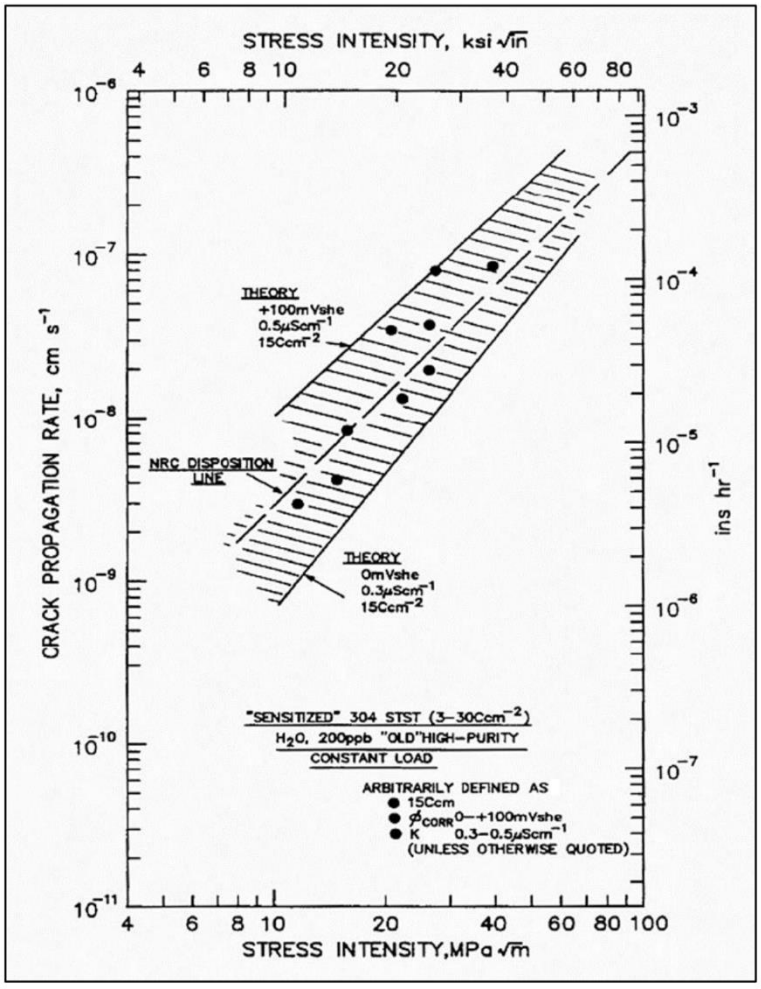

Figure A-25
Crack propagation rate/stress intensity dependence for sensitized stainless steel in water at 288°C water with 0.2 ppm oxygen and conductivity 0.3-0.5 µS/cm [A51]

NOTE:
Note the insertion of theoretical relationships and the NRC regulatory relationship used for structural integrity evaluations.

Changes in the corrosion potential and conductivity (i.e., anionic activity) are known to have a very significant effect on crack propagation rates in stainless steel. The effects of these parameters on how they change the crack tip pH and anionic activity and hence, the passivation rate parameter "n" at the strained crack tip are also predictable. These relationships emphasize the crucial need for water purity control and for the adoption of procedures (e.g., hydrogen injection, noble metal technology) that lower the corrosion potential. The specific effect of water purity control on the predicted and observed cracking at a number of plants for 28" schedule 80 recirculation lines is illustrated in Figure A-26. Similar predictions may be made for the cracking propensity for different system parameters such as changes in stainless steel composition (Type 304 vs. 316NG vs. 321) or the effect of surface grinding and its effect on surface cold work and residual stresses. Obviously, there will be uncertainties in the predictions

associated with uncertainties in the values of the model parameters (e.g., residual stress, coolant conductivity, corrosion potential, sensitization, etc.), but these can be treated using knowledge of the distributions of these parameters and their input, via a Monte Carlo assessment, into the deterministic crack growth equation.

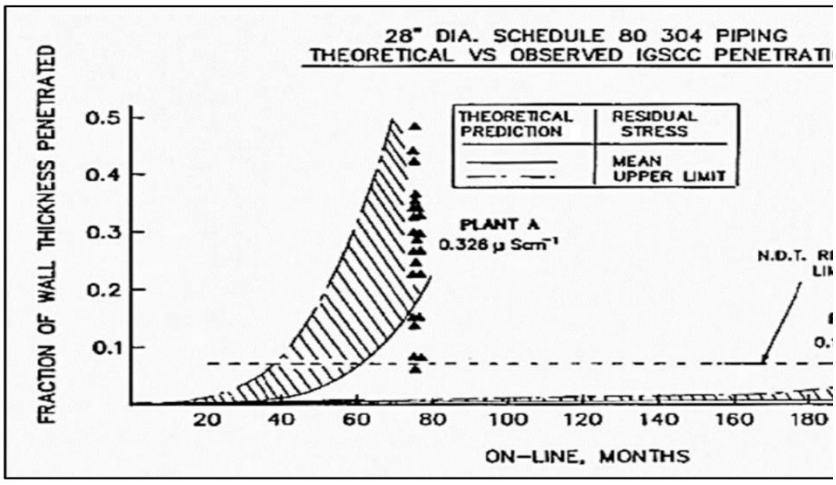

Figure A-26
Theoretical and observed crack depth versus operational time relationships for 28" diameter schedule 80, 304 stainless steel piping for two boiling water reactors operating at different mean coolant conductivities [A119], [A156]

NOTE:
Note the bracketing of the maximum crack depth in the lower purity plant by the predicted curve that is based on the maximum residual stress profile, and the predicted absence of observable cracking in the higher purity plant (in 240 operating months).

This understanding of the mechanism of cracking in stainless steels can be logically expanded to predict the extent of cracking under different combinations of stress, material, and environmental variables. Examples include:

- The incidence of transgranular cracking in stainless steels in LWR systems where the requirement for a sensitized grain boundary is offset by increased yield stress due to surface or bulk cold work, or by dynamic straining [A51]
- The effect of strain localization in weld HAZs
- The effect of irradiation which can affect, to different degrees, the extent of grain boundary chromium depletion, stress relaxation, and irradiation hardening
- The extent of cracking of stainless steels in reducing PWR primary environments which may be exacerbated by cold work, inadvertent oxidizing transients, and chloride and/or sulfate impurities
- The extent of cracking of other austenitic alloys, such as nickel-base alloys, in water reactor environments

A.3.2.6 IGSCC of Nickel-Base Alloys in BWRs

Although IGSCC was initially observed in BWRs associated with sensitized stainless steels, other incidents of IGSCC began to be observed in the late 1970s in nickel-base alloys such as Alloys 600 and 182 used for welded safe ends, access hole covers and shroud head bolts, and in Alloy X-750 jet pump beams. During this period, the importance of water purity control became increasingly obvious, especially with regard to creviced components where the geometry and oxidizing conditions in the bulk environment could give rise to increased anionic activity in the creviced region even though the bulk water purity was acceptable at that time [A49], [A50].

The relationships between the crack propagation rate in austenitic nickel-base alloys and the water conductivity, corrosion potential, grain boundary sensitization, and bulk chromium content are very similar to those observed in austenitic stainless steels. However, the development of mechanism-based prediction models for environmentally assisted cracking of nickel-base alloys in BWR systems was made difficult by the fact that the observed propagation rate data, against which the prediction models are validated, can exhibit extreme scatter due to various analytically intractable factors (e.g., the tortuosity of the interdendritic crack front in the weld metal Alloys 82 and 182) and experimental control issues. These difficulties may be minimized by establishing strict experimental guidelines that are now applied to databases for several cracking systems, including nickel-base alloys [A158]–[A160].

There are factors that suggest that the quantification of the slip-oxidation model developed for austenitic stainless steels in BWR environments may be relevant to life prediction algorithms for nickel-base alloys in the same environments [A161], [A162]. For example:

- Both alloy systems involve ductile face-centered cubic structures with similar mechanical properties. Thus, it is reasonable to use in preliminary model derivations the same crack tip strain rate algorithms for ductile nickel-base alloys as for stainless steels.
- The solubility of the NiCr and FeCr oxides are very similar in BWR NWC water at 288°C and, therefore, from an electrochemical viewpoint, the crack-tip system and rate-determining steps in the bare-surface oxidation kinetics are likely to be similar for the nickel-base alloy and austenitic steel systems.

Given these assumptions, the predictions are in reasonable agreement with the observations of stress corrosion in the nickel-base alloy/BWR systems. For example, the variation in extent of cracking of Alloy 600 shroud head bolts and access hole covers as a function of the average plant conductivity are reasonably predicted (Figure A-27 and Figure A-28, respectively). In Figure A-27, the importance of the detrimental effect of excessive coolant impurity transients during early operation is noted, even if the average conductivity is subsequently maintained at a low average value.

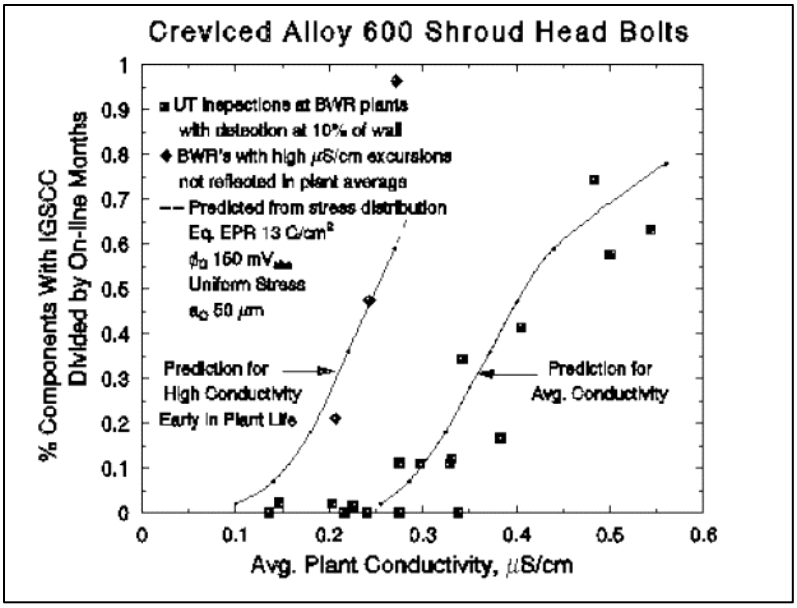

Figure A-27
Predicted and observed effects of average plant water purity on crack incidence in creviced Alloy 600 shroud head bolts [A162]

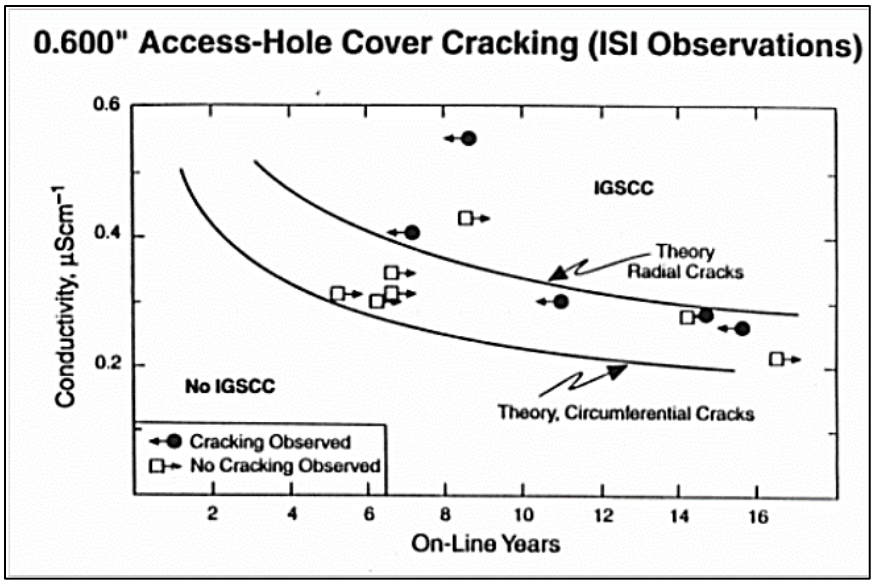

Figure A-28
Predicted and observed effects of average plant water purity on crack incidence in creviced welded access hole covers [A162]

A.3.2.7 SCC of Stainless Steels in PWR Primary Coolant Circuits

Types 304/304L and 316/316L stainless steels, which are widely used in the PWR primary system piping, have a very good record of stress corrosion cracking resistance. Similarly, titanium stabilized stainless steel used in VVER primary circuits has performed very well. This is to be expected given the earlier discussion regarding the predictable sensitivity of cracking of stainless steels in BWRs to the corrosion potential, and the fact that the primary systems in PWRs and VVERs operate at low corrosion potentials due to dissolved hydrogen in the primary coolant. When stress corrosion cracking has occurred, it has been rare. Of the 183 events considered in an evaluation of stainless steel SCC in PWRs, only 30 occurred in free flowing primary water (i.e., water chemistry within EPRI guidelines). The rest occurred in stagnant conditions (i.e., concentrated dissolved oxygen and chlorides) (Figure A-29).

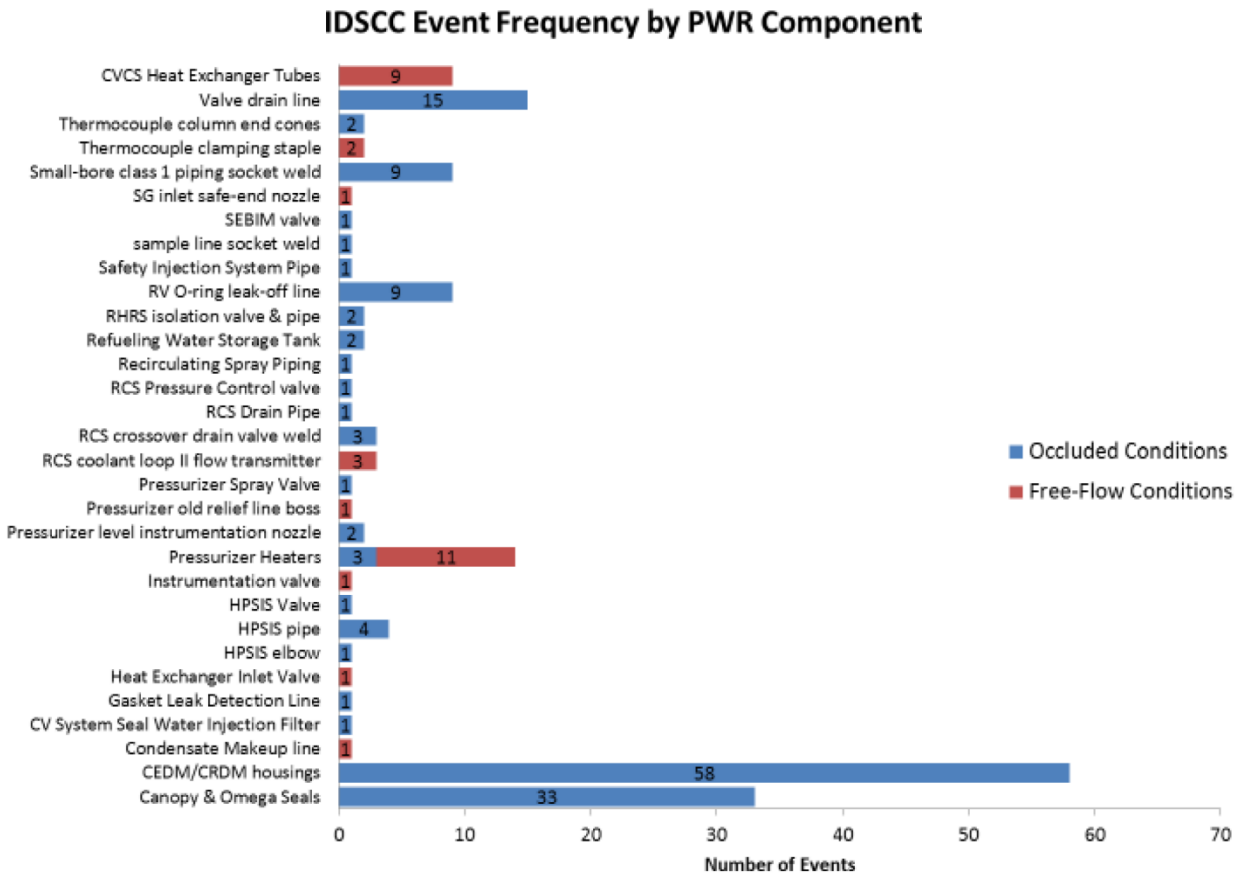

Figure A-29
Summary of SCC of austenitic stainless steels in PWR primary circuits [A163]

The deleterious effects of chloride and the presence of dissolved oxygen for stainless steels are well known [A164], [A165]. PWR primary water chemistry specifications allow, in principle, significant chloride levels (i.e., 150 ppb Cl^-), which could lead to stress corrosion cracking in oxygenated conditions. Consequently, the EPRI guidelines mandate a reduction in chloride level from 150 ppb within 24 hours, or else the reactor would have to be shut down. Typical operational values are much less at < 10 ppb. This may be one reason why the cracking problem with stainless steels is not widespread. The cracking of control rod canopy seals in PWRs, for

example, has been attributed to oxygen–chloride contamination trapped after refueling and maintenance operations, although significant chloride contents are rarely observed in the trapped liquid. It seems likely that sulfate impurities may be equally as damaging in a highly oxidizing environment (Figure A-30).

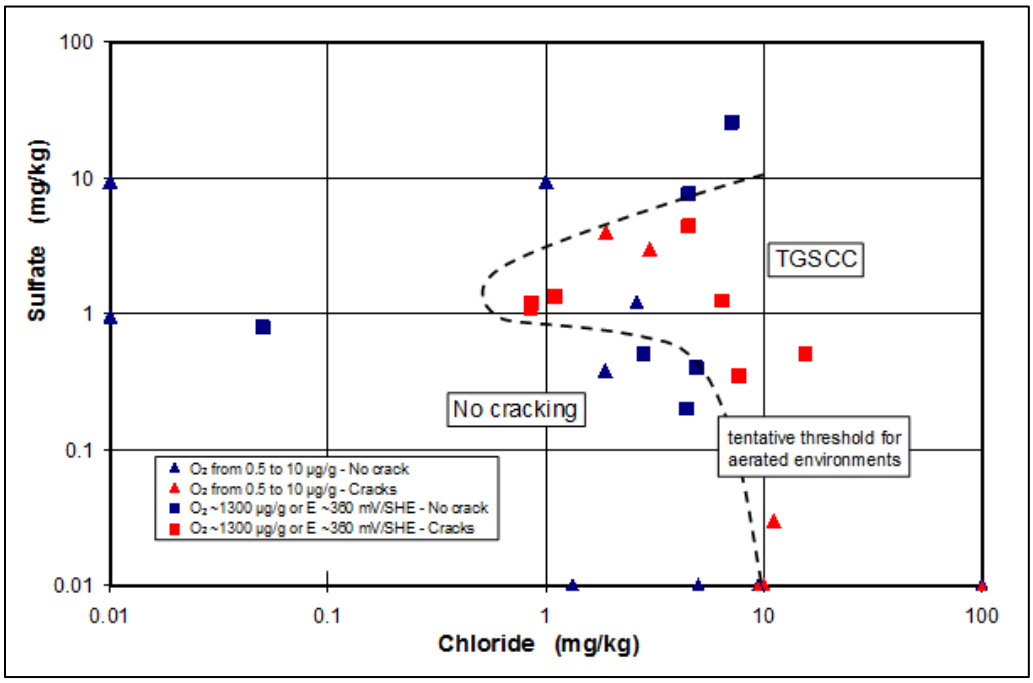

Figure A-30
Tentative SCC domain for Type 304 stainless steel at 200°C in PWR environment containing chloride and sulfate, simulating pressurized aerated conditions [A166]

The remaining 30 cases of SCC of austenitic stainless steels in PWR primary circuits shown in Figure A-29 occurred without any obvious departure from PWR primary water specifications. These cases mainly involved pressurizer heater sleeves or cladding and heat exchanger tubing in the Chemical and Volume Control System (CVCS). There also appeared to be a clear association between the incidence of cracking and hardness > 300 HV (due to cold work) but sensitization was not a risk factor (as expected in PWR primary water). Nevertheless, deliberately strain-hardened stainless steels, mainly Type 316 and to a lesser extent niobium stabilized Type 347, (up to a limit of 90 ksi (or 625 MPa) have been used for many decades in PWRs for bolting and other purposes where moderate strength is required, and without apparent problems except when highly irradiated. In practical terms for non-stabilized austenitic steels with medium carbon content, this corresponds to an upper limit on cold work of ~20% or a hardness of ~300 HV. Much higher cold work ratios would be necessary to reach the same hardness limit in L grade materials. It can be noted that stress corrosion of other hardenable, high strength, stainless steels only becomes apparent in PWR primary water service at hardness values greater than ~350 HV [A57].

There is also a growing body of laboratory data that clearly shows that SCC can propagate in austenitic stainless steels in normal quality PWR primary water if they are sufficiently cold worked (> 20%) or subject to other types of deformation strain (e.g., severe bending, grinding, and weld shrinkage strains). However, crack initiation is difficult and appears to

require either dynamic straining and/or a significant (transient) dissolved oxygen concentration [A167]–[A171], [A346]–[A349]. Attention has also been focused on complex mechanical deformation pathways that occur during component fabrication, which appear to affect the inherent resistance of austenitic stainless steels to stress corrosion cracking in nominal PWR primary water environment.

A.3.2.8 IGSCC of Nickel-Base Alloys in PWR Primary Water (PWSCC)

The wide-ranging problems of stress corrosion cracking of nickel-base alloys in PWR primary water environments have been reviewed in several articles [A172], [A175]–[A178] under the description of either "Primary Water Stress Corrosion Cracking (PWSCC)" or "Low Potential Stress Corrosion Cracking (LPSCC)." In this appendix, the term *PWSCC* is used as a generic term for stress corrosion cracking of nickel-base alloys in PWR primary water systems.

PWSCC of mill-annealed Alloy 600 was first observed in the laboratory in the 1950s and 1960s [A179] and was then initially observed in the early 1970s on the primary side of "recirculating" PWR steam generators (RSGs), in some cases, after extremely short periods of operation (e.g., two years at Obrigheim [A180]). The cracking in RSGs occurred at high residual tensile stress regions where the tubes were expanded into the tubesheet (via mechanical rolling, explosive expansion, etc.) or at the tight radii of the inner two rows of the tube U-bends. The cracking was highly temperature dependent, being observed primarily in the hot legs of steam generator tubing (~310-325°C). The apparent activation enthalpy was high (~180 KJ/mole), leading to a difference of a factor of 4-5x between the times for "crack initiation" (defined as the time to detect a crack in service) in the hot and cold legs that is associated with a typical temperature difference of 30°C between these locations. PWSCC was also eventually observed in roll transition zones of mill-annealed Alloy 600 tubing in once-through PWR steam generators.

PWSCC of nickel-base alloys in primary environments then extended into thicker section components, normally after significantly longer operating times than for RSG tubing described above. The components primarily affected have been:

- Small bore nozzles attached to pressurizers
- Reactor vessel head penetrations
- Reactor vessel outlet nozzle safe-end regions
- Steam generator inlet safe-end regions, drain nozzles, and divider plates

These incidents have been extensively catalogued [A175]–[A178]. Although the crack orientation in most of the cylindrical geometries has been axial, there have been a few cases of circumferentially oriented cracking, which has raised safety issues for these pressure retaining boundaries.

PWSCC of Alloy 132 or 182 and 82 weld metals, the first two having compositions similar to those of Alloy 600, has been observed in many PWRs in several different countries [A176]–[A178], [A181], [A182]. Both J-groove welds and butt welds have been affected, and crack initiation times have often been very long, up to 27 years. Nevertheless, the extent of cracking observed
in service has so far been very much less than in the case of wrought Alloy 600, with most cracking being associated with Alloys 132 and 182.

Material Composition and Microstructural Effects

Heat-to-heat variability has had a large impact on the frequency of cracking of primary side Alloy 600 components in PWRs. In the case of RSG tubing, only a small fraction of heats typically contributes to the total number of tubes that are cracked [A57]. This variability is seen even when the tubes were from the same manufacturer and were in the same steam generator. The reasons for this heat-to-heat variability are only partly understood, but it is known that there is a correlation between the incidence of PWSCC and the morphology of the chromium carbides precipitated during the final stages of tube manufacture. In this case, PWSCC susceptibility is greatest in the absence of grain boundary carbides [A183], [A184]. In fact, grain boundary chromium-depletion that can be associated with carbide precipitation has no detrimental effect at low corrosion potential in PWR primary water. The absence of grain boundary carbides was correlated in the case of steam generator tubing with low mill-annealing temperatures ~980°C that led to fine grain sizes, large amounts of intragranular carbides, and very few intergranular carbides. Given the ranges in carbon content and differing definitions of "mill annealed" (in terms of temperature and time) from one manufacturer to another, there has been a resultant significant variation in crack initiation times.

The observed correlation between PWSCC susceptibility and carbide morphology led to the development of thermal treatment (TT) procedures that produced desirable carbide morphologies in a controlled fashion. Specifically, higher mill-annealing temperatures (1040°- 1070°C) followed by thermal treatment at 705°C for 15 hours enhance intergranular carbide precipitation in Alloy 600 and provide enough time at temperature for any grain boundary chromium-depletion to recover by diffusion and, thereby, avoid sensitization [A184]. The adoption of the TT heat treatments for replacement Alloy 600 tubing in RSGs became widespread and has led to much improved service experience. When cracking has occurred in Alloy 600TT, it has been usually associated with insufficient carbon in solution prior to the thermal treatment or the application of tube straightening prior to heat treatment; the latter condition promotes intragranular rather than intergranular carbide precipitation [A57].

Wrought Alloy 600 products used for thicker section components did not undergo the same optimization of carbide microstructure as steam generator tubes, until relatively recently, and were usually procured only to chemical composition and strength specifications. Consequently, considerable variability in carbide morphologies exists in these wrought materials that are installed in plants, particularly depending on carbon content and final hot working temperature. Considerable effort has been put into categorizing the microstructure and carbide morphologies of wrought Alloy 600 products in service to judge their susceptibility to PWSCC [A185].

PWSCC initiation times also depend strongly on chromium content (Figure A-31). This has led to the replacement of Alloy 600 (14-17% Cr) with much more resistant Alloy 690 (28-31% Cr), which is also thermally treated, typically at ~715°C, to maximize grain boundary carbide precipitation. Similar higher chromium welding Alloys 152 and 52 have also replaced Alloys 182 and 82, respectively.

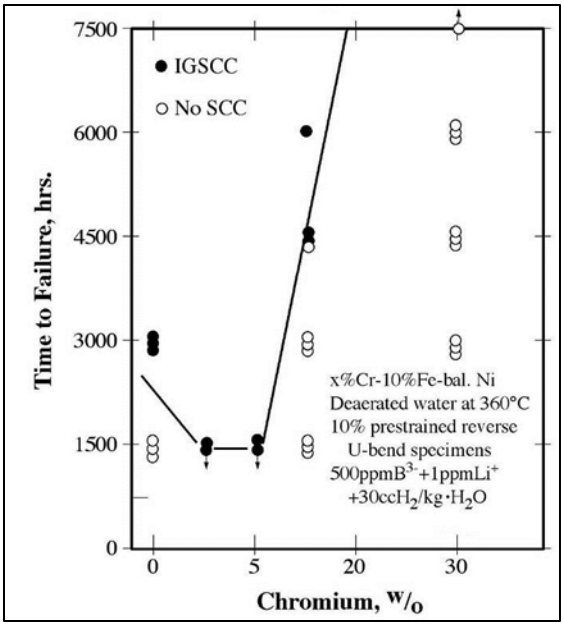

Figure A-31
Time to failure in simulated PWR primary water (500 ppb B, 1 ppm Li, 30 mL [H_2]/kg [H_2O]) at 360°C as a function of Cr content of Ni-Cr-10wt% Fe alloys [A186]

In the case of the weld metal Alloys 132, 182, and 82, dendrites in the weld beads tend to align during solidification in the direction of heat flow toward adjacent cooler materials or surfaces, thus giving rise to microstructural directionality or texture [A181]. Grain boundaries form between packets of dendrites of the same or similar crystallographic orientation and typically have a rather wavy appearance, unlike the rectilinear grain boundaries of wrought materials such as Alloy 600 or 690. In general, PWSCC initiates and propagates preferentially on high angle grain boundaries parallel to the microstructural directionality rather than perpendicular to it. Grain boundaries are typically decorated with fine (Nb,Ti)C and $Cr_{23}C_6$ particles, but no significant grain boundary segregation of the constituent elements has been observed, including impurities such as silicon, phosphorus, and sulfur that have been associated with the risk of hot cracking. No particular link between PWSCC susceptibility and spatial compositional variations has been established. By contrast, the microstructure and mechanical properties in the superficial cold worked layer of ground nickel-base welds can be very different from those of the bulk material and can have a profound influence on PWSCC initiation probability and time.

The introduction of Alloy 690TT as a replacement steam generator tubing alloy for mill-annealed Alloy 600 was made initially at DC Cook in 1989 and soon thereafter in Sweden and France. Steam generators around the world have operated with this grade of tubing since its being first placed in service (i.e., since 1989) without any stress corrosion cracks being reported. Moreover, Alloy 690TT is the replacement material for Alloy 600 thick section components [A187]–[A189], [A350], together with the replacement of the welding Alloys 182/82 with 152/52. In Germany and Canada, because of the uncertainties concerning the cracking susceptibility of nickel-base alloys that arose in the late 1950s and 1960s, an iron-based alloy with 19-23% Cr (Alloy 800) was mainly adopted for PWR and CANDU steam generator tubing. There is no evidence either from service experience or laboratory testing that Alloy 800 is susceptible to PWSCC, as is also the case for VVER stainless steel steam generator tubing [A351], [A352]Environmental Effects

The apparent activation enthalpies for crack initiation and propagation for PWSCC of nickel-base alloys in PWR primary environments are high; typically accepted values are ~180 kJ/mole for crack initiation in Alloy 600 and ~140 kJ/mole for crack propagation [A57]. However, with the improvement in testing techniques over time, particularly in terms of crack detection and taking into account the change in corrosion potential with temperature at constant hydrogen concentration, lower values closer to 130-140 kJ/mole for both initiation and propagation may be more reliable values that should be adopted [A190]. Nevertheless, independent of the precise values of activation enthalpies, it is apparent that a decrease in hot leg temperature of only a few °C can markedly increase stress corrosion cracking resistance, although inevitably with a reduction in thermal efficiency of the unit.

The range of corrosion potentials over which PWSCC occurs in Alloy 600 and its compatible weld metals is very narrow (~100 mV) and is centered on the Ni/NiO equilibrium potential [A57]. The reason for this is not easily explainable via any of the cited mechanistic hypotheses for stress corrosion cracking described earlier. However, the fact that cracking susceptibility and, more particularly, crack propagation rates peak over such a narrow range suggests possible mitigation actions associated with changing the corrosion potential by either increases or decreases in the hydrogen fugacity in the primary coolant. In fact, increases in dissolved hydrogen concentration provide greater benefit over the range of temperatures encountered in PWR hot and cold legs of the primary circuit [A191].

Mitigation of PWSCC has often involved repair and replacement actions using more resistant materials like Alloy 690TT and its compatible weld metal Alloys 152 and 52. Increased attention is also being paid to mitigation measures involving surface treatment (e.g., water-jet, laser, and shot peening) [A353–A355], water chemistry optimization (e.g., adjustment of hydrogen concentration levels [A191] and/or the addition of potentially inhibiting species such as zinc), and various mechanical options to achieve a reduction in tensile stress levels. External weld overlay technology has been adapted from BWR mitigation techniques and applied widely to PWR nickel alloy components, especially dissimilar metal welds (Alloys 82/182), to ensure a compressive residual stress at the water-wetted internal surfaces.
RTF36343235323a204e756d6265

Crack Propagation Rate Studies

Emphasis is often placed on the management and mitigation of the risk associated with the propagation of relatively “deep” cracks that have been detected during in-service inspections. This focuses attention on crack propagation rate versus crack tip stress intensity relationship, which together with the specific stress profile determines how much crack penetration will occur before the next inspection. An example of such “crack growth disposition” relationships is given in Figure A-32 for the nickel-base Alloys 600, 182, and 82 in a PWR primary environment (the data points shown are for the weld metal Alloys 182 and 82).

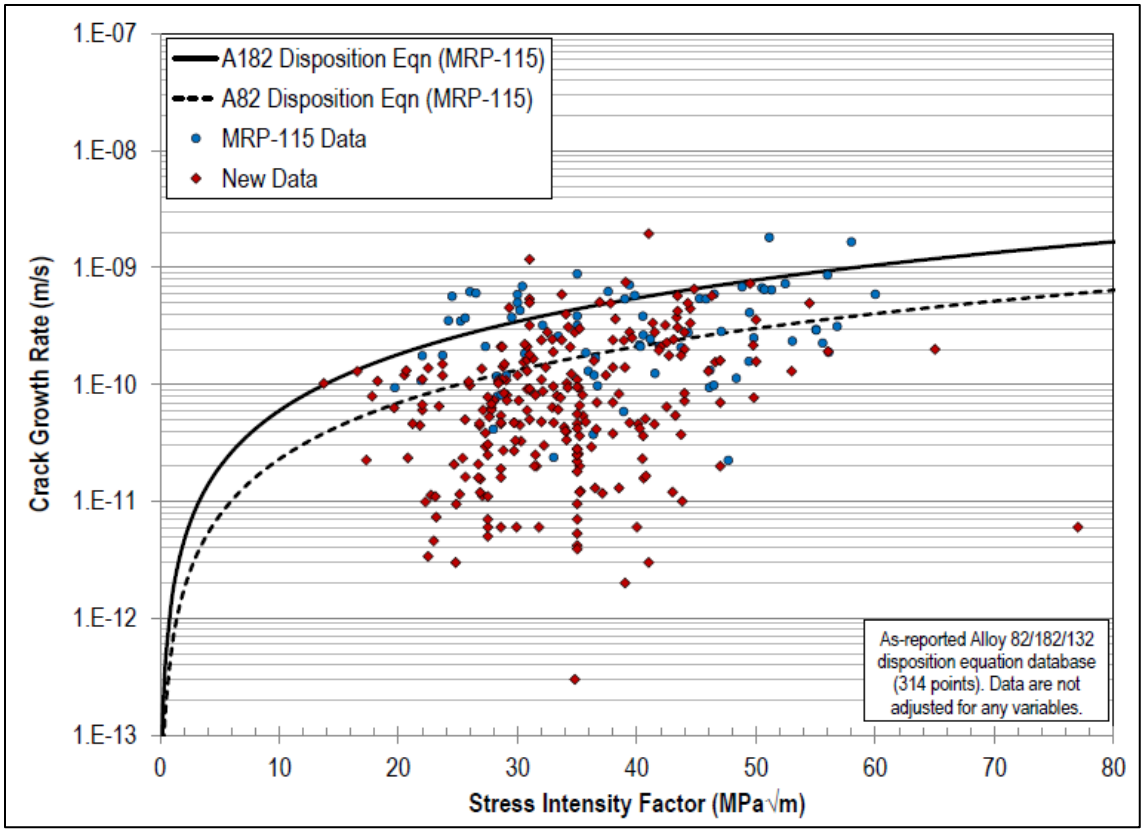

Figure A-32
Crack propagation rate versus stress intensity data and disposition relationships for nickel-base Alloys 600, 82, 182, and 132 in PWR primary water (data adjusted to 325°C) [A369]

Figure A-32 illustrates the scatter in the data upon which the disposition relationships are based. (Similar scattered databases for IGSCC growth rates in cold-worked and/or sensitized stainless steels exist for BWR NWC and HWC environments.) The reasons for this scatter are summarized as follows:

- Aleatory uncertainties that relate to the fact that many of the physical processes are stochastic in nature (such as intergranular oxidation, crack coalescence, and short crack propagation). Since these processes are stochastic, or random, no amount of new data will reduce the scatter in the database.
- Epistemic uncertainties that relate to the completeness in the disposition algorithm or the accuracy of the inputs to that algorithm. In these cases, improvements in the model or the accuracy of the inputs to the model will reduce the scatter in predictions and increase confidence in the model predictions.

Much of the qualification testing of Alloy 690TT has concentrated on crack propagation studies since long-term exposure tests of smooth specimens, even at high stress and high temperatures under similar conditions to those that readily produce cracking in Alloy 600, show no evidence of crack initiation [A193], [A350]. Even in fatigue pre-cracked fracture mechanics specimens of Alloy 690 or Alloys 52 and 152, intergranular crack initiation has predictably proved difficult, except in one-dimensionally deformed materials where the crack plane is in the rolling plane. On the other hand, perpendicular to the rolling or deformation plane, transition to intergranular

cracking and growth are extremely difficult, and usually intergranular crack extension is close to or below the detection limit. Compilations of crack propagation rates as a function of K_I observed in Alloy 690 plates and CRDM nozzles, as well as in Alloys 52 and 152 weld metals are shown in Figure A-33 and Figure A-34, respectively.

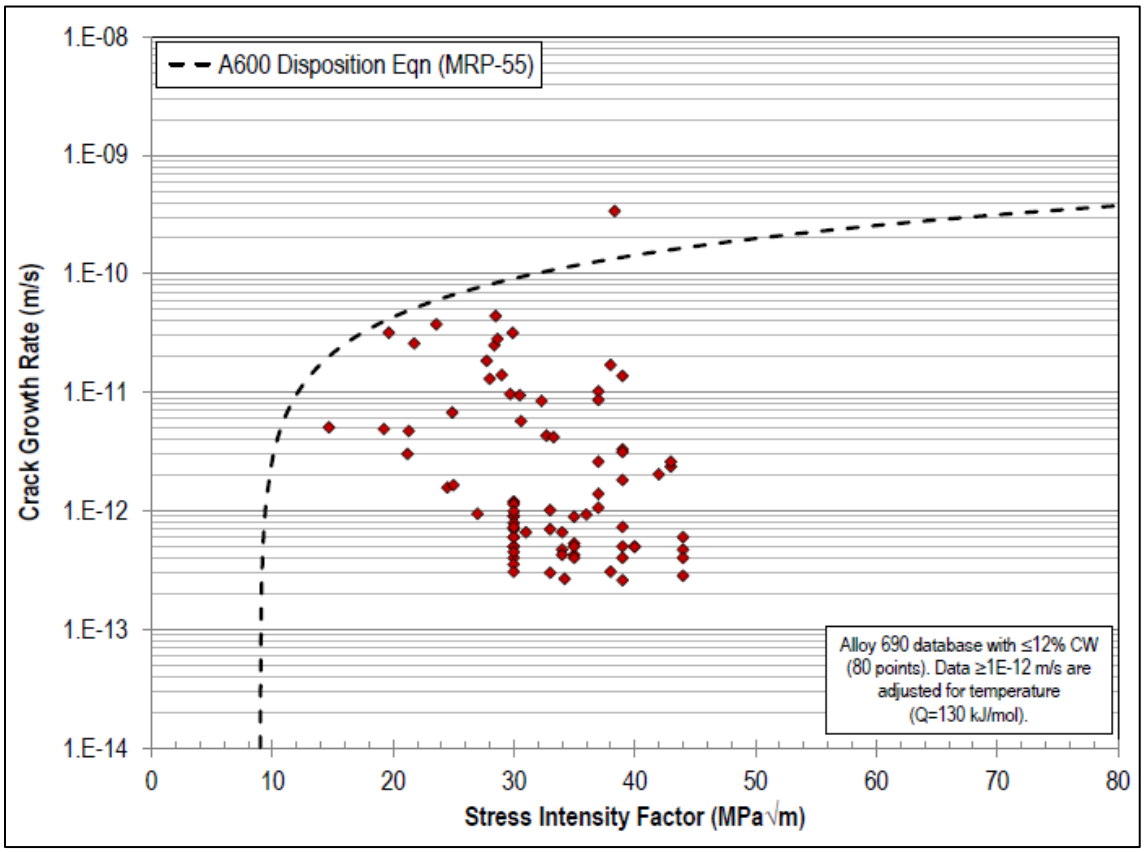

Figure A-33
Summary of PWSCC growth rates at constant K_I in Alloy 690 CRDM and plate materials [A369]

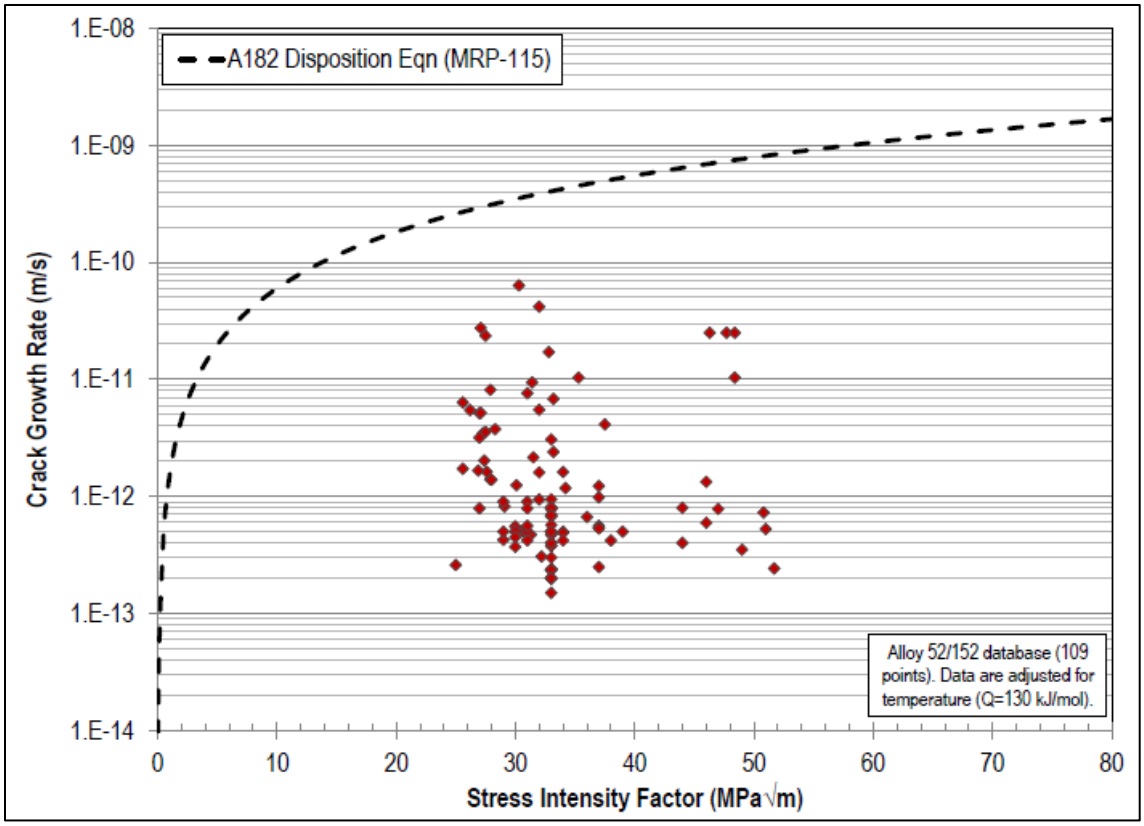

Figure A-34
Summary of PWSCC growth rate data for Alloys 52 and 152 [A369]

The large range in the crack growth data in Figure A-33 and Figure A-34 is a concern and whose origin is important to understand in order to judge the pertinence of these data to components in the field. Most of the qualification testing of Alloy 690 material has concentrated on crack propagation studies since long-term exposure tests of smooth specimens, even in conditions similar to those that readily produce cracking in Alloy 600, show no evidence of crack initiation. However, laboratory testing has shown that PWSCC is possible, albeit with very low crack growth rates for Alloy 690 materials without cold rolling. Without cold rolling, crack growth rates are typically almost unmeasurable, in the range 10^{-12} to 10^{-11} ms^{-1} and, as such, are of little engineering significance. On the other hand, crack growth rates obtained from Alloy 690TT materials that are cold rolled, forged (cold or hot), or strained by tensile loading are significantly enhanced, in some cases by 2-3 orders of magnitude with > 20% cold work. The highest rates of growth that are comparable with the highest data for non-cold-worked Alloy 600 have been measured when microstructural carbide banding seen in some Alloy 690 plate products is aligned with the one-dimensional cold rolling plane and the cracking plane, although some homogeneous materials exhibit growth rates within ~3-4 times as high. However, not all banded or homogeneous materials necessarily exhibit such high growth rates. In one case, very high rates of growth have also been observed in a 31% cold rolled, homogeneous Alloy 690 material, whereas 17% cold work did not give rise to a similar deleterious effect. The weld metal results in Figure A-34 show generally low or very low average rates of growth below 2 x 10^{-12} ms^{-1} with one exception of a weld that was not fabricated by an NSSS vendor.

The effect of temperature on crack growth rates in Alloy 690 varies with microstructure and cold work [A195]. Those materials with moderate to high growth rates show almost no temperature dependence, whereas materials with moderate or lower growth rates exhibit a temperature dependence consistent with that observed in Alloy 600 and Alloy 182/82 weld metals. A similar conclusion has been drawn regarding the effects of dissolved H_2 on crack growth rates. Alloy 690 with moderate to high growth rates shows almost no dependence on dissolved H_2 concentration, whereas in lower growth rate materials some effect is observed.

The justification for working on one-dimensionally deformed Alloy 690TT is that shrinkage strains of 10 to 20% have been frequently observed adjacent to the fusion zones of multi-pass welded, thick section, austenitic materials (usually stainless steels), which are also a zone where intergranular carbides could conceivably be dissolved and rapidly re-precipitate intragranularly during cooling. To date, no experimental evidence of more rapid growth in heat-affected zones of Alloy 690 relative to the bulk material has been found (in contrast to Alloy 600).

It is interesting to note that almost the same dramatic deleterious effect of one-dimensional cold rolling on IGSCC growth rates in austenitic stainless steels has been observed in laboratory tests. However, there is no credible evidence from the field that (non-irradiated) stainless steels strain hardened up to ~20% are susceptible to stress corrosion cracking in properly controlled PWR primary water. Thus, the combination of conditions under which Alloy 690 has shown significant susceptibility to PWSCC growth in the laboratory seems unlikely to present a significant practical threat, although carbide banding in wrought products should clearly be avoided. Perhaps the best demonstration of this conclusion has been the observation that PWSCC initiated in a susceptible material like Alloy 600 or Alloy 182 does not propagate into Alloy 690 or Alloy 152 in welded composite specimens [A196]. By contrast, PWSCC has no difficulty in crossing the fusion boundary between Alloy 600 and Alloy 182 in similar welded composite specimens.

Life Prediction for Nickel-Base Alloys Affected by PWSCC

There is at present no consensus concerning the mechanism of PWSCC for nickel-base alloys among those summarized earlier [A125]. Thus, the prediction of future cracking behavior of Alloy 600 components affected by PWSCC relies mainly on empirical observations of the effects of the material, stress, and environment on the time to observable cracking from initially smooth surfaces or on crack propagation rates. The databases available for PWSCC growth rates in Alloys 600, 182, and 82 were discussed earlier, as shown in Figure A-32 together with the disposition curves that have been derived. However, considerable emphasis has been placed on estimating the lives of Alloy 600 components in PWR service recognizing that crack initiation times plus growth below the detection limit of NDE can be very significant. The databases for such predictions can show considerable scatter, either because of 1) inherently stochastic reasons applicable to surface-dominated phenomena or 2) uncertainty in the definition or control of the system conditions under which the data were obtained.

Practical models for predicting in-service lifetimes of Alloy 600 components affected by PWSCC, where initiation times dominate overall life relative to propagation, have typically been based on empirical models. For example, extrapolations of the Weibull distribution of plant failures of a given component as a function of time or empirical relationships between time to failure and the temperature, stress, and microstructural dependencies of PWSCC discussed earlier have been used.

The Weibull distribution is a well-established tool that has been successfully applied to quantify the dispersion in stress corrosion data of all types, including PWSCC (and IGA/IGSCC) of Alloy 600 steam generator tubing [A197]–[A201]. Its use has also been extended to PWSCC of CRDM nozzles [A202]. The dispersion in times to observe detectable cracks arises from the inherent variability in susceptibility of materials to stress corrosion cracking and, in the case of plant components, to variability in surface finish and uncertainty in the precise operating stress and temperature. This approach has also been adapted to French operating experience of PWSCC in the roll transitions of steam generator tubes and incorporating the method of material susceptibility indices described below [A202], [A203]. An attempt was made to adapt this approach to PWSCC of CRDM nozzles, but it was found to be overly conservative [A202]. Consequently, other approaches were examined that took into account heat-to-heat susceptibility, operating temperature, and stress (see below).

The simplest approach has been taken in the United States where priorities for plant inspection of Alloy 600 CRDM nozzles and J-groove welds have been based uniquely on a strong correlation between time to detectable PWSCC and operating temperature [A176], [A178], [A189]. Although evidence of heat-to-heat variability in susceptibility to PWSCC has been observed in the U.S. operating experience of CRDM nozzle cracking, it has not usually been considered necessary to include this feature for estimating the susceptibility ranking of different plants. Thus, the risk of cracking of CRDM nozzles in the U.S. PWR fleet is judged from a calculation of Effective Degradation Years (EDYs) expressed as a function of operating temperature, as shown in Equation A-17 [A370]:

$$EDY_{600^\circ F} = \sum_{j=}^{n} \left\{ \Delta EFPY_j \exp\left[-\frac{Q}{R}\left(\frac{1}{T_{head,j}} - \frac{1}{T_{ref}} \right) \right] \right\} \qquad \textbf{Eq. A-17}$$

where:

$EDY_{600^\circ F}$ = total effective degradation years normalized to a reference temperature of 600ºF (315.6°C)

$EFPY$ = effective full power years

Q_j = activation energy for crack initiation

R = universal gas constant (1.103 x 10^{-3} kcal/mole-ºR where ºR = ºF + 459.67)

$T_{head,j}$ = upper head temperature at 100% power during time period j T_{ref}

= arbitrary reference temperature (600ºF = 1059.67ºR)

n = number of different head temperatures during plant history

An example of the results for susceptibility ranking of the U.S. PWR fleet as a function of EDY toward the end of 2008 is shown in Figure A-35. This has been the basis for determining appropriate inspection intervals or taking decisions to replace upper heads.

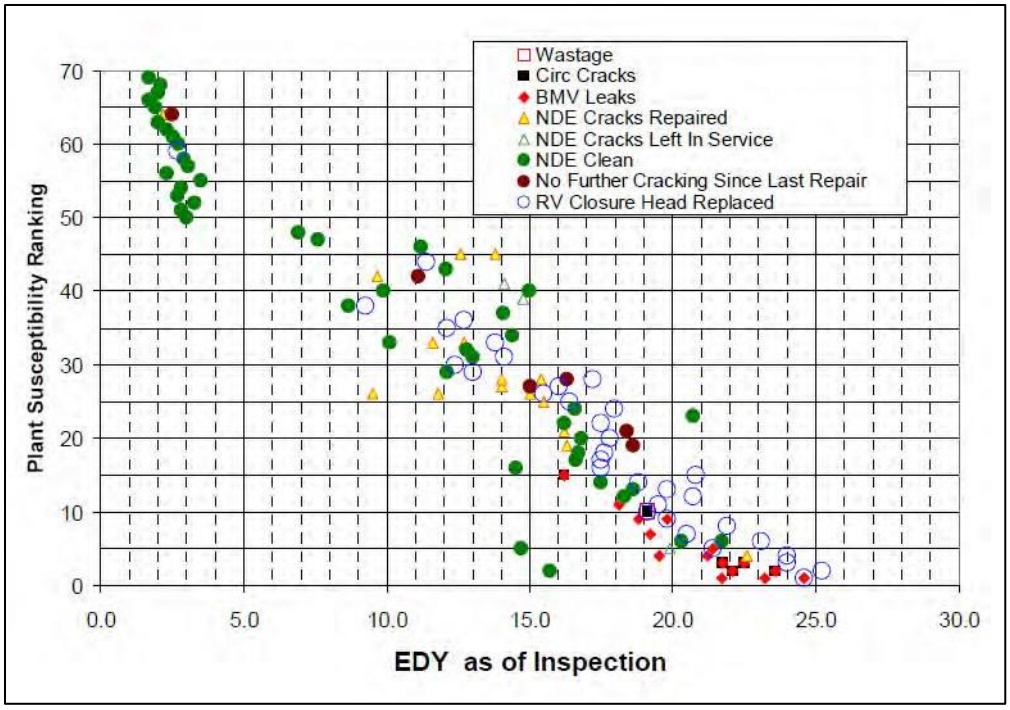

Figure A-35
Results of U.S. reactor vessel head penetration inspections updated late 2008 [A180]

NOTE:
The acronym BMV stands for Bare Metal Visual examination.

More complex models have attempted to include the stress dependency of PWSCC and some measure of the relative susceptibility of different heats of Alloy 600 in service as well as their operating temperature [A185], [A202], [A204]–[A207]. An empirical equation that is commonly used includes the inverse fourth power dependence on applied stress, the temperature dependence with an activation energy set equal to ~44 kcal/mole (~185 kJ/mole) in this case, and a material PWSCC susceptibility factor, or material index, based on the carbide morphologies of different heats of Alloy 600, as shown in Equation A-18:

$$t_f = C\frac{\sigma^{-4}}{I_m}\exp\left(\frac{E}{RT}\right) \qquad \textbf{Eq. A-18}$$

where:

t_f = the time to failure or observable cracking (hours)

σ = the applied stress (MPa)

I_m = the material susceptibility index

E = the apparent activation energy of 44,000 cal/mole

R = the universal gas constant (1.987 cal/mole)

T = the absolute temperature (°K)

C = a constant

For application to Alloy 600 components in French PWRs, a material susceptibility index was defined where a value of unity corresponded to a minimum failure time of 10,000 hours at a temperature of 325°C and an applied stress of 450 MPa [A202], [A205]. The time to failure can then be rearranged, as shown in Equation A-19:

$$t_f = \frac{10{,}000}{I_m I_\theta I_\sigma} \qquad \textbf{Eq. A-19}$$

where a temperature index, I_θ, and stress index, I_σ, are defined, as shown in Equations A-20 and A-21:

$$I_\theta = \exp\left[\left(\frac{-E}{R}\right)\left(\frac{1}{T}-\frac{1}{598}\right)\right] \qquad \textbf{Eq. A-20}$$

$$I_\sigma = \left(\frac{\sigma}{450}\right)^4 \qquad \textbf{Eq. A-21}$$

and I_m is the material susceptibility index defined above. The definitions of temperature and stress indices are therefore defined relative to reference conditions of 325°C (598 K) and 450 MPa.

To assess the likelihood of PWSCC occurring in a plant component, reliable estimates of fabrication stresses for different classes of components like CRDM nozzles are required together with an assessment of their material susceptibility indices and operating temperatures. The first of these objectives was achieved for the assessment of wrought Alloy 600 CRDM penetrations in French PWRs by extensive finite element modeling and by the manufacture and analysis of mockups of generic component items [A208]. This was complemented by a careful analysis of the effects of various surface machining and grinding techniques on surface stresses and cold work that drive PWSCC initiation [A209], [A210].

Determining material indices for the heats used to manufacture the plant components is a bigger challenge. As described earlier, laboratory studies have shown that PWSCC of Alloy 600 is very dependent on carbide morphology. The real carbide morphology of components in service cannot normally be known without destructive metallography, although a method has been developed to take replicas in situ in order to access this information [A206], [A371]. More generally, material susceptibility must be estimated. For example, for wrought Alloy 600 components in French PWRs, the effect of alloy composition and hot working processes (notably carbon content, yield strength after forging or rolling, and the temperature of final heat treatment) on microstructure and carbide morphology was studied. This was combined with accelerated laboratory testing for PWSCC susceptibility of archive materials or other heats comparable to those in service [A205], [A207]. Several different classes of PWSCC susceptibility indices were identified ranging from 1.1 (most susceptible) to 0.2 (least susceptible).

This method of assessment of the risk of PWSCC affecting Alloy 600 components was further developed by using a Monte Carlo approach to evaluate the equation for lifetime to failure (or observable PWSCC) quoted above. This approach allows the inherent dispersions in the input parameters of stress, temperature, activation energy, and material susceptibility index to be taken into account, leading to probabilistic predictions of component failure.

The Monte Carlo simulation technique of randomly sampling distributions of the input parameters in the equation describing lifetime to observable PWSCC to determine a distribution of failure times is illustrated in Figure A-36. Good agreement was obtained in this way between predictions and the results of repeated inspections of CRDM nozzles, which facilitated the timely planning of replacement upper heads. More recently, this analysis has been applied to possible axial PWSCC of BMI nozzles, which, unlike the CRDM nozzles, are often stress relieved with the reactor pressure vessel.

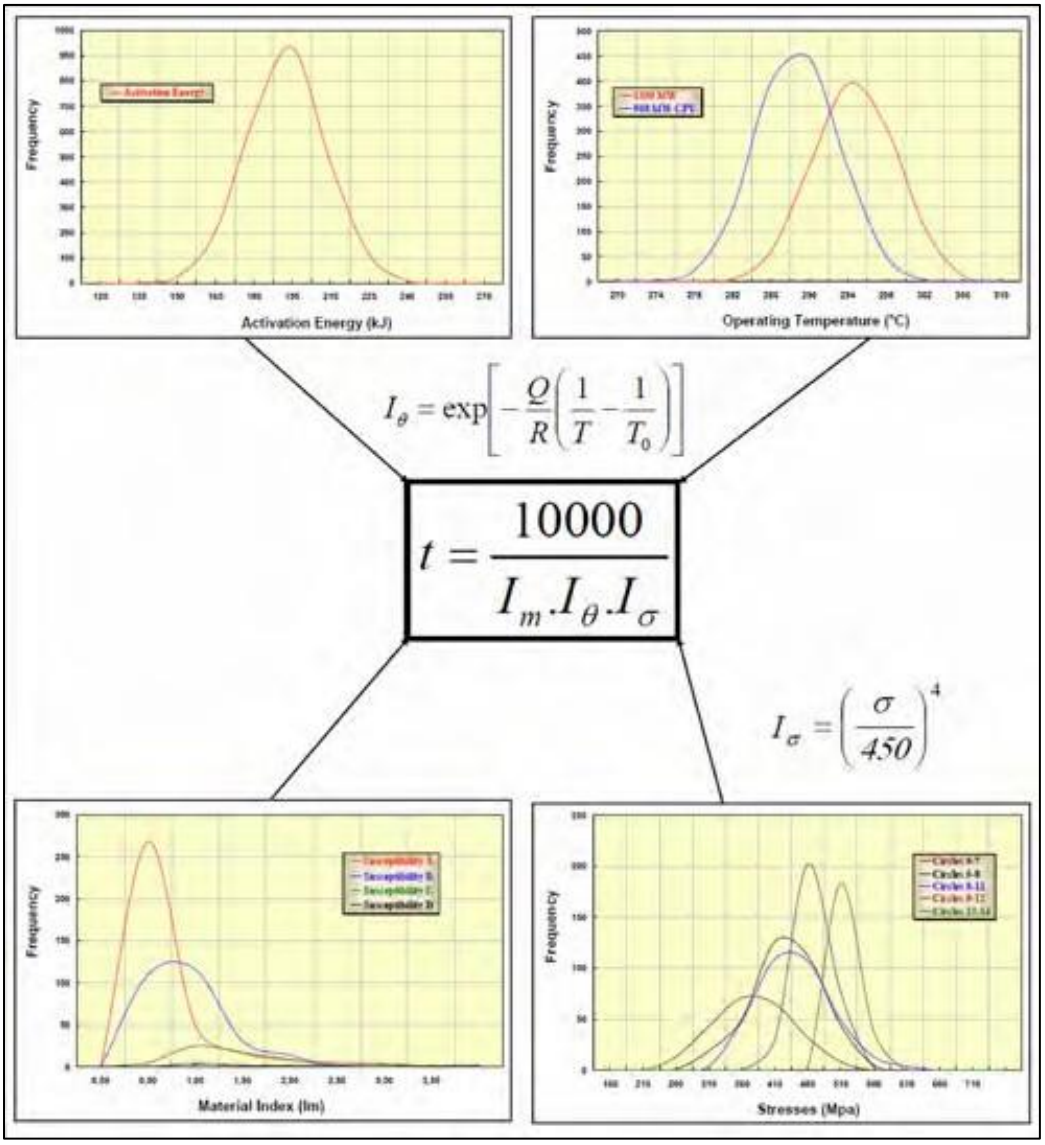

Figure A-36
Illustration of Monte Carlo simulation of upper head penetration cracking [A207]

A.3.2.9 IGA and SCC of Steam Generator Tubing Alloys in Secondary Circuits

There are several corrosion degradation modes that can occur in the steam generators of PWR, VVER, and CANDU systems, and these are mainly related to the presence of crevices around the tubes that are subject to a heat flux (see the earlier section on crevice corrosion). Aggressive environments may be created in these regions by boiling/evaporation concentration of impurities, which leads to localized crevice corrosion of carbon steel support plates (causing tube denting) as well as wastage, intergranular corrosion attack, and stress corrosion cracking of steam generator tubing. This section concentrates on IGA/SCC of PWR steam generator tube alloys, mainly mill-annealed Alloy 600, occurring primarily within the crevices between the tubes and their supports and under sludge piles that accumulate on the tube-sheet.

This topic is an extremely broad one and has been extensively reviewed on several occasions in terms of the various steam generator designs, the materials of construction, the localized environments that can occur, and, finally, the laboratory and field experience associated with mitigating these various cracking problems [A172]–[A174], [A211]–[A214]. Only a brief overview of the subject can be given in this appendix.

Environmental Chemistry Effects

The boiling/evaporation mechanism for concentration of secondary water impurities in superheated secondary side crevices potentially gives rise to remarkably concentrated solutions with concentration factors for different cationic and anionic impurity species of up to a million times depending on their solubilities and volatilities (Figure A-37). Depending on the ionic balance, solution pH values can vary from very alkaline to very acidic, although Na^+ cations often seem to predominate to give rise to highly caustic crevices. In addition, corrosion processes may be assisted by oxidizing species (such as Cu^{2+}) if present.

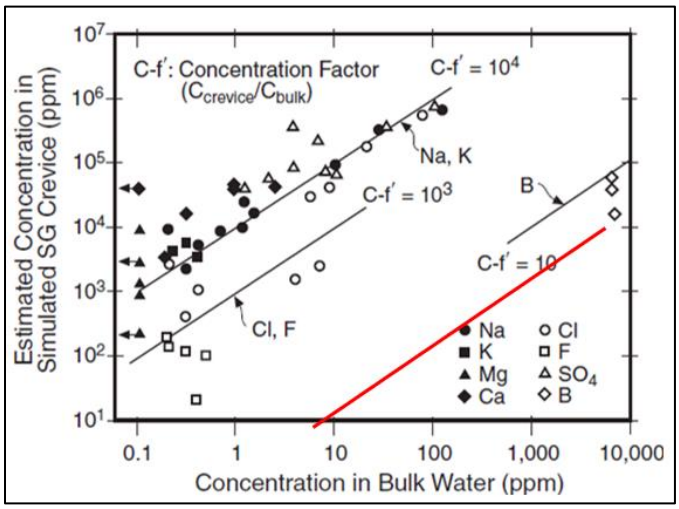

Figure A-37
Estimated concentrations of species in simulated steam generator crevices versus the concentration in the bulk water [A215]

> **NOTE**:
> The broad oblique line to the right of the figure denotes the condition where there is no concentration of species in the crevice.

It is, therefore, not too surprising that a significant amount of the corrosion damage on the secondary side occurs in high superheat crevices on the hot-leg side of the generator, since, intuitively, it would be expected that the cracking susceptibility would increase with local impurity concentration as well as with temperature. Moreover, it is to be expected that deoxidizing additions to the secondary environment, such as hydrazine, would ameliorate the cracking incidence rate, and that buffering additions of boric acid would be beneficial. However, there is no question that it is remarkably difficult to define the crevice chemistry accurately enough to be able to predict the level of SCC susceptibility with any great certitude, despite the development of sophisticated calculation tools such as MULTEQ [A216].

The potential/pH combinations where IGA/IGSCC has been observed in laboratory and reactor experience are shown in Figure A-38, superimposed on the Pourbaix diagram for nickel at 300°C [A217]. All of these modes of IGA/IGSCC are distinguished by predictable traits with respect to the changes in cracking susceptibility with potential, pH, material and environmental impurities [A212], [A214]. The potential pH region that results in the least corrosion is the one marked “Passive Region,” which is the region between pH 5 and 9 and at potentials about 50 mV and higher above the standard hydrogen (1 atm) line where protective oxide films provide the greatest resistance to corrosion and cracking. Note also that most of the degradation modes are very different from PWSCC (or LPSCC as it is described in Figure A-38) that occur in a lower range of corrosion potentials than those typical of the secondary side, due to the large difference in hydrogen concentrations between primary and secondary water.

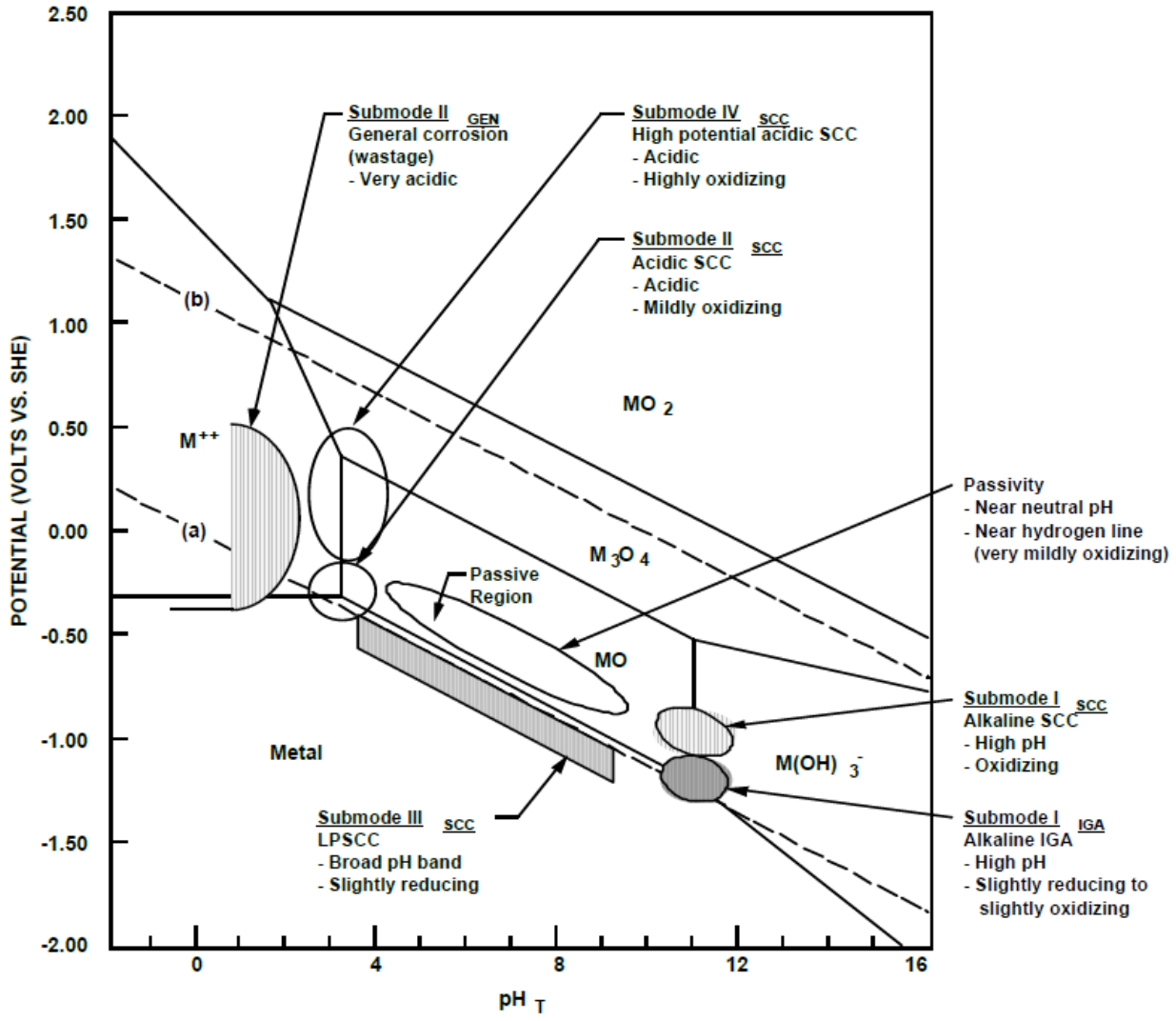

Figure A-38
Mill-annealed Alloy 600 corrosion mode diagram (T~300°C) superimposed on the Pourbaix diagram for nickel [A217]

NOTE:
The presence of lead or reduced sulfur species can lead to IGA or SCC in the passive area and aggravate attack in regions with IGA or SCC.

As noted in Figure A-38, there are fears that IGA/SCC in Alloy 600 exposed to lead impurities (and to a lesser extent, reduced sulfur species and some alumino-silicates) can affect passivity over a wide range of pH_T [A214], [A217] and, consequently, that the contribution of lead, in particular, may have been underestimated previously. In laboratory testing, small amounts of lead from 0.1 ppm upwards, regardless of its chemical form in the liquid phase, have been shown to cause rapid cracking (transgranular or intergranular) in Alloy 600 (and Alloy 800) over a wide range of pH_T (and also in Alloy 690TT, but only at low and high pH_T) [A214]. Further concern was provoked by high resolution ATEM examinations of 17 pulled Alloy 600 tubes with secondary side stress corrosion cracking from both recirculating and once-through steam generators that revealed significant concentrations of up to 20% lead incorporated into the crack

tip and flank oxides in two thirds of the samples examined [A218]. In many of the Alloy 600 pulled tubes examined by high resolution ATEM, the presence of lead had not been suspected from conventional chemical analyses. It also seems likely that the contribution of lead may have been underestimated in prior studies because lead cracking was often mistakenly associated with a uniquely transgranular cracking morphology. These results were the stimulus for a special workshop held in 2005 [A219], [A220]. Work continues to test Alloys 600TT, 690TT, and 800NG to see whether there are threshold corrosion potentials and pH_T, especially in the alkaline range, above which lead-induced stress corrosion cracking occurs [A221]. The only known defense at present is strict control of lead products in the manufacture and operation of steam generators combined with the use of sophisticated analytical techniques to determine lead concentrations in feedwater to ensure the lowest possible levels.

Alloy Chemical Composition and Microstructural Effects

A common feature of Alloy 600 steam generator tube cracking in PWR secondary side conditions and in PWR primary water is that there is a large heat-to-heat variability in the susceptibility of different heats to IGA/SCC [A172]. As in primary water, the reasons for this heat-to-heat variability are not completely understood but good intergranular carbide networks increase resistance [A172]. The favorable effect of good grain boundary carbide coverage is also evident from plant operating experience since Alloy 600 TT has been much less affected by IGA/IGSCC and after much longer periods in service compared to Alloy 600 MA [A222], [A223]. Some of these cases have been shown by examinations of pulled tubes to be due to the thermal treatment not being effective in improving carbide morphology. However, this cannot explain all cases observed to date, and there is concern that IGA/SCC could spread more widely in Alloy 600TT tube bundles remaining in service.

Laboratory testing has also shown that Alloy 600TT has greater tolerance of caustic crevice conditions than Alloy 600MA, as shown in Figure A-39.

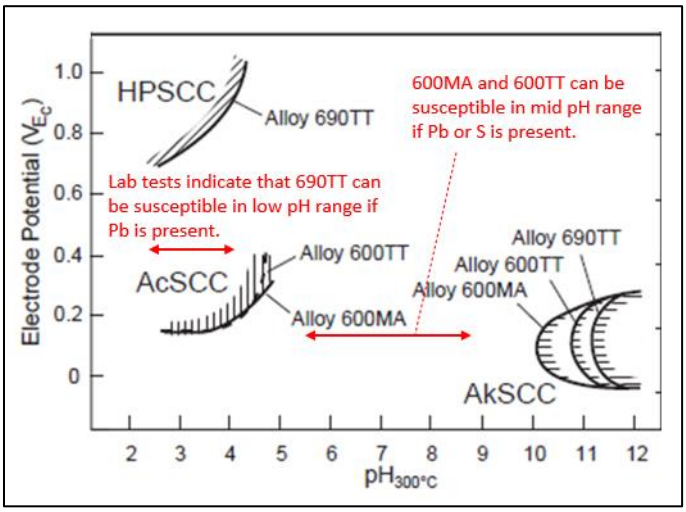

Figure A-39
Comparison of IGA/IGSCC susceptibility between Alloy 690TT and Alloy 600MA or TT at temperatures from 280 to 320°C as a function of pH and electrode potential [A214]

Alloy 690TT has not shown any signs of IGA/SCC in service to date, the first Alloy 690TT tube bundles having entered service in 1989. Laboratory testing has also shown great improvement in resistance relative to Alloy 600MA or 600TT. Indeed, the residual vulnerability of Alloy 690TT seen at high corrosion potentials in strongly acidic environments or at low potentials in very strong caustic environments is unlikely to be a practical threat given current secondary water operating conditions. However, as noted above, the effects of lead impurity accumulation that are not reflected in the experimental studies behind Figure A-38 and Figure A-39 can pose a threat to Alloy 690TT at low and high pH_T [A214], [A217].

Laboratory testing of Alloy 800, particularly the nuclear grade Alloy 800NG, has revealed some susceptibility to caustics and acid sulfates, albeit lower than Alloy 600MA. However, resistance to IGA/SCC is observed in near neutral solutions, even when sulfates or lead is present [A217].

Service performance has been good with KWU-designed PWR steam generators with Alloy 800NG tube bundles since 1972. In the context of secondary side corrosion issues, it is important to note that KWU have always emphasized the importance of the use of the modified nuclear grade specification for Alloy 800NG tubes in conjunction with design features to minimize impurity hideout. Nevertheless, in the first decade of this century, some secondary side IGA/SCC initiating from shallow pitting has been discovered [A224], [A225]. This degradation was observed either near the top of the tubesheet or in tubesheet crevices between the upper and lower roll expansion zones (in SGs where full depth rolling within the tubesheet was not carried out). There is some evidence that the upper roll expansions in the zone of the degraded tubes relaxed sufficiently after many years of operation to allow secondary water access to the crevice below.

Circumferential cracking of Alloy 800NG has also been reported associated with denting above the roll transition under hard sludge on the tubesheet top surface [A225]. These observations provoked a new laboratory study of the species likely to be concentrated by hideout under sludge with the most severe conditions being identified as moderately caustic with added lead oxide.

The use of Alloy 800NG tubing in CANDU recirculating SGs has also been reviewed where it has been used in CANDU 6 steam generators for ~30 years [A226], [A227]. Secondary side performance has also been excellent, although the lower temperatures of the primary (heavy) water coolant of CANDUs relative to most PWRs are probably significant in this context since it lowers the tendency to hideout of secondary side impurities. It is also noteworthy that these steam generators include many cases where the tubes were not expanded into the tubesheet, thus exposing them to potentially aggressive crevice conditions. However, in this case, there is more concern about vulnerability to crevice corrosion during plant shutdown than during high temperature operation.

Similar to German and Canadian experience with Alloy 800, VVER steam generators with titanium stabilized stainless steel tubes have also shown relatively few problems with secondary side cracking. Degradation has usually been attributed to the concentration of chlorides in boiling crevices. However, there remains a significant problem of extrapolating laboratory data developed in concentrated environments to field experience.

Mechanisms and Life Prediction

Crack propagation rates for Alloy 600MA as a function of pH have been observed to follow the trend in NiO solubility dependency over a wide pH range that covers the regions assigned to IGA/SCC [A212]. The stability and morphology of the various oxide films that can form alloys in PWR secondary side environments are also seen having a strong influence on the various mechanisms of cracking of Alloy 600 [A125]. These broad observations suggest that the slip-oxidation (or possibly, in some cases, the internal-oxidation) mechanism of crack propagation is a reasonable working hypothesis around which to interpret the empirical data for IGA/SCC of Alloy 600 in the various localized environments in PWR or CANDU secondary systems. In general, on this basis, it would be expected that:

- Cracking in concentrated local environments would be confined to a narrow potential range where the sides of the crack are protected by a stable oxide and the crack may propagate due to oxidation to a soluble species at the strained crack tip.
- Cracking susceptibility will be very sensitive to the presence of oxidizing or reducing species, which raise or lower the corrosion potential into or out of the cracking range.
- Alloying additions that increase the passivation rate will decrease cracking susceptibility, for example, the higher chromium alloys such as Alloy 690 will generally be more resistant. The same principle applies to local alloy chemical compositions within the microstructure, such as grain boundary chromium-depleted or nickel-enhanced zones.
- Slowly increasing loads associated with denting that increase the oxide rupture rate will increase the cracking susceptibility.
- Local plasticity associated with grain boundary sliding and its dependency on the presence or absence of grain boundary carbides will affect cracking kinetics.

The above deductions, nevertheless, are qualitative and in no way predict quantitative changes in cracking susceptibility of nickel-base alloys in PWR secondary systems. Given the complexity of the environmental chemistry, this is a difficult task [A214]. In the meantime, replacement of the most vulnerable steam generators with Alloy 600MA tube bundles is well advanced using mainly Alloy 690TT tube bundles.

Predicting the likely future development of IGA/SCC of Alloy 600 steam generator tubing on a plant-by-plant or steam-generator-by-steam-generator basis has been largely based on fitting the Weibull distribution to NDE data from the field [A200], [A213]. The number of tubes with NDE indications or the number of plugged tubes at each outage are fitted to the Weibull distribution as a function of operating time. The resulting Weibull plots tend to be steeper than those for PWSCC and have long offsets on the time axis. This is consistent with perceptions of the mechanism of IGA/IGSCC, which requires a significant time for the secondary side tube crevices to become flow restricted by deposits and then to concentrate any impurities. Subsequent development of cracking is then relatively rapid. Another approach that has been used is to try to predict the chemistry of the occluded secondary side crevice environments and then to use empirical relations derived from laboratory data for the time to observable cracking [A228], [A229].

A.3.2.10 SCC of High Strength Alloys

High strength alloys for components such as springs, bolts, tie rods, and valve stems in PWR, VVER, CANDU, and BWR primary coolants are either fabricated from precipitation-hardened nickel-base alloys or high strength stainless steels. For secondary water service and external bolting, low-alloy steels are used. All have had some instances of in-service cracking that is often attributed to hydrogen embrittlement, although for the nickel-base alloys in PWR primary water service, PWSCC probably also plays a major part.

Nickel-Base Alloys

The main high strength, nickel-base materials used in PWR primary circuits, including those in high neutron radiations fields close to the nuclear fuel, are Alloys X-750 and 718. They were originally developed for the aircraft industry and were adopted on the basis of their strength and resistance to general corrosion and stress relaxation [A230]. Yield strengths are in the range 800 to almost 1000 MPa for Alloy X-750 and up to 1400 or even 1500 MPa for Alloy 718, depending on the thermal aging heat treatment and any cold work prior to aging.

An austenitic material is often necessary for the purpose of fastening together austenitic stainless steel components without risk of thermally induced relaxation that would, for example, result from using a martensitic stainless steel with a significantly different coefficient of thermal expansion. The (cheaper) alternative to a precipitation-hardened, austenitic stainless steel is limited to the intermediate strength A-286 grade [A172].

The composition of Alloy X-750 is close to that of Alloy 600 except for higher contents of titanium, aluminum, and additions of niobium required for strengthening [A230], [A231]. High strength is developed by heat treatment after solution annealing that leads to a homogeneous distribution of γ' $Ni_3(Al,Ti)$ precipitates that are coherent with the austenite matrix. Among the choices of heat treatment available for Alloy X-750, two have been used extensively: a two-step thermal treatment at 885°C and 704°C (AH) and a high temperature solution annealing at ~1100°C followed by single-step aging at 704°C for 20 hours (HTH) [A231]–[A234]. The latter has been adopted in both PWRs and BWRs for maximum resistance to SCC, although attention to surface finish, avoiding intergranular oxidation during heat treatments, and in-service stresses are also essential.

Alloy 718 is an age-hardenable nickel-base alloy containing 17-21% Cr and a higher niobium content than Alloy X-750 that can be heat treated to very high strengths due to precipitation of a fine distribution of nanometer size γ', $Ni_3(Al,Ti)$, and γ'', $Ni_3(Nb)$. The standard aeronautical heat treatment has generally been used after solution annealing that involves thermal aging at 720°C for eight hours, furnace cooling at 55°C/h followed by eight hours at 620°C, and then air cooling. It is used extensively for springs and bolts in fuel elements where it can be irradiated to very high neutron doses during the time a fuel element spends in the core. Alloy 718 has proved to be reasonably reliable in PWR primary water, including highly irradiated conditions where it must also resist significant thermal- and irradiation-induced relaxation. Alloy 718 has the reputation of being very resistant to PWSCC initiation but relatively susceptible to propagation once an intergranular crack is initiated. Nevertheless, many fewer incidents of PWSCC of Alloy 718 have been reported compared to Alloy X-750 [A172], [A235]. These have been attributed to intergranular oxidation of the surface during product rolling due to loss of control

of the chemistry of the furnace atmosphere, which then had a severe adverse influence on resistance to PWSCC initiation. Clearly, for optimum PWSCC resistance in service, it is essential to remove any layer affected by oxidation in the furnace atmosphere, as noted previously for Alloy X-750.

One side effect of the heat treatment of Alloy 718 is the formation of the δ phase, which is a thermodynamically more stable form of the γ' strengthening phase. Its formation can lead to γ' denuded zones on either side of grain boundaries that, in principle, may allow strain localization. It has often been commonly accepted that the formation of the δ phase on grain boundaries in Alloy 718 has an aggravating influence on PWSCC susceptibility, particularly intergranular crack growth susceptibility [A236]. However, others have not observed a major effect of δ phase on product performance and indeed noted that it is a necessary feature to avoid excessive grain growth during solution annealing prior to thermal aging [A372]. Such disagreement on the importance or otherwise of the presence of δ phase for PWSCC resistance has prompted studies that reassess its role, particularly the morphology of δ phase formed at different temperatures [A237], [A238].

Stainless Steels

The main high strength, stainless steels reviewed here are Alloy A-286 PH austenitic stainless steel, Type 410 and similar martensitic stainless steels, and Type 17-4 PH martensitic stainless steel. Small numbers of these components have proved to be susceptible to stress corrosion or hydrogen embrittlement in service.

Alloy A-286 is an austenitic, precipitation-hardened, stainless steel that is strengthened by γ' precipitates, $Ni_3(Ti,Al)$, formed during aging at 720°C. It is used when the expansion coefficient relative to other austenitic stainless steels is an important design factor. It is, however, susceptible to IGSCC in PWR primary water when loaded at or above the room temperature yield stress, typically 700 MPa [A239]–[A244]. Cold work prior to aging in combination with the lower of two commonly used solution annealing temperatures of 900 and 980°C has an adverse effect on resistance to IGSCC [A240]. Hot heading of bolts can create a heat-affected zone between the head and shank and is believed to be another adverse factor. However, even if all these metallurgical factors are optimized, immunity from cracking cannot be assured unless the stresses are maintained below the room temperature yield stress, which necessitates tight quality control of the head-to-shank and thread stress concentrations and strictly controlled bolt loading procedures. It is also suspected that superimposed fatigue stresses can lower the mean threshold stress for IGSCC even further. Finally, the available operating evidence indicates that impurities and dissolved oxygen can help crack initiation. Stress corrosion cracks grow relatively easily in Alloy A-286 stainless steel once initiated, even in properly controlled PWR primary water [A241].

Components such as valve stems, bolts, and tie rods requiring rather high strength combined with good corrosion resistance in PWR primary water have often been fabricated from martensitic stainless steels, particularly Types 410 and 17-4 PH. A significant number of failures of martensitic stainless steels such as Type 410 have occurred in PWR service, as noted for example in NRC Information Notices [A245]. In most cases, the affected components have usually entered service in an excessively hard condition due to tempering at too low a temperature. No in-service aging seems to have been involved, these materials being susceptible

to hydrogen embrittlement in the as-fabricated and hardened condition. Galvanic corrosion due to contact with graphite-containing materials in valve packing glands has also occurred, sometimes leading to valve stem seizure. The preferred replacement material has usually been Type 17-4 PH with its higher chromium and molybdenum content that no doubt confers better resistance to crevice corrosion in valve packing glands.

Type 17-4 PH is a precipitation-hardened stainless steel for which a significant number of cracking failures have also occurred in PWR primary water [A246]–[A249]. Initially, intergranular cracking, probably due to hydrogen embrittlement, was associated with the lowest temperature aging heat treatment, at 480°C (900°F) and designated H900, which gives a minimum Vickers hardness value of 435 HV. Such a hardness value is clearly in excess of the limit of 350 HV commonly observed to limit the risk of hydrogen embrittlement in reactor coolants. The 593°C (H1100) aging heat treatment was subsequently widely adopted and should normally yield a hardness value below 350 HV. Nevertheless, a small number of failures, due either to brittle fracture or hydrogen embrittlement, have continued to occur, but after relatively extended periods of service. The origin of these failures appears to be thermal aging embrittlement in service. Corrosion-related failures have also been aggravated by impurities from valve packing gland materials.

Two main thermal aging mechanisms of martensitic stainless steels have been identified. The first "reversible temper embrittlement" is related to the diffusion of phosphorus to grain boundaries at aging temperatures generally above 400°C and can occur in both Types 410 and 17-4 PH stainless steels. The grain boundaries are consequently embrittled and are particularly susceptible to intergranular cracking by hydrogen embrittlement, but no general increase in hardness is observed. Temper embrittlement can be reversed by heat treating around 600°C and, in practice, is largely avoided by reducing the phosphorus content and by small alloying additions of molybdenum.

The second thermal aging embrittlement mechanism is relevant only to PH stainless steels such as Type 17-4 PH. It arises from an intra-granular decomposition of the martensitic matrix into two phases, α-phase which is rich in iron, and α'-phase which is rich in chromium. A generalized increase in hardness is observed with corresponding increases in strength and ductile/brittle transition temperature and loss of fracture toughness. The hardening cannot be reversed without re-solution annealing. This aging mechanism can occur in Type 17-4 PH steels on time scales relevant to the design lives of PWRs at temperatures exceeding 250°C, and quantitative models for component assessment have been developed [A246], [A248].

Low-Alloy Steels

High strength low-alloy steels are used in many external fastener applications in nuclear power reactors, including support bolting and pressure boundary fasteners, and a significant number of failures of this class of component have occurred [A250]. Most have been described as corrosion-related failures. Tempering at too low a temperature to produce overly hard, very high strength structures susceptible to hydrogen embrittlement has played a significant part in such failures. Like the martensitic stainless steels, they can be susceptible to temper embrittlement and consequently to enhanced risk of intergranular hydrogen embrittlement. Remedies for avoiding temper embrittlement are the same as for the martensitic stainless steels.

Support bolting (typically AISI 4340 and 4140 low-alloy steels) with yield strengths greater than 1050 MPa (150 ksi) has failed by hydrogen embrittlement due to a combination of excessive applied stresses and humid or wet environments collecting around the bases of components. Non-stainless component support bolting with lower yield strengths is considered not susceptible to cracking in such environments [A251]. An upper bound strength limit can normally be defined by a hardness level acceptance criterion to guard against hydrogen embrittlement susceptibility in these circumstances.

A second category of bolt failures is concerned with the integrity of the primary pressure boundary at locations such as flanges of manway covers and valves. Most of these incidents have been caused by erosion-corrosion in PWR primary water leaks, as described in an earlier section. A small number of failures among this category of bolts have been associated, however, with hydrogen embrittlement rather than wastage [A250]. The ferritic bolting steels involved were not out of specification but had been in contact with molybdenum disulfide lubricants. It has been suggested that the lubricant dissociated on contact with hot water to yield hydrogen sulfide, which is a severe hydrogen embrittling agent for ferritic steels.

A.3.2.11 Delayed Hydride Cracking (DHC) of Zirconium Alloys

The CANDU design uses a Zirconium alloy (Zr-2.5Nb) as the pressure tube that encloses each fuel assembly and is a part of the primary pressure boundary. A zirconium alloy is used to increase neutron economy. These Zr-2.5Nb pressure tubes have been found to be susceptible to a hydrogen-assisted cracking mechanism, termed *delayed hydride cracking (DHC)*. DHC is a multi-step, diffusion-controlled process (Figure A-40). Over time, there is an uptake of hydrogen (or deuterium) in the pressure tube material. Hydrogen in solution in the zirconium alloy is transported to the crack tip by diffusion processes where it precipitates as a hydride phase. When a critical state is reached, related to the hydride precipitate size and the applied stress intensity factor, K_I, fracture ensues, and the crack extends through the brittle hydride and arrests in the matrix. Each step of crack propagation results in crack extension by a distance approximately the length of the hydride.

The crack tip hydride grows due to the migration of hydrogen from hydrides in the bulk of the material at some characteristic distance from the crack tip. The driving force for the diffusion of the hydrogen is the difference in the chemical potential of hydrogen in the crack tip hydride due to the local hydrostatic stress field and the chemical potential of hydrogen in the hydrides under a reduced hydrostatic stress at a distance from the crack tip. Of most significance for CANDU pressure tubes is the potential for hydride formation and fracture to occur at the tips of existing flaws. The presence of hydrides in the bulk of the material is not a sufficient condition for cracks to grow significantly. However, when formed in the high stress area at a crack tip, fracture of the hydrides can occur, resulting in crack growth by DHC.

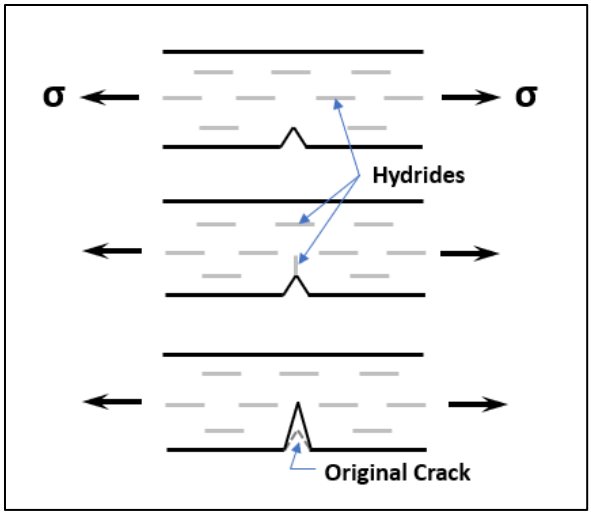

Figure A-40
Illustration of hydride cracking in a pressure tube [A252]

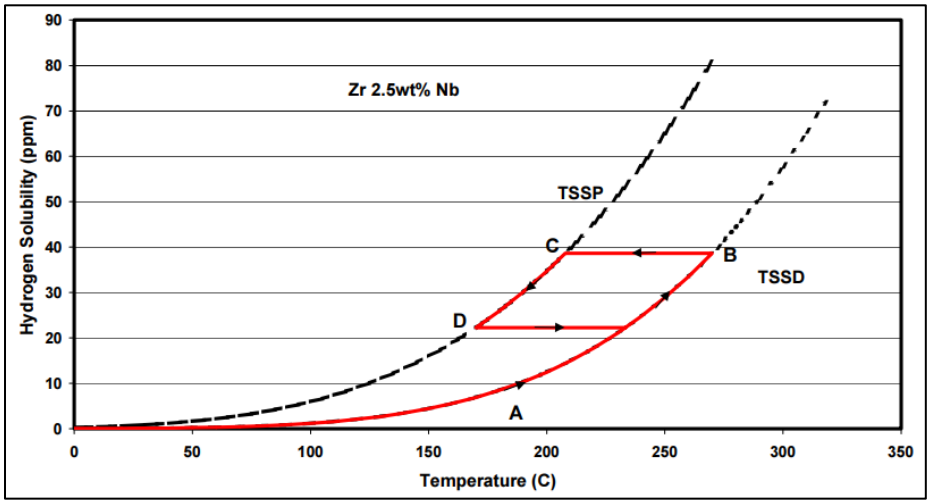

Figure A-41
Hydrogen solubility as a function of thermal history [A252]

A study of the DHC phenomenon has also shown that there is a significant hysteresis effect associated with hydrogen solubility depending upon whether hydrides are dissolving or precipitating. The effect is manifested as a difference between the concentration of hydrogen in solution in the metal in equilibrium with dissolving hydrides at a particular temperature and the concentration in equilibrium with precipitating hydrides at the same temperature. Figure A-41 illustrates this effect, where a temperature progression from A to D and back to A can result in significant differences in hydrogen solubility at the same temperature. Additionally, DHC crack growth rates have been shown to vary depending on thermal history. At the same temperature, the crack growth rate can vary from a maximum possible value down to zero.

Although a number of DHC-related cracking events occurred early in service life, improved design, maintenance and fabrication practices have been successful in preventing subsequent failures in CANDU reactors. The ends of the pressure tubes are of most interest at present. There is an increased probability of hydride formation at these locations, as well as the presence of cold work and increased corrosion associated with the stainless steel pressure tube end fittings.

A.3.2.12 Irradiation-Assisted (IA) SCC of Stainless Steels

Irradiation-assisted stress corrosion cracking (IASCC) is a term that defines SCC of core structural materials in water-cooled nuclear power reactors in which neutron and/or γ irradiation contribute directly to the initiation and propagation of cracks. By implication, in the absence of material damage by fast neutrons and/or modification of the environmental chemistry by ionizing radiation, SCC either does not occur or is significantly less severe.

A summary of observations attributed to IASCC in the austenitic stainless steels of core internals of BWRs and PWRs is shown in Figure A-42 together with an overview of the mechanisms of irradiation damage in austenitic stainless steels as a function of neutron fluence. The difference in the apparent IASCC threshold neutron fluences between BWRs and PWRs (and by analogy VVERs) is primarily attributed to the difference in corrosion potential established in the oxygenated NWC of BWRs and the hydrogenated primary water chemistry of PWRs (and VVERs). Note also the order of magnitude difference in the maximum possible neutron fluences for an initial license period of 40 years, which is in large part due to the difference in the widths of the water gaps between the outermost fuel elements and core support structures in BWRs and PWRs.

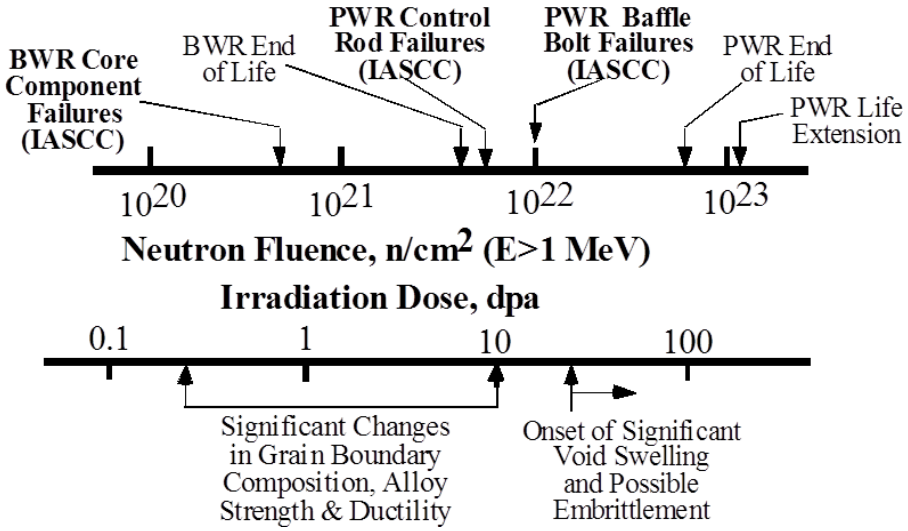

Figure A-42
Summary of IASCC in light water reactors and associated metallurgical changes in austenitic stainless steels as a function of neutron irradiation in n/cm^2 (E ≥ 1 MeV) or displacements per atom (dpa) [A253]

NOTE:	
~15 dpa ≈	10^{22} n/cm^2 E ≥ 1 MeV (for PWR and BWR neutron spectra)
~7 dpa ≈	10^{22} n/cm^2 E ≥ 0.1 MeV (for PWR and BWR neutron spectra)

BWR Core Support Structures

The earliest incidents of IASCC in BWRs occurred during the 1960s and were associated with cracking of Type 304 stainless steel fuel cladding. The driving forces for the cracking were the tensile hoop stress in the cladding due to swelling of the fuel and the highly oxidizing conditions in the NWC environment. Since the mid-1980s, there have been an increasing number of observations of intergranular cracking in stainless steel BWR core components somewhat more remote from the fuel when exposed to fast neutron irradiation. Initially, the observations were on highly stressed components, such as control blade sheaths operating under relatively poor coolant purity conditions. This occurred when an apparent "threshold" fluence level ($>5 \times 10^{20}$ n/cm^2) was exceeded (Figure A-43).

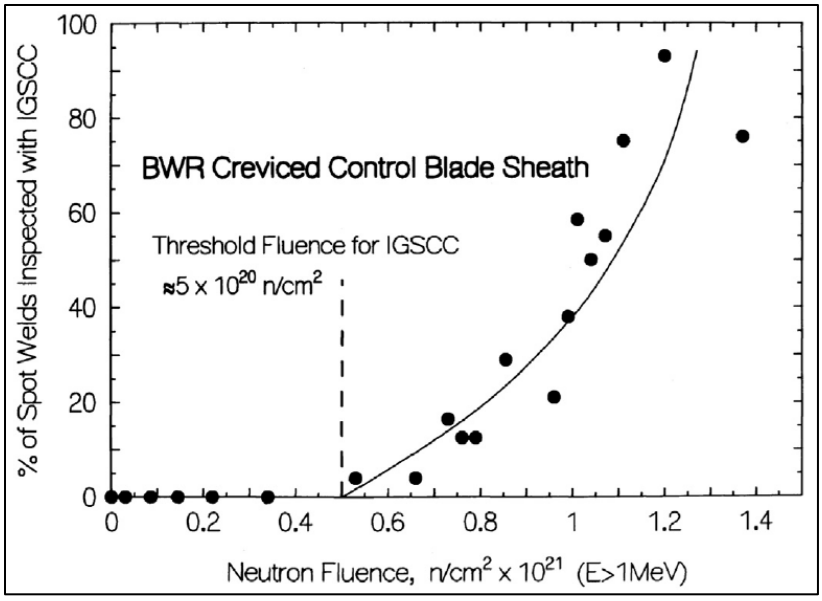

Figure A-43
Dependence of IASCC on fast neutron fluence for creviced control blade sheaths in high conductivity BWR coolants where the tensile stress is high due to spot welds and dynamic due to swelling B4C absorber tubes [A49]

IASCC has since been observed at lower fluences in larger welded BWR core shroud structures, with the extent of cracking depending on specific combinations of prior thermal-sensitization due to the fabrication procedure, fast neutron flux and fluence, weld residual stress, and coolant purity [A254]–[A258]. Thus, it should be noted that full susceptibility to IASCC does not appear suddenly at a threshold level. Instead, susceptibility begins to be measurable at a certain "practical IASCC threshold" neutron fluence level and escalates with increasing neutron fluence over several orders of magnitude of fluence. Interactions with prior fabrication-induced cold work further complicate the practical concept of a threshold neutron fluence.

The substitution of Type 304 stainless steels with L-grade and stabilized alloys (Types 304L, 316L, 347) for irradiated BWR components increased the operating time before cracking was observed. However, IASCC incidents continued to occur after approximately nine effective full power years, especially if the component was severely surface cold worked by grinding, straightening, etc. during manufacture. The IASCC susceptibility of irradiated BWR stainless steel components responded to the various system parameters (i.e., material, stress, and

environment) in much the same manner as observed for non-irradiated stainless steels discussed earlier. Thus, it became accepted that IASCC in BWRs was not a fundamentally new mechanism of cracking but was merely mirroring irradiation-induced changes to the rate controlling parameters for the various phases in crack development described earlier for non-irradiated stainless steels. Such irradiation-induced changes could affect the corrosion potential, stress, grain boundary composition, and yield stress.

PWR Core Support Structures

PWR field experience has also shown that intergranular cracking of highly irradiated, stainless steel core components can occur. The earliest experience of cracking was in Type 304 cladding of both control rods and (now obsolete) fuel pins. The cracks apparently initiated on the external surfaces and showed a clear dependence on neutron dose and cladding strains caused either by swelling of the neutron absorber or fuel pellets [A259].

IASCC was subsequently detected in cold-worked Type 316 core baffle-former bolts of some first generation (CP0 series) 900 MWe French and Belgian PWRs from 1989 onward [A260]. Baffle-former bolt cracking has also been identified in some U.S. PWRs inspected to date [A262], [A263], [A373]–[A375]. Fast neutron doses of > $2x10^{21}$ n/cm^2 (E > 1 MeV) (~3 dpa) and strains > 0.1% have been implicated in the cracking. A small number of IASCC failures of equivalent bolting manufactured from titanium stabilized stainless steel have also been observed in VVER core internals.

Example bolts extracted from PWR baffle bolts with NDE indications have been examined metallographically, which has confirmed the intergranular nature of the cracking typically located between the bolt heads and shanks [A261]. In French CP0 900 MWe PWRs, there are 120 bolts on each former level that fasten the baffles to the formers thereby giving a total number of 960 bolts, so that a Weibull analysis of the evolution of cracking as a function of neutron dose was feasible (Figure A-44). The results showed a strong dependence on neutron fluence and reinforced the conclusion that the cause of baffle bolt cracking was IASCC. The heat of stainless steel used to fabricate the bolts, the number of major power transients (between 15 and 100% full power), and the differential thermal expansion loads applied to the bolts were found to be additional important influencing parameters.

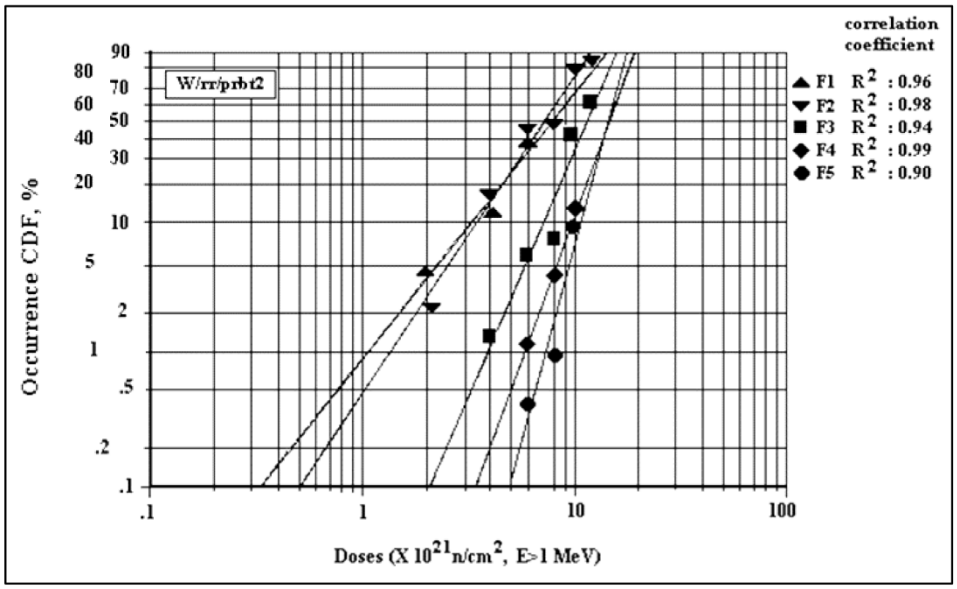

Figure A-44
Weibull plot of the percentage of defective baffle/former bolts on former levels 1 to 5 as a function of neutron dose based on the data for all inspections combined for a French CP0 series PWR [A260]

A factor specific to the PWR baffle-former bolts in the CP0 series of French 900 MWe plants where IASCC was detected is the presence of a closed crevice around the bolt shank [A259], [A260]. Later plants have small holes in the former plates that allow cooling water to flow around the shank of each bolt. This has led to speculation that local radiolytic production of oxidizing species might occur due to limited access of hydrogenated primary water. However, no evidence of oxidizing conditions has been found on extracted bolts. Moreover, laboratory simulations of crevices irradiated by high energy protons that reproduced irradiation intensities and quality equivalent to in-core conditions have also failed to reveal the formation of any oxidizing species within irradiated crevices [A254], [A255]. An alternative hypothesis for PWR baffle bolt cracking is that local boiling due to γ heating could cause the confined environment to become strongly alkaline by concentrating lithium hydroxide in the liquid phase. Again, there is no evidence for this in the form of mineral precipitates containing boron that are observed when PWR primary water is allowed to boil (as, for example, on fuel cladding in the case of the Axial Offset Anomaly).

The conclusion, therefore, is that cracking of PWR baffle-former bolts is caused by IASCC in normal quality PWR primary coolant once the combination of neutron dose and stress exceeds the levels required to initiate intergranular cracking. However, attention is drawn to the potentially very complex evolution of bolt stresses with time as a result of interactions between irradiation creep and differential swelling between cold-worked baffle-former bolts and solution-annealed baffle plates (see later). Moreover, detailed design factors clearly play an important role, for example, lower neutron fluences due to fuel management (aimed primarily at reducing neutron flux to the reactor pressure vessel) and lower temperatures due to reduced gamma heating. The latter are also linked to fuel management, the direction of water flow in the inter-space between the baffle plates and the core barrel, and, where available, cooling water flow around the shank of each bolt. Yet another factor is the detailed design of the baffle-former bolt head to shank junctions that affect the stress concentration factor in this location.

Mechanisms and Life Prediction

Considerable effort and expenditure have been devoted to studying IASCC mechanisms over the last two decades, including a major contribution from an EPRI coordinated international cooperative program on IASCC known as "the CIR program" [A264]. The overall goal was to try and develop better models for life prediction. While not fully successful in that respect due to the complexity of the problem and experimental difficulties associated with working with highly activated stainless steels, considerable progress was made, as outlined below.

Irradiation effects on mechanical properties of austenitic stainless steels and irradiation creep are common to both BWRs and PWRs and are described in more detail later. Clearly, from the earlier discussion of SCC in austenitic stainless steels, both have an important impact on the mechanisms and prediction of IASCC. Irradiation creep can have an obvious effect on relaxation of residual stresses driving IASCC. In addition, in PWRs, the higher projected end-of-life neutron fluences are sufficient for void swelling to be possible, as also described in more detail in a later section. If void swelling occurs, differential swelling between cold-worked baffle-bolt materials and solution-annealed former materials can lead to an increase in stress applied to the bolts. This increase in stress though could be counteracted by irradiation creep, and this complex interaction needs to be evaluated in the context of life prediction.

The effect of yield strength on SCC growth rates was discussed earlier for non-irradiated austenitic stainless steels (see Figure A-24) and was accounted for via its effect on the crack tip strain rate. Such an increase in crack propagation rate with yield stress appears to be a common effect among many materials and many mechanisms of yield strength enhancement (e.g., cold work, martensite formation, irradiation hardening, and precipitation hardening, etc.) [A265]. It can be noted that SCC propagation rates in stainless steels increase with yield strength in both BWR and PWR primary water chemistries.

Other irradiation effects may influence the environmental water chemistry and corrosion potential as well as the microstructural alloy chemical composition of grain boundaries and are described in more detail below.

The increase in corrosion potential associated with radiolysis of BWR NWC coolant and the consequent generation of dissolved oxygen and hydrogen peroxide lead to a predictable (from the slip-oxidation mechanism) increase in IASCC propagation rates if all other parameters are held constant. This is illustrated by the data obtained on pre-cracked specimens of furnace sensitized stainless steel exposed to high temperature water in either a variable energy cyclotron or the core of an operating nuclear reactor [A254], [A255], [A266]. See, for example, Figure A-45, where the observed and predicted crack depth versus time relationships for the furnace sensitized stainless steel exposed in a non-irradiated recirculation line and in an irradiated core instrumentation tube of a BWR are compared. The observed and predicted effect of irradiation in increasing the crack propagation rate via its effect on the corrosion potential alone is apparent.

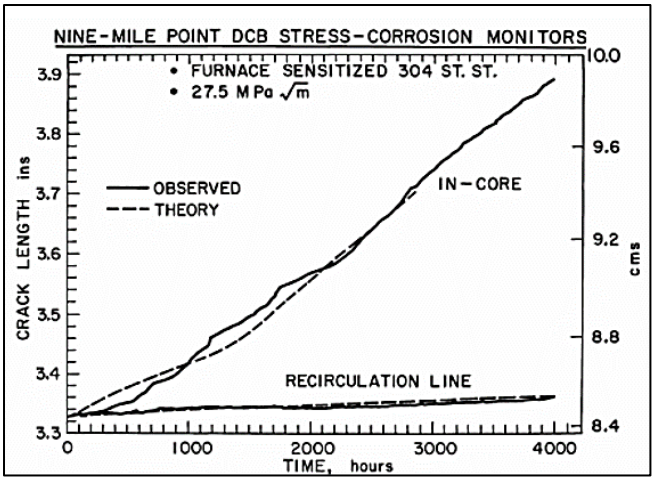

Figure A-45
Crack length versus time for DCB specimens of sensitized Type 304 stainless steel exposed in a BWR core (at high corrosion potential from radiolysis) and in the recirculation line [A254], [A266]

Reducing the corrosion potential via correct application of HWC/NobleChem^{TM} should, therefore, significantly slow down the propagation of cracks in BWR core components [A267], [A268], [A269]. However, this prediction is tempered to a certain extent by the fact that there are clearly other conjoint system conditions that can affect cracking susceptibility even at low corrosion potentials, as evidenced by the cracking of baffle-former bolts in PWRs, albeit with a significantly higher apparent neutron fluence threshold. Candidate additional mechanisms for increasing IASCC susceptibility at high fluences are a rise in hydrogen embrittlement susceptibility associated with increasing tensile strength due to irradiation hardening, and an accumulation of helium from boron and nickel (n, α) transformation reactions. Due to the insolubility of helium in metals, it is trapped in cavities and/or forms many tiny nanometer size gas bubbles as irradiation progresses with a detectable tendency to accumulate on grain boundaries [A270]–[A273]. Hydrogen is also trapped in the bubbles initially created by helium.

Grain boundary chemical composition of irradiated austenitic alloys is, in general, altered by neutron radiation-induced segregation (RIS), which is driven by the flux of radiation-produced defects to sinks. RIS, therefore, is fundamentally different from thermal segregation processes (e.g., sensitization from Cr carbide or boride formation and growth) discussed earlier with respect to IGSCC of non-irradiated stainless steels. Nevertheless, the effect of RIS on cracking of irradiated stainless steels can be very pronounced even though the profiles of Cr, Fe, and Mo depletion and Ni and Si enrichment are very narrow compared to the Cr-depletion profiles that form from thermally induced Cr carbide formation during welding or heat treatment; see for example [A258]. For BWR applications, Cr-depletion was quantified and fitted to an empirical equation in terms of an effective EPR parameter equivalent to that measured electrochemically for the same minimum Cr-depletion on thermally sensitized stainless steels [A256], as shown in Equation A-22:

$$EPR_{eff} = EPR_0 + 3.36x10\text{-}24(fluence)1.17 \qquad \textbf{Eq. A-22}$$

where EPR_0 represents any initial grain boundary sensitization due to thermally activated chromium depletion; the fluence is in units of n/cm^2.

Although radiation-induced Cr-depletion at grain boundaries has a significant and predictable role in increasing cracking susceptibility of austenitic stainless steels in BWRs, it has no effect at low corrosion potential in PWR primary water. Consequently, there has been considerable effort to define the role of other elemental radiation-induced grain boundary segregations/ desegregations [A264], [A274]–[A276]. However, it is still not possible to quantify the effects of the segregation of these other elements on IASCC at low corrosion potential, although there is some evidence that silicon enrichment at grain boundaries may be detrimental.

Based on the discussions above, it is apparent that fast neutron irradiation can affect many controlling parameters for IASCC and that these effects can take place over different time and geometrical scales. For example, the neutron flux will have an immediate effect on the corrosion potential in direct cycle BWRs operating on NWC, whereas radiation-induced segregation at grain boundaries, increases in yield stress, and relaxation of residual stress will all take effect over time as neutron fluence accumulates. Regarding the geometrical aspect, the neutron flux will be attenuated through the thickness dimension of a thick component such as a BWR core shroud. Thus, not only is the fluence changing over time, but also the fluence affecting the crack tip can change as the crack propagates into the irradiated component. Predicting these combined effects and their impact on crack propagation in BWRs is certainly complicated but is made possible by making logical changes to the inputs of the prediction methodology developed for non-irradiated stainless steels based on the slip-oxidation mechanism.

An example of a predicted crack depth versus time relationship is shown in Figure A-46 for a welded BWR core shroud. It is seen that the propagation rate changes with time, i.e., neutron fluence, mirroring both the time-dependent reduction in weld residual stress and the increase in grain boundary Cr-depletion. In this particular case, the Cr-depletion is attributed to the initial thermally induced sensitization at grain boundaries due to the welding process used plus an additional depletion that occurs with neutron fluence at the particular point analyzed in the shroud. In addition, these crack propagation rate responses will change with other parameters known to affect IGSCC in stainless steels such as water purity (conductivity) and extent of surface cold work. It is also apparent that a constant disposition crack propagation rate formulated for ease of application for regulatory purposes may give erroneously high predictions of the real extent of future crack growth.

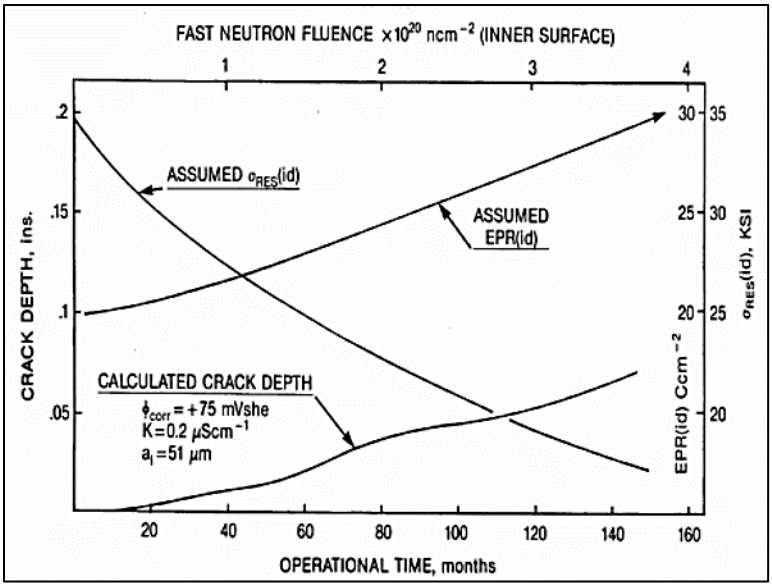

Figure A-46
Predicted crack depth versus time response for cracks propagating in the beltline weld of a core shroud illustrating the non-monotonic variation in crack propagation due to the competing effects of fast neutron irradiation on grain boundary chromium depletion and on residual stress relaxation [A256], [A266]

The comparison between prediction by the slip-oxidation mechanism and observation of IASCC in BWRs is limited by two considerations:

- Uncertainty in the definition of the system, such as the initial material conditions, coolant purity, and corrosion potential, but most significantly, that associated with the definition of weld residual stress
- Uncertainty in defining the observed crack depths and, to a lesser extent, surface lengths

The effect of these uncertainties is shown by the comparison in Figure A-47 (left image) between the observed and predicted crack depths adjacent to a horizontal H4 beltline weld in a BWR core shroud, where the observations have been made during consecutive reactor outages. It is apparent that the best that can be accomplished is to predict the range in crack advance associated with a range in estimated weld residual stresses. This comparison is made in the right image in Figure A-47 for various BWR core shroud welds (H3, H4, H6) manufactured with different stainless steels (Types 304, 304L). Over this population, the agreement between observation and prediction is reasonable, given the uncertainties in observation and definition of the system.

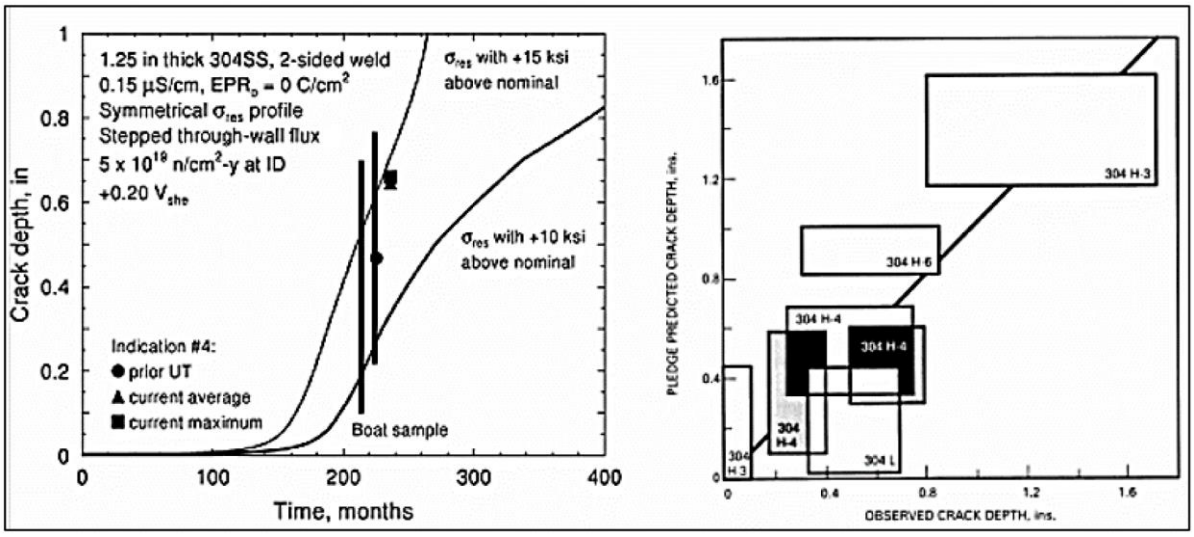

Figure A-47
Crack length versus time predictions and observations for a Type 304 stainless steel BWR core shroud with multiple inspections and multiple cracks (left), and comparison of observed and predicted crack depth for a number of BWR core shrouds (right) [A256]

For PWR applications, where it is not immediately apparent that the slip-oxidation mechanism is always applicable, especially at high neutron fluences, a more empirical approach has been taken to forecasting likely increases in the fraction of baffle-former bolts that might be affected by IASCC. One approach is to use the Weibull equation, as illustrated in Figure A-44. However, the considerable effect of heat-to-heat variability in IASCC susceptibility is difficult to predict in advance of initial inspection results. Another approach adopted by the EPRI MRP has been to assemble all the known time-to-failure data as a function of applied load and neutron fluence and then compare the lower bound of these data to baffle-former bolt stresses and fluences estimated from complex finite element models [A277]–[A279]. Figure A-48 and Figure A-49 show the compendium of laboratory hot cell and test reactor results as a function of test duration and neutron fluence, respectively.

It is immediately apparent in Figure A-48 that IASCC either occurs quite rapidly in PWR primary water conditions, generally within a few hundreds of hours, or not at all, despite the apparent dose/stress combinations for IASCC initiation and growth apparently being satisfied (as shown by the specimens of the same heats of material that did crack and failed rapidly). This means that the lifetime of an irradiated component is dictated by the time required to achieve the necessary dose/stress combination for IASCC initiation. The observations of comparatively short failure times may also indicate that a degree of dynamic straining is required to initiate IASCC in PWR primary water, as also indicated by the effect of transient loads observed during laboratory investigations [A264]. On the other hand, no significant effect of test temperature between 320 and 340°C has been observed to date.

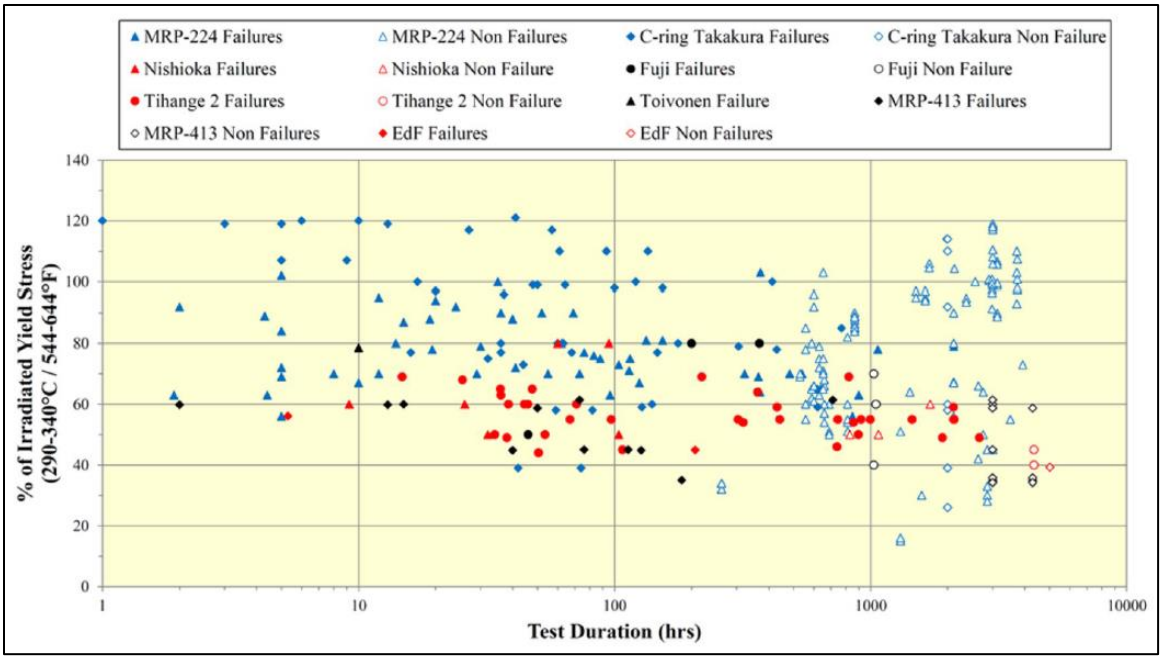

Figure A-48
IASCC initiation data stress versus time to cracking from constant load tests in PWR primary water [A277]

Figure A-49 shows the same compendium of results as a function of neutron fluence. Below a screening level of ~3 dpa, no significant degradation by IASCC is observed at constant load. Above 3 dpa, the effective stress threshold expressed as a fraction of the irradiated yield stress decreases to an apparent asymptotic value between approximately 30 and 35% of irradiated yield strength for neutron dose levels between approximately 10 and 100 dpa. Significant heat-to-heat variability in susceptibility to IASCC is also hidden within this compendium of results, similar to that seen in the field and which is not properly understood. Maximum testing times up to approximately 5000 hours are currently available, but it is noted that these are still several orders of magnitude less than 60- to 80-year operating times in LWRs.

Due to the complexity of potential loading and unloading of stressed components such as baffle-former bolts in PWR core internals caused by interactions between radiation creep, void swelling, thermal strains, and irradiation hardening, the stress-dose trajectory for a given component can be very complex. Sophisticated 3D finite element models are required to evaluate these complex interactions [A278], [A279].

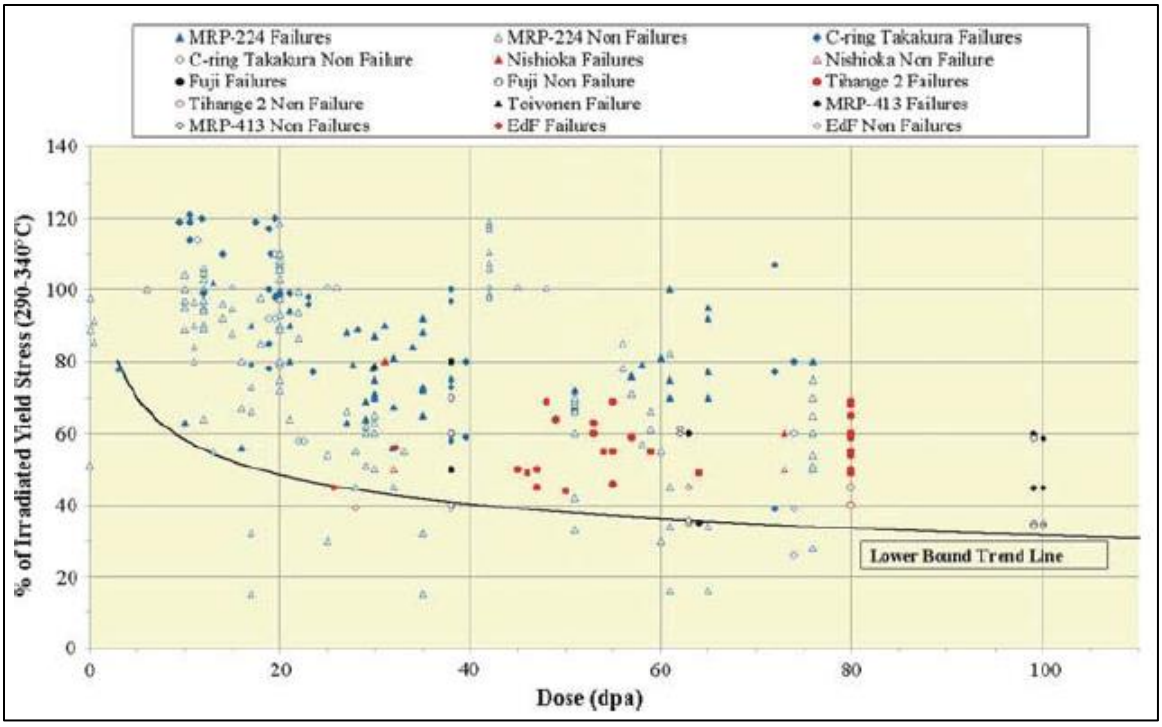

Figure A-49
IASCC initiation stress versus neutron fluence from constant load tests in PWR primary water [A277]

A.4 Fatigue

Metal fatigue cracking occurs as the result of repeated stress/strain cycles caused by fluctuating loads or temperatures and, unlike localized corrosion phenomena, is explicitly taken into account as part of the design basis of water-cooled reactors. Crack initiation can occur after repeated cyclic loading if sufficient localized microstructural damage has been accumulated. Subsequent cyclic loading by thermal or pressure fluctuations can then cause fatigue crack growth.

It should be noted that confusion often arises through the use of different definitions for fatigue crack initiation in terms of the flaw size that constitutes an initiated crack. In laboratory studies of low-cycle fatigue at constant strain amplitude, initiation is usually taken to correspond to a 25% load drop. However, this already corresponds to a relatively deep crack, and recent studies confirm that incipient flaws form much earlier during cycling, although they may often not continue to grow. In the field, “initiation” is usually more arbitrarily defined as the crack length/depth that can be reliably detected during nondestructive examinations.

Mitigation of fatigue damage for existing components is usually accomplished by reducing the magnitude of the applied loads or thermal cycling conditions or reducing the number of loading cycles. For thermal transients, reduction in the rate of temperature change for extreme temperature cycles can be effective. In rare instances, mitigation is accomplished by replacement with a more robust design or by selection of a more fatigue resistant material. However, the normal planned or anticipated operating transients are not generally the source of significant fatigue damage in nuclear plants. When fatigue cracking has occurred, it has usually been due to

conditions that were not anticipated at the time of original plant design or due to the incorrect quantification of the stress/strain/frequency conditions for a specific component under various operational modes. Changes in operating conditions can also introduce new, unanticipated fatigue loads, as has occurred subsequent to power uprates.

Major areas where fatigue damage, and occasionally leakage, has occurred are discussed in the following sections [A280].

A.4.1 Reactor Coolant System and Steam Generator Piping

A significant cause of leakage has been mechanical vibration-induced cracking of small, attached lines (primarily socket welded instrument lines). Power uprates have also contributed to a number of incidents.

Thermal fatigue has caused cracking where relatively colder water is injected into flowing reactor coolant system lines. Thermal fatigue has also occurred in a number of normally stagnant branch lines attached to flowing reactor coolant lines. The source has been thermal stratification/cycling due to valve in-leakage in up-horizontal running safety injection line configurations and swirl-penetration thermal cycling in down-horizontal drain/excess letdown lines. This has been addressed by the EPRI MRP culminating in the issue of management guidelines [A281].

A potential thermal fatigue issue related to PWR surge line stratification was identified in 1988, although no occurrences of leakage have been identified. It was resolved by analysis; however, the computed fatigue usage factors were quite high. Environmental fatigue effects could also be significant for these lines. Other potentially susceptible locations include PWR charging nozzles and BWR RHR tees, where significant thermal transients can occur in some plants.

A.4.2 Reactor Pressure Vessels

The effects of fatigue are managed by adherence to the plant design basis where thermal transients were considered in the original plant designs. Notable exceptions were in BWR feedwater nozzles [A282] and control rod drive return line nozzles, where the effects of cold water injection induced significant thermal cycling and caused cracking early in the life of some plants. Mitigating actions included changes to the feedwater thermal sleeve design to eliminate leakage of the cooler feedwater into the annulus between the thermal sleeve and nozzle and capping of the CRD return nozzles. Subsequent inspections have shown these modifications to be effective.

A.4.3 Pressurizers

There have been no known fatigue failures in PWR pressurizers. However, considerations of cold water in-surge to pressurizers have been identified that may be a contributing factor to leakage that has been observed in some pressurizer heater sleeve welds. The pressurizer spray nozzle is also affected by some significant thermal transients. Pressurizer surge nozzles can be affected by thermal stratification conditions in the surge line, as noted earlier.

A.4.4 Steam Generator Shell, Tubes, and Internals

Steam generator feedwater nozzles have exhibited cracking from thermal stratification and cycling, but high oxygen concentrations in the feedwater during low-power conditions may have caused significant environmental effects. Girth weld cracking of the steam generator shells, and feedwater nozzle blend radii, have also been observed, where both hot/cold water thermal fatigue and an environmental contribution were identified (see the earlier discussion of SICC of C&LAS).

Fatigue failures due to flow-induced vibration (FIV) have also been noted in steam generator tubing, for example:

- The upper span of tubes along the "inspection lane" in OTSGs in the 1970s and early 1980s
- A dented and improperly supported tube at North Anna 1 in 1987
- Fatigue failures at Indian Point 3 and at Mihama 2 in the early 1990s
- More recent incidences arising from flow perturbations due to clogging of broached support plates (See earlier description of fouling and clogging of PWR steam generators.)

A.4.5 RPV Internal Components

A number of fatigue failures have been observed in reactor internals. In most cases, these have been high-cycle fatigue events generated by either FIV or thermal fatigue. A notable case has been high-cycle fatigue issues with BWR steam dryers. Beginning in the 1980s, cracking of drain channel welds, end hood welds, and braces between dryer banks has been seen in a number of units. These occurrences have been attributed to FIV. Subsequently, several units saw significant cracking of end hoods and cover plates resulting from acoustic loads generated by increased steam flow at newly uprated power levels. In some cases, the fatigue damage led to a complete replacement of steam dryers with units designed to resist the acoustic loading. Other relatively recent observations of fatigue cracking in BWR reactor internals include:

- Cracking of BWR steam dryer support brackets attached to the reactor vessel wall. This fatigue cracking resulted from rocking of the dryer in the steam flow in cases where the dryer had not been installed perfectly level. In most cases, cracking has been confined to small areas of the outside corners of the top of the bracket. However, in one case, cracking occurred across the entire top of the bracket and propagated downward through the thickness.
- Some BWRs have observed fatigue cracking at jet pump riser brace to riser pipe welds, with cracking initiating at the toe of the riser brace to riser pipe weld.
- Recent cracking of X-750 clevis insert bolting and stainless steel baffle-former bolting includes evidence of crack propagation by fatigue, although the cracking likely initiated by SCC.

Design against fatigue damage is based on the S-N curves in Section III, Appendix I of the ASME Code. These curves indicate the number of cycles of given amplitude of stress intensity that is required to reach a cumulative usage factor of 1.0. The design fatigue curves upon which this criterion rests are based on test data measured in air at room temperature and then reduced by a factor of 2 on stress range or 20 on cycles to failure, whichever is most conservative, to account for data scatter, size effects, roughness, and (controversially) service environment. For carbon and low-alloy steel materials, the most adverse conditions of mean stress are used to

correct the test data prior to applying these factors. The ASME Code includes analytical approaches and criteria for determining usage factors for Class 1 components, which must be shown to be less than 1.0 for the anticipated component life. However, a fatigue usage factor of unity does not necessarily imply that crack initiation will occur because of the safety factors built into the stress intensity amplitude or number of allowed cycles for the Code fatigue design S-N curves.

The crack growth that follows fatigue crack initiation can be predicted if the crack depth and shape can be characterized and if the cyclic stress field is known. Procedures for performing crack growth analyses are contained in Section XI of the ASME Code. Both ASME Section III and Section XI are currently in a state of flux as work remains in progress regarding the development of fatigue crack growth rate curves that address environmental effects.

A brief description of the relevant fatigue-related degradation modes is provided below.

A.4.6 High-Cycle Fatigue (HCF)

High-cycle fatigue involves a number of stress cycles > 10^5 at relatively low stress amplitudes typically below the material's yield strength but above the fatigue endurance limit of the material. The crack initiation phase is considered dominant since crack growth is usually fairly rapid. High-cycle fatigue may be:

- Mechanical in nature, that is, vibrations or pressure pulses or due to FIV.
- Power uprates are a concern in this context as an increase in flow may change the vibrational characteristics of the system and, in the worst case, excite a resonant frequency mode. Increased flow may also introduce resonant frequency acoustic loads in steam spaces where none were present at lower power levels.
- Thermally induced due to rapid mixing of cold and hot fluids where local instabilities of mixing lead to low-amplitude thermal stresses at the component surface exposed to the fluid.
- Due to combinations of thermal and high-cycle mechanical loads such as those that might occur on pump shafts in the thermal barrier region.
- Aggravated by the presence of an elevated mean stress. There can be cases where the cyclic loading itself is insufficient to initiate a fatigue crack. However, when this cyclic loading is overlaid on to a significant sustained tensile stress, the combined stress at the peak of each cycle may be sufficient to cause fatigue damage and ultimately crack initiation and propagation.

The ASME III design curves for fatigue referred to above are based on data from strain-controlled tension/compression tests on initially smooth specimens. Under these conditions "crack initiation" was defined when the peak stress had relaxed 25% due to crack initiation and early propagation. As indicated earlier in Figure A-17, such an engineering definition of crack initiation encompasses a variety of microscopic precursor surface events, many of which can be affected by the environment. For example, cracks may be initiated on a microscopic level at corrosion pits, intergranular corrosion notches, and so on. Thus, crack initiation is expected at locations where an aggressive environment can be formed. In the example mentioned above where fatigue cracks developed in steam generator tubing under high frequency FIV conditions in once-through steam generators along the inspection lane, the chemistry conditions at the

lower face of the upper tubesheet and at the top tube support plate (locations of circumferential through-wall cracks) were believed to have significantly reduced the stress required to initiate fatigue cracks. This may also have been a factor where fatigue cracks occurred at fouled tube support plate intersections in recirculating steam generators.

In general, however, the environment does not have a major effect on the kinetics of high-cycle fatigue crack propagation since at low stress/strain amplitudes and high frequencies, the extra environmentally assisted increment of crack growth/cycle is small or insignificant relative to the mechanical fatigue contribution. The mechanistic reason for this was discussed earlier in the context of the slip-oxidation mechanism where it was seen that the aqueous environment has a diminishing effect on the time-dependent crack propagation rate as the crack tip strain rate increases.

A.4.7 Low-Cycle Fatigue (LCF)

Low-cycle fatigue cracking is due to relatively high stress/strain range cycling where the number of cycles is less than about 10^4 to 10^5 and plastic strains exceed the yield strength of the material. For reactor coolant system components, the cumulative combined effects of reactor coolant system pressure and temperature changes are considered in the component design analysis. The strain cycling that contributes to low-cycle fatigue is generally due to the combined effects of pressure, piping moments, and local thermal stresses during normal operation. The latter are usually highest for transients such as plant startup, shutdown, or hot standby. Particular attention must be paid to the possibility of locally high component stresses (e.g., from notch effects at welds or from piping restraints) even though nominal system design criteria are met.

The major difference between high- and low-cycle fatigue is that, for low-cycle fatigue, it is the crack growth rate that dominates component life since crack initiation can occur after relatively few strain cycles.

A.4.8 Corrosion Fatigue (Environmentally Assisted Fatigue [EAF])

Corrosion fatigue concerns the reduction in fatigue life that is observed in a reactor water environment compared to that in room temperature air. The subject of environmental (corrosion) fatigue is still evolving and is under considerable discussion in the technical community, Code bodies, and regulatory agencies [A291]. It involves two primary elements: 1) the effects of reactor water on the overall fatigue life of reactor components (as represented by either multiplying the fatigue usage factor by an “environmental factor” to account for aqueous corrosion effects or the use of an environment-adjusted fatigue design curve), and 2) the potential accelerated growth of an identified defect caused by exposure to reactor water environments.

Fatigue crack initiation and growth resistance are governed by a number of material, structural, and environmental factors, such as stress range, temperature, dissolved oxygen or hydrogen concentration, mean stress, loading frequency (strain rate), surface roughness, and number of cycles. Cracks typically initiate at local stress concentrations, such as welds, notches, other surface defects, and structural discontinuities. The presence of an oxidizing environment or other deleterious chemical species in reactor water can accelerate the fatigue crack initiation and propagation processes by, for example, producing pits in the surface that then act as stress

concentrators and potential fatigue crack initiation sites. Corrosion fatigue can also be viewed as an extension of stress corrosion cracking and strain-induced cracking in the overall spectrum of "environmentally assisted cracking" modes, as described in the SCC discussion for C&LAS. In this case, however, it is recognized that the environmental component of crack advance is superimposed on a component of crack advance due to "mechanical fatigue" that would occur anyway in a dry air environment.

For C&LAS, interactions between the various system parameters can have an effect on the extent to which corrosion fatigue can be predicted [A283] (as described earlier in the context of SICC). In this case, the predictive methodology based on the slip-oxidation mechanism may be used to quantify the amount of environmentally induced crack advance during those portions of a fatigue loading cycle when the applied strain rate may be increasing. If it is assumed that low-cycle fatigue component life is essentially determined by crack propagation, the number of cycles to failure may be calculated as a function of the strain amplitude and frequency. A comparison between the observed and theoretical relationships between strain amplitude and cycles to crack initiation is shown in Figure A-50, illustrating the effect of applied strain rate on the fatigue behavior of carbon steel in oxygenated water at 288°C. On the basis of such predictive capabilities, the effect of combinations of system parameters that are relevant to various reactor operating conditions may be evaluated. Such an example is shown in Figure A-51 for a worst-case combination of high dissolved oxygen concentration, slow applied strain rate, and high temperature. Under this combination of conditions, the cycles to crack initiation are less than the ASME III design relationship. However, it should be pointed out that such oxidizing conditions rarely exist in RCS environments. Carbon and low-alloy steels are not normally directly exposed to the reactor water environment in PWR, VVER, and CANDU primary systems, and oxygen levels are relatively low in BWRs operating under hydrogen water chemistry/NobleChem™. Improved models taking this into account are also now available regarding environmental effects on crack growth [A287].

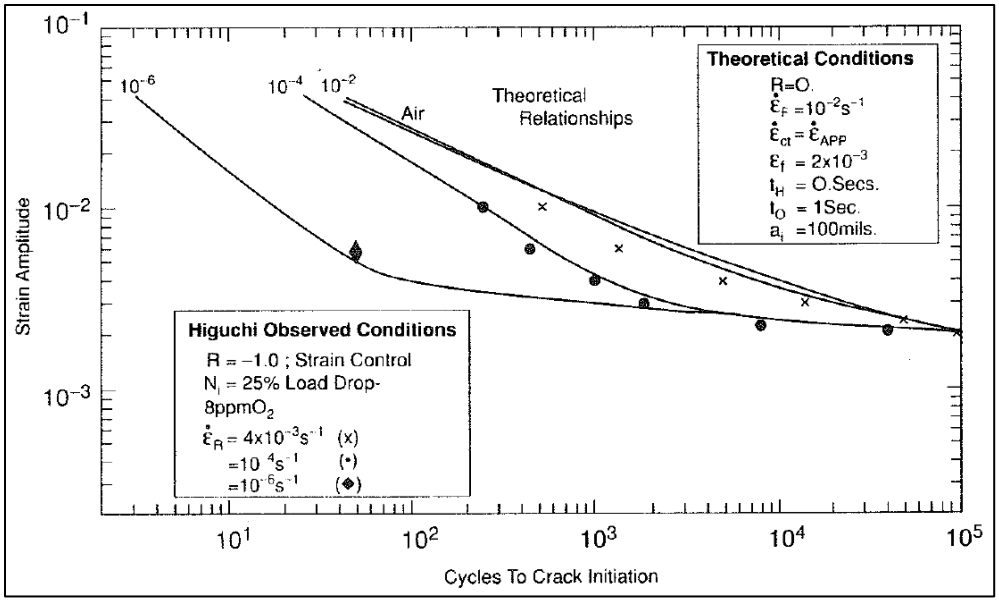

Figure A-50
Predicted [A284] and observed [A285] strain amplitude versus cycles to crack initiation relationships for un-notched carbon steel in 288°C, 8 ppm oxygenated water with strain applied at different rates

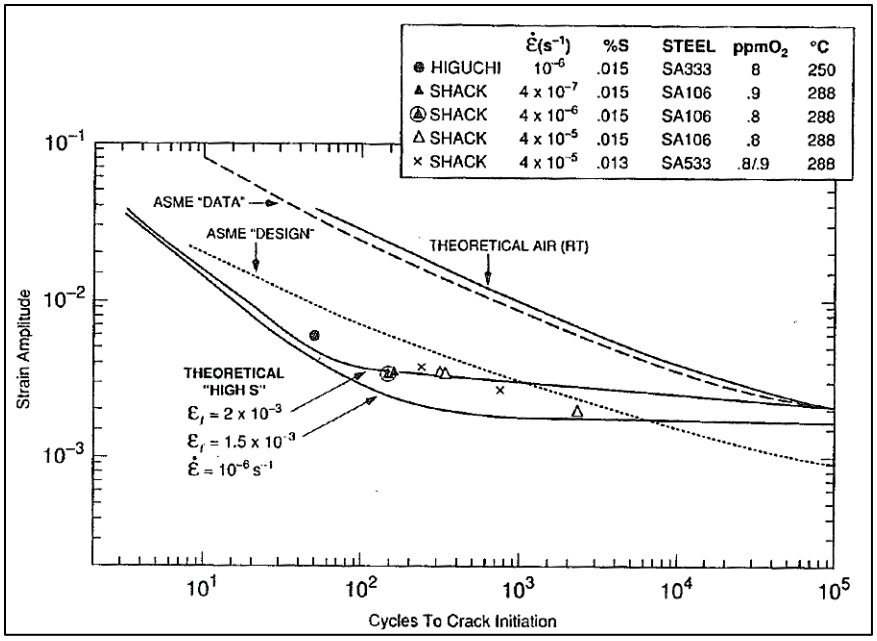

Figure A-51
Predicted [A284] and observed [A285], [A286] strain amplitude versus cycles to crack initiation relationships for un-notched C&LAS in 288°C water under the worst combination of material and environmental conditions

Note the non-conservatism of the ASME III design curve under these conditions at certain strain amplitudes and low strain rates.

A major environmental factor that has not received adequate consideration in laboratory investigations of corrosion fatigue is the flow rate past the specimens. For C&LAS, the high flow rates typical of reactor operation are known to be very beneficial in reducing corrosion fatigue effects regarding both the initiation and growth of cracks. As noted earlier for SICC, this is attributed to the beneficial effect of high flow helping remove sulfur anions from pits and the crack enclave.

By contrast to the deleterious effect of oxygenated BWR NWC on the fatigue life of C&LAS, significant reductions in the fatigue lives of stainless steels and nickel-base alloys have been observed in simulated hydrogenated PWR environments, i.e., at low corrosion potential, compared to room temperature air. Oxygenated BWR NWC only has an effect if the stainless alloys are sensitized. While a general understanding of the underlying mechanism exists for C&LAS, there is currently no adequate mechanistic interpretation of this phenomenon for austenitic alloys in hydrogenated coolants. Studies with austenitic stainless steel uniaxial test specimens (crack initiation and crack growth up to ~ 3 mm) have shown that fatigue lives are shorter in low dissolved oxygen (DO) water than in high DO water. Austenitic stainless steel specimens tested in LWR environments also show well-defined fatigue striations, indicating that crack tip plasticity effects (mechanical factors) are important. Further work is required to understand initiation and growth mechanisms and to understand the reasons for crack growth retardation under some circumstances.

Underlying the issues associated with environmental fatigue is reconciliation of the predicted environmental fatigue enhancement with operating plant experience. The laboratory data supporting NUREG/CR-6909 clearly demonstrate environmental effects, and it is therefore appropriate that such effects should be considered in the design of LWR components. However, predicted lifetimes from NUREG/CR-6909 and similar methods may be excessively conservative when compared with field experience. This may be because there is substantial conservatism included within both design codes and the use of bounding transient definitions, because plant operating cycles are characteristically different from material testing cycles or because the simple test specimens used to establish environmental factors do not adequately represent the complex loading that occurs for plant components.

Regarding crack growth, ASME Section XI provides “in air” fatigue crack growth curves for austenitic stainless steels but does not currently include a comprehensive set of curves for wetted flaws. ASME Code Case N-809 addresses this issue for low ECP environments but does not address the BWR NWC environment. Further, crack growth rates appear to be dependent on the specific material type, and relevant data on environmentally affected crack growth rates for some materials (e.g., Alloys 690, 316LN) are not presently available.

A.5 Fracture—Reduction in Fracture Properties (RiFP)

This section addresses material degradation modes that lead to a reduction in the resistance to fracture of the material, either with increasing time or through contact with the reactor coolant. Because a high level of fracture toughness is a design assumption for most LWR pressure boundary and internal components, degradation modes that lead to reductions in resistance to fracture are of high significance for many components. Thermal aging and environmental effects on fracture toughness are described here. The various irradiation-induced modes of embrittlement and loss of fracture toughness are described in a subsequent section devoted to the effects of neutron irradiation on structural alloys.

A.5.1 Thermal Embrittlement (Th)

Embrittlement associated with specific alloy microstructural/compositional features and exposure over time at elevated temperature is of concern with cast stainless steels, martensitic and ferritic stainless steels, ferritic and low-alloy steels, and some high chromium content nickel-base alloys. The mechanisms of such embrittlement are varied. They range from the precipitation of secondary phases (which increase yield strength and lower fracture toughness) to the segregation of metalloid impurities to grain boundaries (which can induce intergranular fracture) to the pinning of dislocations by interstitial impurities (which inhibit plasticity) to, finally, the formation of brittle long-range ordered phases.

A.5.1.1 Cast Stainless Steels

Cast austenitic stainless steels (CASS) have been used for many pressure boundary components (e.g., pump and valve bodies) in water-cooled reactors due to their high corrosion resistance, strength, ductility, and fracture toughness. CASS components are not normally subject to significant neutron fluxes, although some on the periphery of PWR core support structures may reach fast neutron fluences on the order of 10^{21} n/cm^2 (E > 1.0 MeV) and greater as they continue to operate for periods of extended operations. However, stainless steel weld deposits of PWR core barrels and especially of some designs of welded core support structures can reach significantly higher neutron fluences. Corresponding fluences for BWR core shroud welds are at least an order of magnitude smaller.

The most commonly used CASS materials are SA-351 grades CF-3, CF-3A, CF-3M, CF-8, CF-8A, and CF-8M. They have a duplex γ-austenite/δ-ferrite microstructure and are susceptible to thermal aging embrittlement of the δ-ferrite phase after long exposure times at typical PWR and BWR operating temperatures. The volume fraction of δ-ferrite in CASS is typically less than 25% but can be higher. Stainless steel weld deposits, typically Types 308 and 309 or 316L, have a similar duplex microstructure but with lower volume fractions of δ-ferrite, normally in the range 5 to 15%. The δ-ferrite phase provides resistance to hot cracking during casting or welding, increased strength, and resistance to sensitization.

Thermal aging of the δ-ferrite phase results in an increase in hardness, loss of ductility, and loss of fracture toughness. The mechanisms of thermal aging of CASS and resultant effects on mechanical properties and embrittlement have been reviewed and summarized by the NRC, by several EPRI MRP reports, and in the EPRI Materials Handbook for Nuclear Plant Pressure Boundary Applications [A292]–[A295]. Most of this work date from the 1980s and 1990s and, in the context of PWRs, with the exception of examining possible synergism between thermal aging and irradiation embrittlement, have been pursued mainly in France and in Japan see for example [A296], [A297]. The focus of French studies, in particular, has been on studying CASS after very lengthy aging times of up to 200,000 hours at temperatures ≤ 350°C rather than ≤ 400°C.

Thermal aging embrittlement of CASS at temperatures below about 400°C arises primarily as a consequence of a thermally activated separation of chromium by diffusion in the Fe-Cr solid solution of the δ-ferrite phase that results in the formation of an iron-rich α-phase and a chromium-rich α'-phase. This process is called *spinodal decomposition*. The α'-phase may also

form by precipitate germination and growth, particularly at temperatures > 400°C, but can also contribute at lower temperatures depending on the precise combination of chromium content and temperature. The austenite phase of CASS is unaffected by thermal aging in the same temperature range.

The formation of α' during thermal aging can affect all Fe-Cr solid solutions with Cr-contents >10%. An “oscillation” in the resulting Cr-distribution is observed by very high resolution, microscopic techniques with a “wavelength” measured in a few nanometers and the Cr-content “amplitude” increasing with aging time and temperature. The effect increases notably with the Cr and Mo-content of the δ-ferrite phase so that CF-3M and CF-8M are less resistant to thermal aging than CF-8 or CF-3 without Mo. Static castings have also been observed to be more susceptible to thermal aging embrittlement than centrifugal castings.

Although several sets of screening criteria for embrittlement of CASS have been used since the mid-1990s, the most recent observations and analyses led to Table A-1 being adopted in 2016 by EPRI and the NRC as screening criteria for thermal aging susceptibility for CASS components with service temperatures > 250°C (482°F) [A298]. The demarcation line between “potentially significant” and “non-significant” is based on a fracture toughness criterion (see later discussion). The formation of the embrittling α'-phase from δ-ferrite is enhanced by other alloying elements such as silicon, which, together with Cr and Mo, can be represented by the chromium equivalent. Chromium equivalent (i.e., a function of Cr + Mo + Si) > 23.5 wt% is the preferred metric for potentially significant embrittlement in France rather than the criteria listed in Table A-1.

Table A-1
Thermal aging screening criteria for CASS adopted by the NRC
Source: Final Safety Evaluations of BWRVIP-234 [A298]

Mo Content (wt%)	Casting Method	Ferrite Content	Significance of Thermal Aging
High (2.0–3.0)	Static	> 14%	Potentially susceptible
		≤ 14%	Not susceptible
	Centrifugal	> 20%	Potentially susceptible
		≤ 20%	Not susceptible
Low (0.50 max.)	Static	> 20%	Potentially susceptible
		≤ 20%	Not susceptible
	Centrifugal	> 25%	Potentially susceptible
		≤ 25%	Not susceptible

Other precipitation phenomena occur in the δ-ferrite phase and at the ferrite-austenite interfaces in CASS above about 350°C, particularly the precipitation and growth of the FCC Ni-Si-Mo-rich G-phase, which can reach up to 12% by volume in Mo-containing CASS. Carbon also enhances G-phase precipitation. By their nature, precipitation processes involving the germination of a new phase occur much later in the thermal aging process than spinodal decomposition that only depends on solid state diffusion. Nevertheless, G-phase does not appear to contribute

significantly to hardening and loss of toughness. At higher temperatures between 400 and 500°C, other intermetallic phases precipitate but to a much lesser extent than G-phase. However, extensive carbide (and sometimes nitride) precipitation, particularly at austenite-ferrite interfaces, occurs at these higher temperatures in Mo-free CASS.

Although the microstructural evolution of CASS during thermal aging at water reactor relevant temperatures is fundamentally driven by solid-state diffusion processes, the complexity and changing nature of the phenomena with higher temperatures is such that extrapolation over large temperature ranges using Arrhenius-type relationships can be potentially misleading. Accelerated thermal aging for PWR applications has generally only been carried out up to 400°C where hardening of the δ-ferrite by α' formation is the predominant aging process. Even with this restriction, the observed apparent activation energy for changes in mechanical properties such as hardness and fracture toughness (see later discussion) can be very variable and usually significantly below the activation energies associated with diffusion of metallic species, particularly Cr, in ferrite.

The complexity of the microstructural changes associated with thermal aging of CASS gives rise to very strong material and heat dependencies for the extent and kinetics of evolution of mechanical properties. Consequently, extensive studies have been necessary to determine the range of temperatures, compositions, etc. for which mechanical properties data obtained from accelerated aging tests can be applied to service conditions via Arrhenius-type temperature correlations. The increase in hardness and decrease in ductility of the δ-ferrite phase due to thermal aging promotes premature cleavage in this phase that can extend preferentially through it if there is a continuous δ-ferrite network. Even if the fracture path intersects the austenite, deformation-induced martensitic transformation can allow the brittle fracture to extend beyond the embrittled δ-ferrite.

The main parameter used for characterizing the evolution of mechanical properties due to thermal aging has been the Charpy impact energy, although the most recent work has relied on direct fracture toughness measurements. Measurements of tensile properties, hardness, micro-hardness of the δ-ferrite phase, and J-R fracture resistance curves have also been made and empirical correlations with Charpy impact energy derived. Thermal aging of CASS at BWR and PWR operating temperatures is characterized by an increase in hardness and tensile strength and a decrease in ductility, impact strength, and toughness. In addition, the “brittle-to-ductile” transition temperature increases and the upper shelf decreases. The demarcation criterion between “potentially significant” and “non-significant” thermal aging for the screening criteria in Table A-1 is based on a J-R tearing resistance of 200 kJ/m^2 (1450 $in.\text{-}lb/in.^2$) at a crack extension of 2.5 mm (0.1 inch) [A298]. All components identified as having a potentially significant reduction in fracture toughness due to thermal aging are then placed in an aging management program. A corollary of this classification is that no significant thermal aging is anticipated for stainless steel weld deposits because of their lower δ-ferrite contents relative to CASS.

Examples of Charpy impact energy measurements at room temperature on many heats of CASS are shown in Figure A-52 based on aging times up to 58,000 hours at 400°C. Although the dispersion in the results is large, all heats show a clear trend to a saturation of the aging effect (i.e., a minimum plateau value of room temperature Charpy impact energy) when conditions occur, leading to predominantly brittle fracture. This saturation effect, which decreases with increasing δ-ferrite or chromium equivalent, is associated with the development of channel fracture.

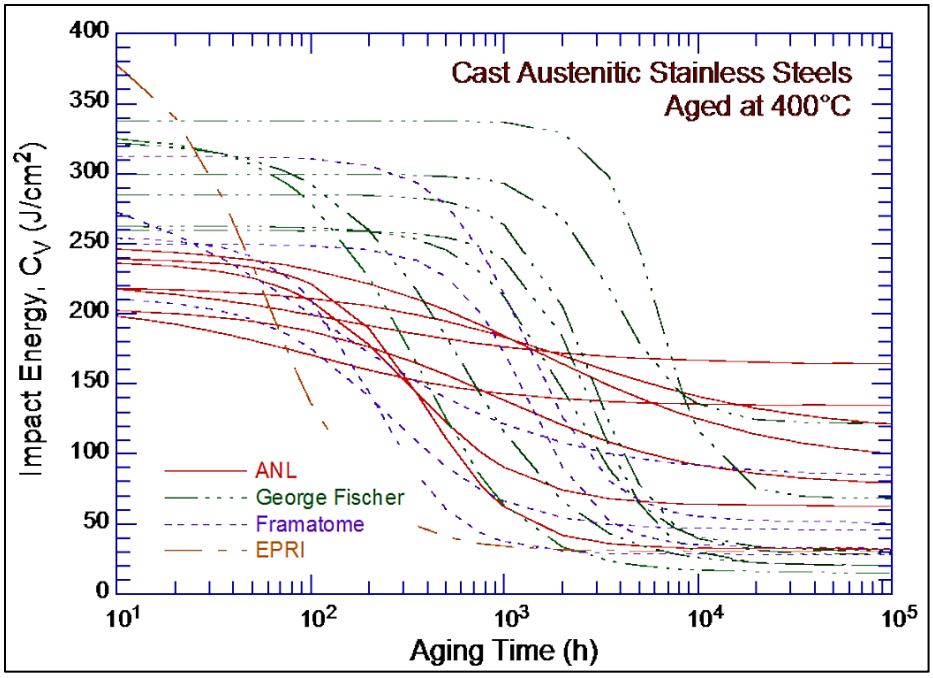

Figure A-52
Decrease in Charpy impact energy for various heats of cast stainless steels aged at 400°C [A299]

The procedure proposed in the United States for estimating the toughness of CASS components in service is based on empirical equations relating room temperature Charpy impact energy to the chemical composition, notably Cr, Mo, Si, and C (i.e., Cr_{eq}), and time and temperature, including accelerated aging data at temperatures up to 400°C [A299]. The kinetics of aging are based on Arrhenius-type correlations derived from data such as those shown in Figure A-53 [A300]. It can also be seen in Figure A-53 that the lower bound plateau is independent of aging temperature, at least up to 400°C. The apparent activation energy for the aging kinetics is observed to depend on the concentrations of the aforementioned elements and to vary between 65 and 250 kJ/mole [A299]. The room temperature J-R curve is then estimated from empirically established correlations with the room temperature Charpy impact energy for the different categories of CASS shown in Table A-1. The J-R curve coefficients can then be linearly interpolated between room temperature and normal operating temperatures. Lower bound estimates of end-of-life toughness are made based only on the chemical composition and lower bound correlations if no further details of the microstructure are available.

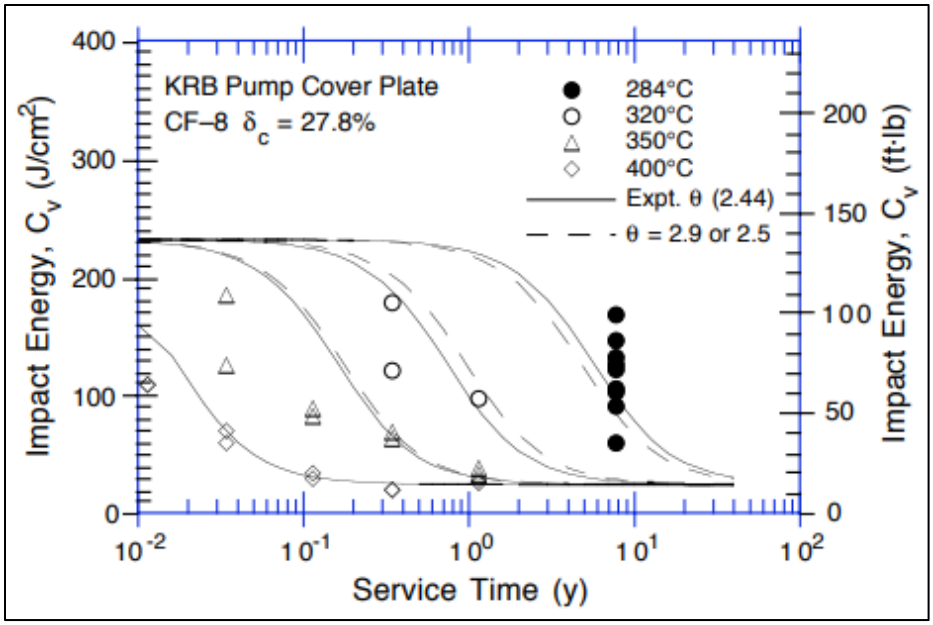

Figure A-53
Comparison of experimental and estimated room temperature Charpy impact energy as a function of aging temperature and time for a CASS pump cover plate [A300]

Some concerns have been expressed about anomalies in the kinetics of thermal aging and embrittlement between 350 and 400°C because, in a database that now extends up to 200,000 hours, embrittlement curves can cross for some heats in this temperature range. As noted earlier, this implies that the mechanism of aging embrittlement may not be the same between 350 and 400°C compared to lower temperatures closer to those in service, and that accelerated aging at temperatures higher than 350°C may not necessarily be conservative.

The issue of possible synergistic interactions between thermal aging embrittlement of CASS and neutron irradiation embrittlement continues to be raised as a potential concern by the NRC for some components of core support structures [A298]. However, presently available data for irradiated, thermally aged CASS support a screening criterion based on the minimum neutron dose for detectable loss of fracture toughness by irradiation embrittlement alone of 6.7×10^{20} n/cm^2, (E > 1 MeV).

A.5.1.2 Ferritic and Low-Alloy Steels

Thermal aging embrittlement of materials other than CASS used in reactor components includes temper embrittlement and strain aging embrittlement. Ferritic and low-alloy steels are subject to both degradation mechanisms, but wrought austenitic stainless steels are not usually affected by either mechanism in the temperature range of interest.

Temper embrittlement of low-alloy steels is caused by the diffusion and segregation of impurity elements (metalloids), such as phosphorous, tin, antimony, and arsenic, to grain boundaries after prolonged exposure to temperatures in the range from 350 to 575°C [A301], [A302]. At temperatures above this range, the impurities tend to dissolve in the ferrite matrix, and little or no grain boundary segregation is observed at temperatures above 625°C. At temperatures below this range, very long exposure times are necessary for the impurities to diffuse to, and segregate in, the grain boundaries. This could, in principle, be an issue for PWR and VVER 1000

pressurizers, for example, with a typical operating temperature up to 343°C, but no convincing experimental evidence is available of temper embrittlement of the grades of C&LAS used. The phenomenon is circumvented for reactor pressure vessels by the fact that the surveillance specimens used to check for irradiation embrittlement automatically integrate the effects of exposure at reactor operating temperatures. The presence of carbon tends to accelerate the embrittlement process due to preferential segregation of impurities at interfaces between grain boundary carbides and ferrite grains. The role of other alloying elements, such as chromium, nickel, magnesium, and molybdenum, in the acceleration or retardation of the temper embrittlement process, has been studied extensively. The principal manifestation of temper embrittlement in low-alloy steels is an increase in the ductile-to-brittle transition temperature, due to a change from predominantly cleavage fracture (before temper embrittlement) to predominantly intergranular fracture along impurity segregation paths (after temper embrittlement). Temper embrittlement also promotes intergranular hydrogen embrittlement susceptibility in high strength steels and caustic cracking in low-alloy turbine steels.

Strain aging embrittlement occurs in cold-worked ferritic steels when they are subjected to strains at temperatures in the range from 260 to 370°C and is caused by the pinning of dislocations by interstitial impurities (nitrogen, carbon, etc.). Ongoing studies of strain aging in low-alloy reactor pressure vessel steels have already been described in the context of SCC and SICC susceptibility in reactor coolant environments [A148], [A151], [A152]. Post-weld heat treatment of reactor vessel components following cold working during fabrication mitigates the embrittlement but does not eliminate it. However, following post-weld heat treatment, residual strain aging embrittlement has only a slight effect on the ductility and fracture toughness of LWR vessel materials under the environmental and loading conditions of interest.

A.5.1.3 Nickel-Base Alloys

A specific form of thermal aging and subsequent embrittlement that can arise in Ni-base alloys containing around 30% chromium (such as Alloys 690, 152, and 52) can occur as a result of long-range ordering by the formation of the intermetallic compound Ni_2Cr [A303]. It was initially thought that this can be avoided if the iron content of the material is > 7% [A304]. It should also be noted that 7.0% minimum iron content was the value specified in the first issue of the Alloy 690 tubing guidelines in accordance with ASTM SB-163 but was revised in 1999 to 9.0% minimum [A305] to minimize concerns about possible long-range ordering reactions that might possibly lead to embrittlement after long times at temperature. However, recent work appears to indicate that the kinetics associated with long-range ordering are complex and need to be better understood, particularly with respect to the potential effect of hardened material on PWSCC [A356]–[A359].

A.5.2 Environmentally Induced Reduction of Fracture Resistance (Env)

- Structural integrity margins that are central to the avoidance of loss of coolant accidents are currently defined using the mechanical properties of the structural materials measured in air in accordance with ASTM standard test procedures. Leak-before-break analyses also use “dry air” mechanical properties. In addition, the rate at which a postulated condition for structural instability is approached is usually evaluated on the basis of crack propagation rates measured under a relatively restricted range of stress intensity control conditions (e.g., constant stress intensity and constant deflection, etc.).

- There are two categories of phenomena that might challenge the conservatism of this approach, namely:
  - An environmentally induced decrease in the apparent fracture toughness or resistance that would lead to an earlier onset of unstable crack growth than in air. This category may be subdivided into decreases in the measured fracture toughness (K_{IC}) or the J-R tearing resistance (J_{IC}) depending on the ductility of the alloy and loading rate.
  - Enhanced subcritical crack propagation rates: 1) as the critical fracture condition is approached (e.g., at high stress intensity factor and/or low temperature) that could reduce the time before mechanical instability occurs; 2) due to a high positive dK/da profile as distinct from quasi-constant K conditions used for most experimental determinations of crack growth rates; and 3) caused by hydrogen absorbed in the metal and dissolved H_2 in the reactor coolant.

As illustrated in Figure A-54, it is likely that interactions exist between these phenomena [A306]. The bold curve in Figure A-54 represents a typical crack growth disposition curve for a given material/environment system, which is normally quantified as a function of water chemistry, temperature, material condition, etc. for a relatively limited range of stress intensities.
If the apparent K_{IC} or tearing resistance values are decreased because of environmental effects on fracture, then accelerated subcritical crack propagation rates are to be expected as K_{IC} is approached (denoted by the shaded oval in Figure A-54) since these rates will be influenced by changes in the strain distribution and an elasticity at the "embrittled" crack tip.

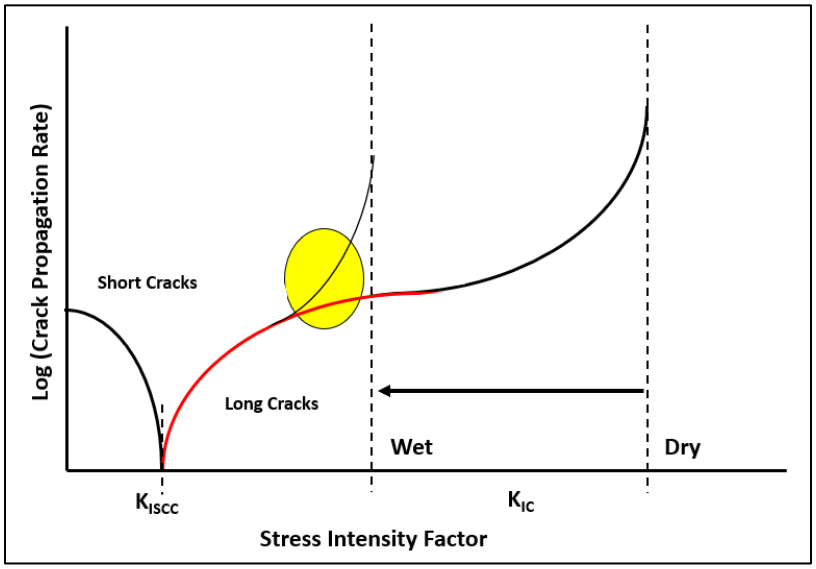

Figure A-54
Schematic stress corrosion crack propagation rate versus stress intensity curves indicating the divergence from the usual relationship at lower stress intensity (denoted by the bold curve) [A306]

A.5.2.1 Unusually High SCC Propagation Rates

There is some evidence that unusually high SCC propagation rates may be observed under specific testing conditions, as described below.

Abnormally high SCC propagation rates have been reported below 150°C in a number of Ni alloys [A307], [A308]. The extent to which this might occur is unknown in cold worked or HAZs of stainless steel, irradiated stainless steel, or low-alloy steel (including post-irradiation).

Abnormally high propagation rates have also been observed in structural alloys in high temperature water under high positive dK/da conditions, e.g., > 10 MPa√m/mm [A309], [A310]. Such situations can exist in components under certain residual stress profiles even under constant displacement. The increase in propagation rate under these conditions can be considerable (over two orders of magnitude) and can be further exacerbated in some materials below 150°C [A307], [A308].

There have been very few investigations into the conditions that give rise to these unusually high SCC propagation rates.

A.5.2.2 Decreased J-R Tearing Resistance and Fracture Toughness

Although the traditional view is that fracture behavior (e.g., J-R tearing resistance or K_{IC} fracture toughness) is affected by microstructure and test conditions (e.g., temperature and strain rate), there are reasons to consider aqueous environmental effects on these properties, given that such exposure is inherent to the practical application.

The study of low temperature crack propagation (LTCP) has its origins in the observation of significant crack extension occurring in high strength Alloy X-750 after PWSCC tests while the specimens were still loaded during cool down of the experimental autoclaves, and which was later reproduced during rising load tests in simulated PWR water [A311][A313]. Rapid intergranular crack propagation rates up to a few millimeters per minute have been observed in specimens at low temperatures that had been pre-cracked by PWSCC. The embrittlement was shown to be due to hydrogen absorbed during prior exposure to the high temperature aqueous environment. Susceptibility to crack extension due to absorbed hydrogen persisted up to 260°C and 338°C in this case.

Experiments designed to study LTCP are typically conducted on pre-cracked specimens in the same way as a classical rising load J-R toughness test, but at a reduced loading rate that is typically approximately two orders of magnitude less than that used in air. The results are normally displayed in the J-R format from which an effective J_{Ic} and tearing modulus are derived. Various investigators have observed large reductions in tearing resistance for pre-cracked specimens of wrought Alloys 600 and 690, nickel-base weld Alloys 182, 82, 152, and 52 (see for example Figure A-55), and thermally aged CF8 CASS. These large reductions in fracture resistance were only observed when the tests were performed in low-temperature (<150°C) water and not at normal operating temperatures [A317][A321], in contrast to Alloy X-750. In these tests, hydrogen was present either as an added constituent of the aqueous environment, or as a result of corrosion at the crack tip, or from prior exposure to high-temperature, hydrogenated water. The effect on apparent toughness diminishes with decreasing hydrogen concentrations in PWR primary water and recovers significantly at a typical

operational concentration of ~30 mL H_2/kg H_2O or close to a shutdown hydrogen concentration of ~5-10 mL H_2/kg H_2O. Carbide interfaces seem to be implicated as preferred traps for hydrogen, and the resulting embrittlement can be aggravated by the presence of sulfur and phosphorus on grain boundaries.

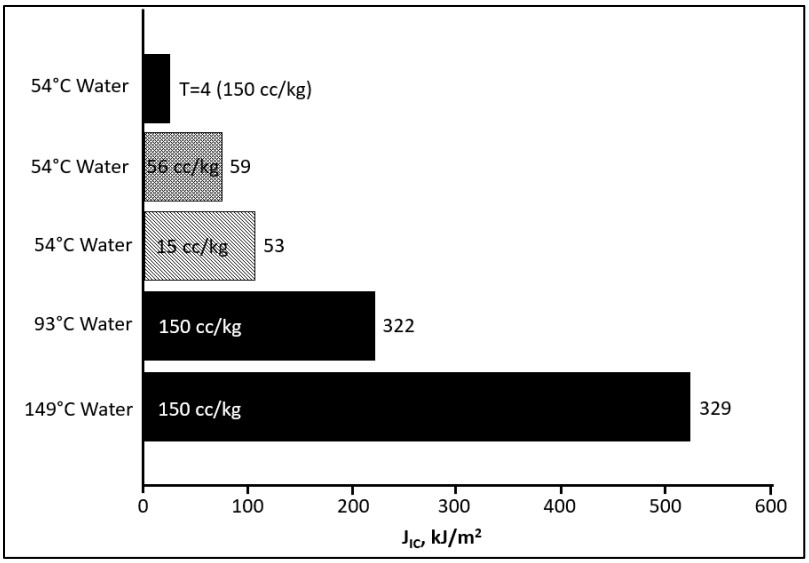

Figure A-55
Elastic-plastic fracture toughness (JIC) of Alloy 52 welds in water (Values of tearing modulus, T, are shown to the right of each bar.) [A314]

Some tests have also been conducted to measure the apparent fracture toughness of the nickel-base weld metals 182, 52, and 152 in simulated PWR shutdown primary water at pH 5 containing 4 to 10 ppm hydrogen peroxide that represents the acidic oxidizing conditions used to maximize nickel ferrite dissolution for decontamination purposes [A360]. Despite the increase in corrosion potential by almost 1 volt relative to normal PWR primary water conditions, all Alloy 182 weld metals tested showed major reductions in fracture resistance, but Alloys 52 and 152 maintained significant apparent toughness. On the other hand, in another investigation, no reduction in apparent toughness was observed in Alloy 182 weld metal in BWR hydrogen water chemistry at 100°C [A321].

There are few data available to evaluate the effect of LWR coolants combined with irradiation embrittlement of stainless steels and low-alloy steels where K_{IC} values are already reduced by the neutron fluence (see later discussion). A recent EPRI-sponsored study on Type 316L stainless steel irradiated to 6.7 dpa did not show any significant reduction in apparent fracture toughness due to exposure to simulated BWR and PWR coolants, although the authors cautioned against generalizing this conclusion based on so few observations and combinations of materials and environmental conditions [A361].

The second type of observation discussed in the context of LTCP concerns is the occasional sudden brittle fracture during measurements of stress corrosion or corrosion fatigue crack growth rates, usually in test conditions simulating the normal reactor coolant operating chemistry and temperature. Fracture toughness (KIC) represents the resistance to sudden, unstable fracture, and is commonly characterized using notched Charpy or pre-cracked CT specimens. Like other mechanical properties, there is no reason to expect that KIC is a function only of material and

test temperature. In particular, the hydrogen content of the material could affect fracture toughness. It is known that hydrogen readily diffuses through Fe and Ni alloys in ~300°C water [A155], and it is reasonable to be concerned for the effect of the presence of hydrogen throughout a metal on its fracture properties.

Isolated and usually unintentional observations of such brittle fracture behavior have been reviewed [A310]. For example, pre-cracked specimens of cold-worked stainless steel and Alloy 182 weld metal exposed in 288°C water suddenly broke apart at stress intensities equivalent to KIC values as low as 68.6 and 82 ksi√in, respectively. All such observations to date have been in high temperature water, and the possibility exists that larger effects would be observed if the materials were cooled to below 150°C, where hydrogen effects on fracture resistance are known to be much more pronounced. Nevertheless, EPRI-sponsored reassessments of these data have shown that a substantial fraction is in fact a manifestation of limit load failures of the test specimens and not caused by specifically environmental effects. This conclusion has been supported by two more recent experimental investigations [A362], [A363], although the second of these reports advised caution on extending this as a general conclusion for the full range of applicable structural materials, temperatures, and water chemistries of practical relevance.

It is a matter of scientific debate whether the LTCP phenomenon represents a genuine reduction in fracture properties of the material or a form of rapid, subcritical crack growth due to the environment [A310]. Nevertheless, the possibility of unstable crack growth at lower values of K_{IC} or J_{IC} than in air needs to be evaluated independent of arguments over the terminology used. It seems likely that hydrogen plays a major role in both abnormally high SCC propagation rates and premature fracture phenomena so that there is a mechanistic basis for expecting effects of strain rate, loading mode, temperature, microstructure, hydrogen concentration, etc. However, there is no quantitative model for predicting the extent of their influence. Nevertheless, the fugacity of hydrogen in the environment, diffusivity of hydrogen within the metal, and their interaction as a function of temperature and mechanical loading rate are likely to be significant factors in determining the practical impact.

In summary, the decrease in apparent fracture toughness due to aqueous environmental effects is expected to be greatest in higher yield strength materials (e.g., Alloy X-750 and Alloy 718) and in materials that are inhomogeneous (e.g., Ni alloy weld metals and thermally aged CASS). Cold-worked and possibly irradiated stainless steels are also potentially of concern. To date, however, there is little (if any) plant experience or evidence of environmentally reduced fracture resistance, although the consequence might be a reduction in structural integrity margins that depends on specific material-component operating conditions. Evaluation of the significance of laboratory LTCP observations has relied on comparing the conditions of test under which apparent fracture toughness is reduced by a large margin with reactor operating conditions, especially at low temperatures during plant heat up or cool down [A364]–[A366][A322]. Only Alloy X-750 and possibly Alloy 718 appear likely to be significantly susceptible to LTCP in PWR service because the instantaneous stress intensities and rising loading rates required for LTCP of the most susceptible weld nickel-base metals do not appear to occur when primary circuit components would be most susceptible [A322].

A.6 Irradiation Effects

A.6.1 Irradiation Embrittlement (Emb)

Irradiation by neutrons results in embrittlement of materials. Its extent depends on several variables, including neutron fluence, neutron flux, irradiation temperature, and material microstructure and chemistry. Irradiation embrittlement of alloys used in nuclear power systems refers to the loss of ductility and fracture toughness from exposure to high-energy neutrons (E > 1.0 MeV). The loss of ductility and fracture toughness is usually accompanied by marked increases in yield and ultimate tensile strength.

Mechanistically, irradiation embrittlement results from lattice defects induced by neutron bombardment. High-energy neutrons displace atoms from their normal lattice positions and create point defects. Although most point defects (interstitials and vacancies) are annihilated by recombination, surviving point defects form various irradiation-induced microstructural features consisting of dislocations, precipitates, and cavities. Cavities, which are three-dimensional clusters of vacancies, can be associated with other microstructural features such as precipitates, dislocations, and grain boundaries. These defects and precipitates from irradiation are obstacles to dislocation movement and result in an increase in yield and tensile strengths and decreased work hardening capacity and ductility, and loss of fracture toughness. The growth of cavities by vacancy condensation can also lead to void swelling and a further deterioration of fracture toughness but only at very high neutron fluences that can only be encountered in PWR core support structures.

The detrimental effect of irradiation embrittlement has long been recognized for low-alloy steel PWR, VVER, and BWR reactor pressure vessels and for Zircaloy-2 and Zr-2.5%Nb alloys used for CANDU calandria and pressure tubes. However, until relatively recently, irradiation embrittlement had not been extensively quantified for PWR, VVER, or BWR core internals. This is partly because the internals are mainly constructed of austenitic stainless steels, which retain high levels of ductility and fracture toughness even after neutron exposure levels that would have caused significant embrittlement in low-alloy steel reactor vessels. However, the proximity of austenitic stainless steel internals to the core in BWRs and especially PWRs means that the neutron flux for many lower internals (core support structures) is one to three orders of magnitude higher than for the low-alloy steel reactor vessels. Because of this large increase in neutron fluence that will be accumulated by core support structures over their lives, the austenitic stainless steels can undergo significant hardening and loss of ductility and toughness as a result of neutron irradiation. A large reduction in fracture toughness of stainless steels due to neutron irradiation can significantly increase the sensitivity to flaws that are either preexisting during construction or developed during service due to SCC, IASCC, or fatigue.

A.6.1.1 Ferritic Steels

Irradiation embrittlement in ferritic low-alloy pressure vessel steels is typically measured by an increase in the ductile-to-brittle transition temperature (RTNDT) and a decrease in the upper shelf energy, as determined by Charpy impact energy tests, and corresponding increases in yield and ultimate tensile strength. Tensile ductility is not affected to the same extent. Embrittlement in the older generation of ferritic low-alloy steels used for LWR reactor pressure vessels is primarily caused by the irradiation-induced formation of copper-rich precipitates that harden the matrix and reduce toughness.

Extensive databases exist for evaluating and predicting embrittlement in this older generation of reactor vessel steels. For specific PWR, VVER, and BWR vessels, data are obtained from specimens of vessel materials in surveillance capsules placed on the inside surface of the reactor pressure vessel at the height of the active core, and from test reactors. Embrittlement trend curve models such as Reg. Guide 1.99, Rev. 2 [A323] are used to predict the shift in RTNDT and drop in upper-shelf energy as a function of copper, nickel, and neutron fluence.

Significant variations in irradiation embrittlement have also been observed between different types of ferritic steels and even between different heats of the same steel. These differences are caused by variations in metallurgical structure and composition. Improved empirical trend models have been developed to describe the combined effects of copper, nickel, phosphorus, irradiation temperature, and neutron flux and fluence on the embrittlement of reactor pressure vessel steels. Steels with a very low copper content show low embrittlement in spite of high radiation doses. The effect of irradiation exposure at low temperatures (below 274°C [525°F]) increases the rate of embrittlement damage. Weld metal is generally more sensitive to irradiation embrittlement than base metal. Chemical impurity level, chemical composition variability, and different microstructure are responsible for the greater sensitivity of the weld metal. In 2015, an updated improved trend curve model was approved in a revision to ASTM Standard Guide E 900 [A324].

A.6.1.2 Austenitic Stainless Steels

PWR, VVER, and BWR internals next to the core are mainly fabricated from wrought austenitic stainless steels. The most commonly used alloys in PWR and BWR core internals are solution-annealed Types 304/304L and cold-worked Types 316/316L, while titanium-stabilized stainless steels are used in VVERs. They may be welded or bolted with, typically, cold-worked Type 316 or 347 stainless steels, solution-annealed Type 304, or titanium-stabilized stainless steel bolting materials. Some components on the core periphery can be made from CASS. The neutron fluences sustained by these materials are at least an order of magnitude greater than those sustained at the beltline of the pressure vessel and can be up to three orders of magnitude greater (see Figure A-42). Other internal components that are made of martensitic stainless steels, austenitic or martensitic precipitation-hardened stainless steels, austenitic nickel-base alloys, austenitic precipitation-hardened nickel-base alloys, and cobalt-base alloys usually do not reach significant neutron exposures during the reactor lifetime to be a concern for irradiation embrittlement but may become a concern for longer periods of extended operations.

Tensile Properties of Irradiated Austenitic Stainless Steels

Tensile properties of irradiated austenitic stainless steels have been widely investigated. However, a 2004 review of available tensile data for irradiated austenitic stainless steels for the EPRI MRP [A325] indicated that most data were from materials irradiated in fast reactors. The review also noted that data exceeding fluences of 15 dpa (~ 1.0×10^{22} n/cm^2, E > 1.0 MeV) in LWRs were limited. Since that time, additional LWR data for austenitic stainless steels have become available for comparison and evaluation [A326], [A327].

Yield strength data as a function of neutron fluence at elevated temperature are plotted in Figure A-56 for solution-annealed and cold-worked austenitic stainless steels as an example of the trends observed. All data (for yield strength, ultimate tensile strength, elongation, etc. between room temperature and operating temperature) consistently indicate a saturation of

irradiation strengthening between 10 dpa (~6.67 x 10^{21} n/cm^2, E > 1.0 MeV) and ~20 dpa (~1.33 x 10^{22} n/cm^2, E > 1.0 MeV) and thereafter the mechanical properties reach a plateau and remain at that level without further change. There is also only a small difference between the saturated irradiated yield and ultimate tensile strengths at constant temperature, and the corresponding uniform elongations of the irradiated austenitic materials are very small (< 1%). Total elongation remains significant, however, and saturates at between 5 and 15% with neutron fluence above 5 dpa (~3.33 x 10^{21} n/cm^2, E > 1.0 MeV). Although there can be significant variability in the initial heat-to-heat tensile properties (e.g., available data show that room temperature total elongation values for non-irradiated Type 304 solution-annealed material vary from 44 to 94%), the variability of tensile properties is reduced considerably after saturation. Overall, the stainless steel tensile test data are complete enough to identify the trend of embrittlement up to a neutron fluence value of 231 dpa (~1.54 x 10^{23} n/cm^2, E > 1.0 MeV). Moreover, no significant difference has been detected between fast reactor and thermal reactor irradiated materials. Therefore, it appears that no additional tensile test data are needed to define the embrittlement trend of austenitic stainless steels, provided that significant void swelling does not occur (see later discussion).

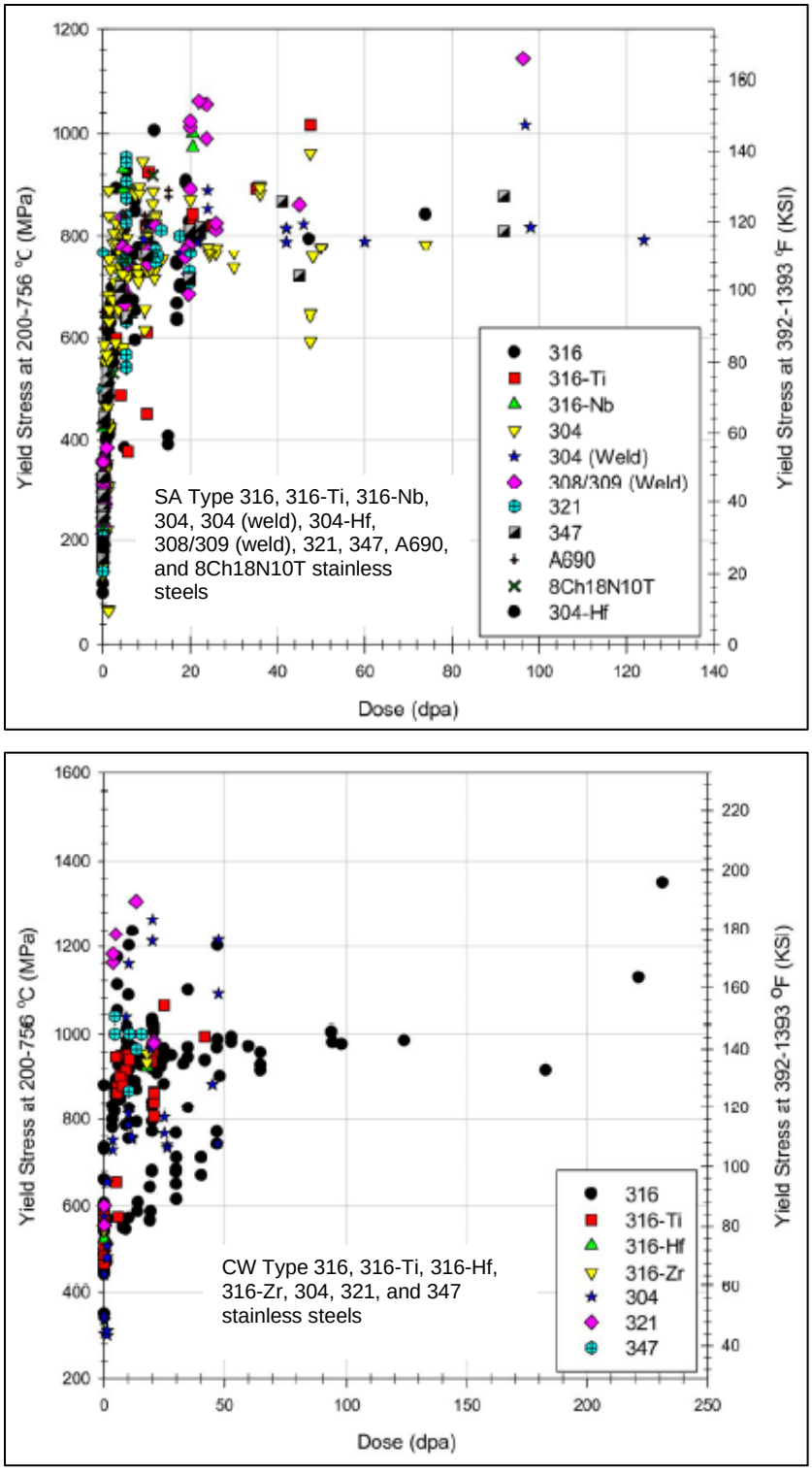

Figure A-56
Effect of neutron fluence on elevated-temperature yield stress, (top) solution annealed (SA) and (bottom) cold worked (CW)

Fracture Toughness Properties of Irradiated Austenitic Stainless Steels

Irradiation embrittlement of austenitic stainless steels has been mostly characterized through standard fracture toughness testing, although some Charpy V-notch data are also available. Data have been generated from materials irradiated in fast and thermal reactors, including decommissioned PWR and BWR reactor core internal components. All known fracture toughness data (converted to equivalent values of K_{IC}) are plotted in Figure A-57 and Figure A-58 for austenitic stainless steel irradiated in fast and thermal reactors, respectively [A326][A329]. All these data are consistent, revealing a saturation of irradiation embrittlement between 5 and 10 dpa (~$3.3x10^{21}$ and $6.7x10^{21}$ n/cm^2, E > 1.0 MeV). The minimum initiation fracture toughness, J_{IC}, is ~10 kJ/m^2 (57 in.-lb/in.^{2}) from which the lower bound fracture toughness, K_{JC}, is calculated as ~38 MPa√m (35 ksi√in) at neutron doses greater than $6.67x10^{21}$ n/cm^2 (E > 1.0 MeV) or ~10 dpa.

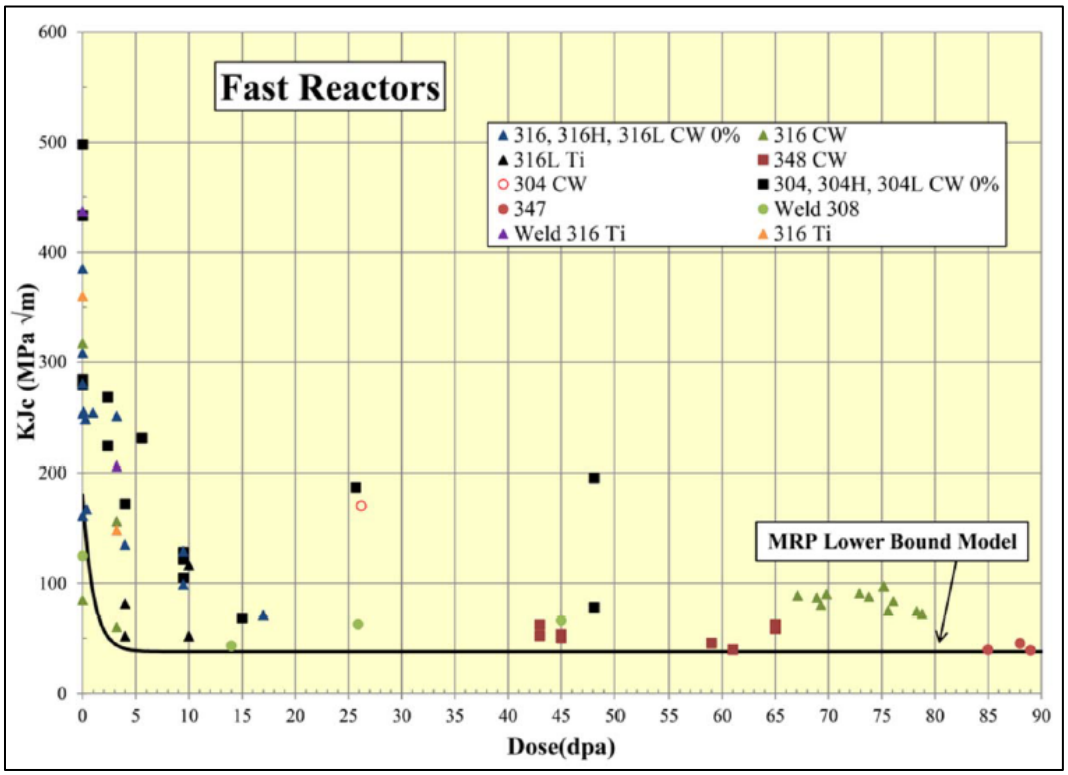

Figure A-57
Effect of neutron fluence on fracture toughness—fast reactors [A326]

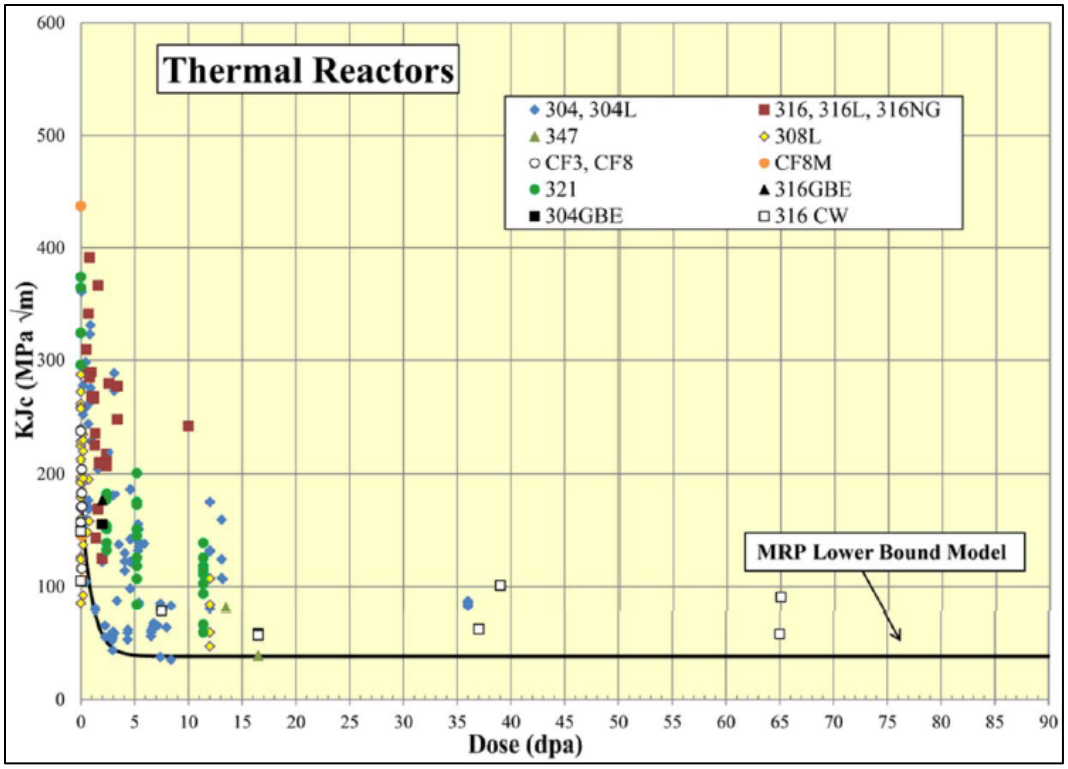

Figure A-58
Effect of neutron fluence on fracture toughness—thermal reactors [A326]

It can be seen in Figure A-57 and Figure A-58 that data taken from specimens irradiated in fast reactors and in thermal reactors are in agreement, indicating a lack of any noticeable flux effect for the embrittlement of austenitic stainless steels. The stainless steel fracture data are sufficiently complete to identify the lower bound plateau at fluences >10 dpa (~6.67×10^{21} n/ cm^2, E > 1.0 MeV) up to ~90 dpa (~6.00×10^{22} n/cm^2, E > 1.0 MeV). For BWRs, it is clear that adequate data are available for life-extended operations, but there remains a lack of fracture toughness data for PWR components at very high dpa (between ~90 and 120 dpa or between 6.0×10^{22} and 8.4×10^{22} n/cm^2, E > 1.0 MeV). It is also noted that some of the data points at very high fluences from material irradiated in the EBR-II fast reactor exhibited significant void swelling (up to 8%) [A330], but this did not have any noticeable impact on the lower saturated plateau of fracture toughness. However, void swelling > 10% will likely cause a significant further reduction in fracture toughness.

Another important observation from fracture toughness testing of highly irradiated stainless steels is that the tearing modulus is reduced to very low values as a result of neutron irradiation [A328], [A329]. Therefore, it appears that when the decrease in fracture toughness properties approaches saturation, linear elastic fracture mechanics (LEFM) evaluations may be more appropriate to establish acceptable flaw sizes.

A.6.2 Void Swelling (VS)

Irradiation-induced void swelling, hereafter called *void swelling (VS)*, occurs under some irradiation conditions in all structural alloys used in various reactor types, but is especially prevalent in austenitic stainless steels and nickel-base alloys under high temperature and fluence conditions. The common feature of these alloys is their FCC crystal structure, which is more prone to swelling earlier and, eventually, at a higher rate than that of BCC and HCP crystal structured metals [A331].

Void swelling is a complex phenomenon that is highly dependent on the material (chemical composition and thermal-mechanical treatment) and on the irradiation conditions (temperature history, neutron spectrum, flux, and transmutation gas production). These factors are often highly interactive and synergistic in determining the path taken by the swelling phenomenon. All contribute to the difficulty of confidently forecasting the level and distribution of void swelling and its associated effects in nuclear reactor internals.

Void swelling is a potential concern for PWR internals and other reactor types operating at elevated temperatures in that it produces volume and thus dimensional changes, and when acting in concert with irradiation creep, it produces distortions of structural components [A330]. For the lower operating temperatures and, particularly, lower fluences of BWRs, void swelling is not considered to be an issue. However, if swelling exceeds a few percent, an additional concern begins to develop regarding mechanical properties and toughness. Whereas the radiation-induced changes in mechanical properties typically saturate at relatively low neutron doses, a new form of embrittlement associated with void swelling arises with increasing swelling above ~5 to 10%. Based on fast reactor data available to date, when ~10% volume change is exceeded, the tearing modulus at PWR operating temperatures of Type 300-series stainless steels is dramatically reduced, producing severe embrittlement with little energy required to propagate any crack [A330].

Swelling in austenitic stainless steels is caused by the creation of small cavities from a few to a few tens of nanometers in diameter that appear under certain conditions of temperature, flux, and fluence. Swelling has typically been a concern for fast reactors because of high fluences and operating temperatures, but a small amount (up to 0.24%) of void swelling has also been observed under PWR conditions, primarily in highly irradiated PWR baffle-to-former bolts, as summarized in Figure A-59 [A326], [A327], [A332]. The available data for the highest fluences are all at estimated temperatures, including the effects of γ-heating, of less than 330°C (626°F). Since void swelling appears to be minimal below 310°C (590°F), more data are needed for high fluences representative of end of life (including life extension) at temperatures higher than 330°C (626°F) and possibly up to ~400°C, to take into account the aggravating effect of γ-heating of thick section components.

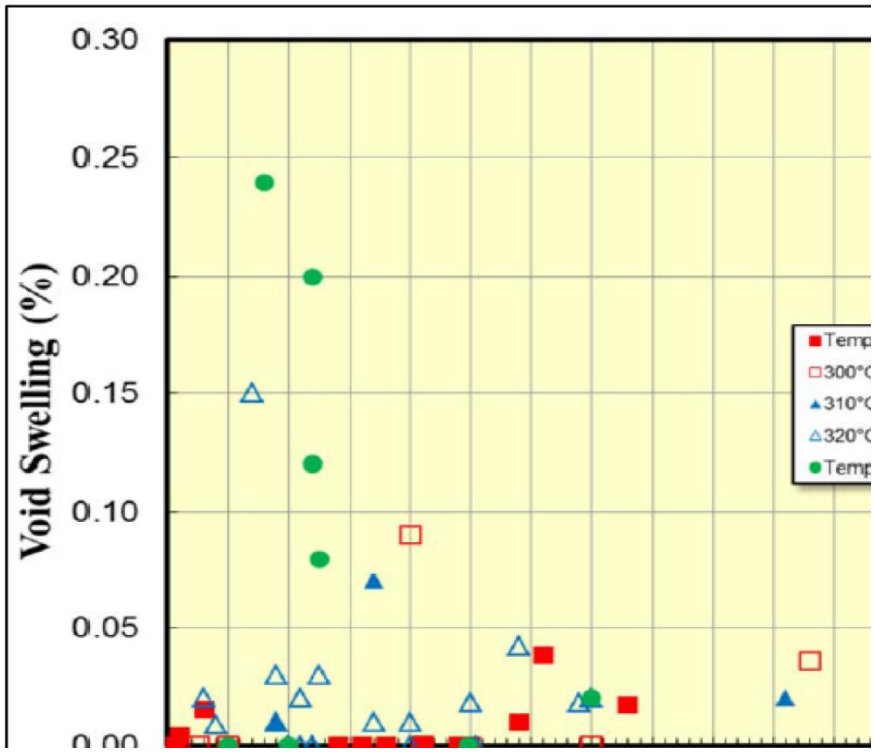

Figure A-59
Void swelling data for austenitic stainless steels irradiated in thermal reactors (mainly PWRs) [A326]

Estimates of the level of void swelling under PWR conditions have been based thus far on empirical extrapolations of data from fast reactor irradiations, albeit from reflector positions where neutron flux values (between $4x10^{-4}$ and 10^{-7} dpa/s) and temperatures (370-430°C/698-806°F) were closer to PWR core periphery conditions [A333]. This empirical model is consistent with the void swelling measurements, albeit small, of the samples from PWR internal components available to date. Although these data fit within the scatter of the available void swelling model being used for PWR internals evaluations, the data set is not sufficient to fully verify or calibrate the model under all PWR irradiation conditions.

A.6.3 Irradiation Creep and Stress Relaxation (IC/SR)

The general mechanisms of stress relaxation (SR) and irradiation creep (IC) are well understood [A335]. Some confusion in discussion of stress relaxation and creep phenomena can arise from overlapping use of mechanisms and behavior terminology. The terms *primary*, *secondary*, and *tertiary creep* are familiar for thermally induced creep, but these terms do not refer to mechanisms or even different types of deformation; they more properly describe regions of a thermal creep curve and then only under constant load conditions (Figure A-60). The mechanisms operative during secondary thermal creep are also operative during primary thermal creep but not vice versa.

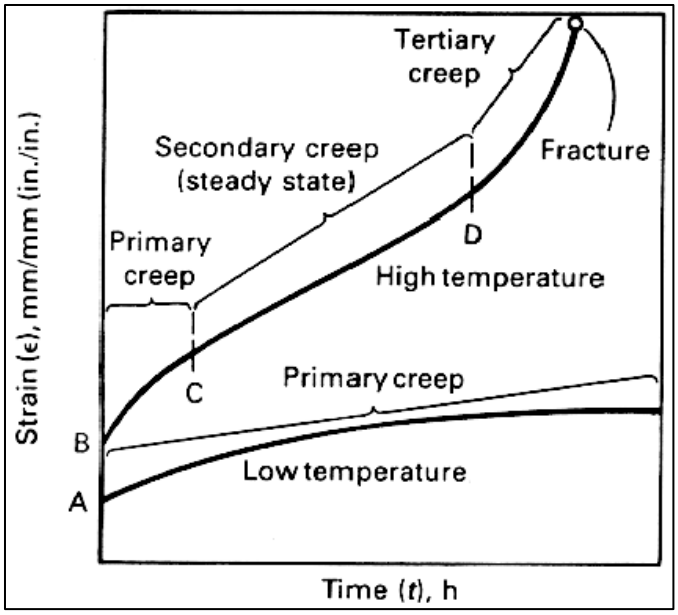

Figure A-60
Schematic representation of creep curves under constant load (A and B denote the elastic strain on loading; C denotes the transition from primary to secondary creep; and D denotes the transition from secondary to tertiary creep.)

Some authors go further in narrowing the definition of thermal creep to that occurring under constant load where a steady deformation rate (secondary creep) is attained. This is usually at temperatures above half the absolute melting point ($> 0.5T_m$); thus, materials creep thermally above $0.5T_m$ but can also relax below $0.5T_m$. Stress relaxation, in reality, is primary creep at a temperature where, by definition, thermal creep does not occur; see for example [A337], [A338].

The real practical issue is whether permanent deformation of the material occurs below the yield point. Thus, stress relaxation refers to the consequences of any plastic deformation under constant strain that occurs below the yield point of a material, and creep is any time-dependent plastic deformation that occurs below the yield point of a material under constant load.

In 2001, the EPRI MRP sponsored a project to evaluate the available data on stress relaxation and creep [A339].

Concern regarding thermal stress relaxation (primary creep in Figure A-60) is associated with bolted joints and coil or leaf springs potentially leading to excessive wear or fatigue failure. Secondary thermal creep in austenitic stainless steels is associated with temperatures higher than those relevant to PWR, VVER, BWR or CANDU internals, even after taking into account gamma heating. Only a few stress relaxation tests by primary creep have been reported in the literature for austenitic stainless steels at PWR internals temperatures (approximately 288°C/550°F to 343°C/650°F).

It has been noted that the available data show that thermal stress relaxation (by primary creep) appears to reach saturation in a short time (< 100 hours) with a maximum reduction of 10-20% of initial bolt preloads at reactor internals temperatures [A335]. This is based on tests that lasted 1000 hours or less. However, there is no physical basis to argue that significant further stress

relaxation will occur at longer times, and with approximately 80% of initial preload remaining in bolting applications, the functionality of a component item will remain intact. It is also worth noting that the conclusion above is consistent with the discussion of creep and stress relaxation, in the absence of a significant radiation environment, found in NUREG/CR-6048 [A367].

Irradiation creep is an athermal process that depends on the neutron fluence and stress and can also be affected by void swelling should it occur. It manifests itself in two ways. In the first case, irradiation creep operates to mitigate potential increases in stress caused by void swelling, especially problems that might be caused by gradients in swelling within a given component. In the second case, however, it is important to note that irradiation creep can occur in the absence of void swelling and that it can cause stress relaxation of preloaded components (possibly leading to excessive wear or fatigue) or affect components with sustained pressure differences (with possible consequences for fluid flow or heat transfer). A large amount of fast and thermal test reactor stainless steel material test data exist for irradiation creep, and empirical equations for the steady-state irradiation creep are well developed. The MRP database consists of data for a variety of austenitic stainless steels, including solution-annealed Type 304 and cold-worked Type 316.

Figure A-61 shows correlations of irradiation-induced creep strain as a function of the composite parameter of effective stress multiplied by the irradiation dose [A336]. The current database indicates that a greater irradiation creep rate occurs for solution-annealed Type 304 materials than for cold-worked Type 316 materials. The recently obtained data are consistent with other literature data, although the slopes are somewhat higher than seen previously with fast reactor data (~ 14% higher). Transmission electron microscope examinations have confirmed that swelling did not contribute to the observed irradiation creep in these more recent experiments.

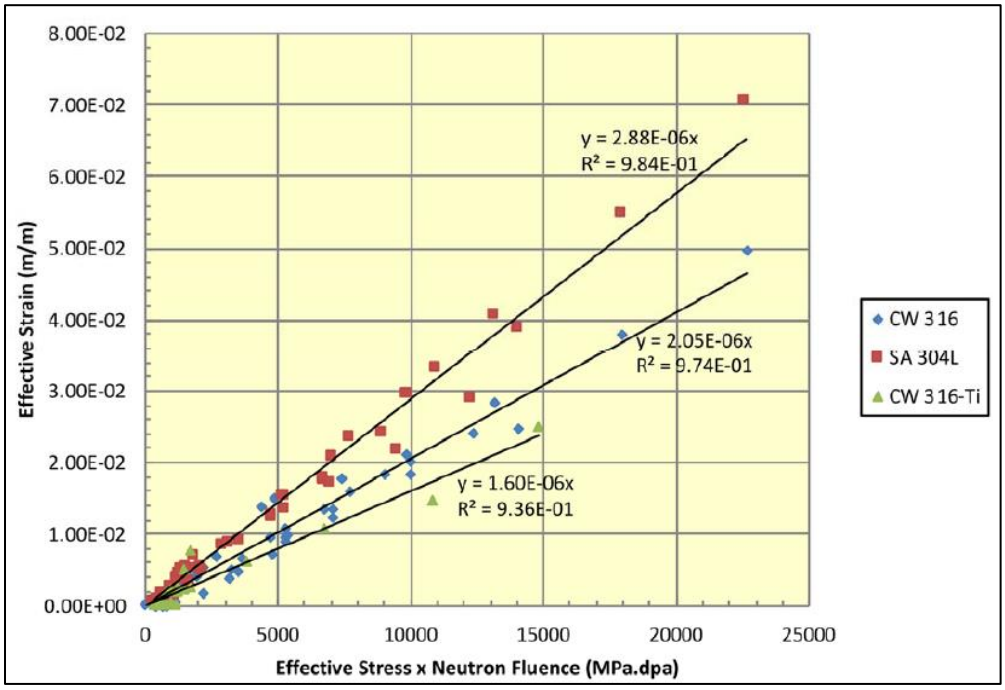

Figure A-61
Irradiation creep and stress relaxation data and model fits [A326]

A.7 References and Bibliography

[A1] "Corrosion: Environments and Industries," *Metals Handbook*, Vol. 13C, ASM International, 1987.

[A2] "Corrosion: Environments and Industries," *Metals Handbook*, Vol. 13C, ASM International, 2006.

[A3] *Uhlig's Corrosion Handbook*, 2nd edition, R. W. Revie (Ed.), John Wiley and Sons, 2000.

[A4] *Corrosion*, 3rd edition, L. L. Shrier, R. A. Jarman, and G. T. Burstein (Eds.), Butterworth-Heinemann Ltd, 1994.

[A5] P. P. Milella, *Fatigue and Corrosion in Metals*, Springer, 2012.

[A6] T. L. Anderson, *Fracture Mechanics, Fundamentals and Applications*, CRC Press, 2005.

[A7] G. S. Was, *Fundamentals of Radiation Materials Science*: *Metals and Alloys*, Springer, 2007.

[A8] M. Pourbaix, *Atlas of Electrochemical Equilibria in Aqueous Solutions*," Ed. NACE, 1974.

[A9] B. Beverskog and I. Puigdomenech, "Revised Pourbaix Diagrams for Iron at 25-300°C," *Corrosion Science*, Vol. 38, No. 12, p. 2121, 1996.

[A10] B. Beverskog and I. Puigdomenech, "Revised Pourbaix Diagrams for Nickel at 25-300°C," *Corrosion Science*, Vol. 39, No. 5, p. 969, 1997.

[A11] B. Beverskog and I. Puigdomenech, "Pourbaix Diagrams for the Ternary System of Iron-Chromium-Nickel," *Corrosion*, Vol. 55, No. 11, p. 1077, 1999.

[A12] G. M. W. Mann, "The Oxidation of Iron-Base Alloys Containing Less Than 12% Cr in High Temperature Aqueous Solutions" in *High Temperature High Pressure Electrochemistry in Aqueous Solutions*, NACE, Houston, pp. 34–47, 1976.

[A13] L. Tomlinson, "Mechanism of Corrosion of Carbon and Low Alloy Ferritic Steels by High Temperature Water," *Corrosion*, Vol. 37, No. 3, pp. 591–596, 1981.

[A14] T. Mizuno, Pednekar, S. Szklarska-Smialowska, and D. D. Macdonald, "Corrosion and Stress Corrosion Cracking Behavior of Carbon Steels in Oxygenated High Purity Water at Elevated Temperatures" (pp. 395–422). In: J. Roberts and W. Berry (Eds.), National Association of Corrosion Engineers, Proceedings of First International Symposium on Environmental Degradation in Nuclear Power Systems – Water Reactors, Myrtle Beach, South Carolina, USA, August 22–25, 1983.

[A15] E. G. Brush and W. L. Pearl, "Corrosion and Corrosion Product Release in Neutral Feedwater," *Corrosion*, Vol. 28, No. 4, pp. 129–136, 1972.

[A16] J. Robertson, "The Mechanism of High Temperature Aqueous Corrosion of Stainless Steels," *Corrosion Science*, Vol. 32, No. 4, pp. 443–465, 1991.

[A17] C. C. Lin, Y. J. Kim, L. Niedrach, and K. S. Ramp, "Electrochemical Potential Models for BWR Applications," *Corrosion*, Vol. 52, p. 618, 1996.

[A18] GE-NE Document 22A1495, Rev. 3, "Pressure Integrity of Piping and Equipment Pressure Parts," February, 1974.

[A19] *Materials Reliability Program (MRP): Crack Growth Rates for Evaluating Primary Water Stress Corrosion Cracking (PWSCC) of Thick-Wall Alloy 600 Materials (MRP-55), Revision 1*. EPRI, Palo Alto, CA: 2002. 1006695.

[A20] USNRC Information Notice 86.108, *Degradation of Reactor Coolant System Pressure Boundary Resulting from Boric Acid Corrosion*, December 29, 1986; Supplement 1, April 20, 1987; Supplement 2, November 19, 1987; Supplement 3, January 5, 1995.

[A21] USNRC Generic Letter 88-05, *Boric Acid Corrosion of Carbon Steel Reactor Pressure Boundary Components in PWR Plants*, March 17, 1988.

[A22] USNRC Information Notice 2002-11, *Recent Experience with Degradation of Reactor Pressure Vessel Head*, March 12, 2002.

[A23] USNRC Information Notice 2003-02, *Recent Experience with Reactor Coolant System Leakage and Boric Acid Corrosion*, January 16, 2003.

[A24] C. J. Czajkowski, "Corrosion and Stress Corrosion of Bolting Materials in Light Water Reactors" (pp. 192–208). In: Proceedings of 1st International Symposium on Environmental Degradation of Materials in Nuclear Power Systems – Water Reactors, NACE, Myrtle Beach, South Carolina, USA, 1984.

[A25] J. F. Hall, "Corrosion of Low Alloy Steel Fastener Materials Exposed to Borated Water" (pp. 711–722). In: Proceedings of 3rd International Symposium on Environmental Degradation of Materials in Nuclear Power Systems – Water Reactors, The Metallurgical Society, Traverse City, MI, USA, 1988.

[A26] J. F. Hall, R. S. Frisk, A. S. O'Neill, R. S. Pathania, and W. B. Neff, "Boric Acid Corrosion of Carbon and Low Alloy Steels" (pp. 9–38 to 9–52). In: Proceedings of 4th International Symposium on Environmental Degradation of Materials in Nuclear Power Systems – Water Reactors, NACE, Jekyll Island, GA, USA, 1990.

[A27] C. A. Campbell, S. Fyfitch, and D. T. Martin, "Boric Acid Corrosion of Carbon and Low Alloy Steels," Corrosion 1994, Paper 166, NACE International, 1994.

[A28] J. M. Gras, D. Noel, B. Prieux, M. Cleurennec, and Y. Rouillon, "Corrosion of Low Alloy Steels and Stainless Steels in Concentrated Boric Acid Solutions." In: Proceedings of EUROCORR 96, Session IX Nuclear Corrosion and Protection, Paper OR 20, Nice, France, 1996.

[A29] *Boric Acid Corrosion Guidebook, Revision 1: Managing Boric Acid Corrosion Issues at PWR Power Stations*. EPRI, Palo Alto, CA: 2001. 1000975.

[A30] J.-H. Park, O. K. Chopra, K. Natesan, W. J. Shack, and W. H. Cullen, "Boric Acid Corrosion of Light Water Reactor Pressure Vessel Materials" (pp. 459–468). In: Proceedings of the 12th International Conference on Environmental Degradation of Materials in Nuclear Power Systems – Water Reactors, TMS, Snowbird, Utah, USA, 2005.

[A31] H. Xu, S. Fyfitch, and J. Hyres, "Boric Acid Corrosion Laboratory Investigation of The Davis-Besse Reactor Pressure Vessel Head" (pp. 855–861). In: Proceedings of the 12th International Conference on Environmental Degradation of Materials in Nuclear Power Systems – Water Reactors, TMS, Snowbird, Utah, USA, 2005.

[A32] C. Marks, A. McIlree, J. Hickling, K. Ahluwalia, J. Lumsden, and D. Lister, "Boric Acid Corrosion Testing of Power Reactor Pressure Vessel Closure Head Material" (pp. 761–774). In: Proceedings of Fontevraud VI, 2006.

[A33] *Establishing an Effective Leak Management Program*. EPRI, Palo Alto, CA: 2001. TR-114761.

[A34] *Survey of On-line PWR Coolant Leak Detection Technologies (MRP-94)*. EPRI, Palo Alto, CA: 2003. 1009062.

[A35] C. Czajkowski, Metallurgical Evaluation of an 18-inch Feedwater Line Failure at the Surry Unit 2 Power Station, NUREG/CR-4868, Brookhaven National Laboratory, March, 1987.

[A36] The Nuclear and Industrial Safety Agency, *Secondary Piping Rupture Accident at Mihama Power Station, Unit 3 of the Kansai Electric Power Co., Inc. (Final Report), Revision 1*, translated by the Japan Nuclear Energy Safety Organization (JNES), May 14, 2005.

[A37] USNRC Information Notice 2006-08, Secondary Piping Rupture at the Mihama Power Station in Japan, March 16, 2006.

[A38] *Flow Accelerated Corrosion in Power Plants, Rev 2*. EPRI, Palo Alto, CA: 2016. TR-106611.

[A39] G. J. Bignold, K. Garbett, and I. S. Woolsey, "Mechanistic Aspects of the Temperature Dependence of Erosion–Corrosion." In: P. H. Berge and F. Kahn (Eds.), Proceedings of Conference of Corrosion Erosion of Steels in High Temperature Water and Wet Steam, Electricité de France, May, 1982.

[A40] G. J. Bignold, C. H. de Whally, K. Garbett, and I. S. Woolsey, "Mechanistic Aspects of Erosion-Corrosion Under Boiler Feedwater Conditions" (pp. 219–226). In: Proceedings of Water Chemistry of Nuclear Reactor Systems III, BNES, 1983.

[A41] B. Poulson, "Advances in Understanding Hydrodynamic Effects on Corrosion," *Corrosion Science*, Vol. 35, pp. 655–665, 1993.

[A42] R. L. Tapping, "Flow Accelerated Corrosion," Appendix B17 in Expert Panel Report on Proactive Materials Degradation Assessment, US NRC NUREG/CR-6923, 2006.

[A43] R. K. Freier, "Operating Experiences with Protective Layers of Metal Oxides, Using Addition of Oxygen" *Vom Wasser*, Vol. 38, Ed. Verlag Chemie Gmbh, Weinheim, Bergstr, 1971.

[A44] *BWRVIP-190 Revision 1: BWR Vessel and Internals Project. Volume 1: BWR Water Chemistry Guidelines – Mandatory, Needed, and Good Practice Guidance*. EPRI, Palo Alto, CA: 2014. 3002002623.

[A45] M. J. Davies, I. S. Woolsey, J. McGuigan, and T. Renwick, "Erosion-corrosion in AGR Boilers." In: Proceedings of Chimie 2002, Avignon, France, April 22–26, 2002.

[A46] A. Bart, H. M. Crockett, L. F. Goyette, J. S. Horowitz, and R. Montgomery, "Flow Accelerated Corrosion – the Entrance Effect," PVP2008-61185. In: Proceedings of PVP2008, 2008 ASME Pressure Vessels and Piping Division Conference, Chicago, Illinois, USA, July 27–31, 2008.

[A47] P. T. Gilbert, "Copper and Copper Alloys," Chapter 4.2. In: L. L. Shreir, R. A. Jarman, and G. T. Burstein, Eds., *Corrosion*, Third Edition, Butterworth Heinemann, 1994.

[A48] *Corrosion Related Failures in Power Plant Condensers*. EPRI, Palo Alto, CA: 1980. NP-1468.

[A49] G. M. Gordon and K. S. Ramp, "Dependence of Creviced BWR Component IGSCC Behavior on Coolant Chemistry" (pp. 14–46 to 14.62). In: D. Cubicciotti and E. Simonen, Eds., National Association of Corrosion Engineers, Proceedings of Fourth International Symposium on Environmental Degradation in Nuclear Power Systems – Water Reactors, Jekyll Island, Georgia, USA, August 6–10, 1989.

[A50] K. S. Brown and G. M. Gordon, "Effects of BWR Coolant Chemistry on Propensity for IGSCC Initiation and Growth in Creviced Reactor Internals Components" (pp. 243–248). In: G. J. Theus and W. Berry, Eds., The Metallurgical Society, Proceedings of Third International Symposium on Environmental Degradation in Nuclear Power Systems – Water Reactors, Traverse City, Michigan, USA, August 30–September 3, 1987.

[A51] *Corrosion-Assisted Cracking of Stainless Steel & Low Alloy Steels in LWR Environments*. EPRI, Palo Alto, CA: 1987. NP5064S.

[A52] B. C. Syrett and R. L. Coit, "Causes and Prevention of Condenser Tube Failures." In: Second Joint ASM/ANS Nuclear Engineering Conference, Portland, Oregon, USA, July 1982.

[A53] R. W. Staehle, "Bases for Predicting the Earliest Penetrations Due to Stress Corrosion Cracking for Alloy 600 on the Secondary Side of PWR Steam Generators," USNRC Report NUREG–CR-6737, 2001.

[A54] D. You, S. Lefevre, D. Feron, and F. Vaillant, "Experimental Study of Concentrated Solutions Containing Sodium and Chloride Pollutants in SG Flow Restricted Areas," Paper 151, Proceedings of Chimie 2002, SFEN, 2002.

[A55] P. M. Scott, "A Discussion of Mechanisms and Modeling of Secondary Side Corrosion Cracking in PWR Steam Generators" (pp. 107–122). In: Ed. R. H. Jones, The Metallurgical Society, Proceedings of Chemistry and Electrochemistry of Corrosion and Stress Corrosion Cracking: A Symposium Honoring the Contributions of R. W. Staehle, 2001.

[A56] A. Baum, "Experimental Evaluation of Tube Support Plate Crevice Chemistry." In: Proceedings of 10th International Symposium on Environmental Degradation of Materials in Nuclear Power Systems – Water Reactors, Lake Tahoe, Nevada, NACE International, 2001.

[A57] P. M. Scott and P. Combrade, "Corrosion in Pressurized Water Reactors." In: *ASM Handbook on Corrosion*, Second Edition, Vol. 13C, pp. 362–385, ASM, 2006.

[A58] Layman, W. H., et al., "Status of Steam Generators," *Combustion*, pp.14–20, 1979.

[A59] W. T. Lindsay, "MULTEQ: What It Is and What It Can Do" (pp. 567–575). In: Eds. R. W. Staehle, J. A. Gorman, and A. R. McIlree, Proceedings of Control of Corrosion on the Secondary Side of Steam Generators, NACE International, 1996.

[A60] G. R. Englehardt, D. D. Macdonald, and P. J. Millet, "Transport Processes in Steam Generator Crevices-I. General Corrosion Model," *Corrosion Science*, Vol. 41, pp. 2165–2190, 1999.

[A61] G. R. Englehardt, D. D. Macdonald, and P. J. Millet, "Transport Processes in Steam Generator Crevices-II. A Simplified Method for Estimating Impurity Accumulation Rates," *Corrosion Science*, Vol. 41, pp. 2191–2211, 1999.

[A62] Z. Szklarska-Smialowska, "Review of Literature on Pitting Corrosion Published Since 1960," *Corrosion*, Vol. 27, pp. 223–233, 1971.

[A63] G. Cragnolino, "A Review of Pitting Corrosion in High Temperature Aqueous Solutions." In: International Conference on Localized Corrosion (NACE Houston), Florida, 1987.

[A64] D. D. Macdonald and G. A. Cragnolino, "Corrosion of Steam Cycle Materials," Chapter 9 (pp. 659–1031). In: Ed. P. Cohen, *The ASME Handbook on Water Technology for Thermal Power Systems*, ASME, 1989.

[A65] H. Bohni, "Localized Corrosion of Passive Metals" (pp.173–190). In: Ed. R. W. Revie, *Uhlig's Corrosion Handbook*, Second Edition, John Wiley and Sons, 2000.

[A66] H. H. Strehblow, "Mechanisms of Pitting Corrosion" (p. 243). In: Ed. P. Marcus, *Corrosion Mechanisms in Theory and Practice*, Second Edition, Revised and Expanded, New York, Basel, Marcel Dekker Inc., 2002.

[A67] G. Wranglén, "Pitting and Sulphide Inclusions in Steel," *Corrosion Science*, Vol. 14, p. 331, 1974.

[A68] A. J. Sedriks, "Role of Sulphide Inclusions in Pitting and Crevice Corrosion of Stainless Steels," *International Metals Reviews*, Vol. 28, p. 295, 1983.

[A69] A. J. Sedriks, "Effect of Alloy Composition and Microstructure on the Localized Corrosion of Stainless Steels" (p. 85). In: Eds. H. Isaacs, U. Bertocci, J. Kruger, and S. Smialowska, *Advances in Localized Corrosion* (Orlando, Florida, USA, June 1987), NACE-9, 1990.

[A70] I. L. Rosenfeld and I. S. Danilov, "Electrochemical Aspects of Pitting Corrosion," *Corrosion*, Vol. 7, pp. 129–142, 1967.

[A71] W. Cieslak and D. Duquette, "The Pit Initiation Resistance of Ferritic Stainless Steel in Chloride Environments from 80 to 260°C" (pp. 438–450). In: Eds. J. Roberts and W. Berry, National Association of Corrosion Engineers, Proceedings of First International Symposium on Environmental Degradation in Nuclear Power Systems – Water Reactors, Myrtle Beach, South Carolina, USA, August 22–25, 1983.

[A72] H. P. Leckie and H. H. Uhlig, "Environmental Factors Affecting the Critical Potential for Pitting in 18-8 Stainless Steel," *Journal of the Electrochemical Society*, Vol. 113, pp. 1262–1267, 1986.

[A73] L. F. Lin, G. Cragnolino, Z. Szklarska-Smialowska, and D. D. Macdonald, "Stress Corrosion Cracking of Sensitized Type 304 Stainless Steel in High Temperature Chloride Solutions," *Corrosion*, Vol. 37, pp. 616–627, 1981.

[A74] W. F. Bogaerts, A. A. Van Haute, and M. J. Brabers, "Relative Critical Potentials for Pitting Corrosion of 304 Stainless Steel, Incoloy 800 and Inconel 600 in Alkaline High Temperature Aqueous Solutions," *Journal of Nuclear Materials*, Vol. 115, pp. 339–342, 1983.

[A75] J. R. Park and Z. Szklarska-Smialowska, "Pitting Corrosion of Inconel 600 in High Temperature Water Containing $CuCl_2$," *Corrosion*, Vol. 41, pp. 665–675, 1985.

[A76] J. Horvath and H. H. Uhlig, "Critical Potentials for Pitting Corrosion of Ni, Cr-Ni, Cr-Fe and Related Stainless Steels," *Journal of the Electrochemical Society*, Vol. 115, pp. 791–795, 1968.

[A77] S. J. Green, "Steam Generator Failure or Degradation" (pp. 937–945). In: "Corrosion in the Nuclear Power Industry," *ASM Handbook, Corrosion*, Vol. 13, 1987.

[A78] M. Karaminezhaad-Ranjbar, J. Mankowski, and D. D. Macdonald, "Pitting Corrosion of Inconel 600 in High Temperature Chloride Solution under Controlled Hydrodynamic Conditions," *Corrosion*, Vol. 41, No. 4, pp. 197–204, 1985.

[A79] J. F. Sykes and M. J. Angwin, "The Causes of Major Pitting of Alloy 600 Steam Generator Tubing in Pressurized Water Reactors" (pp. 624–631). In: Proceedings of 2nd International Symposium on Environmental Degradation of Materials in Nuclear Power Systems – Water Reactors, American Nuclear Society, Monterey, CA, 1986.

[A80] J. Hickling, "Pressure Vessel Steels: Corrosion and Environmentally Assisted Cracking," MIT/EPRI Course on *Materials Reliability in Nuclear Power Systems*, June 2005.

[A81] K. J. Vetter and H. H. Strehblow, "Pitting Corrosion in an Early Stage and Its Theoretical Implications" (p. 240). In: Localized Corrosion, Williamsburg, VA, USA (December 1971), NACE-3, 1974.

[A82] T. R. Beck, "Occurrence and Properties of Anodic Salt Films in Pitting Corrosion" (p. 85). In: Eds. H. Isaacs, U. Bertocci, J. Kruger, and S. Smialowska, *Advances in Localized Corrosion* (Orlando, Florida, USA, June 1987), NACE-9, 1990.

[A83] N. Sridhar, D. S. Dunn, C. S. Brossia, and G. A. Cragnolino, "Stabilization and Repassivation of Localized Corrosion" (p. 1). In: CORROSION 2001, Proceedings of Research Topical Symposium on Localized Corrosion, NACE, 2001.

[A84] Z. Szklarska Smialowska and J. Mankowski, "Effect of Temperature on the Kinetics of Development of Pits in Stainless Steel in 0.5 NaCl + 0.1 N H2SO4 Solution," *Corrosion Science*, Vol. 12, p. 925, 1972.

[A85] D. D. Macdonald and M. Urquidi-Macdonald, "Distribution Functions for the Breakdown of Passive Films," *Electrochemical Acta*, Vol. 31, p. 1079, 1987.

[A86] T. Shibata and H. Takamiya, "Effect of pH and Cl- on the Stochastic Process of Pitting Corrosion of Mo Containing Stainless Steels." In: Eds. H. Leidheiser and S. Haruyama, Proceedings of Critical Issues in Reducing the Corrosion of Steels, USA-Japan Seminar Nikko Japan, 1985.

[A87] T. Shibata and T. Takeyama, "Stochastic Theory of Pitting Corrosion," C*orrosion*, Vol. 33, p. 243, 1977.

[A88] *A Study of Microbiologically Influenced Corrosion in Nuclear Power Plants and Practical Guide to Counter Measures*. EPRI, Palo Alto, CA: 1986. NP-4582.

[A89] D. H. Pope, "Microbiologically-Influenced Corrosion in the Nuclear Power Industry, Case Histories, Methods of Detection, Control and Prevention" (pp. 641–646). In: Eds. G. J. Theus and W. Berry, Proceedings of Third International Symposium on Environmental Degradation in Nuclear Power Systems – Water Reactors, Traverse City, Michigan, The Metallurgical Society, August 30–September 3, 1987.

[A90] G. O. Hayner, D. H. Pope, and B. E. Crane, "Microbiologically-Influenced Corrosion in Condenser Water Boxes at Crystal River-3" (pp. 647–653). In: Eds. G. J. Theus and W. Berry, Proceedings of Third International Symposium on Environmental Degradation in Nuclear Power Systems – Water Reactors, Traverse City, Michigan, The Metallurgical Society, August 30–September 3, 1987.

[A91] S. C. Dexter, "Localized Biological Corrosion" (pp. 114–122). In: *Corrosion, Metals Handbook*, Vol. 13, ASM International, 1987.

[A92] J. Robertson, "The Mechanism of High Temperature Aqueous Corrosion of Stainless Steels," *Corrosion Science*, Vol. 32, p. 443, 1991.

[A93] D. H. Lister, R. D. Davidson, and E. Mcalpine, "The Mechanism and Kinetics of Corrosion Product Release from Stainless Steel in Lithiated High Temperature Water," *Corrosion Science*, Vol. 27, p. 113, 1987.

[A94] F. Carrette, "Relâchement des produits de corrosion des tubes en Alliage 690 de générateurs de vapeur du circuit primaire des réacteurs à eau pressurisée," PhD Thesis, Institut National Polytechnique de Toulouse, 2002.

[A95] D. H. Lister, "Corrosion Product Release in PWR Primary Coolant" (Vol. 2, p. 87). In: Water Chemistry for Nuclear Reactor Systems 4, October 1986, BNES, London, 1987.

[A96] A. J. Sedricks, J. W. Schultz, and M. A. Cordovi, "Inconel 690 – A New Corrosion Resistant Material," *Corrosion Engineering*, Vol. 28, pp. 82–95, 1979.

[A97] T. Yonezawa, K. Onimura, N. Sasaguri, T. Kusakabe, H. Nagano, K. Yamanaka, T. Minami, and M. Inoue, "Effect of Heat Treatment on Corrosion Resistance of Alloy 690" (pp. 593–608). In: Proceedings of 2nd International Conference on Environmental Degradation of Materials in Nuclear Power Systems (Monterey, CA, 1985), ANS, 1986.

[A98] L. Guinard, O. Kerrec, D. Noël, S. Gardey, and F. Coulet, "Influence of the Initial Surface Condition on the Release of Nickel Alloys in the Primary Circuit of PWRs," *Nuclear Energy*, Vol. 39, p. 19, 1997.

[A99] *Effect of Steam Generator Replacement on PWR Primary Corrosion Product Transport*. EPRI, Palo Alto, CA: 2002. 1003601.

[A100] F. Dacquait, P. Ridoux, C. Brun, and N. Engler, "Impact of Steam Generator Replacement on PWR Primary Circuit Contamination by Radioactive Corrosion Products" (p. 53). In: Water Chemistry of Nuclear Reactor Systems 8, BNES, 2000.

[A101] F. Dacquait, L. Guinard, C. Andrieu, J. L. Bretelle, F. Bardet, A. Rocher, and C. Brun, "Status of Primary System Contamination in French PWRs." In: International Conference on Water Chemistry of Nuclear Reactor Systems, San Francisco, CA, USA, October 2004.

[A102] C. C. Lin, "A Review of Corrosion Product Transport and Radiation Field Buildup in Boiling Water Reactors," *Progress in Nuclear Energy*, Vol. 51, p. 207, 2009.

[A103] A. R. Wazzan, H. Procaccia, and J. David, "Thermal – Hydraulic Characteristics of Pressurized Water Reactors During Commercial Operation IV. Saturation Pressure, Circulation Ratio, and Carry-under in a PWR Steam Generator (Tricastin 1 Nuclear Power Plant)," *Nuclear Engineering and Design*, Vol. 80, pp. 79–86, 1984.

[A104] M. Le Calvar, A. Vergnault, H. Bodineau, F. Balestreri, and T. Sollier, "Build-up of Deposits in Steam Generators: A Safety Issue" (pp. 1488–1497). In: 14th International Conference on Environmental Degradation of Materials in Nuclear Power Systems – Water Reactors, Virginia Beach, Virginia, USA, August 23–27, 2009.

[A105] G. Corredera, M. Alves-Vieira, and O. de Bouvier, "Fouling and TSP Blockage of Steam Generators on EDF Fleet: Identified Correlations with Secondary Water Chemistry and Planned Remedies." In: Paper L09-2, International Conference on Water Chemistry of Nuclear Reactor Systems, Berlin, Germany, September 15–19, 2008.

[A106] Z. Amjal, J. Pugh, J. Zibrida, and B. Zuhl, "Polymer Performance in Cooling Water: The Influence of Process Variable." In: Paper No. 160, Corrosion, 1996.

[A107] K. Fruzzetti, P. Frattini, P. Robbins, A. Miller, R. Varrin, and M. Kreider, "Dispersant Trial at ANO-2: Qualification for a Short-Term Trial Prior to SG Replacement." In: International Conference on Water Chemistry in Nuclear Reactor Systems, Avignon, France, April 22–26, 2002.

[A108] K. Fruzzetti, P. Frattini, P. Robbins, A. Miller, R. Varrin, and M. Kreider, "Dispersant Trial at ANO-2: Results from a Short-Term Trial Prior to SG Replacement." In: International Conference on Water Chemistry in Nuclear Reactor Systems, Avignon, France, April 22–26, 2002.

[A109] K. Fruzzetti, M. Kreider, A. Miller, J. Jevec, and P. King, "Dispersant Application for Steam Generator Fouling Mitigation." In: Water Chemistry of Nuclear Reactor Systems, San Francisco, California, USA, October 11–14, 2004.

[A110] D. Rochester, P. Hull, J. Nolin, T. Henrickson, L. Wilson, K. Fruzzetti, M. Kreider, A. Miller, P. King, and J. Jevec, "Dispersant Trial at McGuire Unit 2 for Mitigation of SG Deposit Fouling." In: International Conference on Water Chemistry of Nuclear Reactor Systems, Jeju Island, Korea, October 23–26, 2006.

[A111] K. Fruzzetti, M. Kreider, C. E. Anderson, C. R. Marks, D. Morey, and P. R. Walton, "2009 Industry Update on Dispersant Use for SG Fouling Control." In: Paper 4.02, The 6th CNS International Steam Generator Conference, Hilton Toronto, Toronto, Ontario, Canada, November 8–11, 2009.

[A112] M. Barale, M. Guillodo, M. Foucault, N. Ryckelynck, M. H. Clinard, F. Chahma, C. Brun, and G. Corredera, "Secondary Side TSP Deposit Buildup: Lab Test Investigation Focus on Electrokinetic Considerations." In: International Conference on Water Chemistry of Nuclear Reactor Systems, Quebec, Canada, September 2010.

[A113] F. P. Ford, "Technical and Management Challenges Associated with Structural Materials Degradation in Nuclear Reactors in the Future." In: Eds. P King and T. Allen, Proceedings of Thirteenth International Conference on Environmental Degradation in Nuclear Power Systems – Water Reactors, Whistler, BC, Canada, August 20–24, 2007.

[A114] J. Hickling and D. Blind, "Strain-Induced Corrosion Cracking of Low Alloy Steels in LWR Systems – Case Histories and Identification of Conditions Leading to Susceptibility," *Nuclear Engineering and Design*, Vol. 91, pp. 305–330, 1986.

[A115] Ford, F. P., et al., "The Effect of Dissolved Oxygen, Hydrogen, Carbon Dioxide, Ammonia, Inhibitors, and Dynamic Loads on the Stress Corrosion Cracking of Turbine Disc Steels in Water," General Electric Research and Development Report 84CRD278, November 1984.

[A116] *Stress Corrosion Cracking in PWR and BWR Closed Cooling Water Systems*. EPRI, Palo Alto, CA: 2004. TR-1009721.

[A117] *Status Review of Initiation of Environmentally Assisted Cracking and Short Crack Growth*. EPRI, Palo Alto, CA: 2005. 1011788.

[A118] *Mechanisms of Environmental Cracking Peculiar to the Power Generation Industry*. EPRI, Palo Alto, CA: 1982. NP-2589.

[A119] F. P. Ford, "The Crack Tip System and Its Relevance to the Prediction of Cracking in Aqueous Environments" (pp. 139–165). In: Eds. R. Gangloff and B. Ives, Proceedings of First International Conference on Environmentally Assisted Cracking of Metals, NACE, Kohler, Wisconsin, USA, October 2–7, 1988.

[A120] F. P. Ford, "Quantitative Prediction of Environmentally Assisted Cracking," *Corrosion*, Vol. 52, pp. 375–395, 1996.

[A121] T. Shoji, S. Suzuki, and R. G. Ballinger, "Theoretical Prediction of Stress Corrosion Crack Growth—Threshold and Plateau Growth Rate" (pp. 881–891). In: Eds. R. Gold and A. McIlree, Proceedings of Seventh International Symposium on Environmental Degradation in Nuclear Power Systems – Water Reactors, National Association of Corrosion Engineers, Breckenridge, Colorado, USA, August 7–10, 1995.

[A122] T. Shoji, H. Takahashi, and M. Suzuki, "Corrosion Fatigue Aspects in BWR Pipe Cracking" (p. 58). In: Eds. H. Okada and R. W. Staehle, *Predictive Methods for Assessing Corrosion Damage in BWR Piping and PWR Steam Generators*, Fuji, Japan, May 1978.

[A123] T. Shoji, "Progress in Mechanistic Understanding of BWR SCC and Implication to Predictions of SCC Growth Behaviour in Plants." In: Eds. G. Was and L. Nelson, Proceedings of Eleventh International Conference on Environmental Degradation in Nuclear Power Systems – Water Reactors," Skamania Lodge, Stevenson, Washington, USA, August 5–9, 2003.

[A124] F. P. Ford and P. L. Andresen, "Corrosion in Nuclear Systems: Environmentally Assisted Cracking in Light Water Reactors" (pp. 501–546). In: Eds. P. Marcus and J. Ouder, *Corrosion Mechanisms*, Marcel Dekker, 1994.

[A125] P. M. Scott and P. Combrade, "On the Mechanism of Stress Corrosion Crack Initiation and Growth in Alloy 600 Exposed to PWR Primary Water" (pp. 29–36). In: Eds. G. Was and L. Nelson, Proceedings of Eleventh International Conference on Environmental Degradation in Nuclear Power Systems – Water Reactors, American Nuclear Society, Skamania Lodge, Stevenson, Washington, USA, August 5–9, 2003.

[A126] P. Combrade, P. M. Scott, M. Foucault, E. Andrieu, and P. Marcus, "Oxidation of Nickel Base Alloys in PWR Water; Oxide Layers and Associated Damage" (pp. 883–890). In: Eds. L. Nelson and P. J. King, Proceedings of Twelfth International Conference on Environmental Degradation in Nuclear Power Systems – Water Reactors, The Metallurgical Society, Snowbird, Utah, USA, August 5–9, 2005.

[A127] H. Hanninen, K. Torronen, M. Kempainen, and S. Salonen, "On the Mechanisms of Environment Sensitive Cyclic Crack Growth of Nuclear Reactor Pressure Vessel Steel," *Corrosion Science*, Vol. 23, p. 663, 1983.

[A128] *Fractographic Evaluation of Specimens of A533B Pressure Vessel Steel*. EPRI, Palo Alto, CA: 1984. NP 3483.

[A129] M. M. Hall and D. M. Symons, "Hydrogen Assisted Creep Model for Low Potential Stress Corrosion Cracking of Ni-Cr-Fe Alloys" (pp. 447–466). In: Proceedings of Chemistry and Electrochemistry of Corrosion and Stress Corrosion Cracking: A Symposium Honoring the Contributions of R. W. Staehle, TMS, 2001.

[A130] J. Hickling and D. Blind, "Strain-induced Corrosion Cracking of Low Alloy Steels in LWR Systems – Case Histories and Identification of Conditions Leading to Susceptibility," *Nuclear Engineering and Design*, Vol. 91, pp. 305–330, 1986.

[A131] P. M. Scott and D. R. Tice, "Stress Corrosion in Low Steels," *Nuclear Engineering and Design*, Vol. 119, pp. 399–413, 1990.

[A132] W. J. Bamford, G. V. Rao, and J. L. Houtman, "Investigation of Service – Induced Degradation of Steam Generator Shell Materials." In: Eds. D. Cubicciotti and E. Simonen, Proceedings of Fifth International Symposium on Environmental Degradation in Nuclear Power Systems – Water Reactors, American Nuclear Society, Monterey, California, USA, August 25–29, 1991.

[A133] H. P. Seifert, S. Ritter, and J. Hickling, "Environmentally Assisted Cracking of Low Alloy RPV and Piping Steels Under LWR Conditions" (pp. 73–88). In: Proceedings of 11th International Conference on Environmental Degradation of Materials in Nuclear Power Systems – Water Reactors, American Nuclear Society, Stevenson, Washington, 2003.

[A134] A. Roth, E. Nowak, M. Widera, U. Ilg, U. Wesseling, and R. Zimmer, "Recent In-Service Experience with Degradation of Low Alloy Steel Components Due to Localized Corrosion and Environmentally Assisted Cracking in German PWR Plants." In: Ed. T. R. Allen, P. J. King, and L. Nelson, Proceedings of the 12th International Conference on Environmental Degradation of Materials in Nuclear Power System – Water Reactors, TMS, Skamania Lodge, Stevenson, Washington, USA, August 5–9, 2005.

[A135] J. P. Slade and T. S. Gendron, "Flow Accelerated Corrosion and Cracking of Carbon Steel Piping in Primary Water-Operating Experience at the Point Lepreau Generating Station" (pp.773–782). In: Eds. L. Nelson and P. King, Proceedings of Twelfth International Conference on Environmental Degradation in Nuclear Power Systems – Water Reactors, The Metallurgical Society, Skamania Lodge, Stevenson, Washington, USA, August 5–9, 2005.

[A136] A. Roth and J. Hickling, "Crack Initiation Due to Environmentally Assisted Cracking in Carbon and Low alloy Steels Exposed to High-Temperature Water." In: Proceedings of 13th International Conference on Environmental Degradation of Materials in Nuclear Power Systems, Whistler, British Columbia, Canada, August 19–23, 2007.

[A137] *Environmentally Assisted Cracking of Low Alloy Steels*. EPRI, Palo Alto, CA: 1992. NP7473L.

[A138] F. P. Ford, Trans ASME, *Journal of Pressure Vessel Technology,* Vol. 110, pp. 113–128, 1989.

[A139] F. P. Ford, P. L. Andresen, D. Weinstein, S. Ranganath, and R. Pathania, "Stress Corrosion Cracking of Low Alloy Steels in High Temperature Water" (pp. 561–569). In: Eds. D. Cubicciotti and E. Simonen, Proceedings of Fifth International Symposium on Environmental Degradation in Nuclear Power Systems – Water Reactors, American Nuclear Society, Monterey, California, USA, August 25–29, 1991.

[A140] L. Young and P. L. Andresen, "Crack Tip Microsampling and Growth Rate Measurements in a 0.01%S Low Alloy Steel" (pp. 1193–1204). In: Eds. R. Gold and A. McIlree, Proceedings of Seventh International Symposium on Environmental Degradation in Nuclear Power Systems – Water Reactors, National Association of Corrosion Engineers, Breckenridge, Colorado, USA, August 7–10, 1995.

[A141] H. P. Seifert and S. Ritter, "New Observations of the SCC Crack Growth Behaviors of Low-Alloy RPV Steels Under BWR/NWC Conditions" (pp. 341–350). In: Eds. G. Was and L. Nelson, Proceedings of Eleventh International Conference on Environmental Degradation in Nuclear Power Systems – Water Reactors, American Nuclear Society, Skamania Lodge, Stevenson, Washington, USA, August 5–9, 2003.

[A142] J. Heldt and H.-P. Seifert, "The Stress Corrosion Cracking of Reactor Pressure Vessel Steel Under BWR Conditions" (pp. 901–910). In: Eds. S. Bruemmer and F. P. Ford, Proceedings of Ninth International Symposium on Environmental Degradation in Nuclear Power Systems – Water Reactors, The Metallurgical Society, Newport Beach, California, USA, August 1–5, 1999.

[A143] *Stress Corrosion Cracking in Low Alloy Steels*. EPRI, Palo Alto, CA: 1994. RPC 102-4.

[A144] *BWRVIP-60-A: BWR Vessel and Internals Project, Evaluation of Stress Corrosion Crack Growth in Low Alloy Steel Vessel Materials in the BWR Environment*. EPRI, Palo Alto, CA: 2003. 1008871.

[A145] F. P. Ford, R. M. Horn, J. Hickling, R. Pathania, and G. Bruemmer, "Stress Corrosion of Low Alloy Steels Under BWR Conditions; Assessment of Crack Growth Rate Algorithms" (pp. 855–869). In: Eds. S. Bruemmer and F. P. Ford, Proceedings of Ninth International Symposium on Environmental Degradation in Nuclear Power Systems – Water Reactors, The Metallurgical Society, Newport Beach, California, USA, August 1–5, 1999.

[A146] J. Hickling, H.-P. Seifert, and S. Ritter, "Research and Service Experience with Environmentally Assisted Cracking of Low Alloy Steel," *Power Plant Chemistry*, Vol. 7, pp. 4–15, 2005.

[A147] *BWRVIP-233, Revision 1, BWR Vessel and Internals Project: Evaluation of Stress Corrosion Crack Growth in Low Alloy Steel Vessel Materials in the BWR Environment: Technical Basis for Revisions to BWRVIP-60-1A*. EPRI, Palo Alto, CA: 2011. 1022841.

[A148] H. Hanninen, Y. Yagodzinskyy, O. Tarasenko, U. Ehrnsten, P. A. Aaltonen, and H.-P. Seifert, "Effects of Dynamic Strain Aging on Environment-Assisted Cracking of Low Alloy Pressure Vessel and Piping Steels" (pp. 341–350). In: Eds. F. P. Ford and G. Was, Proceedings of Tenth International Conference on Environmental Degradation in Nuclear Power Systems – Water Reactors, National Association of Corrosion Engineers, Lake Tahoe, Nevada, USA, August 5–9, 2000.

[A149] H. D. Solomon, R. De Lair, and E. Tolksdorf, "LCF Crack Initiation in WB 36 in High Temperature Water" (pp. 865–874). In: Eds. S. Bruemmer and F. P. Ford, Proceedings of Ninth International Symposium on Environmental Degradation in Nuclear Power Systems – Water Reactors, The Metallurgical Society, Newport Beach, California, USA, August 1–5, 1999.

[A150] J. Hickling, "Strain Induced Cracking of Low Alloy Steels Under BWR Conditions; Are There Still Open Issues." In: Eds. F. P. Ford and G. Was, Proceedings of Tenth International Conference on Environmental Degradation in Nuclear Power Systems – Water Reactors, National Association of Corrosion Engineers, Lake Tahoe, Nevada, USA, August 5–9, 2001.

[A151] J. D. Atkinson and J. Yi, "The Role of Dynamic Strain Aging in the Environment Assisted Cracking Observed in Pressure Vessel Steels," *Fatigue & Fracture of Engineering Materials & Structures*, Vol. 20, pp. 1–12, 1997.

[A152] B. Devrient, A. Roth, K. Küster, M. Widera, and U. Ilg, "Influence of Dynamic Strain Ageing on the Crack Growth Rates and Crack Tip Plasticity of Low Alloy Steels in Oxygenated High-Temperature Water." In: Proceedings of 14th International Conference on Environmental Degradation of Materials in Nuclear Power Systems, Virginia Beach, Virginia, USA, August 23–27, 2009.

[A153] P. L. Andresen and F. P. Ford, "Life Prediction by Mechanistic Modeling and System Monitoring of Environmental Cracking of Fe and Ni Alloys in Aqueous Systems," *Materials Science and Engineering*, Vol. A103, pp. 167–183, 1988.

[A154] P. L. Andresen, "Perspective and Direction of Stress Corrosion Cracking in Hot Water." In: Eds. F. P. Ford and G. Was, Proceedings of Tenth International Conference on Environmental Degradation in Nuclear Power Systems – Water Reactors, National Association of Corrosion Engineers, Lake Tahoe, Nevada, USA, August 5–9, 2001.

[A155] P. L. Andresen, P. W. Emigh, M. M. Morra, and R. M. Horn, "Effects of Yield Strength, Corrosion Potential, Stress Intensity Factor, Silicon and Grain Boundary Character on the SCC of Stainless Steels" (pp. 816–831). In: Proceedings of 11th International Symposium on Environmental Degradation of Materials in Nuclear Power Systems – Water Reactors, ANS, 2003.

[A156] P. L. Andresen, P. E. Emigh, and L. M. Young, "Mechanistic and Kinetic Role of Yield Strength / Cold Work / Martensite, H2, Temperature, and Composition on SCC of Stainless Steels" (pp. 215–239). In: Proceedings of International Symposium on Mechanisms of Material Degradation in Non-Destructive Evaluation in Light Water Reactors, Institute of Nuclear Safety System, Osaka, Japan, May 2002.

[A157] F. P. Ford, P. L. Andresen, H. D. Solomon, B. M. Gordon, S. Ranganath, D. Weinstein, and R. Pathania, "Application of Water Chemistry Control, On-Line Monitoring and Crack Growth Rate Models for Improved BWR Materials Performance" (pp. 4.26–4.51). In: Eds. D. Cubicciotti and E. Simonen, Proceedings of Fourth International Symposium on Environmental Degradation in Nuclear Power Systems – Water Reactors, National Association of Corrosion Engineers, Jekyll Island, Georgia, USA, August 6–10, 1989.

[A158] P. L. Andresen, "SCC Testing and Data Quality Consideration" (pp. 411–421). In: Proceedings of Ninth International Symposium on Environmental Degradation of Materials in Nuclear Power Systems – Water Reactors, TMS, 1999.

[A159] P. M. Scott, "Recommended Test Procedure for Studies on Crack Growth in Simulated LWR Water Environments." In: Proceedings of Third International Atomic Energy Agency Specialists Mtg on Subcritical Crack Growth, Moscow, USSR, May 1990; NRC NUREG/CP-0112 (ANL-90/ 22), Vol. 1, pp. 117–128, 1990.

[A160] J. Hickling, "Evaluation of Acceptance Criteria for Data on Environmentally Assisted Cracking in Light Water Reactors," *SKI* Report, Vol. 94, No. 14, September 1994.

[A161] P. L. Andresen, "Modeling of Water and Material Chemistry Effects on Crack Tip Chemistry and Resulting Crack Growth Kinetics" (pp. 301–314). In: Eds. G. J. Theus and W. Berry, Proceedings of Third International Symposium on Environmental Degradation in Nuclear Power Systems – Water Reactors, The Metallurgical Society, Traverse City, Michigan, August 30–September 3, 1987.

[A162] P. L. Andresen, "Observation and Prediction of the Effects of Water Chemistry and Mechanics on Environmentally Assisted Cracking of Inconels 182 Weld Metal and 600," *Corrosion*, Vol. 44, pp. 376–385, 1988.

[A163] *Materials Reliability Program: Stress Corrosion Cracking of Stainless Steel Components in Primary Water Circuit Environments of Pressurized Water Reactors (MRP-236, Rev. 1)*. EPRI, Palo Alto, CA: 2017. 3002009967.

[A164] B. M. Gordon, "The Effect of Chloride and Oxygen on the Stress Corrosion Cracking of Stainless Steel: A Review of the Literature," *Materials Performance*, Vol. 19, p. 29, 1980.

[A165] *Materials Reliability Program: Studies of Stress Corrosion Cracking Initiation in Stainless Steels in Off-Normal PWR Primary Water Chemistry Environments, A Literature Review (MRP-292)*. EPRI, Palo Alto, CA: 2010. 1021016.

[A166] T. Couvant, E. Herms, P. Combrade, F. Vaillant, I. De Curières, J. M. Boursier, O. Raquet, and O. De Bouvier, "Effect of Chlorides and Sulfates on the EAC of Austenitic Stainless Steel in PWR Environment." In: Proceedings of the 13th International Symposium on Environmental Degradation of Materials in Nuclear Power Systems, Canadian Nuclear Society, Whistler, BC, Canada, August 2007.

[A167] O. Raquet, E. Herms, F. Vaillant, T. Couvant, and J.-M. Boursier, "SCC of Cold-worked Austenitic Stainless Steels in PWR Conditions" (pp. 1049–1058). In: Proceedings of the 12th International Symposium on Environmental Degradation of Materials in Nuclear Reactor Systems – Water Reactors, TMS, Monterey, CA, USA, 2005.

[A168] K. Arioka, T. Yamada, T. Terachi, and G. Chiba, "Influence of Carbide Precipitation and Rolling Direction on IGSCC Growth Behaviors of Austenitic Stainless Steels in Hydrogenated High Temperature Water" (pp. 1061–1066). In: Proceedings of the 12th Conference on Environmental Degradation of Materials in Nuclear Power Systems – Water Reactors, TMS, 2005.

[A169] T. Couvant, L. Legras, C. Pokor, F. Vaillant, Y. Brechet, J. M. Boursier, and P. Moulart, "Investigations on the Mechanisms of PWSCC of Strain-Hardening Stainless Steels." In: Proceedings of the 13th Conference on Environmental Degradation of Materials in Nuclear Power Systems – Water Reactors, Canadian Nuclear Society, 2007.

[A170] D. Tice, J. Stairmand, H. Fairbrother, and A. Stock, "Crack Growth Testing of Cold Worked Stainless Steel in a Simulated PWR Primary Water Environment to Assess Susceptibility to Stress Corrosion Cracking." In: Proceedings of the 13th Conference on Environmental Degradation of Materials in Nuclear Power Systems – Water Reactors, Canadian Nuclear Society, 2007.

[A171] Z. Lu, T. Shoji, and S. Yamazaki, "Effects of Loading Mode and Water Chemistry on Stress Corrosion Cracking of 316L Stainless Steel in Simulated PWR Environments" (pp. 207–217). In: Proceedings of the 14th Conference on Environmental Degradation of Materials in Nuclear Power Systems – Water Reactors, ANS, 2009.

[A172] P. M. Scott, "Stress Corrosion Cracking in Pressurized Water Reactors – Interpretation, Modeling and Remedies," *Corrosion*, Vol. 56, pp. 771–782, 2000.

[A173] S. J. Green, "Steam Generator Failure or Degradation." In: *Corrosion in the Nuclear Power Industry, ASM Handbook*, Vol. 13, pp. 937–945, 1987.

[A174] R. W. Staehle and J. Gorman, "Progress in Understanding and Mitigating Corrosion on the Secondary Side in PWR Steam Generators." In: Eds. F. P. Ford and G. Was, Bonus Paper, Proceedings of Tenth International Conference on Environmental Degradation in Nuclear Power Systems – Water Reactors, National Association of Corrosion Engineers, Lake Tahoe, Nevada, USA, August 5–9, 2001.

[A175] W. Bamford and J. Hall, "A Review of Alloy 600 Cracking in Operating Nuclear Plants: Historical Experience and Future Trends" (pp. 1071–1081). In: Eds. G. Was and L. Nelson, Proceedings of Eleventh International Conference on Environmental Degradation in Nuclear Power Systems – Water Reactors, American Nuclear Society, Skamania Lodge, Stevenson, Washington, USA, August 5–9, 2003.

[A176] W. Bamford and J. Hall, "Cracking of Alloy 600 Nozzles and Welds in PWRs: Review of Cracking Events and Repair Service Experience" (pp. 959–965). In: Proceedings of 12th International Conference on Environmental Degradation of Materials in Nuclear Power Systems – Water Reactors, TMS, 2005.

[A177] W. Bamford, G. Elder, B. Perdue, and B. Newton, "Service Experience with Alloy 182 Butt Welds and Weld Overlay Mitigation Process." In: Proceedings of 13th International Conference on Environmental Degradation of Materials in Nuclear Power Systems, Canadian Nuclear Society, Whistler, British Columbia, Canada, 2007.

[A178] W. H. Bamford and N. A. Palm, "Service Experience with Alloy 600 and Associated Welds in Operating PWRs, Including Repair Activities and Regulatory Code Actions" (pp. 1525–1536). In: Proceedings of 14th International Conference on Environmental Degradation of Materials in Nuclear Power Systems, ANS, Virginia Beach, VA, USA, 2009.

[A179] J. Blanchet, H. Coriou, L. Grall, C. Mahieu, C. Otter, and G. Turluer, "Historical Review of the Principal Research Concerning the Phenomena of Cracking of Nickel-base Austenitic Alloys" (pp. 1149–1160). In: Proceedings of NACE-5 Stress Corrosion Cracking and Hydrogen Embrittlement of Iron Base Alloys, National Association of Corrosion Engineers, 1977.

[A180] H. J. Schenk, "Investigation of Tube Failures in Inconel 600 Steam Generator Tubing at KWO Obrigheim," *Materials Performance*, Vol. 15, pp. 25–33, 1976.

[A181] P. Scott, M.-C. Meunier, F. Steltzlen, O. Calonne, M. Foucault, P. Combrade, and C. Amzallag, "Comparison of Laboratory and Field Experience of PWSCC in Alloy 182 Weld Metal." In: Proceedings of 13th International Conference on Environmental Degradation of Materials in Nuclear Power Systems, Canadian Nuclear Society, Whistler, British Columbia, Canada, 2007.

[A182] L. Duisabeau, D. Deforge, Y. Thebault, M. Stindel, and E. Lemaire, "EDF Field Experience of 182 J-groove Welds on CRDMs and SG Channel Head Nozzles." In: Proceedings of Fontevraud 7, International Symposium, SFEN, Avignon, France, 2010.

[A183] G. P. Airey, "The Stress Corrosion Cracking (SCC) Performance of Inconel Alloy 600 in Pure and Primary Water Environments" (pp. 462–476). In: Eds. J. Roberts and W. Berry, Proceedings of First International Symposium on Environmental Degradation in Nuclear Power Systems – Water Reactors, National Association of Corrosion Engineers, Myrtle Beach, South Carolina, USA, August 22–25, 1983.

[A184] A. Stein and A. R. McIlree, "Relationship of Annealing Temperature and Microstructure to Primary Side Cracking of Alloy 600 Steam Generator Tubing and the Prediction of Stress Corrosion Cracking in Primary Water" (pp. 47–51). In: Eds. J. Roberts and J. Weeks, Proceedings of Second International Symposium on Environmental Degradation Systems – Water Reactors, American Nuclear Society, Monterey, California, USA, September 9–12, 1985.

[A185] C. Benhamou and C. Amzallag, "Influence of Manufacturing Parameters on Stress Corrosion Cracking of Alloy 600 Used in Nuclear Power Plants." In: Proceedings of EUROCORR 99, Aix la Chapelle, 1999.

[A186] H. Nagano and H. Kajimura, "Clarification of Stress Corrosion Cracking Mechanism on Nickel Base Alloys in Steam Generators for Their Long Lifetime Assurance" (pp. 291–300). In: Proceedings of 7th International Symposium on Environmental Degradation of Materials in Nuclear Power Systems – Water Reactors, NACE International, Breckenridge, CO, USA, 1995.

[A187] F. Champigny, F. Chapelier, and C. Amzallag, "Maintenance Strategy of Inconel Components in PWR Primary Systems in France." In: Proceedings of Conference on Vessel Penetration Inspection, Cracking and Repairs, Gaithersburg, MD, USA, September 29–October 2, 2003.

[A188] P. Chartier, D. Edmond, and G. Turluer, "The French Regulatory Experience and Views on Nickel-base Alloy PWSCC Prevention." In: Proceedings of Conference on Vessel Penetration Inspection, Cracking and Repairs, Gaithersburg, MD, USA, September 29–October 2, 2003.

[A189] A. Hiser, "US Regulatory Experience and Prognosis with RPV Head Degradation and VHP Nozzle Cracking." In: Proceedings of Conference on Vessel Penetration Inspection, Cracking and Repairs, Gaithersburg, MD, USA, September 29–October 2, 2003.

[A190] E. Richey, D. S. Morton, and R. A. Etien, "SCC Initiation Testing of Nickel-based Alloys in High Temperature Water." In: Proceedings of 13th International Conference on Environmental Degradation of Materials in Nuclear Power Systems, Canadian Nuclear Society, Whistler, British Columbia, Canada, 2007.

[A191] P. L. Andresen, R. Reid, and J. Wilson, "SCC Mitigation of Ni Alloys and Weld Metals by Optimizing Dissolved Hydrogen" (pp. 345–372). In: Proceedings of 14th International Symposium on Environmental Degradation in Nuclear Power Systems – Water Reactors, ANS, Virginia Beach, VA, USA, 2009.

[A192] *Materials Reliability Program: Crack Growth Rates for Evaluating Primary Water Stress Corrosion Cracking (PWSCC) of Thick-Wall Alloy 600 Materials and Alloy 82, 182, and 132 Welds (MRP-420)*. EPRI, Palo Alto, CA: 2017. 3002010758.

[A193] *Materials Reliability Program (MRP): Resistance to Primary Water Stress Corrosion Cracking of Alloys 690, 52, and 152 in Pressurized Water Reactors (MRP-111)*. EPRI, Palo Alto, CA: 2004. 1009801; and U.S. Department of Energy, Washington, D. C.

[A194] S. M. Bruemmer, M. J. Olszta, and L. E. Thomas, "Cold Rolling Effects on Grain Boundary Damage and Stress Corrosion Crack Growth in Alloy 690." In: Proceedings of Fontevraud 7, International Symposium, SFEN, Avignon, France, 2010.

[A195] P. L. Andresen, M. M. Morra, and A. Ahluwalia, "SCC of Alloy 690 and Its Weld Metals in PWR Primary Water." In: Proceedings of EPRI 2010 International Pressurized Water Reactor Conference and Exhibition, June 28–July 1, 2010.

[A196] Y. Vidalenc, O. Calonne, L. Fournier, P. Scott, and P. Combrade, "A Study of the PWSCC Resistance of Alloys 690 and 152 Using Composite Specimens." In: Proceedings of EPRI 2010 International Pressurized Water Reactor Conference and Exhibition, June 28–July 1, 2010.

[A197] *Statistical Analysis of Steam Generator Tube Degradation*. EPRI, Palo Alto, CA: 1991. NP-7493.

[A198] K. D. Stavropoulos, J. A. Gorman, R. W. Staehle, and C.S. Welty, "Selection of Statistical Distributions for Prediction of Steam Generator Tube Degradation" (pp. 731–744). In: Eds. D. Cubicciotti and E. Simonen, Proceedings of Fifth International Symposium on Environmental Degradation in Nuclear Power Systems – Water Reactors, American Nuclear Society, Monterey, California, USA, August 25–29, 1991.

[A199] B. Flesch, P. Pitner, H. Procaccia, T. Riffard, and B. Granger, "Études mécaniques probabilistes appliquées à l'optimisation de la maintenance des faisceaux tubulaires des générateurs de vapeur" (pp. 1–15). Revue Française de Mécanique n° 1993-1.

[A200] R. W. Staehle, J. A. Gorman, K. D. Stavropoulos, and C. S. Welty, "Application of Statistical Distributions to Characterizing and Predicting Corrosion of Tubing in Steam Generators of Pressurized Water Reactors" (pp. 1374–1439). In: Ed. R. N. Parkins, Proceedings of Life Prediction of Corrodible Structures, NACE International, Houston, Texas, USA, 1994.

[A201] P. M. Scott, Y. Meyzaud, and C. Benhamou, "Prediction of Stress Corrosion Cracking of Alloy 600 Components Exposed to PWR Primary Water" (pp. 285–293). In: Eds. T. Shoji and T. Shibata, Proceedings of International Symposium on Plant Aging and Life Prediction of Corrodible Structures, JSCE and NACE, Sapporo, Japan, May 15–18, 1995.

[A202] P. M. Scott and C. Benhamou, "An Overview of Recent Observations and Interpretations of IGSCC in Nickel-Base Alloys in PWR Primary Water." In: Eds. F. P. Ford and G. Was, Proceedings of Tenth International Conference on Environmental Degradation in Nuclear Power Systems – Water Reactors, National Association of Corrosion Engineers, Lake Tahoe, Nevada, USA, August 5–9, 2001.

[A203] I. de Curières and M.-C. Meunier, "Stress Corrosion Cracking of Steam Generator Tubes Made of Alloy 600TT: Analysis of Operating Experience." In: Proceedings of Fontevraud 7, International Symposium, SFEN, Avignon, France, 2010.

[A204] C. Amzallag, S. Le Hong, C. Pagès, and A. Gelpi, "Stress Corrosion Life Assessment of Alloy 600 Components" (pp. 243–250). In: Proceedings of 9th International Symposium on Environmental Degradation of Materials in Nuclear Power Systems – Water Reactors, The Metallurgical Society, Newport Beach, CA, USA, 1999.

[A205] C. Amzallag, S. LeHong, C. Benhamou, and A. Gelpi, "Methodology Used to Rank the Stress Corrosion Susceptibility of Alloy 600 PWR Components." In: Pressure Vessel and Piping Conference, ASME, Seattle, Washington, USA, 2000.

[A206] G. Rao, B. A. Bishop, P. J. Kotwicki, and G. Flukiger, "Probabilistic PWSCC Failure Assessments of the Alloy 600 Reactor Vessel Closure Head Penetrations at Beznau Units 1 & 2 for a Sixty Year Life Extension" (pp. 323–333). In: Proceedings of Fontevraud 6, SFEN, 2006.

[A207] C. Benhamou and C. Amzallag, "Prediction of Stress Corrosion Initiation Time of Alloy 600 Components" (pp. 109–118). In: Proceedings of 14th International Conference on Environmental Degradation of Materials in Nuclear Power Systems, ANS, Virginia Beach, VA, USA, 2009.

[A208] C. Pichon, D. Buisine, C. Faidy, A. Gelpi, and M. Vaindirlis, "Phenomenon Analysis of Stress Corrosion Cracking in the Vessel Head Penetrations of French PWRs" (pp. 1–10). In: Proceedings of 7th International Symposium on Environmental Degradation of Materials in Nuclear Power Systems – Water Reactors, NACE International, Breckenridge, CO, USA, 1995.

[A209] P. Berge, "Importance of Surface Preparation for Corrosion Control in Nuclear Power Stations," *Materials Performance*, Vol. 36, p. 56, 1997.

[A210] S. Le Hong, C. Amzallag, and A. Gelpi, "Modeling of Stress Corrosion Crack Initiation on Alloy 600 in Primary Water of PWRs" (pp. 115–122). In: Proceedings of 9th International Symposium on Environmental Degradation of Materials in Nuclear Power Systems – Water Reactors, The Metallurgical Society, Newport Beach, CA, USA, 1999.

[A211] D. R. Diercks, J. F. Hall, P. C. Bryant, R. H. Keefer, R. W. Staehle, and B. Woodman, "Local Chemistry and Deposit Formation at Upper Bundle Free Span Region" (p. 79). In: Eds. R. W. Staehle, J. A. Gorman, and A. R. McIlree, Control of Corrosion on the Secondary Side of Steam Generators, NACE, Houston, Texas, USA, 1996.

[A212] R. W. Staehle and J. Gorman, "Progress in Understanding and Mitigating Corrosion on the Secondary Side in PWR Steam Generators." In: Eds. F. P. Ford and G. Was, Bonus Paper, Proceedings of Tenth International Conference on Environmental Degradation in Nuclear Power Systems – Water Reactors, National Association of Corrosion Engineers, Lake Tahoe, Nevada, USA, August 5–9, 2001.

[A213] R. W. Staehle, "Bases for Predicting the Earliest Penetrations Due to SCC for Alloy 600 on the Secondary Side of PWR Steam Generators," NUREG-CR-6737, U.S. Nuclear Regulatory Commission, Washington D. C., 2001.

[A214] R. W. Staehle and J. A. Gorman, "Quantitative Assessment of Submodes of Stress Corrosion Cracking on the Secondary Side of Steam Generator Tubing in Pressurized Water Reactors: Parts 1, 2 and 3," *Corrosion*, Vol. 59, pp. 931–994, 2003; Vol. 60, pp. 5–63, 2004; and Vol. 60, pp. 115–180, 2004.

[A215] H. Takamatsu, K. Matsueda, E. Kadokami, K. Arioka, T. Tsuruta, S. Okamoto, and T. Ueno, "Evaluation of SG Crevice Environment by Directly Sampled Method Using an On-Site Autoclave Facility" (p. 752). In: Eds. D. Cubicciotti and E. Simonen, Proceedings of Fifth International Symposium on Environmental Degradation in Nuclear Power Systems – Water Reactors, American Nuclear Society, Monterey, California, USA, August 25–29, 1991.

[A216] *MULTEQ Version 4.0 Desktop Application*. EPRI, Palo Alto, CA: 2006. 1014414.

[A217] *Pressurized Water Reactor Secondary Water Chemistry Guidelines—Revision 8*. EPRI, Palo Alto, CA: 2017. 3002010645.

[A218] L. E. Thomas and S. M. Bruemmer, "Observations and Insights into Pb-Assisted Stress Corrosion Cracking of Alloy 600 Steam Generator Tubes." In: Proceedings of 12th International Conference on Environmental Degradation of Materials in Nuclear Power System – Water Reactors, TMS, 2005.

[A219] *Proceedings: 2005 EPRI/ANL/NRC Workshop on Effects of Lead (Pb) and Sulfur (S) on the Performance of Secondary Side Tubing of Steam Generators in PWRs*. EPRI, Palo Alto, CA: 2005. 1012780.

[A220] A. McIlree, K. Fruzzetti, J. Gorman, W. Shack, R. Staehle, and J. Stevens, "A Case for the Major Influence of Lead and Sulfur in the Secondary Side Degradation of PWR Steam Generator Tubing" (pp. 1247–1256). In: Proceedings of Fontevraud VI, SFEN, 2006.

[A221] *Steam Generator Management Program: Conditions Causing Lead Stress Corrosion Cracking of Steam Generator Tubing*. EPRI, Palo Alto, CA: 2011. 1022829.

[A222] USNRC, Information Notice 2008-07, Cracking Indications in Thermally Treated Alloy 600 Steam Generator Tubes, April 2008.

[A223] E. Shaw, T. O'Brian, S. G. LeBlanc, T. Smith, and R. Mullins, "Vogtle 1 ODSCC." In: Proceedings of Fontevraud 7, International Symposium, SFEN, Avignon, France, 2010.

[A224] R. Kilian, J. Beck, H. Lang, V. Schneider, T. Schönherr, and M. Widera, "Root Cause Analysis of SG Tube ODSCC Indications Within the Tube Sheets of NPP Biblis Unit A." In: Proceedings of Fontevraud 7, International Symposium, SFEN, Avignon, France, 2010.

[A225] D. Gómez-Briceño, M. García-Redondo, and F. Hernández, "Update of Alloy 800 Behaviour in Secondary Side of PWR Steam Generators." In: Proceedings of Fontevraud 7, International Symposium, SFEN, Avignon, France, 2010.

[A226] R. L. Tapping, Y. C. Lu, and M. D. Pandey, "Alloy 800 Tubing: Current Status and Future Challenges." In: Proceedings of 13th International Symposium on Environmental Degradation in Nuclear Power Systems – Water Reactors, Canadian Nuclear Society, Whistler, British Columbia, Canada, 2007.

[A227] J. Slade, V. Moroney, J. Gorman, and T. Gendron, "A CANDU Utility Perspective on Using World Experience to Manage Alloy 800 SG Tube Degradation." In: Proceedings of 13th International Symposium on Environmental Degradation in Nuclear Power Systems – Water Reactors, Canadian Nuclear Society, Whistler, British Columbia, Canada, 2007.

[A228] E.-M. Pavageau, F. Vaillant, P. Lemaire, L. Millet, and I. Rodet, "Secondary Side Corrosion Cracking Models Compared to French Field Experience" (p. 425). In: Proceedings of the 11th International Symposium on Environmental Degradation of Materials in Nuclear Power Systems, ANS, Stevenson, Washington, USA, 2003.

[A229] C. Mansour, L. Legras, H. Catalette, G. Lefevre, M. Fedoroff, and E.-M. Pavageau, "Behavior of Sulfur Species in Steam Generator Conditions of PWRs – Towards an Update of the Secondary Side Corrosion Cracking Model Based on Laboratory Test in Sulfate Environments." In: Proceedings of 13th International Symposium on Environmental Degradation in Nuclear Power Systems – Water Reactors, Canadian Nuclear Society, Whistler, British Columbia, Canada, 2007.

[A230] A. R. McIlree, "Degradation of High Strength Austenitic Alloys X-750, 718 and A-286 in Nuclear Power Systems" (pp. 838–849). In: Proceedings of the 1st International Symposium on Environmental Degradation in Nuclear Power Systems – Water Reactors, NACE, Myrtle Beach, SC, USA, 1983.

[A231] *Material Specification for Alloy X750 for Use in LWR Internal Components (Revision 1)*. EPRI, Palo Alto, CA: 1990. NP-7032.

[A232] C. Benhamou, J. L. Chambrin, P. Todeschini, J. Champredonde, and E. Lemaire, "Evolution de la conception, de la fabrication et du montage des broches de fixation des tubes guides de grappes en Alliage X750." In: Proceedings Convention Nationale, SFEN, 2004.

[A233] B. M. Gordon and G. M. Gordon, "Corrosion in Boiling Water Reactors." In: *ASM Materials Handbook*, 9th Edition, 1987.

[A234] M. Foucault and C. Benhamou, "Influence of Surface Condition on the Susceptibility of Alloy X750 to Crack Initiation in PWR Primary Water" (pp. 791–797). In: Proceedings of 6th International Conference on Environmental Degradation of Materials in Nuclear Power Systems – Water Reactors, TMS, San Diego, California, USA, 1993.

[A235] *Proceedings of the 1986 Workshop on Advanced High Strength Materials*. EPRI, Palo Alto, CA: 1989. NP-6363.

[A236] M. T. Miglin, J. V. Monter, C. S. Wade, J. K. Tien, and J. L. Nelson, "Stress Corrosion Cracking of Chemistry and Heat Treat Variants of Alloy 718, Part 1: Stress Corrosion Test Results" (pp. 815–818). In: Proceedings of 6th International Symposium on Environmental Degradation of Materials in Nuclear Power Systems – Water Reactors, The Metallurgical Society, San Diego, California, USA, 1993.

[A237] J. Deleume, J. M. Cloué, and E. Andrieu, “Influence of Delta Phase Precipitation on the Stress Corrosion Cracking Resistance of Alloy 718 in PWR Primary Water.” In: Proceedings of 13th International Symposium on Environmental Degradation in Nuclear Power Systems – Water Reactors, Canadian Nuclear Society, Whistler, British Columbia, Canada, 2007.

[A238] B. Ter-Ovanessian, J. M. Cloué, J. Deleume, and E. Andrieu, “On the Stress Corrosion Cracking Behavior of Two Age-Hardenable Alloys in PWR Primary Water” (pp. 16–24). In: Proceedings of 14th International Conference on Environmental Degradation of Materials in Nuclear Power Systems, ASM, Virginia Beach, Virginia, USA, 2009.

[A239] G. O. Haynor, R. S. Piascik, D. E. Killian, and K. E. Moore, "Babcock & Wilcox Experience with Alloy A-286 Reactor Pressure Vessel Internal Bolting" (pp. 93–101). In: Proceedings of Fontevraud I, SFEN, 1985.

[A240] R. S. Piascik, J. V. Monter, G. J. Theus, and M. E. Scott, “Stress Corrosion Cracking of Alloy A-286 Bolt Material in Simulated PWR Reactor Environment” (pp. 18–25). In: Proceedings of the 2nd International Symposium on Environmental Degradation of Materials in Nuclear Reactor Systems – Water Reactors, American Nuclear Society, Monterey, California, USA, 1986.

[A241] I. Wilson and T. Mager, “Stress Corrosion of Age Hardenable NiFeCr Alloys,” *Corrosion*, Vol. 42, pp. 352–360, 1986.

[A242] P. J. Plante and J. P. Mieding, “Degradation of Reactor Coolant Pump Impellor-to-Shaft Bolting in a PWR” (pp. 11–45 to 11–55). In: Proceedings of 4th International Symposium on Environmental Degradation of Materials in Nuclear Reactor Systems – Water Reactors, NACE, Jekyll Island, Georgia, USA, 1990.

[A243] USNRC, Information Notice, Stress Corrosion Cracking of Reactor Coolant Pump Bolts, 90-68 (1990) and Supplement 1, 1994.

[A244] J. B. Hall, S. Fyfitch, and K. E. Moore, “Laboratory and Operating Experience with Alloy A286 and Alloy X750 RV Internals Bolting Stress Corrosion Cracking” (pp. 208–215). In: Proceedings of 11th International Conference on Environmental Degradation of Materials in Nuclear Power Systems – Water Reactors, American Nuclear Society, Stevenson, Washington, USA, 2003.

[A245] USNRC, Information Notice, Valve Stem Corrosion Failures, No. 85-59, 1985.

[A246] B. Yrieix and M. Guttmann, “Aging Between 300 and 450°C of Wrought Martensitic 13-17 wt% Cr Stainless Steels,” *Materials Science and Technology*, Vol. 9, pp. 125–134, 1993.

[A247] S. Fyfitch, K. E. Moore, and H. Xu, “Failure Investigation of Type 17-4PH Leaf Spring Material.” In: Proceedings of the 10th Conference on Environmental Degradation of Materials in Nuclear Power Systems – Water Reactors, NACE International, 2002.

[A248] H. Xu and S. Fyfitch, “Aging Embrittlement Modeling of Type 17-4PH at LWR Temperature.” In: Proceedings of the 10th International Conference on Environmental Degradation of Materials in Nuclear Power Systems – Water Reactors, NACE International, Lake Tahoe, Nevada, USA, 2002; August 3–9, 2001.

[A249] H. Xu and S. Fyfitch, “Fracture of Type 17-4PH CRDM Leadscrew Male Coupling Tangs” (pp. 1100–1108). In: Proceedings of 11th International Conference on Environmental Degradation of Materials in Nuclear Power Systems – Water Reactors, American Nuclear Society, Stevenson, Washington, USA, 2003.

[A250] C. J. Czajkowski, "Corrosion and Stress Corrosion Cracking of Bolting Materials in Light Water Reactors" (pp. 192–208). In: Proceedings of 1st International Symposium on Environmental Degradation of Materials in Nuclear Power Systems – Water Reactors, NACE, Myrtle Beach, South Carolina, USA, 1984.

[A251] *Materials Handbook for Nuclear Plant Pressure Boundary Applications (2010)*. EPRI, Palo Alto, CA: 2010. 1022344.

[A252] IAEA-TECDOC-1410, Delayed Hydride Cracking in Zirconium Alloys in Pressure Tube Nuclear Reactors, IAEA, Vienna, 2004.

[A253] S. M. Bruemmer, E. P. Simonen, P. M. Scott, P. L. Andresen, G. S. Was, and J. L. Nelson, “Radiation-Induced Material Changes and Susceptibility to Intergranular Failure of Light-Water-Reactor Core Internals,” *Journal of Nuclear Materials*, Vol. 274, pp. 299–314, 1999.

[A254] P. L. Andresen, F. P. Ford, S. M. Murphy, and J. M. Perks, “State of Knowledge of Radiation Effects on EAC in LWR Core Materials” (pp.1.83–1.121). In: Eds. D. Cubicciotti and E. Simonen, Proceedings of Fourth International Symposium on Environmental Degradation in Nuclear Power Systems – Water Reactors, National Association of Corrosion Engineers, Jekyll Island, Georgia, USA, August 6–10, 1989.

[A255] J. L. Nelson and P. L Andresen, “Review of Current Research and Understanding of Irradiation Assisted Stress Corrosion Cracking” (pp. 10–26). In: Eds. D. Cubicciotti and E. Simonen, Proceedings of Fifth International Symposium on Environmental Degradation in Nuclear Power Systems – Water Reactors, American Nuclear Society, Monterey, California, USA, August 25–29, 1991.

[A256] P. L. Andresen and F. P. Ford, “Modeling and Prediction of Irradiation Assisted Cracking” (pp.893–908). In: Eds. R. Gold and A. McIlree, Proceedings of Seventh International Symposium on Environmental Degradation in Nuclear Power Systems – Water Reactors, National Association of Corrosion Engineers, Breckenridge, Colorado, USA, August 7–10, 1995.

[A257] *Critical Issue Reviews for the Understanding and Evaluation of Irradiation Assisted Stress Corrosion Cracking*. EPRI, Palo Alto, CA: 1996. TR-107159.

[A258] G. S. Was, J. Busby, and P. L. Andresen, “Effect of Irradiation on Stress Corrosion Cracking and Corrosion in Light Water Reactors.” In: *ASM Handbook on Corrosion: Environments and Industries*, Vol. 13C, pp. 386–414, 2006.

[A259] P. Scott, “Review of Irradiation Assisted Stress Corrosion Cracking,” *Journal of Nuclear Materials*, Vol. 211, pp. 101–122, 1994.

[A260] P. M. Scott, M.-C. Meunier, D. Deydier, S. Silvestre, and A. Trenty, "An Analysis of Baffle/Former Bolt Cracking in French PWRs." In: Ed. R. D. Kane, *Environmentally Assisted Cracking: Predictive Methods for Risk Assessment and Evaluation of Materials, Equipment and Structures*, ASTM 1401, American Society for Testing and Materials, West Conshocken, PA, USA, 2000.

[A261] C. Pokor, Y. Thebault, C. Pujol, E. Lemaire, and N. Ligneau, "Metallurgical Examination Update of Baffle Bolts Removed from Operating French PWR" (pp. 545–551). In: Proceedings of Contribution of Materials Investigations to Improve the Safety and Performance of LWRs, Fontevraud 6, 2006.

[A262] J. Conermann, R. P. Shogan, D. R. Forsyth, I. L. Wilson, and H. T. Tang, "Characterization of Baffle-Former Bolts Removed from Service in US PWRs." In: Proceedings of the 10th Conference on Environmental Degradation of Materials in Nuclear Power Systems – Water Reactors, NACE International, 2002.

[A263] H. T. Tang, "Aging Management of Reactor Internals and License Renewal of US PWR Plants" (pp. 507–513). In: Proceedings of Fontevraud VI, SFEN, 2006.

[A264] *Final Review of the Cooperative Irradiation-Assisted Stress Corrosion Cracking Research Program*. EPRI, Palo Alto, CA: 2010. 1020986.

[A265] P. L. Andresen, "Similarity of Cold Work and Radiation Hardening in Enhancing Yield Strength and SCC Growth of Stainless Steel in Hot Water." In: Corrosion/02, Paper 02509, NACE, 2002.

[A266] P. L. Andresen, F. P. Ford, J. P. Higgins, I. Suzuki, M. Koyama, M. Akiyama, T. Okubo, Y. Mishima, S. Hattori, H. Anzai, H. Chujo, and Y. Kanazawa, "Life Prediction of Boiling Water Reactor Internals." In: Proceedings of ICONE-4 Conference, ASME, 1996.

[A267] P. L. Andresen, "Application of Noble Metal Technology for Mitigation of Stress Corrosion Cracking in BWRs" (pp. 563–578). In: Proceedings of Seventh International Symposium on Environmental Degradation of Materials in Nuclear Power Systems – Water Reactors, NACE, 1995.

[A268] S. Hettiarachchi, G. P. Wozadlo, T. P. Diaz, P. L. Andresen, and R. L. Cowan, "The Concept of Noble Metal Addition Technology for IGSCC Mitigation of Nuclear Materials" (pp.735–746). In: Proceedings of Seventh International Symposium on Environmental Degradation of Materials in Nuclear Power Systems – Water Reactors, NACE, 1995.

[A269] P. L. Andresen, T. P. Diaz, and S. Hettiarachchi, "Effect on Stress Corrosion Cracking of Electrocatalysis and Its Distribution Within Cracks." In: Proceedings of 11th International Symposium on Environmental Degradation of Materials in Nuclear Power Systems – Water Reactors, ANS, 2003.

[A270] F. A. Garner, B. M. Oliver, L. R. Greenwood, D. J. Edwards, and S. M. Bruemmer, "Generation and Retention of Helium and Hydrogen in Austenitic Steels Irradiated in a Variety of LWR and Test Reactor Spectral Environments." In: Proceedings of the 10th Conference on Environmental Degradation of Materials in Nuclear Power Systems – Water Reactors, NACE International, 2002.

[A271] F. A. Garner, E. P. Simonen, B. M. Oliver, L. R. Greenwood, M. L. Grossbeck, W. G. Wolfer, and P. M. Scott, "Retention of Hydrogen in FCC Metals Irradiated at Temperatures Leading to High Densities of Bubbles or Voids," *Journal of Nuclear Materials*, Vol. 356, pp. 122–135, 2006.

[A272] K. Fujimoto, T. Yonezawa, E. Wachi, Y. Yamaguchi, M. Nakano, R. P. Shogan, J.-P. Massoud, and T. R. Mager, "Effect of the Accelerated Irradiation and Hydrogen/Helium Gas on IASCC Characteristics for Highly Irradiated Austenitic Stainless Steels." In: Proceedings of the 12th Conference on Environmental Degradation of Materials in Nuclear Power Systems – Water Reactors, TMS, 2005.

[A273] D. J. Edwards, F. A. Garner, S. M. Bruemmer, and P. Efsing, "Nano-Cavities Observed in a 316SS PWR Flux Thimble Tube Irradiated to 33 and 70 dpa," *Journal of Nuclear Materials*, Vol. 384, pp. 249–255, 2009.

[A274] K. Asano, K. Fukuya, K. Nagata, and M. Kodama, "Changes in Grain Boundary Composition Induced by Neutron Irradiation on Austenitic Stainless Steels" (pp. 838–846). In: Eds. D. Cubicciotti and E. Simonen, Proceedings of Fifth International Symposium on Environmental Degradation in Nuclear Power Systems – Water Reactors, American Nuclear Society, Monterey, California, USA, August 25–29, 1991.

[A275] P. L. Andresen, P. W. Emigh, M. M. Morra, and R. M. Horn, "Effects of Yield Strength, Corrosion Potential, Stress Intensity Factor, Silicon and Grain Boundary Character on the SCC of Stainless Steels." In: Proceedings of 11th International Symposium on Environmental Degradation of Materials in Nuclear Power Systems – Water Reactors, ANS, 2003.

[A276] P. L. Andresen and M. M. Morra, "Effects of Si on SCC of Irradiated and Non-irradiated Stainless Steel and Ni Alloys." In: Paper 05591, Corrosion/05, NACE, Houston, Texas, USA, 2005.

[A277] S. Fyfitch, S. Davidsaver, and K. Amberge, "Irradiation-Assisted Stress Corrosion Cracking Initiation Screening Criteria for Stainless Steels in PWR Systems." In: Proceedings of the 18th International Conference on Environmental Degradation of Materials in Nuclear Power Systems—Water Reactors, TMS, 2017.

[A278] T. R. Liszkai, N. S. Yee, J. R. Smotrel, and A. Demma, "Materials Aging Degradation of Reactor Vessel Internals Part I: Thermal Hydraulics Evaluation." In: PVP2008-61804, Proceedings of PVP2008, ASME Pressure Vessels and Piping Division Conference, Chicago, Illinois, USA, July 27–31, 2008.

[A279] T. R. Liszkai, M. Snyder, and A. Demma, "Materials Aging Degradation of Reactor Vessel Internals Part II: Structural Evaluation – Global Finite Element Models." In: PVP2009-77786, Proceedings of PVP2009, ASME Pressure Vessels and Piping Division Conference, Prague, Czech Republic, July 26–30, 2009.

[A280] *Corrosion Fatigue of Water-Touched Pressure Retaining Components in Power Plants*. EPRI, Palo Alto, CA: 1997. TR-106696.

[A281] *Materials Reliability Program: Management of Thermal Fatigue in Normally Stagnant Non-Isolable Reactor Coolant System Branch Lines (MRP-146)*. EPRI, Palo Alto, CA: 2005. 1011955.

[A282] B. M. Gordon, D. E. Delwiche, and G. M. Gordon, "Service Experience of BWR Pressure Vessels." In: Eds. R. Rungta, J. D. Gilman, and W. H. Bamford, Performance of Light-Water Reactor Pressure Vessels, ASME PVP, Vol. 119, San Diego, California, USA, June 1987.

[A283] F. P. Ford, H. D. Solomon, L. M. Young, P. L. Andresen, D. Weinstein, A. Unruh, E. Tolksdorf, and R. Pathania, "Prediction of Corrosion Fatigue Crack Initiation in Low Alloy Pressure Vessel Steels" (pp. 315–325). In: Proceedings of International Symposium on Plant Aging and Life Predictions of Corrodible Structures, Sapporo, Japan, May 15–18, 1995.

[A284] F. P. Ford, "Prediction of Corrosion Fatigue Initiation in Low Alloy Steel and Carbon Steel/Water Systems at 288°C" (pp. 9–16). In: Eds. E Simonen and R. Gold, Proceedings of Sixth International Symposium on Environmental Degradation in Nuclear Power Systems – Water Reactors, National Association of Corrosion Engineers, San Diego, California, USA, August 1–5, 1993.

[A285] M. Higuchi and K. Iida, "Fatigue Strength Correction Factors for Carbon and Low-Alloy Steels in Oxygen-Containing High-Temperature Water," *Nuclear Engineering and Design*, Vol. 129, pp. 293–306, 1991.

[A286] Shack, W., et al., "Environmentally Assisted Cracking in LWRs," NUREG/CR-4667, Vol. 14, 1992.

[A287] H.-P. Seifert and S. Ritter, "Effect of Corrosion Potential on the Corrosion Fatigue Crack Growth Behaviour of Low Alloy Steels in High-Temperature Water." In: Proceedings of 13th International Conference on Environmental Degradation of Materials in Nuclear Power Systems, Canadian Nuclear Society, Whistler, BC, Canada, August 19–23, 2007.

[A288] *Materials Reliability Program: Third International Conference on Fatigue in Reactor Components (MRP-151)*. EPRI, Palo Alto, CA: 2005. 1011958.

[A289] *Materials Reliability Program: Environmental Fatigue Testing of Type 304L Stainless Steel U-Bends in Simulated PWR Primary Water (MRP-188)*. EPRI, Palo Alto, CA: 2006. 1013028; and U.S. Department of Energy, Washington, D. C.

[A290] U.S. NRC Regulatory Guide 1.207, Guidelines for Evaluating Fatigue Analyses Incorporating the Life Reduction of Metal Components Due to the Effects of the Light-Water Reactor Environment for New Reactors, 2007.

[A291] K. Chopra and W. J Shack, "Effect of LWR Coolant Environments on the Fatigue Life of Reactor Materials," NUREG/CR-6909, ANL-0608, 2007.

[A292] U.S. Nuclear Regulatory Commission, License Renewal Issue No. 98-0030, Thermal Aging Embrittlement of Cast Austenitic Stainless Steel Components, May 19, 2000.

[A293] *Materials Reliability Program: A Review of Thermal Aging Embrittlement in Pressurized Water Reactors (MRP-80)*. EPRI, Palo Alto, CA: 2003. 1003523.

[A294] *Materials Reliability Program: PWR Internals Material Aging Degradation Mechanism Screening and Threshold Values (MRP- 175)*. EPRI, Palo Alto, CA: 2005. 1012081.

[A295] *Materials Handbook for Nuclear Plant Pressure Boundary Applications, 2018 Version*. EPRI, Palo Alto, CA: 2018. 3002012420.

[A296] C. Pareige, S. Novy, S. Saillet, and P. Pareige, "Study of Phase Transformation and Mechanical Properties Evolution of Duplex Stainless Steels After Long Term Thermal Ageing (> 20 Years)," *Journal of Nuclear Materials*, Vol. 411, pp. 90–96, 2011.

[A297] T. Yamada, S. Okano, and H. Kuwano, "Mechanic Property and Microstructural Change by Thermal Aging of SCS14a Cast Duplex Stainless Steel," *Journal of Nuclear Materials*, Vol. 350, pp. 47–55, 2006.

[A298] U.S. Nuclear Regulatory Commission Letter, "Final Safety Evaluation of the BWRVIP-234: Thermal Aging and Neutron Embrittlement Evaluation of Cast Austenitic Stainless Steel for BWR Internals (TAC No. ME5060)," June 22, 2016, NRC ADAMS Accession No. ML16096A002.

[A299] O. K. Chopra, "Estimation of Fracture Toughness of Cast Stainless Steels During Thermal Aging in LWR Systems," NUREG/CR-4513 Rev. 2, ANL-1508, 2015.

[A300] O. K. Chopra and W. J. Shack, "Mechanical Properties of Thermally Aged Cast Stainless Steels from Shippingport Reactor Components," NUREG/CR-6275, April 1995.

[A301] W. R. Corwin, R. K. Nanstad, D. J. Alexander, G. R. Odette, R. E. Stoller, and J. A. Wang, "Thermal Embrittlement of Reactor Vessel Steels," Report Conference 950804-3, 1995.

[A302] R. K. Nastad, D. E. McCabe, M. A. Sokolov, C. A. English, and S. R. Ortner, "Investigation of Temper Embrittlement in Reactor Pressure Vessel Steels Following Thermal Aging, Irradiation and Thermal Annealing." In: Proceedings of Effects of Radiation on Materials: 20th International Symposium, ASTM STP 1405, 2001.

[A303] A. Marucco, "Atomic Ordering in the Ni-Cr-Fe System," *Materials Science & Engineering*, Vol. A189, pp. 267–276, 1994.

[A304] F. Delabrouille, D. Renaud, F. Vaillant, and J. Massoud, "Long Range Ordering of Alloy 690." In: Proceedings of 14th International Conference on Environmental Degradation of Materials in Nuclear Power Systems, ANS, Virginia Beach, Virginia, USA, August 23–27, 2009.

[A305] *Guidelines for PWR Steam Generator Tubing Specifications and Repair—Volume 2, Revision 1: Guidelines for Procurement of Alloy 690 Steam Generator Tubing*. EPRI, Palo Alto, CA: 1999. TR-016743-V2R1.

[A306] Shoji, T., et al., "Mechanistic Understanding of Low Temperature Crack Propagation for Alloy 690 in Hydrogenated Water." In: Proceedings of 13th International Conference on Environmental Degradation of Materials in Nuclear Power Systems, Whistler, BC, Canada, August 19–23, 2007.

[A307] C. A. Grove and L. D. Petzold, "Mechanism of SCC of Alloy X-750 in High Purity Water," *Journal of Materials for Energy Systems*, Vol. 7, No. 2, pp.147–162, 1985.

[A308] L. D. Petzold and C. A. Grove, "Mechanism of SCC of Alloy X-750 in High Purity Water" (p. 165). In: Ed. R. C. Scarberry, *Corrosion of Nickel Alloys*, ASM, 1985.

[A309] P. L. Andresen and M. M. Morra, "Effects of Positive and Negative dK/da on SCC Growth Rates." In: Proceedings of 12th International Symposium on Environmental Degradation of Materials in Nuclear Power Systems – Water Reactors, TMS, Snowbird, Utah, USA, August 2005.

[A310] P. L. Andresen and M. M. Morra, "Emerging Issues in Environmental Cracking in Hot Water" (pp. 1–25). In: Proceedings of 13th International Conference on Degradation of Materials in Nuclear Power Systems, Canadian Nuclear Society, 2007.

[A311] W. J. Mills, M. R. Lebo, and J. J. Kearns, "Hydrogen Embrittlement, Grain Boundary Segregation and Stress Corrosion Cracking of Alloy X-750 in Low and High Temperature Water," *Metallurgical and Materials Transactions A*, Vol. 30A, pp. 1579–1596, 1999.

[A312] D. M. Symons, "The Effect of Hydrogen on the Fracture Toughness of Alloy X-750 at Elevated Temperatures," *Journal of Nuclear Materials*, Vol. 265, pp. 225–231, 1999.

[A313] D. M. Symons, "A Comparison of Internal Hydrogen Embrittlement and Hydrogen Environment Embrittlement of X-750," *Engineering Fracture Mechanics*, Vol. 68, pp. 751–771, 2001.

[A314] M. J. Mills and C. M. Brown, "Fracture Behavior of Nickel-Based Alloys in Water" (pp. 167–174). In: Eds. S. Bruemmer and F. P. Ford, Proceedings of Ninth International Symposium on Environmental Degradation in Nuclear Power Systems – Water Reactors, The Metallurgical Society, Newport Beach, California, USA, August 1–5, 1999.

[A315] C. M. Brown and W. J. Mills, "Load Path Effects on the Fracture Toughness of Alloy 82H and 52 Welds in Low Temperature Water." In: Proceedings of 12th International Symposium on Environmental Degradation of Materials in Nuclear Power Systems – Water Reactors, TMS, Snowbird, Utah, USA, August 2005.

[A316] B. A. Young, A. McIlree, and P. J. King, "Reduction of Toughness Results for Weld Metal 182 in a PWR Primary Water Environment With Varying Dissolved Hydrogen, Lithium Hydroxide and Boric Acid Concentrations" (pp. 613–621). In: Proceedings of the 12th International Conference on Environmental Degradation of Materials in Nuclear Power System – Water Reactors, The Minerals, Metals & Materials Society, 2005.

[A317] A. Demma, A. McIlree, and M. Herrera, "Low Temperature Crack Propagation Evaluation in Pressurized Water Reactor Service" (pp. 623–634). In: Eds. L. Nelson and P. King, Proceedings of 12th International Conference on Environmental Degradation in Nuclear Power Systems – Water Reactors, The Metallurgical Society, Skamania Lodge, Stevenson, Washington, USA, August 5–9, 2005.

[A318] A. McIlree, A. Demma, P. Peng, and P. King, "Effects of Dissolved Hydrogen and Temperature on Fracture Resistance of Weld Metals 182 and 152 in Simulated PWR Shutdown Environment" (pp. 463–476). In: Proceedings of Fontevraud VI, SFEN, 2006.

[A319] E. Herms, O. Raquet, I. de Curières, and P. Joly, "LTCP of Alloy 182/152 Tested in PWR Primary Water" (pp. 262–272). In: Proceedings of 14th International Conference on Environmental Degradation of Materials in Nuclear Power Systems, ANS, Virginia Beach, Virginia, USA, 2009.

[A320] M. Ahonen, U. Ehrnstén, and H. Hänninen, "Low Temperature Crack Propagation of Nickel-Based Weld Metals in Hydrogenated PWR Primary Water." In: Proceedings of Fontevraud 7, SFEN, Avignon, France, 2010.

[A321] *Program on Technology Innovation: Scoping Study of Low Temperature Crack Propagation for Alloy 182 Weld Metal in BWR Environments and for Cast Austenitic Stainless Steel in PWR Environments (Revision 1)*. EPRI, Palo Alto, CA: 2010. 1020957.

[A322] *Materials Reliability Program: Low-Temperature Crack Propagation in Pressurized Water Reactor Materials (MRP-293)*. EPRI, Palo Alto, CA: 2011. 1021018.

[A323] Nuclear Regulatory Commission, Reg. Guide 1.99, Revision 2, Radiation Embrittlement of Reactor Vessel Materials, May 1988.

[A324] ASTM E900-15e1, Standard Guide for Predicting Radiation-Induced Transition Temperature Shift in Reactor Vessel Materials, ASTM International, West Conshohocken, PA, USA, 2015.

[A325] *Materials Reliability Program: A Review of Radiation Embrittlement for Stainless Steels for PWRs (MRP-79)—Revision 1*. EPRI, Palo Alto, CA: 2004. 1008204.

[A326] *Materials Reliability Program: PWR Internals Age-Related Material Properties, Degradation Mechanisms, Models, and Basis Data—State of Knowledge (MRP-211, Revision 1)*. EPRI, Palo Alto, CA: 2017. 3002010270.

[A327] *Materials Reliability Program: Testing Gap Assessment and Material Identification for PWR Internals (MRP-320)*. EPRI, Palo Alto, CA: 2011. 1022866.

[A328] A. Demma, R. Carter, A. Jenssen, T. Torimaru, and R. Gamble, "Fracture Toughness of Highly Irradiated Stainless Steels in Boiling Water Reactors." In: Proceedings of the 13th Conference on Environmental Degradation of Materials in Nuclear Power Systems – Water Reactors, Canadian Nuclear Society, 2007.

[A329] S. Fyfitch, H. Xu, A. Demma, R. Carter, R. Gamble, and P. Scott, "Fracture Toughness of Irradiated Stainless Steel in Nuclear Power Systems." In: Proceedings of the 14th Conference on Environmental Degradation of Materials in Nuclear Power Systems – Water Reactors, ANS, Virginia Beach, Virginia, USA, 2009.

[A330] M. Hamilton, F.-H. Huang, W. J. S. Yang, and F. A. Garner, "Mechanical Properties and Fracture Behavior of 20% Cold-Worked 316 Stainless Steel Irradiated to Very High Neutron Exposures" (pp. 245–270). In: Influence of Radiation in Material Properties: 13th International Symposium (Part II), ASTM STP 956, ASTM, Philadelphia, 1987.

[A331] F. A. Garner, "(Chapter 6) Irradiation Performance of Cladding and Structural Steels in Liquid Metal Reactors," *Materials Science and Technology*, Vol. 10A, pp. 419–543, 1994.

[A332] H. M. Chung, "Assessment of Void Swelling in Austenitic Stainless Steel Core Internals," NUREG/CR-6897, 2006.

[A333] *Materials Reliability Program: A Review of Void Swelling Prediction in Irradiated Austenitic Stainless Steels*. EPRI, Palo Alto, CA: 2009. 1018849.

[A334] *Materials Reliability Program: GONDOLE Void Swelling Irradiation and Testing – Phase 1 Results (MRP-327)*. EPRI, Palo Alto, CA: 2011. 1022872.

[A335] *Materials Reliability Program: PWR Internals Material Aging Degradation Mechanism Screening and Threshold Values (MRP-175, Revision 1)*. EPRI, Palo Alto, CA: 2017. 3002010268.

[A336] *Materials Reliability Program: Technical Basis Document Concerning Irradiation-Induced Stress Relaxation and Void Swelling in Pressurized Water Reactor Vessel Internals Components (MRP-50)*. EPRI, Palo Alto, CA: 2001. 1000970.

[A337] M. J. Manjoine and H. R. Voorhees, "Compilation of Stress-Relaxation Data for Engineering Alloys." In: *ASTM Data Series* Publication DS 60, ASTM Philadelphia, PA, 1982.

[A338] Reed-Hill, R. E., *Physical Metallurgy Principles*. New York, New York, D. Van Nostrand, 1973.

[A339] *Materials Reliability Program: Technical Basis Document Concerning Irradiation-Induced Stress Relaxation and Void Swelling in Pressurized Water Reactor Vessel Internals Components (MRP-50)*. EPRI, Palo Alto, CA: 2001. 1000970.

[A340] O. Chopra, "Initial Results of Investigations of Revised Fen Expressions," EPRI EAF Advisory Panel Meeting, Las Vegas, NV, USA, May 10, 2011.

[A341] O. Chopra and Y. Garud (ANL), and G. Stevens (NRC/RES), "Update of NUREG/CR-6909 Methodology for Environmentally Assisted Fatigue (EAF) – Revised Fen Expressions." Presented to ASME Section III Subgroup on Fatigue Strength, May 15, 2012.

[A342] Code for Nuclear Power Generation Facilities, Environmental Fatigue Evaluation Method for Nuclear Power Plants (JSME S NF1-2009), Japan Society of Mechanical Engineers, 2009.

[A343] NUREG/CR-6048, Pressurized-Water Reactor Internals Aging Degradation Study, Oak Ridge National Laboratory, 1993.

[A344] M. Kansaki, Y. Masaki, and T. Kudo, "Effect of Thermal Treatment on Stress Corrosion Cracking Susceptibility in Alloy 600 and Type 316 Stainless Steel Under Simulated Pressurized Water Reactor Primary Conditions," *Corrosion,* Vol. 71, No. 1, pp. 57–64, January 2015.

[A345] M. Kansaki, Y. Masaki, and T. Kudo, "Effect of Cr and Ni on Stress Corrosion Cracking Susceptibility in Ni-CR-Fe Alloys Under Simulated Pressurized Water Reactor Primary Conditions," *Corrosion,* Vol. 71, No. 8, pp. 1027–1035, August 2015.

[A346] Tice, D., et al., "Environmentally Assisted Crack Growth of Cold-Worked Type 304 Stainless Steel in PWR Environments." In: Proceedings of the 12th International Conference on Environmental Degradation of Materials in Nuclear Power Systems—Water Reactors, TMS, 2005.

[A347] M. Tsubota, "Stress Corrosion Crack Growth Behavior of Cold Worked Austenitic Stainless Steel in High Temperature Water." In: Proceedings of the 12th International Conference on Environmental Degradation of Materials in Nuclear Power Systems—Water Reactors, TMS, 2005.

[A348] C. Guerre, "SCC Crack Growth Rate of Cold-Worked Austenitic Stainless Steels in PWR Primary Water Conditions." In: Proceedings of the 13th International Conference on Environmental Degradation of Materials in Nuclear Power Systems—Water Reactors, CNS, 2007.

[A349] M. Tsubota, "Relation Between the Mechanical Properties and SCC Behavior of the Alloys Used in High Temperature Water." In: Proceedings of the 13th International Conference on Environmental Degradation of Materials in Nuclear Power Systems—Water Reactors, CNS, 2007.

[A350] *Materials Reliability Program: Resistance to Primary Water Stress Corrosion Cracking of Alloy 690 in Pressurized Water Reactors (MRP-258)*. EPRI, Palo Alto, CA: 2009. 1019086.

[A351] Kilian, R., et al., "Operating Experience with Alloy 800 SG Tubing in Europe." In: 2007 Env-Deg Conference, 2007.

[A352] Kilian, R., et al., "Corrosion Resistance of SG Tubing Material Incoloy 800 Mod. and Inconel 690 TT," *Werkstoffe und Korrosion*, Vol. 42, pp. 490–496, 1991.

[A353] *Materials Reliability Program: Technical Basis for Primary Water Stress Corrosion Cracking Mitigation by Surface Stress Improvement (MRP-267, Revision 2)*. EPRI, Palo Alto, CA: 2016. 3002008083.

[A354] *Materials Reliability Program: Topical Report for Primary Water Stress Corrosion Cracking Mitigation by Surface Stress Improvement (MRP-335, Revision 3-A)*. EPRI, Palo Alto, CA: 2016. 3002009241.

[A355] *Materials Reliability Program: Specification Guideline for Primary Water Stress Corrosion Cracking Mitigation by Surface Stress Improvement (MRP-336, Revision 1)*. EPRI, Palo Alto, CA: 2016. 3002008084.

[A356] Young, G. A., et al., "Effect of Long-Range Order on the Stress Corrosion Susceptibility of a Nickel-33 at % Chromium Alloy," *Corrosion*, Vol. 72, No. 11, NACE, November 2016.

[A357] Mouginot, R., et al., "Thermal Aging and Short-Range Ordering of Alloy 690 Between 350 and 550˚C," *Journal of Nuclear Materials*, Vol. 485, pp. 56–65, 2017 (Elsevier).

[A358] T. E. Moss, C. M. Brown, and G. A. Young, "The Effect of Hardening via Long Range Order on the SCC and LTCP Susceptibility of a Nickel-30 Chromium Binary Alloy." In: Proceedings of the 18th International Conference on Environmental Degradation of Materials in Nuclear Power Systems—Water Reactors, TMS, 2017.

[A359] B. Stephan, D. Jacob, F. Delabrouille, and L. Legrs, "A Kinetic Study of Order-Disorder Transition in Ni-Cr Based Alloys." In: Proceedings of the 18th International Conference on Environmental Degradation of Materials in Nuclear Power Systems – Water Reactors, TMS, 2017.

[A360] *Materials Reliability Program: Effects of Dissolved Hydrogen, Temperature, and Hydrogen Peroxide on (LTCP) Fracture Resistance of Weld Metals 182, 52, and 152 (MRP-209)*. EPRI, Palo Alto, CA: 2007. 1015005.

[A361] *Effect of Light Water Reactor Environments on Fracture Resistance in Irradiated Stainless Steel*. EPRI, Palo Alto, CA: 2012. 1025124.

[A362] D. J. Pavarenti and W. C. Moshier, "Interaction of Microstructure, Composition, and Cold Work on the Stress Corrosion Cracking of Alloy 82 Weld Metal" (pp. 1087–1101). In: Proceedings of 15th International Conference on Environmental Degradation of Materials in Nuclear Power Systems – Water Reactors, Colorado Springs, Colorado, USA, August 7–11, 2011.

[A363] *Rapid Fracture Phenomenon in High Temperature Water*. EPRI, Palo Alto, CA: 2013. 3002000766.

[A364] *Materials Reliability Program: Evaluation of Potential for Low Temperature Crack Propagation in Reactor Pressure Vessel Outlet Nozzle Dissimilar Metal Butt Welds by Stress and Fracture Mechanics Analysis (MRP-247)*. EPRI, Palo Alto, CA: 2008. 1016606.

[A365] *Materials Reliability Program: Loading Effects on the Low Temperature Crack Propagation Phenomenon in 182 Weld Metal in a Pressurized Water Reactor Environment MRP-285)*. EPRI, Palo Alto, CA: 2010. 1021017.

[A366] K. Sakima, H. Suzuki, and H. Fujiwara, "Research and Evaluation of Low Temperature Crack Propagation of Ni Bases Alloys in Actual Plants" (pp. 315–326). In: Proceedings of 15th International Conference on Environmental Degradation Materials in Nuclear Power Systems – Water Reactors, 2011.

[A367] NUREG/CR-6048, Pressurized Water Reactor Internals Aging Degradation Study, Phase 1, September 1993.

[A368] Troyer, G., et al., "Dissimilar Metal Weld PWSCC Initiation Model Refinement for XLPR Part 1: A Survey of Alloy 82/182/132 Crack Initiation Literature." In: 17th International Conference on Environmental Degradation of Materials in Nuclear Power Systems – Water Reactors, CNS, 2015.

[A369] *Materials Reliability Program: Recommended Factors of Improvement for Evaluating Primary Water Stress Corrosion Cracking (PWSCC) Growth Rates of Thick-Wall Alloy 690 Materials and Alloy 52, 152, and Variants Welds (MRP-386)*. EPRI, Palo Alto, CA: 2017. 3002010756.

[A370] *Materials Reliability Program Inspection Plan for Reactor Vessel Closure Head Penetrations in U.S. PWR Plants (MRP-117)*. EPRI, Palo Alto, CA: 2004. 1007830.

[A371] Fyfitch, S., et al., "Microstructural and Mechanical Property Evaluation of Alloy 600 CRDM Nozzles from B&W-Design Reactor Vessel Heads." In: Proceedings of the International Symposium: Contributions of Materials Investigations to Improve the Safety and Performance of LWRs, Fontevraud 6, SFEN, 2006.

[A372] K. J. Leonard, M. N. Gussev, J. N. Stevens, and J. T. Busby, "Characterization of Materials Properties and Crack Propagation Mechanisms in Damaged Alloy 718 Leaf Springs Following Commercial Reactor Exposure." In: Proceedings of the 17th International Conference on Environmental Degradation of Materials in Nuclear Power Systems—Water Reactors, CNS, 2015.

[A373] J. McKinley, R. Lott, B. Hall, and K. Kalchik, "Examination of Baffle-Former Bolts from D. C. Cook Unit 2." In: Proceedings of the 16th International Symposium on Environmental Degradation of Materials in Nuclear Power Systems—Water Reactors, NACE, 2013.

[A374] Materials Reliability Program (MRP) Letter MRP 2014-009, Subject: Biennial Report of Recent MRP-227-A Reactor Internals Inspection Results, dated May 12, 2014, NRC Accession Numbers ML14135A383, ML14135A384, ML14135A385.

[A375] Materials Reliability Program (MRP) Letter MRP 2016-008, Subject: Biennial Report of Recent MRP-227-A Reactor Internals Inspection Results, dated May 18, 2016, NRC Accession Number ML16144A789.

B
VVER 440 AND 1000 MATERIALS

The objective of this appendix is to provide summaries of relevant information regarding VVER structural materials for use with the Materials Degradation Matrix. The materials covered in this document are used for reactor pressure vessel, pressurizer, primary piping (including static components of valves and pumps), reactor vessel internals, and steam generator (SG) systems.

Summaries of relevant structural base metals, welds, and cladding used in VVER 440 and VVER 1000 reactor designs and steam generators are given in the following sections:

- B.1 Carbon and Low-Alloy Steels
- B.2 Carbon and Low-Alloy Steel Welds
- B.3 Stainless Steels
- B.4 Stainless Steel Welds and Cladding

B.1 Carbon and Low-Alloy Steels

This section covers carbon and low-alloy steels (C&LAS) that are used as pressure boundary materials in pressure vessels, piping, and similar applications in reactor coolant systems of VVERs. The reasons for use of carbon and low-alloy steels for these applications are their combination of relatively low cost, good mechanical properties in thick sections, good weldability, and high resistance to stress corrosion cracking (SCC) under relevant operating conditions. Regarding reactor vessels, the grades of low-alloy steels that are used also have acceptably low rates of thermal embrittlement and irradiation embrittlement when subjected to neutron flux. In many reactor coolant applications, the carbon and low-alloy steels have been welding overlay clad on the inside wetted surface with corrosion-resistant austenitic stainless steels (SS) [B1, B2]. The main exception is the components of the secondary circuit that are usually directly in contact with the secondary coolant. Some early VVER 440 systems used reactor pressure vessels without any internal stainless steel overlay weld cladding, but there are no examples of this type in the countries participating in Revision 5 of the MDM.

Welds in these carbon and low-alloy steels are covered in Section B.2. The term “weld” is intended to cover both the weld metal and the heat-affected zone (HAZ) of the base material.

B.1.1 Service Experience

Carbon and low-alloy steel pressure vessel steels are widely used in nuclear power plants. Service experience has generally been good. However, there have been some problems, as summarized by the VVER expert panel participants below.

Corrosion fatigue has been identified as a potential concern in secondary and feedwater piping applications, but in practice has not been a serious problem except at feedwater connections to some pressurized water reactor (PWR) steam generators.

Steels in the reactor vessel belt line region are subject to embrittlement due to neutron irradiation. Embrittlement of the base materials of western design LWRs has generally not been a serious problem. Some VVERs have experienced sufficient irradiation-induced embrittlement, as revealed by surveillance specimens, as to require remedial actions such as removing some peripheral fuel elements from the core to reduce the neutron flux to the pressure vessel wall or by dry thermal annealing, typically at 475°C [B3].

Generally, carbon and low-alloy steels are sensitive to uniform corrosion, pitting, crevice corrosion, boric acid and microbial corrosion, fouling (resulting in reduction in heat transfer), stress relaxation (loss of pre-load), fatigue, mechanical wear (abrasion), and erosion corrosion. Carbon steels with < 0.3 wt% Cr can be susceptible to flow-accelerated corrosion (FAC). Higher strength LAS are susceptible to SCC and occasionally hydrogen embrittlement if improperly tempered to too high a strength.

B.1.2 Material Composition and Properties

Most of the carbon and low-alloy steels used in VVER coolant service are in the wrought or forged form. Pressure vessel shells were often fabricated in the past, using plates rolled to the correct curvature and then welded. Flanges and nozzles typically are seamless forgings. The trend in more modern plants has been to eliminate as many welds as possible by use of ring forgings for vessel shells and using integrally forged nozzles. Typical carbon and low-alloy steels used in VVERs are:

Reactor Pressure Vessel (RPV)

LAS: *RPV body – 15Ch2MFA (VVER 440); RPV body and head – 15Ch2NMFA 15Ch2NMFAA (VVER 1000); RPV head – 15241*
RPV flange – 25Ch3MFA (VVER 440)
RPV cover and ring – 18Ch2MFA (VVER 440)
Reactor vessel head – 15241 (VVER 1000)
Fasteners and hardware material – 15236.6 (VVER 1000), 25Ch1MF 25Ch3MFA, 38ChN3MA, 14140.9 (VVER 440)
Support ring – 10GN2MFA (VVER 1000)

CS: *Fasteners and hardware material – 12050.1 (VVER 1000)*
Support frame (sheet metal) – 11375.1, 11378 (VVER 440)
Support ring – cast steel 422643.5 (VVER 440)
RPV and head consoles – 22 K (VVER 1000)

Steam Generator (SG)

Primary Circuit Collectors
LAS: *Primary circuit coolant – 10GN2MFA (VVER 1000 – primary water side has stainless steel overlay weld cladding)*
Steam Generator Secondary Side Internals
C+LAS: *Feedwater collector – 11416; 11523; 20; 12022*

Steam Generator Secondary Pressure Boundary

LAS: Fasteners and hardware materials; hot and cold legs (VVER1000) – 38ChN3MFA; 25Ch1MF; 40Ch; 10GN2MFA; SG vessel (VVER 1000) – 10GN2MFA

CS: Nozzles (VVER 440 and 1000); SG vessel (VVER 440); elliptical ends (VVER 440); Steam collector (VVER 440); Pipes between SG and steam collector (VVER 440) – 22K; 20, K22MA

Primary Pressure Boundary

Main Coolant Pump

LAS: External fasteners and hardware materials – 38ChN3MFA
Main coolant pump nozzles, sleeves, flanges – 10GN2MFA (-T) (VVER 1000)

Reactor Coolant Large Diameter Primary Piping

LAS: 10GN2MFA (-T) (VVER 1000 - primary water side has stainless steel overlay weld cladding)

Pressurizer

LAS: Fasteners and hardware materials – 38ChNMFA (VVER 440 and 1000) 25CH1MF (VVER 1000); nozzles – 10GN2MFA (VVER 1000)

CS: Basic material of pressurizer – 22K

The VVER 440 and VVER 1000 reactor pressure vessels are made from low-alloy chromium, molybdenum-vanadium steel with relatively high mechanical properties. Steel according to the Russian standards GOST is marked *15Ch2MFA* for VVER 440 and *15Ch2NMFA* for VVER 1000. Chemical composition and heat treatment of 15Ch2MFA ensure the required strength properties, ductility, and toughness. The steel exhibits high resistance to thermal and temper embrittlement as well as to radiation damage, mostly due to the presence of vanadium (0.30-0.35 wt%). However, preheating for welding (350-400°C) is necessary to avoid "hot," "cold," and "under-clad" cracks. A decreased content of vanadium (max. 0.1 wt%) and the addition of nickel (up to 1.8 wt%) in steel 15Ch2NMFA for VVER 1000 pressure vessels resulted in a simplified welding technology (lower preheating temperature 150-200°C, lower tempering temperature 620-650°C), higher strength properties, and better toughness. Chemical compositions and mechanical properties of the above-mentioned steels are listed in Tables B-1 and B-2. On the inner surface of the RPV, an austenitic stainless steel weld cladding is applied and composed of two layers: the lower layer being Sv-07Ch25N13 and the surface layer, which consists of two identical layers of Sv-08Ch19N10G2B (see Table B-10).

Low-alloy steel 10GN2MFA is used mainly for the SG collector bodies of the VVER 1000. The steel is produced as forgings and is 2X vacuum treated to minimize the dissolved gas concentration and to ensure a homogeneous chemical composition. The sulfur content must be kept lower than 0.005 wt%, and the concentration of phosphorus must be lower than 0.008 wt% to minimize susceptibility to SCC or SICC in high temperature water environments. The requirements for the chemical composition and tensile properties are summarized in Table B-3 and Table B-4. The primary side is also weld clad on the inner surface with austenitic stainless steel.

Low-alloy steels for external fasteners and other high strength hardware (40Ch, 25Ch1MF, and 38ChN3MFA) are produced as forgings from ingots prepared by basic electric arc furnaces according to the selected producer's technology. The materials are delivered in a heat-treated condition (quenched and tempered). Steels 40Ch and 38ChN3MFA exhibit good resistance to thermal shock. The requirements for the chemical composition of the materials are summarized in Table B-5.

Carbon steels 22K and 20 are produced in basic open-hearth or electric arc furnaces according to the selected producer's technology. The materials are used in the following heat-treated condition: normalized and tempered, or quenched and tempered, for 22K material and normalized in the case of Steel 20. The requirements for the chemical composition of the materials are summarized in Table B-6. Steel K22MA has the same chemical composition as 22K steel with the addition of molybdenum.

B.1.3 Main Limitations

The main limitations to the use of carbon and low-alloy steels are as follows:

- Radiation-induced embrittlement of beltline region materials has been found to be sensitive to the chemical composition of the materials. This applies to both base materials and welds, but embrittlement has been more of a problem with welds than base materials. It is important to control the amounts of deleterious elements, especially copper, phosphorus, and nickel, in both the base materials and weld materials.
- Significant numbers of low-alloy steel parts that were clad with stainless steel or nickel-chromium-iron weld deposits experienced under-clad cracking in the base material. Since this problem is specific to cladding, it is covered in Section B.2.

Carbon steel can have low resistance to FAC/erosion-corrosion in both two-phase flow and single-liquid-phase flow conditions, especially if the steel is low in chromium (< 0.3 wt%). In many steels, chromium is not a controlled element and is present only as a tramp element. In such steels, chromium can be very low (< 0.1 wt%), and the steel can be very susceptible to FAC/erosion-corrosion. FAC/erosion-corrosion can result in wall thinning at locations where droplets in two-phase flow impinge on the wall and at locations, such as elbows and other fittings, where liquid at high velocity and turbulence is in contact with the wall. Small amounts of chromium, copper, and molybdenum in the steel significantly increase resistance to FAC/erosion-corrosion, which helps explain the generally good performance of the chromium-molybdenum grades of low-alloy steels—although these require stress relief of weldments. Carbon and low-alloy steels are also susceptible to general and pitting corrosion in uncontrolled aqueous environments.

Table B-1
Chemical compositions of RPV steels 15Ch2MFA (VVER 440) and 15Ch2NMFA (VVER 1000) [wt%]

Steel	C	Mn	Si	P	S	Cr	Ni	Mo	V	Cu	Co	As
15Ch2MFA	0.13 0.18	0.30.6	0.17 0.30	≤ 0.025	≤ 0.025	2.50 3.0	Max. 0.40	0.60 0.80	0.25 0.35	≤ 0.15	≤ 0.02	≤ 0.04
15Ch2NMFA	0.13 0.18	0.30.6	0.17 0.30	≤ 0.02	≤ 0.02	1.8 2.3	1.0 1.5	0.5 0.7	Max. 0.1	≤ 0.15	≤ 0.02	≤ 0.04

Table B-2
Specified room temperature mechanical properties for RPV steels 15Ch2MFA (VVER 440) and 15Ch2NMFA (VVER 1000)

Steel	Tensile Strength [MPa]	Yield Strength (0.2) [MPa]	Elongation [%]	Reduction in Area [%]	Charpy V-notch [$J.cm^{-2}$]
15Ch2MFA	539-735	Min. 431	Min. 14	Min. 50	Min. 59 (49)
15Ch2NMFA	Min. 608	Min. 490	Min. 15	Min. 55	–

Table B-3
Chemical composition of 10GN2MFA steel [wt%]

	C	Cr	Ni	Mn	Si	Mo	P	S	Ti	V	Cu	Al
10GN2MFA	0.08- 0.12	Max 0.3	1.8- 2.3	0.8- 1.1	0.17- 0.37	0.4- 0.7	Max. 0.008	Max 0.005	–	0.03 - 0.07	Max 0.3	–
10GN2MFA-T									5*%C			0.005-0.035

Table B-4
Specified room temperature mechanical properties for 10GNMFA steel

Steel	Tensile Strength [MPa]	Yield Strength (0.2) [MPa]	Elongation [%]	Reduction in Area [%]
10GN2MFA	540-700	Min. 425	18	60

Table B-5
Chemical compositions of LAS 25Ch1MF, 40Ch, and 38ChN3MFA [wt%]

Steel	C	Cr	Ni	Mn	Si	Mo	P	S	Ti	V	Cu	W
25Ch1MF	0.22-0.27	≤ 0.3	≤ 0.3	0.3-0.6	0.17-0.37	0.6-0.8	Max. 0.025	Max. 0.025	–	0.25-0.35	Max. 0.3	–
40Ch	0.36-0.44	0.8-1.1	Max. 3	0.5-0.8	0.17-0.37	–	0.025	0.025	–	–	Max. 0.3	–
38ChN3MFA	0.330-0.4	1.2-1.5	3.0-3.5	0.25-0.5	0.17-0.37	0.35-0.45	0.025	0.025	Max 0.03	0.1-0.18	Max. 0.3	Max. 0.2

Table B-6
Chemical compositions of carbon steels 20, 22K, and K22MA [wt%]

	C	Cr	Ni	Mn	Si	Mo	P	S	Cu
22K	0.19-0.26	≤ 0.3	≤ 0.3	0.75-1.0	0.2-0.4	–	Max. 0.03	Max. 0.03	≤ 0.3
20	0.17-0.24	Max. 0.4	Max. 0.4	0.4-0.7	Max. 0.4	Max. 0.1	Max. 0.045	Max. 0.045	–
K22MA	0.1-0.23	≤ 0.3	≤ 0.3	0.8-1.1	0.15-0.35	0.25-0.4	Max. 0.03	Max. 0.03	≤ 0.3

B.2 Carbon and Low-Alloy Steel Welds

This section covers welds in carbon and low-alloy steel used in VVER nuclear power plants. The welds are mainly used to join pressure boundary material segments to each other to form a continuous pressure boundary but are also used to repair material defects and to attach non-pressure boundary parts (such as internal and external support lugs) to the pressure boundary.

B.2.1 Service Experience

Experience with welds in carbon and low-alloy steels in reactor coolant system service has generally been good, with relatively few service-induced problems. Adverse experience is summarized in the following paragraphs.

Welds in the beltline region are subject to embrittlement due to neutron irradiation. Experience has shown that the rates of embrittlement are not a serious concern for most Western designed LWRs, and the same could be said for modern VVER materials.

A significant number of flaw indications have been detected in pressure vessels by modern ultrasonic testing (UT) performed for baseline or in-service inspections. Most of these flaws have been associated with welding or cladding. Some of the weld- and clad-related flaws have required repairs, especially when the flaws were detected before operation. However, there appear to be no reported cases of service-induced growth of under-clad weld flaws present since initial construction.

B.2.2 Material Composition and Properties

A large variety of welding materials and welding processes are used to join carbon and low-alloy steels, and it is not practical to show typical material compositions and material specifications. It is required of the weld materials to have tensile strength, ductility, and impact properties that match those of either of the base materials being welded together, as demonstrated by tests using the selected weld metal and the same or similar base materials [B1, B2].

The most common welding processes used to join carbon steel and low-alloy steel parts include submerged arc welding (SAW), shielded metal arc welding (SMAW), and gas tungsten arc welding (GTAW). Post-weld heat treatment is generally required after welding of the carbon and low-alloy steels used for reactor coolant system service.

Typical carbon and low-alloy steel filler metals (FM) according to application are:

- FM for automated welding procedures of 22K – Sv-08GS, Sv-08, Sv-08A, Sv-08AA; Sv-08GSMT
- FM for manual welding procedures of 20, 22K – UONI 13/45 A, UONI 13/55, E-B 123 JE; E-B 121 JE
- FM for automated welding of 10GN2MFA – Sv-10GN1MA
- Flux for automated welding – FC-16, AN-42M

- FM for RPV VVER 440 – Sv-10ChMFT; and for VVER 1000 – Sv-12Ch2N2MA, Sv-12Ch2N2MAA
- Butter layer for carbon steel – Sv-06A

B.2.3 Main Limitations

The main limitations of welds in carbon and low-alloy steel pressure boundary materials are as follows:

- Radiation-induced embrittlement of core beltline welds has been found to be sensitive to the chemical composition of the materials. Accordingly, it is important to control the amounts of deleterious materials, especially copper, phosphorus, and nickel. The copper content should be such that the calculated adjusted reference temperature at the 1/4T position in the vessel wall at the end of life is less than 93°C. In selecting the optimum amount of nickel to be used, its deleterious effect on radiation embrittlement should be balanced against its beneficial metallurgical effects and its tendency to lower the initial RT_{NDT} [B2].
- For detection of surface and volumetric discontinuities, all available methods were used, and the extent of nondestructive testing is comparable with the requirements of ASME Code Section III. The basic documents for production, pre-operational, and operational inspections are: 1) Individual quality assurance programs policies 1, 2, 3 (Ae5301/Dok, Ae5302/Dok, Ae5311/Dok), a set of technical conditions of TPE (10-40/1717-1780/CSE, 10-40/1719/80/CSE, 10-40/1720-1780/CSE, 10-40/1725-1780/CSE, and so on); 2) PK 1514-1572 Rules for inspections of welds, cladding and construction of nuclear power, test and research nuclear reactors and facilities; and 3) Program of pre-operational and operational controls Ae 15771/T.
- Radiographic testing (RT) is typically required by the ASME Construction Code for acceptance of welds. However, in-service inspections are typically performed using ultrasonic testing (UT). UT can detect some flaws that are not detected by RT, and this has led to the need to evaluate many flaws detected by in-service UT and, consequently, to perform some weld repair after installation and service.

Table B-7 shows the chemical compositions of selected filler metals for welding of low-alloy steel and carbon steel.

Table B-7
Chemical compositions of selected filler metals for welding of LAS and CS [wt%]

Filler Metal	C	Cr	Ni	Mn	Si	Mo	P	S	Cu	V
Sv-10ChMFT*	0.04-0.12	1.2-1.8	Max. 0.3	0.6-1.3	0.2-0.6	0.35-0.7	Max. 0.042	Max. 0.035	–	0.1-0.35
Sv-12Ch2N2MA*	0.05-0.12	1.4-2.1	1.2-1.9	0.5-1.0	0.15-0.45	0.45-0.75	Max. 0.012	Max. 0.015	–	–
Sv-10GN1MA	0.08-0.12	–	0.8-1.3	0.8-1.1	–	0.4-0.7	Max. 0.02	Max. 0.02	–	–
Sv-08AA	Max. 0.1	–	–	0.35-0.6	Max. 0.3	–	Max. 0.03	Max. 0.03	–	–
Sv-08GS	Max. 0.1	Max. 0.2	Max. 0.25	1.4-1.7	0.6-0.85	0.25	Max. 0.03	Max. 0.025	0.25	0.5

* Weld material for beltline region must fulfill (Sv10ChMFT): P = Max. 0.01%, S = Max. 0.008%, As = Max. 0.006%, Cu = Max. 0.08%, Sb = Max. 0.006%, P + Sn + Sb = Max. 0.017%.

B.3 Stainless Steels

This section covers wrought austenitic stainless steel base materials that are used for primary piping and other pressure boundary applications, as well as for reactor internals and stainless steels used for internal fasteners and similar hardware. Wrought and cast austenitic stainless steels have been widely used in LWR reactor coolant system pressure boundary applications and as structural materials in reactor internals. Pressure boundary applications include use in piping, valve bodies, and pump casings. In reactor internals, wrought stainless steel has been used for applications such as core shrouds, baffle plates, former plates, and core support plates [B1, B2]. A major difference between the austenitic stainless steels used in VVER reactors and those used in Western-designed LWRs is that the VVER reactors employ titanium-stabilized austenitic stainless steels, whereas the Western-designed LWRs employ primarily non-stabilized austenitic stainless steels.

B.3.1 Service Experience

Wrought stainless steels have provided relatively trouble-free service in LWR applications. Titanium-stabilized austenitic stainless steel together with the low oxygen content, water purity specifications, and hydrogen overpressure in VVER reactor primary coolant minimizes the probability of SCC in primary water environments. The relatively limited numbers of problems that have occurred in stainless steel parts in LWRs have generally been due to either mechanical or thermal fatigue, to high levels of cold work, or to the development in stagnant areas of aggressive environments with chloride and sulfur anionic impurities, concentrated boric acid, and entrapped oxygen (due to trapped air bubbles during refueling).

B.3.2 Material Composition and Properties

The stainless steels that have been used for reactor coolant system piping, reactor internals, and fasteners and similar hardware are:

Reactor Pressure Vessel (RPV)

High nickel SS: Fasteners and similar hardware – ChN35VT (VVER 1000)

Steam Generator (SG)

VVER Steam Generator Tubing, Tube Plugs, and Tubesheet
Austenitic SS Ti-stabilized: Heat exchanger tubes – 08Ch18N10T
Primary Circuit Collectors
Austenitic SS Ti-stabilized: VVER 440 primary circuit collector – 08Ch18N10T
High nickel SS: Fastener and similar hardware – ChN35VT
Steam Generator Secondary Side Internals
Austenitic SS Ti-stabilized: Tube support plates, feedwater collector, emergency feedwater collector – 17246, 17248, 17348, 1.4541, 08Ch18N10T
Steam Generator Secondary Pressure Boundary
Austenitic SS Ti-stabilized: Emergency feedwater system (VVER1000), nozzles (VVER1000), bolts (VVER1000) – 08Ch18N10T, 17246, 17248

Pressure Boundary

Main Coolant Pump (MCP)

Austenitic SS Ti-stabilized: MCP hydraulic body, primary piping system – cast 08Ch18N10T (VVER 440); main shut off valve body – cast 08Ch18N12T (VVER 440); MPC internals, reactor coolant pipeline, sleeves – 08Ch18N10T, 12Ch18N10T; fasteners and similar hardware – 10Ch11N20T3R

Martensitic SS: MCP internals – 14Ch17N2; MCP casings – 06Ch12N3DL (VVER 1000)

Main Coolant Piping

Austenitic SS Ti-stabilized: wrought 08Ch18N10T (VVER 440), small bore primary piping (VVER 1000)

Pressurizer

Austenitic SS Ti-stabilized: pressurizer internals, thermal protection sleeves, heaters, nozzles – 08Ch18N10T (VVER 440); pressurizer internals that are not pressure boundary – 17 247 (VVER 440); pressurizer internals, thermal protection sleeves, heaters, nozzles 08Ch18N10T (VVER 1000); heaters – 12Ch18N10T (VVER 1000); pressurizer internals that are not pressure boundary – 17247, 17246, 17248, 17347 (VVER 1000)

RPV Internals

Structural Components

Austenitic SS: Control rod drive system – 0Ch18N5G12AB

Austenitic SS Ti-stabilized: Core barrel and its bottom core support plate, core shroud (core basket + baffle + former + baffle bolts), protective tube unit – 08Ch18N10; control rod drive system – 08Ch18N10T, 12Ch18N10T, 10Ch11N20T3R, 17246.4

Martensitic SS: Fasteners and similar hardware – 14Ch17N2 (VVER 440), control rod drive system – 1Ch13N3, 20Ch17N2B-Š

Ferritic SS: Control rod drive system – 15Ch17M2B

High nickel SS: Fasteners and similar hardware – ChN35VT

Note: Unless otherwise specified with VVER 440 or VVER 1000, the materials identified apply to both VVER 440 and 1000 RPV internals.

Chemical compositions of selected stainless steels are shown in Table B-8. Typical specified mechanical properties are shown in Table B-9. Austenitic steel is produced in the form of forgings, sheets, rods, tubes, and castings.

Titanium-stabilized 18Cr-8Ni austenitic stainless steels exhibit good corrosion resistance in primary circuit water (with corrosion rates of about 0.001 to 0.002 mm/yr), good formability and weldability. Good weldability and formability are ensured by limiting the ferrite phase content – the maximum is 3% ferrite phase in wrought materials, 8 to 10% in weld metals, and 12% in cast materials. This makes these stainless steels highly thermally stable during long-term operations. Stabilization of steel with titanium provides resistance to sensitization and therefore to intergranular corrosion under specific environmental chemistry conditions with dissolved oxygen and anionic impurities like chloride and sulfur present. Irradiation can cause significant increases in strength characteristics, especially the yield strength, of austenitic SS. However, adequate plasticity is maintained.

Corrosion rates of chromium stainless steels with martensitic, martensitic-ferritic, or ferritic stainless structures in VVER primary circuits are about 0.002-0.008 mm/yr. This type of stainless steel has higher strength characteristic due to hardening processes (austenitization and aging). For example, the yield strengths of materials 10Ch11N20T3R, ChN35VT, and 0Ch18N5G12AB are between 350 and 450 MPa. On the other hand, plastic deformation characteristics are substantially lower than for 18-8 type austenitic steel. As a result, this type of steel is used mainly for internal fasteners and hardware material. Poorer weldability and susceptibility to brittle fracture make them suitable only for smaller structural parts. Mechanical characteristics of 13-17% Cr steels (for example, 1Ch13N3, 14Ch17N2, 20Ch17N2B-Š) are mostly determined by their chemical composition (especially carbon content) and heat treatment. Depending on the application, the chromium steels are used in one of two states: after hardening and high temperature tempering (600-750°C) and after hardening and low temperature tempering (250-350°C). The first group of steels is used for components that are uniformly loaded over the entire cross section. The second group is used for high contact friction loaded pairs. Chromium martensitic stainless steel has relatively low impact strength in both states. Neutron irradiation potentially increases the transition temperature and decreases the level of impact toughness.

Table B-8
Chemical compositions of selected stainless steels [wt%]

Type of Material	C	Cr	Ni	Mn	Si	Mo	P	S	Ti	Cu	Co	W
08Ch18N10T	≤ 0.08	17.0-19.0	9.0-11.0	1.0-2.0	≤ 0.8	–	Max. 0.035	Max. 0.02	0.4-0.7	–	–	–
17246	Max. 0.12	17.0-20.0	8.0-11.0	Max. 2.0	Max. 1.0	–	–	–	5*%C, (0.03)	Max. 0.03	–	–
17247	Max. 0.08	17.0-19.0	9.5-12.0	Max. 2.0	Max. 1.0	–	Max. 0.035	Max. 0.02	Min. 5*%C	–	–	–
17248	Max. 0.1	17.0-19.0	9.5-12.0	Max. 2.0	Max. 1.0	–	Max. 0.035	Max. 0.02	Min. 5*%C	–	–	–
17347	0.12	16.0-19.0	9.0-12.0	2.0	1.5	1.5-2.5	Max. 0.045	0.03	5*%C	–	–	–
17348	Max. 0.1	16.5-18.5	11.0-14.0	Max. 2.0	Max. 1.0	2.0-2.5	Max. 0.035	Max. 0.02	Min. 4*%C	–	–	–
1.4541	Max. 0.08	17.0-19.0	9.0-12.0	Max. 2.0	Max. 1.0	–	Max. 0.045	Max. 0.015	5*%C; Max. 0.7	–	–	–
10Ch11N20T3R	Max. 0.1	10.0-12.5	18.0-21.0	Max. 1.0	Max. 1.0	–	Max. 0.035	Max. 0.02	2.6-3.2	–	Max. 0.05	–
0Ch18N5G12AB	Max. 0.08	18.0-19.5	4.5-5.5	11.5-13.5	Max. 0.8	–	Max. 0.045	Max. 0.03	–	–	–	–
ChN35VT	Max. 0.12	14.0-16.0	34.0-38.0	1.0-2.0	Max. 0.6	–	Max. 0.03	Max. 0.02	1.1-1.5	–	–	2.8-3.5
1Ch13N3	0.08-0.15	12.5-14.5	2.2-3.0	Max. 0.6	Max. 0.6	–	Max. 0.030	Max. 0.025	–	–	Max. 0.05	–
14Ch17N2	0.11-0.17	16.0-18.0	1.5-2.5	Max. 0.8	Max. 0.8	–	Max. 0.03	Max. 0.025	–	–	Max. 0.05	–
20Ch17N2B-Š	0.22-0.28	16.3-17.7	2.3-2.8	0.3-0.7	0.3-0.7	–	Max. 0.02	Max. 0.015	–	Max. 0.25	Max. 0.05	–

Notes:

1. 0Ch18N5G12AB: 0.45-0.52 wt% N; 0.2-0.35 wt% V; 0.6-1.1 wt% Nb+Ta
2. 10Ch11N20T3R: Max. 0.8 wt% Al
3. 20Ch17N2B-Š: 0.05-0.1 wt% Nb

Table B-9
Specified room temperature mechanical properties of selected stainless steels

Steel	Tensile Strength [MPa]	Yield Strength (0.2) [MPa]	Elongation [%]	Reduction in Area [%]	Charpy V-notch [J.cm^{-2}]
08Ch18N10T	Min. 490	Min. 196	Min. 38	Min. 50	–
14Ch17N2	Min. 686	Min. 539	Min. 15	Min. 40	Min. 59
ChN35VT	Min. 834	Min. 490	Min. 18	Min. 40	Min. 59

B.3.3 Welding and Heat Treatment

Austenitic stainless steel 08Ch18N10T is used in the solution-annealed condition and, if necessary, supplemented with a stabilizing annealing. All material is tested and must pass the test for resistance to intergranular corrosion in accordance with GOST 6032-84 (method AM with deliberate sensitization at 650°C for 1 hour in the air).

Automatic submerged arc welding (SAW), manual arc welding with EA 400/10T electrodes, and arc welding in a protective atmosphere of argon (TIG) with Sv-04Ch19N11M3 filler metal are used for joining parts made from austenitic stainless steel. Austenitic steels are welded together without preheating.

Production and welding of the reactor internals follow the production drawings, technical conditions, and technological processes, as follows:

- Technical conditions for production of reactor internals: V-213-Č, TPE 10-40/1443/84
- Technical conditions for welding internals, upper block, and control rod system: V-213-NČ, TPE 10-40/1503/76

B.4 Stainless Steel Welds and Cladding

Austenitic stainless steel welds are widely used to join austenitic wrought and cast stainless steel base materials to each other. They are also sometimes used in dissimilar metal welds to join carbon or low-alloy steel nozzles to stainless steel safe ends and piping. In addition, austenitic stainless steel weld-deposited cladding is widely used on carbon steel or low-alloy steel vessels and (VVER 1000) primary piping to separate the steel from the primary reactor coolant to reduce general corrosion rates and corrosion product release into the coolant.

The main welding alloys that are used for joining austenitic stainless steels are:

- Sv-04Ch19N11M3, Sv-04Ch19N10T – the filler metal (FM) for automated welding is 08Ch18N10T
- EA400/10T, EA 898/21B, EA 898/21B/LC – FM for manual welding procedures of 08Ch18N10T

For cladding or buttering layers (BL) and for dissimilar metal welds (DMW), the following materials are used:

- Sv-07Ch25N13, ZIO 8, EA 395/9 – first layer of austenitic stainless cladding (automated welding procedure)
- Sv-04Ch20N10G2B, Sv-07Ch19N10G2B, Sv-08Ch19N10G2B, EA400/10T, EA 898/21B, EA 898/21B/LC – second layer of austenitic stainless cladding (automated welding procedure)
- Sv-10Ch16N25AM6 – austenitic cladding (automated welding procedure)
- Sv-01Ch12N2 – BL on carbon steel
- Sv10GN1MA – weld wire for BL on CS

Automatic submerged arc welding (SAW), shielded metal arc welding (SMAW) with EA 400/10T electrodes, and tungsten inert gas welding (TIG) using Sv-04Ch19N11M3 filler metal are used for joining austenitic stainless steel parts. Austenitic steels are welded together without preheating. The compositions of bare filler electrodes of common grades are shown in Table B-10.

Production and welding of the reactor internals follow the production drawings, technical conditions, and technological processes, as follows:

- Technical conditions for production of reactor internals – V-213-Č, TPE 10-40 / 1443/84
- Technical conditions for welding internals, upper block, and control rod system – V-213-NČ, TPE 10-40 / 1503/76

Table B-10
Chemical compositions of selected FM for welding of SS and BL of DMWs [wt%]

Type of Material	C	Cr	Ni	Mn	Si	Mo	P	S	Ti	Co	Nb	Cu
Sv-04Ch19N11M3	Max. 0.04	15.0-2.00	9.0-14.0	0.8-2.0	Max. 1.0	1.5-3.0	Max. 0.03	Max. 0.02	–	–	–	–
Sv-04Ch19N10T	Max. 0.04	18.0-20.0	8.5-11.0	1.0-2.0	Max. 0.8	–	Max. 0.025	Max. 0.025	0.4-0.7	–	–	–
Sv-07Ch25N13	Max. 0.05	22.0-26.5	11.0-14.5	0.8-2.0	1.10	–	Max. 0.03	Max. 0.02	–	–	–	–
ZIO 8	Max. 0.12	22.5-27.0	11.5-14.0	1.0-2.5	Max. 1.0		Max. 0.03	Max. 0.02	–	–	–	–
EA 395/9	Max. 0.12	13.5-17.0	22.0-27.0	1.0-2.2	Max. 0.7	4.5-7.0	Max. 0.025	Max. 0.018	Max. 0.12	–	–	–
Sv-04Ch20N10G2B	Max. 0.04	19.0-21.0	8.5-11.0	Max. 1.0	1.3-2.5	–	Max. 0.03	Max. 0.02	Max. 0.04	Max. 0.05	0.7-1.2	–
Sv-07Ch19N10G2B	Max. 0.07	Max. 19.0	Max. 10.0	Max. 1.0	Max. 0.67	Max. 0.15	Max. 0.006	Max. 0.002	Max. 0.07	–	0.8	0.07
Sv-08Ch19N10G2B	Max. 0.08	Max. 19.0	Max. 10.0	Max. 1.0	Max. 0.67	Max. 0.15	Max. 0.006	Max. 0.002	Max. 0.08	–	0.8	0.07
EA400/10T	Max. 0.1	16.8-19.0	9.0-12.0	1.15-3.1	Max. 0.6	2.0-3.5	Max. 0.025	Max. 0.025	–	Max. 0.05	–	–
EA 898/21B	Max. 0.1	17.5-20.5	9.0-10.5	0.6-2.5	Max. 0.7	–	Max. 0.025	Max. 0.025	–	–	0.8-1.5	–
Sv-10Ch16N25AM6	Max. 0.12	12.5-17.0	20.0-27.0	0.8-2.0	Max. 1.20	5.5-7.5	Max. 0.025	Max. 0.018	–	Max. 0.05	–	0.3

Notes:

1. Sv-10Ch16N25AM6 – 0.08-0.18 wt% N
2. EA395/9 – 0.08-0.15 wt% N
3. EA400/10T – 0.3-0.75 wt% V

B.5 References

[B1] IAEA-TECDOC-742, "Design Basis and Design Features of WWER-440 Model 213 Nuclear Power Plants. Reference Plant: Bohunice V2 (Slovakia).

[B2] IAEA Status Report 93, VVER–1000 (V-466B) (VVER–1000 [V-466B]), July 21, 2011.

[B3] M. Brumovsky, R. Ahlstrand, J. Brynda, L. Debarberis, J. Kohopaa, A. Kryukov, and W. Server, "Annealing and Re-Embrittlement of RPV Materials," State-of-the-Art Report, ATHENA – WP 4, AMES Report No. 19, 2008.

C
CANDU OWNERS GROUP REPORT ABSTRACTS

Table C-1 contains abstracts of CANDU Owners Group (COG) reports referenced in Section 7, CANDU Reactor Degradation Matrix Results.

Table C-1
CANDU Owners Group (COG) report abstracts

COG ID	Report Title	Abstract
02-4055	Flow-Accelerated Corrosion Rate for Bruce B Steam Generator Secondary Side Internals	A review of failures and significant degradation caused by flow-accelerated corrosion (FAC) for steam generator (SG) internals has been performed and the results are documented in this report. The review covers recirculating steam generators used in CANDU and PWR plants. The review shows that FAC significantly degraded the secondary-side internals in some SGs. Several repairs and replacements of SG internals were carried out in the USA, Canada, South Korea, and France. The most vulnerable internals are those made of carbon steel in the feed water flow path, primary separators, and top tube support plates. The main reasons for degradation are ammonia water chemistry with low pH (below 9), high fluid velocity, and low chromium content in carbon steel (about 0.05% or less). Hydrazine used in the range of about 50 to 300 ppb seems to be a contributing factor. Calculations of FAC rates for Bruce B SG internals have been performed. Unit 5 was selected for detailed analysis. The calculations used the THIRST code for thermal hydraulic results and the CHECWORKS code for FAC rates. The rates for ammonia water chemistry applied for the first 7 years of operation and for morpholine water chemistry for the last 10 years were used for the combined FAC degradation. Although the calculations use the most recent knowledge and best tools available, the accuracy of prediction is not satisfactory. There are examples when 2 units or 2 SGs under apparently the same conditions result in different degradation.
02-4070 R1	The Effect of Neutron Irradiation on the Mechanical Properties of CANDU Calandria Vessel Material	All components of the CANDU calandria vessel, except for the calandria tubes and calandria tube inserts, are made of austenitic stainless steel 304L. Unfortunately there is little experimental data concerning the ductility and none concerning the fracture toughness of SS 304L weld and heat affected zone (HAZ) material irradiated to the end-of-life fluence, 60 years at 90% capacity, under CANDU operating conditions. The limited information that is available indicates that the base material has sufficient ductility and toughness at the estimated end-of-life fluence. The fracture toughness of welds and HAZ in the calandria vessel of a CANDU reactor has been estimated using literature data for SS 304. For these materials the decrease in ductility and fracture toughness is larger than for the base material. The stainless steel 304L base material can be expected to have sufficient ductility and fracture toughness at the estimated end-of-life fluence. There is little information in the literature concerning the ductility and toughness of irradiated SS 304L weld and heat affected zone materials at the end-of-life fluence, 60 years at 90% capacity. The decreases in ductility and toughness of the irradiated weld and HAZ materials are larger than for the base material.

Table C-1 (continued)
CANDU Owners Group (COG) report abstracts

COG ID	Report Title	Abstract
02-4075	Layup-Induced Corrosion of UNS N08800 (INCOLOY 800) Steam Generator Material and Hydrazine Optimization	During wet layup of steam generators, hydrazine is commonly used as an oxygen scavenger to react with excess dissolved oxygen. Dissolved oxygen is undesirable because it accelerates corrosion of steam generator (SG) components. At Darlington Nuclear Generating Station, the steam generator tubes were fabricated from alloy UNS N08800. While having a relatively good pitting resistance at operating temperature, UNS N08800 can suffer from corrosion degradation at low temperature especially when stable deposits are present. At this time, the optimum hydrazine concentration during layup is not known. In recent years, there has been an incentive to optimize the hydrazine concentration utilized in order to provide adequate corrosion protection while minimizing the environmental release and also the cost associated with hydrazine use. The work described in this report is aimed at determining the likelihood of under deposit corrosion occurring during lay up of Darlington steam generators (SG) and the optimum layup chemistry for the mitigation of SG internal component degradation.
03-4043	FAC Degradation of Secondary-Side Internals of a Steam Generator with an Internal Preheater	A previous review of failures and significant degradation caused by flow-accelerated corrosion (FAC) for steam generator (SG) internals (Pietralik, 2002), revealed that FAC significantly degraded the secondary-side internals in some SGs. The most susceptible internals are those made of carbon steel in the feedwater flow path, primary separators, and top tube-support plates (TSP). The main reasons for degradation are water chemistry with low pH_T, high fluid velocity, and low chromium content in carbon steel.
03-4059	Layup-Induced Corrosion of UNS N06600 (Inconel 600) Steam Generator Material and Hydrazine Optimization	During wet layup of boilers, hydrazine is commonly used as an oxygen scavenger to react with excess dissolved oxygen. Dissolved oxygen is undesirable because it accelerates corrosion of boilers components. At Bruce Nuclear Generating Station, the boiler tubes were fabricated from Inconel 600 (UNS N06600). Currently, the optimum hydrazine concentration during layup is not known. In recent years, there has been an incentive to optimize the hydrazine concentration utilized in order to provide adequate corrosion protection while minimizing the environmental release and also the cost associated with hydrazine use. The work described in this report is aimed at determining the likelihood of underdeposit corrosion occurring during layup of Bruce boilers and the optimum layup chemistry for the mitigation of internal component degradation.

Table C-1 (continued)
CANDU Owners Group (COG) report abstracts

COG ID	Report Title	Abstract
05-1064	State of the Art Report (SOTAR) on Corrosion and Deuterium Ingress in CANDU Pressure Tubes	Delayed hydride cracking and fracture toughness of Zr-2.5Nb pressure tubes are potentially life limiting factors in CANDU pressurized heavy water nuclear power reactors. Concerns for delayed hydride cracking and fracture toughness over the reactor life are exacerbated by the buildup of hydrogen isotopes in the tubes, namely deuterium arising from corrosion of pressure tube surfaces. This report describes the measurements of deuterium ingress in CANDU reactor pressure tubes, identifies the key issues of importance, reviews the research and development activities in this area and summarizes the current understanding of the mechanistic processes involved in corrosion and deuterium ingress in pressure tubes. As a State-Of-The-Art-Report (SOTAR) this document provides both new and existing scientists and engineers with a comprehensive overview of the current status of our knowledge in this area.
05-4034	Fatigue of Alloy 800	In this study, low cycle, high strain fatigue tests were performed on Alloy 800. The material tested was manufactured to CANDU specification. However, the grain size of the manufactured material was twice the size of actual tubing material in Darlington Nuclear Generating Station steam generators. Consequently, the grain size was modified by rolling and heat treatment. The treatment was done by heating to 1800 ± 10°F (980 ± 5°C) with a soaking time of less than 15 minutes. This treatment resulted in an average grain size range of 15-19 mm, which is close to 13 mm for the actual in-service tubing material. Fatigue data were generated for the as-manufactured and modified Alloy 800 materials in air at ambient temperature and in neutral crevice chemistry (with the addition of lead) at 250°C. The results indicated a display of typical reduction in fatigue strength in the crevice environment compared to the air data. The effect of grain size was not so pronounced in the crevice environment. The results indicated that such an effect was limited under the selected mechanical, environmental, and temperature conditions. All samples tested exhibited transgranular cracking features; an observation consistent with the absence of any grain size effect.

Table C-1 (continued)
CANDU Owners Group (COG) report abstracts

COG ID	Report Title	Abstract
05-4069	Layup-Induced Corrosion of UNS N04400 (Monel 400) Steam Generator Material and Hydrazine Optimization	During wet layup of boilers, hydrazine is commonly used as an oxygen scavenger to react with excess dissolved oxygen in the secondary side of nuclear power plants. Dissolved oxygen is undesirable because it accelerates corrosion of boiler components. Currently, the optimum hydrazine concentration during layup is not known. At low concentrations of hydrazine, the carbon steel cathodically protects the tube material while at higher concentrations of hydrazine, the protective oxide layer present on the tubes may be compromised. In recent years, there has been an incentive to optimize the hydrazine concentration utilized in the field in order to provide adequate corrosion protection while minimizing the environmental release and also the cost associated with hydrazine use. The work described in this report was initiated to determine the likelihood of under-deposit corrosion occurring during layup of Pickering Nuclear Generating Station steam generators. In addition, it is of interest to provide information to assist in determining the optimum layup chemistry in conjunction with other information for the mitigation of boiler internal component degradation.
06-1003	Engineering Fatigue Crack Initiation Evaluation Curves for Axial Flaws in Zr-Nb Pressure Tubes	The CSA Standard N285.8 and the COG report COG-02-1065 contain procedures and acceptance criteria for evaluation of the structural integrity of CANDU Zr-Nb pressure tubes containing flaws. One of the requirements of these documents is to evaluate the flaw for fatigue crack initiation. Based on results from fatigue crack initiation experiments, the procedure to evaluate flaws for fatigue crack initiation that is in the current versions of the CSA Standard N285.8 and the report COG-02-1065 is considered to be overly-conservative for flaws with very small root radii, such as 15 mm. Improved, flaw root radius dependent engineering fatigue crack initiation evaluation curves have been developed to address this over-conservatism. This report describes experimental results that were used to develop the new engineering curves, as well as the development and validation of the new engineering curves.

Table C-1 (continued)
CANDU Owners Group (COG) report abstracts

COG ID	Report Title	Abstract
06-1065	Ex-service Inconel X-750 and Zr-Nb-Cu Garter Springs	Annulus gap spacers (garter springs) are a key feature of the CANDU reactor fuel channel design. Assured performance of the integrity of the garter springs is required for a fuel channel to perform reliably over the life of the reactor. The garter springs were initially made from Inconel X-750 and were fitted tightly onto the pressure tube. This design was used in NPD and KANUPP. When the Douglas Point reactor was built, the design was changed to a loose fitting spring made from a Zr-2.5Nb-0.5Cu alloy. This design was used for all subsequent fuel channels installed to 1983. The spring material was changed from Inconel X-750 to Zr-2.5Nb-0.5Cu in order to improve the neutron economy of the fuel channel. However, the loose fit of the Zr-2.5Nb-0.5Cu spring allowed it to travel along the channel if excited. Displacement of loose fitting garter springs was a contributory factor in the failure of a pressure tube in Pickering Unit 2 in 1983. Following this failure, the decision was made to return to the tight fitting Inconel X-750, despite the loss of neutron economy. Garter springs in the currently operating CANDU plants are either loose fitting Zr-2.5Nb-0.5Cu springs or tight fitting Inconel X-750 springs, depending on whether the fuel channel was installed before, or after, 1983. Any material exposed to neutron irradiation in the reactor core is expected to exhibit changes in properties as a result. A COG project was initiated to provide more data on the condition of irradiated garter springs. The first task of this project was to identify suitable samples for evaluation. Garter springs cannot be extracted from the fuel channel except as part of a pressure tube replacement. Furthermore, due to the practical requirements of a pressure tube replacement operation, the condition of the garter springs becomes compromised as a result of the removal operation. Garter springs from the Bruce A fuel channel B3Q15, of the Zr-2.5Nb-0.5Cu type, and garter springs from the Bruce B fuel channel B8W19, of the Inconel X-750 type, were available for evaluation as a result of pressure tube replacements for these channels. Additional X 750 garter springs were available from the Darlington Unit-2 fuel channel D2O18 after that pressure tube was removed. However, in all cases each individual garter spring was damaged to a greater or lesser degree by the removal operations. Notwithstanding the limitations imposed by the as-received condition of the samples various examinations including diameter measurement, hydrogen isotope measurement, and metallography examination were performed. In addition, radial compression (crush) testing and stretch testing were also performed. For these mechanical tests the prior condition of the samples was more limiting but extensive efforts have been made to extract as much useful information as possible. A detailed assessment of the compression test indicates that the performance of a spacer section in the crush test is a function of the test rig geometry and loading conditions, which can be understood and quantified analytically.

Table C-1 (continued)
CANDU Owners Group (COG) report abstracts

COG ID	Report Title	Abstract
07-1042	State of the Art Report (SOTAR) on Corrosion and Deuterium Ingress at Rolled Joints in CANDU Pressure Tubes	Delayed Hydride Cracking (DHC) of Zr-2.5Nb pressure tubes at the rolled joint is a potentially life limiting factor in CANDU-PHW nuclear power reactors. Concerns for DHC over the reactor life are exacerbated by the buildup of hydrogen isotopes at the tube ends, namely enhanced deuterium ingress at the rolled joint arising from galvanic coupling between the zirconium alloy pressure tube and the stainless steel end fitting. This report provides a summary the data obtained from analyses of tubes removed from service in power reactors, a review the R&D effort on sources and routes of the enhanced ingress at the tube ends, ideas considered for reducing deuterium ingress at rolled joints, a discussion on the mechanism of enhanced ingress, and a description of the current predictive model. As a State-Of-The-Art-Report (SOTAR) this document provides both new and existing scientists and engineers with a comprehensive overview of the current status of our knowledge in this area.

Table C-1 (continued)
CANDU Owners Group (COG) report abstracts

COG ID	Report Title	Abstract
07-1092	Delayed Hydride Cracking in Zirconium Alloys – State of the Art Report (SOTAR)	Between 1974 and 1986 several zirconium alloy pressure tubes in different CANDU and RBMK reactors failed by a fracture process involving hydrogen. Although hydrogen is essentially insoluble in zirconium at room temperature and has only limited solubility at reactor operating temperatures, these small amounts of hydrogen easily diffuses down hydrogen gradients, down temperature gradients and up stress gradients and this movement leads to accumulations of hydrogen sufficient to form brittle zirconium hydride at the end of the gradient. With sufficiently high tensile stress, the hydride can crack and the diffusion process is repeated. This cracking mechanism is called Delayed Hydride Cracking (DHC). The characteristics of DHC are: - a threshold stress condition has to be met before cracking starts, - the threshold condition is mostly independent of temperature, hydrogen concentration and alloy strength but sensitive to alloy crystallographic texture, - the cracking rate is independent of the stress condition and hydrogen concentration but highly sensitive to temperature, temperature history, temperature gradient, loading history, and alloy microstructure and strength. A mechanism based on hydrogen accumulating at the end of the stress gradient at a crack tip, and invoking the large hysteresis between the hydrogen solubility limits on heating and cooling, explains a large body of the experimental results. Most of the failures in reactors resulted from large residual tensile stresses. No new failures were reported once the source of these stresses was eliminated. Vigilance continues to be necessary as reactors age – the hydrogen concentration continues to increase and some flaws may develop from interaction between the fuel and the pressure tubes. Assessment methods have been developed so that flawed tubes at risk may be replaced while flawed tubes that are not at risk can remain in service in the reactor. Pressure tubes in new reactors should be less likely to fail by DHC since their initial residual stresses and hydrogen concentrations are small, and they will also pick up hydrogen at a reduced rate. Most of the failures did little damage to the reactors because they were detected by water leakage before the crack became unstable; this is the principle of leak-before-break. Should a crack develop in a new tube, it will be tolerated better because the length of an unstable crack is now consistently large because of an improvement in fracture toughness.

Table C-1 (continued)
CANDU Owners Group (COG) report abstracts

COG ID	Report Title	Abstract
07-4030	Fatigue of Alloy 400	In this study, low cycle, high strain-controlled fatigue tests were performed on Alloy 400 to produce fatigue life data. The objective of the overall work package is to produce a database of fatigue properties for Alloy 400 for input into fitness-for-service documentation. The material tested was heat-treated to CANDU specification. Fatigue data were generated for the as-manufactured and heat-treated Alloy 400 materials in air at ambient temperature and in neutral crevice chemistry at 250 °C with and without addition of lead. The results of these tests are presented in this report.
08-4054	Potential Risk of Primary Water Stress Corrosion Cracking in Dissimilar Metal Welds at CANDU Feeder Tube Flow Devices	Dissimilar metal welds (DMWs) involving Alloy 600 and its equivalent weld metal, Alloy 82, are used in the CANDU heat transport system in inlet feeder components, and in a number of outlet feeders at Bruce Nuclear Generating Station, and at Darlington Nuclear Generating Station. Pressurized water reactor (PWR) operating experience has shown welds containing Alloy 600 and its weld metal equivalents to be susceptible to primary water stress corrosion cracking (PWSCC). In response to the PWR operating experience an assessment of the likelihood of PWSCC in the DMWs present in CANDU units has been undertaken. Initially a comprehensive review was conducted, covering industry operating experience, life management strategies, regulatory issues, as well as laboratory studies. Acting on recommendations from that review, example CANDU DMWs have been characterized in terms of residual stress and microstructure.

Table C-1 (continued)
CANDU Owners Group (COG) report abstracts

COG ID	Report Title	Abstract
08-4072	Factors Leading to Corrosion Degradation of Alloy 800	Until recently, operating experience with Alloy 800 Steam Generator (SG) tubes indicated no susceptibility to any long term aging related degradation. Historically, all degradation observed during laboratory testing, and the few instances of corrosion in operating SGs, was clearly associated with exposure of the Alloy 800 tubing to highly corrosive environments during water chemistry excursions that are now precluded by modern chemistry control regimes. However, operating experience in Germany and Canada over the last five years has challenged the assumption that Alloy 800 SG tubes will continue to demonstrate trouble free corrosion performance. Recently, there have been reports of intra tubesheet stress corrosion cracking (SCC) and intergranular attack (IGA) in Alloy 800 SG tubing at some of the older German pressurized water reactors (PWRs). Within the CANDU industry, unexpected (but minor) SG tube wall loss has been recently observed at the Darlington Nuclear Generating Station (DNGS) in Units 2 and 4. In both cases minor corrosion was detected that appears to be coincident with shallow fretting located at the hot leg supports; however, there have been no observations of corrosion in Darlington tubes coincident with U bend AVB (anti vibration bar) fretting elsewhere in the DNGS SGs. The damage observed in the tubes removed from DNGS Units 2 and 4 is associated with plastic strains in the near surface region in the vicinity of the fretting wear scars. In addition, corrosion testing of these removed tubes revealed that they were somewhat more susceptible to pitting corrosion than Alloy 800 tubing that has never been in service. Seen in context with the unexpected cracking observed in some German SG tubes, these findings have led to speculation that Alloy 800 tubing may have some in service aging degradation susceptibility. It is important to note that all the material susceptibility factors in question are subtle, both in nature and in effect. There is no reason to suspect gross changes in the relative corrosion resistance between aged and new tubing. Exposure to known corrosive environments, which can be precluded by water chemistry control, must occur before degradation is a possibility. (continued on next page)

Table C-1 (continued)
CANDU Owners Group (COG) report abstracts

COG ID	Report Title	Abstract
08-4072 (continued)	Factors Leading to Corrosion Degradation of Alloy 800	(continued from previous page) Control of the water chemistry is a key measure for the prevention of degradation during all aspects of SG operation. The current COG work package was undertaken to characterize the corrosion degradation and coincident mechanical damage observed in the Darlington Nuclear Generating Station tubes and to perform corrosion and electrochemical testing of ex-service and archived materials. The general aim of the work is to determine if there is any evidence of aging related corrosion degradation having occurred or whether it might occur in the future. A specific objective of the ongoing work is to determine why even non mechanically damaged SG material displays reduced corrosion resistance, apparently as a result of in service aging. Another objective is to study the interaction of surface mechanical damage and corrosion resistance to determine what level of damage/plastic strain is a cause for concern as a function of corrosive environments possible in SGs. This current report reviews all findings to date.

Table C-1 (continued)
CANDU Owners Group (COG) report abstracts

COG ID	Report Title	Abstract
08-4075	A Survey on the Corrosion Susceptibility of Archived Alloy 800 Tubing from CANDU Steam Generators	This COG report presents the results from a survey on the corrosion susceptibility of archived steam generator (SG) tubes from the Centrale Nucleaire Gentilly 2 (CNG2), Point Lepreau Generating Station (PLGS), Bruce Nuclear Generating Station (BNGS), and Third Qinshan Nuclear Power Co., Ltd (TQNPC). The results were compared with those obtained from the SG tubing D4 SG1 R49C61 removed from Darlington Nuclear Generating Station (DNGS) as part of routine period inspection program requirements. The removed tube R49C61 had shallow less than 5% tw underdeposit corrosion based on the metallography examinations. The corrosion susceptibility of the ex-service DNGS tubing was assessed previously under simulated CANDU crevice chemistry conditions at 300 C. The experimental results suggested that these ex-service SG tubes were more susceptible to pitting corrosion than a reference nuclear grade Alloy 800 tubing. The conditions and the root cause leading to the SG tube degradation at DNGS have been under investigation. The work carried out under this COG WP was to survey the corrosion susceptibility of the archived Alloy 800 tubing from the CANDU SGs under plausible crevice chemistry conditions and to determine whether Alloy 800 SG tube material at other CANDU plants would be susceptible to the same degradation as that found at DNGS. Another purpose of testing archived Alloy 800 tubing was to compare their electrochemical behavior against the reference nuclear grade Alloy 800 and determine whether the reference nuclear grade Alloy 800 is representative for the Alloy 800 CANDU SG tubing in service. Archived Alloy 800 SG tubing samples from four CANDU nuclear power plants, including BNGS, PLGS, CNG2, and TQNPC, were collected for testing. All the archived tubing had no in service exposure. High temperature electrochemical tests were carried out for the archived Alloy 800 tubing under normal neutral SG crevice chemistry conditions both at 300°C and 150°C. The results were compared with those obtained from the ex-service DNGS SG tubing under the same test conditions.

Table C-1 (continued)
CANDU Owners Group (COG) report abstracts

COG ID	Report Title	Abstract
08-4080	Environmentally Assisted Cracking of Alloy 800 – Current Knowledge and Future Work Required for Supporting Steam Generator Life Predictions (SOTAR)	As CANDU plants approach end of design life, refurbishment and life extension of non-refurbished components such as steam generators (SGs) to a 60 year life are being undertaken. Degradation free performance of Alloy 800 SG tubing in the remaining and extended plant life is of critical concern to the nuclear industry. SG long term degradation behavior prediction methodology development, improvements and validation (via field SG inspections) for producing better SG life cycle management plans and for better managing business risks (i.e., time of onset and severity of ODSCC relative to the extended life) is required. The Electric Power Research Institute (EPRI) and Dominion Engineering, Inc. (DEI) have developed probabilistic approaches using a degradation free lifetime Weibull distribution based on operating experience with Alloy 600 SG tubing and a concept of materials improvement factors (MIFs) to justify the long term service behavior of other SG tubing. The University Network Excellence in Nuclear Engineering (UNENE) Waterloo Chair (Pandey) has also proposed a new “Corrosion Stress Cycles Analysis” (CSCA) approach, which is focusing on the degradation of SG Alloy during chemistry excursions and SG transients, for predicting SG tube long term behavior with high confidence. To reduce the uncertainties of the EPRI/DEI probabilistic approaches for predicting the long term behavior of CANDU Alloy 800 SG tubing, it is very important to obtain appropriate MIFs through R&D focusing on the degradation mechanisms of Alloy 800 and Alloy 600 SG tubing under plausible CANDU SG operating conditions. The development of the CSCA approach for predicting Alloy 800 SG tubing long term degradation also requires the support of laboratory tests focusing on the life limiting degradation mechanisms of Alloy 800 tubing under plausible CANDU SG operating conditions. OPEX of Alloy 800 SG tubing in the German Pressurized Water Reactors (PWRs) and in CANDU NGS suggested that outer diameter stress corrosion cracking (ODSCC) is a plausible life limiting degradation mode for Alloy 800 SG tubing. (continued on next page)

Table C-1 (continued)
CANDU Owners Group (COG) report abstracts

COG ID	Report Title	Abstract
08-4080 (continued)	Environmentally Assisted Cracking of Alloy 800 – Current Knowledge and Future Work Required for Supporting Steam Generator Life Predictions (SOTAR)	(continued from previous page) Future R&D focused on the mechanistic process of ODSCC and its precursors including passivity breakdown and localized corrosion such as intergranular attack (IGA) and underdeposit corrosion is required. There were many previous EPRI and COG test programs to study the SG tubing degradation. The purpose of this COG report is to compile and document relevant data generated in COG, EPRI, and other agency programs in order to retrieve useful data or experiences and identify any gaps for future work required to support the development of probabilistic approaches of predicting Alloy 800 CANDU SG tubing long term behaviours. Two separate reviews were performed and are attached to this report as appendices: One is focused on the electrochemical aspect (passivity breakdown) and localized corrosion, including pitting corrosion, IGA and underdeposit corrosion, which may likely be the precursor leading to stress corrosion cracking SCC of SG tubing. The other is focused on environmentally assisted cracking (EAC) of SG tube alloys. Based on these reviews, the degradation modes associated with different SG off specification operations have been verified. The major life limiting degradation mode and the factors leading to Alloy 800 SG tubing degradations were discussed. Future R&D work focusing on the life limiting degradation mode of SG tubing during SG layup, startup and excursions using sufficient test specimens to satisfy certain reliability level for predicting SG long term behavior has been proposed.
08-4081	Implications of Intra-Tubesheet Cracking at Biblis A to CANDU Alloy 800 Steam Generator Tube Performance	Document R 7924 00 01 Rev. 0 was prepared for AECL by Dominion Engineering, Inc. (DEI) and presents a review and analysis of European reports of Alloy 800 crack indications at Biblis A and Unterweser, and the implications of this mode of degradation for CANDU steam generators with Alloy 800 tubes.

Table C-1 (continued)
CANDU Owners Group (COG) report abstracts

COG ID	Report Title	Abstract
08-4082	Summary Notes on an Optimized Materials Improvement Factor Approach for Alloy 800 CANDU Steam Generator Tubing	As CANDU plants approach end of design life, refurbishment and life extension of non-refurbished components such as steam generators (SGs) is being undertaken. New reactors are being designed and built for a 60 year SG life. However, there is insufficient history for Alloy 800 SG tubing in service to predict accurately the expected life. Electric Power Research Institute (EPRI) and Dominion Engineering, Inc. (DEI) have developed probabilistic approaches using a degradation free lifetime Weibull distribution based on OPEX of Alloy 600 SG tubing and a concept of materials improvement factors (MIFs) to justify the long term service behavior of other SG tubing. Attempts were made recently to predict Alloy 800 CANDU SG tubing long term behavior for Point Lepreau Generating Station (PLGS) and Darlington Nuclear Generating Station (DNGS). This is a promising step towards managing SG life in a proactive manner. However, the current EPRI/DEI has some limitations resulting from a few assumptions, which requires further improvements. For example, the approach assumes the degradation of SGs is a function of full power operation. It is not applicable for corrosion related degradation relevant to shutdowns, excursions and SG transients. To improve this situation, UNENE NSERC Chair, M. Pandey of University of Waterloo, started to link the SG tube degradation to the off specification operation using the safe electrochemical corrosion potential (ECP)/pH zone ratio defined for SG Alloys by AECL to estimate the MIFs. Pandey also proposed new probabilistic approaches to predict long term behavior of Alloy 800 SG tubing independent of Alloy 600 OPEX. For example, a new Bayesian approach can be used to predict SG lifetime distribution by combining expert estimates with information available from in service performance of Alloy 800 tubing in CANDU reactors. In addition, a brand new concept “corrosion stress cycle analysis” (CSCA) that is independent of the OPEX of Alloy 600 is also proposed. This alternative approach is based on the concept of “Fatigue Usage Factor” used in mechanical design. The idea of the CSCA approach assumes that an alloy can tolerate a certain number of corrosion stress cycles, i.e., excursions due to poor chemistry conditions and SG transients etc. Using the in service experience, the number of stress cycles that occurred in the history of a SG and in the future can be estimated. Probability distributions can be used to assign uncertainties to the estimates, and then the probability of SG tubing degradation in a specified period of time can be calculated. (continued on next page)

Table C-1 (continued)
CANDU Owners Group (COG) report abstracts

COG ID	Report Title	Abstract
08-4082 (continued)	Summary Notes on an Optimized Materials Improvement Factor Approach for Alloy 800 CANDU Steam Generator Tubing	To ensure a consistent CANDU industry approach to long term service behavior of SG tubing, using the latest EPRI, DEI and the probabilistic approaches proposed by Pandey, work has been funded by COG under WP 40829 to coordinate experts in the nuclear power industry and UNENE to review and discuss the current probabilistic approaches and to provide direction for future R&D work in this area. A workshop titled "AECL COG UNENE Workshop on Probabilistic Approaches for Predicting SG Tubing Degradation," was held on January 15, 2009, at the COG offices in Toronto. A report prepared by DEI is attached in this document (Appendix A) to introduce the probabilistic approaches developed by EPRI/DEI and a summary of the presentations, the discussions and suggestions on future work at the workshop. A summary note by Pandey is also attached to this report (Appendix B) to introduce the probabilistic approaches developed in his group. It is clear that R&D work is required for supporting the further development and application of the above mentioned probabilistic approaches for predicting Alloy 800 CANDU SG tubing long term degradation. It is suggested that experimental work should be performed to determine the following three major characteristics of the alloy: 1. How big is the operating margin? This characteristic can be quantified by the Safe ECP/pH zone, which is verified in terms of all major SG tube degradation modes. The smaller the operating margin, the higher the degradation probability the alloy. 2. How long can the alloy tolerate excursions/upset without initiating degradation? This characteristic can be determined by measuring the degradation incubation time. The probability of initiation of degradation of the alloy increases as the incubation time decreases. 3. How fast does the degradation propagate? Once degradation is initiated, the time to failure will be determined by the degradation growth rate Future R&D work to evaluate Alloy 800 and Alloy 600 in terms of the above mentioned three characteristics may establish an improved material improvement factor (MIF) supporting the application of EPRI/DEI approaches for predicting Alloy 800 CANDU SG tubing long term service behavior using OPEX from Alloy 600 SG tubing. The results from the R&D can also be used for the development of CSCA approach proposed by Pandey for predicting Alloy 800 SG tubing degradation.

Table C-1 (continued)
CANDU Owners Group (COG) report abstracts

COG ID	Report Title	Abstract
09-1008	Interim Approach Fatigue Crack Initiation Evaluation Curves for Axial Flaws in Zr-Nb Pressure Tubes	The CSA Standard N285.8 and the COG report COG-02-1065 contain procedures and acceptance criteria for evaluation of the structural integrity of CANDU Zr-Nb pressure tubes containing flaws. One of the requirements of these documents is to evaluate the flaw for fatigue crack initiation. Based on results from fatigue crack initiation experiments, the procedure to evaluate flaws for fatigue crack initiation that is in the current versions of the CSA Standard N285.8 and the report COG-02-1065 is considered to be overly-conservative for flaws with very small root radii, such as 15 mm. Improved, flaw root radius dependent engineering fatigue crack initiation evaluation curves for the axial components of flaws were developed to address this over-conservatism. The development and validation of the improved engineering curves are described in the report COG-06-1003.
09-4008	The Basis for Chemistry Control in the Steam Generator During Wet Layup and Startup	Literature from key nuclear conferences on water chemistry and the corrosion of nuclear materials, reports prepared under the auspices of EPRI, COG, AECL, and individual nuclear utilities as well as selected journal publications, have been reviewed to establish the optimum chemistry conditions to mitigate corrosion of SG materials under wet lay up and start up conditions. Differences in results reported by various investigators are dispositioned and recommendations are made to address gaps in the knowledge that were identified by this review. Based on our current knowledge, a set of optimum chemistry control measures to mitigate degradation of SG materials during wet lay up and start up is proposed.
09-4058	The Interactive Effects Between Steam Generator Impurities on CANDU Steam Generator Tube Corrosion – A Final Report	This report presents the results obtained from a series of electrochemical experiments carried out to study the corrosion susceptibility of Alloy 800 and Alloy 600 under the influence of different common steam generator (SG) impurities and their interactions in the SG secondary side crevice chemistries. The effect of different lead compounds and other SG impurities such as silicon, copper, aluminum, magnesium, calcium (act alone or in combination with lead) on the corrosion degradation of Alloy 800 and Alloy 600 tubing materials was studied under secondary side SG crevice chemistry conditions. The impact of SG impurities on the corrosion susceptibility has been presented in the safe ECP/pH zones of Alloy 800 and Alloy 600.

Table C-1 (continued)
CANDU Owners Group (COG) report abstracts

COG ID	Report Title	Abstract
09-4078	Examination of Ex-Service DNGS Steam Generator Tubes (Intra-Tubesheet Region)	Recent European operating experience confirmed that cracking of Alloy 800 steam generator (SG) tubing can occur under specific secondary side environments, as observed in the deep intra-tubesheet region. This finding generated interest to re-assess the condition of the material in the intra-tubesheet region of removed and in-service Alloy 800 SG tubes in CANDU plants. The overall objective of this work is to obtain relevant information from removed Alloy 800 SG tubing material to assess the likelihood of the occurrence of stress corrosion cracking (SCC) in CANDU SG tubing within the intra-tubesheet based on factors such as material characteristics, secondary side environmental conditions within the tubesheet, and residual stresses. The findings from this investigation show that some of the known conditions that lead to the SCC degradation in the European nuclear plant are present in the Darlington SGs (i.e., leakage from the secondary side within the gap between the tube and the tubesheet, accumulation of deleterious species, mainly S and Cl, and evidence of minor degradation due to pitting). However, the metallurgical examination showed no signs of intergranular attack (IGA) or SCC degradation. Moreover, Orientation Imaging Microscopy (OIM) analysis did not reveal the presence of significant residual strain within the intra-tubesheet region. Although SCC and IGA has not been an issue for Alloy 800 SG tubes in CANDU plants, the recent European Operating Experience (OPEX) and current findings for the DNGS SG tubes, point to a potential for this mode of degradation. This is a conservative position based on the unknown level of risk for cracking associated with the conditions observed in the DNGS SG tubes in this report.

Table C-1 (continued)
CANDU Owners Group (COG) report abstracts

COG ID	Report Title	Abstract
09-4084	Evaluation of Implications of New Indications of Steam Generator Alloy 800 Tube Degradation	The attached document R 7931 00 01 Revision 1 (Appendix A) was prepared by Dominion Engineering, Inc. (DEI) and presents an updated summary of operating experience related to recent indications of Alloy 800 steam generator tube degradation in several European nuclear plants. This is a supplementary report to COG 08 4081. The European OPEX has been analyzed to evaluate the potential impact of degradation observed in several steam generators tubed with Alloy 800 on steam generator tube life of CANDU (Canadian deuterium uranium) pressurized heavy water reactors. CANDU steam generators tubed with Alloy 800 have more than 25 years of essentially trouble free service, and the steam generators are either expected to provide, or being considered, for a further 30 years' service. Hence it is important to assess whether the European OPEX could have any impact on this extended steam generator life. Based on available information, the deep intra tubesheet intergranular attack/cracking observed in several German reactors is considered to have resulted from off specification low temperature operation, such as at shutdowns, and as a consequence of accumulation of oxidizing and corrosive conditions (sulphur contamination) in deep tubesheet crevices. There has been no report of such degradation in any CANDU steam generator, whether tubed with Alloy 600 or Alloy 800, even though evidence from removed tubes indicates that most Alloy 800 tubes with hydraulic expansions allow inleakage of coolant during shutdowns, and even though a number of CANDU steam generator tube upper expansions were not carried out, leaving open crevices within the tubesheet. Since the intra tubesheet degradation observed in Europe is most likely active or initiated at low temperatures, it is concluded that it also represents a potential threat to CANDU SGs, even though they operate at lower temperatures than European SGs. (continued on next page)

Table C-1 (continued)
CANDU Owners Group (COG) report abstracts

COG ID	Report Title	Abstract
09-4084 (continued)	Evaluation of Implications of New Indications of Steam Generator Alloy 800 Tube Degradation	(continued from previous page) Another degradation mechanism is reported to have occurred at several other European plants with Alloy 800 steam generator tubing is top of tubesheet (TTS) denting, together with signals suggesting the presence of cracks at the top of tubesheet, in two plants. Unlike the deep tubesheet degradation, which appears to have taken many years (> 25) to be detected, and which occurred in plants with initial phosphate treatment, denting and possible cracking have been detected after relatively short in service life (~ 12 to 15 years) in plants operating with AVT chemistry. This observation is based on interpretation of eddy current data, and not on any removed tubes. This denting poses a threat of circumferential cracking at the TTS, but has not been seen in any CANDU units to date. It is noted that this denting and possible cracking is reported to have occurred in SGs with Alloy 800 tubing that has had an external full length shot peening treatment to reduce susceptibility to stress corrosion cracking, with a subsequent upper hydraulic expansion and recessed mechanical roll that produces a complicated stress state at the TTS. It is speculated that this denting and possible cracking may be a consequence of the TTS crevice depth associated with the expansion process and the peening induced cold worked layer. Only G 2 has tubing with similar shot peening treatment, but that treatment was restricted to tubes in rows 19 and below (tight radius tubes), and was carried out above the first support plate only. All CANDU steam generator tubesheets also have very shallow crevices at the TTS, which may explain the difference in denting observations between European and CANDU steam generators.

Table C-1 (continued)
CANDU Owners Group (COG) report abstracts

COG ID	Report Title	Abstract
09-4086	Analysis of Tube Degradation in Steam Generator Preheater of Darlington Steam Generator	Recent inspections show that tubes are degraded in the preheater of the Darlington steam generators (SGs). The degradation occurred on the outside surface of the tube, near the top surface of the baffles and reached up to 50% through wall. Tube R3C51 at preheater baffle P05 was analyzed most comprehensively because it experienced significant damage. The tube degradation coincides with the clearance gap between the tube and the preheater baffle hole. In this narrow gap there is low flow due to the low pressure difference across the baffle plate which reduces the efficiency of the preheater heat transfer. The objective of this study is to understand the Darlington SG preheater tube degradation and to determine the mechanism of the tube degradation. The analysis used the THIRST code for a 3 dimensional thermal-hydraulic simulation of the steam generators and the ANSYS FLUENT code for detailed thermal-hydraulic simulations of flow and heat transfer in the clearance gaps. The flow and heat transfer phenomena in the preheater and the clearance gap were analyzed to examine the possibility of cavitation and cavitation degradation can occur in the Darlington SG preheaters.
10-4075	An Aging Assessment of CANDU Alloy 800 SG Tubing	Steam generator (SG) tubing removed from three CANDU® stations with service life spanning from 2 to 27 years was examined as part of a material aging assessment under COG 40830. This report summarizes the results obtained from laboratory examinations of the tubing, including high temperature electrochemical experiments carried out under the SG crevice chemistry conditions to verify the corrosion susceptibility, metallurgical examinations to check the chemical compositions, grain size, hardness of the ex-service tubing materials and Secondary Ion Mass Spectroscopy (SIMS) analysis to examine for potential surface chromium depletion and grain boundary segregation of the ex-service tubing. These data provide support for SG life extension to 60 years, and for SG life management.

Table C-1 (continued)
CANDU Owners Group (COG) report abstracts

COG ID	Report Title	Abstract
10-4077	Cavitation Susceptibility of Tubes in Steam Generator Preheaters for CANDU 6 Internal and Bruce External Preheaters	Recent inspections show that tubes degraded in the preheater of the Darlington steam generators (SGs). The degradation occurred on the outside surface of the tube, near the top surface of the baffles and reached up to 50% through wall depth. While the Darlington SGs have windowed baffle plates, other CANDU SGs have segmented baffle plates or external preheaters of the segmented design. The objective of this study is to determine if CANDU 6 segmented baffle preheaters and external preheaters have conditions that could make them susceptible to similar tube degradation found in the DNGS windowed baffle preheaters. The Point Lepreau preheater design was used as an example for CANDU 6 specific data. The study consists of a thermal-hydraulic analysis of flow and heat transfer in SG preheaters, an analysis of flow and conditions leading to boiling inside clearance gaps between tube and baffle, and a discussion of factors affecting cavitation degradation probability. For CANDU 6 internal preheaters, the analysis used the THIRST code for a 3 dimensional thermal-hydraulic simulation of the steam generators and the ANSYS FLUENT code for detailed thermal-hydraulic simulations of flow and heat transfer in the clearance gaps. The flow and heat transfer phenomena in the preheater and the clearance gap were analyzed to examine the possibility of cavitation and cavitation degradation. For external preheaters, a one dimensional analytical calculation was used to estimate the local stream velocities and pressures and these parameters were then compared to those predicted in CANDU 6 and DNGS preheaters. The analysis focuses on the possibility of cavitation and cavitation degradation in the clearance gaps.

Table C-1 (continued)
CANDU Owners Group (COG) report abstracts

COG ID	Report Title	Abstract
10-4091	Summary Report on the Interactive Effects of Impurities on CANDU Steam Generator Tube Cracking	The main objective of this summary report is to document the key observations from the previous work conducted in various COG work packages and to identify any gaps that may exist in the understanding of the effect of lead-containing impurities on the corrosion degradation and cracking of steam generator (SG) tubing alloys (specifically, Alloy 600 and Alloy 800). The application of electrochemical and capsule testing methodologies, conducted under complementary work packages (WP 40813 and WP 40814), was successful in the investigation of the corrosion and cracking of Alloy 600 and Alloy 800. The tests were performed in simulated SG secondary side crevice chemistries in the presence of lead using different lead compounds and cationic impurities. The main observations from both types of testing are as follows: 1. There was no evidence to suggest that sulphate could immobilize, and reduce the corrosivity of, lead species under steam generator crevice chemistry conditions. 2. Silica (SiO2) appeared to have an inhibitive effect on SG tube degradation in the presence of lead. 3. Alloy 600 mill-annealed (MA) was susceptible to lead-induced degradation/stress corrosion cracking (SCC) in the presence of any of the lead compounds tested, including lead oxide, lead sulphate, lead sulphide, and lead chloride. 4. Alloy 800 displayed better corrosion/SCC resistance than Alloy 600 MA under SG crevice chemistry conditions in the presence of a variety of SG impurities.

Table C-1 (continued)
CANDU Owners Group (COG) report abstracts

COG ID	Report Title	Abstract
11-4055	Effects of Chloride and Sulfate on SCC Thresholds for Cold-Worked Type 316L Stainless Steel at Intermediate Temperatures	Stress corrosion cracking (SCC) of stainless steel instrument lines, which form part of the pressure boundary of the primary heat transport system, has been a problem at the Darlington Nuclear Generating Station. The instrument lines of austenitic stainless steel, operated at intermediate temperatures (ranging from 150ºC to 250ºC) with a low rate of refreshment, may be subjected to excursions from normal primary chemistry, resulting in their exposure to oxygenated water with chloride and sulphate contamination. It was identified prior to this work package that determination of the chloride threshold for activation and arrest of SCC in austenitic stainless steel as a function of temperature is required. Before undertaking an extended experimental program, a literature review was completed, and information related to the roles of chloride and oxygen in SCC of austenitic stainless steel assessed and documented in COG 09 4056 (see Appendix A), in which earlier work on cracking thresholds was reviewed and gaps identified. Work was then performed to experimentally determine threshold conditions for SCC of Type 316L stainless steel at the intermediate temperatures, especially with respect to effects of chloride and sulphate. Tests were performed by Serco Technical Consulting Services. The material used for the tests was Type 316L stainless steel with 2%, 5%, and 10% cold work, respectively. Long time crack growth testing on compact tension specimens was realized by engaging on line crack growth measurements, and effects of chemistry variations were studied by real time chemistry control using a high temperature water circulation loop.
JP-4363-V067	Effect of Irradiation on Inconel X-750 Fuel Channel Spacers	This report presents data and discusses the effect of irradiation on the properties of the X-750.
JP-4363-V158	Results of He and H analysis in Ex-Service Inconel X-750 Annulus Spacers	The helium concentration in specimens from Inconel X-750 annulus spacers are determined by isotope dilution gas mass spectrometry. The results are reported and compared with the expected He levels for transmutation reactions. Protons are also formed in the Inconel matrix by transmutation reactions and measurement of potential trapped hydrogen was attempted by HVEMS at CRL. Specific results are not reported for hydrogen.

Table C-1 (continued)
CANDU Owners Group (COG) report abstracts

COG ID	Report Title	Abstract
JP-4363-V165	Test Report for Ex-Service Spacer Crush Testing	This test report details the in-cell crush testing performed on ex-service, irradiated spacer samples, taken from Bruce, Darlington, and Pickering. Nineteen (19) crush tests in total were executed; two (2) commissioning tests, sixteen (16) principal tests, and one (1) un-irradiated confirmation test. Crush testing was performed using Flat-Flat platens on spacer sample lengths ranging between 15 and 32 coil turns, taken from the 12 o'clock and 6 o'clock positions. The hooked ends of the spacer was defined as the 12 o'clock position corresponding to the top of the pressure tube and the 6 o'clock position corresponding to the bottom of the pressure tube, where the spacer is in contact between the pressure tube and calandria tube. Testing was conducted inside CRL Building 234 Universal Cell #2, using an AECL designed crush test apparatus.
JP-4363-V185	Assessment of Inconel X-750 Material Degradation	This current assessment combines the insights generated from the complementary work completed and reported to date, with insights from the comprehensive literature review undertaken in 2010. It is anticipated that this framework will provide the context within which to assess the significance of the new crush test results once they are available.

Table C-1 (continued)
CANDU Owners Group (COG) report abstracts

COG ID	Report Title	Abstract
JP-4363-V197	Assessment of Inconel X-750 Spacer De-Tensioning	In order to prevent movement from installed locations Bruce 8 and Optimized Inconel X-750 spacers were designed to be tight-fitting around the pressure tube within CANDU reactor fuel channels. In light of recent assessments on the effects of irradiation on Ni-rich alloys it is conceivable that the spacers (also referred to as garter springs) could become susceptible to movement from their design locations during the initial period of reactor operation provided significant relaxation and swelling were to occur prior to the time when they become loaded as the pressure tube sags to make contact with the calandria tube. The CANDU industry has initiated work to address this issue with the objective of understanding the rate of relaxation and swelling of X-750 spacers relative to the rate of diametral expansion of the pressure tubes, and to assess service loading conditions to evaluate the susceptibility of spacers to movement from their design locations, both prior to, and after being pinched between the pressure tube and calandria tube. At least two of the spacers removed from channel Q13 of the Darlington Unit 3 reactor appeared loose on the pressure tube when extracted from the fuel channel. As the spacers would be expected to conform to the shape of the pressure tube after the initial applied tension had relaxed, the loose fit on removal of the pressure tube from the fuel channel could be attributed to the springs: (i) being stretched during the removal operation; (ii) being pushed from a higher to a lower diameter portion of the tube; (iii) swelling. Material characterization by transmission electron microscopy (TEM) has shown evidence for cavity formation in the material. Whereas swelling will be occurring as a result of the cavity formation, the extent of the swelling is not known accurately. In addition to the observations from transmission electron microscopy modelling of the cavity/bubble evolution provides valuable insights. The extent of Helium production via Ni transmutations has been calculated and subsequently quantified by measurements. The quantity of helium generated (a primary driver for swelling) and the number of times each atom has been displaced (a primary driver for relaxation and swelling) after 14 EFPY of operation for the Inconel X-750 spacers in D3Q13 have been calculated (~ 20000 appm and ~60 dpa respectively). Calculations of time to de-tensioning for spacers in high power and low power channels in Bruce 8 and Darlington reactors have been conducted to support evaluation of Inconel X-750 spacer movement susceptibility. These sample calculations use conservative estimates of spacer stress relaxation and swelling rates coupled with the rate of diametral creep of pressure tubes.

Table C-1 (continued)
CANDU Owners Group (COG) report abstracts

COG ID	Report Title	Abstract
JP-4363-V202	Assessment of the Potential of Stress Corrosion Cracking of Alloy X-750 Fuel Channel Spacers	The CANDU industry has initiated work to address issues associated with X-750 spacer degradation. The overall objectives of the work are to understand the conditions that cause material degradation and to assess service conditions to determine this risk and to demonstrate fitness-for-service. Spacers removed from service were tested to failure in 2006 and failed at reduced loads compared to as-fabricated spacers. Fractures were all entirely intergranular. The possibility that the strength of spacers was compromised by pre-existing cracks was investigated because it was suggested that some form of intergranular stress corrosion cracking (SCC) might have occurred prior to testing. No evidence of stress corrosion cracking having influenced the crush tests was found. The purpose of the current assessment is to determine the significance of SCC as a degradation mechanism for X-750. Circumstances where it is possible to assert that SCC is not credible are identified. Circumstances where some potential for SCC exists are identified.
JP-4363-V203	Assessment of Fuel Channel Annulus Spacer Wear	An assessment of fuel channel annulus spacer wear was requested by COG to address a gap in knowledge about the potential causes and the impact of spacer wear. This document reviews OPEX related to ex-service spacer examinations and in-service inspections to provide context to the frequency and magnitude of spacer wear. The potential causes of wear in spacers are then discussed by reviewing information related to fuel channel and calandria tube vibration. The final sections of this document focus on the impact of spacer wear on the integrity of spacers, and the implications on pressure tube to calandria tube contact time.
JP-4363-V204	Fuel Channel Life Management, Assessment of Delayed Hydride Cracking in Zr-2.5Nb-0.5Cu Spacer	The report provides an evaluation of the susceptibility of Zr-Nb-Cu spacers to DHC under reactor operating and SLAR conditions. The manufacturing, metallurgical properties, design and operating conditions of Zr-Nb-Cu spacers are described. A review on the DHC properties of cold worked and heat treated Zr-Nb pressure tubes and Zr-Nb-Cu material was performed, with an emphasis on the available data and information on KIH, the threshold stress intensity factor for DHC from a crack. Using the approach provided in CSA N285.8 for the evaluation of DHC in Zr-2.5Nb pressure tubes, the susceptibility of the spacers to DHC was evaluated under a conservatively postulated scenario of crack size, spacer movement and a high SLAR load of 450 lb (2002 N).

Table C-1 (continued)
CANDU Owners Group (COG) report abstracts

COG ID	Report Title	Abstract
OP-1084	Inconel X-750 Fuel Channel Annulus Spacer Integrity Assessment	The integrity of the optimizes Inconel X-750 tight fitting annulus spacer is assessed in response to concerns raised over results of crush tests on irradiated spacers generated during a recent COG program and reported in draft report COG-06-1065. The work carried out to complete this assessment includes: a review of the tests carried out during development and qualification and used to establish the static load to carrying capability of the spacer: a detailed reassessment of the test methods and equipment used and results obtained for the irradiated spacers: finite element modelling analysis to quantify any significant differences between the spacer: finite element modelling analysis to quantify any significant differences between the spacer loading during tests and in-reactor operational loads; and, an investigation, by examination of fractures using fractography and metallography of the potential for in-reactor spacer degradation such as stress corrosion cracking having led to the apparently low load test results. The major finding of this assessment is that the finite element modeling of the in-reactor loading, together with a detailed reassessment of the most limiting crush test results provides a load margin of at least a factor of four to spacer failure for the spacer design load of 890N. Careful analysis of the crush test loading curves was required because the geometry and rigidity of the rig used for the crush test results in uneven coil loading in the spacers as they are crushed. The uneven loading can be exacerbated by prior deformation in the irradiated coils due to damage on removal from the reactor and transport to AECL-CRL. The limited ductility of the spacers following irradiation in coil failure prior to the load being spread among the coils of the spacer under test. In the reactor, the loading among coils of the spacer is much more even due to the compliance of the calandria tube. Although no detailed assessment was carried out for fatigue loading, the in- reactor loads are sufficiently low that fatigue due to thermally induced rolling of the spacer with fuel channel expansion and contraction should not be a concern. Examination of fracture surfaces indicated that all the fractures examined appeared brittle and intergranular in nature with little evidence of ductility. (continued on next page)

Table C-1 (continued)
CANDU Owners Group (COG) report abstracts

COG ID	Report Title	Abstract
OP-1084 (continued)	Inconel X-750 Fuel Channel Annulus Spacer Integrity Assessment	(continued from previous page) The fractures from the crush tests show no evidence of pre-existing cracks and all were the result of single overload events. The fractures present in the spacers when they were received in the hot cells appear to be oxidized. On one of the examined fractures, there is evidence of more than one occurrence of crack extension with an intervening period of oxidation. However, the metallographic examination concluded that the fractures were not used by stress corrosion cracking (SCC), as no signs of crack branching were observed. Furthermore, a detailed assessment of SCC concluded that there is no plausible case for SCC in a dry annulus and that the required stress levels are not present. The presence of oxide on the fracture has been judged to likely be the result of oxidation following fractures that occurred as a result of overloading during removal from the reactor and transport to ACEL-CRL, rather than from fracture and oxidation in-reactor. Intergranular fracture surface are expected to be susceptible to corrosion attack in warm, humid, highly radioactive environments and these were most likely present for several months in the station flask following removal of the fuel channel from Darlington. Based on the margins established and the judgement that the oxidation observed likely occurred after removal from the reactor, the optimized Inconel spacers are acceptable for reactor operation Additional work is being planned to confirm the judgement.

D
REVISION LOG

Table D-1 provides an overview of MDM revisions occurring from Revision 0 through Revision 5.

Table D-2 provides a more detailed section-by-section overview of revisions to the MDM for Revision 5.

Tables D-3 through D-6 provide detailed lists of MDM cells for which a change in status occurred for Revision 5. For each cell, a short description of the reason for the change is also provided.

- PWR result changes are listed in Table D-3.
- BWR result changes are listed in Table D-4.
- CANDU result changes are listed in Table D-5.
- VVER result changes are listed in Table D-6.

Table D-1
Revision log

Revision	Description of Change
Revision 0 (2004)	Initial issue.
Revision 1 (2008)	Revision 1 of the MDM is the initial presentation of the material in a traditional EPRI report format. Revision 0 of the MDM was made available to select interested parties but was not published as a technical report. Therefore, Revision 1 established the general approach to the presentation of materials degradation information. Also, all technical information was reviewed by an expert panel and revised to include recent developments in the area of materials degradation for Class 1 components. The key aspects of the presentation of this information established in this revision are as follows: 1. The use of component level results tables as the basis for presentation of information. This represents a consolidation of the multi-level information approach used in Revision 0. 2. The addition of a cover section and introduction. The addition of introductory and summary information aligns the report with a standard EPRI technical report format. 3. The addition of a “Summary of Results” section. This section is added to provide a summary of all the information contained in the report. 4. The development of BWR and PWR component level results tables. As mentioned in item 1, these tables organize information from “levels 1, 2, and 3” tables in Revision 0 into a single-level, hyperlinked presentation of the most recent information. 5. A references section is added to provide an organized presentation of document references in a single location. References in Revision 0 were distributed throughout the document. 6. Appendix A was added as a “Degradation Mechanism Summary.” In Revision 0, this information was found in a series of mechanism information summaries. This new appendix organizes the information in a single location. 7. Appendix B was added as a “Materials Summary.” In Revision 0, this information was found in a series of materials information summaries. This new appendix organizes the information in a single location.

Table D-1 (continued)
Revision log

Revision	Description of Change
Revision 2 (2010)	Revision 2 of the MDM addresses consideration of long-term operations (LTO). In addition to the standard consideration of a 60-year plant operation, the Expert Panel considered potential changes to results from consideration of an 80-year operating window. The result is a new “LTO” tag applied to affected cells in the components results tables as well as discussions of the implications of an 80-year operation. A second fundamental change in the revision is the addition of “implementation” (IMP) tags to some cells. The IMP tag indicates cells where no further research is required but that aspects of R&D findings have not yet been put into practice. In addition to the changes described above, the most significant changes to the MDM Component Results Tables from Revision 1 are summarized below: 1. The PWR and BWR summary results tables were removed. 2. A new column was added to address fouling. 3. A new alpha-numeric explanatory numbering system was used for clarity. 4. The total number of component level results tables were reduced by consolidating similar tables, particularly for pressure boundary components. 5. Nickel alloys are now divided between high- and low-chromium alloys. 6. Separate line items were added to the applicable reactor internals tables for X-750, A-286, XM-19, and martensitic stainless steel. 7. Rows for mill-annealed and sensitized steam generator tubes were removed as these are considered “sunset” materials. 8. A new row for ferritic stainless steel was added to the steam generator internals table. In addition to the component level results table changes above, a new Section 5 was added for strategic issues. Previous strategic issues were presented in Section 2. Most of this content in Revision 2 is new or has been substantially revised.

Table D-1 (continued)
Revision log

Revision	Description of Change
Revision 3 (2013)	Revision 3 of the MDM includes a general update of the BWR and PWR results (Sections 3 and 4) based on recent operating experience and R&D program results. Additionally, this revision expands on conclusions reached for long-term operations (LTO) and introduces a set of MDM results for the CANDU pressurized heavy water reactor design (Section 5). The results table organization was altered to align with the presentation of degradation mechanisms in Appendix A. Columns for SCC were moved to the right of the columns for loss of material (corrosion and wear). Conclusions and strategic issues are now presented in Section 6. Consistent with the changes to the results, the content of Section 6 has been extensively revised. Appendix A: “Degradation Mechanism Summaries” was extensively revised to streamline the text, improve subject matter organization, include new materials/ degradation mechanisms related to CANDU components, and revise/update text to include recent developments in the field of material aging. Appendix B: “Materials Summaries” was updated to include relevant new content from updated versions of the EPRI Materials Handbook. The content has been reorganized to better align with the presentation of results in the degradation matrix results tables. Materials are now grouped into categories for structures and welds, high-strength alloys, and steam generator tubing and tube supports. Additionally, new content was added to address the zirconium alloys used in CANDU fuel assemblies, the content for steam generator tubing was expanded, and new content was added to address ferritic and martensitic stainless steels applied as the material of construction for steam generator tube supports.

Table D-1 (continued)
Revision log

Revision	Description of Change
Revision 4 (2018)	Revision 4 includes a general update of the PWR, BWR, and CANDU results based on operating experience and R&D program results. This revision also introduces a set of MDM results for VVERs. In developing the Revision 4 results, it is noted that a consolidated expert panel elicitation process was not used due to the difficulties in managing these panels for multiple reactor designs. In the case of VVER results development, a small panel was convened. For other results, inputs were solicited from the industry, and a small group of industry experts and EPRI staff managed the actual revisions to the results. An additional objective of this revision was to streamline and simplify the MDM results. Modifications to the MDM to accomplish this objective include the following: 1. The MDM now reflects operations beyond 60 years as the only standard in the evaluation and presentation of results. Conclusions presented in the results sections for BWRs, PWRs, and CANDUs were modified on this basis. As a result, the “LTO” tags used in Revisions 2 and 3 of the MDM to distinguish differences in conclusions for 60-year and 80-year operations are no longer needed and have been removed from the degradation matrix results tables. 2. In most cases, the implementation (IMP) tags (included to denote that, although fundamental R&D is not considered needed, there are implementation issues remaining) have been removed in recognition that the issue management table (IMT) process is adequately capturing and addressing these implementation issues. 3. A decision was made to relocate the strategic issues section to Section 3 of the MDM, a location preceding presentation of results for each reactor design type. This results in the renumbering of the reactor design results sections. 4. Lists of references have been added to the end of each results section, and the consolidated references section has been removed. This change is an effort to facilitate future revisions to the MDM for one or more individual reactor design types without requiring a comprehensive revision of the references. 5. Appendix B of the MDM has been replaced with a link to the EPRI Materials Handbook. This decision was made to reduce the overall content of the MDM document and to avoid duplication of resources. There was extensive overlap between Appendix B of the MDM and the materials handbook. Users may refer to the materials handbook for materials information. 6. A new appendix for VVER materials was added as Appendix D. This information, although analogous to the information provided in the EPRI Materials Handbook, has not yet been incorporated into the handbook. This appendix will remain in the MDM until such time as the materials handbook is updated to include the VVER materials information. Minor updates to Appendix A – Degradation Mechanism Summaries were made to reflect new operating experience and updated expert perspectives. **NOTE**: Revision 4 includes a transition in file structure and software format to facilitate updates from multiple personnel. As a result, there are minor differences in appearance between Revision 3 and Revision 4.

Table D-1 (continued)
Revision log

Revision	Description of Change
Revision 5 (2024)	Revision 5 includes a general update of the PWR, BWR, CANDU, and VVER content based on operating experience and R&D program results. In developing Revision 5, a decision was made to return to the expert panel elicitation process. It was felt that the MDM is a sufficiently mature document such that an expert panel containing two to four subject matter experts per reactor type could appropriately cover revisions to the tables. Efforts were made to form a multi-disciplinary and international panel of experts representing various viewpoints (reactor OEMs, consultants, researchers, etc.), and revisions were vetted by appropriate EPRI nuclear materials experts. The following minor changes were made, which are applicable to the MDM report in its entirety: • Hyperlinks were added to every technical note for easy navigation back to the respective MDM tables. • The statement “No additional R&D is necessary.” was omitted from the abbreviated definition for the green color code that appears in Sections 4 to 7, and hyperlinks to the comprehensive color definitions in Section 2 were inserted. • Removal of the remaining implementation (IMP) tags, included to denote that, although fundamental R&D is not considered needed, there are implementation issues remaining. These were retained in the CANDU MDM tables for Revision 4 but have been removed with the development of issue management tables (IMTs) for CANDU reactors in 2024. • A comprehensive review of Appendix A was performed. • In Revision 4, Appendix B of the MDM was replaced with a link to the EPRI Materials Handbook. This decision was made to reduce the overall content of the MDM document and to avoid duplication of resources. In Revision 5, the readers are referred to the materials handbook for additional materials information in “Section 2.2.2 Material Classes.” Appendix B Materials Summaries was omitted, and the appendices were re-ordered as follows: – Appendix A – Degradation Mechanism Summaries – Appendix B – VVER 440 and 1000 Materials – Appendix C – CANDU Owners Group Report Abstracts – Appendix D – Revision Log

Table D-2
List of significant changes to the MDM, Revision 5

Report Section	Description of Change
Section 1 Introduction	Background was updated as needed to reflect Revision 5.
Section 2 Approach	The content of Section 2 was updated to describe the use of an Expert Panel approach to this MDM revision.
Section 3 Strategic Issues	Strategic issues were updated based on conclusions of experts contributing to Revision 5. With respect to LWRs, strategic issues were added pertaining to the SCC of stainless steel in primary water, the fracture toughness evolution in irradiated stainless steels, the effects of water impurities on the SCC of LAS, and the benefit of updated CGR models to contain continuity across various water chemistries (BWR and PWR). With respect to VVERs, significant changes included a decreased emphasis on EAF due to significant European test programs currently underway and an increased emphasis on void swelling for stainless steel reactor vessel internals. With respect to CANDU reactors, significant changes included a decreased emphasis on the irradiation embrittlement of Alloy X-750 annulus spacers and the addition of text pertaining to the effects of irradiation on martensitic stainless steel pressure boundary components (fracture toughness and SCC resistance).
Section 4 PWR Results Section 5 BWR Results Section 6 VVER Results Section 7 CANDU Results	For the PWR, BWR, VVER, and CANDU reactor types, the results were updated to reflect the consensus of the experts based upon the results or recent research contributing to Revision 5. See Table D-3 for a list of changes to cell results.
Appendix A Degradation Mechanism Summaries	The content of Appendix A was reviewed by EPRI staff in this revision of the MDM and updated as deemed appropriate.
Appendix D Table D-3, D-4 and D-5, D-6	Addition of detailed lists of PWR, BWR, VVER, and CANDU reactor MDM cell changes between Revision 4 and Revision 5.

Table D-3
Detailed list of PWR MDM cell result changes for Revision 5

Cell Description	Rev. 4 Result	Rev. 5 Result	Basis/Notes
PWR Primary Pressure Boundary			
300 Series SS: Base metal, welds & cladding – SCC (p1-6c, p1-6d)	Y	Y	The status was conservatively set to Yellow to reflect potential gaps in knowledge with respect to the identification of susceptible components based on the recent OE with SCC of non-isolable branch piping in the safety injection system of some plants.
CASS – SCC (p1-6e)	Y	Y	The change in status to Green reflects the Expert Panel's opinion that the mode of degradation was sufficiently dispositioned in MRP-236 Rev. 1 and that state of knowledge in this area is considered mature.
C&LAS Base metal & welds – EAF (p1-9a, p1-9b)	Y	Y	The change in status to Green reflects the Expert Panel's opinion that the mode of degradation was sufficiently addressed by the publication of ASME Code Section XI, Appendix Y-3200 and that additional R&D is not warranted at this time.
C&LAS Base metal & welds – RiFP/Th (p1-10a, p1-10b)	?	Y	Thermal aging embrittlement for C&LAS is considered possible in the primary circuit. Based on the review of thermal embrittlement mechanisms, the development of tools to disposition embrittlement, and ongoing research, the R&D status has been set to Yellow.
CASS – RiFP/Th (p1-10e)	Y	Y	Thermal embrittlement processes are generally well understood, and existing R&D indicates that both saturated and partially aged predictions of fracture toughness are very conservative for all but the most extreme cases. The state of knowledge in this area was deemed mature by the Expert Panel.
Alloy 52/152 Welds & Cladding – RiFP/Th (p1-10i)	Y	Y	As a result of the significant ongoing and planned work on the thermal aging of Alloy 52 weld metal variants currently being performed by EPRI, the R&D status was changed from Orange to Yellow.
C&LAS Base metal & welds – Irradiation Effects/Emb (p1-12a, p1-12b)	Y	Y	Considering the high fluence data that will be produced from ongoing neutron irradiation of standard surveillance capsules and the PSSP specimens, this R&D area can be moved to Yellow for 80 years of plant operation.
PWR Reactor Vessel Internals			
300 Series SS: Base metal, welds & cladding – VS (p2-13a, p2-13b, p2-13e)	Y	Y	Based on various testing and evaluation results as well as the reevaluation of the previous data set, which estimates a significant reduction in the predicted swelling rate, the R&D status was changed from Yellow to Green.

Table D-3 (continued)
Detailed list of PWR MDM cell result changes for Revision 5

PWR Steam Generator Tubing, Tube Plugs, and Tubesheet Welds			
Alloys 600TT and 690TT – fouling (p3-4a, p3-4b)	Y	Y	The Expert Panel deemed the state of knowledge with respect to SG fouling to be sufficient to warrant a change in status to Green.
Alloys 600TT and 690TT – HCF (p3-8a, p3-8b)	Y	Y	Except for one particular model SG, other performance issues (level oscillations and loss of thermal performance) appear to manifest sooner than flow-induced vibrations. Mitigation measures taken to address these issues (i.e., chemical cleaning) also fully address the issue of deposit-related flow-induced vibration.
Alloy 690TT – RiFP/Th (p3-10b)	N	Y	Thermal aging tests indicate that Alloy 690 can be embrittled by the formation of an Ni_2Cr phase due to long range ordering. However, this is largely an effect of the Fe content and is mitigated through appropriate material specifications. The issue is considered one of implementation and not a fundamental materials knowledge gap.
Alloy 52/82 Welds – RiFP/Env (p3-11e)	Y	Y	The shift in status to Green reflects the fact that most U.S. utilities have obtained inspection relief for tubesheet welds based on these welds not posing a significant risk to pressure boundary integrity (leakage or pullout).
Row added for Alloy 800 (p3-1c, p3-2c, p3-4c, p3-5c, p3-7c, p3-8c, p3-9c, p3-10c, p3-11c)			In Rev. 4, the PWR SG MDM referred readers to the CANDU MDM for matters pertaining to the degradation of Alloy 800. A decision was made to explicitly re-include Alloy 800 cells in the PWR SG MDM table due to the observations of differing performance of Alloy 800 SG tubing in PWR SGs compared to CANDU. While there is a growing number of instances of Alloy 800 ODSCC in the PWR fleet, there have been zero instances of cracking in SGs of CANDU design, to date. This is considered also to apply to Alloy 800 sleeving.
Row added for Alloy 800 sleeves (p3-1f, p3-2f, p3-7f)			
Alloy 690TT – OD SCC (p3-7b)	N	Y	This change reflects the correction of an error in the past revision, which had the primary side SCC and secondary side SCC cells for Alloy 690TT unintentionally reversed.
Alloy 690 – PS SCC (p3-6b)	Y	N	

Table D-3 (continued)
Detailed list of PWR MDM cell result changes for Revision 5

Cell Description	Rev. 4 Result	Rev. 5 Result	Basis/Notes
PWR External Surfaces and Pressure Retaining Bolting			
C&LAS – SCC (p6-6a)	Y	Y	This change was made in the table to correct an inconsistency in Rev. 4, which had an Orange status assigned in the explanatory note but a Green cell in the table.
LAS Fasteners – RiFP/Th (p6-9f)	?	Y	The change was made as there is OE to suggest the mechanism is possible, and there is limited information to disposition.
C&LAS – Irradiation Effects/Emb (p6-11a)		Y	A new column was added to address the irradiation embrittlement of RPV supports, which may become an issue for 80-year operation and must be addressed in the context of license renewal.

Table D-4
Detailed list of BWR MDM cell result changes for Revision 5

Cell Description	Rev. 4 Result	Rev. 5 Result	Basis/Notes
BWR Primary Pressure Boundary			
C&LAS Base Metal & Welds – SCC (b1-6a, b1-6b)	Y	Y	Although now dispositioned, given that the significant effect of chloride on crack growth rate was unexpected, the status has been set to Orange due to the unknown effects of additional water impurities, which may have elevated importance as some components accumulate fluence, and the lack of ongoing R&D or future plans to address the gap.
Alloy 82/182 – SCC (b1-6g, b1-6h)	Y	Y	The R&D status was changed from Orange to Yellow to reflect planned work related to crack growth rates for Alloys 82/182.
Alloy 52/152 Welds & Cladding – SCC (b1-6i)	N	Y	The change to Y reflects laboratory results that show moderate SCC crack growth rates in BWR environments. However, an Orange status is selected to reflect the lack of ongoing or planned work in this area.
C&LAS Base Metal, Welds & HAZ – IASCC (b1-7a, b1-7b)	?	Y	The change from Blue to Green reflects the Expert Panel opinion that this is a plausible degradation mode. However, since the regions of highest SCC risk (nozzle/penetration weld HAZ) are spatially distant from the regions of significant fluence, applied R&D in this area was not considered necessary.
C&LAS Base Metal, HAZ & Welds – Irr. Emb. (b1-12a, b1-12b)	Y	Y	The change in status from Orange to Green reflects the fact that sufficient data exist to assure that NRC Reg. Guide 1.99, Rev. 2 is adequate for 80 years of BWR plant operation.
BWR Reactor Vessel Internals			
XM-19 – SCC (b2-6h)	Y	Y	The change to Green reflects the very low susceptibility of the material to SCC initiation in BWR environments as demonstrated in lab tests and by a flawless service history. The expert panel consensus is that no further R&D is recommended in this area.
X-750 – SCC (b2-6i)	Y	Y	Recent testing of Alloy X-750 specimens in the HTH condition confirms that, even under HWC conditions, SCC crack growth rates of engineering significance can occur. Given the SCC susceptibility observed, the strategic knowledge gap associated with these materials is the capability to predict component service lifetimes with greater confidence. The status change to Orange reflects the lack of ongoing or planned work to address this knowledge gap.

Table D-4 (continued)
Detailed list of BWR MDM cell result changes for Revision 5

Cell Description	Rev. 4 Result	Rev. 5 Result	Basis/Notes
BWR Reactor Vessel Internals (cont.)			
CASS – TE/IE (b2-10c, b2-12c)	Y	Y	With respect to the irradiation embrittlement of CASS, some key data gaps exist. Most notably, the lack of fracture toughness data for low Mo materials (CF3/CF8) between 1 and 5 dpa as well as a lack of data for CASS materials with concurrent irradiation dose and thermal exposure for greater than 1 dpa. The R&D status of Orange reflects the lack of ongoing or planned work in this area to address these knowledge gaps.
C&LAS – IASCC (b1-7a)	Y	Y	The change in status from Orange to Green reflects the fact that the risk of IASCC initiation and growth in the RPV is considered to be low since the regions most susceptible to SCC (e.g., nozzle/penetration weld HAZ) are distant from the core mid-plane, i.e., spatially removed from the regions of significant flux.
BWR Reactor Fasteners and Hardware			
XM-19 – IASCC and IE (b2-7h, b2-12h)	Y	Y	IASCC and irradiation effects associated with XM-19 are possible due to their locations and fluence levels. Irradiated XM-19 test data indicate that the SCC growth rate increase is small at the relevant fluence levels; however, the data are limited. The status change to Orange reflects the lack of ongoing or planned work to address this knowledge gap.
X-750 – IASCC and IE (b2-7i, b2-12i)	Y	Y	Alloy X-750 BWR internals components are located where end-of-life fluence approaches a level at which IASCC can be a concern and IASCC growth rates in irradiated specimens show a limited enhancement relative to non-irradiated data; however, the data are limited. The status change to Orange reflects the lack of ongoing or planned work to address this knowledge gap.

Table D-5
Detailed list of CANDU MDM cell result changes for Revision 5

Cell Description	Rev. 4 Result	Rev. 5 Result	Basis/Notes
Fuel Channel Assemblies			
X-750 – SCC and Irradiation Effects (c1-6c, c1-7c, c1-12c, c1-13c, c1-14c, c1-15c, c1-16c)	Y	Y	A decision was made to set the R&D status for these cells to Green as there is a sufficient understanding of SCC susceptibility and irradiation effects for X-750 annulus spacers due to the considerable amount of work carried out under the COG Fuel Channel Life Management Joint Project. Furthermore, X-750 spacers are currently effectively managed via a surveillance program and are being phased out during refurbishment and replaced with Zr-Nb-Cu alloy spacers.
Zr-Nb-Cu – Wear (c1-5d)	Y	Y	Examination of ex-service spacers has indicated that Zr-Nb-Cu spacers can be subject to significant wear in pinched regions because of a continuous hydriding/spalling process. A conservative Yellow status was assigned as an insufficient number of spacers have been examined to establish the extent of wear and its impact on component function. Plans are in place to examine future ex-service spacers.
Zr-Nb-Cu – DHC (c1-9d)	Y	Y	DHC is a plausible mode of degradation for Zr-Nb-Cu spacers. A brittle fracture has been observed during recent out-of-reactor component testing of surveillance spacers. R&D is considered necessary to understand the extent and implications of these results. Currently, there are no R&D activities planned. As such, the status was set to Orange.
SS: Martensitic – SCC and Irradiation Embrittlement (c1-6e, c1-14e)	Y	Y	Examination of an ex-service end fitting has indicated that irradiation hardening, without any sign of saturation, appears plausible at the inboard end, counter to previous assessments that assume irradiation effects saturate very early in the component life. Currently, no R&D is planned to investigate the effects of irradiation on the embrittlement of end fittings or the consequence of embrittlement on SCC susceptibility. As such, the status has been set at Orange.

Table D-5 (continued)
Detailed list of CANDU MDM cell result changes for Revision 5

Calandria Vessel and Moderator System			
SS & SS Welds – Localized Corrosion and SCC (c2-2a, c2-2b, c2-6a, c2-6b)	Y	Y	The transition to a Yellow R&D status reflects concerns regarding understanding the mode of degradation of localized corrosion and SCC observed in the calandria relief ducts of CANDU units. There is currently planned and ongoing work in this area that is expected to address this knowledge gap.
SS & SS Welds – IASCC (c2-7a, c2-7b)	N	?	The predicted dose of 60+ EFPY exceeds the engineering thresholds for IASCC susceptibility for LWR internals. The transition from “N” to “?” reflects the possibility that the calandria vessel could be susceptible to IASCC under LTO conditions; however there is a significant lack of SCC test data under relevant environmental conditions (low temperature, highly oxidizing) to determine susceptibility with sufficient confidence.
SS & SS Welds – Irradiation Embrittlement (c2-14a, c2-14b)	Y	Y	The transition from Orange to Yellow reflects the planning and initiation of a comprehensive accelerated irradiation and subsequent test program carried out through the COG Strategic R&D program to address the knowledge gap pertaining to the evolution of mechanical properties in the calandria vessel/tubesheet and its welds.
Primary Heat Transport System			
Ni-Alloy 600 & 82 – IG /TG SCC (c3-6d, c3-6e)	Y	Y	The transition to a Green R&D status reflects the knowledge acquired by the characterization of dissimilar metal weld dilution zones in CANDU feeder flow elements and the sunsetting of these materials in the CANDU fleet upon refurbishment. The Green status is consistent with the corresponding cell in the PWR pressure boundary MDM table.
Addition of Ni-Alloys 690 & 52 (c3-6f, c3-6g, c3-11f, c3-11g, c3-11f, c3-13g)			Alloy 600 feeder flow elements are to be systematically replaced with Alloy 690 equivalents upon CANDU refurbishment. As such, they have been proactively included in the CANDU PHTS MDM table.
All PHTS Materials – EAF (c3-11a, c3-11b, c3-11c, c3-11d, c3-11e)	Y	Y	The conditions in the CANDU primary pressure boundary systems are considered enveloped by the information in NUREG/CR-6909. An R&D status consistent with that for LWRs is deemed appropriate. No additional R&D is needed.

Table D-5 (continued)
Detailed list of CANDU MDM cell result changes for Revision 5

Primary Heat Transport System (cont.)			
LAS – Thermal Embrittlement (c3-12c)	?	Y	The peak temperatures experienced in CANDU LAS components are not deemed to differ significantly from those for PWRs. The cell has been updated to be consistent with the state of knowledge for thermal embrittlement of LAS, as indicated in the PWR MDM cell, p1-10a.
All PHTS Materials – Irradiation Effects	N/A		The three columns relating to irradiation effects (Emb., VS, IC/SR) were omitted. All irradiated materials are addressed in Tables 7-1 and 7-2.
Steam Generator Tubing			
Alloy 800 – Pitting (c4-2a)	Y	Y	The change from Yellow to Green R&D status reflects the opinion of the Expert Panel that the main contributing factors to the pitting of Alloy 800 are known. No additional R&D is warranted in this area.
Alloy 800 – ODSCC (c4-7a)	Y	Y	While this degradation has not been observed in CANDU SGs, there has been considerable recent international operating experience of ODSCC of Alloy 800 SG tubing. The change in R&D status to Orange reflects the Expert Panel's opinion that insufficient R&D is planned or underway to understand the susceptibility of Alloy 800 SG tubing to SCC late in plant life.
Ni-base Alloy 82 Welds – Environmental RiFP (c4-12e)	Y	Y	The shift to a Yellow R&D status reflects the fact that this degradation mode is conservatively bounded by feeder flow element dissimilar metal welds and that R&D in that area is sufficient.
Steam Generator Internals and Secondary Pressure Boundary			
C&LAS – FAC (c5-3a)	Y	Y	The Yellow R&D status reflects the recent and unexpected operating experience of considerable FAC-related degradation of some CANDU SG internals. There is currently work planned under the COG program to address this knowledge gap.
External Surfaces and Pressure Retaining Bolting			
CS – SCC (c6-6a, c6-7a)	Y	Y	Due to the limited operating temperature of CS external surfaces and bolting in CANDUs and the absence of a significant FAC hydrogen flux in comparison to feeder piping, the risk can be reasonably ruled out, and no specific R&D is warranted, and therefore the status has been changed to Green.

Table D-6
Detailed list of VVER MDM cell result changes for Revision 5

Cell Description	Rev. 4 Result	Rev. 5 Result	Basis/Notes
VVER 440 Reactor Pressure Vessel			
Ti-Stabilized SS, Welds & Cladding – EAF (v1-9c, v1-9d)	Y	Y	The Yellow R&D status reflects the ongoing Czech Republic national EAF test program aimed at generating data for VVER materials in simulated primary water.
VVER 1000 Reactor Pressure Vessel			
SS Welds & Cladding – SCC (v2-6d)	N	Y	The change in status reflects an increase in concern for SCC of stainless steel in primary water due to recent operating experience of cracking in safety system piping. The particular concern is the lack of data for VVER materials and chemistry.
Ti-Stabilized SS, Welds & Cladding – EAF (v2-9d, v2-9e)	Y	Y	The Yellow R&D status reflects the ongoing Czech Republic national EAF test program aimed at generating data for VVER materials in simulated primary water.
VVER Primary System Piping Components (Including the Pressurizer)			
Ti-Stabilized SS, CASS & Welds – IGA (v3-5a, v3-5b, v3-5d, v3-5e)		Y	A new column was added for IGA to address a potential concern of long-term sensitization of Ti-stabilized SS at reactor operating temperatures.
Ti-Stabilized SS & Cladding – SCC (v3-7a, v3-7d)	Y	Y	The change in status reflects an increase in concern for SCC of stainless steel in primary water due to recent operating experience of cracking in safety system piping. The particular concern is the lack of data for VVER materials and chemistry.
CASS & Welds – SCC (v3-7b, v3-7e)	N	Y	The change in status reflects an increase in concern for SCC of stainless steel in primary water due to recent operating experience of cracking in safety system piping. The particular concern is the lack of data for VVER materials and chemistry.
Ti-Stabilized SS & Cladding – EAF (v3-10a, v3-10d)	Y	Y	The Yellow R&D status reflects the ongoing Czech Republic national EAF test program aimed at generating data for VVER materials in simulated primary water.
VVER Reactor Vessel Internals			
Ti-Stabilized SS & Welds – IGA (v4-5a, v4-5b)		Y	A new column was added for IGA to address a potential concern of long-term sensitization of Ti-stabilized SS at reactor operating temperatures.

Table D-6 (continued)
Detailed list of VVER MDM cell result changes for Revision 5

Cell Description	Rev. 4 Result	Rev. 5 Result	Basis/Notes
VVER Steam Generator Tube Bundle and Internals			
Ti-Stabilized SS & Welds – Pitting (v5-2a, v5-2b)	Y	Y	The change in status reflects recent operating experience with pitting and SCC of DMWs situated in the lower crevice between the secondary collector and the intermediate austenitic piece where crud accumulates. R&D is in progress due to the observation of defects in DMWs of VVER-440 SG collector-to-shell connections. However, a number of questions remain unanswered.
Ti-Stabilized SS – ODSCC (v5-7a)	Y	Y	Some plants have reported an increased number of plugged tubes due to ODSCC. It is not clear what factor is causing this trend. Some indications point to the impact of the collector DMW weld repairs, which have been postulated to introduce additional stresses in associated tubing. The concern is for LTO, if incidences of ODSCC increase exponentially.
Ti-Stabilized SS – EAF (v5-9a, v5-9d)	Y	Y	The Yellow R&D status reflects the ongoing Czech Republic national EAF test program aimed at generating data for VVER materials in simulated primary water.
VVER Steam Generator Secondary Pressure Boundary			
Ti-Stabilized SS – EAF (v6-9a)	Y	Y	The Yellow R&D status reflects the ongoing Czech Republic national EAF test program aimed at generating data for VVER materials in simulated primary water.
VVER External Surfaces, Supports, and Pressure Retaining Bolting			
All Materials – BAC (v7-4a, v7-4b, v7-4g, v7-4h)	N	Y	The change in status to Y/Green is due to recent operating experience of BAC on RPV external surfaces and bolting due to leaks from the spent fuel pool cooling system, which exists within containment.

About EPRI

Founded in 1972, EPRI is the world's preeminent independent, non-profit energy research and development organization, with offices around the world. EPRI's trusted experts collaborate with more than 450 companies in 45 countries, driving innovation to ensure the public has clean, safe, reliable, affordable, and equitable access to electricity across the globe. Together, we are shaping the future of energy.

PROGRAM

International Materials Research (IMR), P41.01 .01

For more information, contact:

EPRI Customer Assistance Center
800.313.3774 • askepri@epri.com

3002030559 November 2024

EPRI

3420 Hillview Avenue, Palo Alto, California 94304-1338 USA • 650.855.2121 • **www.epri.com**

© 2023 Electric Power Research Institute (EPRI), Inc. All rights reserved. Electric Power Research Institute, EPRI, and TOGETHER...SHAPING THE FUTURE OF ENERGY are registered marks of the Electric Power Research Institute, Inc. in the U.S. and worldwide.